BUDKER INSTITUTE OF NUCLEAR PHYSICS
of Siberian Branch of Russian Academy of Science

ANNUAL REPORT
2013

NOVOSIBIRSK 2014

Contents

INTRODUCTION

In May 1958, the USSR Council of Ministers declared creation of the Institute of Nuclear Physics of the Siberian Branch of the USSR Academy of Sciences. The new institute was created on the basis of the Laboratory of new acceleration methods, headed by G.I. Budker, of the Nuclear Energy Institute, directed by I.V. Kurchatov. Since 1977, the Institute of Nuclear Physics has been directed by academy member A.N. Skrinsky.

Currently, BINP SB RAS with over 2,800 employees is the largest academic institute of Russia. The Institute research staff of 411 people includes 10 members and corresponding members of the Russian Academy of Sciences, 61 Doctors of Sciences and 167 Candidates of Sciences. BINP has a large experimental production department (about 1,000 employees) with high-level engineering and technology equipment.

The Institute is doing much for training of scientific and technical personnel of high qualification. BINP is a base institution for seven subdepartments of the Physics Department of the Novosibirsk State University (NSU) and the Physicotechnical Department of the Novosibirsk State Technical University (NSTU) (in total about 200 students). 60 post-graduate students are pursuing post-graduate studies at BINP, the NSU and the NSTU.

BINP is one of the world's leading centers in a number of areas of high energy physics, accelerator physics, plasma physics and controlled fusion physics. The Institute conducts large-scale elementary particle physics experiments on electron-positron colliders and a unique complex of open plasma traps and develops up-to-date accelerators, high-power sources of synchrotron radiation and free electron lasers. In most of these areas, the Institute is the only one research institution in Russia.

Below are listed the main BINP achievements in science and technology.

In the field of elementary particle physics and nuclear physics:

- pioneering works on the development of the colliding beam technique, which is now the leading one in the high energy physics:
  - first experiments on the electron-electron interaction (simultaneously with the Princeton/Stanford works) (1965),
  - world's first experiments on the electron-positron interaction (1967),
  - world's first observation of double bremsstrahlung (1967),
  - pioneering works in the two-photon physics (1970);
- research on the characteristics of vector mesons on the installations with colliding electron-positron beams VEPP-2, VEPP-2M and VEPP-4 (since 1967);
- discovery of the phenomenon of multiple production of hadrons in electron-positron annihilation (1970);
- precision measurement of the contribution of hadronic vacuum polarization to the value of muon anomalous magnetic moment for one of the most sensitive tests of the Standard Model, which is conducted in cooperation with the Brookhaven National Laboratory (1984 - 2005);
- development of the resonance depolarization method for precision measurement of the masses of elementary particles and achievement of record accuracy in measurements of the masses of K, rho, omega, phi and psi mesons and upsilon mesons (1975 - 2004);
- discovery of parity violation effects in atomic transitions and confirmation to the unified theory of electroweak interactions (1978);
- development of experiments on hyperfine internal targets on storage rings (since 1967) and investigation into the electromagnetic structure of deuteron in polarization experiments (since 1984);
- development of a technique for production of intense fluxes of labeled high-energy gamma quanta through the use of inverse Compton scattering (1980 - 1982); experimental observation of photon splitting in the Coulomb field of nucleus (1997);
- development of new methods for detection of high-energy charged and neutral particles and creation of unique detectors for installations with colliding beams (OLYA, CMD-1, MD-1, CMD-2, CMD-3, ND, SND, and KEDR) (since 1974);
- development of X-ray detectors for medical applications and creation of a low-dose digital radiographic installation on their basis, with an ultra-low level of patient exposure, and the X-ray system "Sibscan" for inspection of people (since 1981).

In the field of theoretical physics:

- development of the resonance theory of dynamical chaos and pseudochaos in the classical and quantum mechanics (since 1959);
- the first-time computation of charge renormalization in the Yang-Mills theory (1969);
- development of the method of the QCD sum rules (1979 - 1984);
- prediction of large enhancement of parity violation effects in neutron resonances in heavy nuclei (1980 - 1985);
- development of the theory of hard exclusive reactions in the QCD (1977 -1984);
- development of an operator approach to quantum electrodynamics in external fields (1974 - 1976);
- development of quantum electrodynamics in periodic structures, including a laser wave (1972 - 1997);
- development of the theory of radiation effects in passage of high-energy charged particles and photons through orientated single crystals (since 1978);
- derivation of evolution equation in the QCD for energy distribution of partons (the BFKL equation) (1975 - 1997);
- prediction of the coherence effect in the emission of gluons in the QCD and investigation into its influence on hadron distribution (1981 - 1982).

In the field of accelerator physics and technology:

- successful long-term experience in the creation of storage rings and installations with colliding beams;

- invention, development and experimental verification of the "electron cooling" method for heavy-particle beams, which is currently used at laboratories around the world; delivery of efficient "coolers" to heavy-ion accelerator complexes in Germany, China and at CERN (1965 - 2005);
- invention and development of new types of high-power RF generators (gyrocon, relativistic klystron and Magnicon) (since 1967);
- suggestion of a technique of linear electron-positron colliding beams for production of super-high energies (1968) and presentation of a physically self-consistent project (1978);
- development of components of intense-field pulsed magnetic optics (X lenses and lithium lenses), which are currently used at different laboratories (since 1962);
- invention and experimental verification of the method of charge-exchange injection, which is currently applied at all the major proton accelerators (1960 - 1964);
- theoretical and experimental investigation into the generation of polarized beams and spin dynamics in accelerators and colliders and conceptual designing and creation of highly efficient spin rotators and "Siberian snakes" for a number of accelerator complexes, (1966 - 1995);
- theoretical and experimental research on the stochastic instability and "collision effects", which impose limitations on the luminosity of colliding-beam installations (since 1966);
- development of the physical concept of a new generation of electron-positron colliders of very high luminosity, so-called electron-positron factories (since 1987);
- suggestion and development of a method of ionization cooling of muons for creation of muon colliders and neutrino factories (1969 -1981 - 2002);
- development and creation of high-power low-energy electron accelerators for a variety of technological applications, including environment protection (accelerators ELV-12 with a power of 500 kW and an energy of 1 MeV and ILU-10 with a power of up to 50 kW and an energy of 5 MeV) (since 1963);
- suggestion and implementation of a scheme of energy recovery linac for high-gain free electron lasers (1979 - 2003).

In the field of plasma physics and nuclear fusion:

- invention (1954) and creation (1959) of the "classical" open magnetic trap (magnetic bottle) for hot plasma confinement;
- invention and development of new schemes of open traps (multiple-mirror, rotating-plasma, ambipolar, and gas-dynamical ones); experimental realization of multiple-mirror confinement of plasma with sub-fusion parameters in the trap GOL-3; experimental implementation of MHD instability stabilization in an axially symmetric gas-dynamic trap (on the installation GDT) (since 1971);
- discovery of collisionless shock waves in plasma (1961);
- development of a technique of plasma heating with relativistic electron beams (since 1971);
- development of high-intensity surface-plasma sources of negative ions, now widespread in the world (1969 - 1981);
- suggestion and development of a concept of a high-power open-trap source of fusion neutrons for materials science (since 1987).
- theoretical prediction of the Langmuir collapse (1972) and experimental discovery of strong Langmuir turbulence and collapse of Langmuir waves in a magnetic field (1989 - 1997);
- creation of a series of unique high-power precision sources of hydrogen atoms for high-temperature plasma investigation for a number of large installations (1997).

In the field of synchrotron radiation and free electron lasers:

- application of synchrotron radiation of the BINP storage rings to science and technology and establishment of the international Siberian Synchrotron Radiation Center based on VEPP-2M, VEPP-3 and VEPP-4 (since 973);
- theoretical and experimental research on particle emission in periodic structures (undulators, wigglers, and crystals) (since 1972);
- development and creation of specialized sources of synchrotron radiation (since 1983);
- development and creation of one- and two-coordinate detectors for experiments with synchrotron radiation (since 1975);
- invention and development of the optical klystron (1977) and generation of coherent radiation in the infrared to the ultraviolet spectrum (since 1980);
- development and creation of a high-power free electron laser (for photochemical research and technological applications, as well as for energy transfer from the Earth to a satellite) on the basis of the most promising scheme, which uses a recuperator microtron; generation of high-power (400 W) laser radiation in the terahertz range (since 1987);
- creation of a series of intense-field superconducting magnetic devices for SR sources and electron storage rings (wigglers and bending magnets with fields of up to 10 T and solenoids with fields of up to 13 T) (since 1996).

Applied works performed by BINP SB RAS rely entirely on the results of the basic research performed by the Institute and are focused on the following main areas:

- industrial high-power electron accelerators for modification of polymers, treatment of industrial and domestic waste, production of nanopowders of pure metals, silica, and oxides, carbides and nitrides of metals, radiation processing of food, sterilization of medical equipment, disposable instruments and garments and other technological applications;
- low-dose scanning-type digital radiographic installations with ultra-low patient exposure for medical and security systems;

- development of nuclear medicine facilities for proton-, ion- and boron-neutron-capture therapy of malignant tumors;
- installations for electron beam welding;
- radiographic equipment for defense research.

During the past 20 years, BINP was financing its basic and applied research from assets received from contract works. The cost of high-tech products developed, manufactured and supplied annually by BINP to customers in Europe, Asia, and North and South Americas (over 20 countries), as well as in Russia, makes hundreds of millions rubles. The so earned money was used for the completion and commissioning of the accelerator complex VEPP-4M with the unique detector KEDR and designing and construction of large unique installations (the electron-positron collider VEPP-2000, the free electron laser and a new injection system for the existing and future BINP facilities). Throughout the post-Soviet period, these funds have been maintaining the continuous work of the BINP facilities and related infrastructure.

BINP excels in long-term international cooperation with most major foreign and international research centers. A striking example is the BINP participation in the largest international project - the Large Hadron Collider at the European Organization for Nuclear Research (Geneva). Within the framework of this cooperation, BINP has developed, manufactured and delivered to CERN unique hi-tech equipment for an amount of over 100 million Swiss francs. Other cases of BINP international cooperation include the participation of the Institute in the projects of B-factories in the U.S. and Japan and the implementation of the following large European projects: the synchrotron-radiation source PETRA-III, X-ray free electron laser (DESY, Hamburg), heavy-ion accelerator facility (GSI, Darmstadt), and some others.

BINP has played a key role in several major Russian projects, including the following: the Center for Synchrotron Radiation at the Research Center 'Kurchatov Institute', the synchrotron radiation source in Zelenograd, the neutron source for the JINR in Dubna, and radiographic equipment for defense research at VNIITF in Snezhinsk.

In 2013, the state task to the Institute included 26 'baseline' projects within 8 programs in two areas of the Program for Basic Research by the State Academies of Sciences for 2013-2020.The Institute was deeply integrated into the work of the Russian Academy of Sciences and its Siberian Branch, implementing 18 projects under programs of the Presidium of the Russian Academy of Sciences and its branches and 23 projects under SB RAS integration programs. The Institute is executing 13 state contracts and agreements under the Federal Target Programs 'Research and development in priority directions of the science-and-technology complex of Russia for 2007 – 2013' and 'Scientific and pedagogical staff of innovative Russia for the years 2009 – 2013' and 49 RFBR projects.

Every year, members of the Institute make about 200 reports at international and Russian conferences, publish about 500 articles in leading Russian and foreign scientific journals and issue monographs and educational aids. According to data published in the review 'Bibliometric indicators of the Russian Science and Russian Academy of Sciences" (RAS Bulletin, June 2009, Volume 79, № 6), the number of references to papers by BINP members that are accounted in the authoritative international database ESI was 28,267 in 1997-2007. In accordance with the survey data, this is a maximum value among all the institutions of the Russian Academy of Sciences. Four members of the Institute are winners of the Elsevier special premium as the most cited authors in the post-Soviet area in the field of natural sciences.

Below are listed works recognized by the BINP Scientific Council as the best in 2013.

In the field of **nuclear physics, elementary particle physics and physics of basic interactions:**

1) In the experiment with the SND detector at the electron-positron collider VEPP-2000, the cross sections of processes with magnetic dipole radiative decays of excited vector mesons rho (1450), phi (1680) -> eta gamma were measured for the first time.

2) In the experiment with the detector CMD-3 on electron-positron collider VEPP-2000, the anomalous behavior of the cross section of electron-positron annihilation into six pions at an energy of colliding beams corresponding to the threshold of production of nucleon-antinucleon pair was measured with a world's best precision.

3) Within the framework of the international collaboration in the experiment MEG (Switzerland), the most sensitive restriction (5.7×10^{-13}) was imposed for the probability of conservation-principle-violating lepton number of neutrinoless decay of a positive muon into a positron and a gamma quantum, which is 20 times better than previous experiment result.

4) In the BABAR experiment (Stanford, USA), in the energy range from the threshold to 6.5 GeV and with the best in the world precision, the cross section of electron-positron annihilation into a proton-antiproton pair was measured, which is the first such measurement at energies above 4.2 GeV.

5) In the experiment with the KEDR detector on the electron-positron collider VEPP-4M, the ratio of the leptonic widths in direct decays of J/psi meson was measured with the world's best precision.

6) A new efficient mechanism was offered for the generation of thermoelectricity in a nonlinear structure of Wigner crystal in a periodic potential.

7) It was first shown that the isoscalar form factor of nucleon is much larger than the isovector one in a time-like region, near the threshold of production of nucleon-antinucleon pair.

8) A high-performance infrastructure was created for processing of data from high-energy physics experiment on the detectors at BINP, the Large Hadron Collider experiments and other foreign facilities using the supercomputers of the Novosibirsk Scientific Center and the NSU.

In the field of **plasma physics:**

1) At the GDT facility, with additional microwave heating of plasma, an electron temperature of 400 eV was at-

tained, which is a record value for open quasi-stationary magnetic traps (in collaboration with the Institute of Applied Physics and the NSU).

2) At the GOL-3 facility, the possibility of controlling the plasma rotation by injecting an electron beam into it was for the first time demonstrated.

3) A scheme of plasma wakefield acceleration with controlled self-modulation of a long proton-beam driver was offered and checked with numerical simulation. It enables increasing the maximum energy of electron and positron beams by two orders of magnitude

4) On the accelerator source of epithermal neutrons, selective destruction of malignant tumors by boron neutron capture therapy was for the first time demonstrated on cell cultures (together with ICG SB RAS and NSMU).

In the field of **the physics and technology of charged particle accelerators, SR sources and FELs:**

1) The physically launch of the unique high-performance source of positrons for accelerators of Institute was executed with attaining a record rate of conversion of electrons into positrons of 0.14 GeV^{-1}.

2) On the electron-positron collider VEPP-2000, in the energy range of 320 - 1000 MeV in the center of mass system, a record value of "the colliding beam parameter" was attained and an experiment with two detectors, SND and CMD-3, was conducted with a record integrated luminosity.

3) A technique of analysis of biomedical samples was developed, and first in Russia experiments on the toxicity and pharmacokinetics of chemical compounds were conducted using an ultra-sensitive method of analysis - accelerator mass spectrometry (together with the Institute of Catalysis and the NSU).

4) An accelerating section with an original accelerating structure for the new LHC injector was developed, manufactured and supplied to CERN (Switzerland); it is the first realization in the low VHF range.

5) During tests of the unique high-temperature electron cooling system, which was fabricated and developed by BINP, at Jülich Research Center (Germany), the temperature of proton beam in the German Synchrotron COSY was 50-fold reduced.

6) Unique cryogenic stands for tests of accelerator modules of the European X-ray free electron laser (XFEL) were developed, manufactured and put into operation at the laboratory DESY (Germany)

7) Unique superconducting multipole wigglers with a field of 4.2 T and 7.5 T to generate intense X-rays for biomedical research were developed, fabricated and installed at international synchrotron radiation centers.

8) An analytical theory was created and experimental research on the propagation of surface plasmon polaritons along metal-insulator interfaces and their diffraction at the border was performed in the terahertz range.

In 2013, F.V. Ignatov and K.Yu. Todyshev were awarded the RF President Prize for young scientists in the field of science and innovations for the year 2012 for a cycle of works on precision study of properties of elementary particles on colliding electron-positron beams (RF President Decree 46 dated February 7, 2013 "On awarding the RF President Prizes in the field of science and innovations to young scientists for the year 2012").

A Russian Academy of Sciences medal for young scientists in 2012 in the field of nuclear physics for the work "Development of theory of elementary particle reggeization in the next-to-leading logarithmic approximation" was awarded to a group consisting of A.V. Grabovsky, M.G. Kozlov, A.V. Reznichenko (Resolution 30 of the Presidium of the Russian Academy of Sciences on February 19, 2013)

The Novosibirsk region Government Award in 2013 in the field of "development or creation of devices, techniques, technologies, and new scientific and technical products" for a cycle of works "Generation of focused atomic beams for fusion facilities" was awarded to a group consisting of A.A. Listopad, A.V. Kolmogorov, and A.A. Tkachev.

The Novosibirsk region Government Award in 2013 in the nomination "engineering sciences" for a cycle of works on "Creation of equipment for research in the field of X-ray pulses" was awarded to a group consisting of G.A. Fatkin and A.V Pavleno.

The Novosibirsk region scholarship for post-graduate students in 2014 was awarded to A.G. Lemzyakov, Yu.Yu. Choporova, D.A. Shemyakin and I.M. Schudlo.

Groups of the BINP scientific schools headed by academy members G.N. Kulipanov and A.N. Skrinsky, and professors A.A. Ivanov and A.P. Onuchin won the 2014 competition of the RF President Council on Grants for support of leading scientific schools (NSh-2014), thus confirming the status of leading scientific schools for 2014-2015.

A.E. Levichev won the 2014 competition of the RF President Council on Grants for support of young Candidates of Sciences (Mk-2014).

A.A. Ivanova, V.N. Kudryavtsev, and T.A. Kharlamova became winners of the competition for the RF President scholarship for young scientists in 2013. Ten young scientists were awarded the RF President scholarship.

V.F. Sklyarov and V.V. Kaminsky became winners of the competition for scholarships from the President and the Government of the Russian Federation, respectively, for graduate schools.

525 members of the Institute were awarded the memorial sign "For work for the benefit of the city" in 2013 in honor of the 120th anniversary of Novosibirsk.

The three Thesis Boards of the Institute, which are entitled to accept Doctor of Sciences (Candidate of Sciences) theses, continued their work in 2013. 15 meetings of the Boards took place, at which 4 Doctor of Sciences and 11 Candidate of Sciences theses were defended

Over 50 tours of the BINP facilities were conducted for school pupils, students, school and university teachers, members of other organizations and guests of the Institute, in total about 2,000 people. Lectures were delivered at Novosibirsk schools.

1
PARTICLE PHYSICS

1.1. CMD-3 DETECTOR

Five sessions of data acquisition were carried out with the CMD-3 detector (see Fig.1.1.1.) in 2013. The luminosity integral amounted to 25 pb^{-1}; about 25 terabytes of data was recorded.

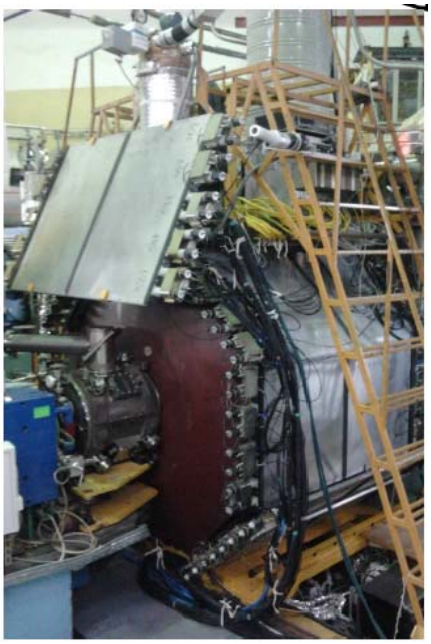

Fig. 1.1.1. CMD-3 detector in the experiment hall of VEPP-2000.

The energy was continuously measured by inverse Compton scattering during the work. A graph of data acquisition with the CMD-3 detector in 2010 - 2013 is shown in Fig. 1.1.2.

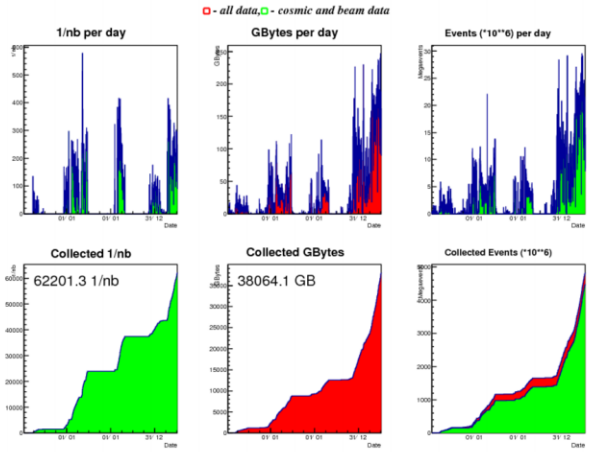

Fig.1.1.2. Graph of data acquisition with CMD-3 detector in 2010 – 2013.

The experiment season of 2013 was the longest one: the CMD-3 detector on the collider VEPP-2000 was continuously collecting data for 7 months. In the first session (November 2012), a small luminosity integral (0.68 pb^{-1}) was accumulated in the area of the $\phi(1020)$ meson energy. Then an experiment (a luminosity integral of 0.23 pb^{-1}) was conducted with the CMD-3 detector in the area of the $\omega(782)$ meson energy. These two sessions allowed us to investigate the parameters of the detector in operation at energies below 1 GeV in the center of mass system and to prepare ourselves to collecting a luminosity integral of 6.2 pb^{-1} in the energy range of 0.32 - 0.98 GeV in the center of mass system, which began in early December 2012 and lasted till mid-April 2013. This energy area is very important in terms of research on the $e^+e^- \to \pi^+\pi^-$ process. The cross section of this process gives the main contribution to the value and the error in the determination of the hadronic vacuum polarization in the calculation of the anomalous magnetic moment of the muon. In accordance with this requirement, one of the main tasks of the experiments with the CMD-3 detector is the measurement of the cross section of the $e^+e^- \to \pi^+\pi^-$ process with a systematic precision of 0.35%. Fig.1.1.3. shows the relative statistical accuracy of the measurement of the cross section of the pion pair production. This accuracy was obtained in the analysis of 2013 data in the energy range of 0.32 - 0.98 GeV. One can see that the accuracy of the CMD-3 experiment throughout the energy range is comparable with the global average value, and is record high in the area of the $\rho(770)$ resonance.

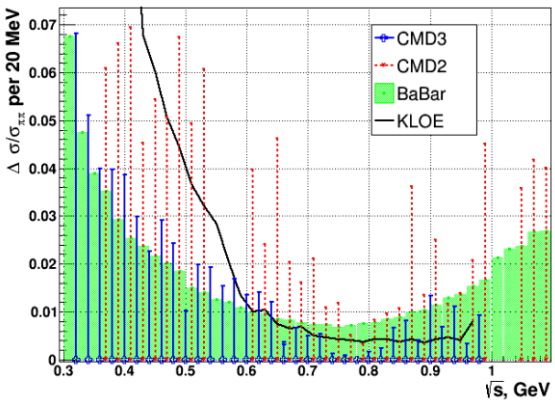

Fig. 1.1.3. Relative statistical accuracy of measurement of $e^+e^- \to \pi^+\pi^-$ cross section in CMD-3 experiment as compared with other similar measurements.

Besides, in the same experiment for the first time in the history of e^+e^- colliders measurements were made at an energy of 0.32 GeV, which is almost equivalent to the threshold of production of hadrons.

After successful scanning of the area of the $\rho(770)$ meson, in April-May 2013 an experimental run was done at the energy of the $\phi(1020)$ resonance, the luminosity integral in which was 6.2 pb^{-1}.

Then, during May-June 2013 a record luminosity integral of 8.6 pb^{-1} was acquired in the area of the $\omega(782)$ meson. At the end of the experiment season of 2013, for two weeks in June the CMD-3 - VEPP-2000 complex was working at one energy point of 0.958 GeV in the center of

mass system. This run resulted in a luminosity integral of 2.7 pb^{-1}. These statistics will be used in analysis of the direct two-photon production of the meson, the mass of which is 0.958 GeV. After this data collection session the complex was shut down for a planned upgrade.

In 2013 some progress was made in the method of luminosity determination. On the CMD-3 detector, the luminosity is found from two processes: $e^+e^- \to \gamma\gamma$ and $e^+e^- \to e^+e^-$. The luminosity values determined using these procedures coincided with those obtained on the CMD-3 detector in 2012 - 2013 with an accuracy better than 0.3%. This allows reckoning on high systematic accuracy of luminosity determination.

The processing of the experiment data collected with the CMD-3 detector in 2011 – 2012 continued. Analysis of the $e^+e^- \to 3(\pi^+\pi^-)$ process in the energy range of 1.5 - 2.0 GeV in the center of mass system was completed and published. A research on the production of six pions in a channel with four charged and two neutral pions, $e^+e^- \to 2(\pi^+\pi^-\pi^0)$, started. Fig.1.1.4. shows preliminary results of the measurement of the cross section of this process.

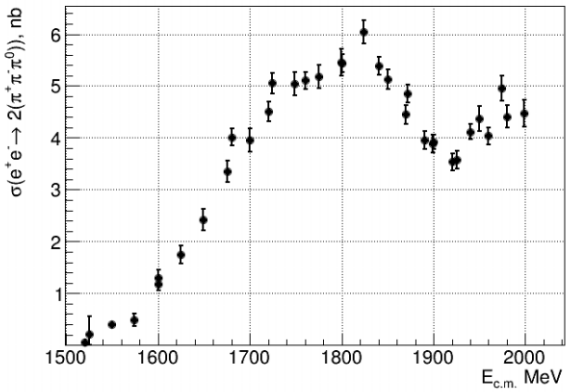

Fig. 1.1.4. Cross section of the $e^+e^- \to 2(\pi^+\pi^-\pi^0)$ process.

In 2013, when analyzing the process of electron-positron annihilation into a proton-antiproton pair near the production threshold, we managed to measure the cross section of this process at a beam energy below 952 MeV. At these energies, the protons and antiprotons do not leave the vacuum chamber of the detector and events of the process are detected by secondary particles resulting from the annihilation.

Fig. 1.1.5. shows a cross section of the $e^+e^- \to pp$ process from the production threshold to the maximum energy of VEPP-2000. The cross section was measured on the CMD-3 detector. For comparison, the figure also shows the results of other experiments on this process. The CMD-3 experiment results are consistent with these measurements.

The CMD-3 collaboration includes analysis of 15 different physical processes, 8 of which had yielded preliminary results, which have been reported at Russian and international conferences.

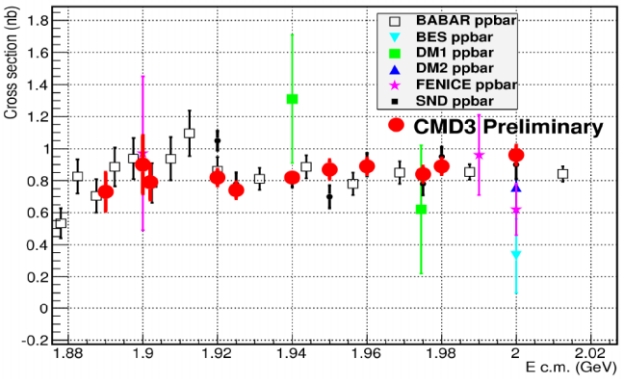

Fig. 1.1.5. $e^+e^- \to pp$ cross section measured on the CMD-3 detector in comparison with results of other experiments.

Works to improve parameters of different detector systems continued in 2013.

The last type of units of the "KLYUKVA" standard in the system for data collection is being replaced now. In-house AWF-32 boards were applied instead of A32 ones for reading information from the cathode channels of the Z-chamber of the detector. The spatial resolution of the Z-chamber that was reached with the new electronics turned out to be not worse than that with the electronics of the "KLYUKVA" standard. When the detector is shut down for upgrade, the new AWF-32 electronics will be installed for reading of information from the liquid-xenon calorimeter. After that, all the electronics of the CMD-3 detector will be made in the new standard, which will reduce the idle time of the data collection system to 70 microseconds instead of 245 microseconds now.

The charged trigger of the CMD-3 detector was modified in 2013. Earlier, the trigger would make a positive decision only if the outer layers of the drift chamber coincided with the adjacent anode sectors of the Z-chamber. Now information of the Z-chamber is excluded from the trigger. The detector systems start registration of event in case of coincidence of the internal and external layers of the drift chamber. This increased the efficiency of the trigger in detection of charged particles. The new configuration of the trigger provided an almost 100% efficiency of detection of slow charged kaons.

Much work was done on the development of algorithms for data reconstruction in the cylindrical electromagnetic calorimeter. The so-called "linkage" of clusters in the liquid-xenon calorimeter with those in the CsI-crystal calorimeter was performed for the purpose of creating a joint cluster. Corrections to photon energies and angles in the calorimeter were developed, which resulted in a decent agreement between the simulation and experiment in the reconstruction of the neutral pion. A joint calibration of the liquid-xenon and CsI crystal calorimeters was performed based on events with cosmic particles and e^+e^- scattering events.

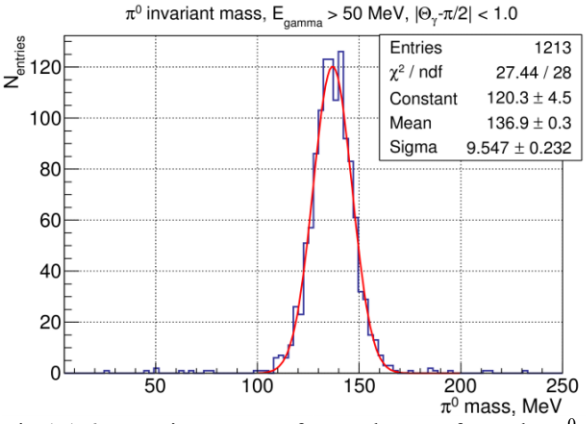

Fig.1.1.6. Invariant mass of two photons from the $\pi^0 \to \gamma\gamma$ decay as detected in cylindrical calorimeter of CMD-3 detector.

As shown in Fig. 1.1.6, the determined resolution in the mass of the π^0-meson that was reconstructed from two photons from the $\pi^0 \to \gamma\gamma$ is $\sigma_m/m = 7\%$.

The calibration and refinement of the reconstruction programs in 2013 resulted in an energy resolution of the end calorimeter of the CMD-3 detector for events of $e^+e^- \to e^+e^-$ and $e^+e^- \to \gamma\gamma$ that is close to the simulation.

Within the upgrade of the detector in 2013 – 2014, the time-of-flight system will be replaced. The new system, which is created in conjunction with the Institute of Theoretical and Experimental Physics (Moscow), will be made on scintillation plates that collect light using spectrum-shifting fiber and SiPM photodetectors. A prototype of one module of the system has been tested on a BINP bench. A time resolution of 0.8 ns was obtained, which is close to the design value. This system will be installed in the detector by the new experiment season.

The works were carried out with a financial support from the Russian Ministry of Education and Science, State Academy of Sciences Basic Research Programs II.15.1.2 and II.15.2.2 and RFBR grants 12-02-31501-a, 12-02-31499-a, 12-02-31498-a, 12-02-01032-a, and 13-02-00215-a.

1.2. THE SND DETECTOR

Experiments at VEPP-2000

Experimental season of 2012 ÷ 2013 data-taking with the SND detector at VEPP-2000 started in November 2012. The aim of the experiment was to scan the energy range below the ϕ meson. The beam energy E varied from 160 to 500 MeV. This experiment was completed in March 2013. Accumulated integrated luminosity was 6 pb^{-1}. A great achievement of the VEPP-2000 collider in this season was the high instantaneous luminosity, 4÷ 5 times the luminosity of VEPP-2M at the same energies. Due to the high luminosity, the experiment was completed ahead of the schedule, and it was decided to conduct two additional experiments in the remaining time: scanning of a narrow energy region near the ϕ-meson resonance with an integrated luminosity of 7 pb^{-1} and an additional data-taking in the region of the ρ- and ω- resonances with an integrated luminosity of 8 pb^{-1}. The first experiment was completed in mid-May, the second experiment — at the end of June.

During these experiments, the collider energy was monitored by the method of the inverse Compton scattering of laser radiation on the beam electrons.

Detector status

During the experiments of the 2012 ÷ 2013 season, all detector systems worked steadily without significant problems.

Work was continued on the production of the second copy of the tracking system. At the present time, wire tensions have been tested and high-voltage distribution was mounted. The inner cathode was manufactured and fixed inside the body of the tracking system. High-voltage boards are being configured.

Experiments in 2012÷2013 years were performed with the completely renewed electronics of the first layer of the calorimeter. In 2013 the production and verification of new electronics for the 2nd and 3rd layers of the calorimeter have been completed. Work was continued on the development of new electronics boards for calorimeter channels: shaper amplifier, ADC and the DeltaT board allowing to measure a time shift (from 0 to 25 ns) between the primary trigger signal and the digitizing step of ADC. The new channel has been tested experimentally. For events with energy deposition in the calorimeter counters more than 200 MeV, time resolution was 1.3 ns. Amplitude resolution for the generator signal, equivalent to an energy deposition of 100 MeV, equals to 350 keV.

In the experiments of 2010÷2013 years, two versions of the threshold Cherenkov counter system were used with different refractive indices of the aerogel: n = 1,05 at the energies E less than 500 MeV for e/π separation, and n = 1,13 at the energies E greater than 500 MeV for K/π separation. Using the experimental data collected above the ϕ-meson resonance, for the system with n = 1.13 detection efficiencies were measured for charged π and K mesons (Fig.1,2). The achieved degree of the system efficiency provides suppression of pions more than two orders of magnitude in the momentum range from 350 to 870 MeV. The average amplitude of the signal for ultra-relativistic electrons is 6-8 photoelectrons. The respective registration efficiency of electrons is equal to 99.7%.

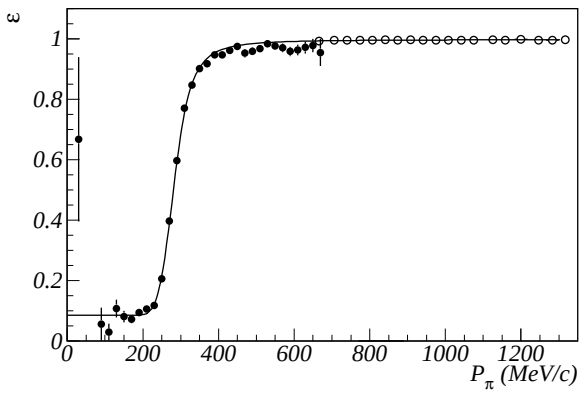

Fig 1.2.1: Dependence of the detection efficiency of the system of aerogel Cherenkov counters with n=1,13 on particle momentum. For pions (filled circles) events of the process $e^+e^- \to \pi^+\pi^-\pi^0$ were used to determine the efficiency. For muons (empty circles) the detection efficiency was obtained by using the events of the process $e^+e^- \to \mu^+\mu^-$. The curve represents an approximating function.

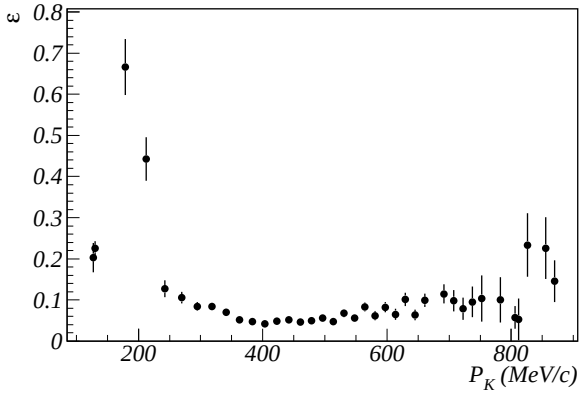

Fig 1.2.2: Dependence of the kaon detection efficiency of the system of aerogel Cherenkov counters with n=1,13 on kaon momentum obtained by using the events of the process $e^+e^- \to K^+K^-$.

In 2013 the Cherenkov counter worked with a refractive index n=1,05. Operability of the system was checked on such $e^+e^- \to e^+e^-$ process events the final state particles of which hit the "good" counter area (excluding hits of particles in the shifter and in the counter edges). Fig 1.2.3 and 4 show the time dependencies of the average number of photoelectrons in the counter and the detection efficiency of the system for ultra-relativistic electrons.

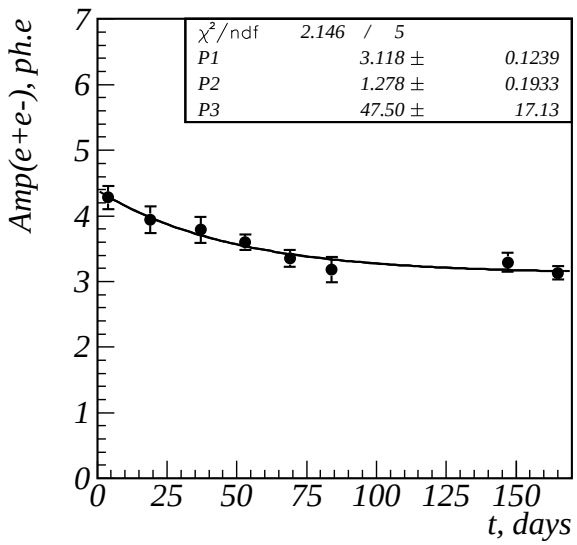

Fig 1.2.3: Time dependence of the average signal amplitude for the entire system of aerogel Cherenkov counters with n=1,05.

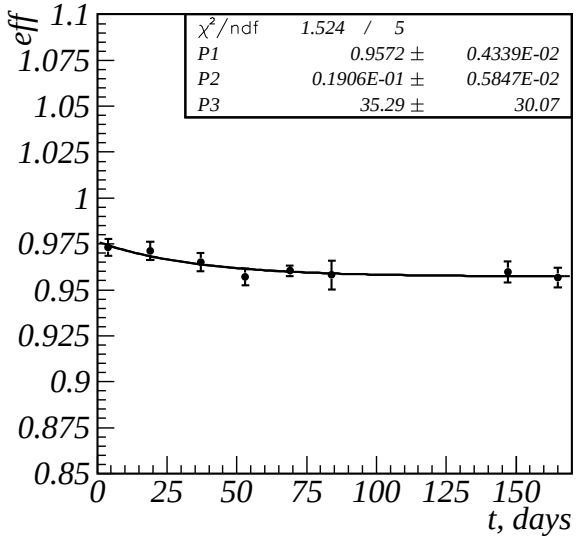

Fig 1.2.4: Time dependence of the detection efficiency of ultra-relativistic electrons for the entire system of aerogel Cherenkov counters with n=1,05.

Software Status

Software of the data acquisition system (DAS) was developing in the direction of supporting new electronics components and improving controllability and reliability of statistics collection. Namely, the following developments have taken place. Readout and saving of the event based information were implemented for new boards digitizing calorimeter signals (A24MM) and for the board that determines the time shift of the trigger signal (DeltaT). Several test runs were carried out with prototype boards. More regular scheme to activate DAS processes (scenario ponline) was adopted. Data exchange with VEPP2000 using the service channel access (VCAS) was implemented. The storage, display and transmission of the beam energy measurement data in VCAS were organized for the laser backscattering system which determines the beam energy from the Compton end-point energy of the scattered photons spectrum. The new mode suspension of run until operator intervention (Pause) was added. In the process of event based online monitoring a new calibration of the interaction point was added which takes into account the inclination of the beam axis, as well as a control of the Z-coordinate measurement. An ability of the cold (complete, after switching) initialization of all DAS control blocks (cold_init) was added.

Of changes in the simulation the following points should be noted: simulation software kernel was switched to Geant4 version 9.5; simulation of the response of the muon system electronics was brought to the operating state; primary generators for the processes $e^+e^- \to e\tau$, with the decays $\tau \to \mu\nu\nu$, $e\nu\nu$ or $\pi\nu$, and of e^+e^- annihilation into 8 particles uniformly distributed over the phase space were developed and integrated into the SND simulation software; the primary generator of the processes $e^+e^- \to 4$ leptons (DIAG36) were also added; A bug was fixed in the simulation of the proportional chamber strips response; in the primary generator Kardapo a new process $e^+e^- \to \eta\phi$ was added.

During 2012-2013, there were several important changes in the system of processing and data reconstruction, in particular: corrections were designed and implemented accounting geometric distortions in the detector, such as shear and rotation of the axis of e^+e^- beams, shear and rotation of the calorimeter hemispheres relative to the drift chamber; package vdkine of the kinematic reconstruction was extended by inclusion of new processes; infrastructure was developed for description of the physical structure of the event and for the automatic generation of the kinematic reconstruction algorithms; in the framework of scientific cooperation, SND group started to use a computer cluster (supercomputer) of the Siberian Supercomputer Center of SB RAS for reconstruction, processing and modeling of the events; for this purpose, we continue to use computing cluster of NSU too; the use of two independent sites allowed to increase overall system reliability; in the object candidate physical particle information was added about the hits in the muon system (external scintillation counters and proportional tubes) and in the particle identification system (threshold Cherenkov counters); new objects were added with information about the normalized ionization density (dE/dx) in the event; software of SND successfully passed the assembly and initial testing on the x86_64 architecture in the regime of 32-bit compatibility, on OS Linux SL6; infrastructure was developed allowing to control the amplitude calibration of the drift chamber; incorrect calibrations found were corrected; a procedure and its applications were developed for obtaining an absolute z calibration in the drift chamber; a procedure for removing artifact tracks in the chamber during reconstruction was

significantly improved; a procedure of accounting for overlaps in the detector events was implemented and tested.

SND data analysis

Analysis of the process $e^+e^- \to n\bar{n}$ have been performed using all experimental data accumulated in 2011-2012. The procedure of the cosmic background subtraction has changed; conditions for selecting $n\bar{n}$ events and background suppression were improved; in the simulation, more correct antineutron absorption cross sections were installed; during the processing of the simulation, recorded beam background events are randomly superimposed. In total, the analysis uses 18 points in the range of the beam energy 900-1000 MeV, including 11 points above the $n\bar{n}$ threshold. Integrated luminosity accumulated above the threshold is $\Delta L = 5,7\text{pb}^{-1}$. It should be noted that only runs with an average luminosity above $3 \cdot 10^{30}$ cm^{-2}sec^{-1} were singled out for the analysis.

As a result of application of the selection criteria, the initial set of more than 10^9 events was reduced to the level of$\sim 5 \cdot 10^3$. Detection efficiency ϵ for the events of the process $e^+e^- \to n\bar{n}$ was about 20%.

The process cross section at each energy point was determined by the following formula:

$$\sigma = \frac{N - xT}{\epsilon L(1+\delta)}, \qquad (1)$$

where N is the number of selected $n\bar{n}$ candidates, x — counting rate of cosmic events, T — duration of the run, ϵ — detection efficiency, δ — radiative correction, L — integrated luminosity. The measured cross section is shown in Fig.5 separately for 2011 and 2012 scans. For comparison, the results of the first and the only previous measurement of the $e^+e^- \to n\bar{n}$ cross section in the FENICE experiment is also shown. The average value of the cross section is $0,73 \pm 0,08$ nb. However, in the energy points closest to the threshold the cross section is close to 1 nb. The error shown in Fig.1.2.5 is statistical one.

The measured distribution over $\cos\theta$, where θ is polar angle of antineutron emission, is shown in Fig.6. The bin width varies for $\cos\theta$, but for θ a constant step of 9° is used, to exclude a differential nonlinearity due to the finite size of the calorimeter crystals. The experimental distribution is approximated by the sum of histograms corresponding to the parts of the differential cross section containing the electric G_E and magnetic G_M form factors, which are correspondingly proportional to $1 - \cos\theta^2$ and $1 + \cos\theta^2$. These histograms, normalized on the number of events obtained in the approximation, and their sum are shown in Fig.1.2.6. Taking into account an additional factor in the cross section $4m_n^2/4E^2$ in the part containing G_E, we can get:

$$|G_E/G_M|^2 = 2,8 \pm 4,6 \qquad (2)$$

We can see from this formula and Fig1.2.6 some dominance of the contribution of G_E over G_M. This is the first measurement of the quantity $|G_E/G_M|$ for the neutron.

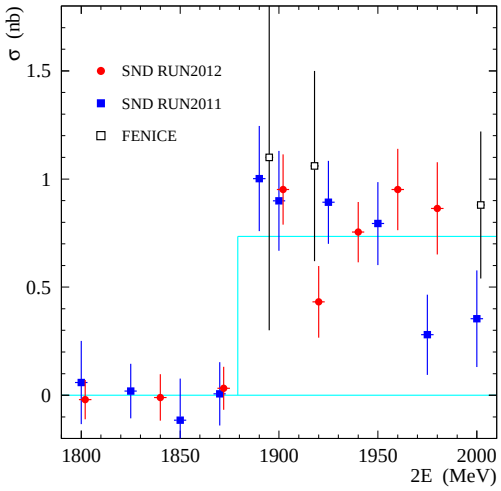

Fig 1.2.5: The measured cross section of the $e^+e^- \to n\bar{n}$ process. By different symbols are shown results of the 2011 and 2012 SND experiments and the data from the FENICE detector.

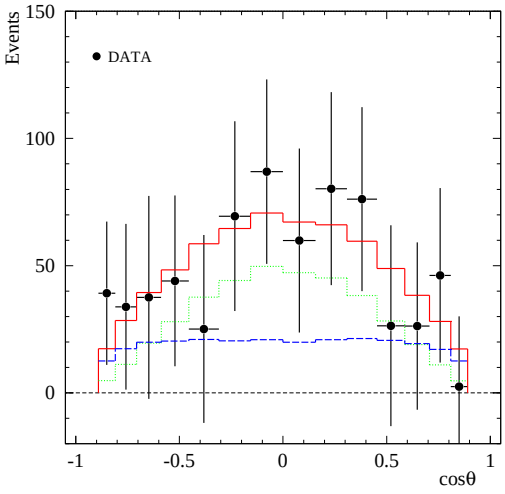

Fig 1.2.6: Distribution of experimental events of the process $e^+e^- \to n\bar{n}$ over $\cos\theta$. Points with errors — experimental data. Solid histogram — result of the approximation. The pointed histogram shows the contribution to the distribution of the term proportional to G_E, and the dotted histogram — of the term proportional to G_M. The upper histogram — the sum of these two contributions.

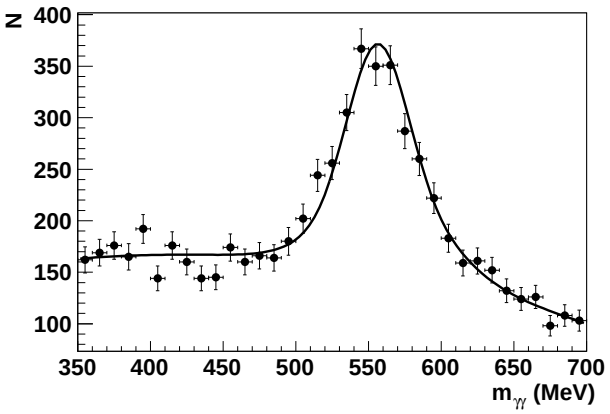

Fig 1.2.7: Two-photon invariant mass spectrum for experimental events in the energy range $2E$ =1450–1550 MeV. The curve shows the result of the approximation of the spectrum by the sum of the effect and background.

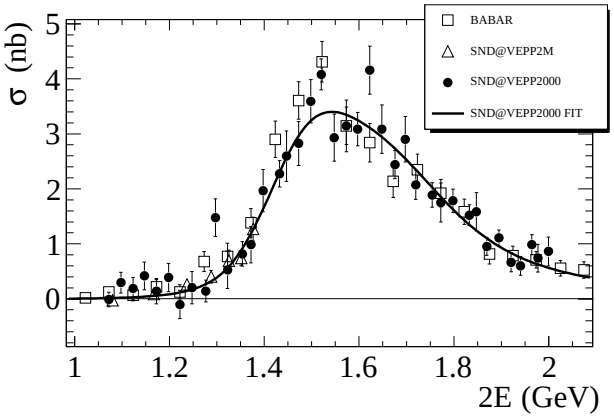

Fig 1.2.8: The Born cross section of the process $e^+e^- \to \eta\pi^+\pi^-$ measured by SND at VEPP-2000, by SND at VEPP-2M and in the BABAR experiment. The curve is the result of approximation of the cross section in the framework of the vector meson dominance model with the sum of contributions from the resonances ρ, ρ', and ρ''.

The main sources of the systematic uncertainties in the measured cross section are errors in the subtraction of the cosmic background (0.1 nb), in the detection efficiency (0.2 nb), in the subtraction of the physical background (0.1 nb) and in the luminosity determination(0.03 nb). The total systematic error is 0.25 nb or $\sim 30\%$.

Cross section of $e^+e^- \to \eta\pi^+\pi^-$ was measured using 2011 and 2012 scans. Events with two charged tracks and with two or three photons were selected. For selected events, kinematic reconstruction under the $e^+e^- \to \pi^+\pi^-\gamma\gamma$ hypothesis was performed. Further, the two-photon invariant mass spectrum was analyzed. The spectrum is approximated by the sum of the functions describing the spectra of the effect and background. An example of the invariant mass spectrum approximation is shown in Fig. 1.2.7.

In the process $e^+e^- \to \eta\pi^+\pi^-$ the dominant intermediate mechanism is $e^+e^- \to \eta\rho$. The energy dependence of the $e^+e^- \to \eta\pi^+\pi^-$ cross section in comparison with the results of previous experiments is shown in Fig. 1.2.8.can be seen that the SND and BABAR results are consistent.

Analysis of the process $e^+e^- \to \eta K^+K^-$ is at an early stage. To investigate the process $e^+e^- \to \eta K^+K^-$, it is supposed to select events with two charged particles tracks and two or more photons. Selection criteria are similar to those for the process $e^+e^- \to \eta\pi^+\pi^-$ described above. However, interaction of kaons with the calorimeter material is characterized by the larger number of clusters which are reconstructed as false photons. In order not to lose the signal events, an upper bound on the number of photons should be less than 10. Choosing a pair of photons from the decay of the η-meson is supposed to be carried out by using a kinematic reconstruction under the $e^+e^- \to K^+K^-\gamma\gamma$ hypothesis.

For simulation of the process $e^+e^- \to \eta K^+K^-$, a primary generator was developed on the basis of the mechanism $e^+e^- \to \eta\phi \to \eta K^+K^-$, which according to the

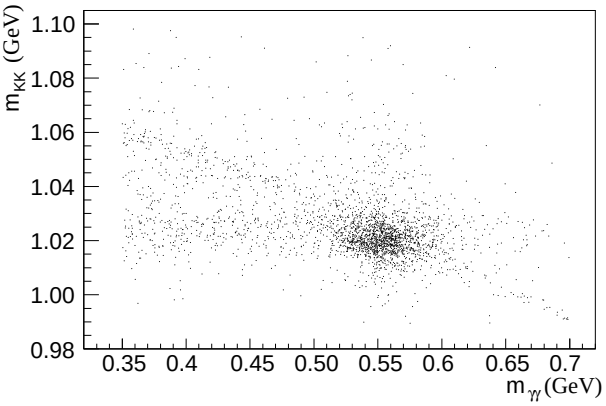

Fig 1.2.9: The two-dimensional distribution over the invariant masses of the systems $\gamma\gamma$ and K^+K^- for simulated events of the process $e^+e^- \to \eta K^+K^-$.

experimental data previously obtained in another experiment is a dominant mechanism. Fig 2.9 shows a two-dimensional distribution over the invariant masses of the systems $\gamma\gamma$ and K^+K^- for simulated $e^+e^- \to \eta K^+K^-$ events at energy $2E = 1.7$ GeV.

The process $e^+e^- \to \pi^+\pi^-\pi^0$ was studied based on the statistics collected in 2011 in the energy range $\sqrt{s} = 1.05 \div 2.00$ GeV. The data, corresponding to the integrated luminosity of about 20 pb^{-1}, were collected in 40 energy points. To select the events under study, the following conditions were required: the presence of two central tracks with the polar angle θ within 30° to 150°, and of two photons with energies greater than 30 MeV. For selected events the kinematic reconstruction was performed assuming that the event comes from the process $e^+e^- \to \pi^+\pi^-2\gamma$. On the parameters obtained in the reconstruction the following restrictions were imposed: χ^2 of the hypothesis that tracks have a common origin is less than 60, χ^2 of conservation

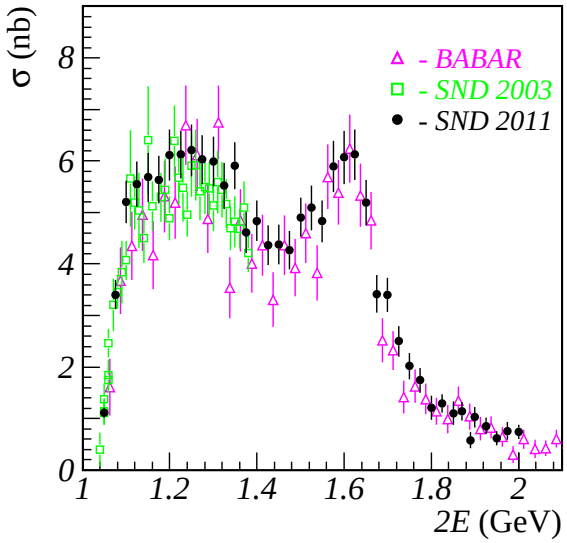

Fig 1.2.10: Cross section of the $e^+e^- \to \pi^+\pi^-\pi^0$ process measured at VEPP-2000 in comparison with the results of previous experiments: SND at VEPP-2M and BABAR.

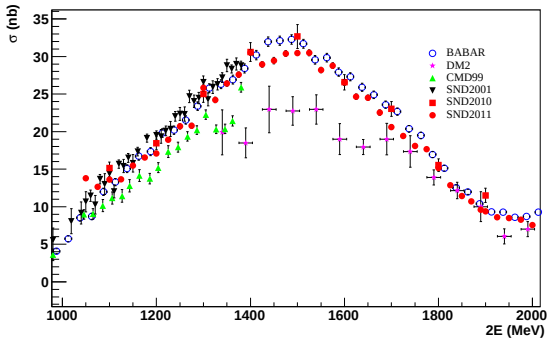

Fig 1.2.11: The measured cross section of the $e^+e^- \to \pi^+\pi^-\pi^0\pi^0$ process in comparison with the results of previous experiments.

of energy and momentum is less than 40. The main source of the background events in the studied energy region is the process $e^+e^- \to \pi^+\pi^-\pi^0\pi^0$. Separation of the effect and the background is carried out in the approximation of the spectrum of the invariant mass of two photons by a sum of the distributions obtained from the simulation for the process under study and for the background process.

To study a systematic uncertainty of the detection efficiency obtained from simulation, $e^+e^- \to \pi^+\pi^-\pi^0$ process was studied in the energy range of the ϕ-meson resonance. In this region desired events can be selected with minimal background impurity using significantly milder selection conditions. Distributions over χ^2 of the kinematic reconstruction were studied and the corresponding corrections to the detection efficiency determined. A correction associated with the strict restrictions on the number of photons was also identified.

The measured cross section of the $e^+e^- \to \pi^+\pi^-\pi^0$ process is shown in Fig. 2.10 together with data from previous experiments: SND at VEPP-2M and BABAR. The results of all three experiments are consistent to each other.

In the energy range $1 \div 2$ GeV, the cross section of the $e^+e^- \to \pi^+\pi^-\pi^0\pi^0$ process is determined by production in e^+e^- annihilation of the ρ, ρ' and ρ'' vector mesons with their subsequent decays into the $\pi^+\pi^-\pi^0\pi^0$ final state. The main mechanism of the decay is provided by the $\omega\pi^0$ and $a_1\pi$, $rho^+\rho^-$, $f_0\rho^0$ intermediate states. In this energy region the $e^+e^- \to \pi^+\pi^-\pi^0\pi^0$ cross section dominates in the total cross section of the e^+e^- annihilation into hadrons and contributes significantly into the hadronic vacuum polarization.

Pre-selected events with two or more charged particles and four or more photons were analyzed. The extra particles were allowed to avoid the loss of events due to superimposed tracks and photons from the beam background and due to emergence of false photons in pion nuclear interactions with the detector material.

Further kinematic reconstruction of the events was performed under the assumption of the $\pi^+\pi^-\pi^0\pi^0$ final state with implementation of the laws of conservation of energy and momentum. No additional assumptions about the intermediate state were introduced. In events with three or more charged particles, or five or more photons, in the kinematic reconstruction all possible combinations is checked and the combination providing the minimum value of χ^2 of the kinematic reconstruction is selected.

Events were selected for which χ^2 of the kinematic reconstruction is less than 100 and masses of the reconstructed π^0 mesons lie in the range 80-200 MeV.

Detection efficiency for the $e^+e^- \to \pi^+\pi^-\pi^0\pi^0$ process was determined from simulation. Radiative correction was calculated by the Monte-Carlo method and varied smoothly with energy from 0.88 at 1 GeV to 1.14 at 2 GeV. The measured cross section is shown in Fig. 1.2.11.

For the separation of the intermediate reaction mechanisms, the $\pi^+\pi^-\pi^0$ invariant mass distribution was used. At that the combination closest to the mass of the ω-meson was chosen to form the distribution. In the energy region below 1.4 GeV, the distribution over this parameter is well described by simulation. The shapes of the distributions over this parameter for each of the four reaction mechanisms were extracted from the simulation. To determine the contribution of the $\omega\pi^0$ intermediate state, the experimental distribution over the $\pi^+\pi^-\pi^0$ invariant mass was approximated by the sum of four distributions with fixed shapes, taken from simulation. There were four free parameters altogether in the fit. Cross sections of the processes $e^+e^- \to \omega\pi^0$ and $e^+e^- \to \pi^+\pi^-\pi^0\pi^0$ (with the contribution of the $\omega\pi^0$ intermediate state subtracted) are shown in figs 1.2.11,13, 14. Using experimental data corresponding to the integrated luminosity of about 25 pb^{-1} collected in the energy range 1050-2000 MeV in 2011, a preliminary study of the process $e^+e^- \to \pi^+\pi^-\pi^+\pi^-$ was conducted.

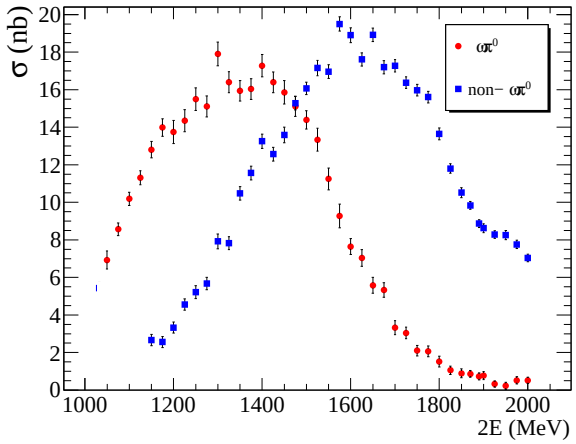

Fig 1.2.12: The measured cross sections of the reactions $e^+e^- \to \omega\pi^0 \to \pi^+\pi^-\pi^0\pi^0$ and $e^+e^- \to \pi^+\pi^-\pi^0\pi^0$ without the contribution of the $\omega\pi^0$ intermediate state.

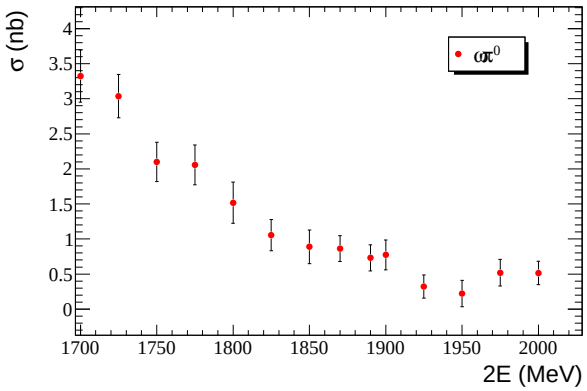

Fig 1.2.13: The measured cross section of the reaction $e^+e^- \to \omega\pi^0 \to \pi^+\pi^-\pi^0\pi^0$.

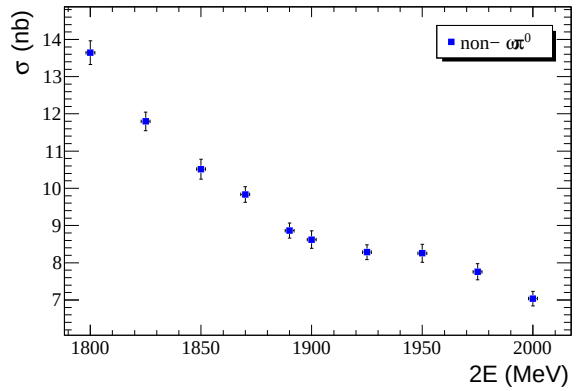

Fig 1.2.14: The measured cross section of the reaction $e^+e^- \to \pi^+\pi^-\pi^0\pi^0$ with the contribution of the $\omega\pi^0$ intermediate state subtracted.

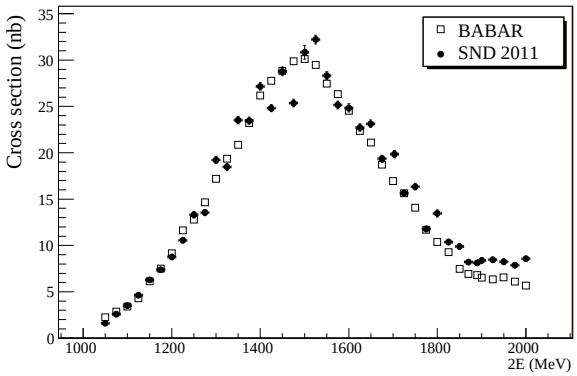

Fig 1.2.15: The cross section of the process $e^+e^- \to \pi^+\pi^-\pi^+\pi^-$ obtained in this work in comparison with results of the BABAR experiment.

Events with four or more charged particles and less than two photons were selected. For the four charged tracks the hypothesis that they all originate from the interaction point was tested and χ^2 of this hypothesis in the $R-\phi$ plane (χ^2_r) and in the $R-Z$ plane (χ^2_z) were calculated. The conditions $\chi^2_r \leq 8$ and $\chi^2_z \leq 20$ were imposed on these parameters. To suppress the beam background, events with too large z-coordinate of the vertex, $|Z_{vert}| > 10$ cm, were rejected. Also we impose conditions on the total energy deposition in the calorimeter ($< 1.75E$) and on the energy of each reconstructed particle ($< 0.75E$). The above selection criteria do not help against the background processes $e^+e^- \to 6\pi$, $e^+e^- \to K^+K^-\pi^+\pi^-$ and $e^+e^- \to K_sK^+\pi^- \to K^+\pi^+\pi^-\pi^-$. Expected numbers of such background events was calculated according to the simulation using experimental data on their cross sections and subsequently subtracted. Preliminary results on the cross section of the process $e^+e^- \to \pi^+\pi^-\pi^+\pi^-$, in comparison with results of the BABAR experiment, are shown in Fig. 1.2.15.

Analysis of the process $e^+e^- \to \eta\gamma$, based on the integrated luminosity of $\sim$32 pb^{-1} accumulated in the energy range 1.07$\div$2.00 GeV in 2010$\div$2012, is near completion. The process $e^+e^- \to \eta\gamma$ is studied in the seven-photon final state, that is in the $\eta \to 3\pi^0$ decay mode of the η meson. Events with seven or more photons and no charged particles were selected for the analysis. The following conditions on the full energy deposition in the calorimeter, E_{tot}, and on the total momentum of photons, P_{tot}, were imposed:

$$0,7 < E_{tot}/2E < 1,2,$$

$$P_{tot}/2E < 0,3/c,$$

$$E_{tot}/2E - cP_{tot}/2E > 0,7.$$

For selected events, a kinematic reconstruction was performed using measured angles, energies of photons and conservation of energy and momentum. The kinematic reconstruction provides refined photon energies and returns

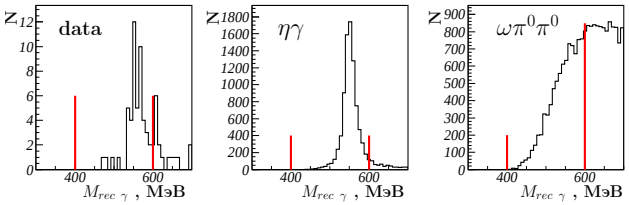

Fig 1.2.16: Distributions over the recoil mass of the most energetic photon in the event for selected experimental events (data), and for simulated events for the processes $e^+e^- \to \eta\gamma$ ($\eta\gamma$) and $e^+e^- \to \omega\pi^0\pi^0$ ($\omega\pi^0\pi^0$).

the value of χ^2, which characterizes the reliability of the hypothesis about the process used in the kinematic reconstruction. Three hypotheses were tested and respectively three χ^2 parameters were calculated:

- $e^+e^- \to n\gamma$ ($n \geq 7$), $\chi^2_{n\gamma}$;
- $e^+e^- \to \pi^0\pi^0\gamma$, $\chi^2_{\pi^0\pi^0\gamma}$;
- $e^+e^- \to 3\pi^0\gamma$, $\chi^2_{3\pi^0\gamma}$.

Further event selection was performed with the following restrictions:

$$\chi^2_{n\gamma} < 30\ ,\ \chi^2_{\pi^0\pi^0\gamma} > 20\ ,\ \chi^2_{3\pi^0\gamma} < 50\ .$$

For selected events, a distribution over the recoil mass M_{rec} of the most energetic photon in the event was formed and it is shown in Fig. 16. The final selection of the events is carried out by the condition $400 < M_{rec} < 600$ MeV.

The measured cross section of the process $e^+e^- \to \eta\gamma$ is shown in Fig.1.2.17The cross section was approximated in the vector meson dominance model taking into account contributions of the vector resonances ρ, ω, ϕ, ρ' and ρ''. Free parameters of the approximation were masses and widths of the ρ', ρ'' resonances and cross sections of the $e^+e^- \to \rho' \to \eta\gamma$ ($\sigma_{\rho'}$) and $e^+e^- \to \rho'' \to \eta\gamma$ ($\sigma_{\rho''}$) processes at the resonance peaks . Unfortunately, because of the small statistics, phases of resonances $\rho\,^{prime}$ and ρ'' cannot be determined in the approximation. For them we used the values $0°$ and $180°$ in various combinations. Parameters of the ρ, ω and ϕ resonances were taken from our previous work.

Approximation that gives the smallest χ^2/ndf corresponds to values $\varphi_{\rho'} = 180°$ and $\varphi_{\rho''} = 0°$. For the cross sections at the resonance maximum the following values were obtained:

$$\sigma_{\rho'} = (55, 7^{+11,2\ +7,1}_{-9,7\ -1,8} \pm 1, 6)\ \text{pb},$$

$$\sigma_{\rho''} = (47, 4^{+72,1\ +4,8}_{-21,6\ -18,1} \pm 1, 3)\ \text{pb},$$

where the first error is statistical, the second is due to model dependence, and the third is the systematic one. The graph of the cross section corresponding to these parameters is shown in Fig.1.2.17.

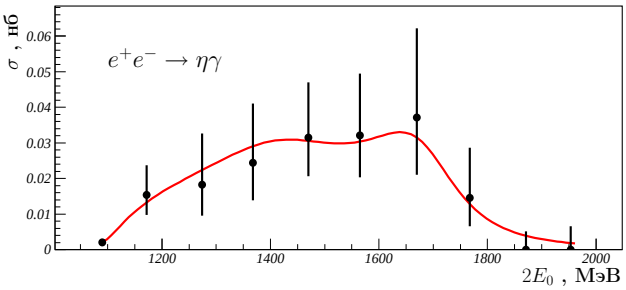

Fig 1.2.17: The cross section of the process $e^+e^- \to \eta\gamma$ measured in this work and the result of approximation by the model described in the text.

This work was financially supported by the Ministry of Education and Science of the Russian Federation, RFBR grants 11-02-00276-a, 12-02-00065-a, 12-02-01250-a, 13-02-00375, 13-02-00418-a, MK-4345.2012.2, 12-02-31488 mol_a,12-02-31692 mol_a, 12-02-31515 mol_a, Russian Federation President Grant for the support of scientific schools NSh-5320.2012.2.

1.3. KEDR DETECTOR

The KEDR detector is a universal magnetic detector, employed in experiments on the e^+e^- collider VEPP-4M in the energy range of 2 to 11 GeV in the center of mass system. The detector also comprises a system for registration of scattered electrons for research on the $\gamma\gamma$ physics and a luminosity monitor. The KEDR detector parameters are at the level of the best world detectors operating in this energy range.

Assembling the KEDR detector.

In 2013, the repair and modernization of the detector was completed and the detector was assembled in full in the experiment interval of VEPP-4M. Most systems installed in the detector have been tested and calibrated in runs with cosmic particles. The serviceability of the accelerator complex has been recovered: the complex is ready to work for luminosity in the energy range of Ψ mesons. It is planned to increase the magnetic field in the detector to 6kGs in February 2014 and start an experiment run.

Status of systems of the KEDR detector.

– Vertex detector. In 2011 34 channels of 310 were turned off; huge crosstalk was observed in the preamplifiers. As a result, attempts to increase the amplification led to «false» tracks and worsening of the detector resolution.

  During the stop, all the tubes were repaired; all leaks were eliminated; the preamplifiers were equipped with additional screens to reduce the crosstalk; the radial wiring diagram for connection of the electronics channels was replaced with a tangential one, which should further reduce the possibility of false tracks; the system of gas splitters on the detector was modified, and now both a group of tubes and individual tubes can be disconnected during operation. The system has been installed in the detector; leaks have been detected in 12 tubes.

– The drift chamber was renovated and set in the detector; tests with cosmic particles were carried out. Before the stop (2011), 2 full layers and 2/3 layer of seven layers were in operating condition. Currently, 6 full layers and 1/2 layer are in operating state. The data for obtaining the parameter X(t)are under processing.

– Aerogel Cerenkov counters (ACC). Before the stop, the detector contained a single layer of the system (80 counters, 17 of the counters out of service); the effectiveness of the system was 80 % in the barrel and 96 % in the ends. Now the system is installed in the detector in full (160 counters in two layers). The system for high-voltage supply and noise control has been commissioned; programs for data collection and reconstruction have been refined. The electronics have been calibrated and statistics with cosmic particles have been collected for geometric alignment of the system and evaluation of its effectiveness.

– Time-of-flight counters have been fixed (gluing of broken light guides and wrapping in aluminized mylar) and installed in the detector. The barrel magnetic screens were equipped with additional screen inserts, which will reduce the effect of amplitude fall in magnetic field injection. 6 electronics channels in the barrel part of the system and one in the end have been repaired. All the counters are operational now (before field injection).

– Liquid-krypton calorimeter. The krypton cleaning system has been assembled and tested. The entire krypton volume has been cleaned of electronegative impurities to a level better than 0.5ppm, which corresponds to a free path in liquid krypton (LKr) of more than 10mm. Maintenance and repair works have been carried out on all the channels of the chamber electronics. The calibration capacity of all the preamplifiers has been measured.

– The CsI calorimeter with a new structure of 4 modules was installed in the detector, which will enable knowing the position of each crystal with accuracy better than 1 mm. 300 channels out of service and 100 channels with reduced efficiency have been fixed. At the moment (before magnetic field injection), 10 channels are out of service.

– Muon chambers. During the shutdown, all the units of the muon system were repaired, which included replacement of all the driver boards and repair of faulty boards of the expansion tanks. 10 wires were replaced.

  The system comprises 544 channels. By the time of the shutdown, there were 46 (9 %) completely defective and 38 (7 %) partially faulty channels.

  The current state of the system is as follows: 10 (1.8 %) completely faulty channels and 8 (1.5 %)partially defective (no longitudinal coordinates) channels. The efficiency in the rest of the system is > 98 %.

– Magnetic system. Cryo wires in the magnetic system of the detector have been remade: a slight inclination was made throughout the length to prevent accumulation of helium gas; the primary winding of the SC transformer will be fed via warm wires passing outside the cryo wire, through a plug in the housing of the cryostat. The control system was supplemented with quick (a discreteness of a few microseconds) check of

currents (voltages) on the primary coil of the SC transformer, on the SC keys, and at some critical points. New SC keys have been manufactured, tested and mounted in the system for powering of the KEDR detector solenoid.

– System for registration of scattered electrons. On the electron and positron lines, a scheme was created and put into operation for calibration of the system for registration of scattered electrons on the basis of precision electro-magnetic calorimeters. The scheme is based on BGO monocrystals and two lasers with wavelengths of 532 nm and 1064 nm. Two calorimeters for the electron and positron shoulders and a system of mirrors to direct laser radiation towards the electron or positron beam were manufactured.

  The system enables calibration of the dependence of the track coordinate on scattered electron (positron) energy and measurement of the energy resolution. An automated procedure for calibration of the system for registration of scattered electrons was put into operation for the electron and positron shoulders, which will enable one to perform calibrations in a few minutes between acquisitions of experimental data.

Development of FARICH technique.

FARICH(Focusing Aerogel RICH, FARICH) is a promising detector for identification of charged particles in a wide range of pulses. It is a ring image Cherenkov detector with a radiator of multilayer «focusing» aerogel. The work has been done by the aerogel group of the KEDR detector together with a group from the Institute of Catalysis SB RAS since 2004. The FARICH methods are in demand in several planned experiments on high-energy physics: Super-c-τ-factiry (BINP SB RAS), $\bar{\text{P}}$ANDA(FAIR, Germany), ALICE (CERN), Belle II (KEK, Japan).

In 2008-2010, BINP created the facility «Extracted electron beam on the VEPP -4M accelerator», which allows research on prototypes of new detectors of elementary particles with beams of electrons and gamma quanta. The electron beam is generated using the bremsstrahlung on a movable probe brought into the halo of the accelerator beam. Conversion of the bremsstrahlung gamma quanta occurs upstream the dipole magnet in the experimental hall. The magnet is used for selection of electrons by their momentum. The resulting electron energy range is 60–3000 MeV. The gamma quantum beam will be generated using a pulsed laser. The laser beam is injected into the vacuum chamber of the collider VEPP-4, where it interacts with the electron beam at the collision point inside the universal magnetic detector KEDR. Laser photons interact with electrons via the Compton scattering. As a result, a beam of gamma quanta is generated in a narrow cone directed along the electron beam. The gamma quanta energy is measured using a unique system for registration of scattered electrons with accuracy of about 0.5 The installation is described in more detail in the BINP report for the year 2011.

The first FARICH prototype was tested on extracted electron beam in 2011. The results were in good agreement with the simulation. They were presented at several workshops, seminars and conferences. The results of the work are described in more detail in the BINP report for the year 2011.

The following was done in 2013 as part of the development of the FARICH technique:

- An automatic system was created for synthesis of aerogels with continuous gradient of the refractive index and possibility of control of the ratio of initial reagents.
- 3 samples of focusing aerogel with continuous refractive index were made. About 10 samples of multilayer aerogels were produced.
- A FARICH prototype№2 with a photodetector consisting of 60 silicon photomultipliers of the CPTA 151-30 type was tested on the beam (Fig.1.3.1). The coordinate resolution of the photodetector is nearly two times better than in prototype №1. 9 samples of focusing aerogels were investigated on beam using the prototype. The data are under processing.

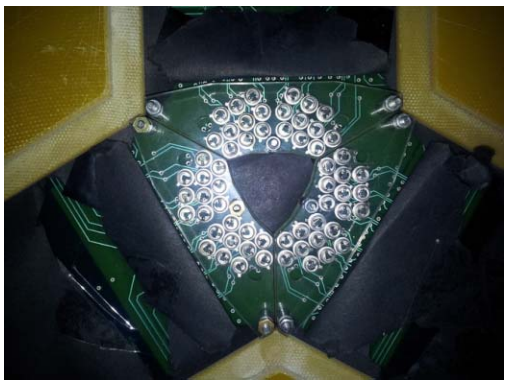

Fig.1.3.1: Photo of 60-channel photodetector based on CPTA 151-30 silicon photomultipliers.

- The processing of the results of the test of the FARICH prototype with DPC photodetector on hadron beam at CERN was completed (see the BINP report for the year 2012). A record high separation of π and K mesons was attained, which reaches 3.5 sigma with a 4 GeV/s pulse, which is almost twice the separation factor achieved with the FDIRC detector prototype for the project of

the Super$B$-factory. The μ/π separation was 5.3 sigma with a 1 GeV/s pulse, which is sufficient for experiments at the planned Super-c-τ-factory. The results were presented at the international conference VCI 2013 and International Forum AFAD 2013 and published in a peer-reviewed journal. Fig.1.3.2shows the resulting factor of separation of π and K mesons as a function of particle momentum.

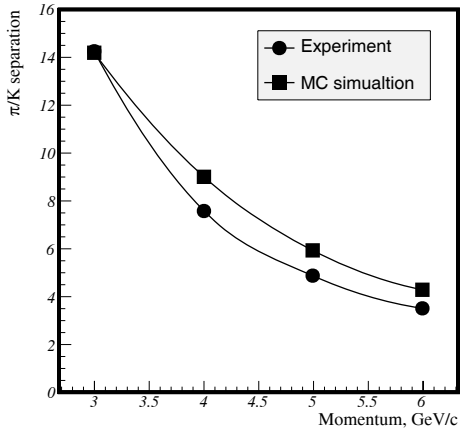

Fig.1.3.2: π/K separation as a function of momentum for the FARICH prototype with DPC as obtained on hadron beam at CERN. Circles: experiment; squares: modeling.

- The FARICH prototype with DPC photodetector was upgraded. In 2013, the prototype was tested on extracted beam of electrons on the VEPP-4M accelerator in the mode of high spatial resolution (a pixel was camouflaged to a 1×1 mm^2 size). Fig.1.3.3 depicts the prototype on the extracted beam. The prototype was used in a measurement of 14 samples of aerogels. Preliminary results were presented at the international RAS conference, Section of Nuclear Physics and at the international conference RICH 2013.

- The state corporation «Rosatom» and Helmholtz association (Germany) awarded a grant for 2014-2017 for development of the engineering design of aerogel RICH detector for the experiment $\bar{\text{P}}$ANDA. Works on the project were begun.

1.4. Results of the KEDR detector operation on the VEPP-4M collider in 2013

In 2013, the statistics collected on the VEPP-4M collider in the KEDR experiment was intensely processed. The main results are summarized below.

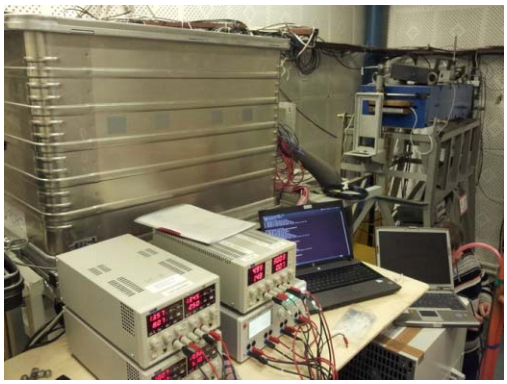

Fig.1.3.3 Photo of FARICH prototype with DPC on extracted electron beam.

- The processing of the experimental verification of lepton universality in decays of J/ψ meson was completed.

- The $J/\psi \to \gamma\eta_c$ process was investigated; the results were passed for publishing.

- A direct measurement of the $\Gamma_{ee}\Gamma_{\mu\mu}/\Gamma\psi(2S)$ value of meson was performed.

- A preliminary measurement of the $\Gamma_{ee}\Gamma_{hadr}/\Gamma_{J/\psi}$ value of meson was performed.

A more detailed description of these papers is given below.

1.4.1. Checking lepton universality in decays of J/ψ meson.

Search for deviations from the Standard Model is one of the urgent problems of modern high-energy physics. Increasing the accuracy of experiments on checking the conservation principles is one of the main directions of the research.

In 2013 the KEDR collaboration completed the experiment on checking the lepton universality in decays of J/ψ meson. The ratio of the partial widths of the $J/\psi \to e^+e^-$ and $J/\psi \to \mu^+\mu^-$ decays was measured; the following result was obtained:

$$\Gamma_{e^+e^-}(J/\psi)/\Gamma_{\mu^+\mu^-}(J/\psi) = 1.0022 \pm 0.0044 \pm 0.0048$$

The accuracy of the result was 0.65%. Fig. 1.3.4 presents a comparison of the lepton widths of the J/ψ resonance which were obtained in different experiments. The article has been passed to the journal Physics Letter B.

1.4.2. Measurement of the probability of the $J/\psi \to \gamma\eta_c$ decay and parameters of η_c meson

Analysis of the data yielded the following values for the mass and width of the η_c meson:

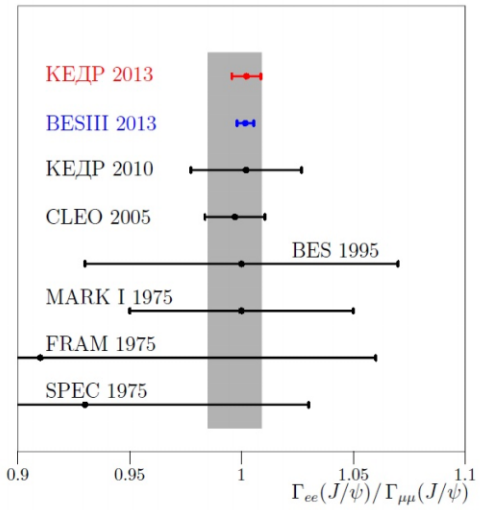

Fig 1.3.4 Comparison of $\Gamma_{ee}/\Gamma_{\mu\mu}$ obtained in different experiments. The position of the band and its width are in agreement with the worldwide average value and uncertainty of $\Gamma_{ee}/\Gamma_{\mu\mu}$ by PDG data.

$$M_{\eta_c} = 2983.5 \pm 1.4^{+1.5}_{-3.6} MeV/s^2 \ ,$$

$$\Gamma_{\eta_c} = 27.2 \pm 3.1^{+5.1}_{-2.8} MeV \ .$$

Within the measurement error, these values are consistent with the worldwide average values. These parameters were earlier measured by other groups in decays of J/ψ mesons and B mesons and $\gamma\gamma$ and pp collisions. In radiative decays of J/ψ mesons, if the resonance is fitted with the Breit-Wigner function, because of the asymmetry of the spectral line, there is a shift in the measured mass towards lower values by a value of about 4 MeV. The Crystal Ball Group took this asymmetry into account, while the MARK3 and BES groups did not. Therefore, we believe that the results of measurements of the mass of the η_c meson by these groups should be corrected by this value, which will result in better agreement with measurements made in other experiments. Our result for the relative probability of the $J/\psi \to \gamma\eta_c$ decay is as follows:

$$B(J/\psi \to \gamma\eta_c) = (3.59 \pm 0.22 \pm 0.25)\%.$$

This result (Fig.1.3.5) is consistent with the recent theoretical calculations on QCD lattices. The article was directed to the journal "Nuclear Physics".

Measuring $\Gamma_{ee}\Gamma_{\mu\mu}/\Gamma$ of $\psi(2S)$ meson

A direct measurement of the product of the leptonic width by the probability of $\psi(2S)$ meson decay into a pair of muons was carried out, and the following preliminary result was obtained:

$$\Gamma_{ee}\Gamma_{\mu\mu}/\Gamma = 9.4 \pm 0.4 \pm 1.1 \text{ eV}.$$

The accuracy of the result (Fig.1.3.6) is about two times better than the "world average" one, which is calculated as the product of $\Gamma_{e^+e^-}$ and $B_{\mu\mu}$.

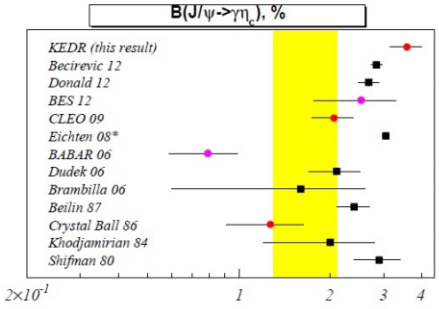

Fig.1.3.5: $J/\psi \to \gamma\eta_c$ decay probability from different experiments and its average value (shown by the vertical stripe).

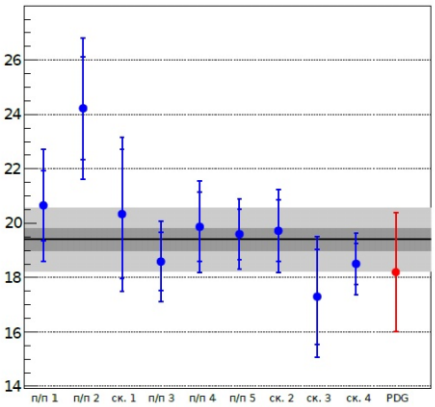

Fig.1.3.6: Comparison of $\Gamma_{ee}\Gamma_{\mu\mu}/\Gamma$ obtained in the KEDR experiment and the "world average" value. The summarized KEDR result is shown with a horizontal line and its errors are indicated with gray stripes.

Measuring the $\Gamma_{ee}\Gamma_{hadr}/\Gamma$ *valueof* J/ψ meson

In 2013, a preliminary result was obtained on the measurement of the product of the leptonic width of J/ψ meson by the probability of its decay into hadrons:

$$\Gamma_{ee} \times Br(J/\psi \to hadrons) = 4.67 \pm 0.04 \pm 0.19 \text{ keV}.$$

This preliminary result has a better accuracy in comparison with previous direct experiments, although is somewhat inferior to the "world average" alue, which is the product of $\Gamma_{e^+e^-}$ and $B_{hadrons}$ (Fig.1.3.7).

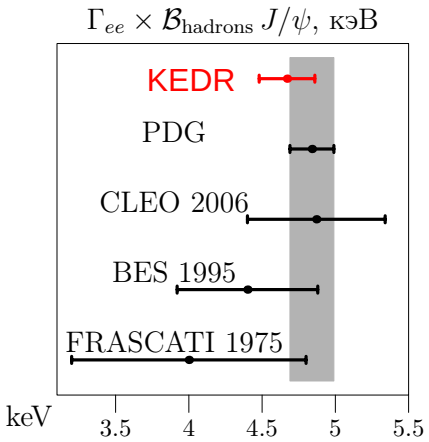

Fig.1.3.7: Comparison of $\Gamma_{ee}\Gamma_{hadrons}/\Gamma$ obtained in various experiments and the world average value.

1.5. ELECTRONICS FOR HEP DETECTORS

In 2013, the following works were performed as part of the upgrade of the electronics of detectors.

1.5.1 KEDR.

The KEDR detector was being repaired. A reconditioning of the electronics of the chambers of the calorimeters in the detector – the krypton and CsI calorimeters – was completed, with partial replacement of amplifiers.

1.5.2 SND.

The electronics for the second and third layers of one hemisphere of the calorimeter have been upgraded.
A prototype of the A24F module with TCP/IP exchange was made; it is under debugging.

1.6. X-RAY DETECTORS

In 2103, within the framework of creation of a multi-line position detector with silicon microstrip structures as recording elements, an agreement was concluded with HAMAMATSU. The company is to manufacture nine coordinate structures of three modifications for tests and selection of optimal parameters.

In 2013, two OD-3M detectors were manufactured and debugged. The first one has a focal length of 1500 mm and is intended for the Siberian Center for Synchrotron and Terahertz Radiation; the second one has a focal length of 700 mm and is intended for a diffractometer.

Made Two copies of the motherboard of the detector OD-4 for wide-angle scattering experiments on SR were made. A multistage gas electron multiplier (GEM) is used in OD-4, unlike OD-3M with wire structure. This allows, along with high gas gain (over 10,000), making an arc detector with arbitrary angular aperture.

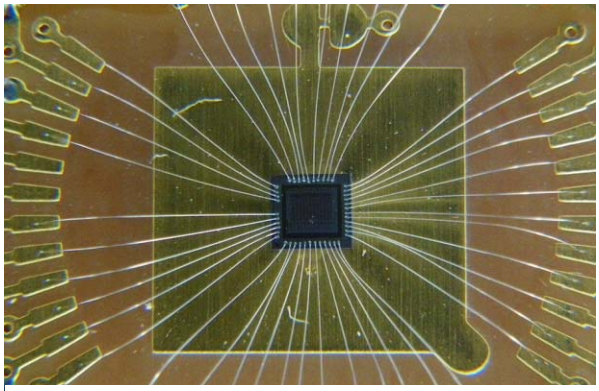

Fig. 1.6.1. Microchip crystal on substrate for testing.

As part of the development of designing of ASICs, for the first time the Institute has developed the topology and obtained working copies (Fig. 1.6.1) of microchips for use in X-ray position detectors of the DIMEX type.

1.7. DATA ACQUISITION SYSTEM FOR DETECTOR BELLE-II

Within the framework of international projects, the BINP members continued their wide participation in the development of the new data acquisition system for the detector BELLE-II (KEK, Japan).

In 2013,

- the high-voltage filters of the preamplifiers of one end of the calorimeter were modernized;
- collective effects for 12x2 recording modules of the cylindrical calorimeter were investigated; modifications to suppress crosstalk of adjacent boards were developed and implemented;
- a design was developed for a programmable logic integrated circuit for the collector module, for data transmission by an optical channel;
- the reading system was checked at a triggering speed of up to 30 kHz; based on the check results, production of a complete set of modules was started;
- a test batch of recording modules for the end part of the calorimeter was designed and ordered.

1.9. THE BELLE EXPERIMENT

1.9.1. Main results.

The main focus of this group is collaboration in the field of elementary particle physics with the High Energy Accelerator Research Organization (KEK), Tsukuba, Japan, which is one of the largest and fastest growing laboratories for high energy physics in the world. In recent years, the KEK management has been actively expanding its international cooperation aimed at making KEK an international centre in this field of physics. One of the key experiments in elementary particle physics in Japan is currently the study of CP violation in B meson decays using the Belle detector at the high luminosity electron-positron storage ring (the so-called B factory).

BINP members have made a significant contribution to the construction of the electromagnetic calorimeter of the Belle detector, both at the design stage and during the manufacture of components of the world's largest calorimeter based on cesium iodide monocrystals, during its assembly and adjustment.

In 2010, the Belle detector was stopped for upgrade. The acquired luminosity exceeds 1040 inverse femtobarns. These experimental data are under processing now, and the detector and the accelerator are being upgraded for increasing the luminosity and preparation for experiments which will enable improvement of the accuracy of CP violation measurements by an order of magnitude and, possibly, observation of manifestation of physical phenomena beyond the Standard Model.

BINP members are actively participating in both the upgrade of the detector and processing of the experimental data.

Below are the main results for 2013.

- Study of mixing of neutral D mesons is going on.
- Search for decays of exotic state X to modes containing η_c meson was performed.
- Parameters of Z_b states were measured.
- The neutral resonance $Z_b^0(10610)$ was first discovered.
- Preliminary results of the study of the $B^0 -> D^{*+}\omega\pi^-$ decay were obtained.
- A search for $\tau^- \to l^- hh'$ decays with violation of the lepton flavor was performed.
- The measurement of the relative probabilities of the decay and mass spectra for τ decays with K^0_S meson in the final state was completed.
- Work on the study of τ lepton decays into three pseudoscalar charged mesons and neutrino was started.
- The measurement of the relative probability of the $\Lambda_c^+ \to pK^-\pi^+$ decay was completed.
- A VME crate for the electronics of the calorimeter was designed and manufactured.
- The first batch of the mass production of shaper-digitizers was manufactured and tested.
- Modified boards for the endcap calorimeter was manufactured and tested.
- A pilot version of the collector module for work with high-rate information transition via optical channel was developed. The new module had been produced, and its operation was tested in high-speed readouts.
- Works on the modernization of the bias voltage filter for the photodetectors of the endcap calorimeter were carried out.

1.9.2. Data analysis.

Model-independent measurement of mixing parameters of neutral D mesons

Within the Belle experiment, work continues on the measurement of parameters of mixing of neutral D-mesons. The mixing parameters and parameters of CP symmetry violation in the mixing are obtained using a model-independent approach suggested in Phys. Rev. D82, 034033. This method uses a three-particle final state but it does not apply the model of the D meson decay which allows one to avoid model uncertainty. The mixing parameters are crucial for charm quark physics. Measurement of CP violation in mixing will enable checking the Standard Model, as these parameters are rigidly constrained in it. In addition, precision measurement of the mixing parameters will reduce the theoretical uncertainty in other measurements, in particular in the measurement of the angle γ of the unitarity triangle. By now, the distributions of kinematical parameters for signal and background events have been studied; a procedure for extraction of the mixing parameters from decay time distribution for D mesons has been developed; correlations between the kinematical parameters of events and the measured D meson decay time are under study (see Fig. 1.9.1).

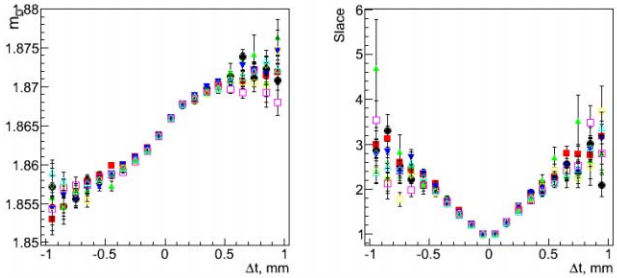

Fig. 1.9.1. Mean value (left) and standard deviation (right) of D meson mass distribution vs. error in measurement of D meson decay time.

Search for decays of X into modes with η_c meson

The Belle collaboration first found the exotic state X(3872) in 2002 in the $B^+ \to K^+\pi^+\pi^- J/\psi$ exclusive decay. The mass of this state is close to the threshold $M(D^0)+M(\overline{D^{*0}})$ which gave rise to a hypothesis that X (3872) may be a $D^0\overline{D^{*0}}$ molecule. Thus, it was suggested that there may be other similar particles, which are also bound states of D(*) mesons. If these states exist, they have quantum numbers different from those of X(3872) and can be found in decays containing η_c meson. If

molecular states of the $D^0\overline{D^0}$ or $D^{*0}\overline{D^{*0}}$ type are possible, such particles have a mass different from 3872 MeV. They were denoted as X(3730) and X(4014), respectively. BINP group performed a search for decays of X-like exotic states into different modes with η_c: $\eta_c\pi^+\pi^-$, $\eta_c\omega$, $\eta_c\eta$, and $\eta_c\pi^0$. An algorithm was developed for separation of events of the $B^\pm\to K^\pm X$ decay with subsequent decays of X into the above modes. No signal was detected so far in any of the studied channels of X decay (see Fig. 1.9.2). So upper limits were set on the products of the branching fractions of X production and decays. The work is ready for publication, and is now in the process of discussion within the collaboration.

Study of exotic states $Z_b(10610)$ and $Z_b(10650)$

In 2010-2011, the BINP group of the Belle collaboration performed a data analysis on e^+e^- annihilation into final states of the $\Upsilon(nS)\pi^+\pi^-$ type, where n = 1,2,3. The most important result was observation of two new charged bottomonium-like states $Z_b(10610)$ and $Z_b(10650)$ (Phys. Rev. Lett. 108, 122001). Fig. 1.9.3 shows the distribution over the invariant mass of the $\Upsilon(nS)\pi$ system where two peaks are clearly visible. The BINP group used the Dalitz analysis technique, which enabled a complete amplitude analysis of the six-dimension phase space of these transitions.

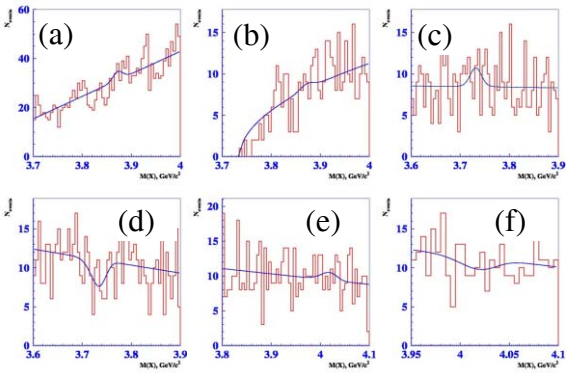

Fig. 1.9.2. Fitting of invariant mass distributions for $\eta_c\pi^+\pi^-$ (a) and $\eta_c\omega$ (b) in the region of the X(3872) resonance, for $\eta_c\eta$ (c) and $\eta_c\pi^0$ (d) in the region of the X(3730) resonance, and for $\eta_c\eta$ (e) and $\eta_c\pi^0$ (f) in the region of the X(4014) resonance.

The most important result of this work is measurement of parameters of Z_b states: mass, width, spin and parity(P), as well as the relative phase between the amplitudes of $\Upsilon(nS)\to Z_b(10610)\pi$ and $\Upsilon(nS)\to Z_b(10650)\pi$.

The existence of decays of the $Z_b\to\Upsilon(nS)\pi^\pm$ type makes it impossible to classify Z_b as two-quark systems. Thus the minimum set is that of four quarks. The authors of this work suggested considering the new states as a weakly bound system of B and $\overline{B^*}$ mesons in the $Z_b(10610)$ case and a system of $B^*\overline{B^*}$ mesons in the Z_b (10650) case, respectively (Phys. Rev. D 84, 054010). Besides of being in good agreement with all the known Z_b state properties, such a model predicts new properties. Some of them can be checked with the existing statistics.

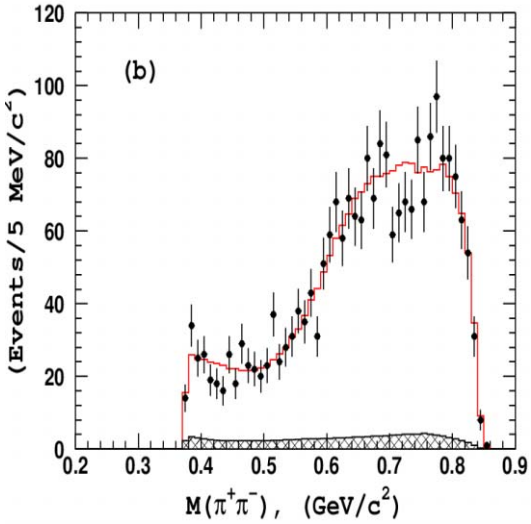

Fig. 1.9.3. Distribution over the invariant mass of the $\Upsilon(2S)\pi^\pm$ system (left) and $\pi^+\pi^-$ system (right) for events from the signal region of the $\Upsilon(5S)\to\Upsilon(2S)\pi^+\pi^-$ decay. Points: experimental data, histogram: result of fitting, shaded histogram: expected level of background events.

From the suggested model it follows that the dominating decay channels for $Z_b(10610)$ and $Z_b(10650)$ will be decays into $B\overline{B^*}$ and $B^*\overline{B^*}$, respectively. Search for these decays is complicated by reconstruction of B mesons that have no dominating decay channels. The large data sample collected by the Belle detector made it possible not only to extract the $\gamma(5S)\to B\overline{B}\pi$ three-particle processes but also to perform preliminary analysis of the dynamics of these decays. Fig. 1.9.4 shows mass distribution of the $B\overline{B^*}$ and $B^*\overline{B^*}$ systems and results of approximation using different models.

The preliminary results are consistent with the hypothesis that the three-particle transitions $\gamma(5S)\to B\overline{B^*}\pi$ and $\gamma(5S)\to B^*\overline{B^*}\pi$ occur mainly through intermediate production of Z_b states. The work has been completed and currently is in the process of discussion within the collaboration.

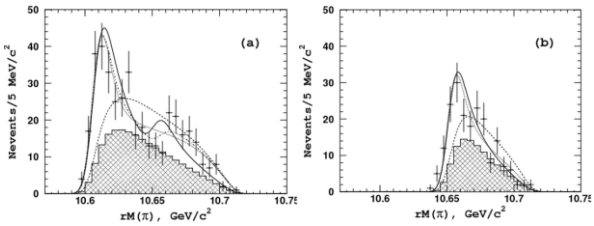

Fig. 1.9.4. Invariant mass distribution of the $B\overline{B^*}$ (left) and the $B^*\overline{B^*}$ (right) systems for events from the signal region for decays $\gamma(5S)\to B\overline{B^*}\pi$ and $\gamma(5S)\to B^*\overline{B^*}\pi$, respectively. Points: experimental data, lines: result of fitting with different models, shaded histogram: expected level of background events.

First observation of $Z_b^0(10610)$ neutral resonance

In 2010-2011, the BINP group of the Belle collaboration performed the first observation of the charged bottomonium-like states $Z_b(10610)$ and $Z_b(10650)$ (Phys. Rev. Lett. 108, 122001). This analysis was extended to the search for neutral isospin partners in the $\Upsilon(nS)\pi^0\pi^0$ final state.

Decays $\Upsilon(10860)\to\Upsilon(nS)\pi^0\pi^0$, n=1,2,3 were found during analysis of the 121 fb^{-1} data acquired at the Belle detector near the $\Upsilon(10860)$ resonance. The cross sections of $\sigma(e^+e^-\to\Upsilon(10860)\to\Upsilon(1S)\pi^0\pi^0) = (1.16 \pm 0.06 \pm 0.10)$ pb, $\sigma(e^+e^-\to\Upsilon(10860)\to\Upsilon(2S)\pi^0\pi^0) = (1.87 \pm 0.11 \pm 0.23)$ pb, and $\sigma(e^+e^-\to\Upsilon(10860)\to\Upsilon(3S)\pi^0\pi^0) = (0.98 \pm 0.24 \pm 0.19)$ pb have been measured. The results are consistent with the prediction for the cross sections of $e^+e^-\to\Upsilon(10860)\to\Upsilon(nS)\pi^+\pi^-$ with consideration of the isospin conservation hypothesis (arXiv: 1209.6450).

Dalitz plot analysis was performed for these processes. The $Z_b^0(10610)$ neutral resonance which decays to $\Upsilon(2,3S)\pi^0$ was first discovered. The significance of the signal including systematic uncertainties is found to be 6.5σ. The measured mass of this resonance is $(10609\pm4\pm4)$MeV/c^2, which is consistent with the mass of the corresponding charged state, $Z_b^{\pm}(10610)$. The results have been published and presented at international conferences.

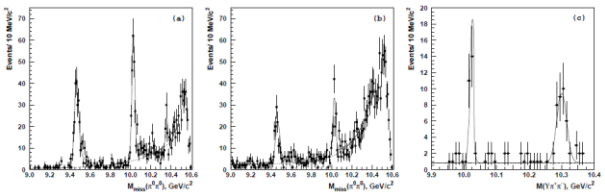

Fig. 1.9.5. Recoil mass to $\pi^0\pi^0$ system for events (a)$\Upsilon(nS)[\mu^+\mu^-]\pi^0\pi^0$ and (b)$\Upsilon(nS)[e^+e^-]\pi^0\pi^0$. (c) invariant mass of $\Upsilon(1S)\pi^+\pi^-$ for events $\Upsilon(2S)[\Upsilon(1S)\pi^+\pi^-]\pi^0\pi^0$. Points with errors show the data; the curves are the fit result.

Dalitz analysis of decay $B^0 -> D^{*+}\omega\pi^-$

BINP members have obtained preliminary results for this study. In particular, the full width of the $B^0 -> D^{*+}\omega\pi^-$ decay has been measured. With the use of the Dalitz analysis, the partial widths of the following resonance decays were determined:

$B^0 -> D^{*+}\rho(770)^- -> D^{*+}\omega\pi^-$,

$B^0 -> D^{*+}\rho(1450)^- -> D^{*+}\omega\pi^-$,

$B^0 -> D_1(2430)^0\omega -> D^{*+}\pi^-\omega$,

$B^0 -> D_1(2420)^0\omega -> D^{*+}\pi^-\omega$.

Contributions of ρ-like resonances and D** states were observed. Effective parameters (coupling constants and phases) were obtained, which describe the dynamics of production of these states with account of interference between them and effects of interaction in the final state. The branching fraction of the color-suppressed $B^0 -> D_2(2460)^0\omega -> D^{*+}\pi^-\omega$ decay has been measured. The widths of the $B^0 -> D_2(2460)^0\omega$ and $B^0 -> D_1(2420)^0\omega$ decays turn out to be comparable, as predicted by the SCET theory. Besides, the upper limit for the $B^0 -> D^{*+}b_1(1235)^- -> D^{*+}\omega\pi^-$ decay was set. This result is the first attempt of observation of $b_1(1235)$ resonances in decays of B mesons. The longitudinal polarizations of D** states have also been measured. The results are consistent with the general picture that is observed in decays forbidden by color. In such decays, violation of the factorization hypothesis is observed. As part of the Dalitz analysis, unbinned fit to experimental data was performed. The results with signal and background distributions are shown in Fig. 1.9.6.

At the moment, the results are being discussed within the Belle collaboration and will be published soon.

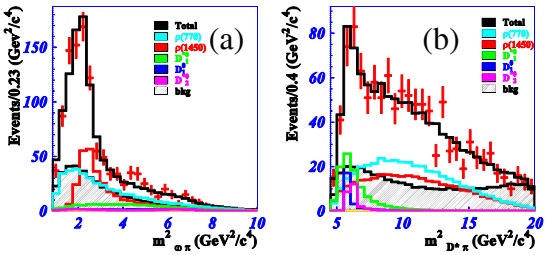

Fig. 1.9.6. Dalitz plot projections of fit results in the signal region. a) Distribution of the squared mass of ωπ pair, b) distribution of the squared mass of $D^*\pi$ pair. Dots: experimental data, dashed histogram: background contribution to the signal area, open histograms: contributions of signal components, black histogram: the overall fit result.

Research on τ lepton decay

Search for $\tau^-\to l^-hh'$ decays with lepton flavor violation was completed, where l = e, μ, and h = π, K. 14 different decay modes were under study. With the use of a large data sample (782×10^6 produced pairs of τ leptons), the upper limits on the relative probabilities of the following decays were set: $B(\tau^-\to e^-hh')<(2.0 - 3.7)\times10^{-8}$, $B(\tau^-\to\mu^- hh')<(2.1 - 8.6)\times10^{-8}$, at the 90% confidence level. These limits are the strongest among all similar studies. Results have been published in the journal Physics Letters B.

Another completed analysis of the experimental data is dedicated to the measurement of the relative decay probabilities and mass spectra of τ decays with K^0_S meson in the final state. The data sample used for this analysis was 669 fb^{-1}, or 616×10^6 produced pairs of τ leptons. The final values of the relative probabilities were obtained for the inclusive decay $\tau^-\to K^0_S X^-\nu_\tau$, as well as for six exclusive modes: $\tau^-\to K^0_S\pi^-\nu_\tau$, $\tau^-\to K^0_S K^-\nu_\tau$, $\tau^-\to\pi^0K^0_S\pi^-\nu_\tau$, $\tau^-\to\pi^0K^0_S K^-\nu_\tau$, $\tau^-\to K^0_S K^0_S\pi^-\nu_\tau$, and $\tau^-\to K^0_S K^0_S\pi^-\pi^0\nu_\tau$. In the latter case, the spectra of invariant masses for the final states $K^0_S K^0_S\pi^0$ and $K^0_S\pi^-$ were also found. In the first case, we see an apparent intermediate structure corresponding to the production of $f_1(1285)$ with a significance of 5.9 standard deviations, and in the second case we see the $K^{*-}(892)$ meson. These results were

reported at the PhiPsi13 conference in Rome. Currently, the final version of the journal article is being prepared.

Another focus is the study of τ lepton decays into three pseudoscalar charged mesons and a neutrino ($\tau^-\to\pi^-\pi^-\pi^+\nu_\tau$, $\tau^-\to K^-\pi^-\pi^+\nu_\tau$, $\tau^-\to\pi^-K^-\pi^+\nu_\tau$, $\tau^-\to K^-K^-K^+\nu_\tau$). There is a disagreement between the measurements of the relative probabilities of these decays in the Belle and BaBar experiments. That is why the BINP group is are carrying out a new measurement on the total available statistics. By now, a modeling of the above decays has been performed and a program for data processing has been written which will allow to obtain preliminary results without considering some corrections and systematic uncertainties so far. The final result is planned for the next year.

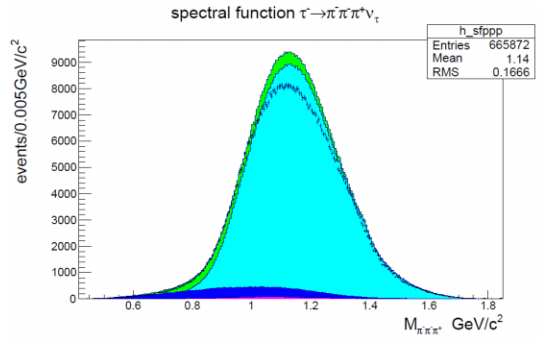

Fig. 1.9.7. Spectral function for $\tau^-\to\pi^-\pi^-\pi^+\nu_\tau$ decay.

Measuring relative probability of $\Lambda_c^+\to pK^-\pi^+$ decay

The absolute value of the relative probability of the $\Lambda_c^+\to pK^-\pi^+$ decay is important for the heavy quark physics theory. Besides, the probabilities of most other decays of Λ_c^+ baryon have been experimentally measured relative to this mode. The absolute probability of this decay has a large uncertainty, mainly because of the dependence of the measurements on theoretical models. The BINP group have developed a model-independent technique for measuring the probability of the $\Lambda_c^+\to pK^-\pi^+$ decay. The technique is based on extraction of exclusive processes of the $e^+e^-\to\Lambda_c^+$ anti-p π^+ $D^{(*)}$- type in the two following ways: (1) reconstruction of Λ_c^+ in the recoil mass and (2) search for the required process with Λ_c^+ registration in the invariant mass of $pK^-\pi^+$. The ratio of (2) to (1) yields the needed result $(6.84 \pm 0.24\ ^{+0.21}_{-0.27})\%$, which is five times more precise than the current value of (5.0 ± 1.3)% . The work has been completed and an article will be published upon approval by the collaboration.

Fig. 1.9.8. Shaper-digitizer modules in rack.

1.9.3. Upgrade of detector.

The ongoing upgrade of the detector (Belle II) and the collider will increase the peak luminosity up to 8×10^{35}cm^{-2}s^{-1}. The new experiment will allow to measure all angles of the unitarity triangle with accuracy of several percents and possibly going beyond the Standard Model. In addition to studying the mechanism of CP violation, the large set of data obtained in this experiment will yield new results in the physics of decays of B and D mesons and τ lepton.

Increase in luminosity and background level of the collider imposes new requirements on the detector systems. The calorimeter also needs upgrade. The BINP group is involved in the development of the upgrade of the calorimeter system of the detector.

In the barrel part of the calorimeter, the electronics will be replaced, which will enable continuous digitization of signals from the counters and subsequent fitting of the data with a known shape. This procedure allows one to determine both energy and time of arrival of signal. Using the time information will enable large suppression of the background rate due to pile-up.

For the endcap part where the background conditions are the most severe, the first phase will be dedicated to upgrade of the electronics. Then the scintillation CsI(Tl) crystals will be replaced with pure CsI crystals with a shorter scintillation time. This will decrease the time of signal integration by a factor of 30. Combined with fitting of the waveform, it will provide an over 150-fold background suppression.

The first batch of the mass production was performed in 2013. It includes 100 shaper-digitizer modules (Fig. 1.9.8). The shaper-digitizer is the basic unit of the new electronics system. This block shapes signals from the counters, digitizes the signal shape every 0.5 microseconds and then performs digital processing with reconstruction of amplitude and time of arrival of signal. In addition, the module generates a fast analogue signal for use in the neutral trigger system. All the modules have been tested on a special stand, developed in 2012. Their characteristics meet all technical requirements (Fig. 1.9.9). An order for mass production of 280 shaper-digitizer units was placed in 2013.

A modification of the board for the endcap calorimeter was manufactured and tested in 2013. The board layout is shown in Fig. 1.9.10. Ten boards will be produced by April 2014. They will be subject to final tests and then the mass production will begin.

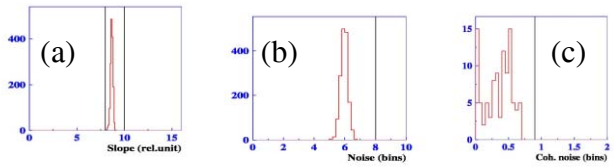

Fig. 1.9.9. Distribution of measured characteristics of the modules: a) conversion factor; b) total channel noise; c) module coherent noise.

In 2013, a VME crate for the electronics of the calorimeter was developed and produced. The appearance of the crate is shown in Fig 1.9.11. The crate, which is equipped with twelve modules of shaper-digitizers, was connected to the barrel calorimeter module. This crate was used for study of the coherent noise behavior and selection of best grounding system. The resulting noise values are consistent with the expected ones.

Fig. 1.9.10. Appearance of shaper-digitizer for endcap calorimeter.

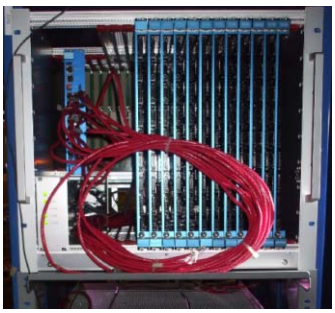

Fig. 1.9.11. VME crate with electronics modules.

In addition to the development of the shaper-digitizer module, the BINP team has developed a pilot version of the collector module for work with high-speed (Gigabit/s) optical channel. The new module has been produced and tested in high-speed readout. A circuit simulating the Belle II data acquisition system has been assembled (Fig. 1.9.12). The FLD projects were loaded to the shaper-digitizer modules (ShaperDSP) from the PC through the collector module (Collector) via a regular Ethernet channel. The data readout is performed by an optical channel from the processor on the board of the data acquisition system (Copper). The triggering was done using the time unit (TTRX) and arriving at the trigger module (FTSW) that synchronizes the operation. It was shown that the module enables operation with loads at frequencies of up to 30 kHz, with no noise increase, as shown in Fig. 1.9.13.

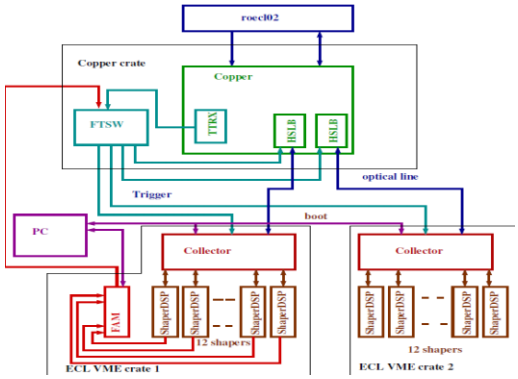

Fig. 1.9.12. Scheme for reading information from calorimeter via optical channel.

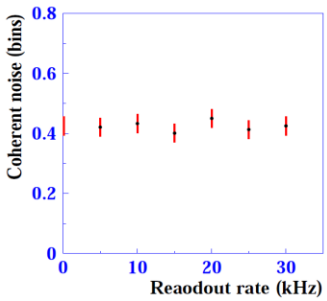

Fig. 1.9.13. Coherent noise on shaper-digitizer board vs. readout rate.

The Belle II experiment is expected to result in a significantly larger neutron flux caused by interaction of lost electrons of the beam with the material of the structure of the accelerator and the detector. The dark current of the semiconductor photodetectors increases proportionally to integrated neutron flux through the detector. The power supply filter for the photodetector of the backward calorimeter was being upgraded in March 2013, which included replacement of preamplifier resistors, for the photodetectors to be able to work after their exposure to a neutron flux. It was necessary to dismantle the calorimeter, to demount the preamplifiers, to replace resistors in them, to test their efficiency, to mount the preamplifiers on the crystals, to close the calorimeter and to make a final check on cosmic particles. The steps of disassembling a sector (1/16) of the calorimeter are shown in Fig. 1.9.14. This work was conducted by a team of 5 persons and took six weeks. As a result, all the filters have been upgraded, and the tests have shown workability of all the 960 channels.

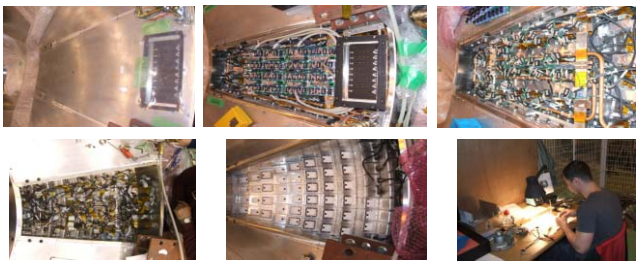

Fig. 1.9.14. Stages of disassembling sector of calorimeter and replacement of resistors.

280 shaper-digitizer modules and 52 collectors will be produced and tested in 2014. Besides, the electronics of the barrel calorimeter will be installed on the detector; all the counters will be connected; the channels will be subject to functional tests. The mass production of the shaper-digitizer modules for the endcap collector will begin. In addition, it is necessary to upgrade the preamplifiers of the forward calorimeter and to test its counters.

1.10. BABAR EXPERIMENT

Experiments with the BABAR detector were carried out at the e^+e^- collider PEP-II at SLAC (USA) from 1999 to 2008. The data collected in the experiment are currently being analized. The BABAR collaboration includes about 300 physicists, wiyth 11 BINP members among them. The BINP members of the collaboration participate in the analysis on the measurement of the CKM matrix element V_{ub}, the measurement of the cross sections of the e^+e^- annihilation into hadrons with the use of radiation return technique and study of two-photon processes with detection of scattered electron. In 2013, the collaboration published 26 articles. The total number of publications is as large as 529.

In 2013, the cross section of the $e^+e^- \to p\bar{p}$ process was measured in the energy range from the threshold up to 6.5 GeV using the radiation return method. Except for a narrow interval near 4 GeV, this is the most accurate measurement to date of the cross section. The data on the cross section was used to derive the energy dependence of the effective proton form factor, which is shown in Fig 1.10.1 in comparison with the existing data obtained both in e^+e^- and $p\bar{p}$ annihilation.

The form factor growth near the threshold is explained by strong final-state interaction. At higher energies, complex behavior of the cross section and the form factor was observed, namely their sharp step-like decrease near 2.2, 2.5 and 3.0 GeV. This behavior is not described by the existing theoretical models. The cross

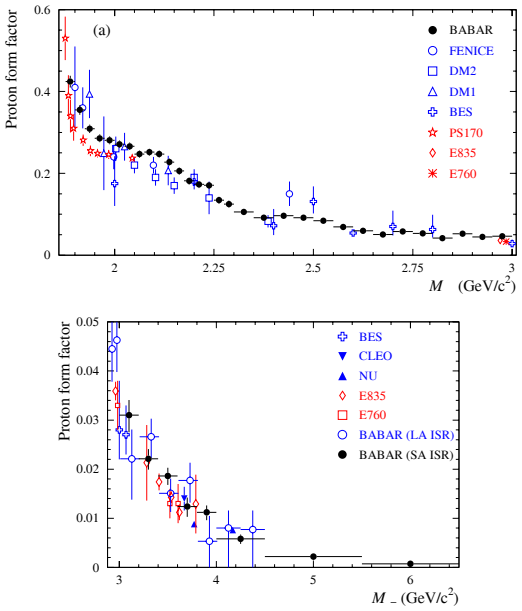

Fig.1.10.1: The measured dependence of the effective proton form factor on the $p\bar{p}$ invariant mass in two mass intervals in comparison with results of previous experiments.

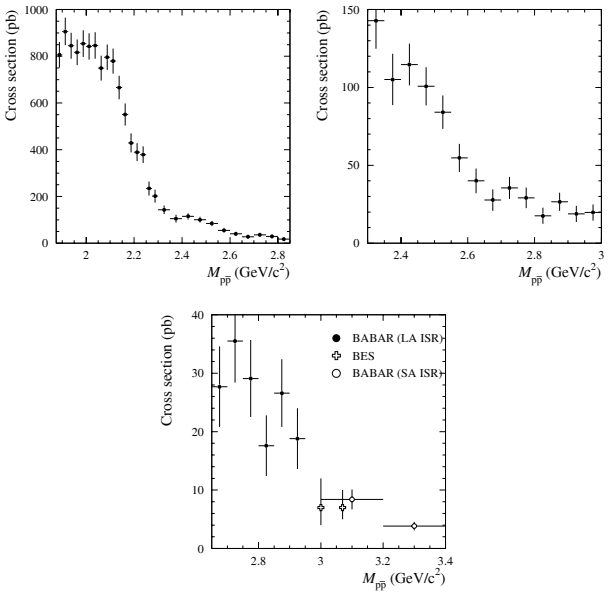

Fig.1.10.2 The cross section of the $e^+e^- \to p\bar{p}$ process near 2.2, 2.5 and 3 GeV/c^2.

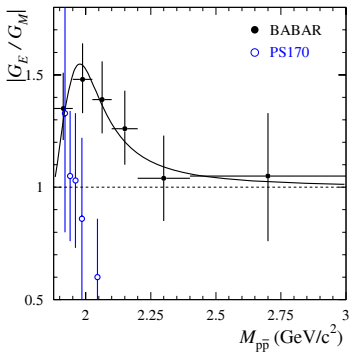

Fig.1.10.3: The ratio of the form factors $|G_E/G_M|$ measured in the BABAR experiment in comparision with the data of the PS170 experiment.

section of the $e^+e^- \to p\bar{p}$ process in the invariantmass regions near the above-mentioned steps is shown in Fig.1.10.2.

From the analysis of the angular distributions of proton-antiproton events, the energy dependence of the ratio of the electric and magnetic form factors $|G_E/G_M|$ was obtained. The result shown in Fig.1.10.3. At energies below 2.2 GeV, the $|G_E/G_M|$ ratio turned out to be significantly larger than unity. This result is in contradiction with the only earlier measurement.

At energies above 4.2 GeV, the cross section and the time-like form factor of proton were measured for the first time. The BABAR results are compared with data on the space-like form factor (Fig.1.10.4, where the "SLAC 1993" squares show the space-like data measured in ep scattering). The curve is the result of the fit to data with the asymptotic dependence

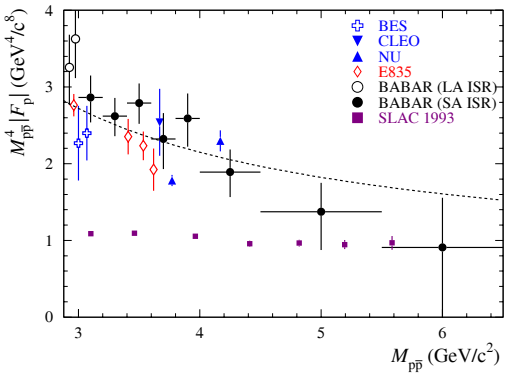

Fig.1.10.4: The normalized (multiplied by $M^4_{p\bar{p}}$) proton effective form factor above 3 GeV/c^2.

predicted by QCD. One can see that the values of the time-like and space-like form factors approach each other at energies above 4.5 GeV, in agreement with the theoretical expectations.

Currently, BINP physicists are working on high-precision measurement of the parameter V_{ub}. Works on the measurement of the cross sections by radiation return method are underway.

1.11. PARTICIPATION IN THE ATLAS EXPERIMENT AT THE LARGE HADRON COLLIDER (LHC).

During 2010-12 the ATLAS and CMS detectors were collecting statistics at a record energy of colliding protons of 7 (in 2010-11) and 8 (in 2012) tera-electron-volt (TeV) in the center of mass system. About 0.04, 4.7 and 20.7 inverse femtobarn were accumulated, respectively.

The most important result is the reliable observation of a signal from a new particle with properties similar to those expected for the Higgs boson. The Nobel Prize in Physics 2013 was awarded to P. Higgs and F. Englert «for the theoretical discovery of a mechanism that contributes to our understanding of the origin of mass of subatomic particles, and which recently was confirmed through the discovery of the predicted fundamental particle, by the ATLAS and CMS experiments at CERN's Large Hadron Collider».

After collecting data at collisions of protons with lead ions in January-February 2013, the Large Hadron Collider and detectors were interrupted for two-year shutdown.
The goal is to prepare for the work at LHC design parameters – energy of colliding protons of 14 TeV in the center of mass system and luminosity of 10^{34} $cm^{-2}s^{-1}$. For the ATLAS detector the list of the actions includes:

- Repair and replacement of broken elements of the detector and electronics
- Installation of new detector elements, in particular, of the insertable layer of the inner detector for detection of particles, containing b-quark
- Improving efficiency and speeding-up the triggering and reconstruction algorithms
- Preparation of entire computing infrastructure (both hardware and software parts) for handling substantially larger amount of data

All this does not revoke the high priority of the work on analysis of the data taken in 2011-12 aiming to swift publication of the results. The most important task is detailed study of the properties of recently discovered particle (the spin, parity, decay branching ratios, and coupling constants). The BINP group participated in the analysis of the Higgs boson decay into four leptons. In Fig. 1.11.1 the distribution over the invariant mass of four leptons for selected candidate events is presented. The contribution of background processes is shown as well as the expected signal for the Standard Model Higgs boson with the mass m_H =124.3 GeV and the signal strength (the ratio of measured cross-section to that in the Standard Model) μ=1.43 (the parameter values were obtained from the fit to data). The analysis of angular distributions in various decay channels of the higgs-like boson shows that the data are compatible with the Standard Model spin-parity $J^P = 0^+$ quantum numbers, whereas all alternative hypotheses studied ($J^P = 0^-$, 1^+, 1^-, 2^+ models) are excluded at confidence levels above 97.8%.

The painstaking work of dedicated groups on detector calibration allowed to significantly reduce the systematic uncertainty on reconstruction efficiency and on the accuracy of the energy scale calibration. The BINP group worked on the calorimeter calibration and on improving the simulation and the reconstruction of electrons and photons. Also a method of the evaluation of the identification efficiency for heavy quarks with large transverse momentum was developed.

The search for new physics goes beyond the Higgs bosons. In particular, BINP physicists continued to search for heavy neutrinos in the channel with leptons and hadronic jets in the final state. Two theoretic models were examined – the Left-Right Symmetric Model, in which the neutrino is generated through the hypothetic right-handed vector boson W_R, and the model with the virtual W boson of the Standard Model. The world's best upper limits have been obtained for the masses (up to the level of 2 TeV), production cross sections and coupling constants of heavy neutrinos. However, further significant improvement is possible only with an increase in the energy of colliding protons in the LHC, which is, as mentioned above, planned for 2015.

After the start of the data taking in 2010, the ATLAS collaboration with participation of BINP authors published 273 papers based on the collision data, including 75 papers in 2013.

In addition, the work on the support and development of the computer infrastructure and software is going on. Due to the 10-gigabit network, BINP physicists are able to analyze data at the NSU and SB RAS computing centers. In 2013, four HP Blade System crates (512 cores) were put into operation at the BINP. The operating system Scientific Linux 6 is deployed, supporting a virtualization technology based on the KVM platform.

Since 2007, BINP experts have continuously participated in the activities of the Trigger and Data Acquisition System administration group, which deals with the maintenance and development of the hardware and software for the High Level Trigger (HLT), Event Builder and other parts of the Data Acquisition System. The equipment includes about 2,300 network booted servers (in total, about 17,000 CPU cores), 50 servers supporting the ATLAS control room, and many other units of the IT infrastructure of the experiment. The main part of the group activity in 2013 was devoted to the migration of the whole software to the OS SLC6, and to the transition from the hardware MS Windows platform to the virtualization scheme "Linux KVM Virtual Host + MS Windows Virtual Machines".

During a scheduled shutdown, significant part of the computing resources of the DAQ system was used for the simulation of events in the ATLAS detector. To make it possible, a special system configuration was deployed with participation of the BINP group.

Of great importance is the work on the support and administration of the ATLAS central computers (~300 units), located in the CERN main computer building. These computers ensure uninterrupted operation of critical services: numerous components of the ATLAS distributed computing system, data bases, electronic logbook

of the detector, data quality monitor, event display etc. In 2013, the work was primarily connected with the transition to new configuration and virtualization systems.

Since 2008, BINP programmers have made a significant contribution to the creation and development of important services and applets to manage the ATLAS Distributed Computing system (ATLAS GRID). The ATLAS GRID Information System (AGIS) has become the basic source of the information on the topology of the ATLAS computing resources and on available software releases. It is integrated with other key components of the distributed computing system: central data replication and data storage system (DDM, ATLAS Distributed Data Management System), a system for distributed analysis and job submission (PanDA, ATLAS Production and Distributed Analysis), monitoring services.

Also the work is going on the preparation of the detector upgrade in future years. The Technical Design Reports (TDRs) for so called "the Phaze 1 upgrade" are written for various detector systems and undergo the endorsement process. The modernization is scheduled to 2018-19 and will mostly concern the trigger electronics. The BINP group plans to participate in developments of the back-end (digital) part of the liquid argon calorimeter electronics (programming of FPGA microchips).

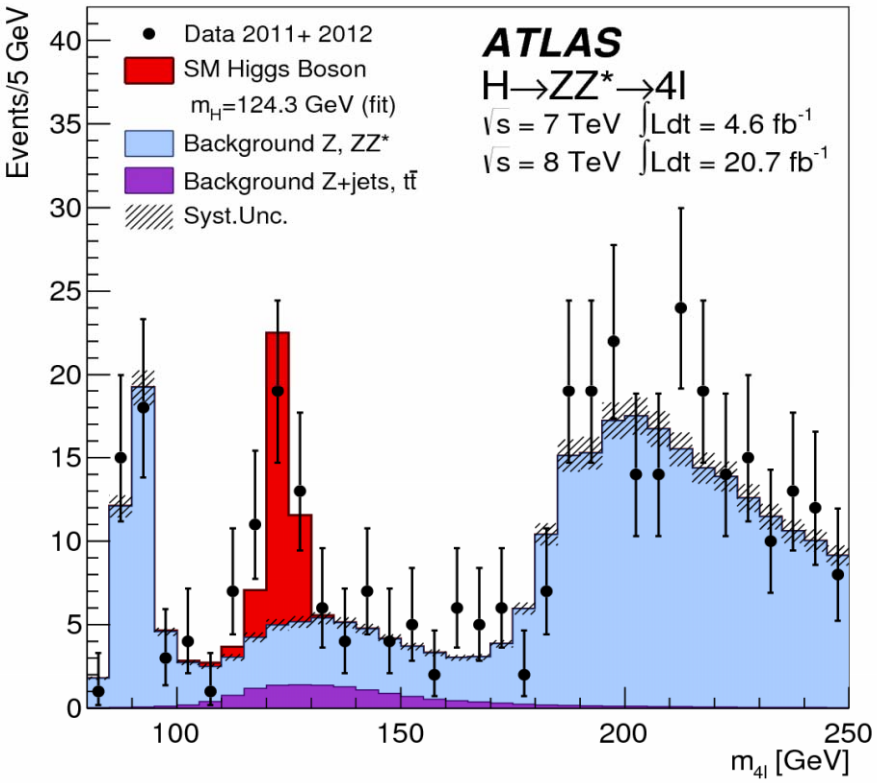

Fig. 1.11.1. Distribution over the invariant mass of four leptons m_{4l} for selected candidate events. Points – experimental data. Histograms show the contribution of background processes as well as the expected signal for the Standard Model Higgs boson with the mass m_H=124.3 GeV and the signal strength (the ratio of measured cross-section to that in the Standard Model) μ=1.43 (the parameter values were obtained from the fit to data).

Also a project for the LHC collider upgrade is being developed at CERN for the purpose of increasing the luminosity by an order of magnitude, up to 10^{35} cm^{-2}s^{-1} . The BINP group takes part in the experiment on the study of operation of the ATLAS liquid argon calorimeters at high rates. In April 2012 and March 2013, another regular data acquisition sessions were carried out at the U-70 accelerator in Protvino with new front-end electronics, much better adapted for high-rate environment. Another important improvement in these runs was better control of parameters of the 50 GeV proton beam. A new secondary-emission chamber made in BINP has allowed more precise measurement of the beam profile (in both transverse coordinates) and of the beam intensity during the spill, with a step of 0.15 s. In previous setup, only one measurement per spill (lasting for about 1.5 s) was possible. Data analysis and comparison with simulation is ongoing.

1.12. LHCB EXPERIMENT

1.12.1. Technical support of the LHCb.

The data flow from the LHCb detector, which is recorded for subsequent storage and processing, consists of about 30 kB events passing through the high-level trigger (HLT2) with a frequency of about 2-5 kHz. Thus, the flow of data to store exceeds 100 MB/s or 1,000 TB per year of operation. This volume is too large to be processed in each separate analysis. Instead, the LHCb experiment applies centralized preliminary offline selection of events (the so-called "stripping"). About 10 % of events are separated from the total data amount and then recorded in a few (5-8) flows. Thus, each data flow that contains similar events (e.g., one flow may group all modes with muons in the final state or events from D meson decays), includes a much smaller number of events, which can actually be processed in the GRID system in a relatively short time. In addition, data files after the "stripping" contain information about candidate particles and their combinations, which further reduces the time for processing and obtaining the physical result. A disadvantage of such approach is that the procedure of preliminary selection shall be applied already at the stage of data acquisition. To some extent, this problem can be solved due to the presence of inclusive selections (such as a muon with large transverse momentum, "topological" selections , and so on).

The BINP group is responsible for the development and maintenance of software environment that preselects events ("stripping") in accordance with selection criteria set by physical analysis developers. Since such pre-selection is in many ways similar to the high-level trigger (which is also programmable), the "stripping" environment is a modification of the programs of the second-level trigger HLT2. Environment for the "stripping" enables simultaneous operation of several hundreds of physical event selection processes, forwards events for recording in a few streams (DST files), and includes modules for debugging the selection criteria and monitoring the results.

Besides that, the BINP group is involved in the support of preselection of events for angle γ measurement in tree decays of B mesons, for analyses, which focus on the study of B decay modes into DX, where B is either a charged ($B^{\pm}$) or neutral (B_d or B_s) B meson; D is a charged or neutral D meson, which is reconstructed in one of the D→hh, D→hhh, D→hhhh, D→$K_S$hh, or D→K$\pi\pi^0$ states (here h is a charged kaon or pion), and X is a kaon, a pion, or a combination of $\pi\pi$, Kπ or KK. Such decay modes cover practically all possible methods of measurements of the angle γ, both from the ratio of amplitudes of allowed and suppressed B→DK decays and with the help of time-dependent analyses or Dalitz distribution analyses.

The BINP members are also involved in the support of experiments and take part in the pilot shifts. In 2013 there was no data taking at the LHCb detector because of a maintenance shutdown of the LHC. However, the ongoing physical analyses, reconstruction of events and modeling still require constant monitoring. In 2013, there were 11 shifts to control the GRID network operation (so-called “production shifts”). These shifts are mainly aimed at the monitoring of ongoing computing tasks and data transfer. These shifts will improve the effectiveness of data reconstruction, modeling and custom tasks.

The BINP members are involved in the work of the department responsible for modeling of backgrounds and doses of radiation loads (the LHCb background simulation group). The simulation results are extremely important; they are used not only for protecting the health of people (induced radiation distribution maps), but also for the maintenance of the equipment (background from neutrons and released energy). In addition to conducting the modeling itself, which requires hundreds of thousands of hours of computer time, the results should be published in a form convenient for the service personnel. In 2013, this work was carried out in two directions:

1) Implementation of web application for visualization of background modeling results.

2) Deployment of the modeling process on the HLT cluster.

The visualization web application is written in the framework WT (www.webtoolkit.eu) and is inlined in most viewed web servers via the FastCGI interface. The system has been installed and is available at cern.ch/lhcbrad (access for the CERN staff only).

Last year, a technique of modeling start on GRID nodes was refined. However, the licensing restrictions for the FLUKA package (www.fluka.org) impose substantial limitations. It was suggested to temporarily (for the time of the stop in data acquisition) use the resources of the HLT on-line cluster. In addition to starting the modeling itself, automation of validation of results was also carried out, as well as averaging of results of multiple runs into a set of files. Data are considered correct if there are no empty files or files completely filled with zeros, there also must be no negative values, which is important for the amount of released energy or an equivalent dose. A two-level system of averaging has been developed. Before running a task, the user sets two values: the numbers of files for averaging at the first and second levels. The total number of modeling streams must be equal to or greater than the product of these two values. As soon as the work of one of the modeling streams ends, the number of output files is checked and then averaging (level 1) is performed. In the end, final averaging (level 2) is done and a file for the visualization Web application is generated. A PVSS panel (www.pvss.com) is used as the frontend, and the backend is a set of scripts in Bash, Ruby and Python.

The Hadron calorimeter HCal is used as an argument of trigger L0. Because of the ageing of plastic and optical fiber and other possible damages, the properties of the calorimeter change. Thus it is very important to perform periodic calibration of the calorimeter. The calorimeter

design is such that a special tube with water passes through all the cells. A capsule with a radioactive cesium source is moved in this tube with simultaneous reading of data, which are used for calibration. The existing calibration program works under the operating system Windows XP. It cannot be transferred to the new versions of Windows because there are no drivers for the EPICS equipment. It was decided to perform migration of the corresponding software to the operational system Linux. According to the long term planning, the full program code will be transferred to the Linux platform. There is, however, a significant obstacle of the large amount of WinAPI-specific code and GUI parts written in MFC. Besides, the client interface of the driver part (API KVASER for SYSTEC devices) also differs significantly from the Linux interface SocketCAN.

As a first step, the operability of the SocketCAN interface was tested, for which a special library Winelib DLL wrapper was written (http://www.winehq.org/docs/winelib-guide/bindlls) to the native interface. Launching of the executable module for the Windows platform in Linux using the WINE emulator demonstrated successful work of the SocketCAN driver. A special server part on the basis of this program will be written for operation within the SCADA system, which is applied in the CERN WINCC (it used to be referred to as PVSS).

1.12.2. Physical results.

The research program of the BINP group in the LHCb experiment is aimed at the observation of effects beyond the Standard Model of electroweak interactions. This common project includes a task of precision measurement of quantities that experience CP violation, i.e. of the angle γ of the unitarity triangle and parameters of mixing of D mesons. Another task is spectroscopy of heavy hadrons.

The amount of data acquired in the LHCb experiment up to 2013 is about 3 fb^{-1}. The corresponding amount of reconstructed decays of B mesons already exceeds by far the statistics collected at the electron-positron B factories (at least in final states not containing π^0 or photons). Besides, there are a lot of available decays of Bs, B baryons and excited states of B, which are either not produced at all at electron-positron machines or are produced in small quantities. This enables study of very rare decays of B hadrons and thereby obtaining good sensitivity to various extensions of the Standard Model.

Below is an overview of the physical results obtained by the LHCb collaboration with participation of the BINP members.

CP violation and measurement of the angle γ

CP violation is responsible for asymmetry of matter and antimatter in the universe. Within the Standard Model, CP violation is described by the Cabibbo-Cobayashi-Maskawa (CCM) matrix, which characterizes transitions between different quark generations due to weak interaction. The CCM matrix can be represented with the so-called unitarity triangle (UT). Various processes are sensitive to the lengths of the sides and values of the angles of the triangle. Effects that are beyond the Standard Model manifest in mismatch in measurements of the UT parameters (e.g., a sum of the angles of the triangle is not equal to 180 degrees). Thus, precision measurements of the UT parameters complement direct searches for "New Physics" effects at high energies in such detectors ATLAS or CMS.

Various CP-violation processes that are most sensitive to the UT parameters are observed in decays of B mesons. At the moment, only one of the angles of the UT (most often referred to as β) has been measured with an accuracy of about 1 degree in the Belle and BaBar experiments at electron-positron colliders. The LHCb experiment will result in more precise determination of many other parameters of the CP violation. In particular, the angle γ can be measured to within a few degrees.

BINP members have extensive experience in conducting analyzes directly related to both measurement of the angle γ in the $B\to DK$ decays and study of other decays of B mesons to open-charm states. These studies were initiated in the Belle experiment at the electron-positron KEKB factory in Japan and are now continued at the LHCb. In addition, BINP members have published several phenomenological papers in this topic with a proposal of new approaches to precision measurements of the angle γ and an investigation into subtle systematic effects. The BINP group coordinated the working group of the LHCb experiment in the investigation into B decays into open-charm states (Beauty to Open Charm Working Group), one of the eight physics working groups of the experiment.

Earlier, in 2011 and 2012, the LHCb experiment yielded several results relating to the angle γ measurement. Those include analysis of the $B\to DK$ decay, where D is reconstructed in a two-particle state, $D \to K\pi$, KK or $\pi\pi$ (so called GLW and ADS methods of measuring γ). In these decays, charge asymmetry of the decay probability (CP-violation) was reliably observed for the first time. That proved that γ is non-zero for sure and gave γ value limitations. In addition, in 2012, the $B \to DK$ decay with the D meson reconstructed to the final states $K_S\pi\pi$ and K_SKK was analyzed by a method first proposed by the BINP group. The analysis, which was performed using all the available LHCb statistics, yielded $\gamma = (57 \pm 16)^\circ$.

Different approaches to the measurement of the angle γ complement each other. In addition to γ, two other unknown parameters are also measured: the amplitude ratio r_B and strong phase δB. Since correlations between these parameters differ in each approach, a combination of several measurements allows a γ measurement accuracy better than that in just averaging. A combined measurement of the angle γ, which resulted in $\gamma = (67 \pm 12)^\circ$ (Fig. 1.12.1), was published in 2013. The results are published in a CERN preprint.

Besides the above decays, the LHCb experiment studies a large number of other processes in which CP violation can manifest itself and that may be sensitive to the angle γ. Although the current amount of data may be insufficient for reliable measurements of CP violation in these processes, they can be used in the future, after the maintenance shutdown of the LHC, as well as after the upgrade of the LHCb detector in 2018. Combining of a large number of independent measurements will result in a better γ measurement accuracy and more reliable monitoring of systematic errors. Study of such processes with the current amount of data will enable debugging the procedures for selection of events and more accurate prediction of the future γ measurement accuracy. In addition, many of these processes are interesting in themselves, as they make it possible to investigate intermediate resonance states of hadrons, seek for new states, and check theoretical predictions of the quark model.

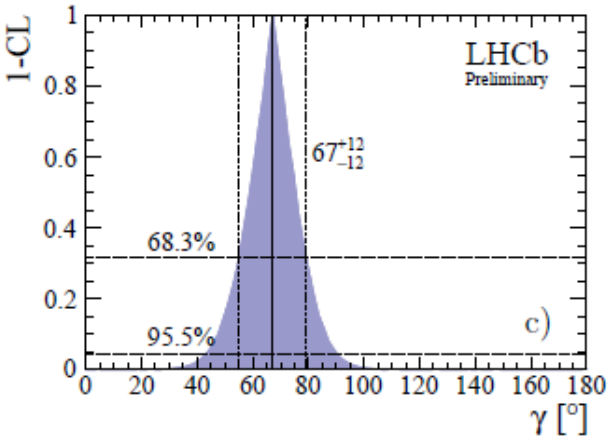

Fig. 1.12.1. Reliability parameter for combined measurement of the angle γ in B→DK decays.

A measurement of CP violation in the same B→DK decay but with the D meson reconstructed in the final state, D→Kππ, was published in 2013. Although the presence of CP violation in such a process was not established reliably because of little statistics, a suppressed process was registered, $B^+ \to D\pi^+$, $D \to K^+\pi^-\pi^+\pi$, as well as a charge-conjugate one, which will make it possible to obtain limitations for angle γ, provided the statistics is large enough.

Another measurement in which the angle γ can be measured is the investigation into the decay of Λ_b^0 baryon into the final state DpK. The BINP group has suggested this method as a promising one for observation of CP violation. This decay was earlier observed, as well as the corresponding "control" decay $\Lambda_b^0 \to Dp\pi$, using some of the LHCB data. The preliminary results were published in a CERN preprint. This analysis was completed in 2013 using statistics collected in 2011 (1 fb^{-1}). An article describing the analysis and its results was submitted for publication in a peer-reviewed journal. The results include the first observation of the $\Lambda_b^0 \to DpK$ decay and its probability measured (see Fig. 1.12.2), as well as the first observation and measurement of the probability of the $\Lambda_b^0 \to \Lambda_c^+ K^-$ decay (Figs. 1.12.3 and 1.12.4). Besides, in the same final states, the baryon Ξ_b^0 was first discovered. It is a bound state of a "beauty" b quark and a "strange" s quark. Earlier this particle was detected in one decay only, into $\Xi_c^+\pi^-$, by the CDF collaboration at the Tevatron collider. We measured the probabilities of corresponding decays of Ξ_b^0 and the mass of this baryon with a precision twice better than that in the previous measurement by CDF.

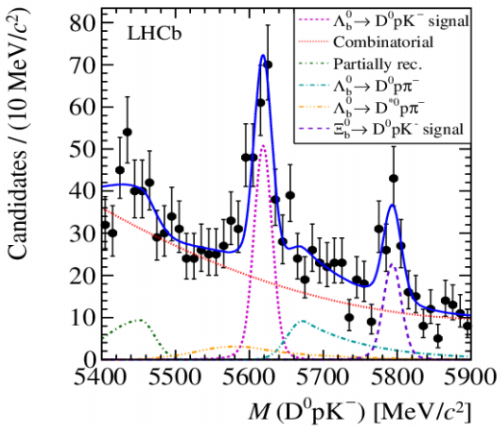

Fig. 1.12.2. Distribution of invariant masses of DpK, which shows signals of $\Lambda_b^0 \to DpK$ and $\Xi_b^0 \to DpK$.

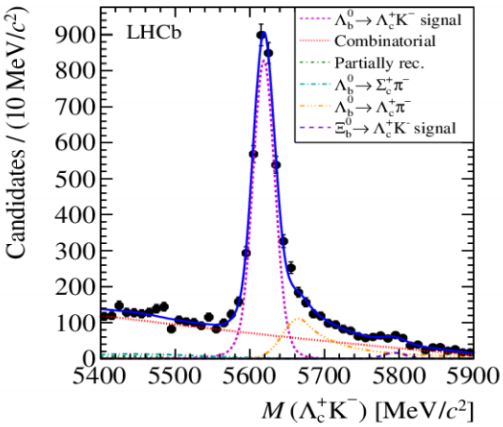

Fig. 1.12.3. Distribution of invariant masses of $\Lambda_c K$, which shows signals of $\Lambda_b^0 \to \Lambda_c^+K^-$ and $\Xi_b^0 \to \Lambda_c^+K^-$.

With all the available statistics of the $\Lambda_b^0 \to Dp\pi$ and $\Lambda_b^0 \to DpK$ decays, the amplitude analysis was started, which will enable identification of intermediate resonance states through which these decays occur. Fig 1.12.5 presents the Dalitz distribution of the $\Lambda_b^0 \to Dp\pi$ decay. In the distribution one can see intermediate resonances in the Dp (excited Λ_c^+ baryons) and pπ (N or Δ baryons) channels. Full amplitude analysis will define the masses, widths and quantum numbers of these intermediate states.

In 2013, a series of studies of three-particle decays of B mesons with a D meson in the final state was carried out. The probability of the $B_s^0 \to DK\pi$ and $B^0 \to DK\pi$ decays

was measured, with $B_s^0 \to DK\pi$ decay registered for the first time. In the future, these decays can also be used for a measurement of the angle γ.

With the use of the $B_S^0 \to D\pi\pi$ final state, a search for the $B_S^0 \to D^{*+}\pi^-$ decay was performed. This decay is interesting because it can occur only in a diagram with exchange of W boson and is thereby expected to be strongly suppressed. Detecting (or failing to detect) this decay provides important information about the mechanism of such $B_s^0 \to \pi\pi$ or $B_s^0 \to DD$ decays, in which both W exchange and rescattering of a pair of ss quarks into cc (or dd) quarks may manifest. The analysis has shown no significant $B_S^0 \to D^{*+}\pi^-$ signal and has given an upper limit for its probability. So one can conclude that the rescattering effects dominate in the $B_s^0 \to \pi\pi$ and $B_s^0 \to DD$ decays.

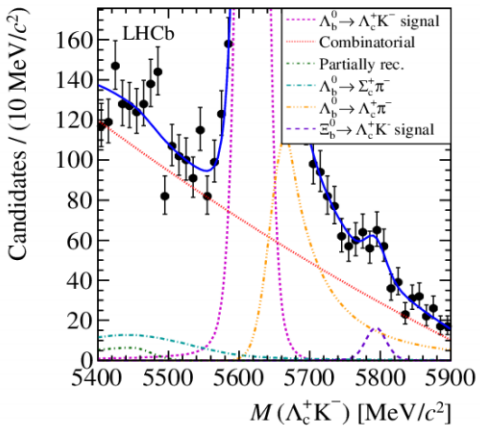

Fig. 1.12.4. The same as in Fig 1.12.3. Fragment enlarged in the Y axis, showing the contribution of $\Xi_b^0 \to \Lambda_c^+ K^-$.

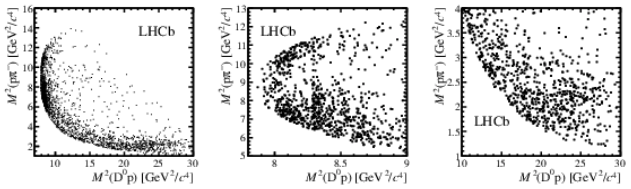

Fig. 1.12.5. Dalitz distribution for $\Lambda_b^0 \to Dp\pi$ decay (total phase space and two areas with intermediate resonances).

Besides the above experimental works carried out with the participation of BINP members, a phenomenological work was completed and published in 2013. It was dedicated to the study of influence of possible CP violation in decays of D mesons on the measurement of the angle γ. A model-independent analysis of the $B \to DK$ and $D \to K_s\pi\pi$ decays was applied. It is known that the fundamental theoretical uncertainty in γ measurement is negligible (about 10^{-7}), and the main uncertainty, except for the purely statistical one, is due to various model effects, such as description of the dynamics of D meson decay, mixing or CP violation in D mesons, and experimental statistical errors. It was earlier suggested to eliminate these difficulties with a model-independent approach to the measurement of the angle γ. In such an approach, all unknown quantities associated with the dynamics of the D decay are obtained from independent experiments with entangled quantum states of D mesons in $\psi(3770) \to DD$ decays. The influence of mixing of D mesons on this approach was considered earlier, and it was shown that its contribution can be taken into account, thus a precision measurement of the angle γ is not limited by the expected uncertainty. The same study found that possible direct CP violation in decays of D mesons can also be considered as a slight modification of the model-independent procedure.

Spectroscopy of heavy hadrons

Among works in the field of spectroscopy of heavy hadrons, analysis of $\Lambda_b^0 \to DpK$ and $\Lambda_b^0 \to \Lambda_c^+ K^-$ has already been mentioned. Decays of Ξb0 baryon were first observed in this analysis. This baryon was observed only in one final state, $\Xi_c^+ \pi^-$.

For the time being, the LHCb detector data contain a large amount of decays of Λ_b baryons, which can be used for exploration of spectroscopy of heavy baryons containing a b quark. In 2012, a group of BINP members analyzed the $\Lambda_b \pi^+ \pi$ spectrum, in which two excited states of Λ_b baryon were revealed: $\Lambda_b^*(5912)$ and $\Lambda_b^*(5920)$. The quark model predicts that these states are radial excitations of Λ_b with a spin of 1/2 and 3/2, respectively. In 2013, this analysis was continued with the use of all the available LHCb statistics. Besides the final state $\Lambda_b \pi^+ \pi$ mentioned, $\Lambda_b^* \to \Lambda_b \gamma$ radiative transitions were revealed. Because of the limited energy resolution in the spectrum of $\Lambda_b \gamma$, the two states, $\Lambda_b^*(5912)$ and $\Lambda_b^*(5920)$, however, cannot be reliably separated. Currently the analysis procedures is under optimization with a view of improvement of the resolving powers in the mass range of $\Lambda_b^* \to \Lambda_b \gamma$. The results of the investigation of radial excitations of Λ_b in the final states $\Lambda_b \pi^+ \pi^-$ and $\Lambda_b \gamma$ with statistics of 3 fb^{-1} will be published in 2014.

In a study of the $B^+ \to K^+ \mu^+ \mu^-$ decay a wide structure in the mass spectrum of the two muons was revealed. This decay is realized through three contributions (decay of B^+ meson into a vector charmonium and K^+ with subsequent decay of the charmonium into a pair of muons) and contributions of loop processes induced by neutral currents, which change the flavor (FCNC). When looking for contributions to the FCNC decays beyond the Standard Model, it is important to correctly take into account the tree contributions. The study of the mass spectrum of the two muons revealed a broad structure that may originate in interference of the decay with the $B^+ \to K^+ \mu^+ \mu^-$ resonance and has a statistical significance of more than 6 standard deviations (see Fig. 1.12.6). Within the errors, the mass and the width of the resonance (4191^{+9}_{-8} MeV and 65^{+22}_{-16} MeV) are consistent with the properties of the ψ(4160) meson. This is the first observation of $B^+ \to K^+ \psi(4160)$ and $\psi(4160) \to \mu^+ \mu^-$ decays.

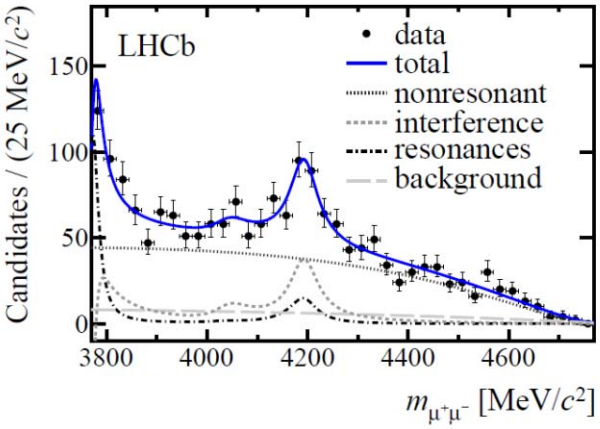

Fig. 1.12.6. Distribution of invariant mass of two muons in $B^+ \to K^+\mu^+\mu^-$ decay.

2

ELECTRO- AND PHOTONUCLEAR PHYSICS

EXPERIMENTS WITH INTERNAL TARGETS

I. Correct account of the contribution of the two-photon exchange (TPE) to the elastic scattering of electron on proton will probably explain the contradiction in the results of measurement of the electromagnetic form factors of proton obtained by various experimental techniques. The three experiments on the determination of the TPE contribution to this process have been conducted worldwide: by the OLYMPUS collaboration (DESY, Germany), by the CLAS collaboration (TJNAF, USA) and by BINP at the VEPP-3 storage ring. In all three cases, the TPE contribution was determined via a measurement of R, the ratio of the elastic scattering cross sections of positron on proton and electon on proton. ?At BINP, the data acquisition was done at energies of electron/positron beams of?1.6 GeV and 1.0 GeV. The data taking was completed in 2012. The results of the experiment were analyzed in 2013. The analysis included various corrections and a study of systematic errors. To suppress the systematic errors it was important to ensure identical conditions in the data acquisition, e.g. the same position of electron/positron beams, their energies, currents level, and so on. Sessions of data acquisition with electron and positron beams were regularly alternated, which allowed significant suppression of the effects of slow drift in time of target thickness , detection efficiency and some other parameters. Two nearly identical detection systems located on the opposite sides of the beam suppressed changes in their total counting rate for small variations of beams position. Negligible magnetic fields in the vicinity of the particle detector eliminated the problem of inequal acceptance of the particle detectors for electron and positron scattering (note that this is a big problem for OLYMPUS and CLAS experiments). In the analysis of the data it was checked how well all these conditions were met. Part of the data (about 5 %) was rejected because of their violation. The contribution of the background inelastic processes to the set of events that were selected as elastic scattering events was taken into account. ?Taking the contribution of radiative corrections into account was an important step in the analysis: it is a significant part of the deviation of the measured value R from the unity. The work on the calculation of radiative corrections was completed, and a publication was prepared.

Preliminary results of the measurement of R vs. ε (virtual photon polarization parameter), obtained in the present experiment are shown in Fig.2.1. Measurements with the highest ε value were used for normalization at both energies. The normalizing value was set equal to 1. In Run II the data were divided into three intervals of ε. The figure also shows the results of previous experiments. They have

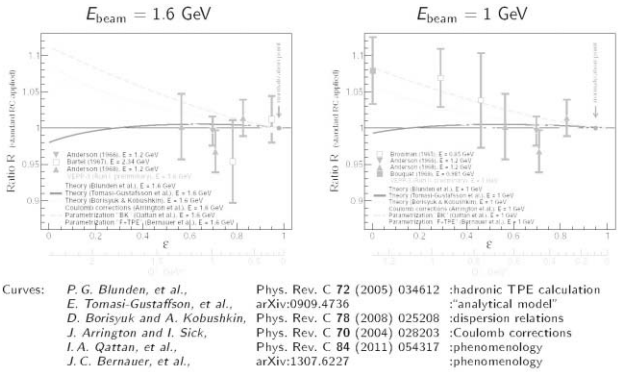

Fig.2.1. Preliminary results of the experiment: R ratio vs. ε. Black circles: data of this experiment.

much larger errors. The lines show some theoretical predictions for R. Note that calculations by P. G. Blunden et al. and D. Borisyuk and A. Kobushkin practically coincide. The experimental points obtained in this work lie approximately in the middle between this pair of curves and the curve by J.C. Bernauer et al. The latter work developed parameterizations of proton form factors, Coulomb corrections and the TPE contribution, which describe well a large set of experimental data, including the results of both unpolarized measurements (by differential cross section data) and polarization measurements (by measured ratios of form factors). That is, this approach removes the above-mentioned contradiction between the proton form factor results obtained by the Rosenbluth method and the polarization transfer one. Calculations by P. G. Blunden, et al. have also shown that the inclusion of the TPE contribution resolves this inconsistency.

The final results of the experiment will be obtained in the coming months.

II. Coherent photoproduction of neutral pion on deuteron is an important process in nuclear physics, which provides valuable information about the structure of deuteron and pion-nucleon and nucleon-nucleon interaction. The presence of only two particles in the final state simplifies the calculations and allows one to make more specific predictions both on their interaction and the intermediate states of the proton-neutron pair. While theoretical studies of the reaction have been carried out for a long time (since the 70s), detailed experimental data on the differential cross sections are relatively recent. Regarding polarization phenomena observed in this reaction, there are only a few measurements of sigma asymmetry. Before our data, there were absolutely no measurements of the tensor analyzing power of the reaction. Our data were obtained from the statistical material of an experiment on deuteron photodisintegration (D.M. Nicolenko et al., JETP 89, 518 (2009)). The accuracy

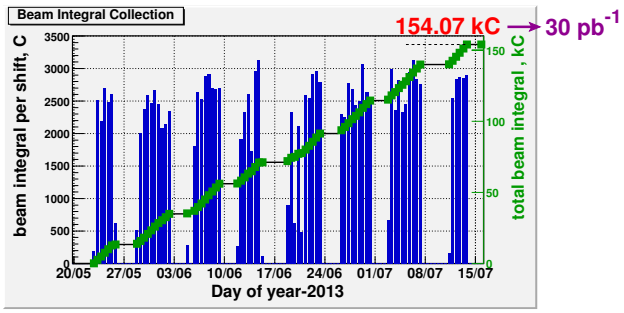

Fig. 2.2: Rate of data acquisition in experiment on coherent production of neutral pion on polarized deuteron. In intervals between the data acquisitions, VEPP-3 was working under synchrotron radiation program.

Fig.2.3: Setting up quasi-real photon tagging system.

of these measurements was low. In this experiment, the accuracy of the measurement of the tensor analyzing power of the T20reaction will be improved several times and data on the differential cross sections will be obtained. In May-July 2013, acquisition of data on coherent production of neutral pion on a tensor-polarized deuteron target was carried out. The integrated charge that crossed the target during the data acquisition was 154 kCoulomb (Fig. 2). The average value of the tensor polarization of the target was 37.3 ± 1.1 %.

III. Works with the quasi-real photon tagging system (PTS) at VEPP-3 were continued. The PTS will greatly expand the possibilities for the study of photoreactions at VEPP-3 and will allow progress towards a photon energy of $1.5 GeV$. Moreover, the transverse polarization of a significant portion of photons will be determined, which will enable experiments with double polarization. Note that, in addition to the new data on deuteron, we will be able to extend such measurements to neutron.

The PTS was assembled for the first time in summer 2013 (Fig. 3) and then installed at VEPP-3. Electron and positron beams were generated in September, with this system in the storage ring. The spectra of bremsstrahlung and annihilation radiation were recorded at a zero angle from the tagging system.

IV. Work continued on the development of a source of polarized molecules of hydrogen isotopes. Calculations were carried out on the focusing of orthohydrogen molecules by the sextupole magnets of the available source of polarized deuterium atoms. These calculations show that at low temperature of the source, two superconducting magnets of the second group can substantially deflect the molecules. The source of molecules will be placed on the tank of the first group of magnets. The tank has the liquid helium temperature, so the temperature of the molecule source can be varied within wide limits adjusted by heat input. The polarized molecules will be accepted by a tube of about 30 mm in diameter placed at 150 cm distance from the magnets. Its size was chosen in such a way that molecules that left the source of molecules cannot reach the interior of the tube if the magnetic field is switched off. When the magnetic field is on, the molecules are affected by a force and molecules with a desired spin projection are focused in the tube. The flow of focused molecules can be estimated by increase of pressure in the tube. The design study of the molecules source and receiver has been completed; some parts have been manufactured.

The experiments with internal targets are carried out in collaboration with groups from Tomsk, NIKHEF (the Netherlands), and ANL (USA).

3
THEORETICAL PHYSICS

NLO evolution of 3-quark Wilson loop operator
I.Balitsky and A.V. Grabovsky
BINP-preprint 2013-25, 39 p.

The NLO evolution equation for the 3-quark Wilson loop operator was obtained. A composite 3-quark Wilson loop operator obeying a quasi-conformal evolution equation was constructed. The linearized quasi-conformal equation is presented.

Evolution equation for 3-quark Wilson loop operator
R.E. Gerasimov and A.V. Grabovsky
JHEP, 04, 102 (2013)

The evolution equation for the 3 quark Wilson loop operator has been derived in the leading logarithm approximation within Balitsky high energy operator expansion.

On the solution to the NLO forward BFKL equation
A.V. Grabovsky
JHEP, 09, 098 (2013)

It is demonstrated that the NLO forward BFKL equation can be solved in the space of its Born eigenfunctions.

Connected contribution to the kernel of the evolution equation for 3-quark Wilson loop operator
A.V. Grabovsky
JHEP, 09, 141 (2013)

The connected contribution to the kernel of the evolution equation for the 3-quark Wilson loop operator was derived within Balitsky high energy operator expansion. Its C-odd part was linearized and transferred to the momentum space.

Multi Regge Amplitudes in non Abelian Gauge Theories
M. G. Kozlov
Nuclear physics and engineering, 4, 853 (2013)

The effective Regge vertices necessary for the proof of the multi Regge form of the amplitudes with gluon exchange within the bootstrap approach have been obtained in the next to Born order within supersymmetric Yang-Mills theories. The one loop contribution of scalar particles to the impact factor of the gluon production has been found for an arbitrary dimension D. The contributions of scalar particles to the eigenfunction of the octet Balitsky-Fadin-Kuraev-Lipatov kernel, as well as additional impact factors appearing in supersymmetric Yang-Mills theories, have been calculated. The fulfilment of all elastic and inelastic bootstrap conditions has been tested, which guarantees the multi-Regge form of multiparticle amplitudes in supersymmetric Yang-Mills theories in the next to leading logarithmic approximation.

Multi Regge Amplitudes in non Abelian Gauge Theories
M. G. Kozlov
Academy of Sciences, 5-8 Nov. 2013

We demonstrated that In Yang-Mills theories of sufficiently general form multiparticle amplitudes had the multi-Regge form in the next-to-leading logarithmic approximation.

Multi-Regge form of amplitudes with gluon exchanges in supersymmetric Yang-Mills theories
M. G. Kozlov, A. V. Reznichenko, V. S. Fadin
BINP-preprint 2012-32 (August 2013), pp. 1-50.

All effective vertices for Reggeon-particle interaction in supersymmetric Yang-Mills theories (SYM) are found both in the leading and next-to-leading logarithmic approximations (LLA and NLLA). Scalar contributions to the eigenfunction of the octet BFKL kernel for the adjoint representation of the gauge group and to impact-factors, analogous to existing in QCD, as well as all additional impact factors, appearing in SYM, are calculated. On this base, the proof of fulfilment of all bootstrap conditions providing the multi-Regge form of the NLLA amplitude with the gluon exchange is carried out. A new method for check of the bootstrap conditions is developed which does not require explicit calculations of effective vertices and impact-factors. It is used to prove bootstrap conditions in the theories with general Yukawa-type fermion-scalar interactions with arbitrary numbers of fermions and scalars in arbitrary colour group representations.

QCD Amplitudes with the gluon exchanges at high energies
A. V. Reznichenko
Nuclear physics and engineering, vol. 4, 857 (2013)

Our paper is devoted to the proof of the hypothesis about the multi-Regge form of the QCD amplitudes with the gluon exchanges at high energies in the framework of next-to-leading logarithmic approximation. The proof in question is based on the relations arising from the compatibility of the multi-Regge form with the s-channel unitarity. These relations are reduced to the verification of the finite number of so-called bootstrap conditions that present non-linear restrictions on the effective Regge vertices and Regge trajectory. Our main calculating goal is to check explicitly the fulfilment of these conditions. In

the paper we put more emphasis on the most difficult bootstrap condition-inelastic bootstrap condition for one-gluon production in the multi-Regge kinematics. There are two main components of the condition: impact-factor of one-gluon production and the matrix element of the jet production operator. We demonstrate the calculation for both of them on one-loop level and check the fulfilment of the bootstrap. As a by-product of the verification process we derive some original mathematical relations for the dilogarithmic function of the complex argument.

Mass spectra in $\mathcal{N}$=1 supersymmetric QCD with additional fields. Part III
V.L. Chernyak
arXiv: 1308.5863 [hep-th], pp. 1-23

This paper continues arXiV:1205.0410 and 1211.1487 [hep-th]. We also consider here the $\mathcal{N}$=1 SQCD - like theories (and their Seiberg's dual) with N_c colors and N_F flavors of light quarks and with N_F^2 additional colorless fields Phi, but now with N_F in the range $2N_c<N_F<3N_c$. The multiplicities of various vacua and quark condensates in these vacua are found. The mass spectra of the direct and dual theories in various vacua are calculated within the dynamical scenario which assumes that quarks in such $\mathcal{N}$=1 SQCD - like theories can be in two standard phases only. These are either the heavy quark phase where they are confined or the Higgs phase. Besides, this scenario implied that, unlike e.g. $\mathcal{N}$=2 SQCD, no additional parametrically lighter particles (like magnetic monopoles or dyons) appear in these $\mathcal{N}$=1 SQCD - like theories without adjoint colored scalar fields. The calculated mass spectra of these direct and dual theories were found to be different, in general. Besides, the mass spectrum of the dual theory with $N_c = N_F - N_C$ colors and $N_c+1<N_F<\frac{3}{2}N_C$ dual quark flavors was calculated.

And finally, the mass spectrum in the direct $\mathcal{N}$=2 SQCD with N_C colors, $N_c+1<N_F<\frac{3}{2}N_C$ flavors of quarks with the mass term $mTr(\Phi\Phi)$ in the superpotential, broken down to $\mathcal{N}$=1 by the mass term $\mu_x X^2$ of the colored adjoint scalar field X, $m << \mu_x << \Lambda_2$, was calculated in vacua of the baryonic branch, and compared with those in the two different Seiberg's dual theories. Our conclusions for this case disagree with those in the recent paper arXiv:1304.0822 of Shifman and Yung.

Decoupling in QED and QCD
A.G. Grozin
Int. J. Mod . Phys. A 28, 1350015 (2013)

Decoupling of a heavy flavor in QCD is discussed in a pedagogical way.First we consider a simpler case: decoupling of muons in QED. All calculations are explicitly done up to two loops.

Introduction to effective field theories, 3. Bloch-Nordsieck effective theory, HQET
A.G. Grozin
arXiv:1305.4245 [hep-ph]

This is a continuation of the lecture series. In this part we discuss interaction of electrons with soft photons in QED and Heavy Quark Effective Theory (HQET).

Effective weak Lagrangians in the Standard Model and B decays
A.G.Grozin
arXiv:1311.0550 [hep-ph]

Weak processes (e.g. B decays) with characteristic energies << M_W can be described by an effective theory which does not contain W, Z and other heavy particles (Higgs, t). Its Lagrangian contains four-fermion interaction operators.

Essentially it is the theory proposed by Fermi and improved by Feynman, Gell-Mann, Marshak, Sudarshan.

Introduction to *Mathematica* for Physicists Graduate Texts in Physics
A.G. Grozin
Springer (2013), 219 pages, ISBN 978-3-319-00893-6; ebook ISBN 978-3-319-00894-3

Mathematica is the most widely used system for doing mathematical calculations by computer, including symbolic and numeric calculations and graphics.

It is used in physics and other branches of science, in mathematics, education and many other areas. Many important results in physics would never be obtained without a wide use of computer algebra. This book describes ideas of computer algebra and the language of the *Mathematica* system.

It also contains a number of examples, mainly from physics, also from mathematics and chemistry. After reading this book and solving problems in it, the reader will be able to use *Mathematica* efficiently for solving his/her own problems.

Towards a synchronization theory of microwave-induced zero-resistance states
O. V. Zhirov, A. D. Chepelianskii and D. L. Shepelyansky
Physical Review B 88, 035410 (2013)

We develop a synchronization theory for the dynamics of two-dimensional electrons under a perpendicular magnetic field and microwave irradiation showing that dissipative effects can lead to the synchronization of the cyclotron phase with the driving microwave phase at certain resonant ratios between microwave and cyclotron frequencies. We demonstrate two important consequences of this effect: the stabilization of skipping orbits along the sample edges

and the trapping of the electrons on localized short-ranged impurities. We then discuss how these effects influence the transport properties of ultrahigh-mobility two-dimensional electron gas and propose mechanisms by which they lead to microwave-induced zero-resistance states.

Our theoretical analysis shows that the classical electron dynamics along the edge and around circular disk impurities is well described by the Chirikov standard map providing a unified formalism for those two rather different cases. We argue that this work will provide the foundations for a full quantum synchronization theory of zero-resistance states for which a fully microscopic detailed theory still should be developed.

Thermoelectricity of Wigner crystal in a periodic potential

O. V. Zhirov and D. L. Shepelyansky
EPL (Europhysics Letters), 103, 68008 (2013)

We study numerically the thermoelectricity of the classical Wigner crystal placed in a periodic potential and being in contact with a thermal bath modeled by the Langevin dynamics. At low temperatures the system has sliding and pinned phases with the Aubry transition between them. We show that in the Aubry pinned phase the dimensionless Seebeck coefficient can reach very high values of several hundreds. At the same time the charge and thermal conductivity of the crystal drop significantly inside this phase. Still we find that the largest values of ZT factor are reached in the Aubry phase and for the studied parameter range we obtain $ZT \leq 4.5$. We argue that this system can provide an optimal regime for reaching high ZT factors and realistic modeling of thermoelecriticy. Possible experimental realizations of this model are discussed.

Elastic enhancement factor as a quantum chaos probe

Ya. A. Kharkov, V.V. Sokolov
Phys. Lett. B 718, 1562 (2013)

Recent development of the resonance scattering theory with a transient from the regular to chaotic internal dynamics inspires renewed interest to the problem of the elastic enhancement phenomenon. We reexamine the question what the experimentally observed value of the elastic enhancement factor can tell us about the character of dynamics of the intermediate system. Noting first a remarkable connection of this factor with the time delays variance in the case of the standard Gaussian ensembles we then prove the universal nature of such a relation. This reduces our problem to that of calculating the Dyson's binary form factor in the whole transition region. By the example of systems with no time-reversal symmetry we then demonstrate that the enhancement can serve as a measure of the degree of internal chaos.

Chaotic Interference and Quantum-Classical Correspondence:Mechanisms of Decoherence and State Mixing

Valentin V. Sokolov, Oleg V. Zhirov
arXiv:1311.1953 [quant-ph]

The famous Nils Bohr's quantum-classical correspondence principle states that the classical mechanics is a limiting case of the more general quantum mechanics. This implies that “under certain conditions” quantum laws of motion become equivalent to classical laws. One of the conditions is fairly obvious: the corresponding classical action should be very large as compared with the Planck's constant. But this condition is ot sufficient. Suppression of effects of quantum nterference (“decoherence”) is the phenomenon of primary importance for understanding of the Bohr's principle. Being, in essence, of quite general nature, this problem takes on special significance in the case of non-linear classically chaotic quantum systems. Whereas the rapid decay of phase correlations is an underlying feature of the classical dynamical chaos, the "quantum chaos" by tself is not capable of destroying the quantum phase coherence. Strictly speaking, any initially pure quantum state remains pure during an arbitrary long unitary evolution. Basically, formation of incoherent mixed states (decoherence) results only from the process of reparation of a mixed initial state or interaction with a poisy environment. Just the decoherence brigdes the uantum and classical worlds. Peculiarities of the time qehavior of Peres fidelity, state purity, Shanon and von Neumann entropies are analyzed in detail. We demonstrate the ways the decoherence shows up in periodically driven systems that can be associated with Ramsey-type interferomentry experiments with ion traps.

Finally, decoherence in ballistic electron quantum transport caused by interaction with a disordered environment is considered.

Final state Coulomb interaction and asymmetry of pair production close to threshold in e^+e^- annihilation

V.F.Dmitriev , A.I. Milstein
Physics Letters B 722, 83 (2013).

We investigate a contribution of the d wave to the cross section of e^+e^- annihilation to the pair of charged eptons or nucleons close to threshold of the process. In contrast to the point of view accepted in literature, due to he Coulomb final state interaction this contribution does not vanish even at zero relative velocity of produced articles. This results in the nonzero asymmetry in ngular distribution at threshold. Though value of the asymmetry is small, observation of this effect is not hopeless.

Relativistic effects in scattering of polarized electrons
O.P. Sushkov, A.I. Milstein, M. Mori and S. Maekawa
Europhysics Letters 103, 47003 (2013)

The side-jump effect is a manifestation of the spin orbit interaction in electron scattering from an atom/ion/impurity. The effect has a broad interest because of its conceptual importance for generic spin-orbital physics, in particular the effect is widely discussed in spintronics. We reexamine the effect accounting for the exact nonperturbative electron wave function inside the atomic core. We find that value of the effect is much smaller than estimates accepted in literature. The reduction factor is $1/Z^2$, where Z is the nucleus charge of the atom/impurity. This implies that the side-jump effect is practically irrelevant for spintronics, the skew scattering and/or the intrinsic mechanism always dominate the anomalous Hall and spin Hall effects.

Kinetics of polarization in non-relativistic scattering
A.I. Milstein and S.G. Salnikov
Nuclear Instruments and Methods in Physics Research B 313, 64 (2013)

An approach is developed, which essentially simplifies derivation of kinetic equation for polarization in non-relativistic scattering. This approach is applicable for collision of projectile particles with a target for any spins of colliding particles. The most detailed consideration is performed for the case of spin 1/2 projectile particle interacting with spin 1/2 particle of a target. The solution of the kinetic equation for the case of zero initial polarization is presented.

Isoscalar amplitude dominance in e^+e^- annihilation to N N pair close to the threshold
V.F. Dmitriev, A.I.Milstein, S.G.Salnikov
arXiv: 1307.0936 [hep-ph]

We use the Paris nucleon-antinucleon optical potential for explanation of experimental data in the process $e^+e^- \to p\bar{p}$ near threshold. It turns out that final-state interaction due to Paris optical potential allows us to reproduce available experimental data. It follows from our consideration that the isoscalar form factor is much larger than the isovector one.

First order representation of the Faddeev formulation of gravity
V. M. Khatsymovsky
Class.Quant.Grav., v.30, p. 095006, (2013)

We study Faddeev formulation of gravity where metric is composed of ten four-dimensional vector fields, that is, of a ten-dimensional tetrad $f^A{}_\lambda$, A=1, …,10 , λ = 1, 2, 3, 4. The Faddeev action can be reduced to the Hilbert-Einstein one using equations of motion. We propose connection representation of the Faddeev gravity, an analog of the Cartan-Weyl form of the Einstein gravity. Now we introduce the SO(10) connection. Excluding this connection via the equations of motion leads to the Faddeev action. In addition, we introduce an analogue of the Barbero-Immirzi parameter used to generalize the Cartan-Weyl form of the Einstein gravity. Now we consider some one-parametric generalization of the connection representation of the Faddeev action which results upon excluding the connection in some one-parametric generalization of the Faddeev action itself which still results upon using the equations of motion in the Hilbert-Einstein action.

On the Faddeev gravity on the piecewise flat manifold
V. M. Khatsymovsky
arXiv:1312.7116[gr-qc], pp. 1-10, (2013)

We study the Faddeev formulation of gravity in which the metric is composed of vector fields. This system is reducible with the help of the equations of motion to the general relativity. The Faddeev action is evaluated for the piecewise flat ansatz for these fields when the metric corresponds to the flat interior of the 4-simplices of the general simplicial complex. Thereby an analogue of the Regge action in the usual general relativity is obtained. A peculiar feature of the Faddeev gravity is finiteness of the action on the discontinuous fields, and this means possibility of the complete independence of the fields in the different 4-simplices or incoincidence of the 4-simplices on their common faces. The earlier introduced analogue of the Barbero-Immirzi parameter for the Faddeev gravity is taken into account. There is some freedom in defining the Faddeev action on the piecewise flat manifold, and the task is set to make use of this freedom to ensure that this discrete system be reducible with the help of the discrete equations of motion to the analogous discrete general relativity (Regge calculus).

Four-loop corrections with two closed fermion loops to fermion self energies and the lepton anomalous magnetic moment
Roman Lee, Peter Marquard, Alexander V. Smirnov, Vladimir A. Smirnov, Matthias Steinhauser;
Journal of High Energy Physics, 1303, 162 (2013)

We compute the eighth-order fermionic corrections involving two and three closed massless fermion loops to the anomalous magnetic moment of the muon. The required four-loop on-shell integrals are classified and explicit analytical results for the master integrals are presented. As further applications we compute the corresponding four-loop QCD corrections to the mass and wave function renormalization constants for a massive quark in the on-shell scheme.

Critical points and number of master integrals

R. N. Lee, A. A. Pomeransky

Journal of High Energy Physics, 1311 , 165 (2013)

We consider the question about the number of master integrals for a multiloop Feynman diagram. We show that, for a given set of denominators, this number is totally determined by the critical points of the polynomials entering either of the two representations: the parametric representation and the Baikov representation. In particular, for the parametric representation the corresponding polynomial is just the sum of Symanzik polynomials. The relevant topological invariant is the sum of the Milnor numbers of the proper critical points. We present a Mathematica package Mint to automatize the counting of the master integrals.

LiteRed 1.4: a powerful tool for the reduction of the multiloop integrals

R.N. Lee

arXiv: 1310.1145

We review the Mathematica package LiteRed, version 1.4.

Gravitational four-fermion interaction in the early Universe

I.B. Khriplovich, A.S. Rudenko

Sov.Phys. Uspekhi, v.184, N 2 (2014);

JHEP 11, (2013) 174

If torsion exists, it generates gravitational four-fermion interaction (GFFI), essential on the Planck scale. We analyze the influence of this interaction on the Friedmann-Lemaitre-Robertson-Walker cosmology. Explicit analytical solution is derived for the problem where both the energy-momentum tensor generated by GFFI and the common ultrarelativistic energy-momentum tensor are included. We demonstrate that gravitational four-fermion interaction does not result in Big Bounce.

On structure of the polarization operator in a magnetic field

V.M. Katkov

arXiv:1311.6205v1 [hep-ph]

The polarization operator is investigated at arbitrary photon energy in a constant and homogeneous magnetic field for the strength H less than the Schwinger critical value. The effective mass of a real photon with a preset polarization is considered in the quantum energy region as well as in the quasiclassical one. Obtained in the quantum region expressions include the singular terms at the creation threshold of electron and positron on Landau levels.

4

PLASMA PHYSICS AND CONTROLLED THERMONUCLEAR FUSION

4.1. ECR PLASMA HEATING IN GDT

The system for electron cyclotron resonance (ECR) plasma heating was commissioned at the gas-dynamical trap (GDT) facility (Fig. 4.1.1).

Two Buran-A gyrotrons produced at IAP RAS operate as radiation sources. The gyrotron power is 450 kW; the pulse duration is up to 100 μs; the radiation frequency is 54.5 GHz. Two power systems have been developed and created for them. The systems generate pulses with a voltage of 70 kV, current of 25 A and duration of up to 5 ms, with an output voltage stability of up to 1%. Each gyrotron is equipped with a transmission line, which consists of a quasi-optical filter, a waveguide line, two bending angles, a universal polarizer and a quasioptical system for radiation injection into the plasma. A quasi-optical filter matches the output mode of gyrotron with the fundamental mode of the corrugated waveguide HE11. It consists of two mirrors with profile specially calculated for a specific gyrotron. The waveguide line consists of separate corrugated waveguides 0.5 m long connected by means of couplings. The bending angle is a planar mirror for 45 degrees. The universal polarizer enables transformation of input linear polarization to any required elliptical polarization. The system of radiation input into the plasma consists of one planar and two parabolic mirrors. It focuses and directs radiation to the desired point of the plasma. The vacuum window is made of quartz. The radiation is input in the near-mirror area of the GDT at an angle of 36 degrees to the axis of the facility. Each line inputs radiation near its magnetic plug. The microwave power loss for transportation in both tracts amounted to ~ 10%. Most devices and parameters of the gyrotron complex are controlled and monitored remotely via an automated control system.

The standard magnetic configuration of the GDT turned out to be unsuitable for the selected scheme of ECR heating because of the too high voltage required for charging of the capacitor bank of the GDT magnetic system and occurrence of parasitic ECR on the periphery of the plasma, from which the radiation is reflected (Fig.4.1.2). In order to solve these problems, we have changed the magnetic configuration. The position of the main EC resonance was left the same; the spurious resonance was shifted towards the wall of the vacuum chamber, where the plasma density is much lower. The voltage of the capacitor banks remains within acceptable limits. The energy properties of the GDT allowed us to create a favorable magnetic configuration for ECR heating on one end of the facility only. For this reason, all experiments were performed with one gyrotron only. A new variant of the reconfiguration of the magnetic system has been developed, in which both the gyrotrons will be used for plasma heating.

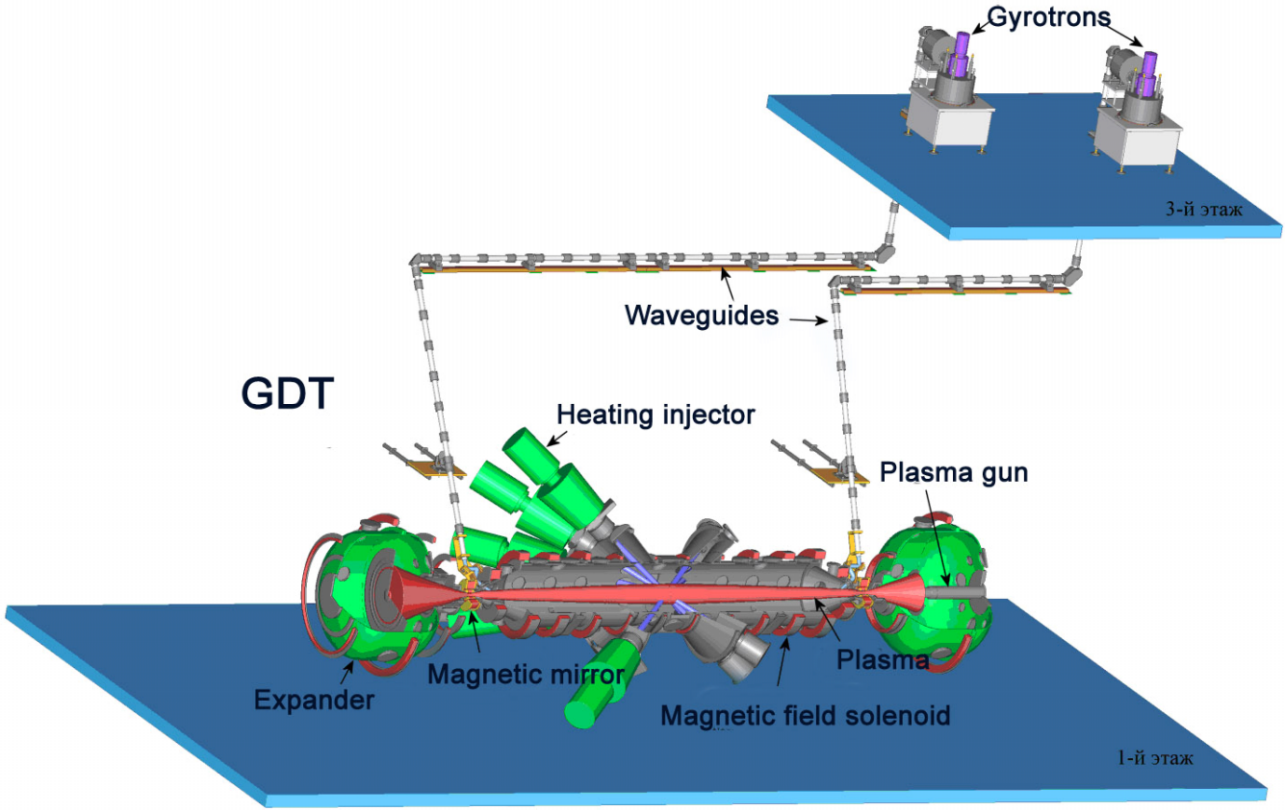

Fig. 4.1.1. System for ECR heating of plasma in GDT.

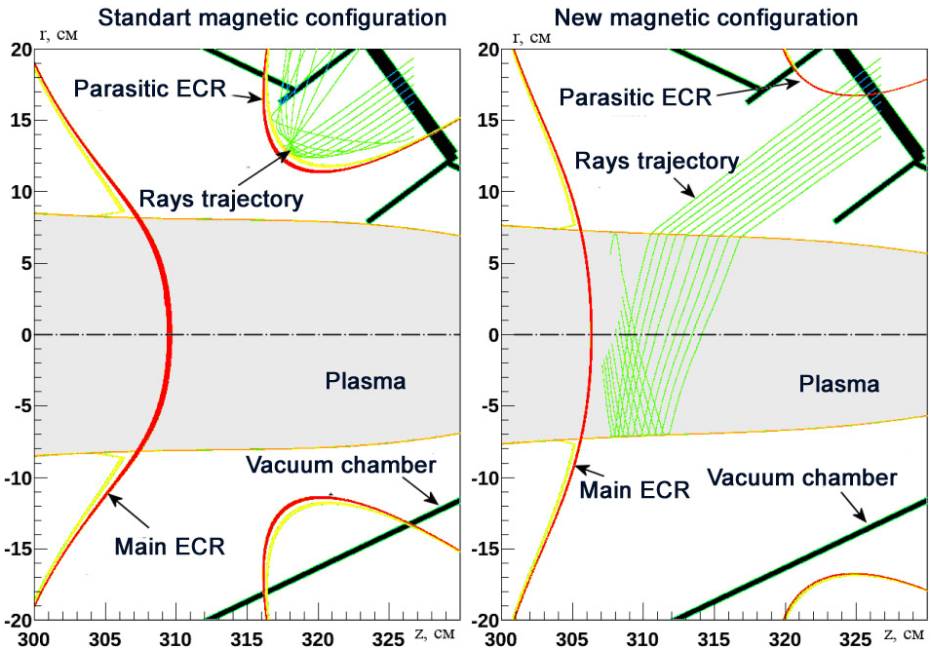

Fig. 4.1.2. Beam trajectories in the standard and new magnetic configurations of GDT.

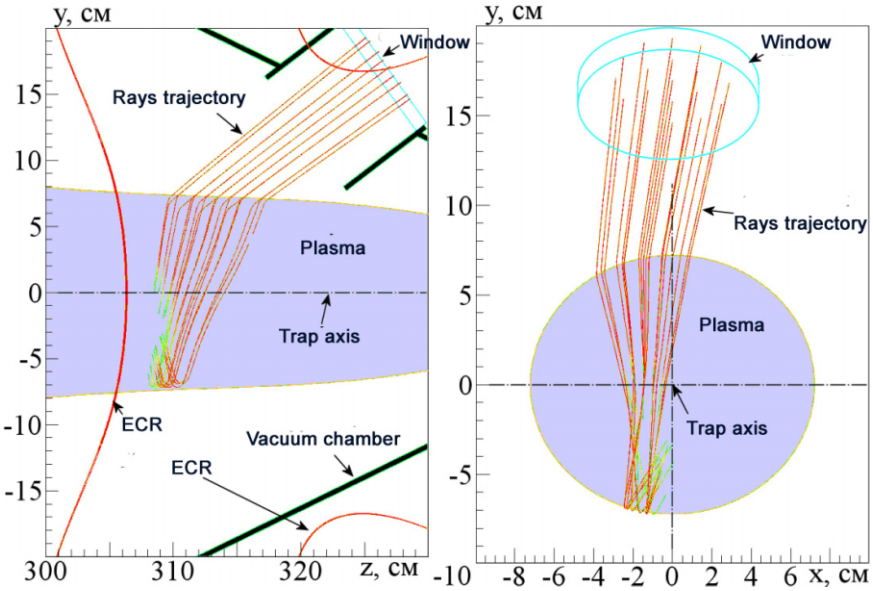

Fig. 4.1.3. Beam trajectories in plasma in GDT.

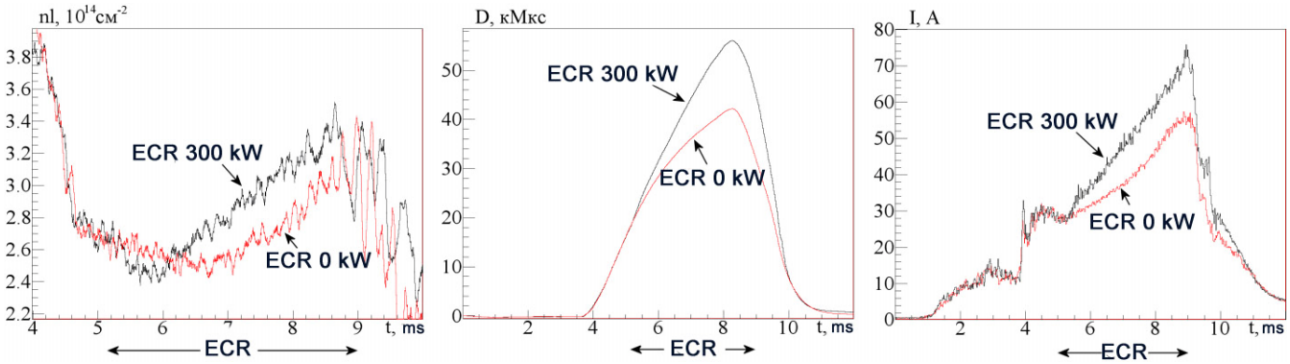

Fig. 4.1.4. Linear density of plasma, plasma diamagnetism and longitudinal ion current.

A 3D numerical code to calculate the wave trajectory and absorption localization in the plasma of the GDT was developed for selection of optimum configuration of the magnetic field and GDT experiment parameters. The wave trajectory is calculated in the approximation of geometrical optics, and the absorption coefficient is calculated from a numerical solution to the dispersion equation for a collisionless warm Maxwellian plasma with motionless ions (Fig. 4.1.3).

With injection of microwave radiation with a powerof ~ 300 kW into the plasma, 1 ms after the start of the atomic injection a growth in the integral plasma parameters is observed, e.g. in the diamagnetism (energy content) of the plasma and the current of ions leaving the trap through the plug (Fig. 4.1.4). The plasma density remains practically unchanged. This evidences a growth in the electron temperature of the plasma due to the ECR heating.

With the help of Thomson scattering, the distribution of plasma density and temperature in shots was measured with ECR heating and without it 2.5 ms after the start of injection of microwave radiation (Fig. 4.1.5). One can clearly see an increase in the plasma temperature during the ECR heating. The off-axial heating is due to the displacement of the center of the beam relative to the center of the plasma.

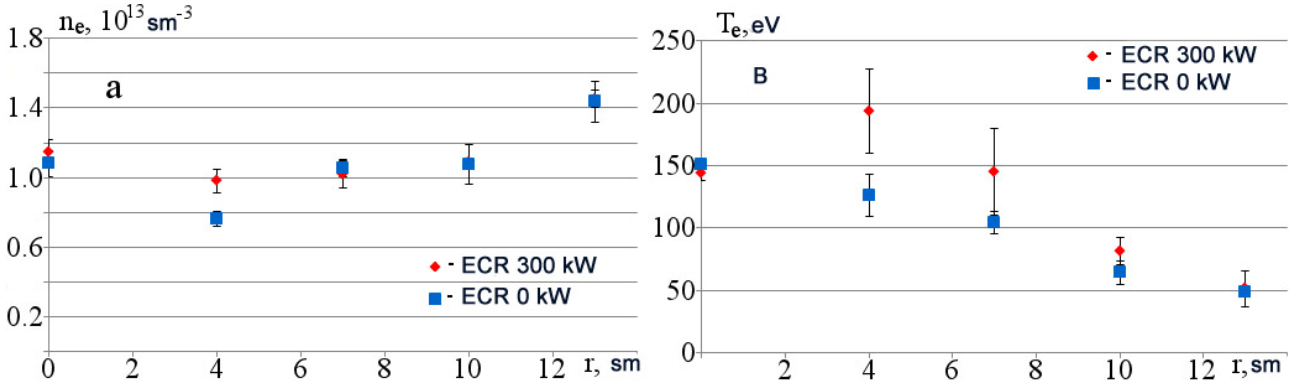

Fig. 4.1.5. Distribution of density and electron temperature of plasma.

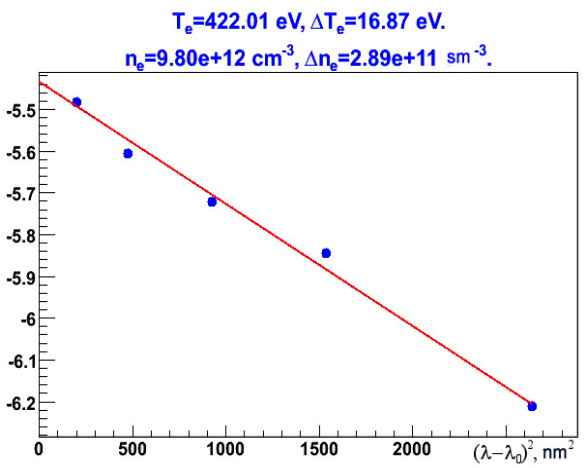

Fig. 4.1.6. Spectrum of scattering of laser radiation on plasma electrons.

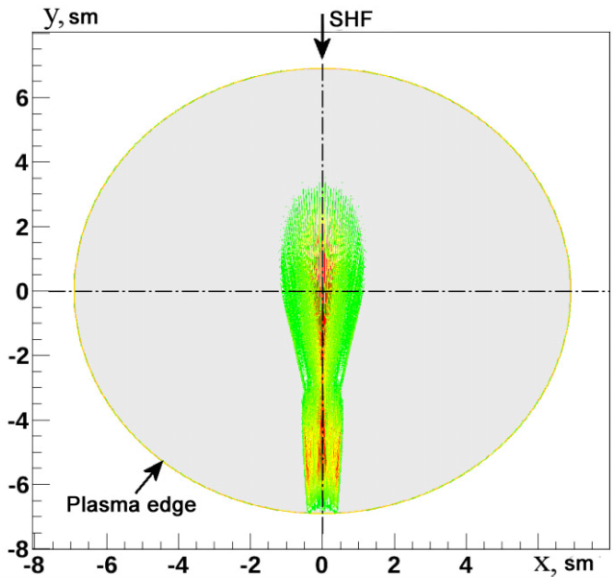

Fig. 4.1.7. Distribution of absorption of microwave radiation in plasma in GDT.

Increasing the ECR heating power up to 400 kW, setting the beam center on the plasma axis, and beginning the microwave radiation injection 3 ms after the start of the atomic injection, we achieved a GDT-record electron plasma temperature, over 400 eV (Fig.4.1.6). This temperature was measured in the center of the plasma using Thomson scattering 0.4 ms after the start of the ECR heating. This temperature is higher than the design estimate of the maximum attainable plasma temperature (350 eV) in absorption of a microwave power of 900 kW in plasma. This evidences a local heating of the plasma. This hypothesis is confirmed by a numerical calculation of the distribution of microwave radiation absorption over the plasma cross section (Fig.4.1.7) and the observed large scatter of measured temperatures between different shots in the GDT at constant integral parameters of the plasma. The attained electron temperature of the plasma is a record one for the quasi-stationary open traps.

4.2. GOL-3 FACILITY

4.2.1. Description and basic operation modes

GOL-3 is a unique engineering-and-physics system for research on the physics of rapid collective plasma heating with a powerful electron beam and physics of high-temperature plasma confinement in a multiple-mirror open trap. The behavior of the plasma in the trap is determined by collective and nonlinear effects. The difference of GOL-3 from other facilities with high-temperature plasma is that plasma is heated with a powerful electron beam. Depending on a certain scientific problem, one of two electron beam sources can be used for this purpose. These sources have quite different parameters. Using a high-current relativistic electron beam with a power of about 20 GW with a duration of around 10 microseconds provides higher plasma parameters. The physics of longer processes is investigated using a weakly relativistic electron beam of submillisecond duration and a power of up to 25 MW.

The scientific program in 2013 included several independent lines of research. One of them was the generation of sub-terahertz electromagnetic radiation in vicinity of double plasma frequency. This radiation arises with strong Langmuir turbulence, accompanying relaxation of high-current relativistic electron beam in a plasma. Another research line is associated with experiments with long-pulse electron beam of moderate power. Besides these programs, the main results of which are set forth in this section, GOL-3 was used in other investigations, aimed at the development of the physics and technology of collective plasma heating with a powerful electron beam and analysis of the influence of high-power plasma flows on structural materials. In parallel with the research experiments, the development of the experiment base was continued in 2013.

The appearance of the facility is shown in Fig. 4.2.1. The main solenoid consists of 103 independent-supply coils and has a total length of about 12 m. In the standard multiple-mirror configuration, the magnetic field has 52 corrugation periods (cells of the multiple-mirror system) with a maximum field of 4.8 T, a minimum field of 3.2 T, and a step of 22 cm. The mirror ratio of the corrugation trap is 1.5, ie, the facility operates in a "weak corrugation" mode. The solenoid ends with single magnetic mirrors with a field of 8 - 9 T. The exit unit of the facility consists of a pre-plasma source and expander tank with end beam

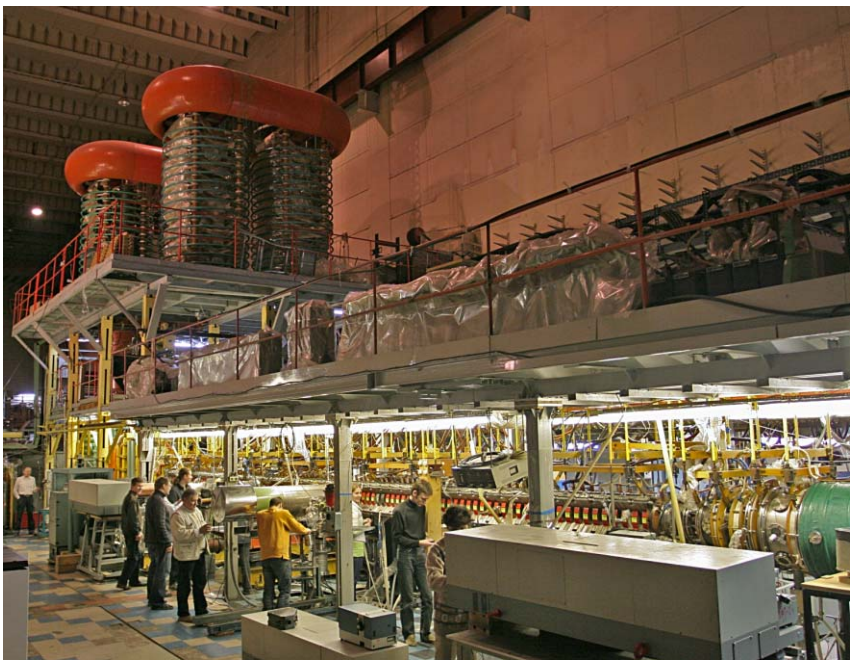

Fig. 4.2.1. Photo of GOL-3.

collector. In the area of the exit expander tank, the magnetic field gradually decreases to 0.05 T, due to which the specific energy density on the surface was decreased to a value that allows application of metals as receiving surfaces in work with a relativistic electron beam. In another experiment set-up, a source of relativistic electron beam is mounted instead of the exit plasma collector.

A typical scenario of experiment in the standard configuration of GOL-3 is as follows. Several pulse valves create a desired distribution of hydrogen or deuterium density over the length. The magnetic system of the facility, which is fed from a capacitor bank with a total energy storage of up to 15 MJ, is switched on. Next, a pre-plasma with the length-average density varying in the range of $(1 - 30)\times10^{20}$ m^{-3} is created using a special low-temperature longitudinal discharge. Then a relativistic electron beam, generated by the U-2 accelerator, is injected into the plasma. The beam has the following parameters: electron energy of 0.5 - 0.8 MeV, current of 20 - 25 kA, base duration of 8 - 12 μs, energy content of up to 120 kJ, and beam diameter of 4.1 cm (for a 3. 2 T magnetic field, corresponding to the minima of the corrugated field). Such a beam is formed in a belt relativistic diode, and then the magnetic system of the accelerator compresses and converts it into a beam of circular cross section. The collective plasma heating can result in a plasma ion temperature of about 2 ÷ 3 keV under optimal conditions (in the hottest part of the plasma column). The multiple-mirror scheme (corrugated magnetic field) allows hot plasma confinement for much longer time than in a simple solenoid trap.

Experiments with weakly relyativistic electron beam were carried without pre-plasma; the beam was injected directly into gaseous deuterium. These experiments are aimed at demonstrating the possibility of injecting a long-duration electron beam into a plasma. The physics research program includes both experiments on achievement of a quasi-stationary plasma state on GOL-3 and works on verification of some assumptions that are in the basis of the physical design of a new-generation open trap, GDMT. The beam parameters can vary widely: the electron energy is 20 - 120 keV; the beam current is 15 - 250 A; the power is 1 - 25 MW; the duration is 30 - 600 μs. The technology of generation of electron beams with the specified parameters, which are suitable for injection into the plasma trap (ie resistant to the high-power plasma flow that exits from the trap), was being refined on a special stand for a few years. This line of research implies the basic possibility of steady-state injection of electron beam. Thus it was necessary to create an electron beam source capable of operating in an incident plasma flow and suitable for at least 100-fold magnetic compression in the current density for the trap to have an acceptable ratio of beam electron density to plasma density.

4.2.2. Polarization of sub-terahertz plasma radiation in injection of relativistic electron beam.

Investigation into the mechanisms of generation, as well as features of the electromagnetic spectrum of radiation, of plasma in strong Langmuir turbulence, which occurs in intense relaxation of electron beam in a plasma, is one of the most fundamental problems of the physics of fusion plasma. This problem is not only important in terms of controlled nuclear fusion, but it is also one of the main tasks of astrophysical observations, because the radio emission of plasma space objects, such as the Sun, is of a plasma nature and these phenomena are based on processes similar to those occurring in turbulent plasma heating in open magnetic systems.

In 2013, experimenters on GOL-3 continued the research on the mechanisms of generation of electromagnetic radiation in the subterahertz range during relaxation of relativistic electron beam in a plasma. Earlier experiments have identifed modes of GOL-3 operation in which the radiation was in the given spectral range.

Experiments with powerful relativistic electron beam were aimed at the research on the spectral properties of electromagnetic radiation in the frequency range of up to 0.5 THz with the following parameters: $n_e = 3.7\cdot10^{20}$ m^{-3}; $E \approx 0.5$ MeV; $I = 20$ kA. The radiation spectrum was analyzed with an eight-channel polychromator. A polarization filter was placed upstream of the polychromator. The filter separated the parallel or perpendicular component of the electric field of the wave. The measurement result averaged over 10 shots is shown in Fig. 4.2.2.

The spectrum of radiation emitted from plasma has three distinct local maxima of intensity. The first is in the range of 100-150 GHz and corresponds to the cyclotron radiation of plasma electrons. Two other local maxima of intensity lie in the areas of frequencies of 170 GHz and 340 GHz. These frequency values coincide with the plasma frequency $f_p = (n_e e^2/\pi m_e)^{0.5} = 175$ GHz and its second harmonic.

The behavior of the polarization of electromagnetic radiation during electron beam injection into the plasma was studied in detail using a radiometric polarimeter consisting of two identical detectors to measure orthogonal polarization radiation. The radiation in the selected frequency range was analyzed with a quasi-optical bandpass filter located upstream of the polarimeter. The result of measurement of the polarization in two areas (near 190 GHz and 315 GHz) is illustrated in Fig. 4.2.3.

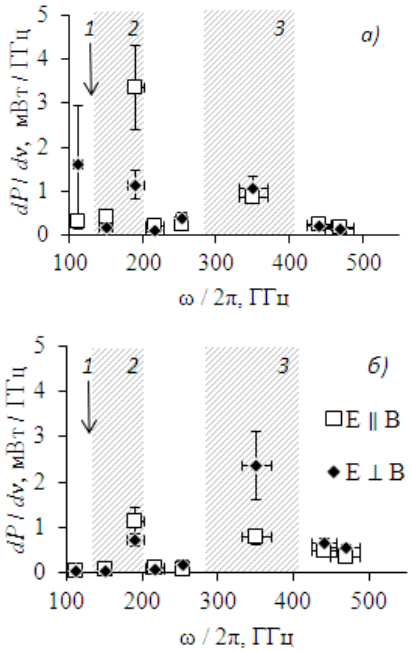

Fig. 4.2.2. Average spectrum of two polarization components of radiation emitted by plasma in beam-plasma interaction:
а) at time $t = 0.5$ μs after beginning of electron beam injection into plasma, *б)* $t = 0.75$ μs. The numerals indicate the frequency ranges relating to 1 – cyclotron frequency, 2 – plasma frequency, 3 – double plasma frequency.

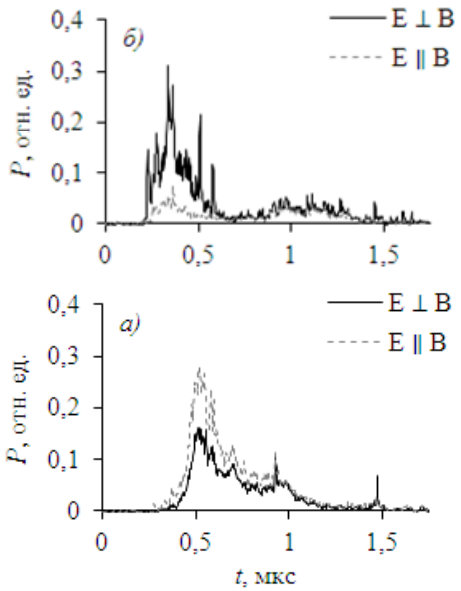

Fig. 4.2.3. Intensity evolution for mutually orthogonal components of electric field of radiation emission in the spectral range $\Delta f / f = 10\%$. Legend: a) plasma frequency neighborhood, $f = 190$ GHz; experiment PL12622;
б) double plasma frequency neighborhood;
$f = 315$ GHz; experiment PL12624.

4.2.3. Pre-plasma arc source.

The objective of this work was to develop a fundamentally new way of filling the facility with low-temperature plasma. This would substantially improve the vacuum and reduce the charge exchange losses from plasma, which is especially important in work with long-pulse beams. The existing system for pre-plasma generation demonstrated high reliability in a wide range of operating pressures of deuterium. The vacuum chamber, however, contained plenty of neutral gas.

It was proposed to use a pulsed arc plasma gun as a new plasma source. The plasma gun was designed and made in 2013. Mandatory requirements to the design included the possibility of work in a strong longitudinal magnetic field and safe work in electron beam injection experiments, in which the plasma gun is also the exit beam collector. The gun consists of a cathode, a hollow anode and an apertured arc channel with the length 130 mm and aperture 40 mm. The gas is puffed in pulses in the area of the cathode and a discharge with a current of 10 kA is ignited. Then the plasma propagates along the magnetic field and fills the area of magnetic confinement.

The gun was mounted on the end of the plasma chamber of GOL-3. The following was measured: the integrated density of the plasma along the central chord (interferometers were placed at distances of 0.4 and 8.3 m), the chord density profile (transverse injection H_0 at a distance of 6.1 m), the local plasma density (Thomson scattering at a distance of 10.8 m), and the optical emission (at different coordinates). Fig. 4.2.4 depicts the plasma density propagation in 40 cm from the gun at a discharge current of 10 kA and magnetic fields of 0.6 T and 1T inside the gun and of 3.2 T and 1.1 Tit outside it. The plasma density was observed to decrease 10 to 100-fold to $nl \approx 10^{14}$ cm^{-2} in 10 meters from the gun. The reason is currently being searched for.

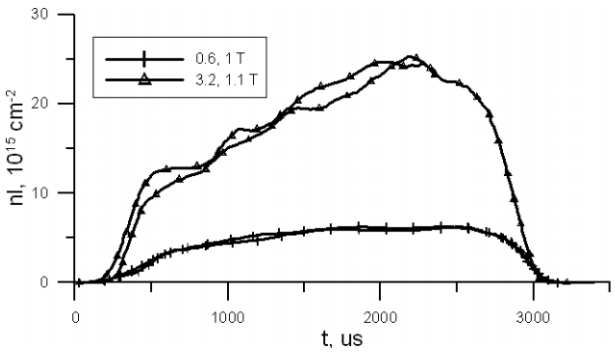

Fig. 4.2.4. Integral of plasma density over the diameter in 0.4 m from the anode of the plasma gun.

4.2.4. Numerical modeling of generation and transport of electron beam on GOL-3.

Modeling of sources of charged particle beams with plasma emitters has a feature of the effect of the electric

fields and particle fluxes on the surface shape of the emitting plasma, which itself is part of the electron-optical system of the source and determines the characteristics of the beam that it forms. For this reason, algorithms for computation of equilibrium shape of plasma surfaces become an essential component of any code for solving problems of plasma emission electronics.

The refinement of the numeral code POISSON-2, which was developed at BINP, was continued in 2013. This code allows calculation of several plasma regions emitting particles of different types and forming charged particle beams in self-consistent electric and magnetic fields. The code identifies the near-emitter potential distribution, which essentially depends on the distribution function of the plasma components. For compliance with the conditions of equilibrium surface, the computer code was supplemented with algorithms for solving the Poisson problem with boundary conditions describing the electric field value on the surface of plasma with a given potential. The equilibrium-surface conditions are met due to calculation of a relevant plasma surface shape at a given emission flux from the surface.

The diode cell of the multiple-aperture electron beam source of the multiple-mirror trap of GOL-3 was modeled. A self-consistent problem of formation of high-current electron beam in a diode with emissive plasma surfaces in an external magnetic field was solved. This will ensure passage of colliding electron and the ion flows through the anode and cathode apertures without current deposition on the electrodes. The solution allowed us to determine the range of density variation for ion current from the anode plasma in which the angular characteristics of the formed electron beam make it 200-fold compressible by the guiding magnetic field and the beam can enter the trap through the magnetic mirror.

Additionally, to check the influence of beam electrons reflected from the entry mirror on the diode operation, we conducted a theoretical analysis and numerical simulation using the computational code "Era" (with ICMMG SB RAS), determined the marginal currents and compared them with earlier experiments on transportation and compression of beam. The resulting currents are in good agreement with the experimental values at which a diode breakdown and pulse length reduction are observed. Thus, it was shown that reflection of beam from the entry mirror is one of the most important mechanisms of the anode plasma density growth, which leads to a breakdown in the diode gap. Nevertheless, an anode plasma of moderate density in the transport line is necessary for compensation for the spatial charge and reduction of the angular spread in the beam from the source. Further progress towards increase in beam duration in the simulation and the experiment is associated with the search for conditions at which the effect of the anode plasma on the diode operation would be minimized.

4.2.5. Development of technology for plasma-emitter sources of long-pulse electron beams.

The works with the source of high-power submillisecond electron beam on the basis of plasma emitter and multiple-aperture electron-optical system (EOS) were continued in 2013. A pulsed arc discharge with cold cathode in low-pressure hydrogen formed a plasma emitter of electrons. The multiple-aperture EOS consisted of a planar diode with molybdenum electrodes with a large number of round-coaxial through holes

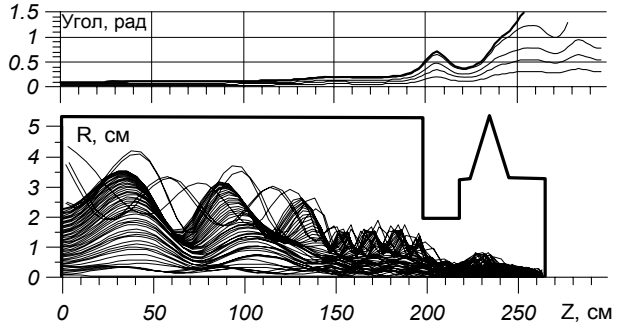

Fig. 4.2.5. Pitch angles and trajectories of 70 A beam electrons in the transport beamline of GOL-3 in regime with electrons reflected from the magnetic mirror (z ~ 260 cm) back to the diode.

forming a hexagonal "lattice". The source was located within the end vacuum tank of the multiple-mirror trap of GOL-3 in an axial magnetic field of ~ 10 mT produced by the external windings of the tank. The electron beam was transported further with adiabatic compression in increasing magnetic field for subsequent injection into the plasma chamber of GOL-3.

This year refinements of the source were aimed primarily at increasing the generated beam current due to augment in the effective area of emission. To this end, the number of apertures of the EOS was increased from 241 to 499 and thus the EOS diameter enlarged from 82 mm to 118 mm. Besides that, a number of changes were made in the plasma emitter design. The length of the emission plasma expander (arc-discharge hollow anode) with the cathode (emission) grid of the diode in the end was increased from 100 mm to 210 mm. The magnetic field in the arc line in the initial part of discharge forming was increased from 0.1 T to 0.8 T. That amplified the magnetic flux divergence over the length of the plasma expander, which should contribute to enlargement of the cross-section of the gas-discharge plasma near the cathode grid and thus extension of the effective area of emission.

The upgraded source was tested experimentally. In test modes, without beam injection into GOL-3, a 2.5-fold increase in the generated beam current as compared with last year was demonstrated. Typical waveforms are shown in Fig. 4.2.6. The average beam power was approximately 20 MW with a duration of to 0.2 μs. With a two-fold

decrease in the emission current, a millisecond generation duration was achieved.

Along with the increased beam current, the modernized source showed a slightly worse trainability and operation stability in experiments on beam injection into GOL-3. The reason may be that, despite the measures taken to increase the area of emission, the emission current density distribution over the cathode grid is markedly heterogeneous, with a maximum near the source axis. Because of this, the peripheral apertures of the EOS work in adverse conditions in terms of the beam optics and are hard-to-train. The beam current density profile was measured on a metal target in 1.5 m from the source using an X-ray pinhole camera (Fig. 4.2.7). The magnetic field in the target area was 1.4 times as high as the field near the EOS. Thus the beam size on the cathode of the EOS was approximately by 20% larger than the beam size at the target.

4.2.6. Control of rotation of plasma via electron beam injection.

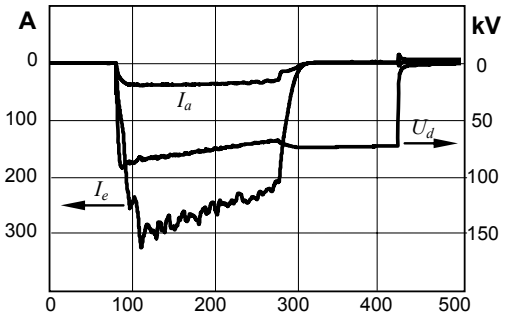

Fig. 4.2.6. Typical oscillograms of electron beam without injection into GOL-3: U_d – voltage across the diode; I_e – emission current; I_a – current deposited on the anode electrode.

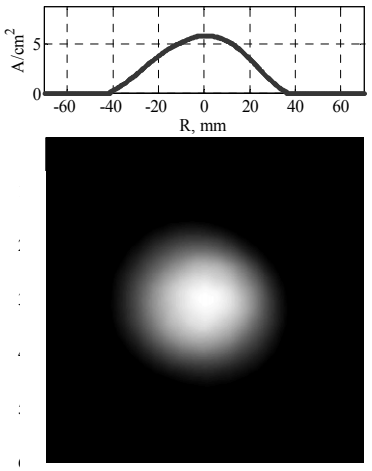

Fig. 4.2.7. X-ray beam obscurogram and reconstructed radial distribution of current density.

Vortex confinement, a method that was suggested theoretically at BINP and then confirmed in experiments on the GDT facility, is one of the promising methods to stabilize a plasma in modern open traps. This method is currently the main way to ensure MHD stability of plasma on the GDT facility. The method consists in giving the central region of plasma confinement a negative potential relative to its periphery. On the GDT facility, this is done with a special system of electrodes to which a voltage is applied. In so doing, the plasma starts rotating around the axis because of the drift in the crossed radial electric field and the longitudinal magnetic one. Another possible way is formation of a negative potential on the axis by means of electron beam injection. Such technology, if successful, may be more acceptable for facilities with large heat fluxes, in which electrodes cannot be used.

Series of experiments on GOL-3 demonstrated the possibility of controlling rotation of plasma by means of injection of electron beam with the following parameters: injection duration of up to 100 microseconds, electron energy of up to 90 keV, and injected current up of to 160 A. The electron beam current was modulated, for the first time with a current modulation depth of 95%. Rapid rotation of magnetic disturbances was observed during the beam injection. A dependence of the plasma rotation speed on the experiment parameters was built. The dependence of the rotation velocity on the $B^{-0.5}$-type guiding magnetic field was determined. The rotation velocity and its functional dependence on external conditions suggest that this effect is caused by the drift in the crossed electric and magnetic fields. The electric field is estimated as E ~ 100 V/cm, which corresponds to an on-axis negative charge with a density of up to 5×10^{-10} C/cm (~5÷10 % of the beam charge). The charge distribution in this dependence is somewhat between a charge concentrated on the axis and a charge uniformly distributed in the plasma. When a modulated beam is injected, the rotation frequency of the second and subsequent sub-beams becomes independent on the magnetic field. The explanation is that the first sub-beam produces plasma, which results in a case corresponding to an approximation of a charge concentrated on the axis of the plasma.

It was shown that the direction of perturbation rotation is inverted upon termination of beam injection. The direction of rotation is inverted if the beam current exceeds a threshold of ~ 10-15 A; with a beam current of 8 A or less, the direction of rotation corresponds to a positive charge of the plasma. The time of rotation direction establishment does not exceed 5.1 μs. This suggests the possibility of introduction of an electric potential into the plasma by means of electron beam, ie without direct contact of the plasma with cold electrodes. Thus, a relatively low-power electron beam can be employed for carrying a potential in the plasma in a controlled way. This achievement allows considering application of such method to control of plasma potential,

as well as to high-power linear traps to confine reactor-grade plasma.

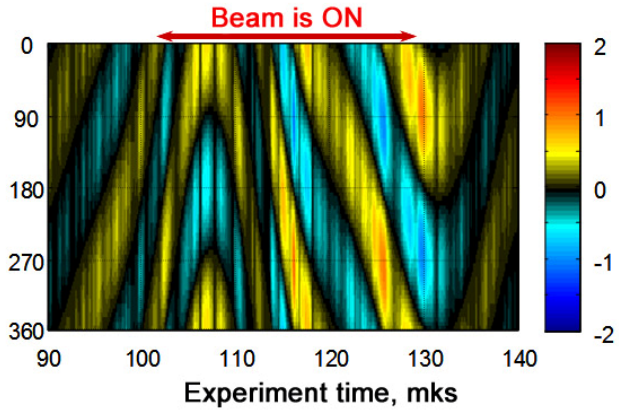

Fig. 4.2.8. Dynamics of perturbation of plasma magnetic surface during injection of modulated electron beam. The slope of lines of equal brightness corresponds to the speed and direction of plasma rotation; the color refelcts the magnitude of plasma boundary deflection from the calculated position. The electron beam was modulated with a depth of over 95% , a relative pulse duration of 2, and a modulation period of 60 μs.

4.2.7. GOL-3 development prospects.

Since the creation of GOL-3, injection of high-power electron beams along the magnetic field has been the main method of heating plasma to high temperatures. Collective interaction of the beam with the plasma results in rapid relaxation of the beam, which is accompanied by occurrence of turbulence and heating of the plasma. Earlier experiments on the multiple-mirror trap of GOL-3 yielded sub-fusion parameters of deuterium plasma with an ion temperature of over 2 keV and lifetime of 1 ms scale at a density of 10^{21} m^{-3}.

Analysis of possible ways of development of the facility has revealed an important line of research on the patterns of quasi-stationary escape of high-temperature plasma from an open trap with multiple-mirror end sections. Such results are in direct need for the program of creation a new-generation open trap. Besides electron beams, other, less traditional, methods of heating and confinement of plasma can be employed in a quasi-stationary system, in particular injection of neutral beams of deuterium with a megawatt-scale power. Preparation of a quasi-stationary experiment with neutral injection on GOL-3 will require designing and manufacturing of injectors with supply systems, as well as creation of a new vacuum chamber.

The GOL-3 system for neutral injection contains two injectors of atomic beams (ABs) with the energy 25 keV, total power 1.5 MW, beam duration up to 5 ms, and geometric beam focusing. The injection is carried out normally to the axis of GOL-3 into the center of a series local trap. The angle between the injected beams is 158°. The purpose of the injection of ABs is creating a population of fast ions in the local trap of GOL-3 and analysis of the transport of these ions in the multiple-mirror trap at conditions of turbulent plasma maintained by a longitudinal REB. The intension was to use an analyzer of charge-exchange atoms, laser diagnostics of Thomson scattering, diamagnetic sensors and other means of plasma diagnostics available at the GOL-3 facility. A possibility is provided for quick switching from injection D to injection H, which allows identification of ions that were injected into the deuterium plasma.

The atomic injectors were mounted and are now under a vacuum of $2 \cdot 10^{-4}$ Pa. The gas supply system for the injectors was assembled. The system allows connection of two gas cylinders and fast selection of gas. The electric supply system is currently being manufactured. The source is composed of 25 series-connected sections. Each section operates autonomously, generates a voltage pulse of 1 kV and has an optical input for start and stop, as well as overcurrent protection. The sections were tuned and tested. A voltage drop caused by a discharge of capacitors is compensated by the additional sections, which are turned on in the middle of pulse. The accelerating voltage is adjusted with a 1 kV step via the amount of turned-on sections. Two 800*800*33U racks that contain a source of 0.3-1 kA controlled arc current for the plasma generator, discharge ignition circuits, and supply of gas valves and a 700 V offset of the exit grid are being mounted. Each injector is equipped with a computer connected by a fiber optic link to the local network of the GOL-3 board room.

The formation of atomic beams was modeled, with due account of defects of actually-fabricated spherical forming grids. The loss of beam intensity in the focus because of defects of the grids is less than 5%.

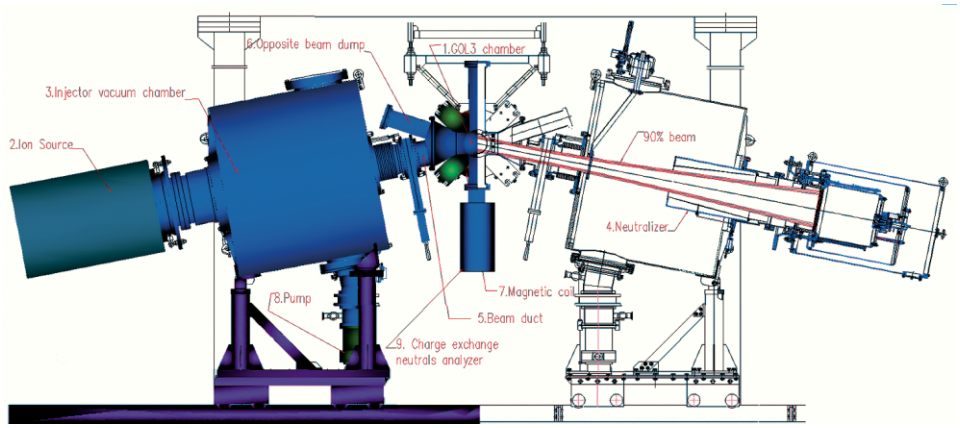

Fig. 4.2.9. Arrangement of neutral beam injectors on GOL-3 (stage 1).

4.2.8. Conclusion.

As earlier, the GOL-3 facility is used in experiments aimed at collecting the physics knowledge required for the construction of an open-trap fusion reactor. The quality of acquired information is improved due to both new diagnostics techniques and conduction of specialized experiments. New technologies of plasma heating are being developed; they will advance the plasma parameters. Applied research in various directions was conducted. Further plans include refinement of the electron beam source and creation of a new source of pre-plasma and a system for neutral beam injection.

4.3. PLASMA THEORY

4.3.1. Alf'ven ion-cyclotron instability.

A threshold for the Alfvén ion-cyclotron (AIC) instability in a mirror trap with passing through weakly-collisional plasma is investigated in the report of Yu.A. Tsidulko, I.S. Chernoshtanov, in proc. of XL International conf. on plasma physics and CTF, Zvenigorod, (2013). Excitation of AIC instability in a multi-mirror trap can provide additional collision-less ion scattering which could be useful for effective multi-mirror confinement.

The unperturbed ion angle distribution is calculated bysolving approximate kinetic equation. Angle scattering, trapped ion bounce oscillations, axial plasma losses and appearing of untrapped ions are taken into account in the kinetic equation. The different angle distributions of inflowing ions are considered.

The AIC instability is driven by inverse population of resonant particles which have longitudinal velocity satisfying the cyclotron resonance condition $v_{\|res} \approx (\omega - \Omega_{ci})/k$. The destabilizing contribution is provided by the particles with pitch-angle near the loss cone boundary. The total contribution of resonant particles can be destabilizing if $v_{\|res} \sim v_T$. The stability margin strongly depends on angle scattering frequency and mirror trap length.

The used approximation of distribution function makes possible to expand dispersion relation to the complex planes of z, ω and k, which is necessary to study absolute stability margins and searching for turning points in the WKB method.

It is shown that the AIC instability can develop in a mirror trap with flowing through plasma and provide collision-less ion scattering with frequency significantly higher than ion-ion collision frequency.

4.3.2. Modulational instability of a Langmuir wave in plasmas with energetic tails of superthermal electrons.

The impact of superthermal electrons on dispersion properties of isotropic plasmas and on the modulational instability of a monochromatic Langmuir wave is studied for the case when the power-law tail of the electron distribution function extends to relativistic velocities and contains most of the plasma kinetic energy. Such an energetic tail of electrons is shown to increase the thermal correction to the Langmuir wave frequency, which is equivalent to the increase of the effective electron temperature in the fluid approach, and has almost no impact on the dispersion of ion-acoustic waves, in which the role of temperature is played by the thermal spread of low-energy core electrons. It is also found that the spectrum of modulational instability in the non-maxwellian plasma narrows significantly, as compared to the equilibrium case, without change of the maximum growth rate and the corresponding wavenumber.

4.3.3. Exact kinetic theory for the instability of an electron beam in a hot magnetized plasma.

Efficiency of collective beam-plasma interaction strongly depends on the growth rates of dominant instabilities excited in the system. Nevertheless, exact calculations of the full unstable spectrum in the

framework of relativistic kinetic theory for arbitrary magnetic fields and particle distributions were unknown until now. In this paper, we give an example of such a calculation answering the question whether the finite thermal spreads of plasma electrons are able to suppress the fastest growing modes in the beam-plasma system. It is shown that nonrelativistic temperatures of Maxwellian plasmas can stabilize only the oblique instabilities of relativistic beam. On the contrary, non-Maxwellian tails typically found in laboratory beam-plasma experiments are able to substantially reduce the growth rate of the dominant longitudinal modes affecting the efficiency of turbulent plasma heating.

4.3.4. Theoretical studies of improved axial plasma confinement in a corrugated field.

A new system for improvement of axial confinement in open traps or pumping of hot plasmas along the magnetic field is proposed. It is based on rotation of the plasma column in a helicoidally corrugated magnetic field.

(A.D.Beklemishev, Helicoidal System for Axial Plasma Pumping in Linear Traps, Fusion Science and Technology, V. 63 1T (2013) p.355-357.)

Theoretical studies of dynamical processes that may cause anomalous ion scattering in cells of multiple-mirror traps were conducted. Such scattering is crucial for effective operation of the multiple-mirror trap at low plasma densities consistent with magnetic confinement.

It is shown that quasi-parallel sound modes in mirror traps may be sufficiently localized. Predicted frequency of sound modes is in good agreement with experimental data from the GDT trap.

(D.I.Skovorodin, A.D.Beklemishev, Flow-Driven Drift Instability in a Multiple-Mirror Trap, Fusion Science and Technology V. 63 1T (2013) p.256-258 .

D.I.Skovorodin, K.V.Zaytsev, A.D.Beklemishev, Global sound modes in mirror traps with anisotropic pressure Phys. Plasmas 20, 102-123, 2013)

4.4. BEAM INJECTORS OF HYDROGEN ATOMS AND IONS

4.4.1. Beam Injectors of Hydrogen Atoms.

Diagnostic injector of hydrogen atoms has developed for the world's largest stellarator Wendelstein 7-X, which is under construction in the Max Planck Institute of Plasma Physics (Greifswald, Germany). This branch of the Institute is one of Europe's leading centers for controlled fusion research. The W7-X experiments will allow to study the behavior of plasma parameters close to the reactor and to conclude about fusion power plant based on the stellarator concept.

The injector was commissioned at the IPP test bed. In accordance with the plans in a year the injector has to be installed on the stellarator. Injector generates beam of hydrogen atoms with an equivalent current of 2.4 A and an energy of 60 keV. Pulse width of the beam is up to 2.5 s with different modulation modes during 10 s beam.

With the help of the atomic beam and diagnostics based on energy analysis and charge exchange recombination spectroscopy one can to define a wide range of plasma parameters such as ion temperature, impurity density, plasma potential, radial electric field and others.

4.4.2. Development of powerful continuous injector of beam of fast hydrogen atoms.

Works under the project of powerful continuous injector of beam of fast hydrogen atoms with 500-1000 keV energy on the basis of negative ions are continued. The project is based on separate formation and acceleration of negative ion beam. Basic elements of the injector are manufactured. At experimental stand prototype of hydrogen negative ion source with beam current up to 1 A is tested. Large experimental stand for acceleration of hydrogen negative ion beam with ~ 5 A current to energy ~ 800 keV is under preparation.

4.5. RESEARCH ON DYNAMICS OF SPECTRUM OF HIGH-POWER MILLIMETER WAVE RADIATION ON ELMI INSTALLATION

4.5.1. Introduction.

Experiments on generation of millimeter wave radiation in the two-channel planar free-electron maser (FEM) with two-dimensional distributed feedback conducted on the ELMY installation in 2012 demonstrated the possibility of simultaneous generation of high-power pulses of 4 mm wave radiation in the channels with synchronous phases of the oscillation of the channels at a given frequency. Radiation pulses generated in the channels had the following parameters: the characteristic power of pulse from one channel was ~ 10-20 MW; the pulse duration was up to 250 ns; the oscillation frequency in the middle of the emission line was 74.6 GHz (one of the longitudinal modes of the resonator); the spectral width was 10-20 MHz, close to the natural line width. A series of experiments in the same year yielded dependences of the millimeter-wave power in the frequency band corresponding to the longitudinal modes of the resonator (74.5-75.5 GHz) on the magnitude of the transverse component of the undulator magnetic field at several fixed values of the guiding longitudinal field (see BINP annual report for the year 2012). From the above experiments it was concluded that generation of high-power mm-wave radiation is possible with static undulator field varying in a rather wide range. However, precise measurements of the radiation spectrum using heterodyne diagnostics showed that variation of the

undulator field in the FEM resonator within acceptable limits is as a rule associated with generation of several longitudinal modes in a radiation pulse duration. At the same time, one can expect that if the undulator resonance condition is met, ie $\omega - hv_{\|} = \Omega_b$, where $v_{\|}$ is the longitudinal velocity of the electron, and $\Omega_b = 2\pi v_{\|} / d_u$ is the frequency of the bounce oscillations of electron in the undulator magnetic field with the period d_u, stable single-frequency generation at the frequency of one of the natural modes of the resonator is experimentally attainable. Thus the experiments in 2013 were aimed at reaching a stable single-frequency generation throughout a pulse of mm-wave radiation due to meeting the undulator resonance conditions, which can be done via a right choice of the values of transverse and longitudinal components of the undulator magnetic field, in accordance with the energy of the beam electrons.

4.5.2. Experiment conditions.

The scheme of experiments on radiation generation in the two-channel planar FEM is shown in Fig. 4.5.1. A detailed description of the scheme, as well as the diagnostics of microwave radiation, is given in the BINP report for the year 2012.

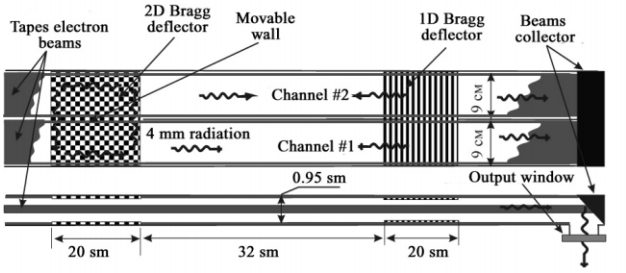

Fig. 4.5.1. Scheme of experiments on mm-wave radiation generation in the two-channel planar FEM.

In the experiments in 2013, as in the previous year, the FEM channels along their entire length were separated by a metal bar. Nevertheless, there was electrodynamic coupling between the channels because of the penetration of small part of radiation flows from one channel to another in the area of graphite collectors for absorption of beam electrons.

Since the experiments were aimed at single-frequency generation of radiation without hopping from one longitudinal mode to another, it was necessary to select such an operation mode for the surge generator in which the diode voltage was maintained constant for a few hundred nanoseconds. In so doing, it was necessary to ensure good repeatability of the pulse shape and amplitude from shot to shot. From a preliminary numerical simulation, it was found that deviation of diode voltage during the pulse should not exceed 2 %.

The surge generator of the ELMI facility consists of two independent in-series connected parts. Its lower part consists of six Fitch cells connected in series, which form a pulsed voltage that varies in time as $U = U_0\left[1 - \cos(2\pi t / T)\right]$. The upper part consists of 12 levels of in-series connected capacitors and is charged up to 600 kV by a DC voltage source. This surge generator scheme allows one to control the amplitude and, to some extent, the shape of diode voltage via varying the charge voltages of both parts of the generator and selecting the time of switching the megavolt gas-filled spark gap that connects the generator to the diode of the accelerator. Before the experiments, the surge genreator was subjected to an essential upgrade, which included several steps. First, the previous gas-filled spark gaps with field escalation were replaced by new in-house multiple-gap devices, RUM 50x2 (50 kV, 120 kA, 0.6 Cl). Second, their triggering system was replaced. Currently, these spark gaps reliably switch voltage on the 42 kV capacitors of the surge generator at a maximum current of 100 kA and an oscillation period T = 30 μs. Thirdly, the triggering system of the megavolt spark gap was subjected to an essential remodeling, the main element of which was the creation of an isolated system for starting an intermediate Marx generator (72 kV, 30 kA, τ~100 ns), which initiates a breakdown in the megavolt spark gap. The new triggering system has significantly improved the reliability of response of this spark gap and reduced the response time scatter to 0.5 μs.

4.5.3. Research results.

In this series of experiments on the generation of mm-wavelength radiation in the two-channel FEM, we varied from shot to shot the amplitude and shape of the accelerator diode voltage at fixed values of the transverse and longitudinal components of the magnetic field in the channels. For instance, in one of the shots with weak attenuation of radiation entering the heterodyne diagnostics, there was observed simultaneous generation of radiation at all longitudinal modes of the resonator, as illustrated in Fig. 4.5.2. In this figure, the result of registration of the spectral density of the generated radiation power is compared with the results of "cold" measurements of the Q-factor of Bragg resonator at its eigenmode frequencies. The latter measurements were conducted prior to this series of "hot" experiments with electron beams. It should be noted that the spectral density amplitude at a frequency of 74.6 GHz is presented disproportionately low for visibility of radiation at other frequencies.

As seen from the figure, the experiment distribution of the spectral density of the generated radiation power agrees well with the position of the eigenmodes of the resonator and is qualitatively consistent with the Q-factor values of the resonator at these frequencies.

In subsequent experiments on the single-frequency regime of mm-wave generation, we selected the diode voltage pulse shape such that the voltage drop during the radiation generation (150 to 250 ns) did not exceed 10 to 20 kV. Under these conditions, we conducted

simultaneous recording of spectra of radiation emerging from the two channels of the FEM.

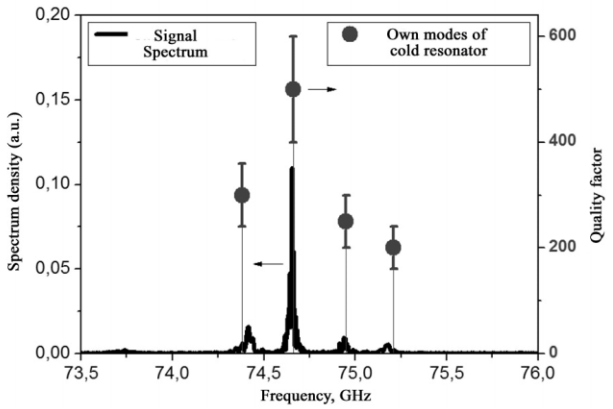

Fig. 4.5.2. Spectrum of millimilter-wave radiation in FEM channel in comparison with results of "cold" measurements of frequency and Q-factor of longitudinal modes of the resonator.

Figs. 4.5.3 and 4.5.4 show typical waveforms of the diode voltage, strip beam currents, and dynamics of the radiation spectrum in a shot in the single-frequency regime at the frequency of the highest Q mode of the resonator (74.6 GHz).

In a series of experiments with beams generated with a voltage pulse form suitable for single-frequency generation with a longitudinal component of the undulator field of 1.13 T and a transverse component amplitude of 0.138 T, we selected only shots with a single-frequency generation mode in at least one channel of the FEM generator. Thus, if the voltage across the diode during the generation of radiation was in the range of 840 kV ± 20 kV, the single-frequency regime was registered at the frequency of the highest Q mode of the resonator, 74.6 GHz. As for the voltage across the diode in the range of 875 ± 20 kV, the single-frequency generation in most shots occurred at another longitudinal mode of the resonator, with a frequency of 77.7 GHz.

The initial energy of electron entering the undulator was determined from the diode voltage in the middle of the voltage value range at which a longitudinal mode with the frequency ω_m was generated. Based on this energy and using computer simulation of electron motion in the undulator magnetic field of the maser, its average longitudinal velocity in the resonator $v_{||}$ was calculated. As a result, substituting this electron velocity in the expression for the undulator synchronization detuning, we obtain $\Delta = \left(\omega_m - hv_{||} - \Omega_b\right)/\omega_m C$, where C is the Pierce parameter ($C \approx 4 \cdot 10^{-3}$ in our case). The detuning value Δ = 1.5 was found, which is optimal for our experiment conditions. This value agrees well with the detuning value at which the electron efficiency maximum is achieved in the numerical simulation [Technical Physics, 2014, vol. 84, iss. 2, p. 98-105]. This agreement between the experiment and theoretical values of the undulator synchronism detuning proves the adequacy of description of radiation generation in a planar FEM two-dimensional feedback distribution.

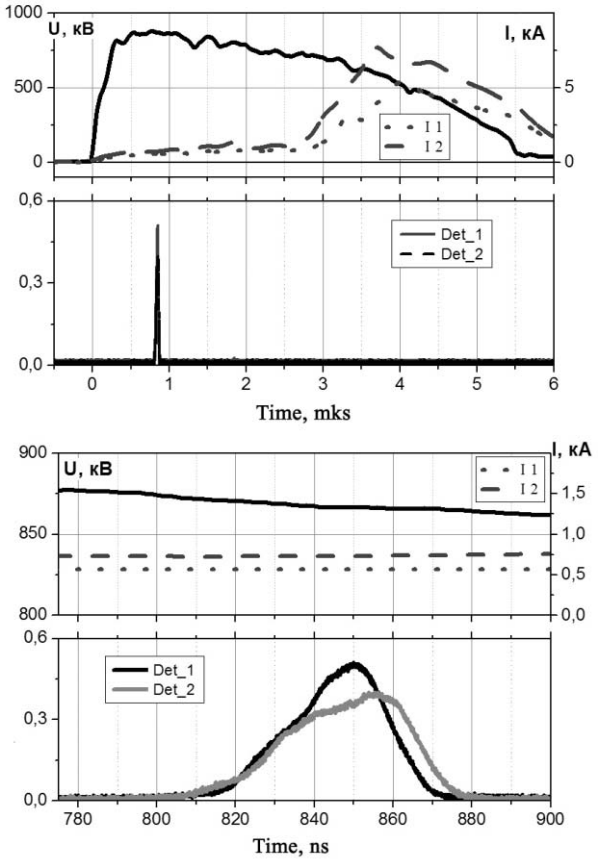

Fig. 4.5.3. Diode voltage U oscillograms, strip beam currents (I1 and I2), and power of mm-wave radiation from the two channels of the FEM (Det_1 and Det_2) in a typical shot with single-mode single-frequency generation at a frequency of 74.6 GHz. The two upper and two lower patterns differ in the time scale only.

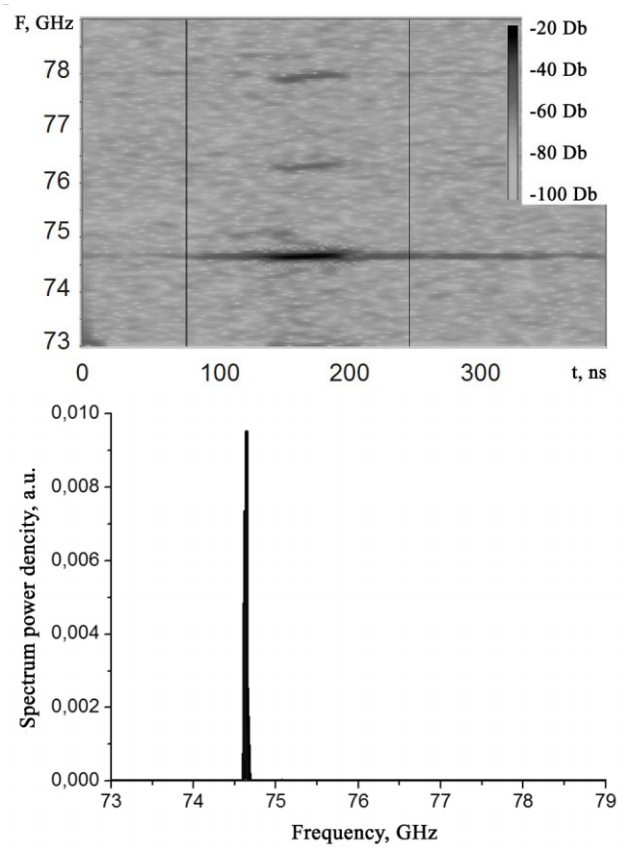

Fig. 4.5.4. Dynamics of mm-wave radiation spectrum (shot 7986) in single-frequency regime (top) and radiation frequency spectrum in the time interval of 70-250 ns (bottom).

4.5.4. Preparing experiments on two-phase generation of terahertz radiation.

To conduct experiments on two-stage generation of THz radiation, we perform upgrade of the ELMI installation. A new vacuum channel (Fig. 4.5.5, a) with a longitudinal guiding magnetic field of up to 2.5 T for transport of two strip beams was manufactured, as well as a new active magnetic undulator (Fig. 4.5.5, b) for build-up of the transverse component of the electron velocity. The basic units of the connection of the new channel to the U-3 accelerator and the system for electron dump and extraction of THz radiation into the atmosphere were designed and are now being fabricated.

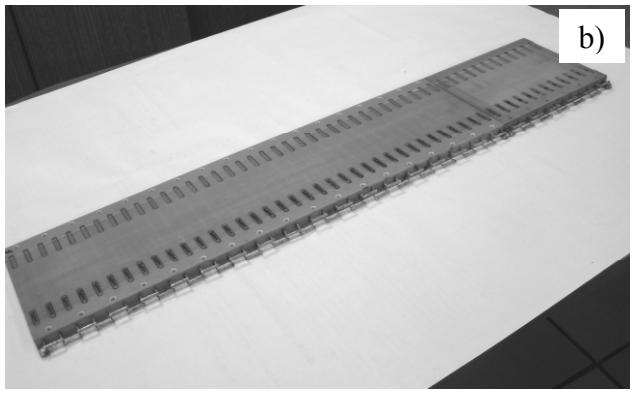

Fig. 4.5.5. Photos of a) new vacuum channel and b) new undulator for two-phase THz radiation generation.

4.6. GDMT-T FACILITY

4.6.1 Introduction.

Plasma-surface interaction is a critical issue of a fusion reactor. It is generally recognized now that namely processes on plasma receivers will determine the effectiveness of a fusion reactor and the possibility of its industrial use. However, the today's fusion facilities do not allow achieving energy and particle flows that are expected in the ITER and DEMO reactors. Thus, within works on these projects, a network of specialized facilities is created for research on various aspects of plasma-surface interaction. BINP works on the creation of a new GDMT-T facility for research on the effects of plasma-surface interaction at plasma parameters close to those expected in a tokamak-based fusion reactor. The GDMT-T facility will simulate conditions on plasma receivers of the reactor in the quasi-stationary operation regime with pulse-periodic load (ELM mode). Research at this facility will be useful in solving the following tasks:

- test of the resistance of samples of the ITER and DEMO plasma receivers under the influence of quasi-stationary plasma flow,
- analysis of the erosion of materials of the ITER and DEMO plasma receivers under the influence of pulse-periodic load,
- investigation into the propagation of impurities and diffusion of surface plasma,
- refinement of technical solutions for creation of the elements of open-trap fusion reactor (superconducting solenoid, plasma receivers, and system for production of stationary plasma),
- training of staff for research by the fusion program.

The GDMT-T facility differs from the existing and projected stands for plasma-surface interaction in the strong magnetic field corresponding to the field in the ITER tokamak and the possibility of testing samples under simultaneous action of stationary and pulse-periodic loads. The components and systems of the facility area under design now.

4.6.2. GDMT-T design.

A scheme of the GDMT-T facility is shown in Fig. 4.6.1. In the central part, there are three identical superconducting solenoids with a magnetic field of up to 5 Tesla. From both sides the central solenoid is connected with expansion tanks, one of which accommodates a pulse-periodic electron beam generator. One of the diagnostics sections of the central solenoid houses a system for production of stationary plasma flow based on helicon microwave discharge at a frequency of 915 MHz. This system generates a plasma with a density of up to $10^{20}m^{-3}$ and a temperature of 1-10 eV.

The second diagnostics module comprises targets to investigate and diagnostics for research on surface plasma. When a target is placed inside the superconducting solenoid, the system will produce a plasma flow with a power density of up to 10 MW/m^2 and a particle flux density of 10^{24} m^2 on a 7 cm^2 sample. Additional pulse-periodic plasma heating by injection of electron beam (100 keV and 100 A) leads to a hundred-fold increase in the power density on the target during the time of injection (1-5 ms), which allows one to simulate the impact of plasma on the divertor plates of a reactor-grade tokamak in pulse-periodic load modes (ELM modes). A gyrotron-based system for electron-cyclotron heating is considered as an alternative method of creating pulse-periodic loads.

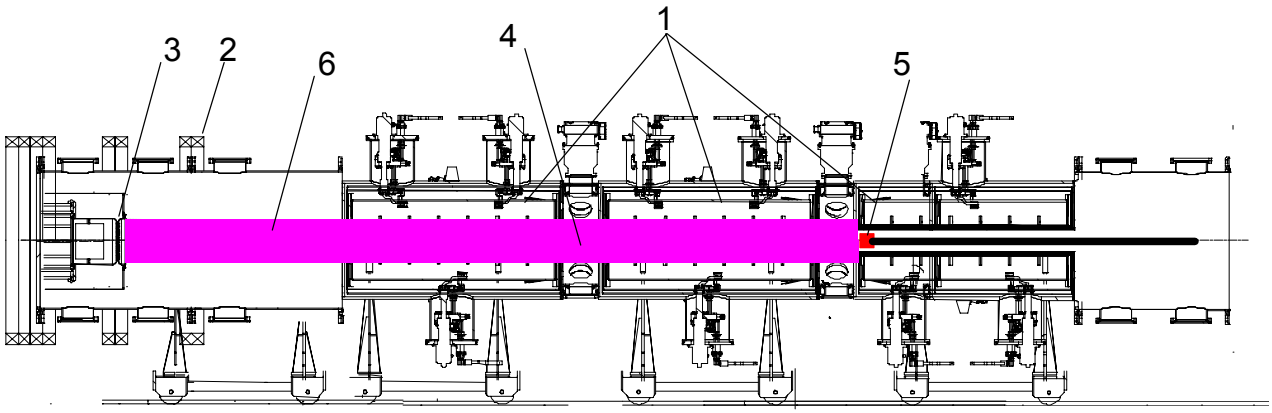

Fig. 4.6.1. GDMT-T scheme: 1 – the superconducting solenoids, 2 – the solenoid of the electron beam generator, 3 - electron beam pulse-periodic generator, 4 - plasma creation system, 5 – the test chamber with the unit for attachment of targets, 6 – the plasma column.

4.6.3. Development of magnetic system of GDMT-T facility.

Designing of the superconducting solenoid is of interest for both the realization of the GDMT-T project and projects of fusion reactor based on linear magnetic systems. All the existing projects of fusion reactors on the basis of linear traps implies plugs, i.e. areas of intense magnetic field, the efficiency of plasma confinement determined substantially by the magnitude of magnetic field in the plugs. To create such plug sites it is necessary to use superconducting solenoids with ultimately achievable magnetic field.

The design of such solenoids has some features that distinguish them from commercially available analogs. The main difference is the action of non-compensated magnetic field from the main part of the facility, and as a consequence, the effect of large longitudinal forces on the solenoid, as well as the large aperture and high heat loads from plasma to the inner wall of the solenoid. In addition, the project is to include the option of generation of both a homogeneous field and a spatially variable (multiple-plug) one, which is promising in terms of improving the plasma confinement.

The general view and design of the superconducting solenoid are shown in Fig. 4.6.2 and 4.6.3. Since the solenoids are assumed to be used in future as the end sections of the GDMT facility, the solenoids allow obtaining both a corrugated field and a quasi-homogeneous one. Each solenoid includes two coils: external, which creates the main constant magnetic field, and the internal, which consists of seven subsections with opposing connection of neighboring subsections, which allows generation of a multiple-plug magnetic field.

The internal and external subsections of the SP solenoid are powered by various-value currents from independent current sources. The subsections are powered so that all external subsections on the axis of the system create a magnetic field in one direction, while all the internal radial subsections generate an alternating magnetic field. This results in a corrugated magnetic field on the axis of the solenoid section with four maxima and three minima; the maximum and minimum values of the field are 7.3 T and at 2.7 Tesla, correspondingly. A configuration with quasi-homogeneous field, when only the external winding of the solenoid is switched on, is more preferable for

experiments on plasma-surface interaction. In this case, changing the current in the winding of the third (output) solenoid, one can adjust the magnetic field and, therefore, the power density on the target.

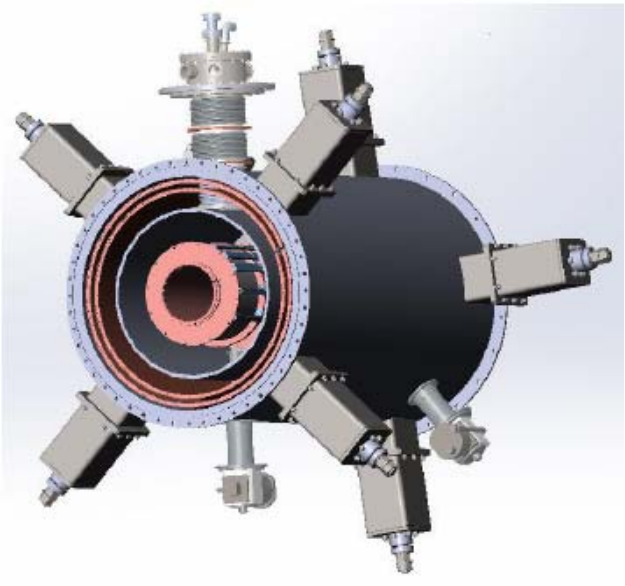

Fig. 4.6.2. Superconducting solenoid.

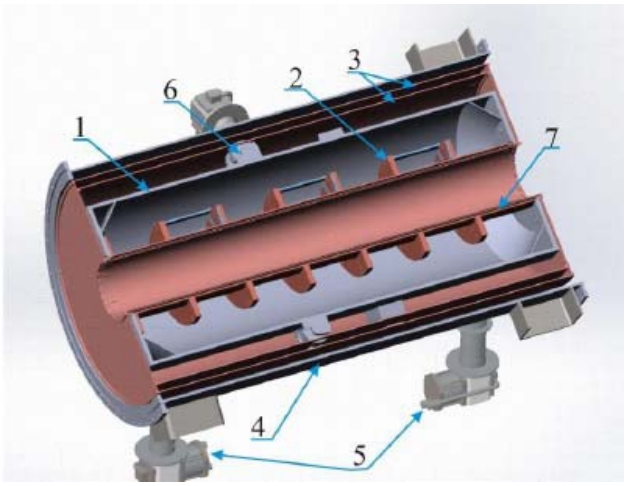

Fig. 4.6.3. Scheme of SP solenoid module.

1 – the cryogenic volume, 2 – the frame of coil of the SP solenoid, 3 - the heat shields, 4 – the wall of the vacuum chamber, 5 – the cryocoolers, 6 - one of the points of attachment of Kevlar rope, 7 – the water-cooling inner wall of the vacuum chamber.

The magnetic fields and thermal regime of the solenoid were calculated in a two-dimensional axisymmetric geometry using the package ANSYS. It was revealed that the largest forces of about 250 kN act on the end sections of the superconducting solenoid in its axis direction, and decrease rapidly towards the center of the solenoid. The mechanical forces are transmitted from the outer housing to the cryogenic volume via eight pre-tensioned Kevlar cables, which ensure the required stiffness at low heat inleaks.

The designed cryogenic volume, which is protected with radiation shields and has room temperature surfaces with super-insulation against heat, as well as the design of the current leads and the supportive cables, should provide a minimum heat input into the cryogenic volume. The heat fluxes to the cryogenic volume with a temperature of 4.2 ° K come from the following sources:

- current leads: ~ 0.3 W;
- thermal bridges via the supports: ~ 0.5 W (depends on the design of the bridges);
- thermal radiation from the radiation screens: ~ 0.1 W;
- sensing wires from temperature sensors and level meter: ~ 0.05 W at most;
- residual gas in the vacuum chamber: ~ 1 mW at most.

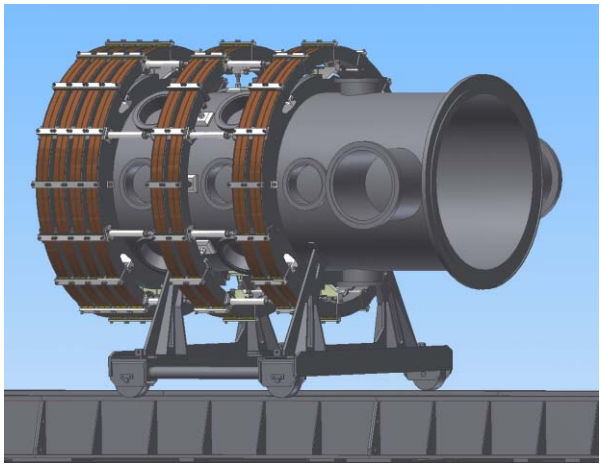

Fig. 4.6.4. Exit section of GDMT-T.

Reducing the heat input below 1 W provides the heat balance of the cryogenic volume using embedded cryocoolers, and thus no liquid helium is required in the system, which greatly simplifies the design of the solenoid and facilitates its use.

A general scheme of the solenoid has been defined so far, and its individual units are being designed. In addition, a design of the exit section of the GDMT-T facility has been developed and its production has started (Fig. 4.6.4).

4.6.4. Conclusion.

The implementation of the project of GDMT-T facility will results in an up-to-date stand at BINP for studying the plasma-surface interaction, which is necessary for the implementation of the ITER project and development of an open-trap reactor. Within this project, technical decisions to be used in a reactor-grade plasma facility will be tried and the physical aspects of plasma confinement in a magnetic field and the interaction of high-power electron beams with plasma will be investigated.

A physical design of the facility and main technological units has been developed. Preparation of design documentation for components of the facility is underway.

5
ELECTRON-POSITRON COLLIDERS

5.1. WORK OF VEPP-2000 IN 2013 AND INJECTION PART MODERNIZATION.

5.1.1. Statistics gathering in the range 2×(160–500) MeV with CMD-3 and SND detectors.

Experimental work of VEPP-200 in 2013 was devoted to data gathering by two detectors in the low energy range from 160 to 510 MeV per bunch. Besides of beam-beam effects suppression, the use of round beams significantly weeks the Touschek effect, which limits beam lifetime at low energy. This allowed VEPP-2000 to work at 160 MeV — extremely low energy for electron-positron colliders. In 2013 we collected 24pb^{-1}, the luminosity integral gathered during all work of VEPP-2000 is 60pb^{-1} per detector. In Fig. 5.1.1 the comparison of VEPP-2000 luminosity and data from BaBar experiment is shown. One can see that at energies corresponding to φ-meson our collider leaves BaBar statistics behind. And after upgrade for operation with projected parameters on high energies we will be able to exceed BaBar data.

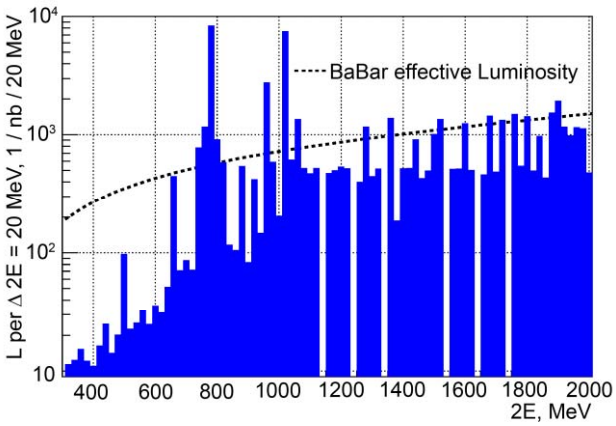

Fig. 5.1.1. Luminosity from CMD-3 detector.

Let's briefly list the main stages of VEPP-2000 complex operation in 2013. In January we finished RHO2013 experiment in the range of 490–360 MEV. Then there was a short break for measurement of the BEP's 13th magnet after its upgrade, and the energy calibration of VEPP-2000 by a method of resonant depolarization. From February till March we went to low energies, 360–160 MeV. From April till beginning of May there was a work in the range of 440–530 MeV, in May and June — 410–370 MeV. At the end of June experiment ETAPRIME2013 was curried out: the work in one precisely tuned point of 478.89 MeV, the considerably integral of luminosity was gathered. At the end of the experimental season we studied the possibility of bunch lengthening to increase the luminosity. It became possible after φ-dissectors were installed on the ring. In August of 2013 VEPP-2000 was stopped on upgrade.

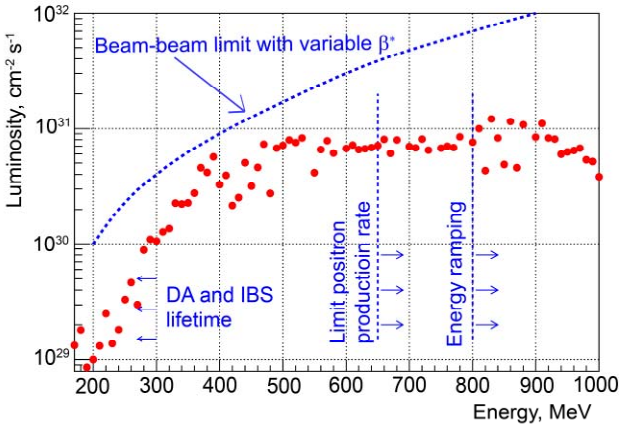

Fig. 5.1.2. Luminosity of VEPP-2000.

The luminosity of collider (Fig. 5.1.2) is limited by positron production rate in energies higher than 500 MeV. In case of energies higher than 800 MeV additional limitations arise from need to accelerate the beam in VEPP-2000 ring. In the middle energies (300–500 MeV) peak luminosity is restricted by beam-beam effects, mainly flip-flop effect.

Starting from energies of 400–450 MeV the field of CMD-3 detector is beginning to have significant impact: with decreasing energy the fields of magnetic elements are recalculated, but the CMD-3 field is remaining unchanged, and at low energies the effect of this strong magnetic element becomes more and more noticeable. To compensate for CMD-3 field we need big field in short compensating solenoids. This leads to increase of orbit corrections in remaining part of the ring; the symmetry of the ring is broken, injection becomes worse. All these factors lead to decrease of luminosity.

At low energies because of weak radiation damping the problems of non-linear dynamics are worsen, dynamic aperture is reduced, higher-order resonances are shown up. Besides, the lifetime caused by particles' scattering inside the beam is decreased.

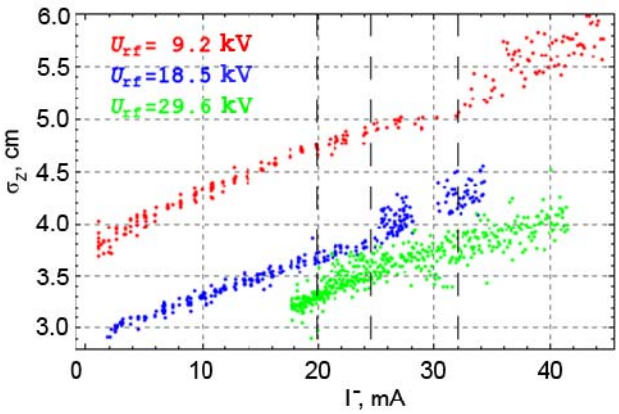

Fig. 5.1.3. Measurement of beam longitudinal size by φ-dissector at different currents.

In 2013 the measurement of bunch lengths with an accuracy of 2 mm by means of installed phi-dissectors was implemented on VEPP-2000 collider. At that the effect of microwave instability was observed, which arises in collisions of short bunches. The threshold of this instability depends on accelerating voltage of RF cavity. At first time the microwave instability was observed when measuring longitudinal size of the beam. From the Fig. 5.1.3 one can see that the rise of longitudinal size spread has clear threshold.

"Achieved" beam-beam parameter is determined as:

$$\xi_{lumi} = \frac{N^- r_e \beta^*_{nom}}{4\pi\gamma\sigma^{*2}_{lumi}},$$

where the value of beta-function at interaction point is taken as nominal (without perturbation by counter bunch), but the beam size is real, it is calculated from experimentally measured luminosity.

In the Fig. 5.1.4 the correlation between "achieved" and so called "nominal" beam-beam parameters is shown by using the complete data gathered at specific energy of 392.5 MeV. "Nominal" beam-beam parameter is defined as:

$$\xi_{nom} = \frac{N^- r_e \beta^*_{nom}}{4\pi\gamma\sigma^{*2}_{nom}},$$

in which all incoming parameters are calculated, hence this is a measure of beam current. The value of achieved beam-beam parameter is $\xi \sim 0.09$ per one interaction point.

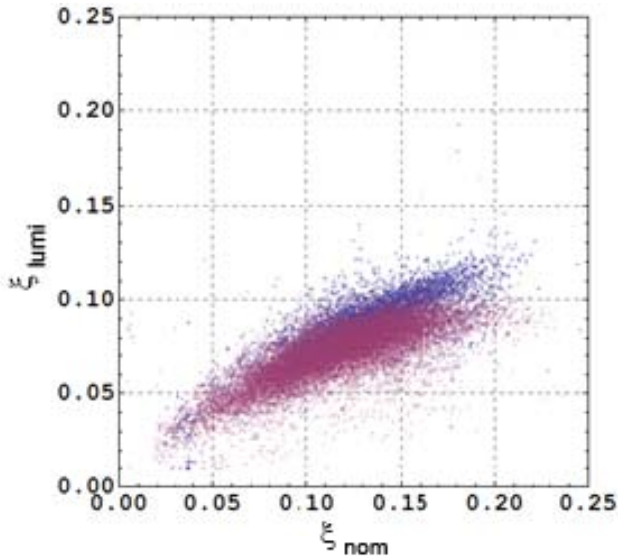

Fig. 5.1.4. Achieved vs. nominal beam-beam parameters at 392.5 MeV.

When studying the influence of bunch length on beam-beam effects there was observed that lowering the voltage of RF cavity from 30 to 17 kV allows one significantly increase peak value of beam-beam parameter up to $\xi \sim 0.12$ per one interaction point (Fig. 5.1.4). Probably, this effect is connected to additional suppression of beam-beam effects when the bunch length slightly exceeds the value of beta-function at interaction point. In our case the bunch lengthening is provided not only by decrease of the accelerating voltage, but also by the microwave instability, which was observed at low voltage and bunch intensity being higher than a certain threshold value.

In addition we can compute the beam-beam parameter from the spectrum of beams' coherent oscillations. In the Fig. 5.1.5 two peaks of σ- and π-modes with betatron tunes of 0.165 and 0.34 are clearly seen. The complete tune shift $\Delta\nu = 0.165$ corresponds to the beam-beam parameter per one interaction point:

$$\xi = \frac{\cos(\pi\nu_\sigma) - \cos(\pi\nu_\pi)}{2\pi\sin(\pi\nu_\sigma)} = 0.124,$$

that is in good agreement with the value taken from luminosity and is an absolute world record. In this estimation the Yokoya parameter was supposed to be 1, because the coherent oscillations of small amplitude were generated by quick kicker and were observed during 8000 turns. Within such short time interval the particle transverse distribution has not enough time to be deformed and thus remains Gaussian.

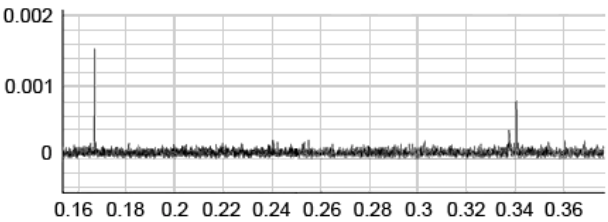

Fig.5.1.5. Spectrum of coherent oscillations at energy of 479 MeV.

On VEPP-2000 complex three methods of energy measurement are implemented: control of field in bending magnets by means of NMR sensors; method of Compton backscattering, which requires relatively big currents (more than 20 mA, hence it can't be used at low energies), and the third is the method of resonant depolarization. In 2013 season we carried out the measurement of beam energy by resonant depolarization in special regime of VEPP-2000: so called "warm" optics without CMD-3 and solenoids. Comparison of data taken showed good agreement of all three methods; this allows us quickly control the beam energy during experimental work.

5.1.2. BEP upgrade and K-500 channel.

The need of VEPP-2000 accelerating complex modernization is caused by several factors. First is the lack of positrons that did not allowed us to achieve the threshold of beam-beam effects. At low energies the problems arise, which are connected to beams' lifetime. This means that we need excess positrons from VEPP-5. Secondly this is the need to boost beams in VEPP-2000 ring to the experiments energy, because the booster ring BEP is not able to accelerate the beams higher than 800 MeV. Addi-

tional acceleration in VEPP-2000 is bad in terms of "dead" time (there is no statistics gathering) and problems of intensity bunches acceleration. Besides it is impossible to achieve threshold values of beams' intensities when injecting not on energy of experiment.

Upgrade of injection part of VEPP-2000 complex to work with beams at the energy of 1 GeV consists of several stages. First we need beams from injection complex VEPP-5, that means we have to build and put into operation K-500 channel. There is need in upgrade of booster ring BEP to avoid troubles with increase and decrease of beams' energy in VEPP-2000. And, of course, there should be modernization of BEP–VEPP-2000 channel and preparation of VEPP-2000 ring to accept the beams at energy of 1 GeV.

In July of 2013 after the end of experimental season the VEPP-2000 complex was stopped for upgrade. Before this stop big amount of preparation work was carried out within two years.

At the moment on K-500 channel the installation and preliminary geodesic alignment of all magnetic elements is complete. This includes 4 horizontal magnets, 4 pulse magnets of the rise, 55 pulse quadrupoles, additional bending and injecting into BEP magnets, 27+12 dipole correctors, 23 pickups and 12 phosphor sensors. Power supplies and all the electronics for sensors are manufactured and ready for installation into the channel. Vacuum chamber is assembled and pumped.

Fig. 5.1.6. Injection channel K-500.

In the Fig. 5.1.6 (a part of rise into BEP) one can see assembled vacuum chamber, quadrupoles and magnets installed, cables are connected. The overall management and concept of injection complex, channel and VEPP-2000 collaboration is worked out.

New injection magnet was manufactured (H = 17.5 kGs, L_{eff} = 42.8 cm, $R_{кр}$ = 980 mm, ∅ 9 mm).

Modification of bending magnets is carried out, including change of pole gap 40 mm → 32 mm; pole restriction 120 mm → 90 mm; plates of 50 mm are installed on internal radius of yoke. As a result magnetic field of 26 kGs is reached, which is needed for energy of 1GeV.

Quadrupoles are modified by decreasing inscribed diameter (D-lens: 56 mm → 52.89 mm, F-lens: 84 mm → 74.8 mm); poles' profile is changed to increase chromatic sextupole component of the magnetic field.At the energy of 1 GeV gradients in quads will be 3.214 kGs/cm and -4.512 kGs/cm.

Aluminum vacuum chamber in magnets and quadrupoles is modified. Vertical size of vacuum chamber is decreased by pressing in the range of dipole magnet and D-lens.

The replacement of vacuum chambers in two straights to the simple elliptic chambers is made (with synchrotron radiation receiver and pumping port. Then we installed in these straights two special C-shaped layer long-pulse magnets, which provide 25 mm distortion of the horizontal orbit before beam ejection ("BUMP" element).

As far as main magnetic elements of BEP are fed from one high-current power supply (10 kA) and high values of their magnetic fields lead to strong iron saturation, special attention during calculation was carried to equality of saturation curves of all the multipoles. For example, in the Fig. 5.1.7 the central curve shows the difference in saturation between D-lens and dipole magnet in relative units. Other curves set "window" available for correction by correcting coils in lens. In this "window" we have to "inscribe" the main curve.

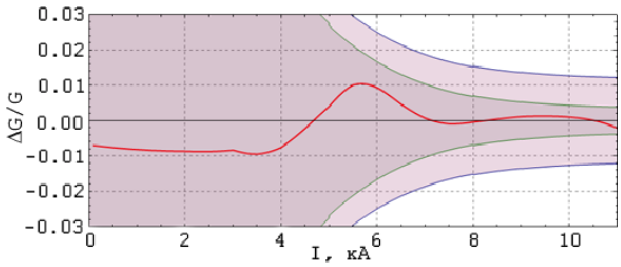

Fig. 5.1.7. Superposition of saturation curves for dipole magnet and quadrupole.

In Fig. 5.1.8 upgraded bending magnet is shown being on test bench. The results of measurements by NMR sensor and Hall probe are presented in Fig.5.1.9, 5.1.10.

Fig. 5.1.8. New dipole magnet of BEP.

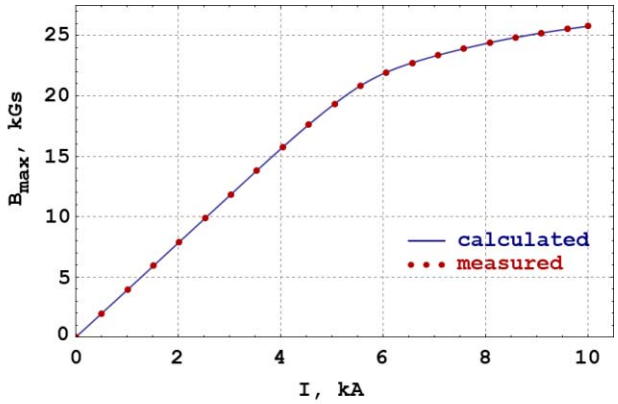

Fig. 5.1.9. Measurement of dipole magnet by NMR sensor.

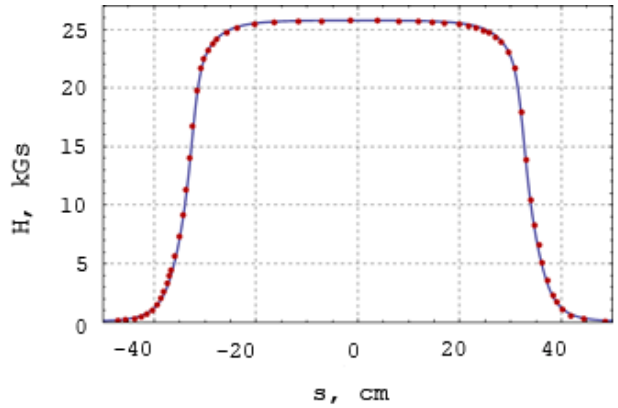

Fig. 5.1.10. Measurement of bending magnet with Hall probe, current is 9.9 kA.

In the channel BEP–VEPP-2000 magnets M2, M3, MP4, ME4, MP5, ME5 will be replaced. They are fed in series with BEP magnetic elements and the magnetic field should also be 26 kGs In VEPP-2000 ring additional inflector plates have to be installed in vacuum chambers of 1M1 and 2M2 magnets for injection on maximal energy.

New RF system of BEP is supposed to work at frequency of 174 MHz (13th harmonic of BEP revolution frequency) and consists of accelerating cavity, RF generator and control system. Accelerating cavity of coaxial type at maximal voltage of 120 kV has mechanism for tuning main and higher modes. Parameters of RF cavity are listed in Table 5.1.1.

Table 5.1.1. Parameters of BEP RF cavity

Harmonic number	13
Working frequency, MHz	174.3755
Characteristic resistance $\rho\tau^2$, Ohm	127
Q-factor	14900
Accelerating voltage, kV	112
Power to the beam, kW	6.9
Power losses in cavity, kW	3.5
Complete power, kW	10.4

In 2013 new RF cavity was manufactured, RF parameters of main and higher (up to 1500 MHz) modes were measured. At the present time new cavity is installed on BEP ring, is warmed up and pumped.

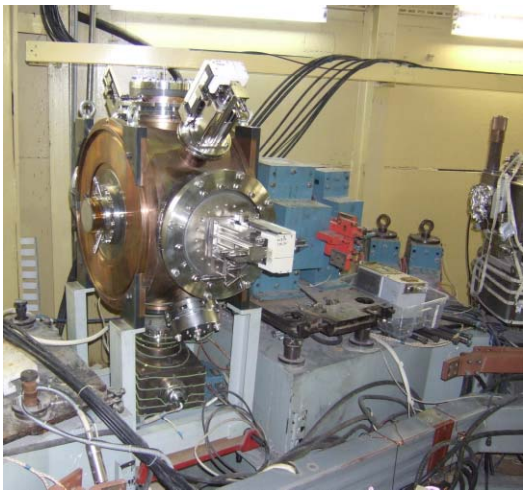

Fig. 5.1.11. New BEP RF cavity.

5.2. VEPP- 4 ACCELERATOR COMPLEX

Accelerator complex VEPP-4 is a unique installation for experiments with colliding high-energy electron-positron beams. The complex includes injector "Positron", multipurpose storage ring VEPP-3 and electron-positron collider VEPP-4M with the universal magnetic detector KEDR. The main purpose of the VEPP-4 collider is experimental studying of the properties of elementary particles, the parameters of resonances and the cross-sections of electron-positron annihilation processes.

5.2.1. Distribution of working time.

In 2013 the planned reconstruction of the KEDR detector was continued, thus, the high-energy physics experiments at the VEPP-4 collider were not carried out.

This year working hours of the complex are distributed mainly between the experiments with synchrotron radiation (24,9 % VEPP-3 + 4,4 % VEPP-4), and also the DEUTERON experiment at VEPP-3 (16,5 %). Regular maintenance works (2,5 %) are carried out weekly. The accelerator physics experiments at VEPP-4 were performed to increase a luminosity and to develop the research on CPT invariance testing. The series of experiments with a beam of high-energy γ-quanta obtained by conversion at the internal target («the output beam») is also continued at VEPP-4M.

5.2.2. DEUTRON experiment at VEPP-3.

Two series of experiments were performed at “Deutron” installation in 2013:

1. Experiment on measuring T_{20} tensor asymmetry in reaction of a coherent photoproduction of neutral pi-meson with deuteron is carried out. The works were performed in March-July, 2013 (Fig. 5.2. 1).

After the period of installation, assembly, commissioning and adjustment of the equipment of the polarized gas target and the equipment of the particle detection system, a collection of experimental data (from the middle of May to the middle of July) was performed.

The work was carried out at the electron beam energy of 2 GeV. As a result, the beam current integral of 154 kilocoulombs was achieved - this corresponds to the planned value of luminosity integral of 30 inverse picobarns.

2. The first test switching-on of a new equipment of "Deuteron" installation, quasi-real Photon Tagging System (PTS) is carried out. Besides, conditions of operation of the PTS particle detector parts with a hydrogen target and an electron/positron beam with energy of 600 MeV were studied.

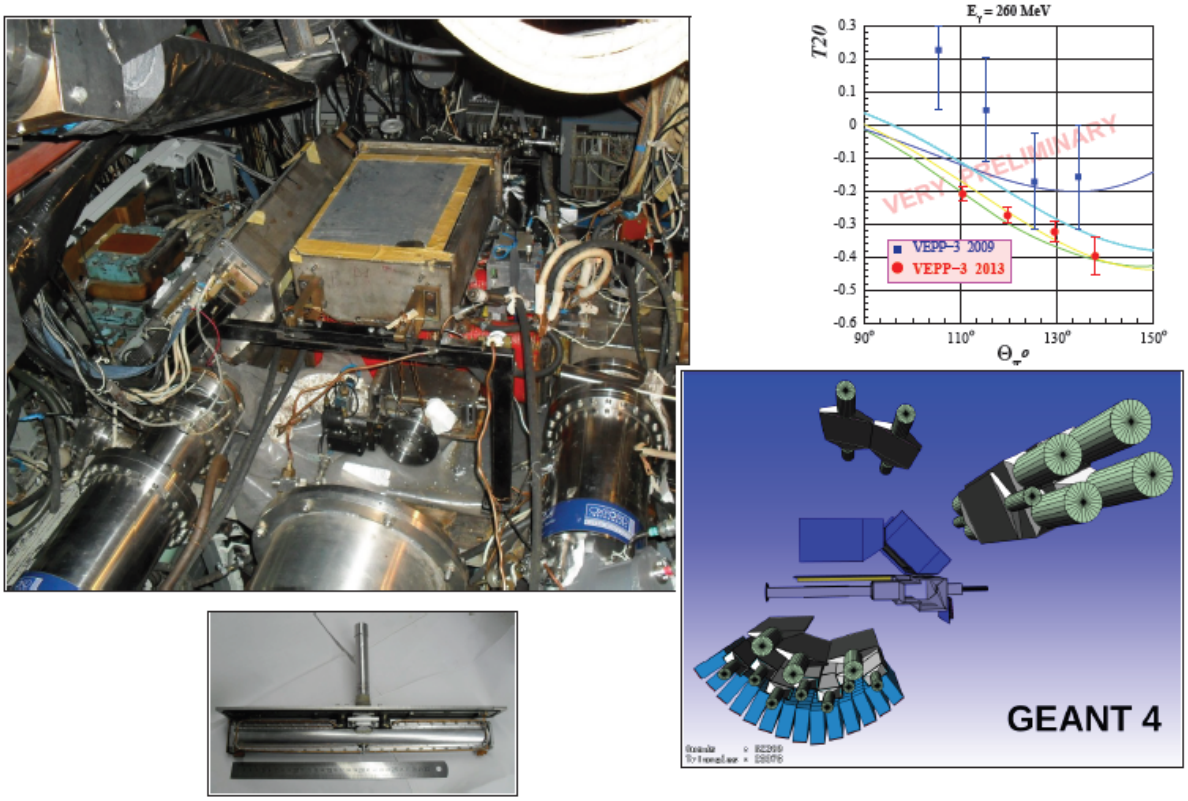

Fig. 5.2.1. T_{20} measurement in $\gamma+d \rightarrow \pi^0+d$ reaction.

5.2.3. CPT test experiment.

Study on efficiency of RF separation of electron and positron bunches at the parasitic interaction point at the VEPP-4M collider – at the centre of its technical section – is continued.

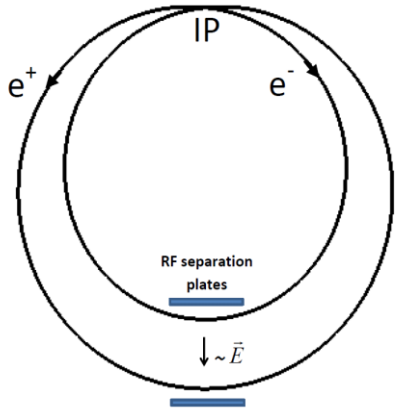

Fig. 5.2.2. Schematic two-turn closed orbit in the form of the Pascal Snail curve, represented as a 4-th order flat curve. IP - main interaction point; RF separation plates – plates of radial separation of the orbits with ac voltage at the frequency equal to a half of the revolution frequency.

The usual electrostatic system of orbit separation used for similar purposes in the high-energy physics experiments at the KEDR detector is a necessary means to provide electron-positron colliding beam stability. At the same time our methodic experiments have showed that electrostatic fields used for orbit separation yield a systematic error of 10^{-6} of CPT experiment against the required one of not worse than 10^{-9}.

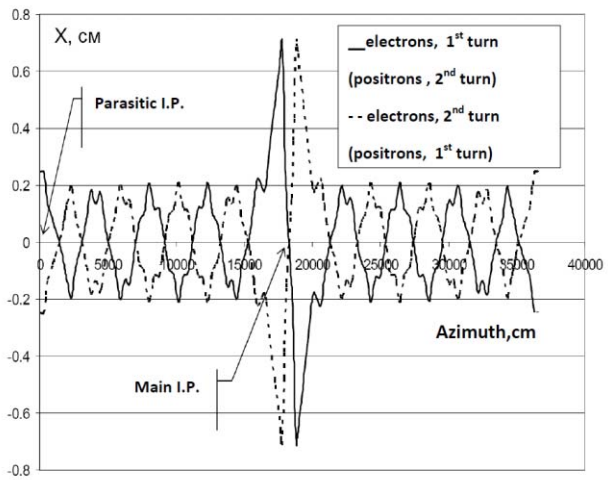

Fig. 5.2.3. Designed radial orbit with RF separation vs azimuth: E=1.85 GeV, the amplitude of plate voltage =5 kV, the orbit separation at the centre of technical section is 5 mm.

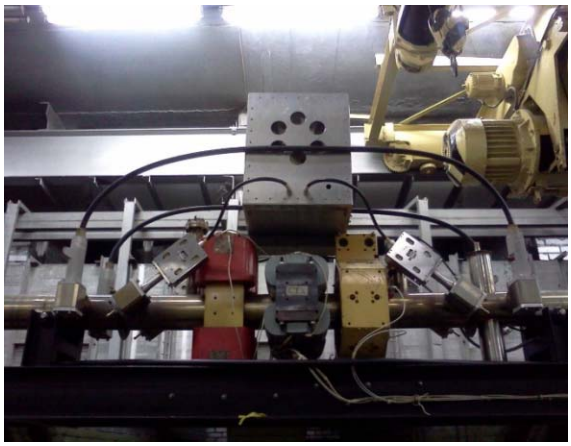

Fig. 5.2.4. Placement of the resonant circuit block and its connection to the orbit separation plates in the VEPP-4M technical section.

To cope with this problem an alternative orbit separation system has been proposed: beam separation at a certain point by horizontal RF electric field with the frequency equal to a half of the VEPP-4M revolution frequency.

Fig. 5.2.5. Image of the electron bunch with energy of 1.85 GeV on the SR monitor at the RF voltage amplitude on the plates of about 6.5 kV.

In 2013 a more precise calibration of separation using orbit measurements by means of “fast” pickup-stations located in the experimental section was performed. Fig.5.2.6 represents the data on horizontal co-ordinate of either of the two electron bunches in the experiment with a turned-on RF separation system.

In 2013 an experiment in precise comparison of bunch energies in the specified case using the method of resonance depolarization was carried out. In the experiment, the measured energies of the bunches have agreed within 10^{-6} in accordance with the theoretically proved property of RF orbit separation.

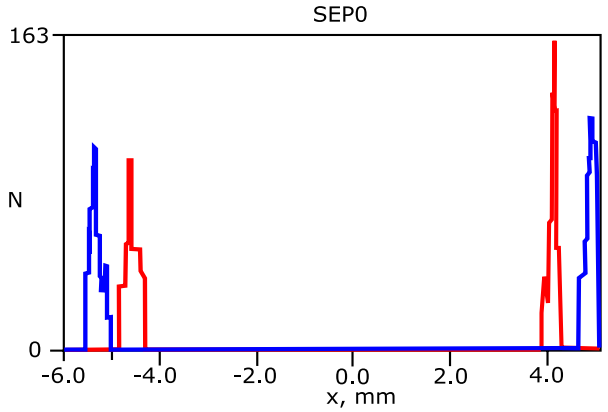

Fig. 5.2.6. Measured distribution of two-turn orbit horizontal position in the experiment with two electron bunches.

In 2013 the most important experiment for the system testing was performed – the experiment with colliding beams. At current of 1.1 mA (electrons) and 0.3 mA (positrons), beam-beam effects were not observed, though the electrostatic separation system unlike its RF analogue was completely turned off (Fig. 5.2.7).

Fig. 5.2.7. Images of 1 electron (left) and positron (right) bunches on the SR monitors at turned-on RF separation. Electrostatic separation system is completely turned off.

5.2.4. Method for increasing the luminosity of the VEPP-4M collider at low energy.

Luminosity for the collider with flat colliding beams (such as VEPP-4M) can be written as follows:

$$L = \frac{\gamma}{2er_e}\frac{I\xi_y}{\beta_y^*}$$

where betatron frequency shifts are equal to:

$$\xi_x = \frac{Nr_e}{2\pi\gamma}\cdot\frac{\beta_x^*}{\sigma_x^2} \qquad \xi_y = \frac{Nr_e}{2\pi\gamma}\cdot\frac{\beta_y^*}{\sigma_y^*\cdot\sigma_x}$$

Figure 5.2.8 shows the VEPP-4M work point, and the corresponding footprint, in a betatron frequency plane. The width and altitude of the footprint are approximately equal to values ξ_x, ξ_y. Thus, in the magnetic structure, ξ_x is determined only by a beam current, and ξ_y depends also on a vertical size of a beam at IP which depends on a betatron coupling and beam-beam effects.

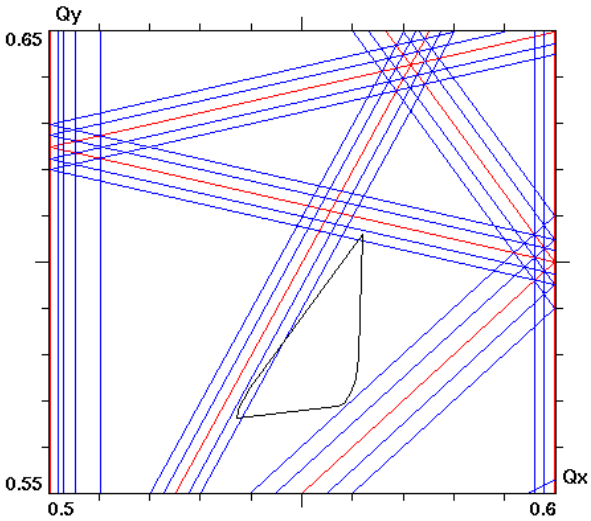

Fig. 5.2.8. Betatron resonances up to the 6th order (red lines) and their synchro-betatron satellites (blue lines). Black triangle is a footprint –frequency spread in a beam.

If to reduce β_x at IP so that σ_x is not changed (i.e. it is necessary not to decrease η_x, but on the contrary – to increase it a bit), then ξ_x will also decrease. It will allow increase of the maximum current by the same factor, thus, of the luminosity as well.

We have found an alternative modification of the VEPP-4M magnetic structure in the experimental section (close to IP), at which β_x at the interaction point decreases by a factor of 2-3, and a full horizontal size of a beam σ_x does not change. Thus, we have a possibility to increase the VEPP-4M luminosity by a factor of 2-3 at low (1.5 – 2.0 GeV) energy in a rather simple way.

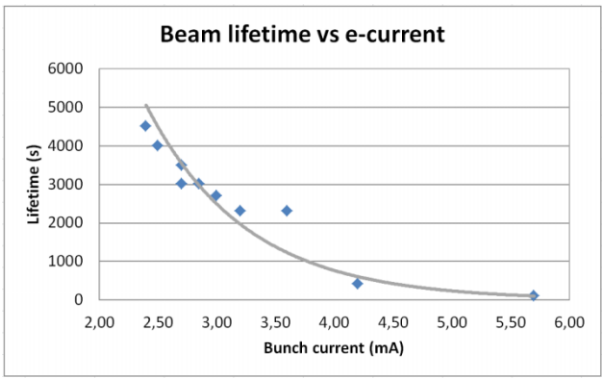

Figure 5.2.9. Beam lifetime (luminosity mode) vs the electron beam current.

Experimental test of the above-stated ideas was carried out during December, 2013. Preliminary results are presented in Fig.5.2. 9, 10. In the future, continuation of works in this direction is planned.

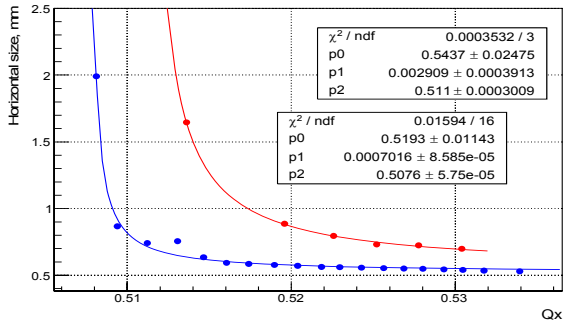

Fig. 5.2.10. Horizontal size of electron beam vs betatron frequency Q_x.

5.2.5. VEPP-4 modernization.

Temperature control system. The temperature control system is also implemented at the injection part of the installation, new "wiggler" for SR generation and the thermal pump (Fig. 5.2.12).

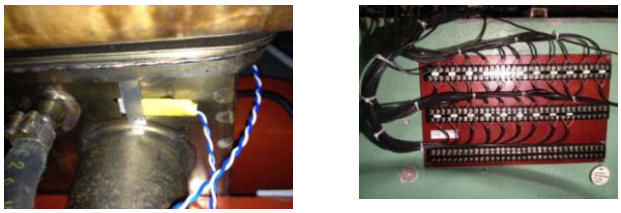

Fig. 5.2.11. Components of the Temperature control system.

Injection complex – VEPP-3 channel. The vertical section of the electron-optical channel from the injection complex to VEPP-3 is completed (Fig. 5.2.12). Magnets 5 and 6 are assembled and aligned, are power- and water-connected. A new injection magnet is ready for installation.14 pulse power supplies are assembled in racks.

Fig. 5.2.12. Vertical section of the injection channel to VEPP-3.

Magnetic field stabilization in the VEPP-4M magnets. As a result of modernization of DACs, controlling the powerful power supplies, a slow drift of magnets is almost eliminated and noises in the band down to 1 Hz are reduced by the factor of 1,5 – 2 (Fig. 5.2.13).

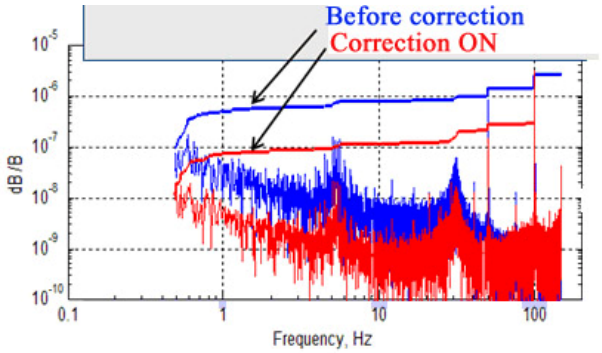

Fig. 5.2.13. Dispersion of field pulsations of the VEPP-4M calibration magnet before and after turning-on of correction.

Modernization of the pickup-system of VEPP-3, VEPP-4M. In 2013 a partial replacement of the electronics of pickups-stations is carried out. At VEPP-3 7 out of 19 pickups are replaced, at VEPP-4 - 18 out of 54 pickups. As a result, accuracy of measurements of an orbit with pickup-electrodes has essentially increased (Tab. 5.2.1).

Table 5.2.1. Parameters of pickup-electrodes after modernization.

Parameter	*Unit.*	Value
Resolution of turn-by-turn measurements	*μm*	30 / (beam current, mA)
Resolution of slow measurements at beam current more than 1 mA	*μm*	3-8
Dependence of the result on a bunch current in 0.5-20 mA current range (for every bunch)	*μm*	40-80
Temperature dependence of the measurement result	*μm / degree*	1-2

New pickups are characterized by:

a) Ability to measure separately position of electron and positron bunches close to interaction points.

b) Turn-by-turn measurements for each pickup.

c) A higher resolution of measurements.

d) Absence of electromechanical switches (magnetic switch), with a limited resource.

5.3. INJECTION COMPLEX VEPP-5

In 2013, work was carried out on the physical launch of the injection complex with positrons and electrons. Electron and positron beams have been generated at the output of the linear accelerator; the initial configuration of the linear accelerators enabled an increase in the beam energy at the output of the linear accelerators to the operating values. The capture and storage of the beam in the cooling storage have been realized.

The magnetic system and the beam diagnostics system in the cooling storage ring have been thoroughly tested and put into operation. Measurement of betatron frequencies in the cooling storage ring has been organized. Orbit and optics correction in work with electron beam has been performed, which enables a considerable increase in the available aperture and beam capture in the cooling storage ring.

Trial extractions of electron beam from the cooling storage ring were carried out using local orbit distortion and an extraction kicker.

For improvement of the accuracy and reliability of the diagnostics, new electronics to measure the beam position in the linear accelerators and cooling storage ring have been developed (pick-up stations). The electronics set for the linear accelerator is ready and is currently being implemented on the accelerator. A pick-up station prototype has been made for the cooling storage ring and is under tests now.

The synchronization system has been substantially changed; the timing of the RF system of the linear accelerator has been decoupled from beam injections. This significantly reduces the radiation load on the linear accelerators during their adjustment without changing the thermal modes. This alteration also includes changes required for work with beam users.

5.4. COMMISSIONING OF NSLS - II BOOSTER

A contract for construction of the booster for the synchrotron NSLS-II, being created at the Brookhaven National Laboratory (BNL), USA, was signed in May 2010. Table 5.3.1 presents the main parameters of the booster.

In 2012, all components of the booster were delivered to and assembled at BNL. All the systems were tested before the commissioning. In 2012, the BNL started a campaign to improve the safety of labor, which postponed the booster commissioning by a year. This time was used for additional advanced integration tests of all the systems of the booster and writing of the top-level software.

Table 5.3.1. Design parameters of the booster

Perimeter	158.4 m
Rated/ minimum injection energy	200 MeV/170 MeV
Rated/ minimum extraction energy	3 GeV/3.15 GeV
Repetition frequency	1 or 2 Hz
RF	499.68 MHz ± 10 kHz
Horizontal emittance at 3 GeV	<40 nm*rad
Pulse spread in extraction	<0.1%
Charge (long pulse/single pulse mode)	> 10 nCl/0.5 nCl
Efficiency of charge transfer from the linac to the main ring	> 75%
Operation time per year	6000 hours
Unplanned stop time	0.4 % (24 hours per year)

Fig. 5.3.1. Third arch of the assembled booster ring.

In December 2013, the commissioning of the booster was approved. By the New Year, a circulating beam was generated and ramped to the design energy of 3 GeV.

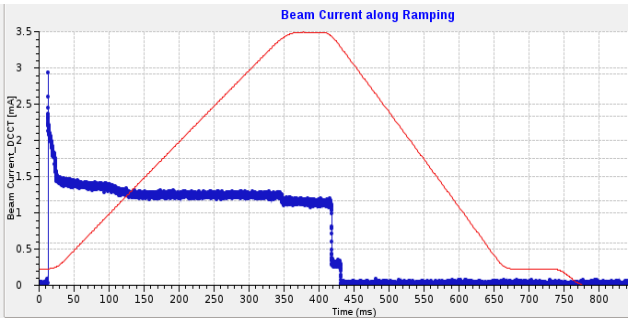

Fig. 5.3.2. Energy of 3 GeV was attained. Red line: current in the dipole magnets (1 Hz); blue line: current in the booster.

5.5. LINEAR INDUCTION ACCELERATOR LIA – 20R

As part of the creation of linear induction accelerator LIA-20R for the promising X-ray complex at VNIITF, works were started last year on making test benches for the accelerating and deflecting modules of the installation LIA-20.

Below are described the works performed.

A scheme of modulator to power the inductors in a mode of two-pulse series with adjustable time interval between the pulses starting from 2 microseconds was offered. Variants of capacitive storages having properties of forming lines were considered, as well as options for high-voltage high-current switches for use in the pulsed modulator; the pulse modulator was designed.

A bench was created for testing the basic components of the switched power supply of the inductors.

The completion of the development of the switched power supply of the accelerating module will require additional and deeper practical research of the pulse properties of the power supply scheme as a whole, as well as of its individual components. First of all, it is necessary to check the pulse characteristics of the forming lines, to study the work of the hydrogen thyratrons in the mode of electric strength reconstruction from reverse voltage in a time of the order of hundreds of nanoseconds. After the research, it will be necessary to perform a detailed elaboration of the structure of the pulse modulator. To verify the properties of the power supply system it is extremely important to refine the test bench and develop a load able to simulate a complex current load on electron beam.

An accelerating module has been designed for the regular structure of the accelerator LIA-20. Strap rings of amorphous alloy 2NSR will be used as the yokes. For reversal magnetization losses to be small, the strap shall have an insulation coating of sufficient dielectric strength and shall not degrade the magnetic properties of the material. The technology of production of such magnetic yokes developed at the MRTI will enable production of magnetic yokes required for the accelerator LIA-20.

Data for designing the components of the short accelerating section (calculations of dielectric strength and evaluation of the parasitic parameters of the inductors) have been prepared. The designing and the start of the production of the accelerating section is planned for 2014.

As part of the works on the electron-optical system of LIA-20, two software products, "Emittance" and "Envelope", were developed for evaluation of beam emittance growth on the LIA-20 elements and the influence of the beam emittance on the beam envelope. The programs were used in all the calculations required for the development of electron-optical system of the LIA.

The position of the elements of the LIA-20 magnetic system will be monitored with a combined system for measuring the horizontal and vertical displacements of the elements. The system is based on a hydrostatic system for level measurement and a stretched-thread system. Such systems have already been used at other facilities. This experience and the existing schematics and designs suggest adaptability of these solutions to monitoring of the position of components of the LIA-20 magnetic system.

Below are listed works performed on the creation of the test bench.

Simulation of particle motion in the magnetic components of the system have shown that, in terms of fundamental physical phenomena, there are no principle restrictions that exclude the possibility of creation of deflecting modules for an electron beam with the given parameters. At this stage, a concept that enables creation of a prototype for the kicker has been developed.

For the septum and the dipole magnet with adjustable quadrupole component, it is necessary to perform additional studies to optimize the geometry to provide magnetic fields of sufficient quality in accordance with the developed technical specifications.

5.6. ELECTRON BEAM WELDING

5.6.1. Experiments on "electron beam welding bench".

On the "Electron beam welding bench", BINP together with Sobolev Institute of Geology and Mineralogy SB RAS simulated the processes of electron beam melting of rock analogues of meteorites and gaseous and drip spray of the melting products. The observed structural and compositional zones of the thermal influence of electron beam are similar to those in fragments of the Chelyabinsk bolide that are at the Mineralogical Museum of Sobolev Institute. It is essential that the borders of the melting zones and melt films investigated with electron microscope are identical to the real structures of the melting boundaries in the fragments of this stony meteorite. Analysis of the composition of melt drops on glass and metal plates revealed their similarity with glassy droplets collected at the site of spray of the bolide destruction products. These observations enabled formulation of a mathematical model of melting of stony meteorites with a numerical scheme to describe the dynamics of combustion of solid fragments of cosmic bodies entering the Earth's atmosphere.

Test experiments were conducted for identification of the capacities of the "Electron beam welding bench" in study of mechanisms of extraction of partial and complete melt products from real rocks in bulk samples of the main rocks that form deep layers of the continental mantle beneath the craton of Siberia.

The bench was also used for experiments on electron beam application, carried out with students of the Novosibirsk State University. As a result, the students executed terms projects and an RF patent application for the invention of "A method of electron beam welding of non-magnetic metals and alloys" was filed.

5.6.2. Development of vacuum system for high-intensity electron-positron colliders and technology for its production.

Below are listed works under the ISTC project "Development of vacuum system for high-intensity electron-positron colliders and technology for its production" that were continued at the "Electron beam welding installation" in the 14th building of BINP.

1. A system for visualization and aiming of beam of secondary electrons was designed to finding the joint trajectory.

For this purpose an electronic unit for visualization and aiming of beam was manufactured. It is intended for viewing of the surface to weld during preparation for the welding process and making necessary corrections to the electron beam position during welding.

Surface monitoring is done with the unit switched to the mode of one-dimensional (a moving or rotating item) or two-dimensional (a fixed one) scanning of the beam of electron gun working at a small (~ 100 μA) current. The secondary-emission and scattered electrons that arise on the surface deposit on the collector electrode; the resulting current is amplified by a special amplifier, and the signal is applied to entry of the ADC of the visualization and monitoring unit.

A preliminary version of microprogrammed control codes for the visualization and monitoring unit has been developed. These codes have been loaded into the ROMs of the unit. Two stages of testing of the unit have been conducted with the loaded codes, both in autonomous mode and in conjunction with the control computer and a test program.

2. Control software has been developed for electron-beam welding. It has a three-level design:

- lower level: drivers of devices,
- upper level: application and operator software,
- medium level: connection; it provides data exchange between the software applications and hardware.

3. A system was made of two linear-motion modules (ZAO "Servotechnika"), which enables travel of a piece to weld without piece rotation mechanism.

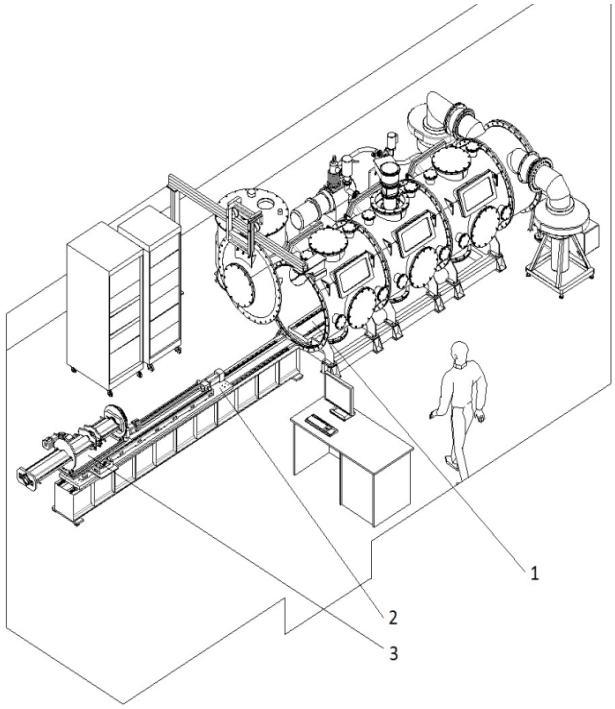

Fig. 5.6.1. Scheme of the electron-beam welding installation. 1 – lower (fixed) platform; 2 - upper (movable) platform; 3 - mechanism to rotate the piece to weld about its longitudinal axis and linear modules.

Table 5.6.1. Main parameters of the linear motion modules.

No	Parameter name	Longitudinal motion module	Transversal motion module
1.	Minimum possible stroke, mm	70	
2.	Maximum possible stroke, mm	1930	310
3.	Positioning accuracy, mm	+/- 0.05	
4.	Positioning repeatability, mm	+/- 0.02	

The transverse module for linear motion is equipped with a mechanism to rotate the part to weld. This ensures the movement of the part in the plane and its rotation around the longitudinal axis.

Fig. 5.6.2. XY movement mechanism

4. Vacuum pumping of the working chamber with two oil-vapor diffusion pumps was replaced by evacuation with two more efficient, up-to-date turbo-molecular pumps with a performance of 1400 l/s each.

Besides, joint experiments with colleagues from Italy (LNL, INFN) were conducted at the "Electron beam welding installation". The aim was to determine the efficiency of the protective device for the fission target of the installation SPIRAL-2 (France). The protective window was a tantalum plate. The time in which the plate is burnt through was determined for different electron beam parameters.


Fig. 5.6.3. Vacuum pumping system.

5.7. CONNECTION MODULE FOR EUROPEAN XFEL (DESY)

In the European XFEL project it was suggested for the first time to use powerful horizontal multi-beam klystrons as RF power sources for the superconducting sections of the accelerator. The horizontal type of klystrons made it possible to significantly reduce the cost of the building of the XFEL tunnel, but complicated by far the mechanism of connection and powering of klystrons inside the tunnel, because of the limited volume of the tunnel and large weights and dimensions of the klystrons and pulse transformers.

To solve this problem, BINP has developed a connection module (Fig. 5.7.1).

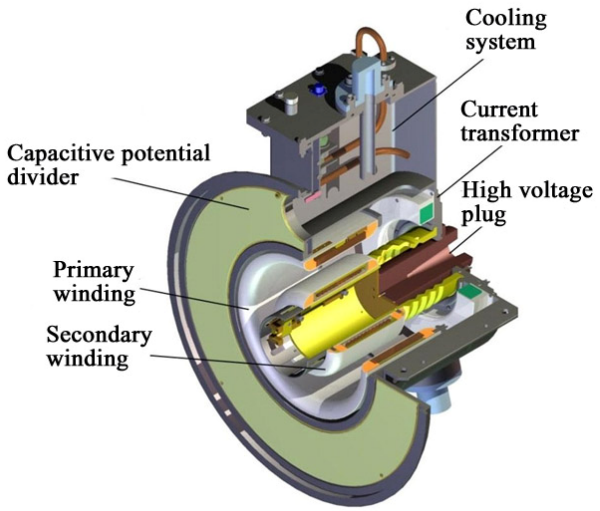

Fig. 5.7.1. Three-dimensional view of the connection module.

The original design of the connection module made it possible

- to power the horizontal klystrons (Toshiba, Thales, CPI) from a pulsed transformer through a flexible cable connection;
- to stably power the filament supply of the klystrons through a separation dividing resonant transformer from a specially designed invertor, which is controlled remotely via Ethernet protocol;
- to execute pulsed measurement of the current and voltage of the klystrons;
- to cool the cathode volumes of the klystrons.

In the period from May 2012 to November 2013, BINP delivered 27 sets of the connection modules to DESY. Most of the modules have been successfully tested on the test stands at DESY (see. Fig. 5.7.2).

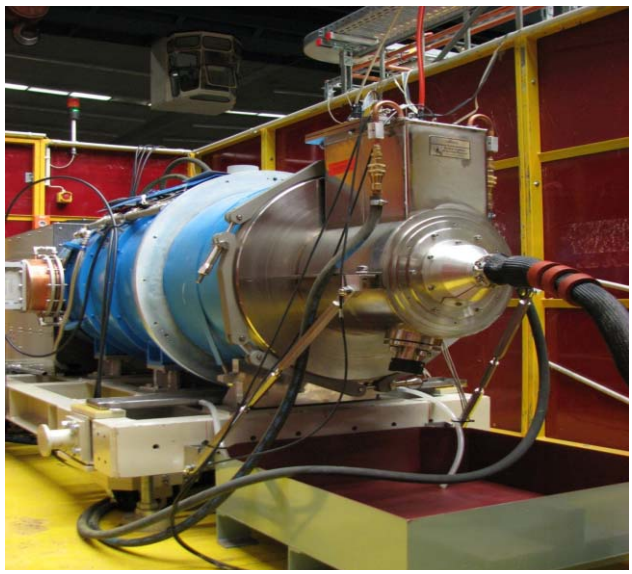
Fig. 5.7.2. Connection module on test bench at DESY.

Fig. 5.7.3. Transport of first SHF stations to the building of the XFEL injector.

The XFEL injector has been under assembly since September 2013. The first two SHF stations with connection modules have been successfully assembled and tried during tests of the SHF photo-gun of the injector.

Fig. 5.7.4. First assembled SHF station of the XFEL injector (September 2013).

5.8. NEW GUIDEBOOKS FOR THE ACCELERATOR SUB-DEPARTMENT OF THE NSU PHYSICS DEPARTMENT

In 2013, three guidebooks on the specialty "Collective effects in beam dynamics" at the accelerator subdepartment of the physics department of the NSU were published. They essentially expand the range of literature available to Russian undergraduates, graduate students and young scientists who study the features of development of coherent oscillations and beam stability in the today's and future storage rings and colliders.

The first guidebook (N.S. Dikansky, D.V. Pestrikov "Theory of coherent beam oscillations in storage rings", NSU, 2013) contains a description of the modern state of the theory of coherent beam oscillations in storage rings for charged particles. It is based on enriched texts of the lectures that have been read at the NSU since 1987. It also contains tasks. The guidebook will be useful for strengthening of practical knowledge of coherent effects in the current and future colliders and storage rings.

The second guidebook (D.V. Pestrikov, "Influence of spatial charge on dipole oscillations and fluctuations of continuous ion beam", NSU, 2013) describes calculation of stability conditions for coherent dipole oscillations and noise spectra of a continuous intense ion beam moving in a storage ring. In solving such problems, nontrivial predictions appear thanks to the fact that particle oscillations are under joint action of nonlinearities of the focusing fields of storage ring and nonlinearities of the fields of the spatial charge of beam. The guidebook is intended for the course "Collective effects in beam dynamics". The guidebook will be useful for strengthening of practical knowledge of coherent effects on the current and future colliders and storage rings.

The third guidebook (D.V. Pestrikov, "Rapid transverse dipole oscillations of bunches in storage rings", NSU, 2013) describes the properties and features of development of dipole transverse oscillations of bunches of stored charged particles, the rate of change in the amplitude and phase of which significantly exceeds the frequencies of small synchrotron oscillations of the particles. Many of the properties of such rapid coherent oscillations of beams resemble the features of beam chopping instability, which was originally observed only in linear accelerators. In storage rings, the possibility of storing fields induced by bunches can lead to additional important effects. The guidebook is intended for the course "Collective effects in beam dynamics." The guidebook will be useful for strengthening of practical knowledge of coherent effects on the current and future colliders and storage rings.

5.9. ELECTRON COOLING INSTALLATION

5.9.1. Electron cooling installation for synchrotron COSY (Germany).

The works on the creation and shipment to Germany of the fundamentally new 2 MV electron cooler for the German accelerator center COSY were completed in 2012. In 2013 this installation was mounted on the accelerator ring. In October 2013, the installation was started and the first cooling was done. This electron cooler enables unique experiments with an elementary particle detector with suppression of effects induced by scattering on the target nuclei and by spread of pulses caused by fluctuations in the ionization losses. The high-voltage cooler was designed using the scientific research and developments by BINP listed below.

1. Laser compass operating in vacuum for precision control of straightness of force lines in the cooling section.
2. Correction of position of the coils of the cooling section.

3. A four-electrode electron gun with controlled beam profile. Modulation of different parts of electron beam enables measurement of the position and size of electron beam.
4. Embedded electron beam profile meter.
5. Sectional design of electrostatic accelerator, consisting of unified modules. Each module is capable of providing generation of high voltage of up to 60 kV, contains electronics for generation of magnetic field along the accelerator column and is equipped with electronics control module.
6. High-power cascade transformer enables feeding of the high-voltage terminal and generation of solenoidal field along the accelerating and decelerating tubes.

The design of the 2 MeV electron cooler includes an acceleration column for acceleration and deceleration of electron beam, beam lines for transport of electrons to the cooling section and back, and a cooling section, where energy is transferred from hot ions to the cool electron beam. For the electron cooling to be applied in a wide energy range from 25 keV to 2 MeV, it was proposed to design a modular electrostatic accelerator. Each new installation is assembled from ready unified modules for any preset energy.

In the course of the commissioning of the installation, the electron cooling was performed with electron energies of 100, 200, 300 and 900 keV. First successful experiments on combined electron and stochastic cooling were carried out. The maximum attained current was 0.5 A. In high-voltage tests, an energy of 1450 kV was achieved. Figs. 5.9.1 - 5.9.3 show the installation under assembly.

Figs. 5.9.4-5.9.6 show the first results on electron cooling at an energy of 198 keV. One can see that the electron beam reduces the transverse size of the proton beam. From the measurements of the spectral width of the Schottky noise, one can also see that variations in the longitudinal pulse also become much smaller.

Fig. 5.9.1. June 2013: assembling and adjustment of the electron cooler, control electronics and power supply in Germany.

Fig. 5.9.2. Assembling the electrostatic accelerator in Germany.

Fig. 5.9.3. Assembling the cooling section on the accelerator ring.

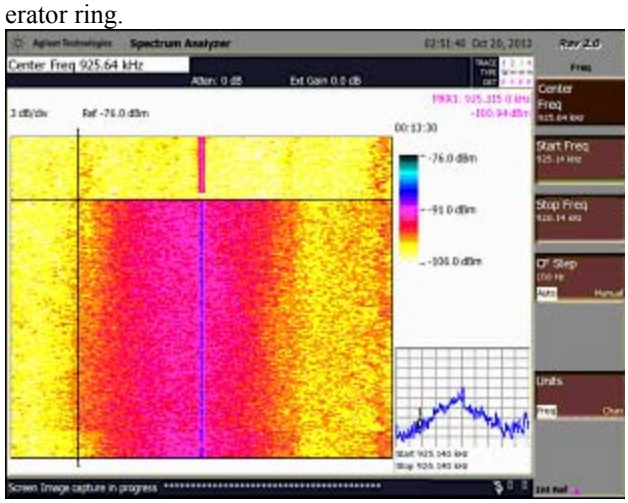

Fig. 5.9.4. Schottky noise from protons without electron cooling.

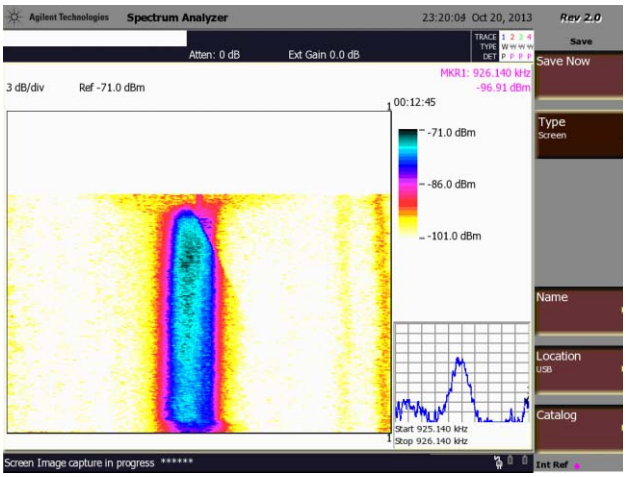

Fig. 5.9.5. Schottky noise from protons with electron cooling.

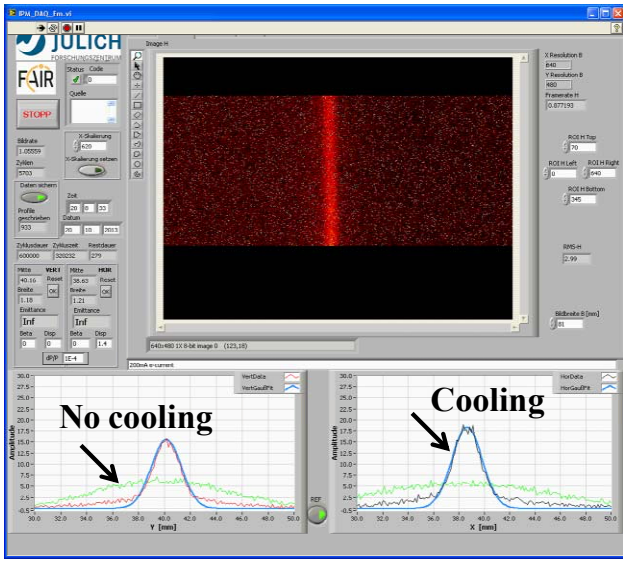

Fig. 5.9.6. Change in transverse profile of beam under the influence of electron cooling. Vertical (to the left) and horizontal (to the right) size of proton beam.

5.9.2. Electron cooling system for booster NICA

BINP participates in the creation of heavy-ion collider under the NICA project (JINR, Dubna). The booster, which is required for storage and acceleration of $^{197}Au^{31+}$ ions to an energy of 400 MeV/nucleon and reducing the beam emittance due to electron cooling, is one of the key elements of the collider. BINP and JINR have contracted to design, manufacture and commission the electron cooling system (ECS).

Technical requirements: The ECS shall ensure efficient cooling of heavy charged particles - from protons to $^{197}Au^{31+}$ ions and have the follow basic parameters:

Electron energy , keV: 1.5 ÷ 50;
Electron beam current I, A: 0.2 ÷ 1.0;
Energy adjustment accuracy $\Delta E/E$: $\leq 1 \cdot 10^{-5}$;
Electron beam energy recovery mode;
Electron beam loss current, $\delta I/I$: $\leq 3 \cdot 10^{-5}$;
Magnetic field strength, T: 0.1 ÷ 0.2;

Permissible axial magnetic field inhomogeneity in the cooling section, $\Delta B/B \leq 3 \cdot 10^{-5}$ over a length of 15 cm (3 periods of the Larmor spiral of an electron with an energy of 50 keV in a field of 0.1 T);

Transverse electron temperature in the cooling section (in the particle system), eV ≤ 0.3;

Correction of the orbit of ions entering and leaving the ECS: displacement, mm ≤ 1.0; angular deviation, mrad ≤ 1.0.

The period of the contract performance: August 2013 to December 2015. All research and design works have been done by March 2014; working drawings have been passed for production of components of the system.

5.10. ACCELERATOR MASS SPECTROMETER

In recent years the number of works on the application of the accelerator mass spectrometer (AMS) to biomedicine is growing steadily. The high sensitivity of the AMS enables research with very low biochemical and radiation doses of substances introduced into living systems. AMS analysis is used for investigation into the toxicity and metabolism of drugs, analysis of damage to DNA molecules, testing new medicines and so on.

In 2013, the BINP AMS was adapted for biomedical research without limitations on dating of natural objects. Tests confirmed the reliability of AMS analysis in an expanded range of radiocarbon concentration in samples. It was demonstrated that the "memory effect" influence is unimportant in the analysis of samples. BINP together with the Institute of Catalysis made a stand for preparation of biomedical samples for AMS analysis.

BINP together with the NSU conducted first biomedical research using the BINP AMS on the subject "Development of promising techniques for analysis of biomedical samples for studies on toxicity and pharmacokinetics of chemical compounds using an ultra-sensitive method of accelerator mass spectrometry". The pharmacokinetics of methanol in male laboratory mice was studied. Despite the small number of radiocarbon tags in methanol (20Bq), the measured concentration of methanol several times exceeded the natural one in the mouse organs under study. In AMS analysis, the statistical straggling in piece-by-piece counting of radiocarbon tags is much smaller than the natural spread for separate individuals due to individual metabolic features.

All archeological and geological samples (about 400 pieces) graphitized by the sample preparation group of the shared-equipment center "Geochronology of the Cenozoic" were subjected to AMS analysis in 2013.

Thus, some works in 2013 were aimed at broadening the field of application of the BINP AMS and at radiocarbon analysis of archaeological and geological samples.

5.11. VACUUM SYSTEMS

5.11.1. Application of bulk getters to production of high vacuum in future thermonuclear fusion installations.

The load on the vacuum system in future sources of high-energy hydrogen atoms is expected to be 1 Pa·m^3/s for up to 10^3 seconds. To get the desired degree of vacuum of 10^{-3} Pa, a hydrogen pumping speed of about 1000 m^3/s is required. Standard solutions, using well-proven cryosorption pumps, may be uneconomical because they require constant maintenance of cryogenic temperatures with a significant heat load. Otherwise, even with a slight warming of the cryopanel, desorption of the hydrogen that condensed on it will begin. Furthermore, the entire path of the beam is under high voltage (up to 10^6), which requires special isolation of the injector with the cryopumps from the container of cold helium gas.

Using bulk getters can provide the required dynamic pressure in the vacuum chambers. The potential benefits are as follows:

- operation at room temperature;
- the structure will not become more complicated and no additional electrical isolation of the injector from the getter will be required; a possibility of getter activation via applying power to the heater will be enough.

Below are presented results of a study of the gas-absorbing and activation properties of the domestic TiZrAl getter made by OAO Polema.

The TiZrAl getter is made in the form of tablets of 1.7-0.2 mm in diameter and a thickness of 3.5 mm. BINP made a prototype of getter pump cartridge (Fig.5.10.1) containing 285 tablets (weight: 0.450 kg) and a built-in heater. The cartridge is a cylinder with the outer diameter of 90 mm and the length of 140 mm. The tablets are arranged in a regular manner with spacings of 1 ÷ 1.5 mm between cylindrical grids. The geometric active area of the getter (the outer wall of the cylinder) is 395 cm^2. The ends of the cartridge were closed for uniform heating of the tablets. Fig.5.11.1 presents a cartridge placed on a Conflat-type flange.

Fig. 5.11.1 Prototype of cartridge based on TiZrAl tablets.

Since there is no detailed information on the properties of the TiZrAl getter, BINP conducted additional research of the getter pumping speed and hydrogen sorption capacity in dependence on activation temperature.

The gas-absorption and activation properties of the getter were investigated using the following sequence of measurements:

1) Activation No1 at 300 °C (measurement of hydrogen pumping speed and sorption capacity)/passivation (24 hours under the air atmosphere);
2) Activation No2 at 350 °C (measurement of hydrogen pumping speed and sorption capacity);
3) Regeneration No1 at 400 °C (measurement of hydrogen pumping speed and sorption capacity)/passivation (72 hours under air atmosphere);
4) Activation No3 at 500 °C (measurement of hydrogen pumping speed and sorption capacity);
5) Regeneration No2 at 500 °C (measurement of hydrogen pumping speed and sorption capacity);
6) Regeneration No3 at 520 °C/passivation (12 hours under air atmosphere).
7) Study of the pumping speed versus operating temperature (after activation at 350 ° C).
8) Study of the pumping speed versus operating temperature (after activation at 400 ° C).

The activation (regeneration) was carried out for 24 hours.

Tables 5.11.1 and 5.11.2 present values of quasi-equilibrium hydrogen pressure at room temperature after the activation or regeneration and quasi-equilibrium pressure in the system vs. absorbed hydrogen dose at room temperature after activation, respectively.

Table 5.11.1. Quasi-equilibrium hydrogen pressure at room temperature after activation or regeneration (at different temperatures).

	Activation No1	Activation No2	Regeneration No1	Activation No3	Regeneration No2	Regeneration No3
T_{activ}, °C	300	350	400	500	500	520
P_{equil}, Torr	2.06 E-8	2.18 E-9	3.3E-9	4.8E-9	8.4E-10	5.04E-10

Table 5.11.2. Quasi-equilibrium pressure in system when saturated with hydrogen at room temperature after activations.

	Activation No1	Activation No2	Regeneration No1	Activation No3	Regeneration No2	Regeneration No3
Dose, l·Torr	450	1440	1440	1550	1560	-
P_{equil}, Torr	3.12 E-5	1.39 E-6	4.8E-8	2.4E-7	2.64E-7	-

The dependences of the getter pumping speed on injected gas flow were measured (Fig. 5.11.2) for different activation temperatures. Because of the strong outgassing by the getter, it is impossible to state with confidence that the getter was fully activated at the initial temperature of 350-400 °C. Subsequent activations/regenerations at 500-520 °C have fully confirmed this assumption.

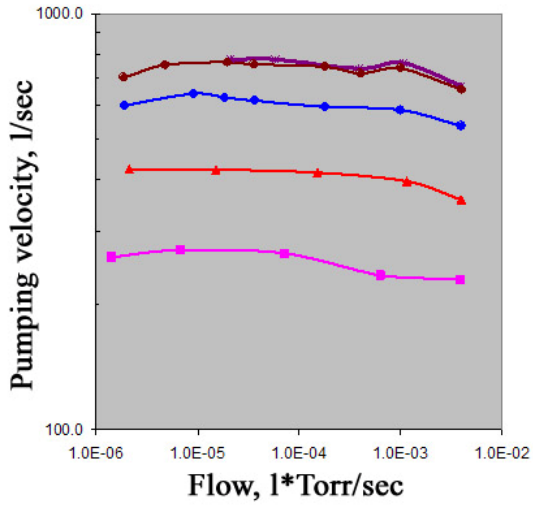

Fig. 5.11.2. Pumping speed vs. injected gas flow at different activation temperatures.

Fig 5.11.3 shows the measured dependences of the hydrogen pumping speed of the getter on the operating temperature of the getter (experiments 7 and 8).

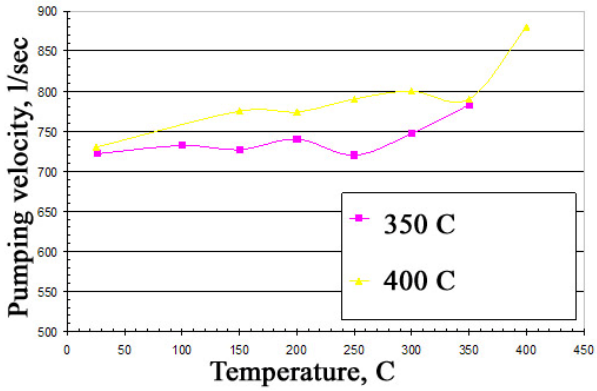

Fig. 5.11.3. Pumping speed vs. working temperature of TiZrAl getter. Gas flow: (2÷4)•10^{-5} l•Torr/sec.

Further increase in the activation temperature did not raise the pumping speed. Thus, the relatively high activation temperature (500 °C) is actually required for preliminary degassing of the getter, which can be done on a dedicated vacuum bench before the cartridge is installed in the injector.

6

SYNCHROTRON RADIATION AND FREE ELECTRON LASERS

6.1. INTRODUCTION

The shared-equipment Siberian Center for Synchrotron and Terahertz radiation (SCSTR) started its work at Budker Institute of Nuclear Physics more than thirty years ago. Works at the center are going in two directions: using synchrotron and terahertz radiation.

The "Synchrotron radiation (SR)" direction includes works on the VEPP-3 and VEPP-4 storage rings, development and creation of SR generation systems for Russian and foreign SR centers.

Works in the terahertz direction are conducted at the Novosibirsk free electron laser (FEL).

Besides, the center in engaged in educational and training programs for students and post-graduates.

In 2013, there were allocated 2076 hours for work on SR beams from the VEPP-3 storage ring (1590 hours in 2012) and 348 hours on beams from VEPP-4 (48 hours in 2012). The experiments involved 10 stations on 7 SR extraction beamlines on VEPP-4 and 2 SR stations on beamlines from VEPP-4. In 2013 the Novosibirsk FEL worked for the users for about 1000 hours, the same as in 2012.

6.2. WORK ON SR BEAMS FROM VEPP-3

6.2.1. Station "Experimental state of matter".

The station is intended for analysis of fast explosive and shock-wave processes. The station is equipped with an explosion chamber and a system for detection of passed SR and small-angle X-ray scattering (SAXS) of SR.

Participating organizations :

- Institute of Hydrodynamics,
- Russian Federal Nuclear Center “All-Russian Research Institute of Experimental Physics (VNIIEF), Sarov,
- Russian Federal Nuclear Center “All-Russian Research Institute of Technical Physics (VNIITF, Snezhinsk,
- Institute of Solid State Chemistry and Mechanochemistry SB RAS,
- Budker Institute of Nuclear Physics SB RAS.

In 2013, works at the station were carried out by the scientific plans of the participating institutions and had financial support from the following projects and contracts:

• SB RAS Integration project No. 65 "Study of scale effects in detonation of explosives", 2012-2014.

• RAS Program No. 2.5 “Research on the dynamics of condensation of nanoparticles in detonation of TATB-based mixtures by small-angle scattering of synchrotron radiation ", RAS Presidium program on basic research "Matter at high energy densities", 2012-2014.

• RFBR 12-01-00177- “Tomography of mechanical parameters of detonation flow and the equation of state of explosion products”, 2012-2014 (guided by E.R. Pruuel).

• RFBR 11-03-00874- “Research on the dynamics of condensation of nanoparticles in HE detonation by small-angle scattering of synchrotron radiation, 2011-2013 (guided by V.M. Titov).

• Contract 6/2013 from 15 April 2013 "Research on detonation wave parameters with application of synchrotron radiation". Customer: Zababahin All-Russian Science-Research Institute of Technical Physics, (Russian Federal Nuclear Center VNIITF).

Examples of works in 2013.

1. Exploration of TEN + soda mixture.

Experiments with SR were conducted on samples of bulk detonating TEN + soda 35/65 mixtures with diameter 15-20 mm. This explosive mixture has a very low initial density of ~ 0.5 g/cm^3) and low detonation velocity (~ 2 km/s). With a low critical diameter (~ 3 mm) this mixture is very promising for use in explosion welding. All samples of this explosive mixture were prepared at VNIIEF (Sarov). The experiments were performed in two set-ups: longitudinal and transverse measurement of X-ray absorption (the detector was placed across the detonation direction). SR was detected with the in-house detector DIMEX. The first set-up experiments yielded density distributions in the front during detonation of this mixture. Density values in the Neumann peak (1.15 g/cm^3) were obtained at a detonation velocity of 2.3 km/s. The chemical peak width is 1.2 - 1.5 mm. Transverse measurement of absorption yielded volumetric distributions of pressure, density and velocity field of spread of detonation products.

2. Measurement of absorption of synchrotron radiation (SR) along propagation of detonation.

Longitudinal measurements yield mass distribution along the SR beam. Fig. 6.2.1 shows an experimental assembly with charges of TEN + soda mixture. In the detonation front there is observed a characteristic mass increase, which is associated with the compression of the matter. zt-charts of front start position in the compounds under study were drawn. An approximation line z=Dt+c was drawn through the resulting points, where the z is the coordinate of the front; t is time; D is the derived front velocity; c is a constant. The uncertainty of the determination of D is at the level of 1 - 2% in most cases.

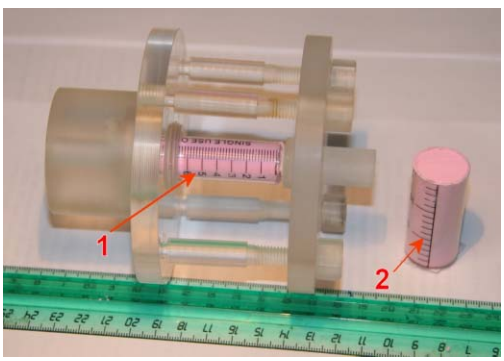

Fig. 6.2.1. Assemblies with ten + soda mixture prepared for experiments. 1 – a 10 ml syringe; 2 – a 20 ml syringe.

In the experiments with soda, a syringe was filled with the mixture and then tapped until complete disappearance

of cavities. The resulting density of the mixture ranged from 0.7 to 0.8 g/cm^3. Fig. 6.2.2 shows a recorded detonation front position. The detonation velocity is stable in the density range of 0.5 - 0.85 g/cm^3.

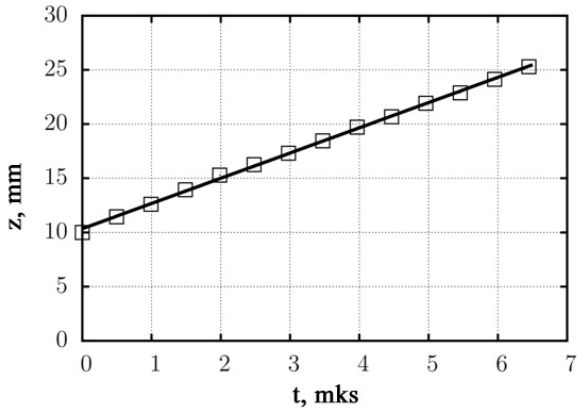

Fig. 6.2.2. z - t diagram of the detonation wave front. No significant fluctuations in the speed.

After calibration of the detector, the dynamic dependence of on-beam mass on channel number (distribution of mass on the axis, Fig. 6.2.3) is reconstructed from the records. The reconstruction of density distribution in the axial part of HE sample in experiments of this type is done in several steps. First, the dependence of the integral value

$$m(X)=2\int_0^R \rho(X,r)dr$$

on distance is determined ($m(X)=$ is the explosive mass along the SR beam, which passes through the axis of symmetry of the charge and is perpendicular to it) , where R is the radius of the explosive charge. Since the value m varies significantly in the detonation of the explosive and the subsequent expansion of the explosion products, the SR absorption spectrum also changes. Therefore each channel of the detector was subjected to pre-calibration, which revealed how the value m is linked with the relative absorption of radiation by the HE under study, J/J_0, where J is the recorded flow and J_0 is the incident SR flow. HE samples of different thicknesses were used for this purpose. The result of this calibration, presented as a $\ln(J/J_0)$ dependence on m, is close to a linear function and is interpolated with a parabola $\ln(J/J_0)=a_0-a_1\cdot m+a_2\cdot m^2$.

The density profile in the detonation front near the axis of symmetry of the HE sample is determined from m values that correspond to the channels that register the signal in the near-front zone. A number of the following simplifying assumptions are applied:

 The front of the detonation wave is part of a sphere of radius $R=d^2/8b+b/2$, where d is the diameter of the charge; b is the bulge of the central point of the front;

 the HE compressed behind the front is composed of layers of constant density separated by spherical surfaces of radii that successively decrease by the width of the measurement channel;

 Each of the channels that got behind the detonation front is attributed a value of HE density on the axis of symmetry of the charge.

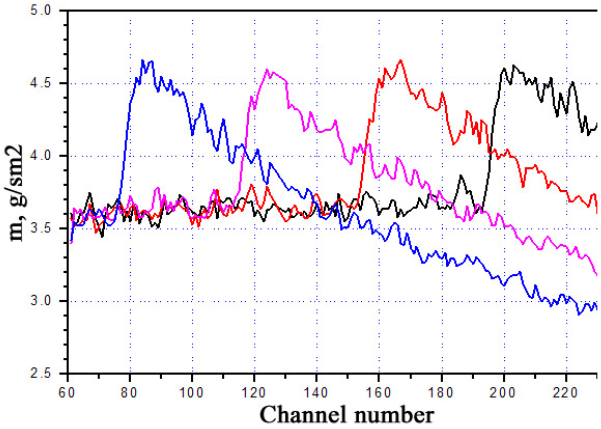

Fig. 6.2.3. On-beam mass distribution $m(n)$ in ten + soda sample. The profiles are given with an interval of ~ 2 μs.

The resulting smoothed dependence $\rho(X)$ that was averaged over several experiments is shown in Fig 6.2.4, where X=0 corresponds to the shock jump.

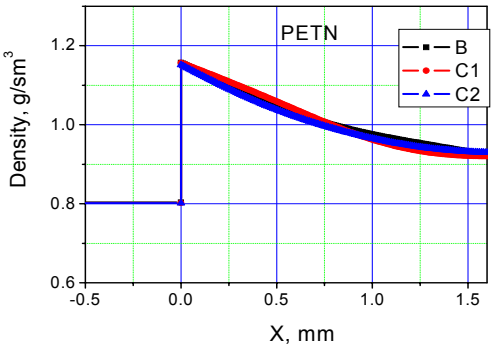

Fig. 6.2.4. Density profile in the front of detonation of ten+soda mixture. The initial density is 0.8 g/cm^3.

This experiment set-up has an essential feature of the curvature of the detonation front in combination with its axial symmetry. This results in an error in density reconstruction from the results of registration of radiation that passed through the sample, this error increasing sharply with the distance from the front because of the assumption of spherical equal-density layers. As a result, the area with acceptable accuracy of reconstructed density is not more than 1 mm.

3. Transverse measurement of absorption.

In this set-up, the spread of the products of detonation of cylindrical explosive charge is investigated. The transverse distribution of absorption is measured with a time period between SR pulses. The transverse distribution of

mass is reconstructed after calibration of the absorption by the detector.

The developed specialized methods of density reconstruction using regularization of the desired solution through intensive use of *a priori* information about the structure of the flow under study have greatly improved the accuracy of density reconstruction and allowed starting reconstruction of other mechanical parameters of flow: distribution of mass velocity and pressure.

The results obtained allow detailing the spatial density distribution of scattering products. Figs. 6.2.5 and 6.2.6 show the obtained pressure and density distributions, as well as their values in the axis of the charge in detonation of ten+soda mixture (density = 0.75 g/cm^3). Fig. 6.2.7 presents distributions (and directions) of the mass velocity vector.

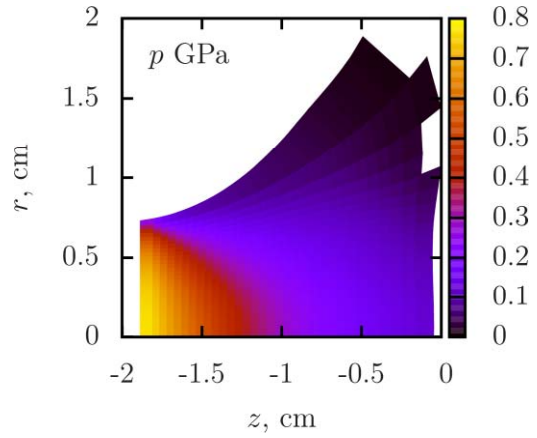

a

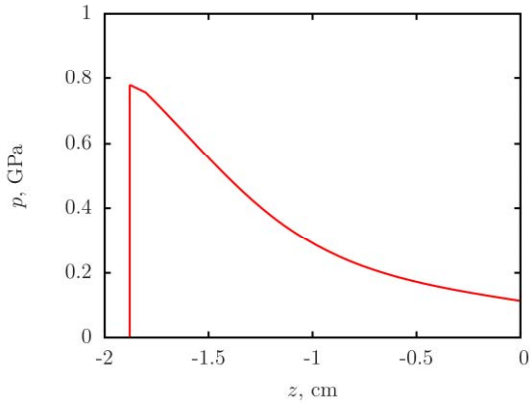

b

Fig. 6.2.5. Spatial distribution of pressure with a density of 0.85 g/cm^3 (a); pressure distribution along the axis of the charge (b).

The obtained detailed information about the flow structure allows one to construct an unloading adiabat (or an equation of state of spreading explosion products) from the experimental data. The derivative $c = \left(\frac{\partial p}{\partial \rho}\right)^{1/2}$ will be interpreted as the speed of sound. After reconstruction of the equation of state, it is calculated explicitly as

$$c = \left(\frac{\partial p}{\partial \rho}\right)^{1/2} = \left[p_0(\rho/\rho_{00})^{\gamma(\rho)}(\gamma(\rho)/\rho + \ln(\rho/\rho_{00})\gamma'(\rho))\right]^{1/2}$$

Knowing it, one can accurately reconstruct the zone of influence of the chemical reaction on the parameters in the detonation wave front.

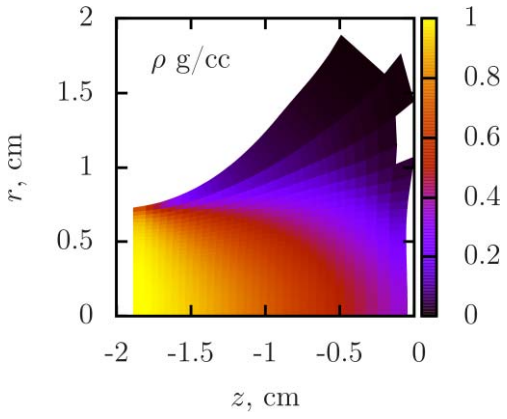

a

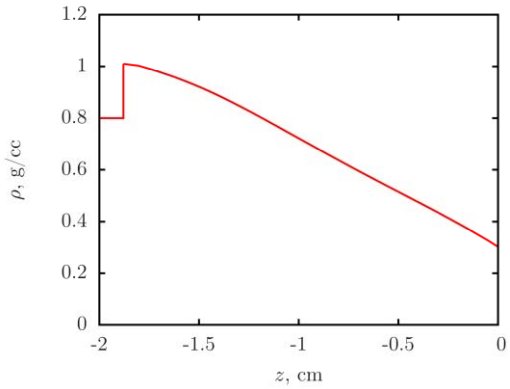

b

Fig. 6.2.6. Spatial density distribution (a), density distribution along the axis of charge (b).

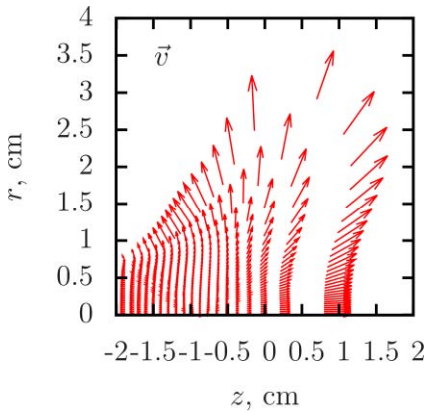

Fig. 6.2.7. Spatial distributions of the mass velocity.

6.2.2. Station "LIGA technology and X-ray lithography".

The station is intended for experiments on X-ray lithography in thick resistive layers for fabrication of microstructures, including X-ray masks.

Participating organizations:

- Budker Institute of Nuclear Physics SB RAS, Novosibirsk;
- Institute of Cytology and Genetics SB RAS, Novosibirsk;
- Institute of Solid State Chemistry and Mechano - chemistry SB RAS;
- Institute of Automation and Electrometry SB RAS;
- Vorozhtsov Institute of Organic Chemistry SB RAS;
- Institute for Automation and Control FEB RAS, Vladivostok.

In 2013, works at the station were carried out by the scientific plans of the participating institutions and had financial support of the following projects and contracts:

- RFBR project No. 12-02012071 (2012-2014) ofi_m "Development of methods to make high-resolution phase-contrast images using X-ray diffraction optics";
- SB RA and FEB RAS interdisciplinary integration project No. 92 (2012-2014) "Materials and LIGA technology to create microfluidic analytical systems to record fluorescence".

Examples of works in 2013:

In 2013, the activity at the LIGA station on the VEPP-3 storage ring was aimed mainly at the development of manufacturing of X-ray masks for subsequent production of high-aspect microstructures for applied research (biochips and diffraction gratings). To this end, researchers at the SCSTR have implemented a prototype of micro-beam X-ray lithographer (MBXL), a new device for direct formation of microstructures in deep layers of X-ray resist. It performs vector drawing of an arbitrarily given topology using SR microbeam (without X-ray patterns with topological figure of the structure). Special software was developed for precise motion of a substrate with resist relative to the X-ray mask diaphragm with control of dose accumulated. As a result, polygonal and multiple-arc microstructures were produced directly in a layer of negative resist SU- 8 several hundred micrometers thick. The resulting microstructure of resist SU-8 on a conductive (glass-carbon) substrate are used as masks for electrochemical deposition of gold coating 25 - 50 microns thick, which is radiopaque in the "hard" SR range of 1-10 Å. Now this method is used at SCSTR for manufacturing of X-ray masks on substrates of glass-carbon or beryllium.

The MBXL capabilities were enhanced substantially and the time of formation of microstructures was decreased considerably due to a modernization of the MBXL and implementation of the ability to change the microbeam size in the course of drawing of a structure. To this end, the MBXL was equipped with an independent precision coordinate table, which was to move a set of X-ray diaphragms in a plane parallel to an X-ray mask substrate. In the course of X-ray lithography, a selected diaphragm is brought in coincidence with a tentative diaphragm 500 mm in diameter, which is fixed at the beam entry to the chamber, and thus a microbeam is formed for drawing of a structure. The change of diaphragms and movement of substrate with resist are controlled automatically. The optimization of the SR microbeam size selection for any element made it possible to fast build topologies in which elements of different sizes are combined.

The effect of contrast of the forming micro-diaphragms in conjunction with the required density of elements of topological pattern on the quality of microstructures to form was assessed. Limitations of the method were identified and recommendations on optimizing the use of MBXL were elaborated.

The MBXL can be used in solving various user tasks which require microstructures with minimum dimensions over 20 μm (Fig. (6.2.)8), e.g. diffractive elements for optics in the X-ray, visible, terahertz and IR ranges, microfluid modules for rapid biological assays, test structures for imaging X-ray microscopy etc. A number of experimental high-aspect microstructures were made. Those include high-contrast X-ray masks for hard (~ 10 keV) SR: an X-ray mask for microfluid module with minimum channel dimensions of 25 microns, an X-ray mask for 1 cm^2 diffraction lattice with period 135 microns with 25-micron gold coating, and a 10 × 3 mm^2 grating of SU-8 resist with period 30 microns (Fig. 6.2.9, Fig. 6.2.10, Fig. 6.2.11).

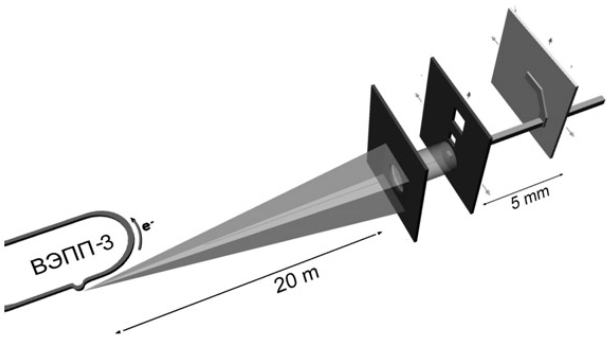

Fig. 6.2.8. Scheme of the prototype of the microbeam X-ray lithographer (MBXL).

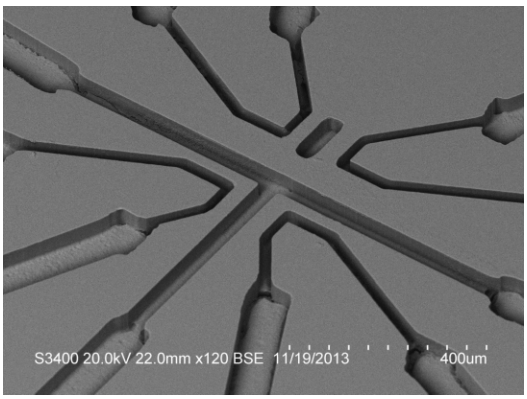

Fig. 6.2.9. Microfluid module made of PMMA using deep X-ray lithography with a mask made by the MBXL after deposition of a 30- micron gold layer on a blank; channels in PMMA are 50 microns deep.

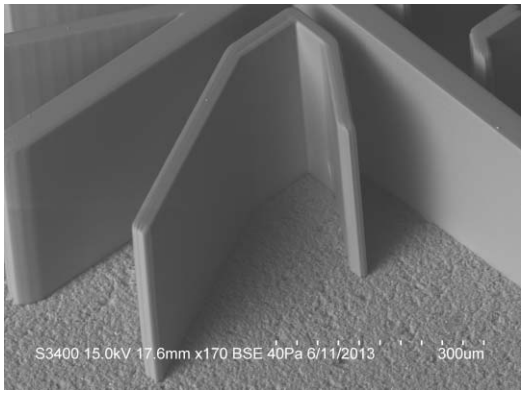

Fig. 6.2.10. High-aspect micro-lamellas drawn by X-ray microbeam in a thick layer of SU-8 resist; the minimum width of the lamellas is 23 microns; the structure height is 330 microns.

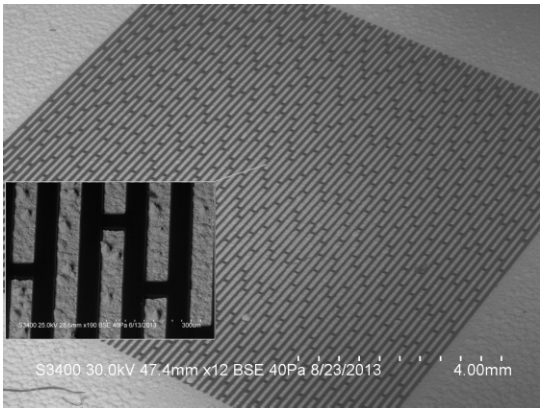

Fig. 6.2.11. SU-8 resist micro-lattice on glass-carbon substrate with gold plating about 50 microns thick. The period of the structure is 130 microns; the line width is 65 microns; the total field of the lattice is 1×1 cm^2.

6.2.3. Station "Anomalous Scattering" and "Precision diffractometry".

Station "Anomalous Scattering".

Below are listed works that were carried out at the station.

1. Analysis of the phase composition and structure of Au/γ-Al_2O_3catalyst calcined at different temperatures by resonant scattering near the absorption edge of AuL_{III} (Institute of Catalysis SB RAS);
2. Analysis of the stability of metal-organic framework (MOF) of MIL-125 in reactive medium (Institute of Catalysis SB RAS);
3. Analysis of the phase composition and structure of polymer-carbon nanocomposites (Institute of Catalysis SB RAS);
4. Research on the structure of mixed perovskite-structure oxides (Institute of Chemistry of Solid State Chemistry and Mechanochemistry SB RAS);
5. Research on the phase composition of ion-plasm-sputtered titanium-nitride hardening coatings (Tomsk Polytechnic University);
6. Analysis of the structural features of mayenite-type calcium-aluminum oxide (Institute of High-Temperature Electrochemistry UB RAS);
7. Research on the structure of high-*k* hafnium-oxide materials (Institute of Inorganic Chemistry SB RAS).

Research on the structure of high-*k* hafnium-oxide materials (Institute of Inorganic Chemistry SB RAS).

Currently HfO_2 and double oxides based on it (HfO_2-Ln_2O_3, where Ln is a rare earth element) have been widely researched as optical, heat-resistant and super-hard materials, which are important for development of new technologies. In addition, these materials have a high dielectric constant (*k*), which allows using them as a gate insulator in micro- and nano-electronic new-generation devices. In this context, the research on thin films based on these compounds is of a special interest.

At atmospheric pressure, hafnium oxide occurs in several structural modifications. At room temperature, the monoclinic phase (k = 16) is the equilibrium one. The monoclinic modification becomes tetragonal (k = 70) at 1300 K, and at a temperature of about 2700 K it turns into cubic (k = 29). Thus films of tetragonal or cubic structure are preferable for practical use. These structures, which are nonequilibrium at T < 1300K, can be are stabilized in a nanocrystalline material, as well as by doping rare and rare earth metals, including lanthanum, in HfO_2.

As compared with HfO_2, films of double oxides $La_xHf_{1-x}O_y$ have an advantage of higher crystallization temperature. One can use lanthanum concentration for efficient modulation of the magnitude of flat-band voltage (V_{FB}) in structures where such films are used as the gate dielectric. Many researchers pay attention to $Hf_2La_2O_7$ films of pyrochlore structure. When used in MOS field-effect transistors (MOSFETs), these films allow adjustment of the work function in contact with the metal gate.

It is known that doping a heterovalent impurity in HfO_2 initiates additional generation of oxygen vacancies. These defects cause rise of charge state levels in the energy gap of the dielectric, which can significantly increase the ionic conductivity of the material. However, some publications have shown that doping lanthanum in HfO_2 leads to a shift of these levels to the conduction band, and charge and leakage currents that are detected in structures with $Hf_{1-x}La_xO_y$ films are smaller. There was also proposed a mechanism of passivation of oxygen vacancies in HfO_2 films doped with elements of Group III.

Thin $Hf_{1-x}La_xO_y$ films are produced through physical sputtering of targets in atmosphere of oxygen or chemical vapor deposition (MOCVD and ALD). The functional properties of such films depend on their chemical and phase composition and structure. Although $Hf_{1-x}La_xO_y$ films are actively researched in recent years, the dependence of their chemical and phase composition, structure and properties on the preparation conditions has not been understood enough so far.

When synthesized by the MO CVD method under non-equilibrium conditions, the films are formed in co-precipitation of volatile precursors from the vapors, the precursors already having Ln-O and Hf-O ties and free valence remaining for some time in case of abstraction of ligands. These synthesis conditions contribute to formation of non-equilibrium phase at T < 600 ° C.

The aim of this work was to develop a method of producing films of double oxides $La_xHf_{1-x}O_y$ from beta-diketonate complexes of La and Hf, characterization of their chemical structure, and research on the phase formation with La concentration varying in wide limits.

Fig. 6.2.12 presents diffractograms of HfO_2 powders of the monoclinic (1) and cubic (2) modifications and $La_2Hf_2O_7$ compound (3), as well as characteristic diffractograms of $La_xHf_{1-x}O_y$ films, in which the La concentration is 4, 11 and 18 at. % (diffractograms 4, 5, and 6, respectively).

It was found earlier that HfO_2 films synthesized from Hf $(thd)_4$ at temperatures ≤ 600 ° C are of the equilibrium monoclinic structure. Comparison of diffraction patterns (1) and (2) with diffractogram (4) shows that the reflections at 2θ = 30.08, 34.7, 50.13, and 59.23° are close in position to the reflections at 2θ = 30.03 (111), 34.2 (002), 50.29 (202), and 59.6 (311), which correspond to the tetragonal phase (ICDD PDF-2 No.00-008-0342). It should be noted that we cannot completely exclude formation of the cubic phase (ICSD No.2-033), since the positions of reflections for these phases are close. Thus, the research has shown that doping lanthanum in HfO_2 at ~ 4 at. % modifies the equilibrium monoclinic structure and forms non-equilibrium tetragonal or orthorhombic structures, which are equilibrium only at high temperatures (> 1700° C). The large half-widths of the diffraction lines are determined by the small size of the nanocrystals the film consists of. Their size as estimated from the Scherrer equation is ~ 10nm.

One can see in Fig. 6.2.12 that the reflections in the diffraction patterns are gradually shifted towards lower 2θ values. This systematic shift of maxima is an evidence of formation of solid solutions. Displacement towards lower 2θ values occurs when an element with a large ion radius (r_{La} = 1.04 Å) is introduced into the HfO_2 lattice (r_{Hf} = 0,82 Å).

Analysis of diffraction patterns of films with La concentration from 7 to 16 at. % showed that films of solid solutions have a cubic fluorite structure and belong to the Fm-3m space group. Thus, the resulting solid solution of fluorite structure occupies an area extending from ~ 7 to 16 at % La.

With increasing La concentration, the lattice parameter *a* increases from 5.14 to 5.3 Å. Comparison of diffraction pattern (6) for a film with a La concentration of 18 at. % with diffraction pattern (3) for $La_2Hf_2O_7$ compound of pyrochlore structure reveals their identity.

Fig. 6.2.13 (1) shows a diffractogram of a film with La concentration 30 at. % in comparison with $La_2Hf_2O_7$(3) and α-La_2O_3 (2) powder patterns.

Comparing the diffractograms, one can see that reflections in the diffractogram of the film reflections at 2θ = 27.5, 28.7, 33.1, 47.7, and 56.4° coincide with those of the $La_2Hf_2O_7$ compound, and the reflections at 2θ = 45.2 and 53.7° are close to reflections of La_2O_3. The 2θ = 27.5° reflection has an arm that can also be attributed to the La_2O_3 phase. Thus, we can conclude that the film that contains ~ 30 at.% of La is biphasic and consists of $La_2Hf_2O_7$ and α-La_2O_3. Using the structural data base (ICDD) for indexing of the reflections in diffractogram (1) is ambiguous, as the database contains two $La_2Hf_2O_7$ phases with the same values of lattice spacings, but with different lattice constants a = 10.77 Å and a = 5.38 Å.

For the La_2O_3 cubic phase there are two known structures with the lattice constants (a = 11.327 Å and 4.51 Å) for which the lattice spacings differ. As can be seen from Fig. 6.2.13, X-ray pattern (1) has a feature of dual reflections in the area of 2θ = 40 - 60° and an arm in the reflection at 2θ = 27.5°, which is typical to materials consisting of two isomorphic phases with similar lattice parameters. A consistent indexing of the reflections at 2θ = 27.5, 28.7, 33.1, 47.7, and 56.4 ° can be taken for a cubic $La_2Hf_2O_7$ structure with the lattice parameter 10.77 Å.

Thus these studies have revealed that

– The films are nanocrystalline; the size of coherent scattering region (CSR) is ~ 10 nm.

– When the La concentration in the diffraction patterns increased, the reflections shifted towards smaller 2θ values. A systematic displacement of the positions of maxima is a signature of formation of solid solutions.

– The forming solid solution has a fluorite structure and occupies an area of ~ 7 to 16 at. % La. At a La concentration of 18 at. % a film with a pyrochlore structure ($La_2Hf_2O_7$) forms.

– The film with a La content of ~ 30 at.% is biphasic and consists of $La_2Hf_2O_7$ and α-La_2O_3.

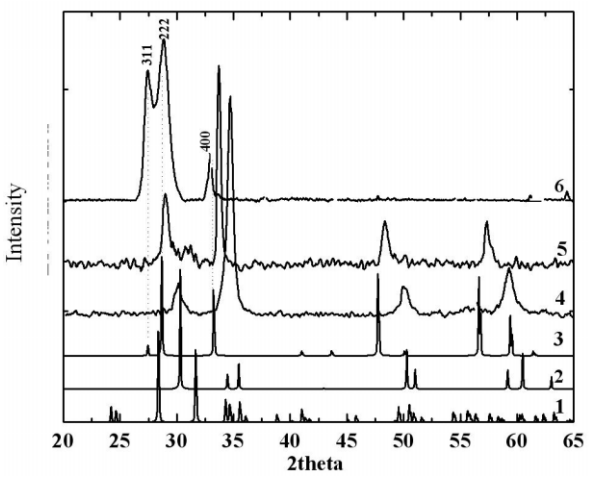

Fig. 6.2.12. Calculated and experiment X-ray patterns: 1 - HfO_2 (monoclinic structure, ICDD PDF-2 No.070-2831); 2 - HfO_2 (cubic modification, ICDD PDF-2 No.070 28312); 3 - $La_2Hf_2O_7$ (pyrochlore structure, ICDD PDF-2 No.037-1040); 4, 5, and 6 - diffractograms of films with La concentrations of 4, 11, and 18 at.%, respectively.

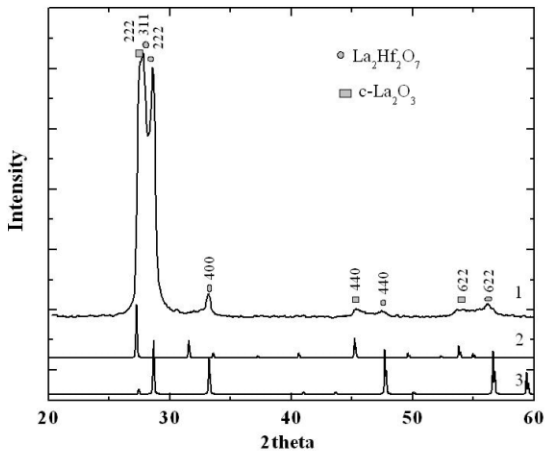

Fig. 6.2.13. Comparison of diffractogram of film with La concentration of 30at.% (1) with powder patterns of □-La_2O_3 (2- ICDD PDF-2 No.004-0856) and $La_2Hf_2O_7$ (3- ICDD PDF-2 No.037-1040).

Station "Precision diffractometry".

Works performed at the station:

1. Analysis of the structural stability of systems $LaCa_x(Fe,Co)_{(1-x)}O3$ (x= 0 – 0.7), $LaMn_xFe_{(1-x)}O3$(x = 0.2 – 0.8) under vacuum in the temperature range of 25 - 900 ° C;
2. Regeneration of catalytic systems with Cu, Ni, and Mo oxides on Al_2O_3 substrate in hydrogen stream in the temperature range of 25-700 ° C;
3. Analysis of autooscillating reactions of the CH_4/O_2 system on nickel in various conditions (partial pressure, temperature, and relative content of reactants);
4. Analysis of the response of oxide systems with high oxygen mobility $Pr_{(2-x)}NiO_4$(□=0-0.3) to changes in oxygen partial pressure at various temperatures;
5. Analysis of the response of the oxide system with oxygen high mobility $Ba_{0.5}Sr_{0.5}Co_{0.8}Fe_{0.2}O_3$ to changes in oxygen partial pressure at different temperatures;
6. Analysis of the structural and phase changes in polymer-carbon nanocomposites near the melting point of the polymer;
7. Analysis of combustion of aluminum nanopowder in air;
8. Analysis of Co reduction in the Co-Al system in hydrogen stream.

***In Situ* X-ray diffraction research on the relaxation of the crystal structure of $Pr_{2-x}NiO_{4-\delta}$ (x=0.0 – 0.3) oxides because of loss of oxygen.**

Mixed electron-ion conductors of K2NiF4-type structure, namely nickelates $Ln_2NiO_{4\pm\delta}$ (Ln=La, Nd, and Pr), have high oxygen mobility and high activity in the reaction of dissociative adsorption of oxygen. In this context, they are of some interest as cathodes for moderate-temperature fuel cells and oxygen-conductive membranes. Among the nickelates, praseodymium-containing oxides have the highest coefficients of chemical oxygen diffusion. Namely the scarcity of data on the oxygen conductivity of these systems with varying oxygen chemical potential made them objects of study.

The starting oxides $Pr_{2-x}NiO_{4-\delta}$ (x = 0.0 – 0.3), hereinafter referred to as PNO-(2-x), were synthesized at the Laboratory for Deep Oxidation Catalysts of the Institute of Catalysis using an original method of polymerized ester precursors (the Pechini method). Fine powders of the oxides were compressed into tablets with diameter 12 mm and thickness 1.5 mm and then annealed in air at 1300 ° C for one hour until reaching 92 - 96 % of the theoretical density. For ensuring of desired reproducibility of properties, after annealing the samples were rapidly cooled in air to room temperature.

The oxygen mobility of the samples was investigated in a high-temperature X-ray flow reactor chamber Anton Paar XRK-900 and apparatus for mixing gases. The experiments on relaxation included several stages. First, the samples were heated to the desired temperature in a flow of N_2/O_2 mixture with the initial pO_2 ~ 0.2 atm with a rate of 15ºC/min. When this temperature was reached, the sample was kept for some time in these conditions, until it attained equilibrium state. Then pO_2 in the mixture was changed to 0.01 atm, and relaxation of the sample structure was observed. Diffractograms were recorded using the position-sensitive parallax-free detector OD-3M. The detectable range of diffraction angles was ~ 48 ÷ 79 °. The radiation wavelength was determined by a single reflection from the monochromator crystal Ge(111) and was 1.7239 Å.

From the X-ray diffraction data, all the starting samples were single-phase systems with orthorhombic symmetry (space group Fmmm), the symmetry of the samples in-

creasing to tetragonal (space group I4/mmm, Fig. 6.2.14) in heating in an atmosphere with $pO_2 \sim 0.2$ bar. In the relaxation the symmetry of the samples did not change.

A typical relaxation curve is shown in Fig. 6.2.15 with the normalized unit cell volume V_t/V_∞, i.e. the ratio of volume at a time t to the equilibrium one, taken as a parameter. The data were processed in the approximation of infinite plate model, in which the normalized relaxation curves were described by the following equation:

$$\frac{V - V_0}{V_\infty - V_0} = 1 - \sum_{n=1} \frac{2L^2}{\beta_n^2(\beta_n^2 + L^2 + L)} \exp\left(-4\beta_n^2 t D_{chem}/l^2\right) \quad (6.2.)\ 1$$

$$L = lk_{chem}/2D_{chem}\ ,\ \beta_n \tan(\beta_n) = L \quad (6.2.)\ 2$$

where V is the unit cell volume; t is the time; l is the effective depth of radiation penetration in the sample; indices 0 and ∞ indicate the initial and equilibrium states of the sample, respectively; D_{chem} and k_{chem} are the chemical diffusion and surface exchange coefficients, respectively. Evaluation of the chemical diffusion coefficient at 470 ° C gives $\log(D_{chem}) = -4.8 \pm 0.3$, which is close to the values obtained by mass relaxation of the sample.

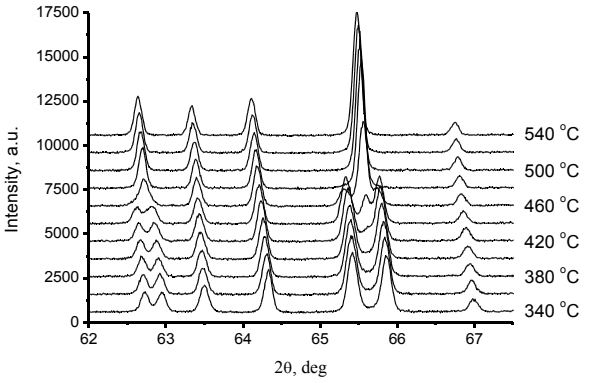

Fig. 6.2.14 Diffractograms of PNO-1.8 in heating in an atmosphere with $pO_2 \sim 0.2$ atm; the wavelength is 1.7239 Å.

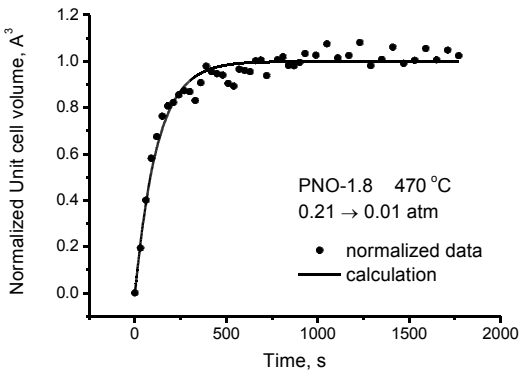

Fig. 6.2.15. Relaxation curve of normalized unit cell volume for PNO-1.8 sample with varied pO_2; the solid line shows the calculated curve for determination of the diffusion and surface exchange coefficients.

"*In Situ* analysis of auto-oscillations in reaction of methane oxidation on nickel by methods of X-ray diffraction."

At the station "Precision diffractometry" of the SCSTR, researchers were investigating *in situ* the auto-oscillations in methane oxidation on nickel by X-ray diffraction. The station was equipped with a system for gas puffing with a gas flow regulator (GFR) Smart-Trak 50 (Sierra) and a mass spectrometer SRS UGA-100 to analyze the gas phase composition at the outlet of the high-temperature X-ray reactor chamber XRK-900 (Anton Paar). Arrangement of the installation is shown in Fig. 6.2.16.

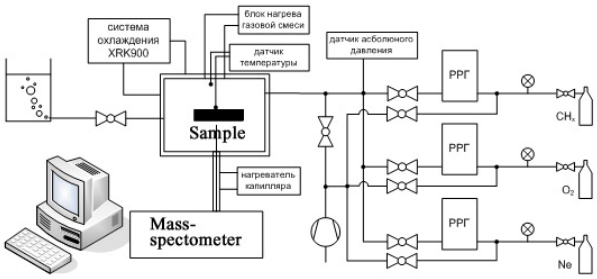

Fig. 6.2.16. Arrangement of installation with reactor camera XRK-900 for *in situ* XRD research and mass spectroscopy.

The application of *in situ* X-ray diffraction made it possible to show changes that occur in the chemical and phase composition of catalyst surface layer in auto-oscillations. Typical diffraction patterns are shown in Fig. 6.2.17. It was found that nickel in the surface layer is in the metallic state when in high-activity state, while transition to low activity is accompanied by formation of a NiO layer on the surface. Analysis of the gas mixture leaving the reactor shows that in the active half-period the reaction is mainly partial oxidation of methane to CO and H_2 with byproducts of CO_2 and H_2O.

Thus, this research has clearly shown that occurrence of auto-oscillations in catalytic oxidation of methane is determined by periodic oxidation/reduction of nickel.

6.2.4. Station "X-ray fluorescence analysis".

The station is intended for determination of the elemental composition of samples of different origin –geological rocks, biological tissues, aerosols, etc. – by XFA elemental analysis using synchrotron radiation (SR XFA). The elemental analysis can be implemented both in a local and a scanning mode.

Participating organizations:

- Sobolev Institute of Geology and Mineralogy SB RAS, Novosibirsk,
- Vinogradov Institute of Geochemistry SB RAS, Irkutsk,

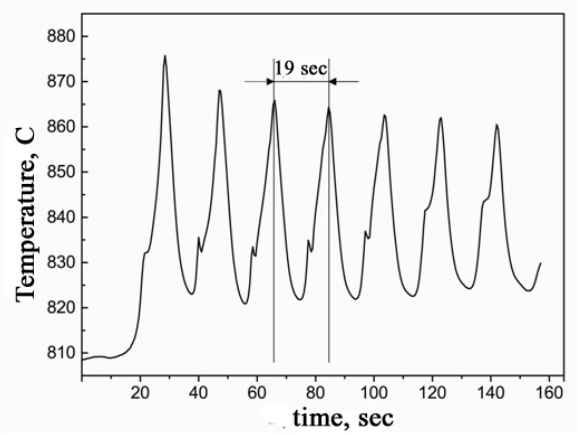

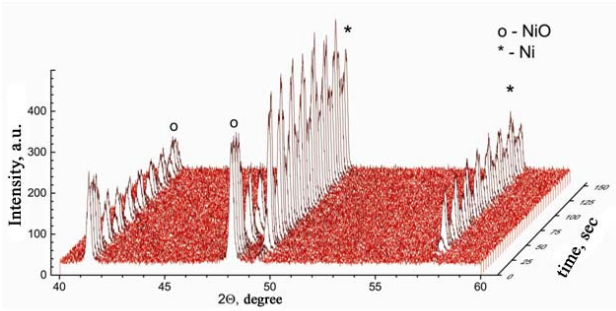

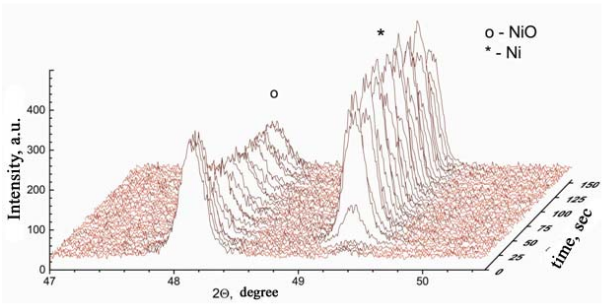

Fig. 6.2.17. Catalyst temperature oscillations observed during oxidation of methane on nickel and co-corresponding changes in X-ray patterns.

- Budker Institute of Nuclear Physics, SB RAS, Novosibirsk,
- Institute of Solar-Terrestrial Physics SB RAS, Irkutsk,
- Institute of Biophysics SB RAS, Krasnoyarsk,
- Sukachev Institute of Forest SB RAS, Krasnoyarsk,
- Institute of Archaeology and Ethnography SB RAS, Novosibirsk,
- Nikolaev Institute of Inorganic Chemistry SB RAS, Novosibirsk,
- Voevodsky Institute of Chemical Kinetics and Combustion SB RAS, Novosibirsk,
- Institute of Internal Medicine SB RAMS, Novosibirsk,
- Institute of Plant and Animal Ecology UB RAS, Ekaterinburg.

In 2013, the works carried out at the stations had financial support of the following projects:

- SB RAS Presidium Interdisciplinary integration project No. 34 "Cyclicity in bio-geological sedimentation systems of Central Asia in the Holocene absolute time-line: global response of Sun-Earth relations"
- RFBR No.13-05-00871_A "Natural climatic cycles in lithological and geochemical characteristics of tape clays of Central Asia lakes "
- RFBR 13-06-00782 "Comprehensive study of the Xiongnu culture articles in elite and ordinary combs in Northeast Mongolia and Transbaikalia"
- SB RAS Presidium interdisciplinary integration project No. 50: "Reconstruction of year-to-year dynamics of glaciers of Eastern Siberia over the past millenniums based on the study of bottom sediments of proglacial lakes and terrestrial sections"
- SB RAS Basic Research Program for 2013 - 2016 Research project V.46.5: "Research on physicochemical processes in formation, distribution, transformation, and migration of dispersed substances in environmental medium"
- RFBR No. 12-05-31324 «Research on the regularities of distribution of uranium and phosphorus in sediments of Lake Baikal, oceanic ferromanganese nodules and sediments of Uzon caldera for identification of short-period climate oscillations (by nuclear-physical methods of analysis)"
- RFBR No. 12-05-00057 «Natural analogues of cement clinker: mineralogy, geochemistry and hydration and corrosion processes"
- SB RAS Programs "Substitution of import" 2013, project 54 "Scanner with high spatial resolution based on polycapillary optics for XRF analysis."

Examples of works in 2013:

Search for natural cyclicity in lake sedimentation systems for medium-short predictive models of climate dynamics.

The promising character of this research area can be exemplified by earlier works on lake Teletskoe (the Altai Mountains). A climate dynamics prediction function based on the identified cyclicity was created in 2010 for the next decade. These estimates turned out to be in good agreement with the actual changes in the temperature in the region in 2010-13.

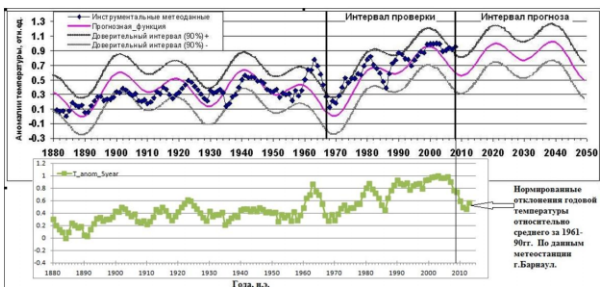

Fig. 6.2.18. Prediction of year-to-year temperatures changes from natural periodicity of paleotemperature reconstructions in the Altai Mountains region as compared with actual meteorological data in 2009 to 2013.

For analysis of distribution of geochemical indicators over bottom sediment cores, their composition was measured with a step corresponding to 1 year in the timeline. The resulting time series were processed by mathematical methods with the aim of finding natural cycles with periods ranging from 3-5 years up to 1000 years.

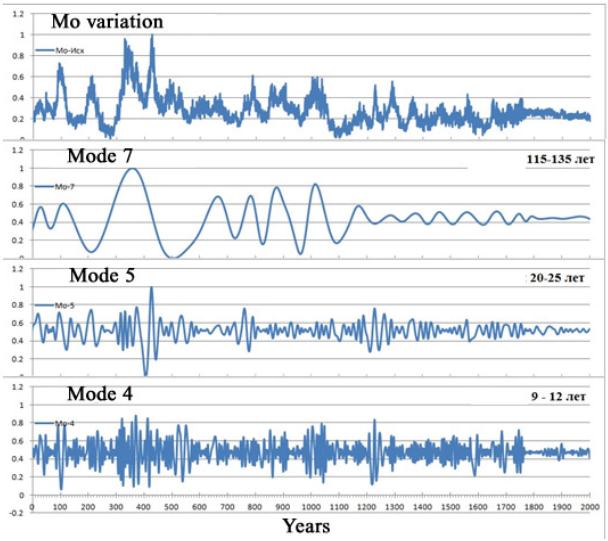

Fig. 6.2.19. Profile of Mo content variations in core of sediments of lake Telmen in the time period from 0 to 2000 AD and empirical modes describing cycles with periods of 120, 20 and 10 years separated by the Hilbert-Huang method [Huang, Wu, 2008].

Analysis of seasonal precipitation in lakes with annually-laminated (varve) sediments.

Varve lakes Shira and Bele in Khakassia were the main objects of the analysis. The annual layer thickness in the studied samples ranged from 0.3 to 2 mm. Detailed scanning was conducted both at the elemental analysis station of the SCSTR using X-ray optics and at the micro-Spot station (BESSY, Berlin). The results obtained made it possible to construct a model of the annual sedimentation cycle, to find indicators that mark the beginning and end of the cycle and to reveal basic links of the sediment structure and composition with weather-and-climate parameters of the environment.

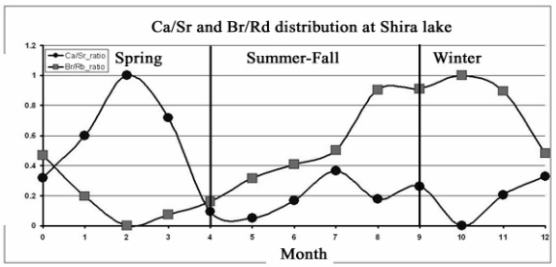

Fig. 6.2.20. Geochemical indicators marking the beginning (Ca/Sr) and end (Br/Rb) of annual layer in sediments of lake Shira, from experimental measurements of distribution of micro-elements within 16 annual layers. The step of scanning is 20-50 microns.

A time model for sediments containing annually-laminated layers is built either by direct counting of all visual layers (optical sections) or based on estimates of the average rate of sedimentation for several intervals of core. The results are then verified by data of isotope studies (^{137}Cs, ^{210}Pb, ^{14}C, and ^{32}Si). We also used geochemical markers. Fig. 6.2.21 presents an example of time model for modern sediments of Lake Shira that was built by geochemical markers.

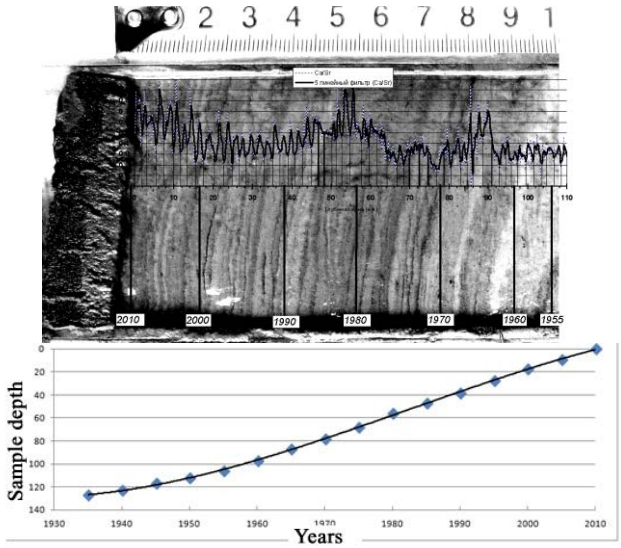

Fig. 6.2.21. Above: counting of annual layers by geochemical marker of Ca/Sr ratio in core of sediments of Lake Shira. Below: time model for the interval of 0 - 140 mm.

The absolute timescale, exact separation of annual layers and detailed intra-year analysis allow finding quantitative relationship of regional climatic parameters and lithological and geochemical properties of sediments.

Comprehensive study of the Hsiung-nu culture media.

We used the SR XFA method to analyze 41 samples of hair strands from mound 22. Extremely high content of Cu was found in all hair samples, as well as high content of Hg. Copper concentration in the hair varies in the wide range from 750 to 20,000 μg/g. Most of the hair (35 out of 41 samples) has a copper concentration of 1,050 to 4,700 μg/g. Copper concentration in the rest 6 samples is significantly higher (9,300; 7,200; 7,100; 8,400; 9,300; 20,000 μg/g), which may indicate a close contact with copper objects.

The mercury content in the hair also varies in a wide range, from 2.3 μg/g to 1,100 μg/g. In 6 hair samples the Hg concentration is 4.8, 3.9, 4.8, 2.3, 5.9, and 5.2 μg/g, which is 2-5 times higher than in the clay taken from the burial. The rest 35 samples have even higher mercury concentration: 20 samples contain mercury in the range of 10-100 μg/g; and the rest 15 samples, 100 to 1,000 μg/g. It follows from the collected data that the hair contains much more mercury than the clay the hair was taken from. In most samples (86%) the mercury concentration is

2-3 orders higher as compared with the clay (1.1 μg/g). Consequently, the clay in the mound could not be a source of mercury in the hair.

In general, the data obtained as well as some literature data indicate the exogenous character of accumulation of copper in hair samples, which can be associated with the presence of various bronze and copper articles in the burials.

Reconstruction of year-to-year dynamics of glaciers in Eastern Siberia over last millenniums from data on bottom sediments of proglacial lakes and terrestrial sections.

The distribution of elemental composition of cores from proglacial lakes adjacent to the glaciers of the Kodar and Baikal mountain ranges and the East Sayan Mountains was investigated. That allowed determination of the pattern of ice slurry arrival because of the response of the hydrological balance in the glaciers to climate change over the past 400 years. The lowest intensity of the ice slurry arrival was in 1700 - 1770 and 1945 - 1960, which may indicate low ablation of glaciers in these periods. The greatest amplitude of hydrological balance oscillations was observed in Sygyktinsky glacier (the Kodar range); the smallest one, in the glacier of Cherski mountain (the Baikal range). Records show a stable trend towards increase in the intensity of their deglaciation in the 2000s.

Instrumental measurements of the temperature regime near Peretolchin glacier showed the minimum temperature to stay practically unchanged, while temperature variations increased 2-fold, which indicates transient climate regimes. This is confirmed by glacial and climate phenomena in the area of Peretolchin glacier. Year 2012 was abnormally unfavorable for processes of glaciation; the glacier significantly shrank, especially in thickness, and crashed into fragments, having exposed ridges of recent terminal moraines. Year 2013 was abnormally favorable for nival-glacial processes – the glacier almost kept its winter forms, and areas that were exposed last years were filled with snow and ice masses. This may be a manifestation of transitional weather patterns in the middle of the interglacial period. A new singular rock glacier (flow) was found in the mountain-taiga area of Munku-Sardyk landmass.

Analysis of the role of atmospheric aerosols in migration of chemical elements in tissues of living organisms and in the environment media.

Works to identify the content of a set of chemical element in atmospheric aerosols and environment and their relationship with human health parameters were continued within studies of migration of dispersed substances in the environment.

Collaborative research with the Institute of Internal Medicine SB RAMS showed that the senile age (80 - 89 years old) and cardiovascular diseases are associated with excess of certain chemical elements (Ca, Fe, Cu, Zn, Br, and K) and decrease in Se and Zr in the blood of patients.

Analysis of bottom sediments in thermal lakes of the Uzon caldera.

Non-destructive layer- scanning yielded distributions of chemical elements along the profile of sediment cores from thermal lakes "Fumarole", "Chloride ", "Sizogo kotla". Most elements have irregular distribution over a section; there are peak concentrations that may differ from the section-average values 4 to 5-fold. Such elements as Ca, Sr, As, Sb, C, S, and Zn are the emost interesting in terms of their concentration non-uniformity; especially Cs, the concentration of which increases abruptly more than 5-fold at a depth of 27.5 cm. Data obtained by the SR XFA method correlate well with atomic absorption results.

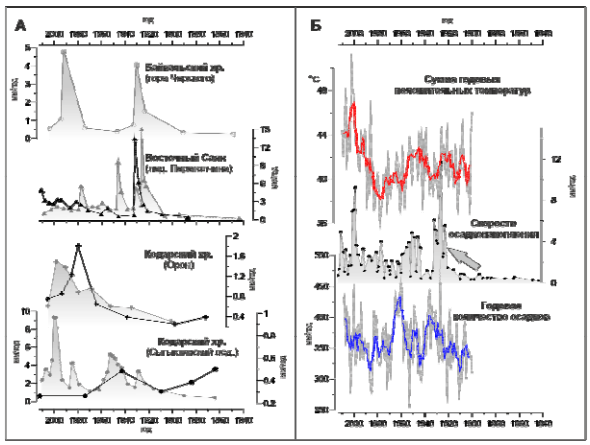

Fig. 6.2.22. А - distribution of sedimentation rates (SRs) in proglacial lakes, Б – comparison of common SRs with average climatic parameters of the region.

The behavior of zinc content against depth is worth special mentioning. It is a monotonically increasing function with a mean zinc concentration of 70 ppm and three "point" maxima, consisting of really one point each. As the scanning step was equal to 1 mm, one can conclude that the anomaly that is responsible for the high zinc content has negligible geometric dimensions, not exceeding 0.1 mm in vertical. The micro-particles are easily detectable by the SR XFA method.

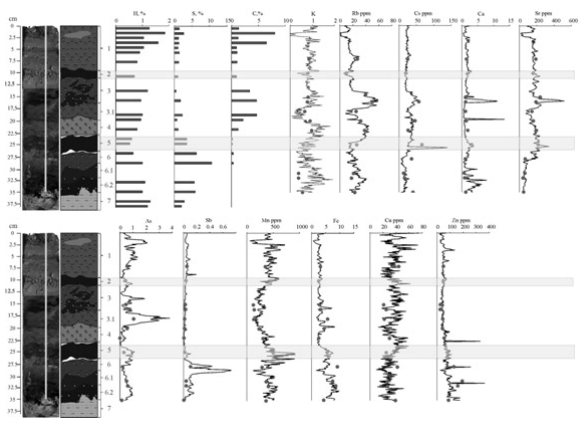

Fig. 6.2.23. Distribution of chemical elements along SR XFA profile of core sediments from lake Fumarole.

Research on natural analogues of cement clinker.

The features of phase formation and fractionation of P, S, Se, F, Br, I, Li, Na, K, Sr, Ba, Zr, Ti, V, Cr, Ni, Cu, Zn, and U in the processes of natural calcination of mixtures of phosphate-silicate-carbonate rocks were determined; elements were identified that contribute to long-term stabilization of the clinker minerals.

Comprehensive analysis of natural pirometamorphic rocks – analogues of sulfoaluminate cement clinkers – revealed the features of the phase formation and fractionation of elements between mineral phases. Experimental and technological simulation of these features would have required much time and money. Large (as compared with man-made products) dimensions of mineral components of natural analogues of sulfo-cement clinker made it possible to quantitatively characterize features of fractionation of these 20 elements during calcination of complex raw-material mixtures. This approach offers the possibility of cement production from natural raw materials of complex phase composition.

Creating scanner with high spatial resolution based on polycapillary optics for XFA.

A scanner with high spatial resolution based on polycapillary optics is needed for research of sediment cores by X-ray fluorescence elemental analysis. Analysis of the elemental composition of lake sediments is necessary for determination of patterns of change in the relative element content in dependence on the surrounding conditions. The high spatial resolution provided by the polycapillary optics and mechanical characteristics of the scanner are required for most complete determination of these patterns and their comparison with other indicative characteristics, which will allow deciphering "paleoclimatic records", resolving the boundaries of changes in climatic conditions, and revealing lower-order fluctuations within individual periods of cooling/warming.

A prototype scanner was developed and put into operation at the experimental station SR XFA. Tests showed the spatial resolution of the X-ray optics system to be less than 10 microns.

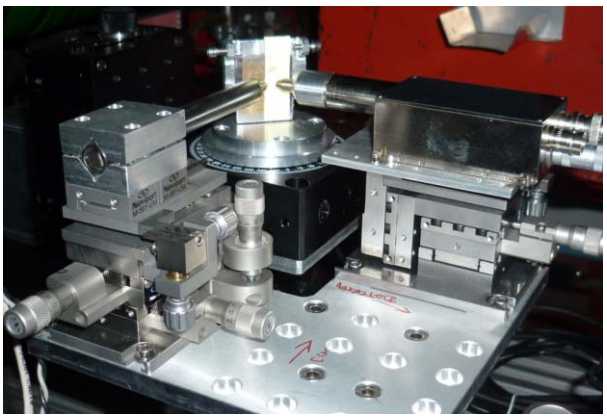

Fig. 6.2.24. Scanner with high spatial resolution at the station SR XFA.

6.2.5. Station "Hard X-ray diffractometry".

The station is intended for hard X-ray diffraction research on the structure of substances.

Participating organizations:

- Institute of Solid State Chemistry and Mechanochemistry SB RAS;
- Institute of Geology and Mineralogy SB RAS;
- Budker Institute of Nuclear Physics SB RAS;
- Institute of Catalysis SB RAS;
- Institute of Metal Physics UB RAS.

In 2013, works on the station were supported by the following projects and contracts:

- RAS basic scientific research program "Petrology, mineralogy and geo-chemistry of metamorphic rocks formed at different P-T parameters, fluid regime and geodynamical conditions (exemplified by Central Asia)", 2012-2014;
- RFBR project 11-05-01121-a, "Dynamics of lattice of microporous minerals during their interaction with water medium at high pressures", 2011-2013;
- RFBR project 12-05-31431-a-mole "Source of potassium in subducting oceanic lithosphere and its behavior during subduction metamorphism " 2012-2014;
- RFBR project 12-05-00841-a "Conditions for stability of hydrocarbon compounds at high pressures and temperatures and their implications for deep structure of the Earth and the planets", 2012-2014;
- RFBR project 13-05-00185-a, "Mechanisms of formation and stability of water-containing high-baric silicates of the MgO-SiO2-H2O system under conditions of subduction of the oceanic lithosphere" 2013-1015;
- RFBR project 13-05-00457-a "Microporous aluminosilicates at high pressure: the influence of framework topology and extra-framework subsystem composition on the compressibility and structural transformations" 2013-1015;
- RF Government Grant No. 14B25.31.0032 "Experiments on matter at ultrahigh pressures and creating harmonized thermodynamic model of deep structure of the Earth" (headed by D.Sc. K.D. Litasov at IGM SB RAS, Prof. E. Ohtani at Tohoku University, Japan). 2013-2015;
- State contract No.14.513.11.0056 "Development of scientific and technical basics for production of nanoprecursors and radiation-thermal synthesis of ferrite ceramics for electronics and instrument engineering using intense electron beam with energy up to 5 MeV and synchrotron radiation methods for analysis of products."

Examples of works in 2013:

1. Analysis of stages of phase formation in chemical interaction of metals, alloys and their mechanocomposites with melts of other metals and alloys.

The aim of the work is to study the physical and chemical interaction between solid-state metals, alloys, and mechanocomposites with melts of metals and alloys. Currently, there is no consistent theory for such interac-

tions. *In situ* X-ray diffraction analysis with "hard" (photon energy 33.7 keV) synchrotron radiation will be used for analysis of the processes of phase formation in systems with nickel and its alloys with tin-based melts. Accumulation of experimental data will allow developing an approach to a theory of physical and chemical interactions in different "solid metal - liquid metal" systems. Such a theory would allow a focused approach to the creation of new materials. Interest in the research on the stages of phase formation in the nickel-tin system is caused by the fact that intermetallic compounds of nickel and tin can be used as anode elements in lithium batteries. Furthermore, understanding the processes of interaction of nickel with lead-free tin-based solders is also very important for the electronics industry.

The samples were prepared by repeated rolling of nickel powder or nickel-based solid solution with tin foil or tin-based alloys.

Analysis of the staging of phase formation in a mixture of nickel powder and tin foil of equiatomic composition showed that the formation of the Ni_3Sn_4 intermetallic begins after melting of tin. An intermetallic compound arises, with maximum content of the low-melting component, Ni_3Sn_4. Heating to 380°C begins transition to the Ni_3Sn_2 phase, which ends in 2 hours at a temperature of about 600 ° C. Interaction of tin with nickel and tin mechanocomposite goes in the same way as the interaction of nickel and tin, with the exception of origin of a small amount of the Ni_3Sn phase. No full transition of Ni_3Sn_4 to Ni_3Sn_2 occurs.

It should be noted that the interaction of nickel and tin occurs at temperatures above the melting point of tin; no halo from the liquid phase is observed in the diffractograms. Perhaps, this effect is due to the presence of degenerate eutectics in the system, and the intermetallic compounds in the Ni-Sn system form via nickel dissolving in a thin layer of eutectic melt, where the crystallization occurs.

The interaction of nickel with alloy of tin and eutectic-composition indium was investigated. When the sample is heated above the melting temperature, a rapid increase in the β phase from the In-Ni system is observed. The β phase contains 56 at. % indium (on average) and exists in the temperature range of 950 - 770 ° C. Further heating to 160°C leads to origin of the In_7Ni_3 phase and extinction of the β phase. With heating above 400°C, there is observed formation of the In_3Ni_2 phase. No tin-containing phases were detected. One can assume that tin is in the structure of phases formed on the basis of indium and replaces indium in the lattice.

The interaction of copper with alloy of tin and eutectic-composition indium was investigated. The samples were prepared three years ago by repeated rolling of indium-tin foil and copper powder. Emergence of a new, unknown phase was recorded in a sample, in addition to the pre-existing phases of copper, In_3Sn and $InSn_4$. When the sample is heated up to 100°C, reflections from this phase disappear. Thus, using eutectic compositions and various mechanocomposites, one can produce materials of new properties.

2. Compressibility and structural behavior of naphthalene, a model compound of polycyclic aromatic hydrocarbons, at 0-6 GPa.

The interest in these compounds is associated with their presence in the deep matter of the Earth (inclusions in the mantle minerals) and meteorites, on the one hand, and insufficient knowledge of their behavior at high pressure. The obtained diffraction data show regular compression of the naphthalene structure and conservation of the original monoclinic phase (spatial group $P\ 2_1/c$) till 6 GPa. The pronounced anisotropy of the compression (Fig. 6.2.25) is due to the difference in the orientation of $C_{10}H_8$ molecules within and between the layers that form a "herringbone" structure in Fig. 6.2.26. The naphthalene structure, including the coordinates of hydrogen atoms, was refined by the Rietveld method. In the investigated range of pressures, the intra-molecule distances C-C and C-H decrease by 3.5%, whereas the intermolecular distances within and between the "herringbone" layers decrease by 18 and 10 %, respectively. The dependence of the interlayer distances on pressure (Fig. 6.2.26) has a distinct inflection at 2 GPa, and with further pressure increase their compressibility is greatly reduced due to the approach of hydrogen atoms of neighboring molecules. Intermolecular distances within the layers are, in contrast, reduced regularly throughout the pressure range. This implies a change in the structural compression mechanism towards dominating reduction of intermolecular distances within the layers at $P > 2$ GPa. Structural abnormalities that are observed at 2 GPa are consistent with the high-frequency shifts of some lattice naphthalene phonons associated with librational oscillations of molecules and C-H valence vibrations, which were observed in this pressure range.

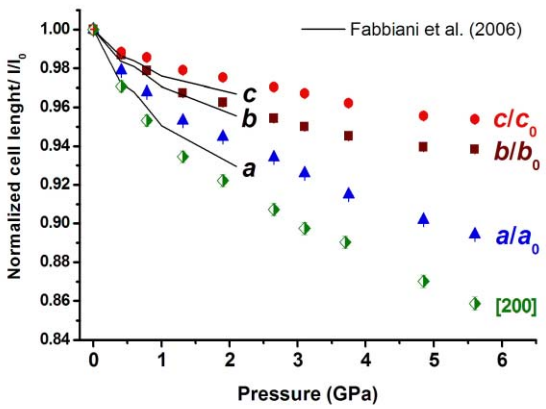

Fig. 6.2.25. Pressure dependence of parameters of naphthalene unit cell (spatial group $P\ 2_1/c$) as compared with literature data.

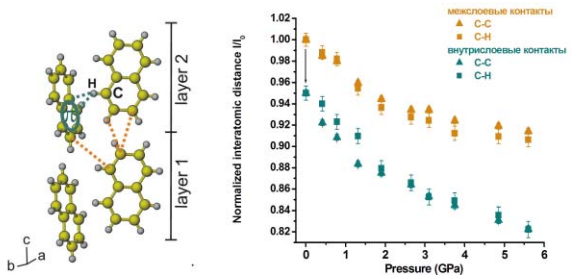

Fig. 6.2.26. Naphthalene structure with marked intralayer (green) and interlayer (orange) intermolecular contacts and dependence of their distances on pressure.

3. Radiation-thermal synthesis of nickel-zinc and manganese-zinc ferrite ceramics.

Experiments were conducted on the SR diffraction, as well as phase analysis of the products of radiation-thermal synthesis of ferrite ceramics of the $(Ni_{0.75}Zn_{0.25})Fe_2O_4$, $(Mn_{0.6}Zn_{0.4})(Fe_{0.75}Mn_{0.25})_2O_4$ and other compositions, obtained in different modes of industrial accelerator ILU-6. Dependencies of the degree of transformation on the synthesis temperature, beam pulse power and time of exposure were constructed. Kinetic curves of *ex-situ* synthesis of nickel-zinc ferrite under an intense 2.4 MeV beam of electrons were built. It was shown that the temperature dependence of the radiation effect is consistent with the active site model of the chemical reaction rather than with the whole-system perturbation model. Analysis of the kinetics of radiation-thermal synthesis of ferrospinels and characterization of the reaction products are presented in published papers.

4. Analysis of the nano-domain structure of highly-oxygen-deficient perovskite-type oxides based on strontium ferrites.

The phase composition and characteristics of the nano-domain state of the strontium ferrite series $SrFe_{1-x}M_xO_{3-\delta}$ (M = V; Mo; x = 0 ÷ 0.2) with high oxygen non-stoichiometry ($2.5 \leq 3 - \delta \leq 2.7$) were investigated. Computer modeling of defect structures and X-ray diffraction on them showed that, the resulting diffraction effects have different characteristics depending on the structure of the nano-domains and extended defects in the structure. Systematic analysis of the experimentally-produced diffraction effects showed that with increasing degree of substitution by highly charged cations and oxygen nonstoichiometry the nano-domains system evolves towards lesser size of the domains and more complicated internal organization of them. The nano-domain states of nonstoichiometric oxides were investigated by unique methods and approaches.

5. Testing of non-standard diffraction methods on SR using two-coordinate detector.

Hard SR and the two-coordinate detector were successfully applied to testing of the following nonstandard diffraction methods:

a) Experimental diffraction patterns of test samples in the range of reciprocal space vectors Q of up to 19 $Å^{-1}$ were recorded, and good-quality radial distribution functions (RDF) of atoms were calculated. As compared with the conventional Bragg – Brentano methods, recording of transmission diffraction patterns with the two-coordinate detector has advantages of non-destructive examination of the structure in the material volume, lenient requirements to the sample volume (up to 1 mm^3), good statistics of diffraction patterns, and relatively small shooting times. In the future, all these qualities will make it possible to investigate the structure of such complex objects as colloid solutions or nanoparticles stabilized in a polymer matrix, which is impossible with the conventional diffractometers.

b) There was also a series of experiments on shooting of thin films in grazing incidence geometry. This method was shown to allow examination of the crystalline structure of thin films ~ 200 microns thick deposited on glass. This structure is indistinguishable in a transmission geometry: peaks from the structure of the film itself are visible on the background of signal from the amorphous glass. Despite the successful testing, this method has few prospects as compared with implementation of grazing incidence geometry on a diffractometer intended for reflection-mode shooting of samples.

6.2.6. Station "Diffraction movies".

The station is intended for time-resolved diffraction experiments, including those at small angles, and general purpose diffractometry.

Participating organizations:

- Institute of Solid State Chemistry and Mechanochemistry SB RAS;
- Novosibirsk State Technical University;
- Institute of Inorganic Chemistry SB RAS
- Institute of Thermophysics SB RAS

Examples of works in 2013:

Characterization of thin films of silicon.

Thin films of amorphous, nanocrystalline, microcrystalline, and polycrystalline silicon are widely used in the instrument engineering and solar power engineering. These films are used as active layers in active-matrix liquid-crystal displays (LCDs), solar cells, etc. The structural properties of the films are important parameters and significantly affect characteristics of such devices. The structural properties of these films are usually investigated using Raman spectroscopy and X-ray analysis, the latter providing more detailed and accurate information about the size of crystallites and their crystallographic orientation. Thin crystalline silicon films on a glass substrate are useful in production of cheap solar cells of large area and high efficiency. There is a promising way of making such films in two steps: 1) high-speed deposition of amorphous silicon films, 2) solid-state crystallization of these films with formation of the necessary degree of crystallinity and crystallite size.

We investigated the solid-state crystallization of amorphous hydrogenated silicon films synthesized by gas-ejection chemical deposition with electron-beam plasma

activation. This method provides high rates (up to 2.3 nm/s) of deposition of thin films from amorphous silicon in a standard vacuum chamber. The films were deposited on quartz substrates and annealed under vacuum at a temperature of 700 °C. We investigated the structural and optical properties of as-deposited amorphous films and the nano-crystal films after annealing.

The crystallite size can be estimated from the broadening of diffraction peaks. Laboratory facilities were found to be unsuitable for these samples because of the low intensity and large divergence of beam and weak scattering power of the thin films. Therefore, the films were investigated on beamline 5b using the one-coordinate detector OD-3M. It would be established in a position with maximum coverage of the diffraction lines of crystalline silicon (2θ ~25 - 56 °). The wavelength was 1.516 A. In view of the already noted weak scattering ability, the sample exposure time was 20 minutes. After normalization, a signal from the clean substrate was subtracted from the diffraction data on the films, for elimination of the background signal (Fig. 6.2.27). Then the diffraction peaks were approximated with Gaussians (Figure 6.2.28). The particle size was estimated by the Debye-Scherrer formula.

Table 6.2.1. Results of processing

Sample	Peak number	Position	Width	CSR, A
TQA2	1	27.90	1.07	83
	2	46.63	2.25	42
	3	54.96	2.11	46
TQA4	1	27.93	1.31	68
	2	46.72	2.67	35
	3	54.9	2.,67	37
TQA6	1	27.9	1.,59	56
	2	46.77	2.87	33
	3	54.92	2.79	35
TQA8	1	27.99	1.46	61
	2	46.79	2.15	44
	3	55.15	2.06	47

It is interesting that for all the samples the CSR size is slightly larger in the (111) plane, which may evidence presence of texturing.

Thus, we measured the dependence of the properties of amorphous (as-precipitated) crystalline (after annealing) films on the deposition temperature in the range of 190 °C to 415 °C. The average crystallite size was measured via X-ray analysis; the degree of crystallinity (59 - 46%) was estimated by Raman scattering. The optical properties and thickness of the films were determined via measurement of the optical transmission spectra. The refractive indexes and optical band gap were measured for both amorphous and nanocrystalline films. The behavior of the refractive index of nanocrystalline silicon in dependence on deposition temperature is correlated with the degree of crystallinity. Thus it was shown that this method can be used for production of nanocrystalline silicon films with a crystallite size of 4 - 8 nm and varying degree of crystallinity.

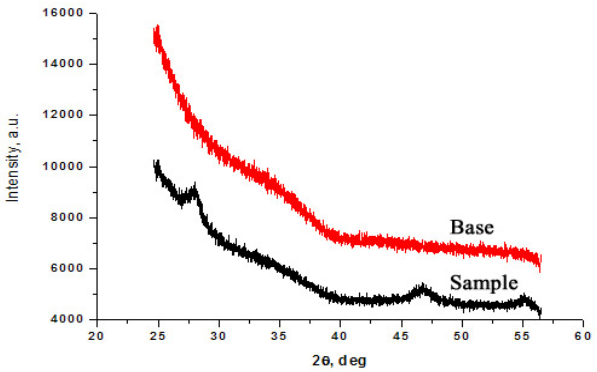

Fig. 6.2.27. Diffractograms of clean substrate (top) and substrate with sample of deposited silicon (bottom).

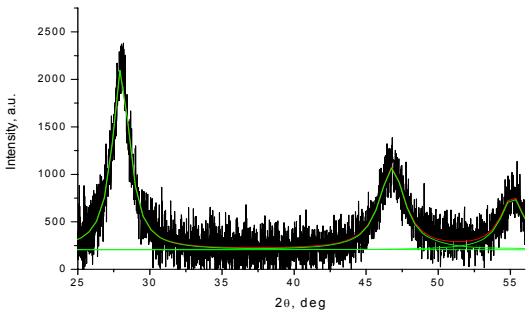

Fig. 6.2.28. Result of subtraction of substrate signal from sample signal and approximation of resulting peaks with Gaussians.

6.2.7. Station "EXAFS spectroscopy".

The station "EXAFS spectroscopy" is intended for recording of X-ray absorption spectra (EXAFS and XANES) of different (usually X-ray amorphous) samples in liquid and solid phase state. The results allow one to determine the electronic structure and parameters of the nearest local environment (coordination number and interatomic distances) of ions of interest, including samples that cannot be investigated by radiographic structural methods.

- Participating organizations:
  - Institute of Semiconductor Physics SB RAS;
  - Institute of Inorganic Chemistry SB RAS;
  - Institute of Solid State Chemistry and Mechanochemistry SB RAS;
  - Siberian Federal University, Krasnoyarsk;
  - Institute of Chemistry and Chemical Technology SB RAS, Krasnoyarsk;
  - Budker Institute of Nuclear Physics SB RAS.

In 2013, works on the station were supported by the following projects and contracts:

- Program No. 24 "Basics of fundamental research on nanotechnology and nanomaterials", project No. 69, "Application of EXAFS and XANES spectroscopy to analysis of microstructure of SiGe quantum rings on Si

(100) surface, GaN/AlGaN quantum dots and AlGaN/AlN superlattices with quantum wells".

- RFBR 12-02-00262-a. Analysis of the microstructure and electronic structure of calibrated clusters of gold in cucurbit[n]urils using XAFS spectroscopy.
- RFBR 11-03-00219-A. Intercalation compounds of complexes and clusters of nickel and copper in cavitand cucurbit[8]uril: chemical experiment, spectroscopic analysis and quantum-chemical modeling.
- Nonequilibrium phase formation in ternary oxide films made by doping rare-earth elements to HfO2.
- Synthesis of AlGaN/AlN structures with quantum dots and analysis of their luminescence and generation properties in excitation with low-voltage electron beams.
- Experiment and theoretical research on the optical, vibrational, structural and electrical properties of heterostructures and nanostructures based on nitrides of group III metals.

Examples of works in 2013:

1. Analysis of the microstructure and electronic structure of calibrated clusters of gold in cucurbit[n]urils using XAFS spectroscopy.

As compared with bulk metals, particles of 10 nm or less in size exhibit new or substantially modified properties, including parameters of the crystal lattice, interatomic distances, mobility of atoms, electronic structure, magnetic, optical and electrochemical properties, and morphology of the surface. The special properties of nano-structures offer unique opportunities for improving already-existing or developing innovative products and nanotechnologies. Gold has always been considered one of the most inert metals. However, it was found recently that in the CO oxidation reaction, gold dispersed to a particle size less than 5 nm exhibits higher catalytic activity than metallic palladium and platinum, which are conventional catalysts in this reaction. The synthesis and analysis of the structure and properties of systems containing metal clusters is associated with key problem of production of nanoparticles homogeneous in size and shape. Thus, it seems very promising if the role of "hosts" for monodisperse metallic "guests" is played by cucurbit[*n*]urils, which are a family of organic molecules $C_{6n}H_{6n}N_{4n}O_{2n}$ (CB[*n*]) with n = 6, 7, and 8 and calibrated cavity sizes d = 5 - 9 Å.

The synthesis of intercalation compounds of nanoparticles of gold in cucurbit[n]urils (n = 6, 7, 8) was performed. Intercalation compounds of metal nanoparticles with CB [7] were synthesized via chemical reduction in water/ethanol solution of chloroauric acid $HAuCl_4 \cdot 3H_2O$ with sodium borohydride ($NaBH_4$). Besides, intercalation compounds of Au@CB[7] were synthesized in aqueous solution (without ethanol) and, for the first time, of Au@CB[6] by a new procedure, in aqueous solution (without ethanol) with addition of $MgCl_2$. Step-by-step synthesis was carried out, through reduction of gold complexes synthesized within cavities of CB[8] and aggregation of Au clusters in them.

The EXAFS, XANES and HERFD XAS spectra of the synthesized compounds were measured in the area of X-ray absorption edges of AuL_{III}. The experimental material was processed using the software packages FEFF 9.0 and DL_EXCURV 98; parameters of the local structure were determined (interatomic distances, local symmetry, partial coordination numbers, and Debye-Waller factors); electronic characteristics were evaluated (charge states of atoms and structure of free electron states) for the system under study, which contains gold nano-particles of calibrated size.

A detailed comparison of the experimental XANES and HERFD spectra of fine-grained samples with the spectra of samples containing larger applied particles of Au and spectra of massive Au showed that, within the accuracy of our experiments (≤ 10%), the spectra are indistinguishable in the initial region. Comparison of the experimental spectra with model calculations by the program FEFF 9.0 suggests that, within our accuracy, the electronic state (in particular, the charge one) of finely-grained gold is also indistinguishable from metallic state.

A comparative analysis of data obtained for intercalation compounds Au@CB[7], Au@CB[6], andAu@CB[8], a reference sample of massive gold foil and finely-dispersed samples that were synthesized earlier by other methods was carried out. The analysis of the experimental data on the finely-dispersed samples revealed that all the samples contain gold in a bidispersed form: 1) fine-dispersion gold inside the cavities of cucurbituril with narrow size distribution, and 2) larger gold particles. For gold clusters inside the cavities of cucurbiturils: 1) CB [7]: coordination numbers $N_{Au\text{-}Au}$ ~ 6; the average Au cluster size d ~ 0.8 nm; 2) CB[6]: $N_{Au\text{-}Au}$ ~ 5, the average cluster size is also less, d ~ 0.7 nm. It was found that gold clusters in the cavities of cucurbiturils CB[7] and CB[6] are characterized by significantly less (by ~ 0.03 Å) interatomic distances and significantly larger (three-fold at 12 K) values of the Debye-Waller factor as compared with massive Au. Thus, it was found that the structural stresses and disordering of the crystal structure become substantial for small gold particles, and this may determine the change in the reactivity of gold when the latter is dispersed.

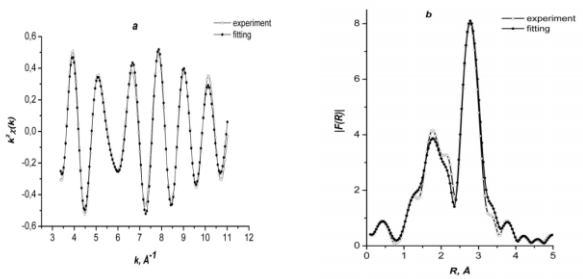

Fig. 6.2.29. Modeled bidispersed system for one of the samples: $k^2\chi(k)$ AuL_{III} EXAFS spectra filtered in the region ΔR = 1.5 – 3.5 Å (a); modules of the Fourier transform of the function $k^2\chi(k)$ AuL_{III} EXAFS (b): ○ - experiment; ● - model calculation.

2. Analysis of the spatial and electronic structure of complex compounds of Fe (II) with pyrazole at temperatures above and below the structural and magnetic phase transitions.

At a certain ligand field force, the coordinate compound Fe (II) with FeN_6 coordination octahedron can exist in two spin states: low-spin (LS) and high-spin (HS) ones. Transition from one spin state to another involves a change in the structure of the complex as the temperature or pressure varies or under light of a specific wavelength. Researchers are always interested in compounds with thermally induced spin transition, because of their practical application, among other things.

Synchrotron radiation (SR) from VEPP-3 at BINP was used for the very first measurement of EXAFS spectra of a number of Fe (II) complexes with pyrazole: 1) $Fe(t(DMPz)M)(tz)_3(NO_3)_2$, 2) $Fe(t(DMPz)M)_2(ClO_4)_2$, 3) $Fe(t(DMPz)M)_2Cl_2 \bullet H_2O$, and 4) $Fe(t(DMPz)M)_2(NO_3)_2$ at temperatures above (~ 300 K) and below (~ 125 K) the temperature of alleged structural and magnetic phase transitions. Analysis of the measured EXAFS spectra yielded description of changes in the molecular and electronic structures of these complexes. Results for some of the samples turned out to be in correspondence with previous results on single-crystal phases; the contribution of these phases into the systems under study was determined.

The $Fe(t(DMPz)M)(tz)_3(NO_3)_2$ sample was found to have a new low-temperature phase; its microstructural characteristics were determined. Thus, only some molecules (~ 50 %) in the $Fe(t(DMPz)M)(tz)_3(NO_3)_2$ sample change their structural characteristics with decreasing temperature and probably turn to the low-spin state. At T ~ 125 K in the spectrum there arise additional features associated with the origin of the distance of 1.97 Å, which is typical to the Fe-N distance in the low-spin complex. A double first maximum is observed in the Fourier spectrum of the transformant. The distance to the second sphere of nitrogen varies slightly at a distance of ~ 3 Å. The microstructure of the first sphere of the neighboring of Fe atoms in the $Fe(t(DMPz)M)_2(ClO_4)_2$ and $Fe(t(DMPz)M)_2Cl_2 \bullet H_2O$ samples did not change in cooling to 125 °C, and the complexes apparently did not change their spin states, because the edge absorption spectra of Fe, the EXAFS spectra and the dependences of the Fourier transformant on the interatomic distances are identical at the two temperatures and correspond to the same structural models. Analysis of the spectra measured for the $Fe(t(DMPz)M)_2(NO_3)$ complex sample and their comparison with model calculations showed that its microstructure changed in the cooling and the complex turned to the low-spin state.

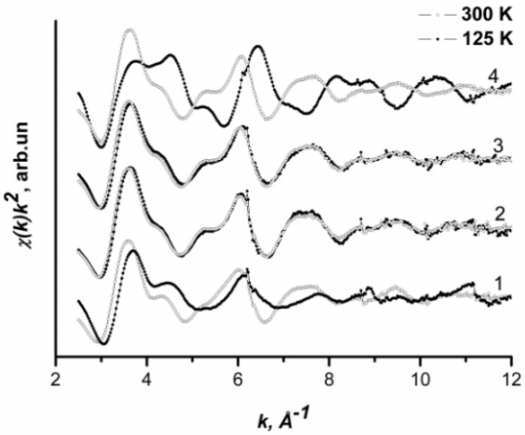

Fig. 6.2.30. Fe K EXAFS absorption spectra for samples of Fe (II)- pyrazole complexes 1-4: at temperatures above (300 K; -○-) and below (125 K; -●-) the temperature of the structural and magnetic phase transitions.

3. Microstructure of SiGe quantum rings, GaN/AlGaN quantum dots and superlattices with quantum wells from EXAFS and XANES spectra.

Switching to the optical methods of generation, transmission and reception of signals is a promising way to increase the rate and volume of data transmission. Its implementation requires effective and fast photonic equipment, including photodetectors and modulators of radiation operating at wavelengths in the near and medium IR spectral ranges. Such devices are necessary for creation of terabit optical fiber communication systems, on-ground communication with flying and space objects, registration of the radiation dynamics of atomic, molecular and solid-state systems, and in chemical and biological sensors. As concerns high-speed terahertz photonic devices, heterostructures based on gallium nitride have good prospects due to the very strong electron-phonon interaction in these ionic materials, which provides femtosecond times of recovery to the initial state, which is much faster than in other semiconductors. The large band offsets in the conduction band of the GaN/AlGaN heterostructures (2 eV in the GaN/AlN heteropair, which is a record for semiconductor heterostructures) allow designing of electrooptical switches and photodetectors on intersubband electronic transitions in quantum wells or quantum dots for the middle and near IR spectral ranges, up to 1.3 microns. Ring-like structures (quantum rings (QRs)), i.e. quantum molecules consisting of a few immediately adjacent quantum dots (QDs) of SiGe on the Si (100) surface, also exhibit some interesting electronic and optical properties, which are very promising for application to nano- and optoelectronics.

GaN/AlN multilayer superlattices with a number of periods of up to 300 and extremely narrow (to 1 nm) quantum wells (QWs) were synthesized by the MBE method, as well as ring-like structures (quantum rings (QRs)) con-

sisting of closely spaced several quantum dots (QDs) of SiGe in the Si(100) surface.

The synthesized nanostructures (QWs, QDs, and QRs) were characterized by atomic-force scanning microscopy (ASM), high-resolution transmission electron microscopy (TEM), small-angle scattering (SAXS) and photoluminescence (PL).

EXAFS and XANES spectra of the synthesized systems were measured near the K-absorption edges of Ge and Ga at the EXAFS station on the synchrotron radiation (SR) beamline on VEPP-3 (BINP). Local structure parameters (interatomic distances and partial coordination numbers) were determined; the influence of the growth conditions and morphology of the synthesized systems on the interlayer diffusion, stresses and relaxation in the nanostructures and their optical properties were investigated.

The growth conditions and the thickness of the superlattices were found to influence the mixing in the border layers, deformations, stresses and optical properties of GaN/AlN. It was revealed that more intense luminescence peaks shifted towards the short-wave side are typical to samples with more appreciable mixing at the interfaces. A substantial decrease in the Ga-Ga interatomic distances (~ 0.03 – 0.04 Å) was found in samples with "thin" superlattices (20 - 40 layers) and extremely small (~ 1nm) thicknesses of GaN and AlN layers, which evidences substantial deformations and stresses in the layers. A minimum decrease (~ 0.01 Å) in Ga-Ga interatomic distances R(Ga) was found in multilayer samples with "thick" superlattices (130 - 260 layers), which agrees with the observed plenty of dislocations and the corresponding stress relaxation in the GaN layers. In samples with "thin" superlattices and extremely thin layers of GaN and AlN, the dependence of the interatomic distances and coordination numbers on temperature was determined. In such systems, the Ga-Ga and Ga-Al distances are close to those typical to solid solutions, except for certain differences associated with the nonequilibrium of the systems under study. When the synthesis temperature is increased from 800 °C to 900 °C, the Ga-Ga and Ga-Al distances decrease somewhat with augment in the Al coordination numbers, as it occurs in equilibrium solid solutions with increase in the Al concentration. With temperature increased from 800 °C to 850 °C and then to 900 °C, the Ga-Al mixing in the boundary layer amounted to 25, 30, and 35 % , respectively.

It was found that in the first stage of growth of SiGe quantum rings (application of a Si/Ge seed layer at ~ 700 ° C), the Ge concentration is ~ 25%. With further growth (application of the basic layer), the Ge concentration increases up to 35-45% depending on the temperature (610-550 °C). In the investigated samples, with the molecular formula Ge_xSi_{1-x} ($0.25 < x < 0.45$) the Ge-Ge and Ge-Si interatomic distances correspond to the values found for solid solutions and Ga/Si quantum dots.

6.3. WORKS ON SR BEAMS FROM VEPP-4

6.3.1. Station "Space".

Station for metrology in soft X-rays on the VEPP-4 storage ring.

Modernization of station equipment.

A new two-mirror monochromator was made and commissioned. The kinematic scheme of the new monochromator allows higher dimensional stability of monochromatic beam. The energy range that can be covered in a single scan without opening of the vacuum volume of the monochromator to the atmosphere was expanded. A supplementary remotely-controlled adjustment of parallelism of the mirrors in the transverse direction was added. The compatibility of the mechanisms of the monochromator with the high vacuum of the station was improved. A control software package for the new monochromator was developed and is being debugged now.

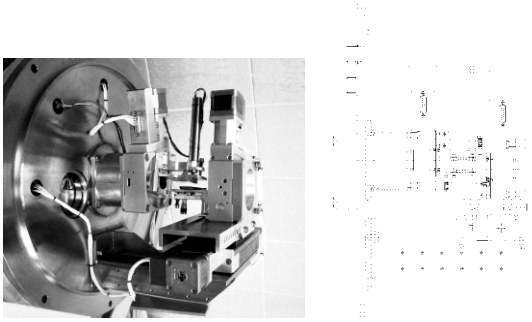

Fig. 6.3.1. Appearance of the monochromator and its assembly drawing.

A new two-coordinate detector based on "back illuminated" CCD matrix was purchased and put into operation. It is intended for control of the quality of monochromatic SR beam.

Development of methods to study the radiation degradation of semiconductor detectors.

In 2013, there were 27 joint shifts with Ioffe Physical-Technical Institute (St. Petersburg) at the station "Space". The radiation degradation of silicon photodiodes under soft X-rays was investigated. Photons with energies within a limited bandwidth were isolated from the "white" SR beam using total external reflection mirrors and thin-film filters. The filters limited the photon flux in the soft region of the spectrum, and the mirrors removed high-energy photons from the beam. Besides, spherical focusing mirrors were used for increasing of the photon flux. A small area on the surface of the detector under testing was exposed to a quasi-monochromatic SR beam through a round 2 mm aperture until a certain dose was received. After that the homogeneity of the detector sensitivity was studied over the entire surface as follows. The detector scanned a relatively thin (about 200 microns) monochromatic SR beam. Then the sensitivity maps of the detector before and after the irradiation were compared. The shape

and place of the arrival of the quasi-monochromatic beam on the detector were additionally controlled by an express-visualization method, suggested by Lebedev Physics Instittute RAS (Moscow): the detector was cooled to negative temperatures and then, under normal conditions, formation of condensation droplets was observed on its surface. Due to the electro-wettability phenomenon, the irradiated area would become visually contrasting to the rest surface of the detector.

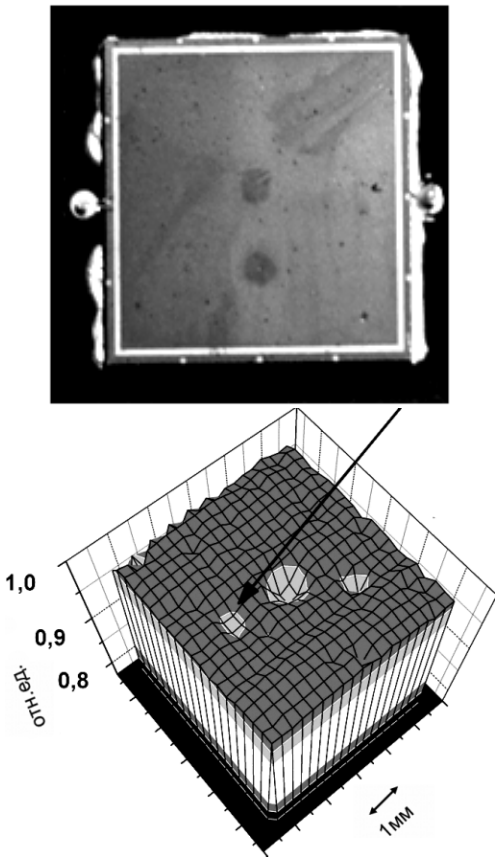

Fig. 6.3.2. Visualization of irradiated region of the detector; its sensitivity map (made at photon energy 100 eV). The arrow shows region exposed to 10.2 eV photons with a surface dose of 9.5 mJ/cm^2.

6.3.2. Station "Flame".

Development of station for diagnostics of combustion processes using SR in VUV range at the VEPP-4M storage ring.

Under agreement with the Ministry of Education and Science of the Russian Federation No. 8186, a station was designed for diagnostics of combustion processes using synchrotron radiation in the VUV range. The station will use the radiation from a bending magnet of the VEPP-4M storage ring and be located on the 1st floor of the SR bunker. The station "Flame" will provide fundamental research on flame, including the kinetics and mechanism of elementary chemical reactions in flame, as well as the mechanism and kinetics of transformations in thermal decomposition of condensed substances.

The plant operation is based on mass spectrometry analysis of intermediate combustion products taken from different parts of flame. Ionization of products to analyze will be performed using synchrotron radiation (SR) of the VUV range (photon energy of 5-20 eV). The station is based on an UHV SR beamline with differential pumping. The optics scheme of the station includes a monochromator with plane grating and focusing mirrors.

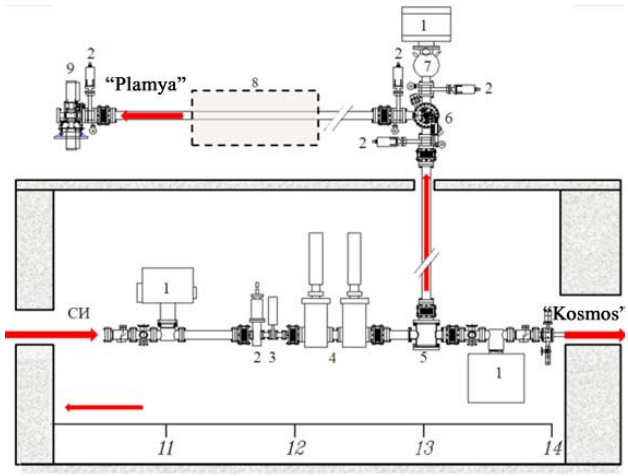

Fig. 6.3.3. Beamline arrangement.

1 - ion pumps; 2 - vacuum gate valves; 3 - fast (10 μs) gate for emergency protection of vacuum; 4 - radiation shutters; 5 – unit of insert focusing mirror; 6 - diffraction grating unit; 7 - nitrogen trap; 8 - gas filter; 9 - exit slit. Distance to the radiation point in meters is shown in the bottom of the figure.

.

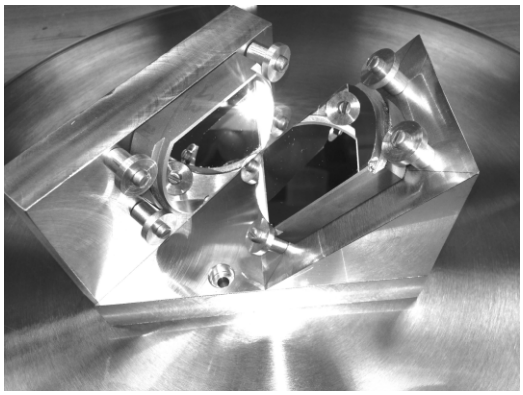

Fig. 6.3.4. Focusing system of the station: 10 m crossed spherical mirrors.

The first results on SR beam are expected to be received in the fall of 2014. The station will be the only one in Russia and one of three similar stations in the world.

6.4. WORKS WITH TERAHERTZ BEAMS

6.4.1. Novosibirsk terahertz free electron laser.

The Novosibirsk free electron laser (FEL) remains the world's most powerful source of terahertz radiation. The maximum value of the average output power achieved at a pulse repetition frequency of 11.2 MHz amounts to 500 W. In 2013, the Novosibirsk FEL worked for users for around 1000 hours. In the standard mode of operation for users at a repetition rate of 5.6 MHz, the average radiation power at the user stations depended on the wavelength and tuning of the accelerating system and was about 100 W. In this mode the FEL radiation is linearly polarized and fully spatially coherent; the wavelength is varied in the range of 40 to 240 microns; the relative spectral width is less than 1% (full width at half maximum); the pulse duration is less than 100 ps (full width at half maximum).

A scheme of the energy recovery linac (ERL) with three FELs installed on the first, second and fourth (the third-stage FEL) tracks is shown in Fig. 6.4.1.

In 2013 there were two main tasks: organization of regular work at six user workstations and preparation for commissioning of the third stage of the Novosibirsk FEL.

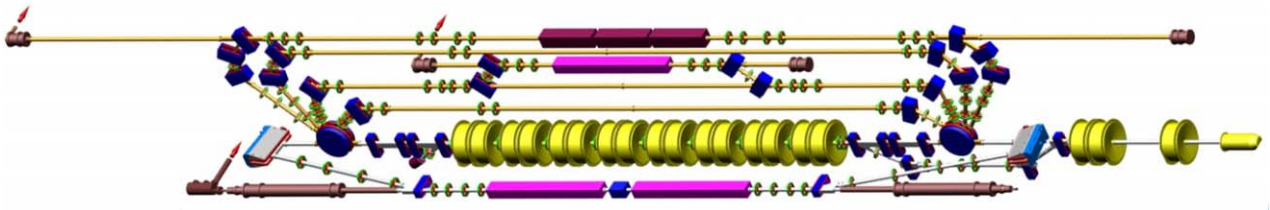

Fig. 6.4.1. General view of the ERL with three FELs installed on the first, second and fourth tracks.

6.4.2. Experiments on THz beams.

At the Siberian Center for Synchrotron and Terahertz Radiation (SCSTR), works with terahertz radiation involve 20 groups from 12 scientific organizations of Novosibirsk, Moscow and South Korea.

Below are listed some of the works in 2013 and performing organizations.

1. Detailed research on the propagation of surface plasmon polaritons on flat and curved metal-insulator-air interfaces were conducted, as well as on their "hops" through long air gaps, which are of interest for development of planar integrated circuits of the terahertz range (Budker Institute of Nuclear Physics SB RAS and the Science-and-Technological Center of Unique Insturment Engineering RAS (Moscow)).
2. Optoacoustic effect in silicon was investigated using the terahertz free electron laser (Moscow State University and Budker Institute of Nuclear Physics SB RAS).
3. Research on the magneto-optical effects in magnetic materials using terahertz radiation FEL yielded first results (Kirensky Krasnoyarsk Institute of Physics SB RAS and Budker Institute of Nuclear Physics SB RAS).
4. A set of binary silicon diffractive optical elements was created and tested. It is intended for controlling the FEL radiation and radiation from other monochromatic sources that allow a variety of experimental designs for a broad class of fundamental and applied research (Samara State Aerospace University, Institute of Systems for Image Processing RAS and Budker Institute of Nuclear Physics SB RAS).
5. A prototype of terahertz near-field optical microscope was created (Technological Design Institute of Scientific Instrument Engineering SB RAS and Budker Institute of Nuclear Physics SB RAS).
6. A prototype of terahertz ellipsometer was created and put into operation (Rzhanov Institute of Physics of Semiconductors SB RAS and Budker Institute of Nuclear Physics SB RAS).
7. The development of unique methods of ultrafast spectroscopy in the terahertz range was continued. In particular, this technique was applied to spectral analysis of the Novosibirsk FEL radiation in unstable modes. Spectra (instability modes) of FEL single pulses (100 ps) were obtained for the first time. These spectra cannot be measured correctly by other known spectral methods. With this method applied to the field of high-resolution gas spectroscopy, signals of molecules associated with the precession of their magnetic moment in a magnetic field were recorded for the first time in real time. These experiments allow high-sensitivity and fast recording of various important radical species (Budker Institute of Nuclear Physics SB RAS and Voevodsky Institute of Chemical Kinetics and Combustion SB RAS).
8. Experiments on the research on combustion and detonation of hydrogen-oxygen mixture by water vapors and OH radicals that arise in these reactions were continued. At transitions of these molecules, terahertz radiation absorption of about 30% was detected in the hot phase of detonation and stronger absorption of up to 100%, in the subsequent cooling phase. Two-dimensional distribution of water vapor in combustion of hydrogen-oxygen flame was measured in a pyroelectric camera (Budker Institute of

Nuclear Physics SB RAS, Lavrentiev Institute of Hydrodynamics SB RAS and Voevodsky Institute of Chemical Kinetics and Combustion SB RAS).

9. Experiments were begun on backscattering of terahertz radiation on water mist. First scattering signals at a wavelength of 118 microns were recorded (Budker Institute of Nuclear Physics SB RAS, Zuev Institute of Atmospheric Optics and Voevodsky Institute of Chemical Kinetics and Combustion SB RAS).
10. A new record power was generated at the Novosibirsk FEL, 220 W at a repetition frequency of 5.6 MHz. That allowed generation of a powerful optical discharge at the diagnostics station. This experiment can be a basis for many other user experiments (Budker Institute of Nuclear Physics SB RAS).
11. Research on the nonthermal effects of terahertz radiation on living systems of different levels of organization (Institute of Cytology and Genetics and Budker Institute of Nuclear Physics SB RAS).
12. Development of a new method of mass spectrometry based on nondestructive soft ablation under the influence of terahertz radiation (Institute of Cytology and Genetics and Budker Institute of Nuclear Physics SB RAS).

6.4.3. Upgrade of the FEL and ERL.

An optical cavity for third-stage FEL was designed. The key components of the optical cavity were fabricated at the BINP experiment workshop. The unit of the mirror is shown in Fig.6.4.2.

Fig. 6.4.2. Unit of the mirror of the optical resonator of the third stage of the FEL.

The assembling of the optical cavity was started. The vacuum chamber of the optical cavity was suspended in the accelerator hall, see Fig. 6.4.3.

Fig. 6.4.3.Vacuum chamber of the optical cavity of the third-stage FEL, suspended in the accelerator hall.

The measurement electronics of the RF generator of the accelerating system of the ERL was upgraded. Control cables for transmission of signals from the measuring loops of the RF cavities out of the accelerator hall were replaced with air-insulated cables. That resulted in a several-fold reduction of the dependence of the phase shift on the temperature of the cables.

A new high-voltage rectifier (Fig. 6.4.4) for the electrostatic electron gun of the ERL was designed and fabricated.

A 90 MHz RF generator for the RF electronic gun for the ERL was put into operation (Figure 6.4.5). The rated voltage across the resonator of the gun and an average electron current of 25 mA were attained after RF training.

Fig. 6.4.4. New high-voltage rectifier for the electrostatic electron gun.

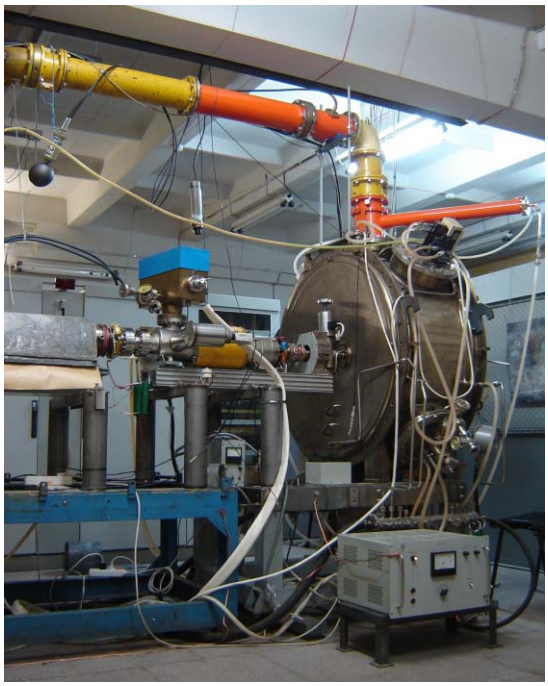

Fig. 6.4.5. RF electron gun with diagnostics beamline.

Magnetic fields in all three undulators for the fourth-track FEL were measured. Then the trajectory of electrons in the measured field and amplitudes of spontaneous emission were calculated. The calculation results were used in the field correction by replacement of some blocks of magnetic material by blocks with the required magnetization components. The magnetic measurements were repeated, and the undulators were installed on the fourth track of the ERL (Fig. 6.4.6).

Fig. 6.4.6. Undulators of the third stage of the FEL on the fourth track of the ERL.

Calculations and experiments were done for optimization of the process of electron beam energy recovery in its four-time deceleration in the RF accelerating cavities. A circulating current sufficient for radiation generation in the FEL was attained.

6.4.4. Meeting on energy recovery linacs.

The International Meeting "Energy Recovery Linacs 2013" was held at Budker Institute of Nuclear Physics from 9 to 12 September 2013.
These international meetings are held every two years with the support of the International Committee on Future Accelerators (ICFA). The previous two meetings were held in the United States and Japan.

The meeting was devoted to the new type of charged particle accelerators, energy recovery linacs (ERLs). It is often that most part of high-current beams of charged particles (usually electrons) is left in the exhausted beam. This power can be returned to the accelerating system if the exhausted beam is directed to it. An accelerator that not only accelerates charged particles but also slows already used ones is called ERL. The ERL was proposed by M. Tigner (USA) in 1965 for creation of electron-electron collider. There are only three ERLs working now the world: at Thomas Jefferson National Laboratory (USA), at Budker Institute of Nuclear Physics (Russia), and at Daresbury laboratory (England). The first two ERLs are used in high-power free electron lasers. Projects of super-high-brilliance X-ray sources based on ERL are developed in Germany, Russia, the USA and Japan. Besides, the possibility of using ERLs in nuclear physics (Germany) and elementary particle physics (the U.S. and the European Centre for Nuclear Research, CERN) is considered.

ERLs can be applied not only to science. ERL-based high-power lasers can transmit power into space for communication satellites, produce isotopically pure materials, treat various surfaces and selectively affect living systems. Technologies developed for ERLs can be used in other promising applications of charged particle accelerators, e.g. decontamination of radioactive waste.

Participants of the meeting visited the Novosibirsk ERL, which differs greatly from the "mainstream" devices by the electron gun with control grid, long-wave non-superconducting accelerating structure, branched magnetic system with tracks, bypass and three FELs, as well by the fact that it operates at a shared-equipment center created on the basis of the FEL.

6.4.5. Results in 2013 and plans for 2014.

Main results of works in 2013:
1. An optical cavity was mounted; undulators of the third stage of the FEL were installed.

2. Construction of new stations and improvement of the FEL systems continued.
3. Experiments using THz radiation at user workstations continued.

Plans for 2014 год:

1. Commissioning of the third stage of the FEL.
2. Continuation of works on the development of new stations and improvement of the FEL.
3. Continuation of experiments using THz radiation at the user workstations.

6.5. DEVELOPMENT AND CREATION OF DEDICATED SR GENERATORS

6.5.1. Superconducting wigglers.

The development and manufacturing of several cryogenic superconducting magnetic systems for SR generators were preformed in 2013, under contracts with various acceleration centers of the world.

A 63-pole 4.2 T wiggler with period 52 mm was installed and put into operation on the Australian Synchrotron (AS) storage ring in January 2013. The temperature of the magnet was lowered to 3.5 K in a cryostat, with no flow of liquid helium and reduced residual gas pressure. That allowed achieving the maximum value of magnetic field in the wiggler of 4.5 T due to thermal bias in the load characteristics of the superconducting wire. The wiggler is used on the Imaging and Medical Beamline (IMBL) for Micro-beam Radiation Therapy (MRT). Fig. 6.5.1 shows the wiggler on the AS storage ring.

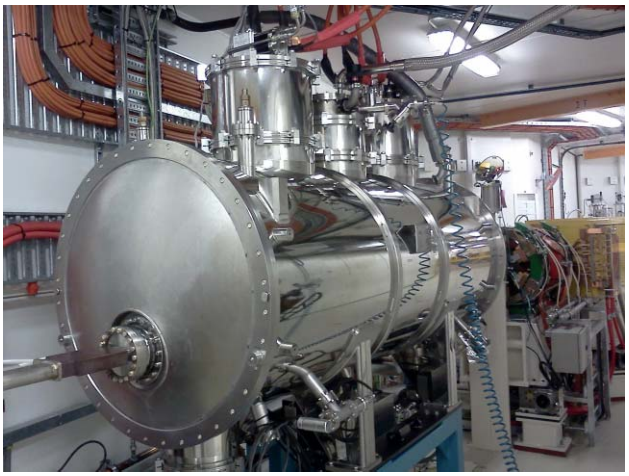

Fig. 6.5.1. 63-pole 4.2 T wiggler with period 52 mm, installed on the storage ring of the Australian Synchrotron (AS) in Melbourne for biomedical research.

A 15-pole 7.5 T wiggler with period 200 mm was built in the territory of the LSU-CAMD storage ring (Louisiana, USA) in May 2013. It has a feature of high stored magnetic field energy (~ 850 kJ), which required a special reliable protection of the wiggler windings from damage in quench. The maximum achieved magnetic field is 7.7 T. The wiggler was installed on the storage ring (Fig. 6.5.2) and is used for research on protein crystallography.

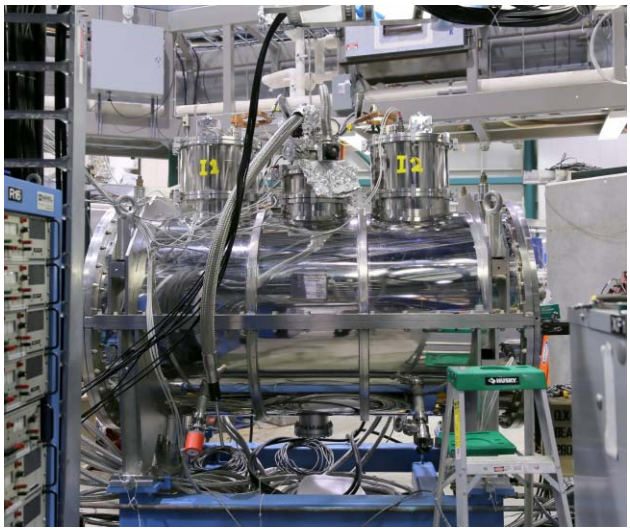

Fig. 6.5.2. 15-pole 7.5 T wiggler with period 200 mm, mounted on the LSU-CAMD storage ring (Louisiana, USA) for research on protein crystallography.

The wigglers that have been developed at BINP in recent years have very low consumption of liquid helium and require maintenance once a year at most. Thus lot of wigglers that were manufactured by BINP earlier and operate now on different storage rings could be upgraded in line with modern requirements. The cryostat of the 49-pole 3.5 T wiggler that was in operation on the ELETTRA () storage ring Italy since 2002 was upgraded in June 2013. The magnetic system was not changed. Fig. 6.5.3 shows the process of testing the upgraded wiggler.

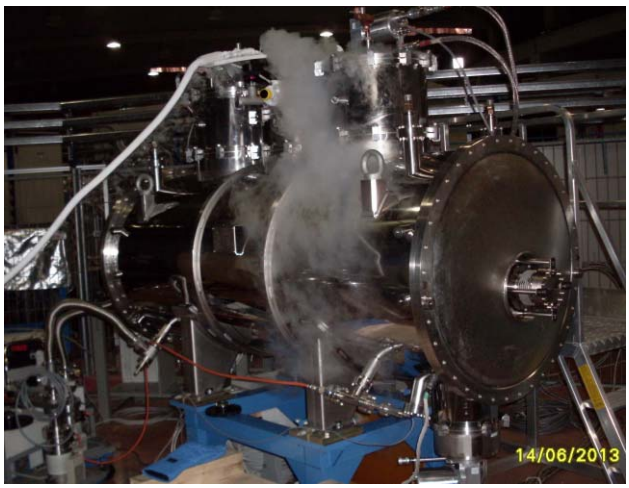

Fig. 6.5.3. Upgraded 45-pole 3.5 T wiggler on the ELETTRA storage ring (Italy).

The upgrade of the cryostat of the 17-pole 7 T HMI (HBZ) wiggler, which has worked on the BESSY-II storage ring since 2002, was completed in August 2013. Fig. 6.5.4 shows transportation of the modernized wiggler back to the storage ring.

Fig. 6.5.4. Transportation of the upgraded 7 T HMI (HBZ) wiggler to the BESSY-II storage ring.

A test commissioning of the 40-pole 2.5 CATACT wiggler with period of 48 mm for the ANKA storage ring (Karlsruhe, Germany) was carried out on the customer's site in December 2013 (Fig. 6.5.5.). A helium temperature decrease to 3.5 K was demonstrated with no liquid helium consumption and negative pressure in the helium vessel. That allowed obtaining a magnetic field of 2.9 Tesla, which exceeds the planned value. Currently this wiggler is being prepared for installation on the ANKA storage ring. The final commissioning is scheduled for July 2014.

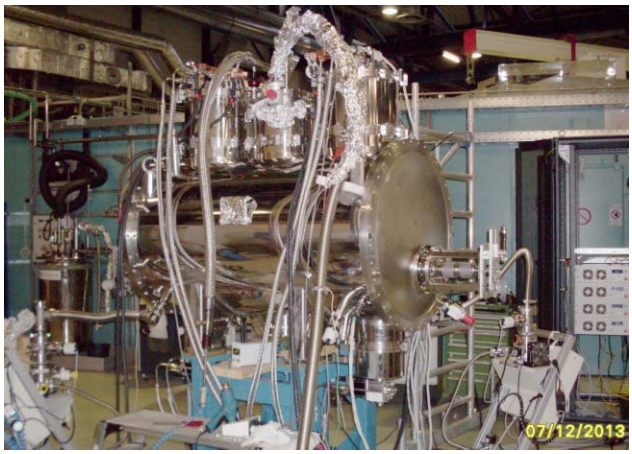

Fig. 6.5.5. Testing the 40-pole 2.5 T CATACT wiggler on the ANKA storage ring (Karlsruhe, Germany).

The 3 T CLIC wiggler with period 51 mm and magnetic gap 18 mm for the ANKA storage ring (Karlsruhe, Germany) radically differs in design from all previous wigglers. This wiggler is cooled to low temperature not with liquid helium but by refrigeration machines through mechanical thermal contacts. The magnetic system itself is in vacuum. A short prototype of such a magnet was tested. It was cooled to a temperature of 3 K and a magnetic field of 3.3 T was achieved. Now the testing of the prototype is continued in various modes of operation and the 72-pole full-length magnet is being produced. The commissioning of the full-size magnet with indirect cooling is scheduled on May 2014.

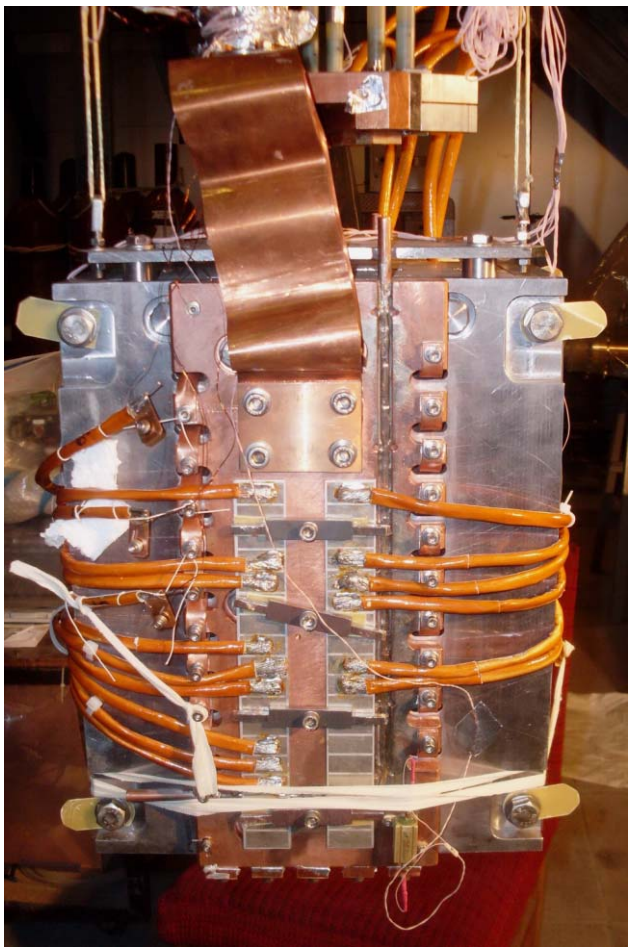

Fig. 6.5.6. Appearance of prototype of superconductive 3 T wiggler for the ANKA storage ring (Karlsruhe, Germany).

6.6. DEVELOPMENT OF MAGNETIC STRUCTURE OF NEW SR SOURCE

6.6.1. General concept

The popularity and demand for research methods using SR at the Novosibirsk Scientific Center has resulted in the appearance of an active user community, which became a

basis for the Siberian Center for Synchrotron and Terahertz Radiation (SCSTR).

Currently researchers at the Center work with SR beams from VEPP-3 and VEPP-4, the parameters of which do not meet today's requirements. In addition, the necessity to share the operation time with other physics programs that are carried out at the complex severely limits the usage of SR methods.

So, the absence of a dedicated SR source is the main problem of the center.

Since 2005, researchers at the center have been developing a new concept of the SR source. A few options have been reviewed so far, including a relatively inexpensive project of SR source to be placed in the tunnel of the VEPP-4M collider and to utilize the existing infrastructure of the complex as much as possible.

• Basic parameters of the proposed source are presented in the table below.

Table 6.6.1. Main parameters of the new SR source for the SCSTR.

Parameter	**Value**
Perimeter	360 m
Electron energy	3 GeV
Design horizontal emittance	< 1 nm rad
Operation current	Up to 500 mA
RF	180 MHz

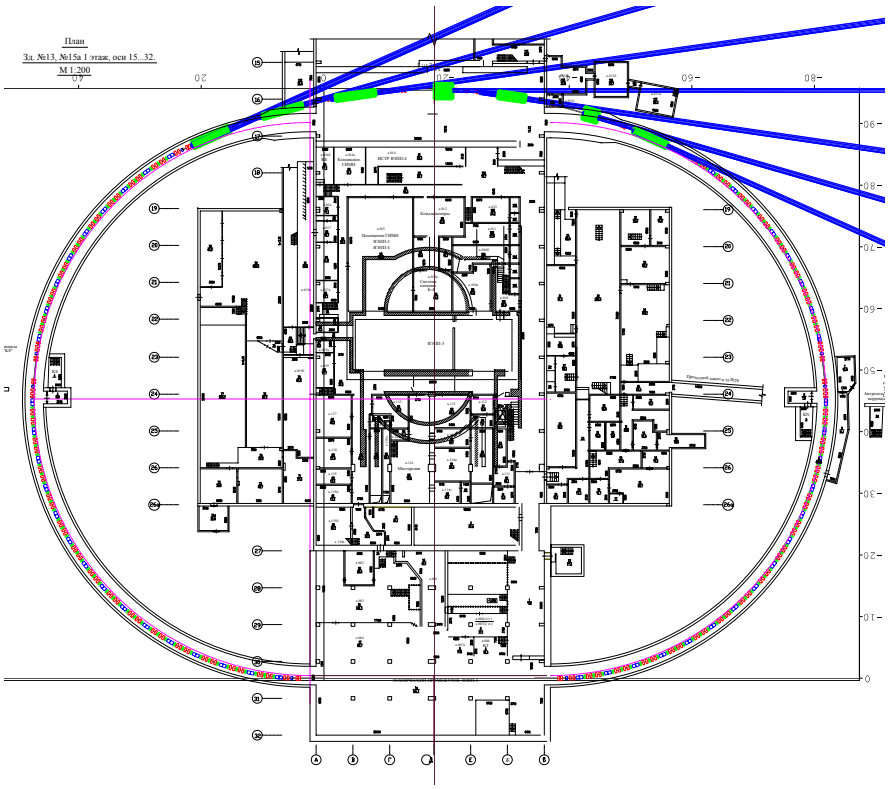

Fig. 6.6.1. Arrangement of the SR source, generation units and radiation extraction lines.

The dimensions of the proposed source are determined by the currently existing tunnel of the VEPP-4 collider.

This approach has an undoubted advantage of a lower project cost because there is no need in construction of a new building. However, the underground location of the tunnel poses a problem of extraction of SR beams.

This project suggests concentrating the SR generation devices in the area of the existing experiment interval of VEPP-4. A rough plan of the proposed structure of the SR source is shown in Fig. 6.6.1.

Six multi-pole devices for generation of SR (superconductive wigglers and undulators) are to be installed. The radiation extraction beamlines are shown with blue lines. Beams transported through these beamlines can be used in the existing and new (specially designed) premises of building 13.

The possibility of using the currently existing experiment hall in building 28 for work with SR beams is also considered.

Besides, a long (up to 10 m) undulator can be mounted at the end of the engineering span of VEPP -4.

6.6.2. Magnetic structure.

The TME (Theoretical Minimal Emittance) structure suits rather well for a low-emittance embodiment of the magnetic structure in this case. The ring contains long bending arcs, and filling them with TME cells allows most efficient use of the advantages of the sufficiently large perimeter of the ring and the absence of extraction of radiation from the bending arcs. Special cells can make the dispersion function be zero at places where wigglers (or undulators) are to be placed. Such places are few, and thus their contribution into emittance increase will be small.

Limiting the gradients of the sextupole and quadrupole lenses with realistic values will allow implementation of the TME-based structure with emittances about 150 pm rad. Unfortunately, high sextupole lenses cause significant decrease in the dynamic aperture, which excludes the possibility of successful realization.

Optimization of the magnetic structure in this case means search for an optimal balance between these two values (emittance and dynamic aperture). Thus, realistic aperture values imply a reasonable deviation from a minimum emittance. Therefore, the design emittance value was chosen at the level of 1 nm rad.

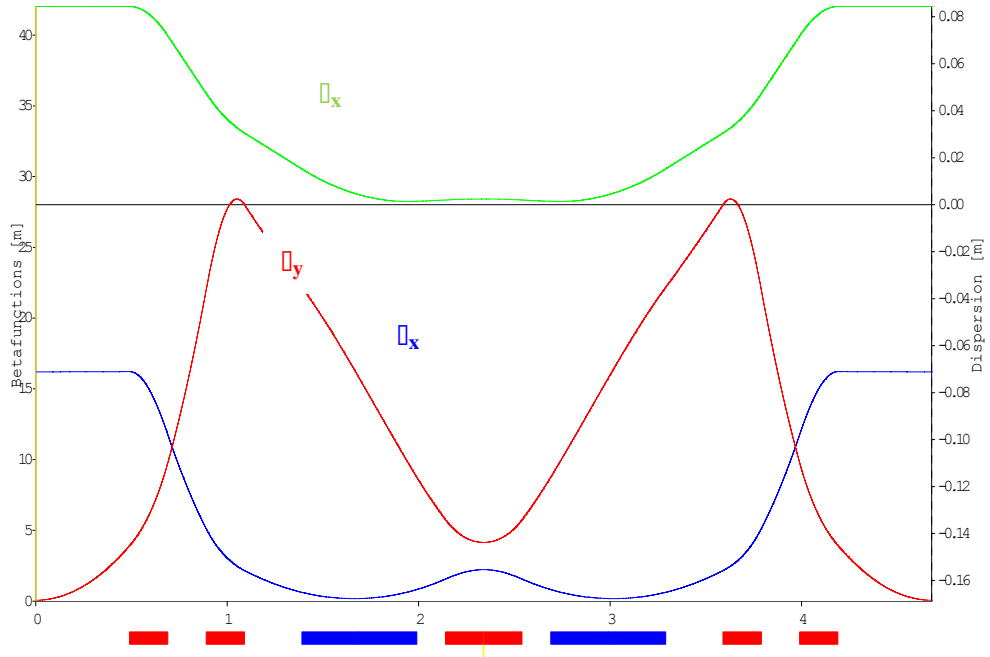

Fig. 6.6.2. Example of cell (SplitTME) in bending arc of the SR source.

The so-called SplitTME variant has substantial advantages among the possible implementations of the TME structure. The essence is the possibility of using one quadrupole lens between two adjacent magnets instead of a universal triplet. A variant of such structure is shown in Fig. 6.6.2. Although the TME conditions in the magnets are met not exactly in this case, at reasonable deviations from the minimum emittance this does not play a decisive role.

This approach has an undoubted advantage of the compactness of the resulting cell, which is very important in the sufficiently narrow tunnel of VEPP-4.

Another advantage of this cell is its flexibility, i.e. parameters of individual elements can be changed, while the entire cell stays operable. In particular, choosing the phase shift on the cell, one can optimize the dynamic aperture: with the phase shift π, which is quite realizable, the transport matrix of the cell becomes equal to (*–I*). Placing two identical sextupole lenses with such spacing leads to compensation of geometric and chromatic aberrations induced by these sextupoles, which in turn provides a dynamic aperture growth.

At present, the search for the optimal parameters of the cell is underway.

7
RADIOPHYSICS AND ELECTRONICS

7.1. POWER SUPPLIES FOR ELECTRO-PHYSICAL INSTALLATIONS

7.1.1 Sources of stable current.

Development of precision sources of stable current for electro-physical installations is one of the main tasks of the Radiophysics Laboratory. Precision DC sources are intended mainly for powering electromagnets of charged particles storage rings. The output current of such sources varies from several amperes to tens of kiloamperes. Thus the output power is from tens of watts to several hundred kilowatts and several megawatts. Current sources tend to have a wide range of current regulation and high accuracy of regulation and stabilization (error of 0.01% and less). Below are listed the main results of works performed in 2013 for designing and manufacturing of stable current sources:

- The upgrade of the electronics of precision thyristor power sources of the IST series was continued. An IST stable current source consists of a mains reducing three-phase transformer, a controlled thyristor rectifier with LC filter, a channel for active ripple suppression and electronics for current control and stabilization. The power output of the current sources of the IST series is up to 200 kW. The IST-type current sources of new modification with an output current of up to 400 A and power OF up to 200 kW made it possible to test the electron cooling facility that was developed and manufactured by BINP for the COSY accelerator, Germany. Permanent technical support for more than 30 IST-type power sources on VEPP-5 and K-500 is provided. A unit for rapid output current reversal has been developed and put into operation.

Fig. 7.1.1. IST-type stable current sources.

- A number of power sources specially designed for powering of the electromagnets of the booster accelerator of the synchrotron radiation source NSLS-II (BNL, USA) were successfully launched in 2013. The booster is capable of operating at a repetition rate of up to 2 Hz, so the requirements to the power sources are quite unique. While meeting high stabilization accuracy requirements, the current power sources have high dynamic characteristics. In particular, the current rise time from the minimum value to the nominal one does not exceed 0.26 s in all the current sources. In total, over 50 current sources were developed and manufactured for powering of the electromagnets of the booster. Table 7.1.1 presents the main parameters of these power supplies.

Table 7.1.1

Power supply	Q-ty	Max current, A	Max voltage, V	Max power, W
BR-QF	1	157	207	32, 496
BR-QD	1	85	49	4, 200
BR-QG	1	126	73.2	9, 229
BR-SXV	8	18	17.4	2, 507
BR-SXH	8	18	17.4	2, 507
BR-Corr	32	7	8.8	1, 963
DC septum	1	400	15	6, 000


Fig. 7.1.2. Power supplies for quadrupoles and DC septum of the booster accelerator at NSLS-II.

The development and manufacturing of precision current sources with an output power of up to 30 kW and a current of up to 1,000A, made using high-frequency (about 20 kHz) converters were continued in 2013. A series of such sources is being produced for replacement of obsolete thyristor current sources of the B-1000 type.

•As part of contract works, a precision current source with current stability of about 20 ppm was designed for the correction magnets at the XFEL installation, Germany.

Fig. 7.1.3. Precision current source for correction magnets.

7.2. HV SOURCES OF HIGH STABILIZED DIRECT VOLTAGE

The Institute has successfully conducted development of HV sources of high stabilized direct voltage with a wide power range:

- tens of watts: for powering of electrostatic deflection devices or those for focusing of charged particles beams;
- hundreds of watts to tens of kilowatts: for supply of various HV “direct action” accelerators;
- hundreds of kilowatts: HV power supply of ion sources and atomic injectors.

The high-voltage power supplies have high stability and regulation accuracy; they are protected against short circuits and breakdowns.

7.2.1. HV sources for atomic injectors for diagnostics and heating of plasma in plasma facilities

Development and production of high-power HV sources for atomic injectors for corpuscular diagnostics and heating of plasma in plasma experiment facilities remains one of the main directions of the activity of the Laboratory. In particular, in 2013

- the development and manufacturing of units of the HV PS for the high-power source of negative ions to be developed under a contract with TAE, USA was continued. The HV PS has the following parameters: U (output) = - 880 kV, I (output) = 10 A, T (pulse) = 100 s. The HV PS consists of eight series-connected high-voltage rectifiers with an output voltage of - 110 kV placed in one volume filled with an insulating gas. The sources of controlled AC voltage (2 kHz, 3 kW) in these rectifiers are 2 kHz voltage inverters with an output power of up to 350 kW each.
- a HV source (120 kV, 100 mA) for a stand of the source of negative ions to design under a contract with TAE, USA has been developed, manufactured and put into operation. The HV PS consists of a stage generator, or "voltage multiplier", operating at a frequency of 20 kHz, and an adjustable high-frequency (20 kHz) voltage inverter (20 kHz);
- a HV PS with an output voltage of up to 60 kV and a power of 600 kW for the diagnostics injector of the RUDI-x facility, Germany was put into operation.

Fig. 7.2.1. HV PS for the diagnostics injector at RUDI-x.

7.2.2 HV PSs for electron acceleration tubes.

In 2013 the development and fabrication of units of HV PSs for electron acceleration tubes was continued.

- A HV PS for the electron tube for Novosibirsk the free electron laser was made using a stage generator (a two-stroke voltage multiplier). The output voltage of the FEL HV PS is up to -300 kV at an output current of over 50 mA.

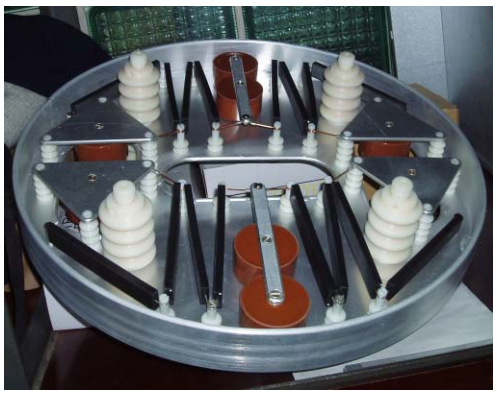

Fig.7.2.2 Section of stage generator for voltage multiplication .

- A new high-voltage rectifier was designed and made with an output voltage of up to -60 kV and a power of up to 60 kW. It will be used in new electron-beam welders.
- The commissioning of the HV PS for the electron cooling installation of the COSY accelerator, Germany was completed. The output voltage of the HV PS is up to 2 MW.
- Under a contract with TAE (USA), a HV PS with an output voltage of -110 kV and an output current of over 100 mA was manufactured and put into operation. This HV PS is based on a stage generator operating at a transformation high frequency of 20 kHz.

7.2.3 Switching Power Supplies for electromagnets of accelerator complexes.

The manufacturing and adjustment of pulsed current generators for transport beam lines K-500 was continued in 2013; 75 switching power supplies of the GID-25 type were made and adjusted.

Fig. 7.2.3. Switching power supply of the GID-25 type.

7.2.4 Electronics for diagnostics and control of charged particle beam position.

Below are listed main works in 2013 on the creation of electronics for diagnostics and control of charged particle beam position:

- Manufacturing and adjustment of the new electronics for pick-ups at the VEPP-2000, VEPP-4, and injection complexes. Over 40 units were made and are being put into operation.
- The electronics for pick-ups for the electron cooling facility of the COSY accelerator, Germany, were manufactured and delivered.
- Under a contract with JINR (Dubna), the electronics for the ion beam phase measurement system for the NICA booster was supplied. This system supplements the booster RF system, which is under manufacturing at BINP. The system allows measurement of beam phase relative to the accelerating voltage of the RF system with an error below 1 degree. The measurement can be done every 10 μs. The system was successfully tested on the JINR accelerator "Nuclotron" in the spring of 2013.
- Under a contract with PINP (Gatchina), a new 4-channel NMR magnetometer was made and delivered. The magnetometer is a 1U Euromechanics standard module and is connected to the computer via Ethernet. The new magnetometer differs from the old one in a response time, which was improved due to faster processing of NMR signals. The error of measurement of homogeneous fields (with gradient less than 10^{-4}/cm) does not exceed 1 ppm (10^{-6}). A new software was developed for the new magnetometer. Another such NMR magnetometer was made and provided for operation on the magnetic measurements stand at BINP.

7.3. DEVELOPMENT OF NONSTANDARD AND SPECIAL ELECTRONICS

The Institute develops a lot of non-standard and special electronics. In particular, the following was developed in 2013.

- A semiconductor RF generator with an option of output voltage amplitude modulation for powering of the plasma emitter of the ion source was designed, fabricated and tested successfully. Its prototype, which provides an output power of up to 20 kW of 4 MHz high voltage, was tested in operation with the atomic injector. The production of a similar generator for a power of up to 40 kW was started.
- A contract of supply of twenty hydrostatic capacitive level sensors of the SASE type to Toyota Tsuho Corp. was completed in 2013. The sensors allow one to determine a mutual vertical displacement of vessels at the accelerator complex from water levels in communicating vessels. The calibrated range of water level measurement with an accuracy of 1 micron is 5 mm; the measurement frequency is up to 0.5 Hz. The measured displacement of vessels allows one to control the vertical adjustment of elements of the accelerator complex.

Fig. 7.3.1. Semiconductor RF generator for atomic injector driver.

7.4. RESEARCH RELATED TO MODELING AND SOLVING ELECTROSTATIC AND ELECTRO-DYNAMIC PROBLEMS OF ACCELERATOR PHYSICS

The calculation and designing of elements of accelerators for the Institute and under international contracts was continued in 2013. Computational methods and programs for calculation and designing of elements of accelerator technology and computer modeling of the dynamics of charged particle beams were also being developed and modernized:

- Under a contract on the construction of a powerful source of neutral particles - an atomic injector - an optimization of the magnetic field configuration in a plasma charge-exchange target was done; the electron fluxes to the chamber walls were evaluated; the final version of the magnetic system was passed to the BINP designing bureau.
- Under a contract on construction of a high-voltage installation for electron cooling for COSY, Germany, works on the computer modeling of the design of the electron gun and collector were done. The results showed good agreement of the measured and calculated parameters.
- Further development of programs for calculation of electrostatic and magnetostatic fields and electron and ion guns was continued. The work of the pre- and postprocessors in the program set UltraSAM was significantly improved; the revealed errors were eliminated.

Within the framework of the designing of the future high-power atomic injector the following was done:

- calculation and optimization of field in the expansion plasma chamber with peripheral multipole permanent magnets;
- calculation and optimization of field of the magnetic filter of plasma electrode;
- calculation and optimization of the deflecting magnet in the ion-optical system;
- calculation of electric fields in the ion-optical system of the prototype atomic injector with one driver and "single-aperture extraction";
- calculation of trajectories of accelerated negative ions and associated electrons.

7.5. NEW RF SYSTEM FOR STORAGE RING OF BOOSTER OF ELECTRONS AND POSITRONS

The Institute is working to create a new radio frequency (RF) system for the storage ring of the booster of electrons and positrons (BEP), which operates as an injector for the accelerator complex VEPP-2000. The new RF system will increase the energy of particles in the BEP from 0.9 GeV to 1 GeV. The RF system works at 174 MHz (the 13th harmonic of the BEP revolution frequency) and consists of an accelerating cavity, RF generator and control system.

The accelerating cavity is of coaxial type and is designed for a maximum voltage of 120 kV. The cavity has mechanisms for tuning of the fundamental and higher modes. Parameters of the cavity are given in Table 7.5.1.

The RF generator is designed for a maximum power of 20 kW and has an output stage on tetrode GU-92A and transistor prestages. Power transfer from the generator to the cavity is performed via a copper coaxial feeder of 160 mm in diameter with a characteristic impedance of 75 Ohms. The feeder kit includes a set of replaceable elements of different lengths for a "trombone"-shape knee bend. One can select the feeder length with an accuracy of 1/32 of the wavelength that would be optimal for both the generator output stage regime and beam stability against synchrotron oscillations.

The control system adjusts the amplitude and phase of the accelerating voltage and provides synchronization in filling of the separatrices of the storage ring.

Table 7.5.1. BEP cavity parameters.

Parameter	Value
Number of harmonics	13
Operation frequency, MHz	174.3755
Frequency hopping, kHz	±130
Transit time factor τ	0.996
Characteristic impedance $\rho\tau^2$, Ohm	127
Unloaded Q	14,900
Accelerating voltage, kV	112
Power to beam, kW	6.9
Power loss in cavity, kW	3.5
Total power, kW	10.4

The fabrication of the cavity and components of the feeder line connecting the generator to the cavity was completed in 2013. An apparatus complex was prepared for testing of the cavity in the ring and for work with beam in the BEP. The RF parameters of the operation and higher (up to 1500 MHz) modes of the cavity (Fig. 7.5.1) were measured. A warming of the cavity was performed; a working vacuum of $1.5 \cdot 10^{-10}$ Torr was attained.

Fig. 7.5.1. RF measurements of parameters of the new BEP cavity.

The cavity will be tested in the storage ring with a standard RF generator. The installation of the cavity in the ring and the mounting of the feeder line and generator are currently close to completion (Fig. 7.5.2).

Fig. 7.5.2. Output stage of the BEP RF generator.

7.6. 816 MHZ PASSIVE SINGLE-MODE CAVITY

. In 2013, the Institute successfully completed works under a contract with the National Synchrotron Radiation Laboratory, Hefei city, China on the development and fabrication of a passive single-mode RF cavity for a frequency of 816 MHz (Fig. 7.6.1). The cavity will be used in the storage ring for increasing the bunch length. This will reduce the "Touschek effect" and increase the beam lifetime.

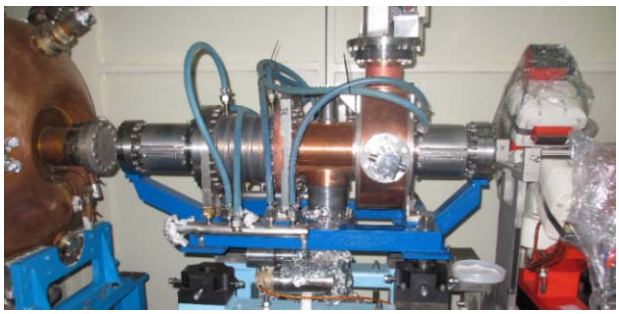

Рис. 7.6.1. Passive single-mode cavity mounted on the storage ring at National Synchrotron Radiation Laboratory, Hefei city, China.

The cavity operates at the fourth harmonic of the accelerating RF voltage. The cavity is excited directly by beam. The cavity voltage level is adjustable via detuning of the cavity relative to the RF harmonic. The maximum voltage is 80 kV. The main parameters of the cavity are shown in Table 7.6.1. The higher modes of the cavity are damped by means of an RF load based on RF ceramic dampers placed inside the vacuum chamber. For decoupling of the load and the main mode, the load is connected

to the cavity through a section of an evanescent waveguide.

Table 7.6.1. Cavity parameters.

Frequency, MHz	816
Maximum voltage, kV	80
Q factor	20,000
Characteristic impedance, Ohm	135
Shunt resistance, MOhm	2.7
Fundamental frequency tuning range, MHz	5.2
Losses in cavity walls, W	1,500
Losses in RF load, W	1,000
Impedances of higher modes, Ohm	≤ 700

The fabrication of the cavity was completed in 2013; the RF parameters of the operation and higher modes were measured. The cavity was warmed; the operation vacuum was attained. The cavity delivered to the customer and mounted at its place on the accelerator ring.

7.7. INSTALLATION FOR DYNAMIC BEAM SEPARATION ON VEPP-4

In 2013, the Institute developed and successfully tested a device for dynamic separation of accelerator beams on the VEPP-4 accelerator. Counter beams of electrons and positrons are separated by means of high voltage applied to deflecting plates when the beams fly by. The orbits of the electrons and positrons are changing at a rate twice as small as the revolution frequency, ie 409 kHz.

The block diagram of the device is shown in Fig. 7.7.1.

The deflection plates are located along the vacuum chamber and have a length of ~ 1 m. Each side of the plate has a lead through a ceramic insulator and contains external ballast devices to suppress high frequency oscillations caused by the flying beams. This is necessary for exclusion of the possibility of synchrotron oscillation build-up due to parasitic resonances on the deflection plates.

The resonant circuit is made using a high-Q coil (Fig. 7.7.2). Stability of tuning to the resonance frequency is provided by heat-stable capacitors and special technology of winding coils on ceramic frame. The oscillation circuit is shielded and has forced air cooling from a source of compressed air. The voltage on the exits of the resonant circuit is controlled using 4 capacitance-resistance voltage dividers. These signals are used in the voltage and phase feedback, as well as for monitoring of the deflecting voltage and control of the moment of beams pass through this section of the accelerator.

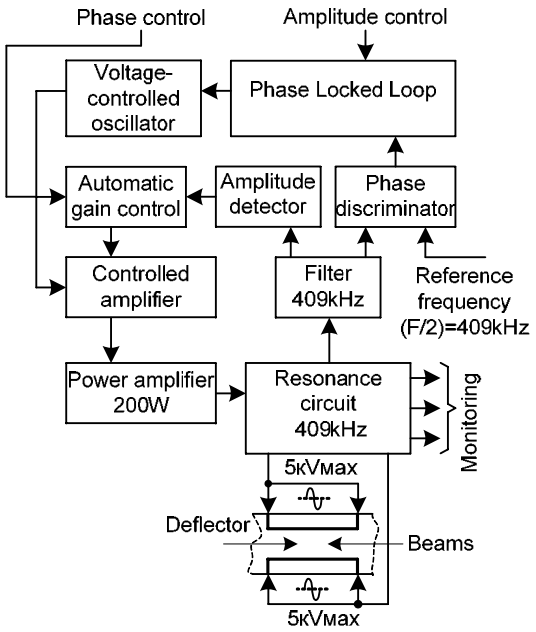

Device for swinging bunch. Block-scheme.

Fig. 7.7.1. Block diagram of device for separation of beams.

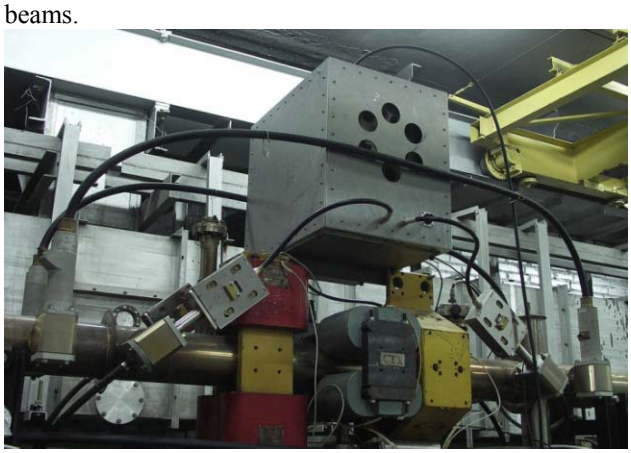

Fig. 7.7.2. Resonant circuit and section of the VEPP-4 accelerator with leads of deflection plates.

The power amplifier provides up to 200 W at a frequency of 409 kHz and is located next to the resonant circuit. The amplifier and power supply are controlled remotely.

The amplitude-phase modulator is placed at a distance, in a served room, and is a controllable element of the device. It is a circuit that sets the amplitude and phase of voltage on the deflecting plates. The circuit comprises two auto-regulation loops, by amplitude and by phase. The phase and amplitude of the signal are adjustable over a wide range. The amplitude adjustment corresponds to a voltage change from 0 to 10 kV across the gap of the deflection plates; in phase it is 0÷360˚ at the revolution rate. These parameters can be controlled manually, e.g. in debugging, and from the computer, through a DAC. The unit is based on a self-oscillator controlled by a phase-lock loop (PLL). The PLL synchronizes the voltage on

the resonant circuit of the separation system with a reference voltage of 409 kHz, i.e. half the accelerator revolution frequency. The phasemeter has a phase characteristic stable and linear within ±180°. It is made by a circuit of frequency-phase detector using high-speed CMOS triggers. The circuit is stable due to its powering from a precision source and shielding against possible external interference. A signal from the phase detector is compared with a set reference voltage and controls the autooscillator to make their difference closer to zero. Varying the reference voltage, one can shift the phase of the output voltage. Thus the device can be tuned so that the maximum voltage on the deflection plates corresponds to the moment of pass of beams. The amplitude on the gap is adjusted by means of a stage for amplification adjustment, which can be operated in manual mode, i.e. without feedback, and in automatic control regime, when the voltage across the gap is used for feedback. An automatic control circuit matches this value to the reference voltage. The computer control of phase and amplitude is the main operation regime. Two DAC channels are used in this regime.

7.8. DEVELOPMENT OF RF SYSTEMS FOR HIGH-POWER INJECTORS OF NEUTRAL ATOM BEAMS FOR PLASMA PLANTS

. In 2013, the Institute continued works on the creation of a high-power continuous injector of hydrogen atom beams with energies up to 1,000 keV on the basis of negative ions. The prototype of the source of negative hydrogen ions will be investigated on the following test benches under construction: one to form a 120 keV beam of negative hydrogen ions in the source and the second to accelerate a 1.5 A beam of negative hydrogen ions to energies of 500÷1,000 keV.

Experiments on the first-bench will be carried out in two stages, with a beam current of 1.5 A (the first stage) and with a current of 9 A (the second phase, after modification of the equipment). An RF discharge is the plasma source. The sources will be fed from a specially-designed RF system. A master clock generator forms a 4 MHz signal at a low power level.

The frequency of the master clock generator is tuned within ±3.5% by means of a self-tuning system and thus tracks the resonance frequency of the circuit made by an inductor and ceramic capacitors placed on the screen of the RF emitter. The signal from the oscillator is amplified by an adjustable amplifier (AA), which regulates the output power level and maintains a stable amplitude. From the AA output the signal arrives at the pre-amplification transistor stage. The output stage is made on a cermet tetrode 4CW50000E made by Eimac (USA) with a common cathode circuit. From the output of the stage the RF power is supplied to the inductor of the plasma emitters through an isolating RF transformer. In operation with a beam current of 1.5 A one channel of the system is used; with a current of 9 A, four independent channels will be used. Parameters of the system are given in Table 7.8.1.

Table 7.8.1. Main parameters of the RF system of experimental stand with beam current of 9 A.

Operating frequency, MHz	4 (± 3.5%)
Number of channels	4
Load power, kW	4 × 40
Mode	Continuous
DC voltage on the "antenna" relative to the platform, kV	120
Anode supply power, kW	400

One channel of the above RF system is used for the second bench. All equipment of the RF system for the second bench is located on a platform under a 880 kV potential.

The first phase of the RF system was put into operation in 2013. Experiments with beam started. The housings of the tube stages and the box and the internal elements of the isolating transformers for the second phase of the system were made. The mechanical mounting of the anode rectifier for the second bench was done.

7.9. ACCELERATING CCDTL STRUCTURES FOR LINAC4, CERN

The European Organization for Nuclear Research (CERN) implements an upgrade of the injection complex of the Large Hadron Collider (LHC). The aim of the upgrade is to ensure reliable operation of the LHC with a luminosity of up to 5×10^{34} $cm^{-2}s^{-1}$. The upgrade program provides, in particular, construction of Linac4 – a new linear accelerator of H^- ions to an energy of 160 MeV (Fig. 7.9.1) – instead of the outdated Linac2 (energy 50 MeV).

Linac4 consists of accelerating structures of various types, optimized for the relevant energy ranges of accelerated particles.

BINP together with VNIITF has developed and produced seven accelerating CCDTL (Coupled Cavity Drift Tube Linac, a linear accelerator with drift tubes and coupling cells, see Fig. 7.10.2) modules for acceleration of particles in the energy range of 50 to 104 MeV. The total length of a Linac4 CCDTL section is ~ 25 m. The operating frequency is 352.2 MHz.

An accelerating CCDTL module is a π/2 structure consisting of 3 accelerating cavities (with 2 drift tubes in each) and 2 side coupling cells between them. The cavities are made of stainless steel. The inner surface of the cavities is electrochemically covered with a copper layer 30÷50 50 microns thick. The drift tubes are made of copper. Each module is installed on its support frame.

The drift tubes, accelerating cavities, coupling cells, and support frames for all the 7 accelerating CCDTL modules were made in 2013.

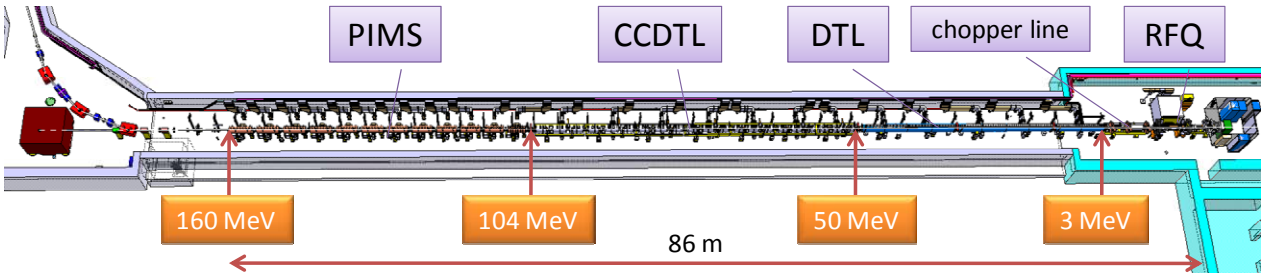

Fig. 7.9.1. Linac4 scheme.

• BINP conducted "cold" (low power) measurements of the RF parameters of the 7 CCDTL modules in the operating mode. The frequency and the quality factor of the fundamental mode were measured ($4.1 \div 4.5 \cdot 10^4$); the non-uniformity of the field (the difference in the maximum field strengths in the central gaps of tanks of one module) is <3%; the range of resonance frequency tuning with a movable tuner and the range of adjustment of the coupling coefficient of the module with the waveguide were also measured. The measured parameters correspond to the technical task.

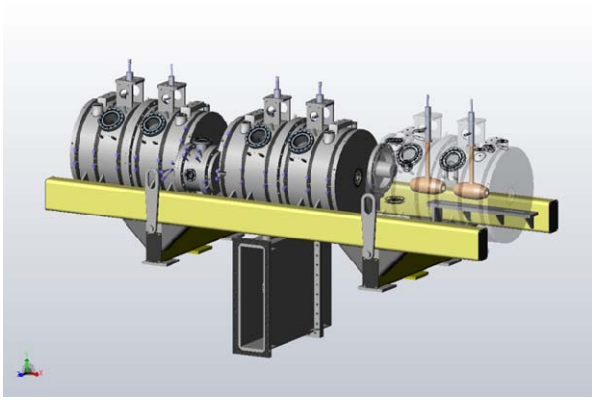

Fig. 7.9.2. Accelerating CCDTL module.

Vacuum tests of the modules were conducted (Fig. 7.9.3). The cavities of the modules were tuned basing on the frequency shifts in the cavities during pumping.

Fig. 7.9.3. Accelerating CCDTL module during vacuum tests at BINP.

All the 7 CCDTL modules had been delivered to CERN, where they were assembled and subjected to vacuum tests and geodesic measurements, the results of which correspond to the design parameters.

• All the modules have been prepared for "hot" tests with a powerful RF generator (Fig. 7.9.4). Tests of module 2 resulted in attainment of the peak power (870 kW) in the cavities of the module in 1 μs (RF pulse duration) at 2 Hz (RF pulse repetition frequency) and a vacuum of $3 \cdot 10^{-8}$ mbar, which corresponds to the nominal parameters of Linac4 in the regime of injection in the PSB.

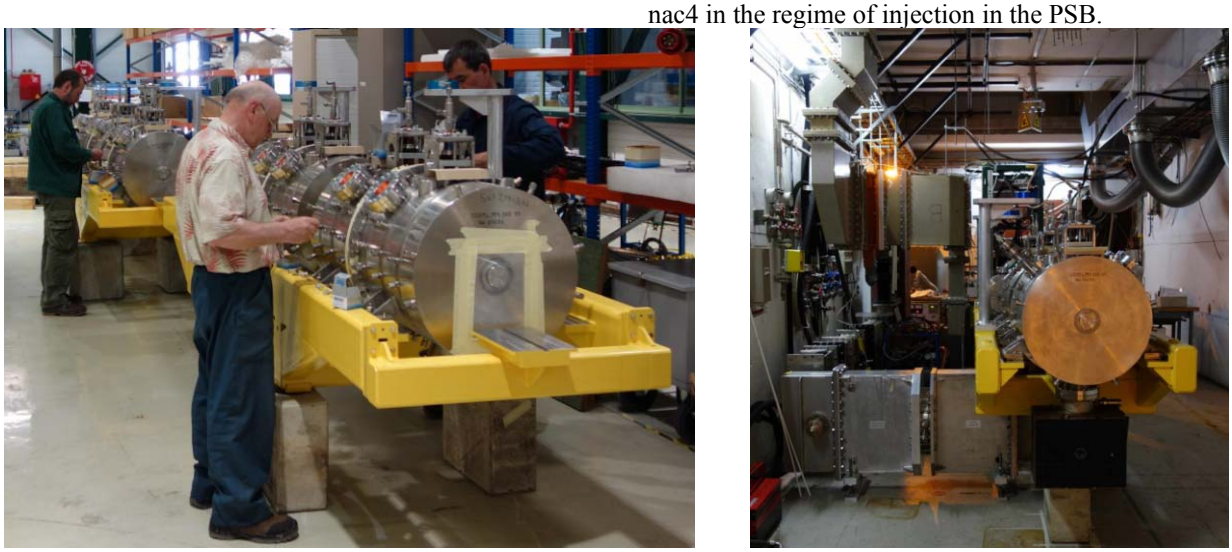

Fig. 7.9.4. Left: preparation of CCDTL modules 5 and 6 to tests at CERN. Right: module 2 secure bunker during "hot" tests.

7.10. ACCELERATING RF STATIONS OF THE ION BOOSTER OF THE NICA-MPD COLLIDER

In 2013, works under a contract with the Joint Institute for Nuclear Research (JINR), Dubna were continued. Under the contract, the Institute is to deliver to JINR two accelerating RF stations for the booster of the NICA-MPD collider. The fabrication of both accelerating cavities was completed in 2013. The cavities were warmed at 350°C, and a design vacuum of $4 \cdot 10^{-11}$ Torr (Fig.7.10.1) was attained. The cavities are ready for connection to RF generators. A cavity is formed by two coaxial line segments that are short-circuited at their ends and connected to each other in the center via an insulator. For reduction in the dimensions and increase in the shunt resistance in the operating frequency band of 0.55÷5.5 MHz, the coaxial space between the conductors is filled with rings of amorphous iron.

Fig. 7.10.1. Cavity with attached ion pump.

The permeability module of the material of the rings is at least 2,000 at a frequency of 1 MHz. Ring sizes: ∅500 x ∅250 x 15 mm. 90 such rings were made for the cavities at the Asha metallurgy factory.

Each accelerating cavity is set on 4 supports. A power amplifier with power supplies and a semiconductor broadband preamplifier will be assembled in a separate compartment under the cavity.

The assembling of the RF power amplifier is close to completion (Fig.7.10.2). The connection of the accelerating cavities with the power amplifiers and RF tests of the stations are planned for the beginning of 2014.

The output stage of the amplifier is set up as a common-cathode circuit on two GU-36B-1 tetrodes. The tubes are excited by paraphase RF voltages. The anodes of the tubes are connected directly to the free ends of the coaxial lines of the cavity near the insulator. The RF voltage amplitude on the anode of each tube is 2.5 kV and thus the accelerating voltage of each station is 5 kV in the operating frequency range. The DC anode voltage coming from the anode rectifier is 4 kV. The semiconductor preamplifier for excitation of the tubes is placed in the power amplifier compartment. The maximum output power of the preamplifier is 500 W.

Fig. 7.10.2. RF power amplifier during mounting.

The control system is made in the Euromechanics standard and is located in a separate rack. There is an oscillator driving the frequency of revolution of the particles, which is connected with the Control Center of the Booster. This master oscillator uses the DDS technology. The output frequency of DDS chip varies in a program-set dependence on synchronizing signals and also depends on feedback signals from magnetic field sensors in the Booster and gauges of position of the equilibrium orbit of the accelerated beam.

The electronics provides correct phasing of the accelerating voltages of the stations and controls the accelerating voltage amplitude by a certain program. Multichannel ADCs and DACs set and control operating regimes of the stations. The control unit is connected with the control center of the accelerator via Ethernet.

7.11. RESTORATION OF 325 MHZ RF SYSTEM OF ELECTRON ACCELERATORS AT KAERI, SOUTH KOREA

In June-July 2013, a group of BINP experts traveled to South Korea to perform the final stage of a contract with the Korean Atomic Energy Research Institute (KAERI) for restoration of the RF systems of the electron accelerator that were damaged by fire in April 2009. The accelerator has two RF systems, for frequencies of 176 and 352 MHz. The first part of the contract – restoration of the 176 MHz RF system – was completed in 2012. Below are listed works the BINP specialists performed in 2013 for the restoration of elements and performance check of the 352 MHz RF system:

1. The power supplies for the RF generators made at BINP were assembled and put into operation. The anode power supply has a constant output voltage of 9.2 kV at a current of 45 A in continuous mode (Fig. 7.11.1). The ripple voltage does not exceed 0.5%. The source has an op-

tion of fast (<30 μs) switch-off of the output voltage at a breakdown in the tetrodes of the generator.

2. The two existing RF generators for 50 kW each were revised and relevant parts were replaced. The generators had been developed and delivered by the Institute.

3. A small-signal RF control system was mounted and tested. It performs adjustment of the amplitude of the superconducting accelerating cavities and phasing of the RF voltages of the cavities with each other and with the RF voltage of the injector that is functioning now. The control system also performs auto-tuning of the superconducting accelerating cavities.

Fig. 7.11.1. Anode power supply (9.2 kV, 45 A).

The cryogenic system at KAERI was not ready and thus it was impossible to cool the cavities. The RF system was tested at maximum allowable conditions. The tests have been successfully completed.

7.12. RF INJECTOR OF MICROTRON RECUPERATOR

In 2013, the Institute continued tests of the new RF injector for the microtron recuperator of the Novosibirsk free electron laser. The tests were conducted on a stand equipped with instrumentation for beam diagnostics, a 30 kW beam dump, and radiation protection.

The RF injector includes a 90 MHz accelerating cavity with an integrated grid thermal cathode assembly and a plug-in control unit for the grid thermal cathode assembly.

The control unit sums up four types of voltages on the control grid of the thermal cathode assembly: two AC voltages with frequencies of 90 and 360 MHz and an amplitude of 20 V, constant cutoff bias of up to 120 V, which regulates the bunch charges, and a surge voltage of 60 V with a pulse duration of 4 ns and an adjustable pulse repetition rate of up to several MHz.

With this control unit electron bunches with energies of up to 300 keV, a regulated duration in the range of 0.5÷1.5 ns, a charge of up to 1.5 nC and a repetition rate of up to 2 MHz were produced. At a repetition rate of 90 MHz a maximum average current of 55 mA of a 250 keV beam was attained.

The works on the sand will be continued in 2014. In particular, tests and refinement of the existing control block are planned. There are also plans to apply the new assembly with a view to obtain an average beam current of 100 mA and more. The new assembly is based on voltage switching by RF transistors. The assembly generates pulses 1 ns long with an amplitude of up to 120 V and adjustable repetition rate of up to 100 MHz.

Besides, the analysis and measurements of beam characteristics, such as bunch duration, emittance, energy spread etc, will be continued.

7.13. RF INJECTOR FOR ACCELERATOR AT VNIIEF

The design average current of the RF injector is 40 mA and more; the electron energy is 50÷100 keV. The bunch duration is 1 ns; the bunch repetition frequency is adjustable from 0 to 100 MHz.

- The RF injector consists of a 100 MHz accelerating cavity (Fig. 7.13.1) with an integrated grid thermal cathode assembly and a plug-in control unit for the thermal grid cathode assembly. The coaxial cavity is loaded with a capacitor. The cavity is excited by a 15 kW tube RF generator (on a tetrode GU-92A) through a loop power input (Fig. 7.13.1, top). The control unit operates via voltage switching by RF transistors.

Fig. 7.13.1. RF cavity of injector for VNIIEF.

The RF generator was assembled and prepared for operation at the workshop of the Institute in 2013. The fabrication of the RF cavity units was completed using advanced technologies, such as electron beam welding, diamond turning on numerical-control machines, and thermal diffusion brazing in vacuum oven of the bimetallic (copper - stainless steel) housing with silver plating inside.

- The cavity was assembled, checked for vacuum leaks and moved to the stand for further testing, including RF training and work with beam. The latter is planned for early 2014.

7.14. UPGRADE OF RF SYSTEM FOR MICROTRON RECUPERATOR

The RF system of the microtron recuperator of the Novosibirsk free electron laser includes two 180 MHz continuous-wave RF generators with a maximum output power of up to 600 kW each. The output stage of each generator sums up the power of 4 GU-01A tubes.

Long-term experience of work with GU-01A tubes showed the tube life to be over 4,000 hours if the power generated per tube is below 120 kW. At the same time, if the output power of the generator is increased up to 120÷150 kW per tube, its lifetime decreases to 1,000 hours and even to a lesser value in some cases. The main causes of tube failure after the specified time are short-circuits between the grids or between the control grid and cathode and quickening breakdowns between the anode and the screen grid. Therefore it was decided to upgrade the RF generators, replacing the GU-101A tubes by TN781 tubes made by THALES. The guarantee period of these tubes is 3,500 hours. At a less filament voltage and an output power of 150 kW, the expected lifetime is over 7,000 hours.

The adaptation of the stages of the generators to the TH781 tubes and replacement of tubes began in 2012. The remaking of the stages addressed only intra-stage elements. In 2013, the upgrade of the RF generators of the FEL microtron was completed. All the 8 GU-101A tubes were replaced by TN781 ones in the output stages of both generators feeding the accelerating cavities of the microtron. For increase in the output power of the generator, the following optimization of the power supplies for the generators on TN781 tubes was performed: the filament voltage was decreased (8.5 V); the anode voltage was increased (up to 10 kV); the bias voltage of the tubes was augmented (up to –250 V). Certain steps were made for suppression of self excitations of the stages at non-operating frequency. Currently, each generator is working stably at a continuous power output of 550 kW.

7.15. 100 MHZ GENERATOR WITH OUTPUT OF 540 KW IN CONTINUOUS MODE

Under a contract with VNIIEF the Institute developed a design of RF generator with an output power of 540 kW at 100 MHz in continuous mode. The required power capacity is attained via summing-up of the powers of three generator units on domestic tubes GU-101A. A similar scheme of power combining has been successfully used for many years in 180 MHz modular generators that were developed at the Institute for different installations. The combining of the powers of the three tube modules is done by their direct connection with the output line with loads in cross sections of the line at distances that are multiples of half the wavelength. Each generator module provides an output power of 180 kW at the least.

Each generator module is excited independently. A module includes a semiconductor preamplifier with an input power of up to 3 W and an output power of 500 W at the least. The power from the preamplifier arrives at the input of an intermediate amplification stage made on a GU-92A tetrode. The output power of this stage, 12 kW, is applied to the input of the output stage of the generator, which uses a GU-101A tetrode (Fig. 7.15.1).

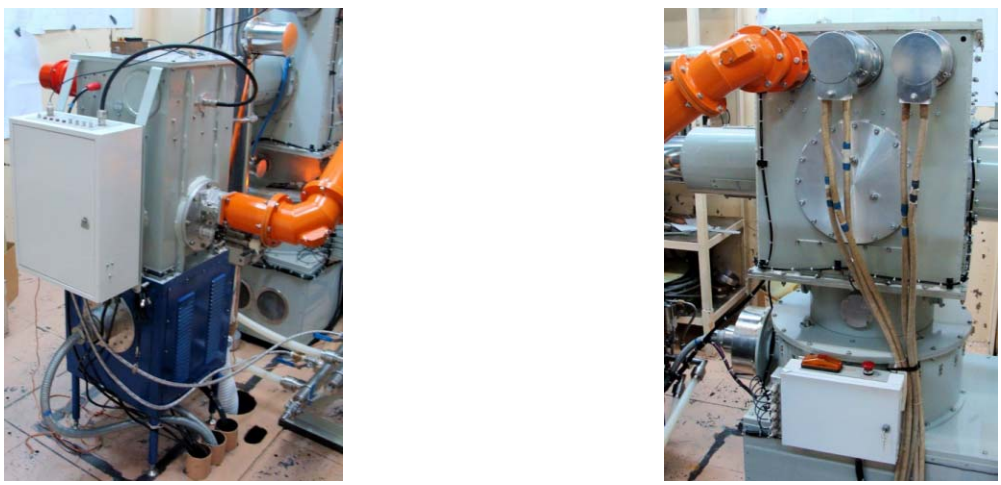

Fig. 7.15.1. Left: – transistor preamplifier and pre-output stage on GU-92A; right: output state on GU-101A.

An optimal balance of phases and amplitudes of excitation voltages is achieved with a system for controlling the amplitude and phase of input signals of the generators. The system requires no tuning in the frequency range of 100 ± 1 MHz, except for resonance tuning of the anode circuit common for the three tubes (coupling line).

The load coupling is adjusted by change in the wave impedance of a quarter wave section at the output of the combining line. The coupling adjustment system allows attaining a power of 540 kW at a VSWR of 1.3 at most in the operating frequency range. The output of the combining line is designed for connection of a hard coaxial copper feeder with an impedance of 50 Ohm and diameters of the internal and external conductors of 70 mm and 160 mm, respectively.

Each of the three tube modules has its own system of high-voltage and low-voltage power supply. The high-voltage PS applies the operating voltage to the anode and screen grids of the tetrodes and ensures smooth rise of the voltage at switching-on or a rapid shutdown at a breakdown in the tubes and circuits of the RF generator. The anode power supply is an adjustable high-voltage source with input controlled by a regulator on thyristors that operates at the mains frequency. The GU-101A anode supply voltage is −13 kV and that of GU- 92A is −6 kV. The output of the GU-101A tube source (− 13 kW) has a fast protection circuit for breakouts and overloads with a response time of ≤50 μs.

The first generator module was fabricated and tested at the Institute and then delivered to VNIIEF and commissioned in 2010. In 2013, the Institute started the fabrication of the second generation module. Some elements of the stages of the generator were fabricated; the assembly of the cabinets for the power electronics was begun. A set of control electronics was prepared, which includes a variable gain amplifier and a modulator, which are used in a feedback loop that regulates the amplitude of RF voltage on the cathode of the output GU-101A tube. The required phase of this voltage is stabilized by another feedback circuit – a phase meter measures the phase difference between the reference RF signal and the RF voltage from the GU-101A cathode. The output of the phase meter controls a phase shifter in the variable-gain amplifier. The construction of a test bench for the generator and the power combining system on the coupling link was started. Tests of the second generator module are to be carried out at the Institute in 2014, and a contract for fabrication of the third generator module and the power combining line will be concluded.

7.16. UPGRADE OF RF GENERATORS OF COMPLEX "SIBERIA-2"

In 2013, the Institute fabricated and delivered to Kurchatov Institute, Moscow elements for upgrade of the output stages of the RF generators of the complex "Siberia-2". The upgrade will be performed with the aim of replacement of the domestic tubes GU- 101A by TN781 tetrodes made by THALES, which in turn will increase the tube lifetime and the reliability of the generators. The three accelerating cavities of the complex "Siberia-2" are excited by two generators, operating in continuous mode. In the output stage of each generator, the powers of two GU-101A tubes are summed up. Thus, four tubes are to be replaced. In 2014, the output stages are to be remade; the TN781 tubes are to be mounted; the generators are to attain the operating regime with beam in the "Siberia-2" storage ring.

7.17. DEVELOPMENT OF EQUIPMENT AND SYSTEMS FOR AUTOMATION OF PHYSICAL RESEARCH

7.17.1. Electronics for monitoring and control of COSY cooler.

The following developments were carried out for the electronic cooling facility of the COSY accelerator (Germany):

- control crate for the high-voltage terminal (HVT);
- a "Compass" system;
- a set of control and interface modules.

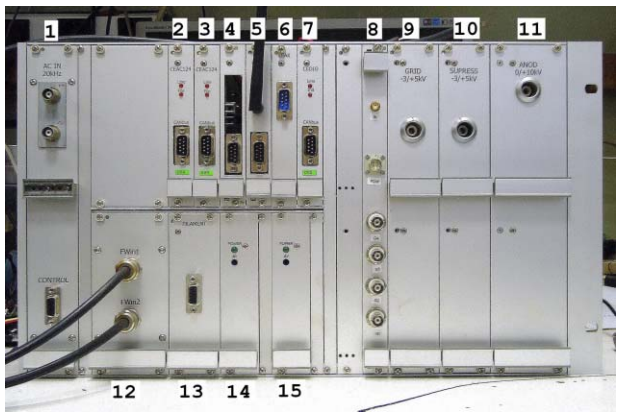

Fig. 7.17.1. Control crate for the high-voltage terminal of the COSY cooler.

The HVT crate is shown in Fig. 7.17.1. It contains 15 modules, some of which (modules 9, 10, 11, and 12) provide stable power supply for the high-voltage electrodes of the gun and collector with an accuracy of 0.1%, and an 8-ampere filament supply (modules 13, 14, and 15). Besides, the crate comprises a beam diagnostic module (8) and a module for optical communication with the PS of the collector (4). The collector current and the leakage current are measured via module 6; modules CEAC124 (2 and 3) and CEDIOB (7) control the crate via a CAN communication line.

Because of the extremely large potential across the HVT (up to 2 MV), the CAN control is transmitted via a radio link (module 5) and the crate (module 1) is fed via a

25 kHz stage transformer of the accelerating column. The four-fold range of allowable input voltages that can be applied to the primary source (1) ensures reliable operation under any column-feeding loads.

Links with the "ground" are realized via standard Wi-Fi access points with an operating frequency of 5 GHz. To this end, an additional module has been developed and installed in the HVT. This module houses an Ethernet-CAN gateway and PSs for the gateway and the Wi-Fi access point inside the HVT. The second access point, which is connected to the control computer, is located under the stage transformer of the accelerating column.

Effective electron cooling of proton beam requires high homogeneity of magnetic field on the axis of the solenoid – its transversal component should not exceed a value of 10^{-5} from the longitudinal constituent. This is achieved via mechanical adjustment of solenoid sections after measurement of actual inhomogeneity using the system "Compass".

The system "Compass" (Fig. 7.17.2) includes optomechanical and electronic parts. Gimbaled planar movable mirror 3, which is placed on the axis of solenoid 1 in vacuum volume 2, is the sensitive element of the system. The planar mirror is oriented across the force lines using a ferromagnetic core. A mechanical drive can move the sensitive element by guides along the axis of the solenoid.

Parallel light beam 4, which is generated by semiconductor laser 5, falls on the mirror. Mirror-reflected beam 6 passes backward and gets to four-quadrant photodiode 7.

The system is adjusted so that, when the mirror is oriented straight across the solenoid, the light spot is formed in the center of the photodiode, causing equal signals from its sectors. Deflection of the mirror that occurs when a magnetic field transverse component appears makes the spots on the photo-diode shift and changes the output currents from the sectors. Because of the large length of the system, a deviation by an angle of 10^{-5} causes a displacement of about 0.1 mm.

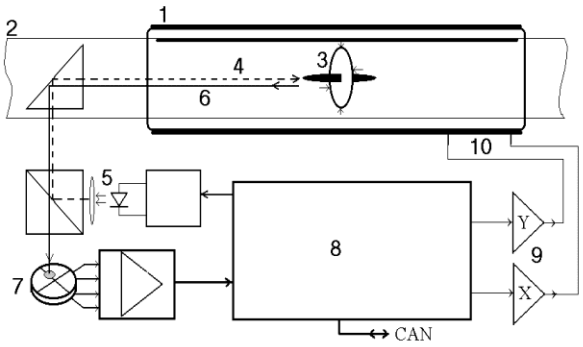

Fig. 7.17.2. Structure of "Compass".

The amplified output signals from the sectors arrive at main electronics unit 8 behind the radiation protection. The unit forms signals corresponding to the vertical and horizontal displacements of the light spot.

Then these signals with given amplitude coefficients are delivered to actuators of the PID controller and from its output, to external power amplifiers 9, which form currents in two elongated pancake coils, stacked vertically and horizontally along the solenoid.

At the beginning of the measurements, the sensor is moved to a specified area of the solenoid. Next, with the PID controller circuit opened, the light beam is directed at the photodiode (either manually or by computer). Then the PID controller is switched on, closing the feedback loop and outputting the light spot in the center. The corresponding currents in the pancake coils are recorded, fields induced by them compensating the stray transverse magnetic field components in this area of the solenoid.

These measurements are repeated at a set of points along the solenoid. Thereafter, based on the resulting heterogeneity profile, the position of solenoid sections is adjusted.

A set of control and interface modules was prepared by the members of the Radiophysics Laboratory for interaction of the control computers with subsystems of the cooler. These modules are presented in Table 7.17.1.

Table 7.17.1. Control and interface modules for the COSY cooler.

Unit	Q-ty	Purpose
CAN-Ethernet	5	Link with CAN modules
CEAC208	1	Compass
CEAC208	10	Operation with MPS-6
CEAC124	7	Operation with 20 PSs
CEAC124	2	Operation in HVT
CEAD20	6	Temperature meter and signal meter
CEDIO_B	1	Input/output register
CEDIO_C	16	Control of heaters and gathering of interlocks
Total	43	

7.17.2. Measurement electronics for NSLS II booster.

Members of the Institute have created a system to measure parameters of pulsed fields of the injection and extraction magnets of the NSLS-II booster. In the spring of 2013, these electronics were integrated into the overall control system of the booster and tested on real signals under control of engineering programs (Fig.7.17.3).

The first group of modules in the system (module VsDC 3) is intended for measurement of magnetic fields in the septum and bump magnets. The error they induce while working with microsecond pulse signals does not exceed $3 \cdot 10^{-5}$, which is much better than the accuracy requirements for measuring the field in the magnet. This allows one to use the module VsDC 3 to adjust the current of the high-power switched PSs of the magnets, ensuring high stability of their work.

The second group of modules consists of digital ADC-200ME recorders and is intended for oscillography of operating currents in the windings of the injection and extraction kickers. The recording accuracy shall be about $\pm 10^{-3}$, while the pulse width is only 300 ns. Options of the ADC-200ME modules enable if necessary feedback to adjust currents of the kickers.

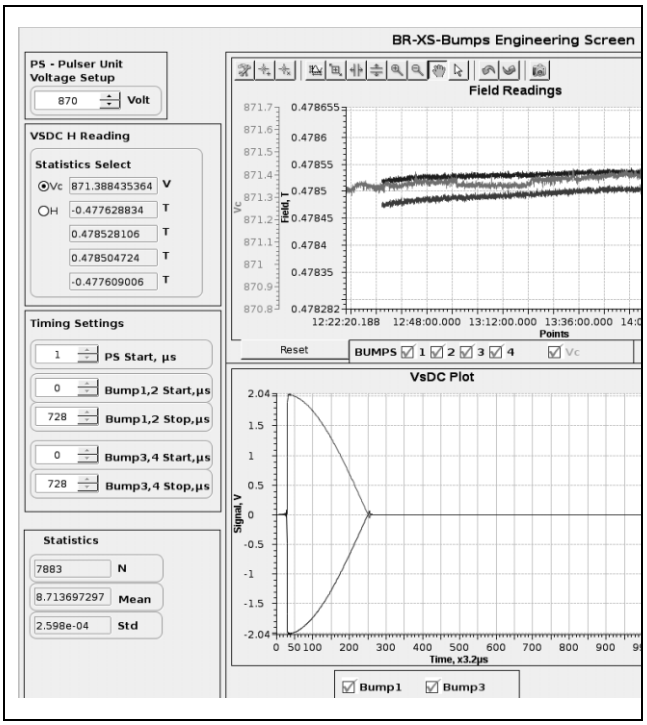

Fig. 7.17.3. Engineer screen for controls of field in bump magnets. The upper graph shows that the measurement noise is about $3 \cdot 10^{-5}$, and the field stability is better than 10^{-4}. The lower graph shows waveforms from induction sensors.

7.17.3. Controller of accelerating RF stations of NICA booster.

Under the contract on the development and fabrication of the RF stations for the NICA booster, the development of the controller of the stations started in April 2013.

The most important function of the controller is high-precision measurement of magnetic field in the aperture of the booster magnets and generation of master sinusoidal signal, which is in link with the measured field value. The error of keeping the field/frequency ratio should be better than 10^{-4}, which implies that the error of field measurement and dynamic errors of the master oscillator should be $5 \cdot 10^{-5}$ at least.

Besides the above task, the controller adjusts the amplitude of the accelerating voltages of the cavities by a given law, depending on the booster operation phase, and controls the modes of the high-power stages of the stations. In addition, the controller measures about twenty signals characterizing the behavior of elements of the stations during an acceleration cycle.

The structure of the controller is shown in Fig. 7.17.4.

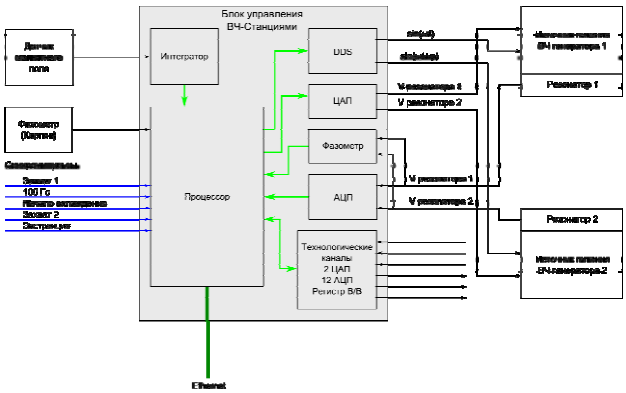

Fig.7.17.4. Structural schematics of RF controller of stations.

The device is based on a single-board computer with 536 MHz microcontroller ARM Cortex-A5 Atmel SAMA5D31. The peripherals are controlled via SPI and I^2C buses with clock frequencies of 50 MHz and 400 kHz, respectively.

The controller software is implemented as two co-routines. The first co-routine is Linux with installed server Tango and is for integration with the control system of the booster. The second co-routine is activated upon start of acceleration cycle and provides all the necessary measurements and real-time operation of the master oscillator.

7.17.4. Precision devices.

The Institute is a leader in the field of development of precision devices of grade 10^{-5} and higher. Below are described two works performed in this direction in 2013.

A controller of PSs for correction magnets for the European free-electron laser (European XFEL) realizes all the functions of control of the high-power units of the source. It contains a 18-bit DAC that sets the output current, a multichannel 24-bit ADC that provides measurements of some voltages, I/O registers, and a CAN bus interface with the control system of the installation.

The controllers were developed subject to the following requirements:

– DAC accuracy grade: 10^{-5} (100 µV);
– DAC stability over year: $5 \cdot 10^{-5}$ (500 µV);
– stability over 8 hours: 10^{-5} (100 µV);

– DAC temperature stability: 1.5 ppm/°C;
– MTBF 10^5 hours (12 years!)
– DAC error: 10^{-5} (100 μV)

The electrical specifications did not look fantastic as BINP applies controllers with even better parameters in its installations, e.g. sources of the CANDAC-20 type. However, the requirements of long-term stability and reliability, as well as on meeting them for the entire series of controllers (400 pieces), made us solve the problem of designing and tracing of PCBs in most thorough way, find a manufacturer of PCBs, select component types and suppliers and agree them with the customers.

Fig.7.17.5. Photo of controller.

A few controllers (Fig.7.17.5) were made in 2013, two of which were shipped to DESY for preparation and testing of programs. Programmers at DESY found the system of commands (based on a similar one that is conventional at BINP) of this controller to be rational and convenient. At the same time, our collaborators had some suggestions on enhancing the functionality of the device. As a result, now the controller functionality is markedly superior to the previous designs. The serial production of these units and equipping the manufactured sources with them will be started in 2014.

The wide-range current meter of ionization chambers should also be classified as a high-precision device. Ionization chambers (ICs) are used in works with synchrotron radiation for SR beam monitoring. The level of output signal of IC is usually small. Depending on the chamber design and the interior medium (vacuum/gas), the output current may be in the range of tens of femtoamperes to a few microamperes.

Three experimental devices were made in 2013. They are capable of measuring currents from 10^{-15} A to 10^{-6} A and have two identical channels, each with a "current-voltage" converter and a 24-bit ADC. Besides these elements, which transform current into a digital code, the devices comprises a controllable high-voltage source with low noise level, connected to the chamber, and a communication module by which the device is linked with the user computer through the Ethernet interface. With the two synchronously-operating channels in the current meter one can create a system to stabilize the SR beam position.

Due to the functionality of the device, it can also be used in other investigations associated with ultra-low current measurements, for example in PH-metering or in research on semiconductor structures.

Fig. 7.17.6 shows the device without housing and directly connected to the IC, which allows perform all electrical links with it directly, without the use of cables and plug connections.

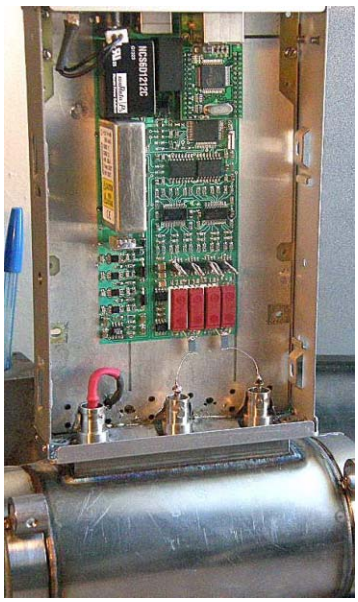

Fig. 7.17.6. Photo of femto-ampere current meter mounted on ionization chamber.

7.17.5 Research to improve stability and reduce ripple of field in magnets of VEPP-4 to $5 \cdot 10^{-7}$.

The need in this work is linked with the preparation of new experiments in high-energy physics. This work was divided into two phases. In the first phase, the possibilities of CANDAC-20 modules, which are controllers of sources of the IST type and first of all determine the accuracy parameters of magnet current in the frequency range of up to 1 Hz, were thoroughly investigated.

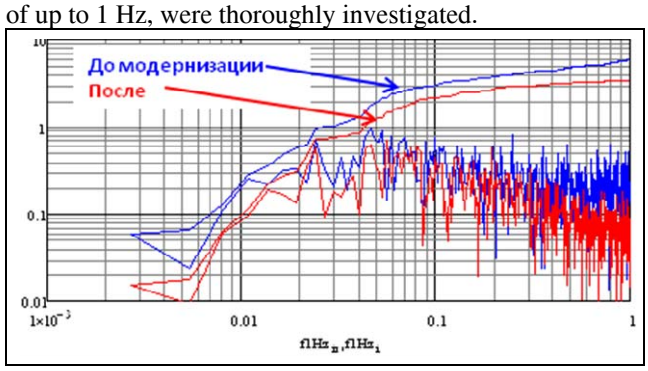

Fig. 7.17.7. Ripple spectrum and ripple voltage of CANDAC-20 (microvolts) vs frequency range before and after modernization.

Then a thorough revision of the CANDAC-20 circuitry was carried out, which allowed refinement of a few units. The results are presented in Fig. 7.17.7.

The figure shows that in the frequency range of up to 1 Hz the ripple level was reduced 2-fold on average and became equal to 2 μV ($2 \cdot 10^{-6}$).

In the frequency range of 1÷100 Hz, a decisive contribution to the instability comes from the high-power elements of the IST source. The ripple level is no longer dependent on the CANDAC-20 control voltage quality, and thus it was proposed to investigate the possibility of suppressing high-frequency pulsations by an induction method.

The essence of the proposal was in the measurement of field ripple with an induction sensor with subsequent adjustment of current into the winding of the magnet by means of a generator that is connected to the IST source in parallel and has a current opposite to the measured ripple. First of all, it was necessary to make sure that the ripple of magnetic field with an amplitude of $5 \cdot 10^{-4}$ G (δB/B ~ $3 \cdot 10^{-7}$) in the 100 Hz frequency band can be measured. Then it was necessary to close the feedback and check whether the ripple can be corrected on a local site of the magnetic structure, which seems to be simpler than working with all magnets of the ring simultaneously.

The experiments on ripple correction were performed with a separate so-called gauge magnet, which was connected in series to the structure. The results in Fig. 7.17.8 include two types of graphs: spectral composition of the ripple and field ripple levels vs. frequency band obtained as the square root of the sum of squared amplitudes of the spectrum components.

For both types of graphs, the situations before and after the correction are shown. One can see that in the gauge magnet the ripple was reduced by almost an order of magnitude. In 2014, these experiments will continue with the whole magnetic system.

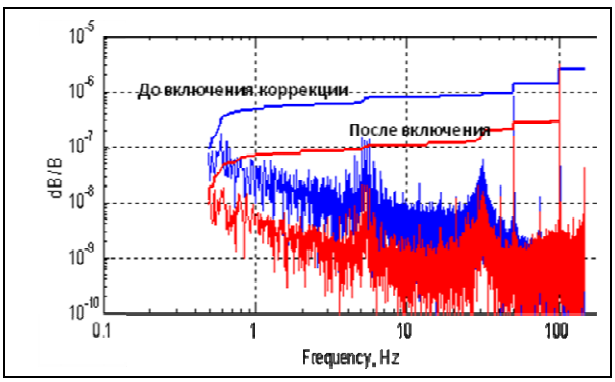

Fig. 7.17.8. Field ripple levels vs. frequency band (upper curves) and ripple spectra (lower curves) (in units) before and after the correction. All graphics are in the units δB/B; B = 1,800 G.

7.17.6. Magnetic measurement systems based on inductive method.

It is known that magnetic measurements based on the induction method imply signal integration. In recent years, the Institute has created for such measurements a new generation of electronics that uses the digital integration method. Solutions that were found in the course of the development enable creation of precise and yet wideband and multifunctional integrators VsDC 2 and 3 VsDC (Volt-second to Digital Converter), which have been widely at the Institute since 2012. Below are presented examples of works in 2013.

Upgrade of the system of measurement of pulsed fields of the bypass from the BEP storage ring to the VEPP-2000 collider. The bypass is equipped with 22 pulsed magnets, 4 pulsed bending dipole magnets and 2 septum magnets. The stability of fields generated by the magnetic elements of the bypass is controlled with induction sensors. It should be noted that only the high-power dipole magnets and septum magnets are equipped with sensors that measure the magnetic field itself. As for the other elements of the bypass, it is not field that is measured but the current in the bus that feeds the magnet. The measurement is done using belts in the PSs of the AC-CORD type. The measurement system is made on the basis of VsDC2 integrators and has 40 measurement channels.

The equipment for **pulsed measurements in the magnetic elements of beam line K 500** is made in a similar way. The pulsed magnets are fed by new-generation PSs of the GID-25 type.

These PSs are placed in Euromechanics crates and are functionally complete devices with modules for control and communication with the computer, power devices and VsDC2 integrators. A photo of the control and measurement modules of the PS GID-25 is shown in Fig. 7.17.9.

Fig.7.17.9. Control and measurement modules of GID-25PS.

7.17.7. Manufacture and operation of earlier-made equipment.

Every year the Institute produces series of earlier-designed units, which are needed for upgrade of the existing equipment or for newly created systems. The follow-

ing was manufactured, adjusted and put into operation in 2013:

14 CEAC-124 units,
10 CEAC-208 units,
5 CEAC-51 units,
15 CGVI-8ME units,
7 CAC-208 units,
40 VsDC 2 units,
5 VsDC 3 units, and
20 IPP-32 units.

Fig.7.17.10. New controller for ovens.

The Laboratory keeps maintaining the electronics of various experiment and production stands at the Institute. For instance, the Laboratory ensures the manufacture and measurement of numerous magnetic components made at the Institute. The Laboratory maintains the control systems for four ovens for hot gluing of magnetic elements. In recent years, the control electronics of the ovens has been based on new up-to-date controllers (Fig.7.17.10).

The systems for precise measurement of magnetic element parameters on benches require constant and very thorough maintenance. Five Hall systems and three induction-method systems are in use at the Institute now.

The Radio-physical Laboratory is also responsible for the technical servicing and repair of hundreds of electronic units that were created at the Laboratory and are in service on installations at the Institute and other organizations.

Since in previous decades the mass automation was based on the CAMAC standard, most of the devices operated are CAMAC units. For information, Table 7.17.2 presents the amount of CAMAC electronics on VEPP-4 only.

Significant quantities of CAMAC modules and systems are used on VEPP-2000, FEL, GOL-3, GDT, KEDR detector, and various stands. The "youngest" CAMAC unit – ADC-333 – is 13 years old, and the "oldest" ones are about 35 years old. The Laboratory staff show a lot of resourcefulness in search for microcircuits made in the 80s, repair of peeling-off conductors on printed circuit boards, restoration of connectors, etc. Apparently, it is high time to take a decision to develop a new generation of electronics for the numerous automation systems of the installations of the Institute.

Table 7.17.2. Amount of CAMAC equipment in the VEPP-4 control system in 2013.

Odrenok	Purpose	Number of CAMAC modules
MSVEPP-4	Control of VEPP-4M magnetic system	70
BEAMV-4	VEPP-4M beam diagnostics	90
MSV3	Control of VEPP-3 magnetic system	40
RFV3	Control of VEPP-3 RF system	20
BEAMV-3	VEPP-3 beam diagnostics	40
UPO	Control of "Positron" injector	80
IPO	Monitoring of "Positron" injector	40
CHAN	Control of VEPP-3/VEPP-4M beam line	70
BEAMPO	Beam diagnostics in transport beam lines	20
CONTROL	Vacuum and temperature control	20
FOTHSCAN	Control of position of SR beam from VEPP-3	6
Total:		**496**

8

POWERFUL ELECTRON ACCELERATORS AND BEAM TECHNOLOGIES

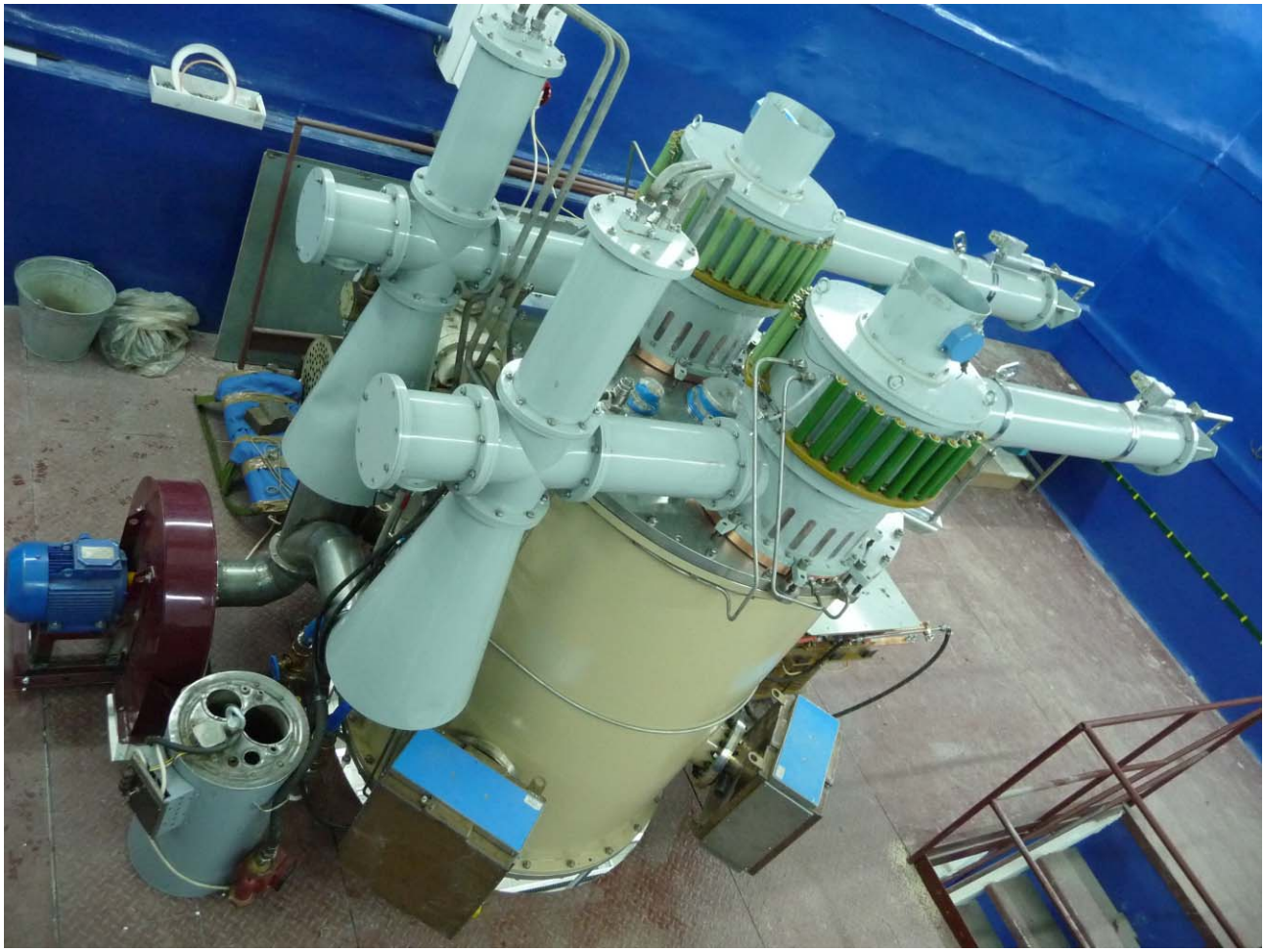

Fig. 8.1.1 ILU-10 accelerator for joint BINP-NSU laboratory.

8.1. ACCELERATOR SUPPLIES

Since 1983 the ILU accelerators are supplied abroad where they are used for researches and are working in the industrial lines. Some of these machines are working round the clock for years. The reliability and technical level of these machines is confirmed by the new supplies.

The manufacturing of the ILU-8 machine for radiation treatment of cables was started according the contract with public corporation OKB KP, Mytischi, Moscow region.

2 converters with collimators for X-rays generation were shipped and mounted on the accelerator in Korea according the contract with the Korean firm EB-TECH Co., Ltd. The converters are purposed for 2 electron accelerators with beam power up to 10 kW and electron energy range of 5 – 7.5 MeV. The presence of the controlled collimators was stipulated by the customer from the very beginning.

The adjustment works were carried out on the ILU-10 machine mounted in the Park for Nuclear Technologies, town of Kurchatov, Kazakhstan.

The new RF cavity was manufactured according the contract for modernization of the ILU-6 accelerator signed with BARC, Mumbai, India. The planned upgrading result – the accelerator ILU-10M with maximum energy of 5 MeV and beam power up to 15 kW, the ILU-6 accelerator has the energy range up to 2.5 MeV. The new RF cavity was tested in the BINP, accepted by the representatives of the BARC and shipped to India.

The preparation works for the joint BINP and Novosibirsk State Univercity research and educational laboratory on radiation technologies are going on. The electron accelerator ILU-10 (Figure 8.1.1) with the power supply system (Figure 8.1.2) were manufactured for this laboratory.

Fig. 8.1.2. ILU-10 power supply system for joint BINP-NSU laboratory.

8.2. RADIATION-THERMAL FERRITE SYNTHESIS PROCESS DEVELOPMENT

Radiation-thermal process for ferrites synthesis was developing in collaboration with the Institute of Solid State Chemistry, Siberian Branch of RAS, according the state contact titled "Development of scientific and technical basis for nanoprecursors production and radiation-thermal synthesis of ferrite ceramics purposed for radioelectronics applications and instrument engineering by means of intensive electron beam with energy up to 5 MeV and synchrotron radiation diagnostics methods for products analyses".

The preparation of the initial reaction mixtures was elaborated as well as the ways and temperature regimes of the ferrite ceramics radiation-thermal synthesis.

The thermal synthesis of the same ferrite ceramics was carried out for comparison.

The parameters of the experimental samples were measured by different methods.

The reaction mixtures for the ferrites synthesis were prepared from the purchased fine chemicals (metal oxides) and from the oxides nanopowders produced by evaporation by intensive electron beam generated by ELV-6 accelerator and the following vapor condensation. Also the mechanochemic activation in the mills was used for oxides mixtures to properly mix them and to diminish the particle sizes. The measured particle sizes after the milling were from 30 to 100 nm.

The structure and phase composition of the ferrite ceramic samples were studied by different methods including the synchrothron radiation.

The tomographic images of the ferrite samples were obtained on the synchrotron radiation source VEPP-3 on the station "Microscopy and Tompgraphy".

The difractometry studies of the samples' surfaces were carried out on the VEPP-3 second synchrotron radiation channel.

The samples' edges peek-a-boo difractometry was carried out on the VEPP-3 forth synchrotron radiation channel.

The small size of the initial particles and the radiation-thermal process allow to carry out the ferrite ceramics synthesis for short time – up to some minutes at temperature of 900 °C. The ferrite synthesis reaction in these conditions are fully completed – the initial oxides content in the ferrite ceramics samples after the synthesis ended can be very close to zero. The zero initial oxides concentration was fixed by the studies. The high resolution roentgen tomography studies (the most sensitive method) proved the zero content of the initial oxides with accuracy of less than 0,1%. (The initial oxides content can be up to 30% in the commercial ferrites.)

The grain sizes in the ferrite ceramics samples produced by radiation-thermal process were measured by electron backscattering diffraction, the sizes were 0.3-0.5 micrometers. The industrial RF ferrite type 100VCh was studies also by the same method, its grains were less than 5 micrometers.

The ferrite ceramics with grain size of 0.5 micrometers has rather low magnetic permeability – from 10 to 80. Such ferrites are suitable for work in the superhigh frequency range.

The comparison of the radiation-thermal and thermal ferrite synthesis showed the advantages of the radiation-thermal process – synthesis temperature decreased and the synthesis duration reduced from 18-20 hours to 20-30 minutes.

8.3. NEW RADIATION TECHNOLOGIES DEVELOPMENT

The radiation treatment of the beneficated ores was carried out in collaboration with the Institute of Mining, Siberian Branch of RAS. The radiation treatment resulted in the energy consumption for the following ore reduction and increase in the output of the useful minerals containing the nonferrous metals.

The iron ore radiation-thermal treatment resulted in the phase transitions and appearance of the magnetic properties – the magnetite formation was observed. It permits to use this process for following ore benefication.

The mixed feed electron beam treatment was carried out in collaboration with the Institute of Experimental Veterinary for Siberia and Far East, Siberian Branch of Russian Agricultural Academy, to prolong the keeping time for the products delivered to the Northern Territories of Russia.

The irradiation influence on samples made of various polymers (polyethylene, fluorocarbon polymer, polymethylmethacrylate, etc.) was carried out to study the changes in strength properties (plasto-elastic deformations). The work was performed in collaboration with the Institute of Hydrodynamics, Siberian Branch of

Russian Academy of Science, to set the data for deformation analysis models.

The irradiation influence on samples made of specially prepared nylon films with various impregnations was carried out to create the blood vessels prothetics. The work was performed in collaboration with the Institute of Chemical Biology and Fundamental Medicine, Siberian Branch of Russian Academy of Science. The first prothetics were successfully implanted in mice. The final goal – the growth of the body's own tissues on these prothetics.

The possibilities of electron beam treatment for the heavy hydrocarbon compounds (including tar oil and pitch) were studied in collaboration with the Institute of Solid State Chemistry and Mechanochemistry, Siberian Branch of Russian Academy of Science.

The electron beam treatment of the silver stearate and the silver salts solutions was carried out in collaboration with the Institute of Solid State Chemistry and Mechanochemistry, Siberian Branch of Russian Academy of Science, to obtain the silver nanoparticles

The chemical reactions mechanisms in the incapsulated systems based on the nanostructured oxides formed by the mechanochemical and radiation thermal processes were studied aiming the formation of materials with the set functional properties. The work was carried out in collaboration with the Institute of Solid State Chemistry and Mechanochemistry, Siberian Branch of Russian Academy of Science, within the framework of the SB RAS Integration Project.

8.4. APPLICATIONS OF INDUSTRIAL ELV ACCELERATORS IN SCIENCE AND TECHNOLOGIES

8.4.1. Accelerators supply.

The main activity of the laboratory is to manufacture and supply of ELV accelerators. In 2013 laboratory team delivered 10 ELV accelerators. At the same time 15 accelerators were assembled, installed, put to commissioning and started up. 6 accelerators were delivered in complete assembly, 4 accelerators were supplied to the customers in cooperation with companies from South Korea and Republic of China).

The energy distribution is shown in Table 8.4.1.

Table 8.4.1.

ELV-4 (1.0 MeV, 1.5 MeV)*100 kW	6
ELV-8 (2.5 MeV)*100 kW	4

Distribution by countries is given in Table 8.4.2.

Table 8.4.2.

Country	Supply 2013	Startup and commissioning
China	4	9
Korea	3	3
India	1	0
Germany	1	1
Russia	1	2
Indonesia	0	1
Total	10	15

8.4.2. Experiments in cooperation and collaboration.

Currently, the National Laboratory of Superconducting Cyclotron at Michigan State University, East Lansing, USA (Michigan State University National Superconducting Cyclotron Laboratory) developed a new generation facility to obtain beams of rare isotopes FRIB (Facility for Rare Isotope Beams). Its main purpose is to obtain and study of new isotopes of chemical elements for the study of fundamental matter properties. Introduction of the facility is planned for 2018 - 2019 years. In FRIB facility the scheme of fragmentation of implemented primary ion beam at a solid target is implemented. Ion beam (from oxygen to uranium inclusively) with 400 kW power, the energy of up to 200 MeV/nucleon and the transverse size of about 1 mm is splited into fragments in a collision with a carbon target, producing new isotopes, which further are sent to an experimental area for study.

The target for isotope production is a multiple-section disc made of graphite, with 5000 rev / min rotating speed. Its specific feature is the high (up to 1900^0C) temperature. This is due to the release of primary beam power in the form of heat from it. During the development of the target design the special attention was focused on its reliability in operation. To this end, a target prototype was produced to test it under the electron beam of up to 50 kW power, and 700-keV energy.

Fig. 8.4.1. The vacuum chamber of prototype target.

Fig. 8.4.2. Set slices of target graphite.

In the framework of cooperation between the INP and the University of Michigan in INP the graphite target for FRIB under focused electron beam of ELV-6 accelerator were tested. During joint experiments with participation of Michigan State University specialists the calculated temperature was achieved and operating mode of target operation is FRIB facility was simulated.

During the tests, the graphite targets were placed in a sealed vacuum chamber made of stainless steel, which was attached directly to the extraction device of electron ELV accelerator. Electron beam generated by ELV accelerator and having a size of few millimeters, was absorbed in the graphite target and heated it to the required high temperatures. To remove power the target was rotated at a speed of several thousand revolutions per minute. In collaborative experiments the mechanical resistance of a graphite target was studied as to short-term (up to 1 hour) and to stationary (a few hours) heating. The heating modes, the least destructive to the target material were chosen. Furthermore, the temperature distribution was measured in a radial direction.

For remote control of target temperature the vacuum chamber was equipped with optical windows. Temperature control was carried out by optical sensor through a set of optical mirrors. To remove the heat power from the target the water cooled panels were placed into vacuum chamber.

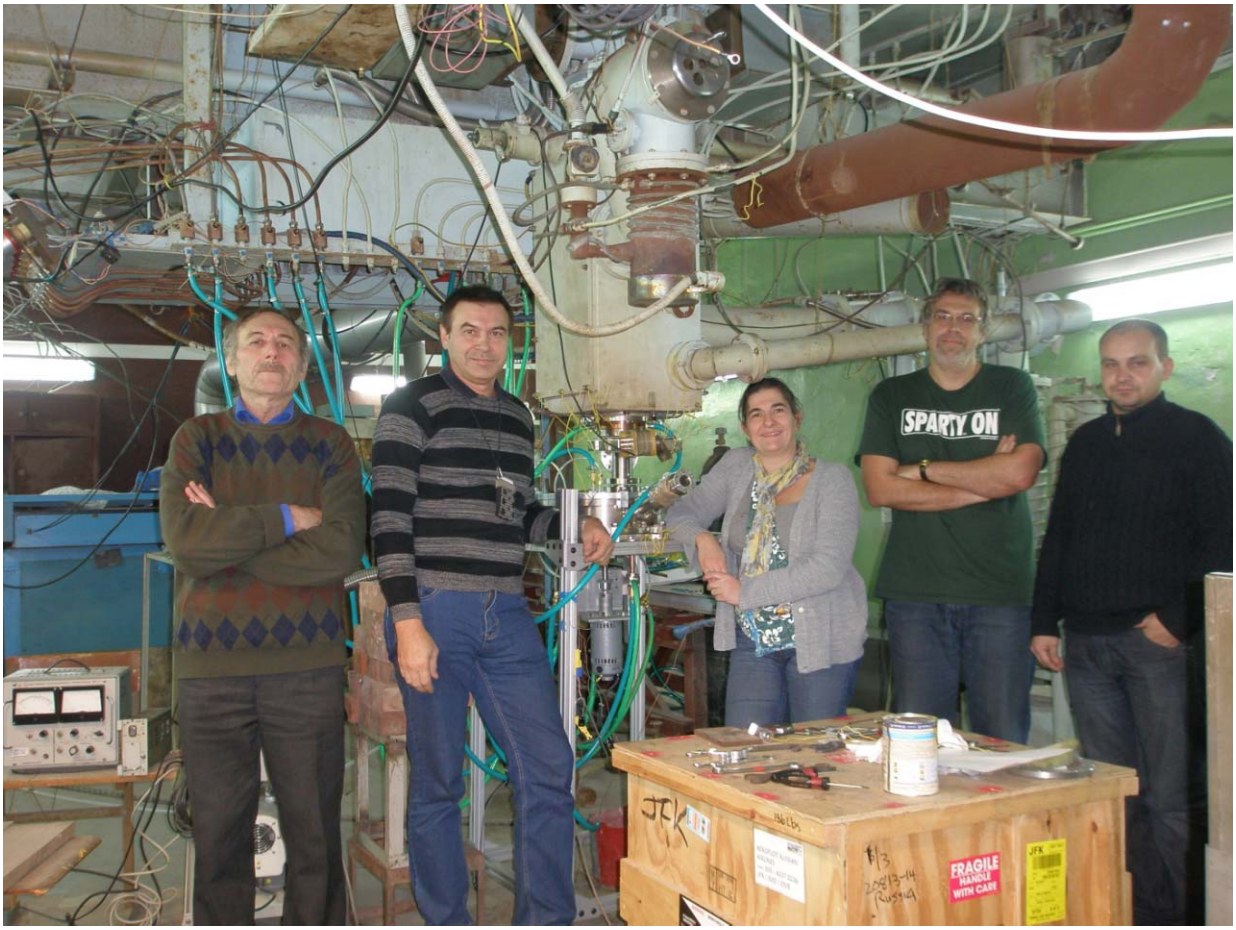

Fig.8.4.3. Specialists of the Laboratory № 12 and University of Michigan after successful experiments on the laboratory test facility.

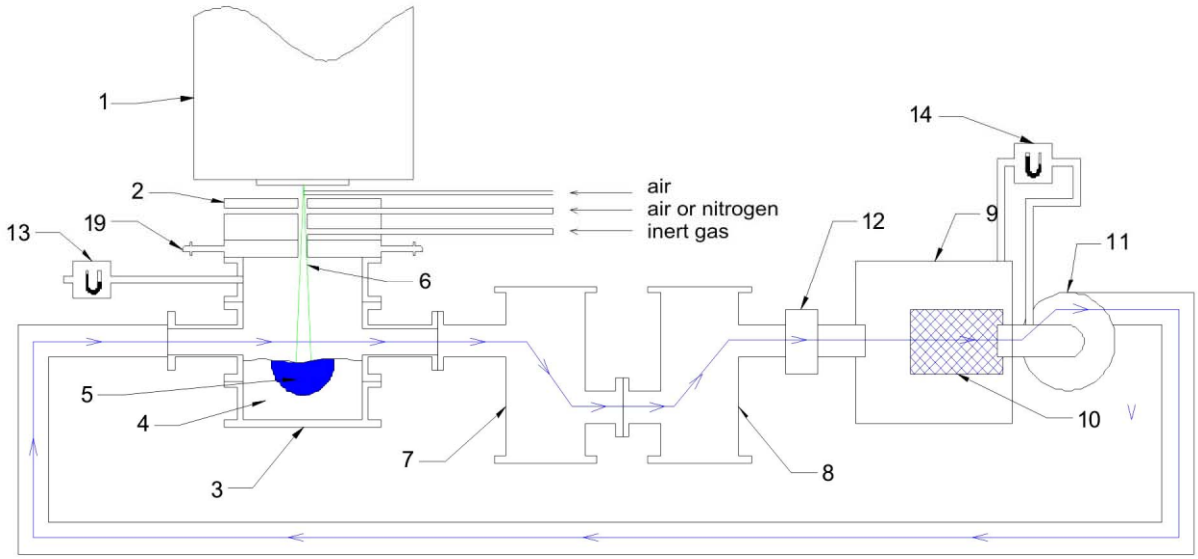

Fig. 8.4.4. - Scheme of modified laboratory facility with closed carrier stream.
1 –ELV-6 accelerator extraction device, 2 – gas seal flange, 3 - water-cooled reactor, 4 - evaporated material,- 5 - molten material, - 6, – electron beam, 7 – tank №1 for aerosol cooling and coarse fraction separation, 8 - aerosol cooling and coarse fraction separation reservoir №2, 9 – filtration box, 10 - bag filter, 11 - fan, 12 – nanopowder production control module, 13 - differential pressure gauge PROMA-IDM to measure pressure in reactor, 14 - differential pressure gauge to measure the pressure difference before and after the filter bag .

8.4.3. Nanopowders production using focused electron beam extracted into atmosphere.

In order to improve productivity and the quality of nanopowders the laboratory facility for nanopowders production was modified. The modification included the automation of facility parameters record, in particular, the flow discharge of cooling water flow, control of carrier gas flows and monitoring of pressure difference across the transport path of nanopowder. To improve the purity of obtained nanopowders the insulation in area of the beam inlet hole protecting the air entering into evaporation chamber was improved. Insulation was achieved by intercepting gas flows (Fig. 8.4.4). The closure of inert gas flow from the path output to the facility input into evaporation chamber made possible to reduce the evaporation consumption of inert gas in the process of nanopowders production. Before modification, inert gas was extracted into ventilation system.

8.4.4. Metal nanopowder surfacing.

In 2013, the studies on surfacing of modifying powders onto metal surfaces using the focused electron beam extracted into atmosphere were continued. The studies were made in collaboration with the Department of Materials Science in Mechanical Engineering of Novosibirsk State Technical University.

Through these studies, the technique of surfacing the refractory and heavy metals such as tantalum, niobium, zirconium onto titanium base was developed. The purpose of forming such the coatings is to strength the surface layer material by particularly high corrosion resistance against some strong acids such as nitric acid and sulfuric acid. Furthermore, because of its high biocompatibility, alloys of Ti-Ta-Nb are of interest for medical applications as a material for implants.

The developed surfacing method has high a efficiency up to 7 cm^2 /s (2.5 m^2 /h) , the thickness of the coating being formed is 2 - 3 mm. The concentration of the alloying components in coatings at single layer surfacing reaches, depending on the kind of the alloying component, the 20 - 25 % weight, the thickness of the modified layer is 1.8 - 2.2 mm. By increasing the number of surfaced layers alloying concentration is increased up to 40 - 50 % weight, and the layer thickness is up to 3 mm. Table 8.4.3 shows some examples of concentration of chemical elements in the surfaced layers.

The studies have shown that the formed coatings have a good complex of mechanical properties, they are practically free of defects and have adhesion to the substrate, which is not weaker than the strength of the basis itself. Figure 8.4.5 shows a diagram of the test on adhesive strength of coatings. The material breakage in the zone of jointing of coating with the basis occurred at a voltage of 410 ... 430 MPa that corresponds to titanium strength.

Several tests on the corrosion resistance in boiling concentrated nitric acid (Figure 8.4.6) showed that the corrosion resistance of the coating material is increased by more than 100 times faster than the resistance of the titanium substrate.

Table 8.4.3.

Mode №	Initial powder composition, weight %, the rest is flux			The number of treatments	Melted layer chemical composition, weight %. The rest is titanium		Depth of melted layer, mm
	Ta	Nb	Ti	1	Ta	Nb	
1	22	0	38	1	10.5±1.5	0	1.4
2	40	0	24	1	22.3±1.1	0	2.2
3	51	0	18	3	34.3±5.1	0	2.6
4	20	15	26	1	5.8±0.8	11.0±0.6	2.5

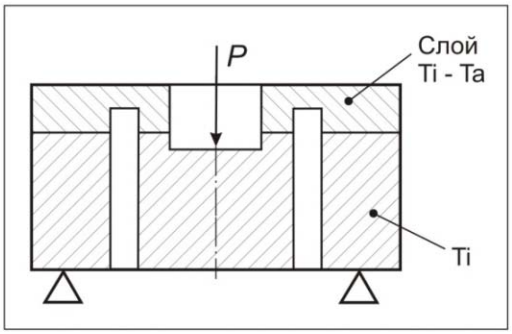

Fig.8.4. 5. Diagram of the test on adhesive strength.

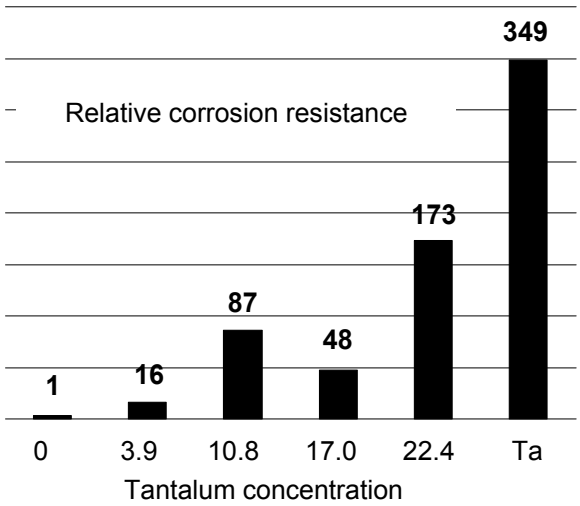

Fig.8.4. 6. Results of tests on corrosion resistance of the coating material with different tantalum concentration.

8.4.5. Potential application of nanopowders.

In process of searching of activators and organic basis for nanocomposite plastic fiber amplifiers of one and a half micron range, the possibility to reduce the opalescence and increase the refractive index due to the component index matching and reducing the size of erbium-containing nanoparticles of activator was investigated.

The luminescence decay of solid solution of thiophosphonate and fluoruquinolone complexes of terbium, erbium, ytterbium and europium in organic glass was investigated.

The perspective of using LED UV pumping of gel and fiber-glass lasers with rare earth activators is noted.

Light output of plastic X-ray phosphor with addition of ultrafine activator of barium fluoride powder (the perspective of which being a UV subnanosecond scintillator for time-of-flight positron tomography was found by Ya. Valbis in 1986) was measured. Unfortunately, volume plastics (except polyolefins, which are getting muddy quickly because of crystallisation) are not sufficiently transparent to UV light, so we had to add terphenyl and anthracene, transfoming original ultraviolet into radiation that is able to spread in polystyrene, to the composition.

9
PHYSICS FOR MEDICINE

9.1. VITA CURRENT STATUS

9.1.1. Introduction.

Nowadays boron neutron capture therapy is regarded as a promising method for the treatment of malignant tumors. Clinical trials at the reactors showed that BNCT can treat glioblastoma and brain metastases of melanoma. These types of malignant tumors are impossible to treat with any other methods. Progress of the boron neutron capture therapy in clinical trials at the reactors and the potential relevance of techniques have led to intense discussions on the development and creation of a neutron source based on a compact and low-cost accelerator.

At BINP it was proposed an original epithermal neutron source based on vacuum insulation tandem accelerator (VITA). During 2013 the study of parameters of generated neutrons was conducted, namely: energy distribution, neutron flux density and spatial distribution of neutron dose. *In vitro* studies clearly demonstrating the effect of BNCT were carried out. Negative effect of charge-exchange gas on tandem accelerator operation was discovered. Solution of this problem was proposed.

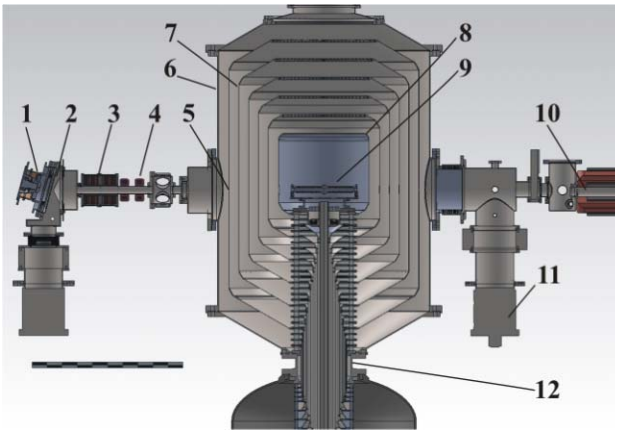

Fig. 9.1.1. Vacuum insulation tandem accelerator (VITA). 1 – H^- ion source, 2 – diaphragm, 3 – magnetic lenses, 4 – magnetic corrector, 5 – first electrode, 6 – vacuum tank, 7 – second electrode, 8 – central electrode, 9 – charge-exchange tube, 10 – high energy beam channel, 11 – vacuum pump, 12 – insulator.

General scheme of the accelerator is shown in Fig. 9.1.1. Negative hydrogen ions are generated by H^- ion source, and are accelerated to 1 MeV. After that they lose two electrons in charge-exchange target and are accelerated again for total energy 2 MeV. Pumping is carried out by cryogenic and turbomolecular pumps through the blinds system. High voltage is applied to the electrodes from a high voltage source through the insulator.

9.1.2. Neutron spectrum measurement.

The results achieved in the long stable generation of neutrons at a proton beam current of 1.5-2.5 mA allowed us to measure the spectrum of neutrons using TOF technique. To create short neutron pulses it is applied a new technical solution, which is briefly described below. Accelerator operates in a stationary mode, generating protons with energy 1.875 MeV, just below the neutron production threshold. Protons with subthreshold energy hit the electrically insulated lithium target, which at the same time is supplied by short 200 ns square pulses of 40 kV high voltage. During each high voltage pulse the energy of protons increases to 1.915 MeV and neutrons are generated. The energy of emitted neutrons is calculated after measuring the time interval between high-voltage pulse and neutron pulse in the remote neutron detector.

Previously this method of generating short pulses of neutrons was not applied by anybody, so we had to solve a number of problems that hinder to conduct measurements. An interesting problem was the noise signal to the resulting neutron spectrum. It was discovered several sources of noise, namely: 1) scattered neutrons; 2) neutrons generated in the reactions $^{55}Mn(p,n)^{55}Fe$ and $^{63}Cu(\alpha,n)^{66}Ga$, caused by proton beam interaction with construction materials; 3) high intensity γ-ray flow; 4) insufficient stability of the proton energy, which leads to unwanted neutron generation when the threshold 1.882 MeV is exceeded. Original technical solutions to suppress this noise and a special method of controlling signal-to-noise ratio were registered as know-how.

As a result of applied solutions we were able to measure spectrum of the neutron flux at a proton energy 1,915 ± 0,005 MeV. The spectrum is shown in Fig. 9.1.2 in comparison with calculated spectrum.

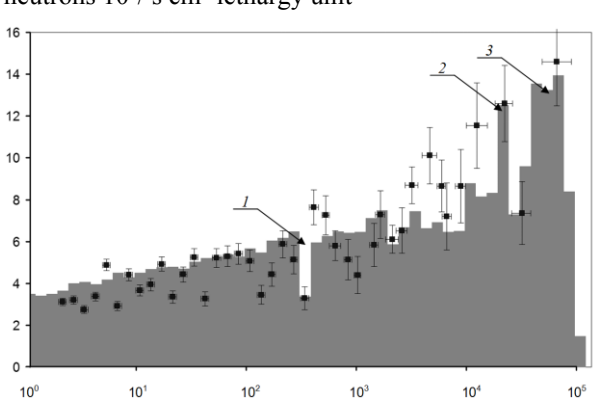

Fig. 9.1.2. Solid columns show the calculated spectrum. Points show the measured spectrum. *1* - 340 eV line is due to the scattering of neutrons by ^{55}Mn. *2*, *3* - transmission lines of ^{55}Fe: 24.5, 72.9 and 82.0 keV.

9.1.3. Spatial distribution and intensity of the generated radiation.

Spatial homogeneity of the neutron flux was determined using neutron activation diagnostic and dosimeter DKS-96 (Corp. "Dose", Russia). As the activation detectors indium pills were used. Each pill had a diameter of 10 mm and weight 0.2 g, so the average thickness was 400 microns. Activation detectors were located at different distances from neutron producing target. When the detectors are placed at 15 cm from the target, the received data is presented in Figure 9.1.3.

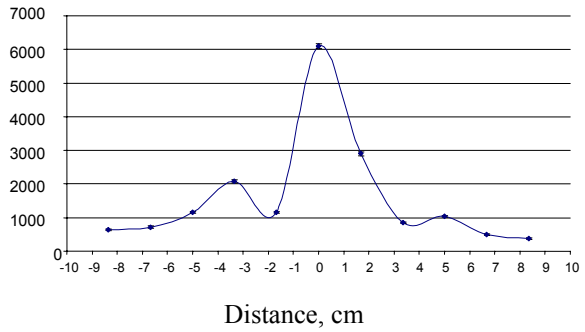

Fig. 9.1.3. The spatial distribution of the neutron flux intensity near the target..

Measurement allows us to understand that the greatest density of the neutron field is concentrated in the region with a diameter of about 5 cm. This heterogeneity can be explained by water cooling system of the target having a minimum thickness near the axis, as well as the presence of structural elements, leading to further reflections of neutrons (splash on the left part of the graph).

The intensity of the neutron flux depending on the distance to the target is shown in Fig. 9.1.4.

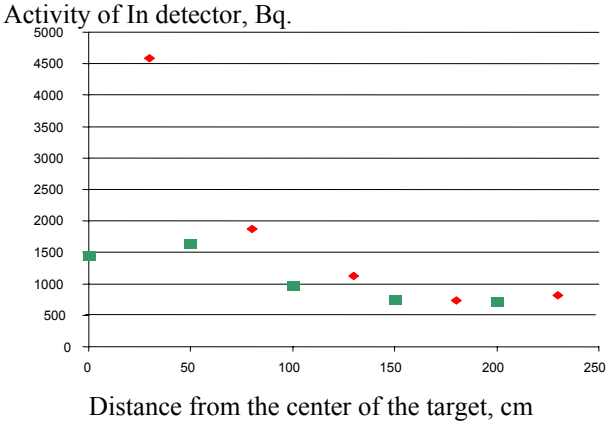

Рис. 9.1.4. The intensity of the neutron flux on the distance to the center of the target for activation of indium. Squares – horizontal alignment, rhombs – vertical alignment..

The results show that the neutron flux generated in the near-threshold mode has a noticeable direction. While starting from a distance of about 1.5 meters we can see a significant contribution of the scattered neutrons, the intensity of which is practically independent of the direction and distance from the target.

Spatial distribution of the neutron dose was measured by the dosimeter DKS-96 at different distances from the target along the proton beam axis and outside the axis. Fig. 5 shows the measured values (the distance from the lithium layer to the center of the detector is shown, the target thickness is assumed to be 6 cm) normalized to 1 mA of proton current and the curve close to $1/r^2$, adopted knowing the size of target. The calculated curve fits well with the measured points, assuming the presence of a background level of 50 mSv/h @ 1 mA (from scattered neutrons). Measurement of doses closer than 20 cm from the target was physically impossible due to the large diameter of the spherical moderator of dosimeter DKS-96. Extrapolation of the graph closer to the target gives a value of 20 Sv/h @ 1 mA at a distance of 2 cm from the target.

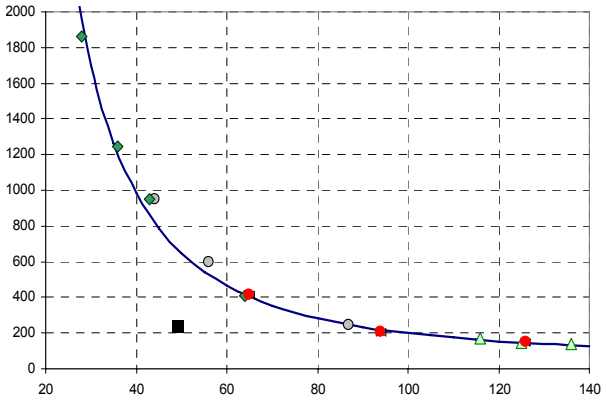

Fig. 9.1.5. Neutron dose depending on the distance from the target measured using dosimeter DKS-96.

9.1.4. Influence of charge-exchange gas on tandem accelerator operation.

During operation it was discovered an unusual effect: the degree of stripping decreased when the charge-exchange gas puffing exceeded a certain value, while the theoretical dependence goes to stable value of 99.998% stripping. Explanation of this effect was found in the analysis of the interaction of the beam with argon in the stripping tube. Conducting of the high-power proton beam through the charge-exchange gas leads to ionization of the gas. Positively charged argon ions penetrate into the acceleration channel from both sides of the charge-exchange tube and the electric field accelerates them up to the full potential of high-voltage electrode. Formation of a

beam of accelerated argon ions leads to the following problems. First, part of the high voltage power is consumed by the acceleration of the argon beam. Second, when the accelerated argon beam hits electrodes of accelerator it leads to a redistribution of their potentials, changes in the conditions of acceleration and focusing of the injected beam of H^- particles. Third, argon beam hit leads to modification of electrode surfaces (Fig. 9.1.6.). And at high argon beam currents the electrodes can even be melted or deformed.

To solve this problem, we propose to use a magnetic field deflecting the flow of positively charged argon ions inside the high voltage electrode in order to prevent them from passing through the electrode diaphragm and go to the acceleration channel.

Рис. 9.1.6. The imprint of argon beam on a rotatable diaphragm located at the entrance of the H^- beam into the accelerator.

Because in a transverse magnetic field not only flowing ions of stripping gas, but also high-energy ions (negatively charged at the entrance of the stripping tube and positively charged at the exit of the stripping tube) will be deflected, it is proposed to tilt or shift the tube. Examples of possible realizations are illustrated in Fig. 9.1.7.

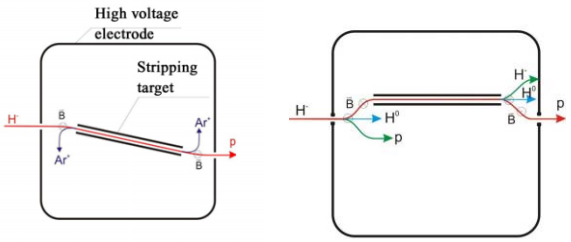

Fig. 9.1.7. The concept of magnetic suppression of argon ions in the embodiment of tilted (left) or shifted (right) charge-exchange tube.

9.1.6. Modernization of the facility.

To ensure stable operation of the accelerator it is necessary to provide high enough vacuum in the beam path. If the vacuum is not good the high-energy beam ionizes the residual gas. Formed electrons and ions are accelerated and hit the high voltage electrodes, causing secondary emission. If the gas pressure is not sufficient to form the avalanche ionization in the high voltage gap, breakdowns can still occur due to not uniform load of the high voltage divider. This parasitic current on the high voltage electrodes "shorts out" one or more high-voltage gaps, resulting in increased voltage on the remaining gaps, which may cause breakdown of the insulator. Breakdown along the insulator surface also may be produced by the ultraviolet radiation due to beam interaction with the gas.

The main sources of residual gas in the accelerator are the source of negative ions and the stripping tube, which produce 0.1 - 0.2 l·Torr/s of hydrogen and 0.05 - 0.1 l·Torr/s of argon respectively. With the help of differential pumping the hydrogen flow in high voltage gap dropped to $5 \cdot 10^{-3}$ l·Torr/s, at a pressure in the low energy channel ~ 10^{-2} Pa. At the first stage of experiments additional gas pumping inside the high-voltage electrode is not provided, pumping is performed only through the blinds. Maximum outgassing from the walls, electrodes and beam receiving targets falls on moment of switching on the beam, and should decrease in time.

Previously, the accelerator vacuum volume was pumped by 01AB1500 turbomolecular pump (TMH 1500) with total pumping speed of 600 l/s, which provided pressure $5 \cdot 10^{-3}$ Pa at 1.5 mA beam current. While stripping gas flow rate was 0.016 l·Torr/s, which corresponded to more than 60% stripping of the beam.

To increase the stripping gas flow rate and the degree of beam charge exchange, as well as to improve the vacuum conditions enhancing the operation stability of the accelerator, the vacuum system has been fully modernized. Old pumps were replaced with new high-speed oil-free turbomolecular and forevacuum pumps. We are preparing to install a new cryogenic pump with a closed helium cycle.

In addition to the vacuum system we modernized accelerator apertures. Previously performed analysis of the beam transport showd that current deposition on three output apertures can reach 16%. New apertures were installed with a diameter 5 mm higher than the calculated beam envelope. This replacement allows us to expect that the maximum value of the accelerated current will increase from 2.5 mA to 3 mA. The first experiment on the ion beam transportation after modernization has shown value 3.2 mA of the resulting output current (Fig. 9.1.8).

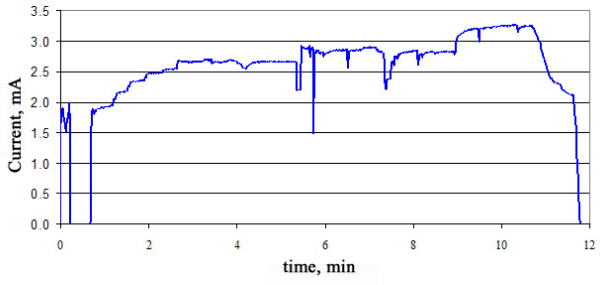

Fig. 9.1.8. Transported current after modernization of the accelerator.

9.1.7. Results and prospects

As result of conducted research we have measured the spectrum, intensity and spatial distribution of the neutron flux generated at the accelerator source of epithermal neutrons. It is shown that during experiments on irradiation of cell preparations, which are located at a distance of 2 cm from the bottom edge of the target, neutron dose rate can reach 20 Sv/h @ 1 mA.

A new effect is discovered: the influence of charge-exchange gas on accelerator operation, limiting further increase of accelerated beam current. Technical solutions were proposed to overcome it.

The results of this research allowed making applications for two patents and know-how.

Upgrade of the facility allowed moving to higher accelerated currents at high operational reliability of the accelerator.

The work is carried out in the framework of the research project II.13.3.7 "Neutron source for neutron therapy of cancer based on the electrostatic tandem accelerator" Program of Fundamental Research of SB RAS on the physics and technology of charged particle accelerators. Partial support is assured by government contracts № 14.518.11.7039 and 14.512.11.0105.

Results of the work are presented at the IV International Conference on Charged Particle Accelerators (IPAC 2013, Shanghai, China), 7th meeting of young BNCT researchers (7th YBNCT Meeting, 2013, Granada, Spain) and published in [1-13].

9.2. X-RAY DETECTORS FOR MEDICINE AND INSPECTION

9.2.1. Micro-doze Digital Radiographic Installation (MDRI) "Siberia".

A direct-quantum-counting detector and associated registration electronics were being developed in 2013. The detector is made based on lines of micropixel avalanche photodiodes coated by a scintillator layer. The number of actuated cells in each photodiode depends on the amount of light generated in the scintillator and therefore the energy of detected quantum. The achieved energy resolution allows implementation of the counting mode and elimination of the self-noise of the detector, as well as energy separation of registered quanta. These properties of the new detector will improve the X-ray image quality (for example, through the use of weighting coefficients). Epy detector can also be used for densitometry in osteoporosis diagnosis. An application for a patent "Method and installation for making projective radiographs" was filed.

9.2.2. X-ray inspection system (XIS) "Sibscan".

In 2013 the Institute was developing a new XIS version, which differs from the earlier modifications produced in the city of Orel by ZAO "Nauchpribor" and in China by Nuctech (under BINP license) in its smaller dimensions and weight and lower cost. That was achieved via reduction of the "emitter - detector" distance from 2 to 1.5 m and using a compact and cheap monoblock IRI-160/2 of domestic production instead of a high-voltage generator and Italian medical X-ray tube (and high-voltage cables connecting them). The image quality will be better because of a fixed tube anode applied in new radiation source.

BIBLIOGRAPHY

List of publications 2013

[1] E.A. Mesyats, A.V. Snytnikov, K.V. Lotov. Choice of particle number in particle-in-cell simulations of plasma physics problems. // Computational Technologies, 2013. - V.18. N6. - P.83-97 (in Russian).

[2] M.G. Kozlov. Multi Regge Amplitudes in non Abelian Gauge Theories. // Nuclear Physics and Engineering. - 2013, Vol.4. - P.853.

[3] A.V. Reznichenko, QCD Amplitudes with the gluon exchanges at high energies. // Nuclear Physics and Engineering. - 2013. - Vol.4, p.857.

[4] Grozin A.G. Introduction to Mathematica for physicists, Graduate texts in physics. // Springer. - 2013, 219 pages; ISBN 978-3-319-00893-6; ebook ISBN 978-3-319-00894-3.

[5] M.N. Achasov, K.I. Beloborodov, A.V. Berdyugin, A.G. Bogdanchikov, A.A. Botov, A.V. Vasiljev, V.B. Golubev, T.V. Dimova, V.P. Druzhinin, D.P. Kovrizhin, I.A. Koop, A.A. Korol, S.V. Koshuba, A.E. Obrazovsky, E.V. Pakhtusova, S.I. Serednyakov, Z.K. Silagadze, A.G. Kharlamov, Yu.M. Shatunov, L.V. Kardapoltsev, A.S. Kupich, K.A. Martin, K.A. Grevtsov, I.K. Surin, K.Yu. Skovpen, D.A. Shtol, A.N. Skrinsky, Yu.A. Tikhonov, Yu.M. Usov, A.Yu. Barnyakov, D.E. Berkaev, D.B. Shwartz, Yu.A. Rogovskii, A.S. Kasaev, A.N. Kirpotin. Study of $e^+e^- \to \pi^+\pi^- \pi^0\pi^0$ in the energy range $1< \sqrt{s} < -2$ GeV with the SND detector. // Nuclear Physics and Engineering. - 2013. - Vol.4. – P.837-841.

[6] A.Yu. Barnyakov, M.Yu. Barnyakov, K.I. Beloborodov, V.S. Bobrovnikov, A.R. Buzykaev, A.F. Daniluk, V.B. Golubev, V.V. Gulevich, S.A. Kononov, E.A. Kravchenko, A.P Onuchin, K.A. Martin, S.I. Serednaykov, V.M. Vesenev. Particle identification system based on dense aerogel for the SND detector. // Nuclear Physics and Engineering. - 4 (2013), 890-893.

[7] M.N. Achasov, V.M. Aulchenko, A.Yu. Barnyakov, K.I. Beloborodov, A.V. Berdyugin, D.E. Berkaev, A.G. Bogdanchikov, A.A. Botov, T.V. Dimova, V.P. Druzhinin, V.B. Golubev, K.A. Grevtsov, L.V. Kardapoltsev, A.S. Kupich, A.G. Kharlamov, D.P. Kovrizhin, I.A. Koop, A.A. Korol, S.V. Koshuba, K.A. Martin, A.E. Obrazovsky, E.V. Pakhtusova, Yu.A. Rogovskii, S.I. Serednyakov, Z.K. Silagadze, K.Yu. Skovpen, A.N. Skrinsky, I.K. Surin, Yu.A. Tikhonov, A.V. Vasiljev, P.Yu. Shatunov, Yu.M. Shatunov, D.A. Shtol, D.B. Shwartz, Yu.M. Usov, I.M. Zemlyansky. Results and perspectives on Baryon Form Factors from SND and CMD-3. // To be published in Intern. Journal of Modern Physics: Conference Series.

[8] M.N. Achasov, V.M. Aulchenko, A.Yu. Barnyakov, K.I. Beloborodov, A.V. Berdyugin, D.E. Berkaev, A.G. Bogdanchikov, A.A. Botov, T.V. Dimova, V.P. Druzhinin, V.B. Golubev, K.A. Grevtsov, L.V. Kardapoltsev, A.S. Kupich, A.G. Kharlamov, D.P. Kovrizhin, I.A. Koop, A.A. Korol, S.V. Koshuba, K.A. Martin, A.E. Obrazovsky, E.V. Pakhtusova, Yu.A. Rogovskii, S.I. Serednyakov, Z.K. Silagadze, K.Yu. Skovpen, A.N. Skrinsky, I.K. Surin, Yu.A. Tikhonov, A.V. Vasiljev, P.Yu. Shatunov, Yu.M. Shatunov, D.A. Shtol, D.B. Shwartz, Yu.M. Usov, I.M. Zemlyansky. Hadronic cross sections measurement at SND. // To be published in Intern. Journal of Modern Physics: Conference Series.

[9] D.V. Pestrikov. Fast dipole transverse oscillations of bunches in storage rings. // Textbook. - Novosibirsk: NGU. - 2013. - 126p.

[10] D.V. Pestrikov. Effects of the space charge on the dipole oscillations and fluctuations of a coasting ion beam. // Textbook. - Novosibirsk: NGU. - 2013. - 96p.

[11] I.A. Ivanov, A.V. Arzhannikov, A.V. Burdakov, V.S. Burmasov, M.V. Ivantsivsky, S.A. Kuznetsov, K.I. Mekler, S.S. Popov, S.V. Polosatkin, V.V. Postupaev, A.F. Rovenskikh, S.L. Sinitsky, V.F. Sklyarov, M.K.A. Thumm. Generation of Thz-radiation on GOL-3 facility. // IX All-Russian Seminar on Radio Physics of Millimeters and Sub-Millimeters Waves, Nizhni-Novgorod, Institute of Applied Physics, 26 February - 1 March, 2013: Abstracts. - P.17-18 (in Russian).

[12] Popova A.A., Sobachkin A.V., Nazarov I.V., Yakovlev V.I., Loginova M.V., Sitnikov A.A., Sharafutdinov M.R., Lyakhov N.Z. Dynamic diffractometry of phase transformations in high-temperature synthesis in powder mechanoactivated systems under volime combustion (in Russian). // Bulletin of the Russian Academy of Sciences. Physics. - 2013. - V.77, N2. - pp. 140-143. (Proc. of XIX National Conference on Synchrotron Radiation "SR-2012" and the All-Russia Youth Conference "Synchrotron Radiation Application").

[13] V.V. Gerasimov, G.N. Zhizhin, B.A. Knyazev, I.A. Kotelnikov, A.K. Nikitin, V.S. Cherkassky. Study of diffraction of surface plasmon polaritons at a rectangular of metal-dielectric interface in the terahertz range (in Russian). // Bulletin of Novosibirsk State University. - 2013. - V.8, N1. - P.6-15.

[14] M.G. Fedotov, V.V. Maksimovskaya, M.R. Sharafutdinov. SR-beam investigations of ultradispersed silver obtained by shock-wave synthesis under cryogenic conditions. // Bulletin of the Russian Academy of Sciences: Physics. - 2013. - Vol.77, N2. - P.107-110. (2013. - T.77, N2. - P.126-130).

[15] K.A. Ten, V.M. Titov, E.R. Pruuel, L.A. Lukyanchikov, B.P. Tolochko, V.V. Zhulanov, L.I. Shekhtman, Yu.A. Aminov, A.K. Muzyrya, O.V. Kostitsyn, E.B. Smirnov. Investigation into detonation wave parameters and condensation processes in benzotrifuroksane by synchrotron methods (in Russian). // Scientific Bulletin of NSTU. - 2013. - N1 (50). - P.128.

[16] V. Aleynik, A. Kuznetsov, I. Sorokin, S. Taskaev, M. Tiunov, I. Schudlo. Calibration of the stripping target of tandem accelerator with vacuum insulation. // Scientific Bulletin of Nosibirsk State Technical University. - 2013. - №1 (50). - P.83-92.

[17] S.A. Kuznetsov, M.A. Astafiev, A.V. Arzhannikov, A.V. Gelfand. Quasi optic frequency-selective structures of millimeter and teraHerz band. // Abstracts of IX All-Russian Seminar on Radio Physics of Millimeters and Sub-Millimeters Waves, Nizhni-Novgorod, Institute of Applied Physics, 26 February - 1 March, 2013, p.91.

[18] E.F. Reznikova, B.G. Goldenberg, V.I. Kondratiev, G.N. Kulipanov, V.P. Korol'kov, R.K. Nasyrov. LIGA technology for synthesis of diffractive refractive intraocular lenses (in Russian). // Bulletin of the Russian Academy of Sciences. Physics. - 2013. - V.77, N2. - P131-135. (Proc. of XIX National Conf. on Synchrotron Radiation "SR-2012" and the All-Russia. Youth Conference "Synchrotron Radiation Application").

[19] B.G. Goldenberg, E.F. Reznikova, A.G. Lemzyakov, V.F. Pindyurin. Micro-beam X-ray lithographer for direct formation of deep LIGA structures (in Russian). // Optoelectronics. - 2013. - V.9, N1. - P.96-102.

[20] G.M. Skuridin, O.V. Chankina, A.A. Legkodymov, V.K. Kramer, N.V. Baginskaya, K.P. Koutsenogii. Trace element content of sea buckthorn (Hippophae rhamnoides L.) tissues (in Russian). // Bulletin of the Russian Academy of Sciences. Physics. - 2013. - V.77, N2. - P.229-232. (Proc. of XIX National Conf. on Synchrotron Radiation "SR-2012" and the All-Russia Youth Conf. "Synchrotron Radiation Applocation").

[21] Fedotov M.G. Modeling a tunable multispectral X-ray SR detector with time-division bands. // Bulletin of the Russian Academy of Sciences: Physics. 2013. - Vol.77, N2. - P.103-106 (2013. - T.77, N2. - P.122-125).

[22] Daryin A.V., Kalugin I.A., Rakshun Ya.V. Scanning X-ray fluorescence microanalysis using synchrotron radiation applied to studying variations of element content in annual layers in sections of sediments of Lake Teletskoe (in Russian). // Bulletin of the Russian Academy of Sciences: Physics. 2013. - Vol.77, N2. - P.210-211. (Proc. of XIX National Conf. on Synchrotron Radiation "SR-2012" and the All-Russia Youth Conference "Synchrotron Radiation Applocation").

[23] Y.V. Getmanov, N.A. Vinokurov, O.A. Shevchenko. Longitudinal stability in energy recovery linac with two accelerating structures (in Russian). // Scientific Bulletin of NSTU. - 2013. - N1 (50). - P.119.

[24] N.A. Timchenko, R.M. Galimov, A.M. Leader, B.G. Goldenberg, A.N. Shmakov. Decay of hydrogenic phases in palladium and titanium under synchrotron radiation beam irradiation in the X-ray spectrum range (in Russian). // Bulletin of the Russian Academy of Sciences. Physics. - 2013. - V.77, N2. - P.181-183. (Proc. of XIX National Conf. on Synchrotron Radiation "SR-2012" and the All-Russia Youth Conf. "Synchrotron Radiation Application").

[25] E.R. Pruuel, K.A. Ten, B.P. Tolochko, L.A. Merzhievsky, L.A. Lukyanchikov, V.M. Aulchenko, V.V. Zhulanov, L.I. Shekhtman, V.M. Titov. Application of synchrotron radiation capabilities to research in detonation processes (in Russian). // Proc. of the Russian Academy of Sciences. - 2013. - V.448, N1. - P.38-42.

[26] Russia at CERN: Participation of research institutions and industrial enterprises of the Russian Federation in the creation of the Large Hadron Collider (in Russian). - Dubna: JINR, 2013. – 160 pages.

[27] A.V. Arzhannikov, P.V. Kalinin, S.A. Kuznetsov, K.I. Mekler, S.S. Popov, S.V. Polosatkin, V.V. Postupaev, A.F. Rovenskikh, S.L. Sinitsky, V.F. Sklyarov, M.K.A. Thumm. Synchronous generation of high power pulses of 4-mm radiation in two-channel planar FEM. // Abstracts of IX All-Russian Seminar on Radio Physics of Millimeters and Sub-Millimeters Waves, Nizhni-Novgorod, Institute of Applied Physics, 26 February - 1 March, 2013, p.57.

[28] V.S. Arbuzov, E.I. Gorniker, E.V. Kozyrev, A.A. Kondakov, V.M. Petrov, A.M. Pilan, A.G. Tribendis. RF high-power supply system for accelerating cavities Novosibirsk microtron recuperator for the FEL. High continuous power divider based on rectangular waveguide (in Russian). // Bulletin of NSU. - 2013. - V.8, N1. - P.32-43.

[29] A.V. Daryin, I.A. Kalugin, Ya.V. Rakshun. Scanning X-ray spectrum microanalysis of samples of bottom sediments using synchrotron radiation from VEPP-3 at BINP SB RAS (in Russian). // Bulletin of the Russian Academy of Sciences. Physics. - 2013. - V.77, N2. - P.204-206. (Proc. of XIX National Conf. on Synchrotron Radiation "SR-2012" and the All-Russia Youth Conf. "Synchrotron Radiation Application ").

[30] A.V. Daryin, I.A. Kalugin, M.A. Maksimov, G.A. Tretyakov, Ya.V. Rakshun. Scanning X-ray fluorescence microanalysis of annual layers in samples of bottom sediments in Lake Shira (in Russian). // Bulletin of the Russian Academy of Sciences. Physics. - 2013. - V.77, N2. - P.207-209. (Proc. of XIX National Conf. on Synchrotron Radiation "SR-2012" and the All-Russia Youth Conf. "Synchrotron Radiation Aplication").

[31] E.I. Palchikov, A.V. Dolgyh, V.I. Kondratiev, A.D. Matrosov. Spectrozonal digital X-ray diagnostics of explosive processes based on absorber-separated imageplate detectors (in Russian). // Bulletin of the Russian Academy of Sciences. Physics. - 2013. - V.77, N2. - P.118-121. (Proc. of XIX National Conf. on Synchrotron Radiation "SR-2012" and the All-Russia Youth Conf. "Synchrotron Radiation Application").

[32] Yu.A Zakharov, V.M. Pugachev, V.V. Kriventsov, A.N. Popova, B.P. Tolochko, A.S. Bogomyakov, V.G.

Dodonov, Yu.V. Karpushkina. Structure of nanoscale Fe-Co and Fe-Ni bimetals (in Russian). // Bulletin of the Russian Academy of Sciences. Physics. - 2013. - V.77, N2. - P.164-167. (Proc. of XIX National Conf. on Synchrotron Radiation "SR-2012" and the All-Russian Youth Conf. "Synchrotron Radiation Application").

[33] A.V. Arzhannikov, I.V. Timofeev. Theoretical consideration of generation of radiation in THz-band in a High Electron Current - Dense Plasma System. // IX All-Russian Seminar on Radio Physics of Millimeters and Sub-Millimeters Waves, 26 Feb. - 1 March 2013, Nizhni-Novgorod: Institute of Applied Physics, Nizhni-Novgorod: Abstrcts. - P.32.

[34] N.S. Dikansky, D.V. Pestrikov. // Theory of coherent oscillations of the beams in storage rings. // Textbook. - NGU. - 2013. - 224p.

[35] K.A. Ten, E.R. Pruuel, L.A. Lukyanchikov, B.P. Efremov, E.V. Bespalov, B.P. Tolochko, V.V. Zhulanov, L.I. Shekhtman. Shock compression of nano-structure porous materials (in Russian). // Scientific Bulletin of NSTU. - 2013. - N1 (50). - P.139.

[36] Edward P. Kruglyakov (22.10.1934-06.11.2012). Bibliographical reference list (in Russian). // Bulletin of Novosibirsk State University. - 2013. - V.8, N2. - P.130-131.

[37] A.V. Kosov, M.A. Sheromov. Experimental study of spatial position of SR beams in channels 13 and 7 of the VEPP-4M storage ring (in Russian). // Bulleting of the Russian Academy of Sciences. Physics. - 2013. - V.77, N2. - pp.110-112. (Proceedings of XIX National Conference on Synchrotron Radiation "SR-2012" and the All-Russia Youth conference "Synchrotron Radiation Application").

[38] I.N. Meshkov, B.V. Chirikov. Electromagnetic field. Part 1. Electricity and magnetism (in Russian). - 2nd ed., rev. and add. - M.; Izhevsk: SRC Regular and chaotic dynamics, 2013. - 544 pages.

[39] I.N. Meshkov, B.V. Chirikov. Electromagnetic field. Part 2. Electromagnetic waves and optics (in Russian). - 2nd ed., rev. and add. - M. Izhevsk: SRC Regular and chaotic dynamics, 2013. - 416 pages.

[40] Kotelnikov I.A., Gerasimov V.V., Knyazev B.A. Diffraction of a surface wave on a conducting rectangular wedge. // Physical Review A. - 2013. - T.87, N2. - P.023828-1-11.

[41] Kulipanov G.N., Getmanov Ya.V., Shevchenko O.A., Skrinsky A.N., Tribendis A.G., Volkov V.N., Vinokurov N.A. Multiturn ERL X-ray source (MARS) feasibility study. // ERL 2011: The 50th ICFA Advanced Beam Dynamics Workshop on Energy Recovery Linacs, KEK, Tsukuba, Japan, Oct. 16 - 21, 2011. - Tsukuba: ICFA&JAEA, 2013. - P.60-63.

[42] Demidova E.V., Goryachkovskaya T.N., Malup T.K., Bannikova S.V., Semenov A.I., Vinokurov N.A., Kolchanov N.A., Popik V.M., Peltek S.E. Studying the non-thermal effects of terahertz radiation on E. coli/pKatG-GFP biosensor cells. // Bioelectromagnetics. - 2013. - Vol.34, N1. - P.15-21; P.345-350.

[43] Science and ultimate reality. Quantum theory, cosmology and complexity (in Russian). - M-Izhevsk: SRC "Regular and Chaotic Dynamics", Institute of computer-related research, 2013. - 642 pages. - (Z.K. Silagadze edited chapters 18, 19, 23, and 24, wrote notes and made lists for supplementary reading to these chapters; I.B. Khriplovich edited chapter 22).

[44] I.A. Kraineva, M.Yu. Mikhailov, T.Yu. Mikhailova, Z.A. Cherkasskaya, Yu.B. Rumer. Physics in XX century (in Russian). // Novosibirsk: Publishing House "ARTA", 2013. - 592 pages.

[45] S.T. Belyaev. Theoretical physics is my profession (in Russian). // Moscow: SRC Kurchatov Institute, 2013. - 188 pages: illustrated.

[46] Gerasimov V.V., Knyazev B.A., Kotelnikov I.A., Nikitin A.K., Cherkassky V.S., Kulipanov G.N., Zhizhin G.N. Surface plasmon polaritons launched using a terahertz free-electron laser: propagation along a gold-ZnS-air interface and decoupling to free waves at the surface edge. // Journal Optical Society of America B. - 2013. - Vol.30, №8. - P.2182-2190.

[47] B.L. Ioffe, L.N. Lipatov, V.S. Fadin Quantum chromodynamics. Perturbative and nonperturbative aspects. Book 2 (in Russian). // Moscow: CSFM, 2013. - 346 pages.

[48] G.M. Skuridin, O.V. Chankina, A.A. Legkodymov, N.V. Baginskaya, V.K. Kramer K.P. Koutsenogy. Element content and intensity of accumulation of chemical elements in buckthorn (Hippiophae rhamnoides L.) fruits (in Russian). // Chemistry for Sustainable Development. - 2013. - V.21. N5. - P.525-532

[49] Bondar A.E., Koop I.A., Kulipanov G.N., Levichev E.B., Parkhomchuk V.V., Perevedentsev E.A., Serednyakov S.I., Skrinsky A.N., Tumaikin G.M., Fadin V.S., Khazin B.I., Khriplovich I.B. Yury Mikhailovich Shatunov (on his 70th birthday). // Physics - Uspekhi. - 2013. - V.56. №9. - P.951-952. – (Uspekhi Fizicheskikh Nauk 183 (9) 1007-1008 (2013).

[50] N.S. Dikansky. Integration of science, education and industry; mainstream development of Russia (in Russian). // About time and us. NSU Physics Department 1963-1968 - Novosibirsk: RRC NSU, 2013. - pp.63-70.

[51] A.E. Bondar. We have a lot to be proud of (in Russian). // About time and us. NSU Physics Department 1963-1968 - Novosibirsk: RRC NSU, 2013. - P.94-99.

[52] V.T. Astrelin. And here the frog jumps into the water (in Russian). // About time and us. NSU Physics Department 1963-1968 - Novosibirsk: RRC NSU, 2013. - P.178-181.

[53] S.I. Serednyakov. Onset of NSU delayed by decades (in Russian). // About time and us. NSU Physics Department 1963-1968 - Novosibirsk: RRC NSU, 2013. - P. 455-456.

[54] Zhirov O.V., Shepelyansky D.L. Thermoelectricity of Wigner crystal in a periodic potential. // EPL. - 2013. - Vol.103, №6. - P.68008.

[55] Sushkov O.P., Milstein A.I., Mori M., Maekawa S. Relativistic effects in scattering of polarized electrons. // EPL. - 2013. - Vol.103, №4. - P.47003.

[56] Bladwell S., Dmitriev V.F., Flambaum V.V., Kozlov A. Color-octet bound states, induced by Higgs mechanism. // Intern. Journal of Modern Physics A. - 2013. - Vol.28, №2. - P.1350009.

[57] Grozin A. Decoupling in QED and QCD. // Intern. Journal of Modern Physics A. - 2013. - Vol.28, №5/6. - P.1350015.

[58] Abelev B., ALICE Collab., Pestov Y. Centrality dependence of π, K, and p production in Pb-Pb collisions at root s(NN)=2.76 TeV. // Physical Review C. - 2013. - Vol.88, № 4. - P.044910.

[59] Abelev B., ALICE Collab., Pestov Y. Centrality determination of Pb-Pb collisions at root s(NN)=2.76 TeV with ALICE. // Physical Review C. - 2013. - Vol.88, №4. - P.044909.

[60] Yi L., Shen B., Lotov K., Ji L., Zhang X., Wang W., Zhao X., Yu Y., Xu J., Wang X., Shi Y., Zhang L., Xu T., Xu Z. Scheme for proton-driven plasma-wakefield acceleration of positively charged. // Physical Review Special Topics - Accelerators and Beams. - 2013. - Vol.16, №4. - P.071301.

[61] Lotov K.V., Lotova G.Z., Lotov V.I., Upadhyay A., Tuckmantel T., Pukhov A., Caldwell A. Natural noise and external wakefield seeding in a proton-driven plasma accelerator. // Physical Review Special Topics - Accelerators and Beams. - 2013. - Vol.16, №4. - P.041301.

[62] Abe T., Perevedentsev E., et al. Achievements of KEKB. // Progress of Theoretical and Experimental Physics. - 2013. - №3. - P.03A001.

[63] Abe T., Perevedentsev E., et al. Commissioning of KEKB. // Progress of Theoretical and Experimental Physics. - 2013. - №3. - P.03A010.

[64] Lizunov A., Donin A., Savkin V. Note: Spectral motional Stark effect diagnostic for measurement of magnetic fields below 0.3 T. // Review of Scientific Instruments. - 2013. - Vol.84, №8. - P.086104.

[65] Vasserman I. B., Strelnikov N.O., Xu J.Z. Some aspects of achieving an ultimate accuracy during insertion device magnetic measurements by a Hall probe. // Review of Scientific Instruments. - 2013. - Vol.84, №2. - P.025004.

[66] Getmanov Ya.V., Kulipanov G.N., Shevchenko O.A., Skrinsky A.N., Tribendis A.G., Volkov V.N., Vinokurov N.A. Full spatially coherent multiturn ERL x-ray source (MARS) based on two linacs. // Journal of Physics: Conference Series. - 2013. - Vol.425. - P.04219. (11th Intern. Conference on Synchrotron Radiation Instrumentation (SRI 2012)).

[67] Golkovski M.G., Bataev I.A., Bataev A.A., Krivizhenko D.S., Losinskaya A.A., Lenivtseva O.G. Structure of surface layers produced by non-vacuum electron beam boriding. // Applied Surface Science. - 2013. - Vol.284. - P.472-481.

[68] Grishnyaev E. S., Polosatkin S.V. Yield determination for a titanium neutron-forming target. // Atomic Energy. - 2013. - Vol.113, №5. - P.345-350.

[69] Khatsymovsky V.M. First-order representation of the Faddeev formulation of gravity. // Classical and Quantum Gravity. - 2013. - Vol.30, №9. - P.095006.

[70] Fadin V.S. NLO BFKL kernels for the adjoint representations of the gauge group. // DIFFRACTION 2012. - Melville: AIP Conference Proc, 2013. - P.239-242. (Intern. Workshop on Diffraction in High Energy Physics (DIFFRACTION), Puerto del Carmen, SPAIN, Sept. 10-15, 2012. - (AIP Conference Proc.; Vol.1523).

[71] Pruuel E.R., Ten K.A., Tolochko B.P., Merzhievsky L.A., Luk'yanchikov L.A., Aul'chenko V.M., Zhulanov V.V., Shekhtman L.I., Titov V.M. Implementation of the capability of synchrotron radiation in a study of detonation processes. // Doklady Physics. - 2013. - Vol.58, №1. - P.24-28.

[72] Erni W., Baldin E., Kotov K., Peleganchuk S., Tikhonov Yu., et al. Technical design report for the PANDA (AntiProton Annihilations at Darmstadt) Straw Tube Tracker. // European Physical Journal A. - 2013. - Vol.49, №2. - P.25.

[73] Soldatkina E. I., Arakcheev A.S., Bagryansky P.A. Experiments in support of the Gas Dynamic Trap based facility for plasma-material interaction testing. // Fusion Engineering and Design. - 2013. - Vol.88, №11. - P.3084-3090.

[74] Stankus S.V., Savchenko I.V., Agadzhanov A.Sh., Yatsuk O.S., Zhmurikov E.I. Thermophysical properties of MPG-6 graphite. // High Temperature. - 2013. - Vol.51, №2. - P.179-182.

[75] Grigoriev D.N., Akhmetshin R.R., Kazanin V.F., Kuzmenko A.E., Yudin Yu.V. Upgrade of the CMD-3 BGO Endcap Calorimeter. // IEEE Transactions on Nuclear Science. - 2013. - Vol.60, №1, pt.2. - P.259-264.

[76] Makarov A.N., Taskaev S.Yu. Beam of monoenergetic neutrons for the calibration of a dark-matter detector. // JETP Letters. - 2013. - Vol.97, №12. - P.667-669.

[77] Bychanok D.S., Shuba M.V., Kuzhir P.P., Maksimenko S.A., Kubarev V.V., Kanygin M.A., Sedelnikova O.V., Bulusheva L.G., Okotrub A.V. Anisotropic electromagnetic properties of polymer composites containing oriented multiwall carbon nanotubes in respect to terahertz polarizer applications. // Journal of Applied Physics. - 2013. - Vol.114, №11. - P.114304.

[78] Veber S.L., Fedin M.V., Maryunina K.Yu., Boldyrev K.N., Sheglov M.A., Kubarev V.V.,

Shevchenko O.A., Vinokurov N.A., Kulipanov G.N., Sagdeev R.Z., Ovcharenko V.I., Bagryanskaya E.G. Influence of intense THz radiation on spin state of photoswitchable compound Cu(hfac)(2)L-Pr. // Journal of Physical Chemistry A. - 2013. - Vol.117, №7. - P.1483-1491.

[79] Getmanov Ya.V., Kulipanov G.N., Shevchenko O.A., Skrinsky A.N., Tribendis A.G., Volkov V.N., Vinokurov N.A. Full spatially coherent multiturn ERL x-ray source (MARS) based on two linacs. // 11TH Intern. Conference on Synchrotron Radiation Instrumentation (SRI 2012), Lyon, France, July 09-13, 2012. - 2013. - P.042019. - (Journal of Physics Conference Series; Vol.425).

[80] Aaij R., Bobrov A., Bondar A., Eidelman S., Krokovny P., Kudryavtsev V., Poluektov A., Shekhtman L., Vorobyev V., et al. Exclusive J/ψ and ψ(2S) production in pp collisions at root s=7 TeV. // Journal of Physics G-Nuclear and Particle Physics. - 2013. - Vol.40, №4. - P.045001.

[81] Sadykov V., Usoltsev V., Yeremeev N., Mezentseva N., Pelipenko V., Krieger T., Belyaev V., Sadovskaya E., Muzykantov V., Fedorova Yu., Lukashevich A., Ishchenko A., Salanov A., Okhlupin Yu., Uvarov N., Smorygo O., Arzhannikov A., Korobeynikov M., Thumm M.K.A. Functional nanoceramics for intermediate temperature solid oxide fuel cells and oxygen separation membranes. // Journal of the European Ceramic Society. - 2013. - Vol.33, №12 Special Issue. - P.2241-2248.

[82] Gerasimov V.V., Knyazev B.A., Kotelnikov I.A., Nikitin A.K., Cherkassky V.S., Kulipanov G.N., Zhizhin G.N. Surface plasmon polaritons launched using a terahertz free-electron laser: propagation along a gold-ZnS-air interface and decoupling to free waves at the surface edge. // Journal of the Optical Society of America B - Optical Physics. - 2013. - Vol.30, №8. - P.2182-2190.

[83] Chesnokov E.N., Kubarev V.V., Koshlyakov P.V., Kulipanov G.N. Very long terahertz free induction decay in gaseous hydrogen bromide. // Laser Physics Letters. - 2013. - Vol.10, №5. - P.055701.

[84] Golkovski M.G., Bataev I.A., Bataev A.A., Ruktuev A.A., Zhuravina T.V., Kuksanov N.K., Salimov R.A., Bataev V.A. Atmospheric electron-beam surface alloying of titanium with tantalum. // Materials Science and Engineering A - Structural Materials Properties Microstructure and Processing. - 2013. - Vol.578. - P.310-317.

[85] Milstein A. I., Salnikov S.G. Kinetics of polarization in non-relativistic scattering. // Nuclear Instruments & Methods B. - 2013. - Vol.313. - P.64-67.

[86] Kotelnikov I. A., Gerasimov V.V., Knyazev B.A. Diffraction of a surface wave on a conducting rectangular wedge. // Physical Review A. - 2013. - Vol.87, №2. - P.023828.

[87] Zhirov O.V., Chepelianskii A.D., Chepelianskii D.L. Towards a synchronization theory of microwave-induced zero-resistance states. // Physical Review B. - 2013. - Vol.88, №3. - P.035410.

[88] Kotelnikov I. A., Popov S.S., Rome M. Photon neutralizer as an example of an open billiard. // Physical Review E. - 2013. - Vol.87, №1. - P.013111.

[89] Bondar A.E. Project of a Super Charm-Tau factory at the Budker Institute of Nuclear Physics in Novosibirsk. // Physics of Atomic Nuclei. - 2013. - Vol.76, №9. - P.1072-1085.

[90] Anashin V.V., Aulchenko V.M., Baldin E.M., Barladyan A.K., Barnyakov A.Yu., Barnyakov M.Yu., Baru S.E., Basok I.Yu., Bedny I.V., Beloborodova O.L., Blinov A.E., Blinov V.E., Bobrov A.V., Bobrovnikov V.S., Bondar A.E., Buzykaev A.R., Vorobiov A.I., Gulevich V.V., Dneprovsky L.V., Zhilich V.N., Zhulanov V.V., Karpov G.V., Karpov S.V., Kononov S.A., Kotov K.Yu., Kravchenko E.A., Kudryavtsev V.N., Kuzmin A.S., Kulikov V.F., Kuper E.A., Levichev E.B., Maksimov D.A., Malyshev V.M., Maslennikov A.L, Medvedko A.S., Muchnoi N.Yu., Nikitin S.A., Nikolaev I.B., Onuchin A.P., Oreshkin S.B., Orlov I.O., Osipov A.A., Peleganchuk S.V., Pivovarov S.G., Poluektov A.O., Pospelov G.E., Prisekin V.G., Rodyakin V.A., Ruban A.A., Savinov G.A., Skovpen Yu.I., Skrinsky A.N., Smalyuk V.V., Snopkov R.G., Sokolov A.V., Sukharev A.M., Talyshev A.A., Tayursky V.A., Telnov V.I., Tikhonov Yu.A., Todyshev K.Yu, Usov Yu.V., Kharlamova T.A., Shamov A.G., Shwartz B.A., Shekhtman L.I., Shusharo A.I., Yushkov A.N. The KEDR detector. // Physics of Particles and Nuclei. - 2013. - Vol.44, №4. - P.657-702.

[91] Shiltsev V., Nesterenko I., Rosenfeld R. Replicating the discovery of Venus's atmosphere. // Physics Today. - 2013. - Vol.66, №2. - P.64-65.

[92] Ivanov A. A., Prikhodko V.V. Gas-dynamic trap: an overview of the concept and experimental results. // Plasma Physics and Controlled Fusion. - 2013. - Vol.55, № 6. - P.063001.

[93] Lotov K.V., Maslov V.I., Onishchenko I.N., Yarovaya I.P. Mechanisms of synchronization of relativistic electron bunches at wakefield excitation in plasma. // Problems of Atomic Science and Technology. - 2013. - №4(86). - P.73-76.

[94] Gauzshtein V.V., Dusaev R.R., Loginov A.Yu., Nikolenko D.M., Sidorov A.A., Stibunov V.N. Negative charged pion production on a deuteron by quasi-real photons. // Russian Physics Journal. - 2013. - Vol.56, №8. - P.878-881.

[95] Zabrodskiy V.V., Aruev P.N., Belik V.P., Ber B.Ya., Kazantsev D.Yu., Drozdova M.V., Zabrodskaya N.V., Lazeeva M.S., Nikolenko A.D., Sukhanov V.L., Filimonov V.V., Sherstnev E.V. Photoresponse recovery in silicon photodiodes upon VUV irradiation. // Semiconductors. - 2013. - Vol.47, №2. - P.213-216.

[96] Koukarine A., Nesterenko I., Petrunin Yu., Shiltsev V. Experimental reconstruction of Lomonosov's discovery of Venus's atmosphere with antique refractors during the 2012 transit of Venus. // Solar System Research. - 2013. - Vol.47, №8. - P.487-490.

[97] Bryzgunov M.I., Ivanov A.V., Panasyuk V.M., Parkhomchuk V.V., Reva V.B. Efficiency improvement of an electron collector intended for electron cooling systems using a Wien filter. // Technical Physics. - 2013. - Vol.58, №6. - P.911-918.

[98] Nishimura K., Dey B., Aston D., Leith D.W.G.S., Ratcliff B., Roberts D., Ruckman L., Shtol D., Varner G.S., Va'vra J.A detailed study of FDIRC prototype with waveform digitizing electronics in cosmic ray telescope using 3D tracks. // Nuclear Instruments & Methods A. - 2013. - Vol.701. - P.115-126.

[99] Allmendinger T., Solodov E.P., Telnov A.V., et al. Track finding efficiency in BABAR. // Nuclear Instruments & Methods A. - 2013. - Vol.704. - P. 44-59.

[100] Va'vra J., Arnaud N., Barnyakov A.Yu., Barnyakov M.Yu., Beigbeder C., Benettoni M., El Berni M., Borsato M., Breton D., Burmistrov L., Collazuol M., Dey B., Gargano F., Giordano F., Jawahery H., Kravchenko E.A., Kononov S.A., Lebbolo H., Leith D.W.G.S., Loparco F., Mazziotta M.N., Maalmi-Di Bello J., Nishimura K., Onuchin A.P., Posocco M., Puill V., Ratcliff B., Roberts D., Simi G., Stocchi A., Shtol D., Stroili R., Tocut V., Twedt E., Varner G.S. Progress on development of the new FDIRC PID detector. // Nuclear Instruments & Methods A. - 2013. - Vol.718. - P. 541-545.

[101] Anisenkov A.V., Aulchenko V.M., Barkov L.M., Bashtovoy N.S., Bondar A.E., Epifanov D.A., Epshteyn L.B., Erofeev A.L., Grebenuk A.A., Ignatov F.V., Karpov S.V., Khazin B.I., Kovalenko O.A., Kozyrev A.N., Kuzmin A.S., Logashenko I.B., Mikhailov K.Yu., Pestov Yu.N, Pivovarov S.G., Razuvaev G.P., Ruban A.A., Ryzhenenkov A.E., Shebalin V.E., Shemyakin D.N., Shwartz B.A., Solodov E.P., Titov V.M., Talyshev A.A., Yudin Yu.V. Barrel calorimeter of the CMD-3 detector. // Nuclear Instruments & Methods A. - 2013. - Vol.732. - P. 463-465.

[102] Barnyakov A.Yu., Barnyakov M.Yu., Beloborodov K.I., Bobrovnikov V.S., Buzykaev A.R., Danilyuk A.F., Golubev V.B., Gulevich V.V., Kononov S.A., Kravchenko E.A., Onuchin A.P., Martin K.A., Serednyakov S.I., Vesenev V.M. Particle identification system based on dense aerogel. // Nuclear Instruments & Methods A. - 2013. - Vol.732. - P.330-332.

[103] Barnyakov A.Yu., Barnyakov M.Yu., Bobrovnikov V.S., Buzykaev A.R., Danilyuk A.F., Degenhardt C., Dorscheid R., Finogeev D.A., Frach T., Gulevich V.V., Karavicheva T.L., Kononov S.A., Kravchenko E.A., Kurepin A.B., Kuyanov I.A., Muelhens O., Onuchin A.P., Ovtin I.V., Razin V.I., Reshetin A.I., Schulze R., Talyshev A.A., Usenko E.A., Zwaans B. Beam test of FARICH prototype with digital photon counter. // Nuclear Instr. & Methods A. - 2013. - Vol.732. - P.352-356.

[104] Bondar A., Buzulutskov A., Dolgov A., Grebenuk A., Shemyakina E., Sokolov A., Breskin A., Thers D. First demonstration of THGEM/GAPD-matrix optical readout in a two-phase Cryogenic Avalanche Detector in Ar. // Nuclear Instruments & Methods A. - 2013. - Vol.732. - P.213-216.

[105] Aubert B., BABAR Collab., Blinov V.E., Bukin A.D., Buzykaev A.R., Druzhinin V.P., Golubev V.B., Korol A.A., Kravchenko E.A., Onuchin A.P., Serednyakov S.I., Skovpen Yu.I., Solodov E.P., Telnov V.I., Todyshev K.Yu., Yushkov A.N. The BABAR detector: Upgrades, operation and performance. // Nuclear Instruments & Methods A. - 2013. - VolA729. - P.615-701. [arXiv:1305.3560 [physics.ins-det]].

[106] Blinov V.E., Buzykaev A.R., Druzhinin V.P., Golubev V.B., Kravchenko E.A., Onuchin A.P., Serednyakov S.I., Skovpen Yu.I., Solodov E.P., Todyshev K.Yu, Yushkov A.N. Time-integrated luminosity recorded by the BABAR detector at the PEP-II e+e– collider. // Nuclear Instruments & Methods A. - 2013. - Vol.726. - P.203-213. [arXiv:1301.2703 [hep-ex]].

[107] Polosatkin S., Belykh V., Davydenko V., Clary R., Fiksel G., Ivanov A., Kapitonov V., Liu D., Mishagin V., Tiunov M., Voskoboynikov R. Neutral particle analyzer for studies of fast ion population in plasma. // Nuclear Instruments & Methods A. - 2013. - Vol.720. - P.42-44.

[108] Popov S.S., Burdakov A.V., Ivantsivskiy M.V., Kasatov A.A., Polosatkin S.V., Postupaev V.V., Vyacheslavov L.N. Two-pulse Thomson scattering system for measurements of fast fluctuations of electron density in multimirror trap GOL-3. // Nuclear Instruments & Methods A. - 2013. - Vol.720. - P.39-41.

[109] Sulyaev Yu.S., Puryga E.A., Khilchenko A.D., Kvashnin A.N., Polosatkin S.V., Rovenskikh A.F., Burdakov A.V., Grishnyaev E.S. Multi-purpose fast neutron spectrum analyzer with real-time signal processing. // Nuclear Instruments & Methods A. - 2013. - Vol.720. - P.23-25.

[110] Arnaud N., Barnyakov A.Yu., Barnyakov M.Yu., Beigbeder C., Benettoni M., El Berni M., Breton D., Burmistrov L., Collazuol G., Dey B., Gargano F., Giordano F., Jawahery H., Kravchenko E.A., Kononov S.A., Lebbolo H., Leith D.W.G.S., Loparco F., Mazziotta M.N., Maalmi-Di Bello J., Nishimura K., Onuchin A.P., Posocco M., Puill V., Ratcliff B., Roberts D., Simi G., Stocchi A., Shtol D., Stroili R., Tocut V., Twedt E., Varner G.S., Va'vra J. A particle identification detector for the forward region of the Super B experiment. // Nuclear Instr. & Meth. A. - 2013. - Vol.718. - P.557-559.

[111] Assiro R., Cappelli L., Cascella M., De Lorenzis L., Grancagnolo F., Ignatov F., L'Erario A., Maffezzoli A., Miccoli A., Onorato G., Perillo M., Piacentino G., Rella S., Rossetti F., Spedicato M., Tassielli G., Zavarise G. Ultra-low mass drift chambers. // Nuclear Instruments & Meth. A. - 2013. - Vol.718. - P.443-445.

[112] Beigbeder C., Breton D., Arnaud N., Barnyakov A.Yu., Barnyakov M.Yu., Benettoni M., El Berni M., Burmistrov L., Collazuol G., Delagnes E., Dey B., Gargano F., Giordano F., Jawahery H., Kravchenko E.A., Kononov S.A., Lebbolo H., Leith D.W.G.S., Leterrier L., Loparco F., Mazziotta M.N., Maalmi-Di Bello J., Nishimura K., Onuchin A.P., Posocco M., Puill V., Ratcliff B., Roberts D., Rouet S., Simi G., Stocchi A., Shtol D., Stroili R., Tocut V., Twedt E., Varner G.S., Va'vra J. Front-end electronics for the SuperB charged particle identification detectors. // Nuclear Instruments & Methods A. - 2013. - Vol.718. - P.186-188.

[113] Gargano F., Arnaud N., Barnyakov A.Yu., Barnyakov M.Yu., Beigbeder C., Benettoni M., El Berni M., Breton D., Burmistrov L., Collazuol G., Dey B., Giordano F., Jawahery H., Kravchenko E., Kononov S.A., Lebbolo H., Leith D.W.G.S., Loparco F., Mazziotta M.N., Maalmi-Di Bello J., Nishimura K., Onuchin A.P., Posocco M., Puill V., Ratcliff B., Roberts D., Simi G., Stocchi A., Shtol D., Stroili R., Tocut V., Twedt E., Varner G.S., Va'vra J. Study of H-8500 MaPMT for the FDIRC detector at Super B. // Nuclear Instruments & Methods A. - 2013. - Vol.718. - P.563-565.

[114] Aad G., ATLAS Collab., Anisenkov A.V., Beloborodova O.L., Bobrovnikov V.S., Bogdanchikov A.G., Kazanin V.F., Korol A.A., Malyshev V.M., Maslennikov A.L., Maximov D.A., Peleganchuk S.V., Skovpen K.Yu., Soukharev A.M., Talyshev A.A., Tikhonov Yu.A. Dynamics of isolated-photon plus jet production in pp collisions at root s=7 TeV with the ATLAS detector. // Nuclear Physics B. - 2013. - Vol.875, №3. - P.483-535.

[115] Aaij R., LHCb Collab., Bondar A., Eidelman S., Krokovny P., Kudryavtsev V., Poluektov A., Shekhtman L., Vorobyev V. Observation of $B^0_S \to \chi(c1)\ \varphi$ decay and study of $B^0 \to \chi$ Kc1, $K_2^{*(0)}$ decays. // Nuclear Physics B. - 2013. - Vol.874, № 3. - P. 663-678.

[116] Fadin V.S., Fiore R., Lipatov L.N., Papa A. Mobius invariant BFKL equation for the adjoint representation in N=4 SUSY. // Nuclear Physics B. - 2013. - Vol.874, №1. - P.230-242.

[117] Aaij R., LHCb Collab., Bondar A., Eidelman S., Krokovny P., Kudryavtsev V., Poluektov A., Shekhtman L., Vorobyev V. Measurement of the effective $B^0_S \to J/\psi\ K_S^{(0)}$ lifetime. // Nuclear Physics B. - 2013. - Vol.873, №2. - P.275-292.

[118] Aaij R., LHCb Collab., Bondar A., Eidelman S., Krokovny P., Kudryavtsev V., Poluektov A., Shekhtman L., Vorobyev V. Observations of $B_S^{(0)} \to \psi(2S)\ \eta$ and $B^0_S \to \psi(2S)\ \pi^+\pi^-$ decays. // Nuclear Physics B. - 2013. - Vol.871, №3. - P.403-419.

[119] Aaij R., LHCb Collab., Bobrov A., Bondar A., Eidelman S., Krokovny P., Kudryavtsev V., Poluektov A., Shekhtman L., Vorobyev V. Prompt charm production in pp collisions at root s=7 TeV. // Nuclear Physics B. - 2013. - Vol.871, №1. - P.1-20.

[120] Aaij R., LHCb Collab., Bobrov A., Bondar A., Eidelman S., Krokovny P., Kudryavtsev V., Poluektov A., Shekhtman L., Vorobyev V. Evidence for the decay $B^0 \to J/\psi\ \omega$ and measurement of the relative branching fractions of B_s^0 meson decays to $J/\psi\ \eta$ and to $J/\psi\ \eta'$. // Nuclear Physics B. - 2013. - Vol.867, №3. - P.547-566.

[121] Bartelt J., Fadin V.S, Lipatov L.N., Vacca G.P. NLO corrections to the kernel of the BKP-equations. // Nuclear Physics B. - 2013. - Vol.867, №3. - P.827-854.

[122] Skovorodin, D. I., Zaytsev K.V., Beklemishev A.D. Global sound modes in mirror traps with anisotropic pressure. // Physics of Plasmas. - 2013. - Vol.20, №10. - P.102123.

[123] Postupaev V.V., Burdakov A.V., Ivanov I.A., Sklyarov V.F., Arzhannikov A.V., Gavrilenko D.Ye., Kandaurov I.V., Kasatov A.A., Kurkuchekov V.V., Mekler K.I., Polosatkin S.V., Popov S.S., Rovenskikh A.F., Sudnikov A.V., Sulyaev Yu.S., Trunev Yu.A., Vyacheslavov L.N. Temporal structure of double plasma frequency emission of thin beam-heated plasma. // Physics of Plasmas. - 2013. - Vol.20, №9. - P.092304. [http://dx.doi.org/10.1063/1.4821608].

[124] Timofeev I.V., Annenkov V.V. Exact kinetic theory for the instability of an electron beam in a hot magnetized plasma. // Physics of Plasmas. - 2013. - Vol.20, №9. - P.092123.

[125] Lotov K.V. Excitation of two-dimensional plasma wakefields by trains of equidistant particle bunches. // Physics of Plasmas. - 2013. - Vol.20, №8. - P.083119.

[126] Anderson J.K., Almagri A.F., Den Hartog D.J., Eilerman S., Forest C.B., Koliner J.J., Mirnov V.V., Morton L.A., Nornberg M.D., Parke E., Reusch J.A., Sarff J.S., Waksman J., Belykh V., Davydenko V.I, Ivanov A.A., Polosatkin S.V., Tsidulko Yu.A., Lin L., Liu D., Fiksel G., Sakakita H., Spong D.A., Titus J. Fast ion confinement and stability in a neutral beam injected reversed field pinch. // Physics of Plasmas. - 2013. - Vol.20, №5. - P.056102. [http:. //dx.doi.org/10.1063/1.4801749 (8 pages)].

[127] Lotov K.V., Pukhov A., Caldwell A. Effect of plasma inhomogeneity on plasma wakefield acceleration driven by long bunches. // Physics of Plasmas. - 2013. - Vol.20, №1. - P.013102.

[128] Timofeev I.V. Modulational instability of a Langmuir wave in plasmas with energetic tails of superthermal electrons. // Physics of Plasmas. - 2013. - Vol.20, №1. - P.012115.

[129] Abbas E., ALICE Collab., Pestov Yu, Performance of the ALICE VZERO system. // Journal of Instrumentation. - 2013. - Vol.8. - P.P10016.

[130] Aad G., ATLAS Collab., Anisenkov A., Beloborodova O., Bobrovnikov V.S., Bogdanchikov A., Kazanin V.F., Kolachev G.M., Korol A., Malyshev V., Maslennikov A.L., Maximov D.A., Orlov I., Peleganchuk

S.V., Schamov A.G., Skovpen K., Soukharev A., Talyshev A., Tikhonov Y.A. Characterisation and mitigation of beam-induced backgrounds observed in the ATLAS detector during the 2011 proton-proton run. // Journal of Instrumentation. - 2013. - Vol.8. - P.P07004.

[131] Aad G., ATLAS Collab., Anisenkov A., Beloborodova O., Bobrovnikov V.S., Bogdanchikov A., Kazanin V.F., Korol A., Malyshev V., Maslennikov A.L., Maximov D.A., Peleganchuk S.V., Skovpen K., Soukharev A., Talyshev A., Tikhonov Yu.A. Triggers for displaced decays of long-lived neutral particles in the ATLAS detector. // Journal of Instrumentation. - 2013. - Vol.8. - P.P07015.

[132] Akimov D.Yu., Akindinov A.V., Alexandrov I.S., Belov V.A., Bolozdynya A.I., Burenkov A.A., Buzulutskov A.F., Danilov M.V., Efremenko Yu.V., Kirsanov M.A., Kovalenko A.G., Stekhanov V.N. Two-phase xenon emission detector with electron multiplier and optical readout by multipixel avalanche Geiger photodiodes. . // Journal of Instrumentation. - 2013. - Vol.8. - P.P05017.

[133] Polosatkin S. Effect of sublevel population mixing on the interpretation of doppler-shift spectroscopy measurements of neutral beam content. // Journal of Instrumentation. - 2013. - Vol.8. - P.P05007. [http://dx.doi.org/10.1088/1748-0221/8/05/P05007].

[134] Bondar A., Buzulutskov A., Dolgov A., Grebenuk A., Shemyakina E., Sokolov A., Akimov D., Breskin A., Thers D. Two-phase Cryogenic Avalanche Detectors with THGEM and hybrid THGEM/GEM multipliers operated in Ar and Ar+N-2. // Journal of Instrumentation. - 2013. - Vol.8. - P.P02008.

[135] Logachev P.V., Kuznetsov G.I., Korepanov A.A., Akimov A.V., Shiyankov S.V., Pavlov O.A., Starostenko D.A., Fat'kin G.A. LIU-2 linear induction accelerator. // Instruments and Experimental Techniques. - 2013. - Vol.56, №6. - P.672-679.

[136] Aleinik V.I., Ivanov A.A., Kuznetsov A.S., Sorokin I.N., Taskaev S.Yu. Dark currents of a tandem accelerator with vacuum insulation. // Instruments and Experimental Techniques. - 2013. - Vol.56, №5. - P.497-505.

[137] Bryzgunov M.I., Ivanov A.V., Panasyuk V.M., Parkhomchuk V.V., Reva V.B. A high-efficiency collector for a high-voltage electron cooler. // Instruments and Experimental Techniques. - 2013. - Vol.56, №3. - P.256-264.

[138] Bosch H.-S., Davydenko V.I, Ivanov A., Shikhovtsev I.V., et al. Technical challenges in the construction of the steady-state stellarator Wendelstein 7-X. // Nuclear Fusion. - 2013. - Vol.53, №12. - P.126001.

[139] Kaneko O., Vyacheslavov L., et al. Extension of operation regimes and investigation of three-dimensional currentless plasmas in the Large Helical Device. // Nuclear Fusion. - 2013. - Vol.53, № 10. - P.104015.

[140] Sarff J.S., Belykh V., Davydenko V.I., Deichuli P., Ivanov A.A., Polosatkin S., Stupishin N.V., et al. Overview of results from the MST reversed field pinch experiment. // Nuclear Fusion. - 2013. - Vol.53, №10 Special Issue. - P.104017.

[141] Ablikim M., BESIII Collab., Achasov M.N., Muchnoi N.Yu., Nikolaev I.B. Measurement of the integrated luminosities of the data taken by BESIII at root s=3.650 and 3.773 GeV. // Chinese Physics C. - 2013. - Vol.37, № 12. - P.123001.

[142] Ablikim M., BESIII Collab., Achasov M.N., Muchnoi N.Yu. Determination of the number of psi ' events at BESIII. // Chinese Physics C. - 2013. - Vol.37, №6. - P.063001.

[143] Meng L.J., BESIII Collab., Achasov M.N., Muchnoi N.Yu., Nikolaev I.B., Parkhomchuk V.V., et al. Research on the detuning system of a cooling electron beam for the dielectronic recombination experiment at CSRm. // Chinese Physics C. - 2013. - Vol.37, №1. - P.017004.

[144] Aad G., ATLAS Collab., Anisenkov A.V., Beloborodova O.L., Bogdanchikov A.G., Kazanin V.F., Kolachev G.M., Korol A.A., Malyshev V.M., Maslennikov A.L., Orlov I.O., Peleganchuk S.V., Schamov A.G., Skovpen K.Yu., Soukharev A.M., Talyshev A.A., Tikhonov Yu.A., Zaytsev A.S. Measurements of top quark pair relative differential cross-sections with ATLAS in pp collisions at root s=7 TeV. // European Physical Journal C. - 2013. - Vol.73, №1. - P.2261.

[145] Aad G., ATLAS Collab., Anisenkov A.V., Beloborodova O.L., Bogdanchikov A.G., Kazanin V.F., Kolachev G.M., Korol A.A., Malyshev V.M., Maslennikov A.L., Maximov D.A., Orlov I.O., Peleganchuk S.V., Schamov A.G., Skovpen K.Yu., Soukharev A.M., Talyshev A.A., Tikhonov Yu.A. Search for pair-produced massive coloured scalars in four-jet final states with the ATLAS detector in proton-proton collisions at root s=7 TeV. // European Physics Journal C. - 2013. - Vol.73, №1. - P.2263.

[146] Aad G., ATLAS Collab., Anisenkov A.V., Beloborodova O.L., Bobrovnikov V.S., Bogdanchikov A.G., Kazanin V.F., Kolachev G.M., Korol A.A., Malyshev V.M., Maslennikov A.L., Orlov I.O., Peleganchuk S.V., Schamov A.G., Skovpen K.Yu., Soukharev A.M., Talyshev A.A., Tikhonov Yu.A. Measurement of the flavour composition of dijet events in pp collisions at root s=7 TeV with the ATLAS detector. // European Physics Journal C. - 2013. - Vol.73, №2. - P.2301.

[147] Aad G., ATLAS Collab., Anisenkov A.V., Beloborodova O.L., Bobrovnikov V.S., Bogdanchikov A.G., Kazanin V.F., Kolachev G.M., Korol A.A., Malyshev V.M., Maslennikov A.L., Maximov D.A., Peleganchuk S.V., Skovpen K.Yu., Soukharev A.M., Talyshev A.A., Tikhonov Yu.A. Multi-channel search for

squarks and gluinos in root s=7 TeV pp collisions with the ATLAS detector at the LHC. // European Physical Journal C. - 2013. - Vol.73, №3. - P.2362.

[148] Aad G., ATLAS Collab., Anisenkov A.V., Beloborodova O.L., Bobrovnikov V.S., Bogdanchikov A.G., Kazanin V.F., Kolachev G.M., Korol A.A., Malyshev V.M., Maslennikov A.L., Maximov D.A., Orlov I.O., Peleganchuk S.V., Schamov A.G., Skovpen K.Yu., Soukharev A.M., Talyshev A.A., Tikhonov Yu.A. Measurement of the tt-bar production cross section in the tau plus jets channel using the ATLAS detector. // European Physical Journal C. - 2013. - Vol.73, №3. - P.2328.

[149] Aad G., ATLAS Collab., Beloborodova O.L., Bobrovnikov V.S., Bogdanchikov A.G., Kazanin V.F., Kolachev G.M., Korol A.A., Malyshev V.M., Maslennikov A.L., Maximov D.A., Orlov I.O., Peleganchuk S.V., Schamov A.G., Skovpen K.Yu., Soukharev A.M., Talyshev A.A., Tikhonov Yu.A., Zaytsev A.S. Jet energy measurement with the ATLAS detector in proton-proton collisions at root s=7 TeV. // European Physical Journal C. - 2013. - Vol.73, №3. - P.2304.

[150] Aad G., ATLAS Collab., Anisenkov A.V., Beloborodova O.L., Bogdanchikov A.G., Kazanin V.F., Kolachev G.M., Korol A.A., Malyshev V.M., Maslennikov A.L., Orlov I.O., Peleganchuk S.V., Schamov A.G., Skovpen K.Yu., Soukharev A.M., Talyshev A.A., Tikhonov Yu.A., Zaytsev A.S. Jet energy resolution in proton-proton collisions at root s 7 TeV recorded in 2010 with the ATLAS detector. // European Physical Journal C. - 2013. - Vol.73, №3. - P.2306.

[151] Adam J., Grigoriev D.N., Ignatov F., Khazin B.I., Popov A., Yudin Yu.V., et al. The MEG detector for $\mu^+ \to e^+\gamma$ decay search. // European Physical Journal C. - 2013. - Vol.73, №3. - P.2365. [e-print: arXiv:1303.2348 [physics.ins-det]].

[152] Aad G., ATLAS Collab., Anisenkov A.V., Beloborodova O.L., Bobrovnikov V.S., Bogdanchikov A.G., Kazanin V.F., Korol A.A., Malyshev V.M., Maslennikov A.L., Maximov D.A., Peleganchuk S.V., Soukharev A.M., Talyshev A.A., Tikhonov Yu.A. Measurement of k(T) splitting scales in $W \to l\ \nu$ events at root s=7 TeV with the ATLAS detector. // European Physical Journal C. - 2013. - Vol.73, №5. - P.2432.

[153] Aaij R., LHCb Collab., Bobrov A., Bondar A., Eidelman S., Krokovny P., Kudryavtsev V., Poluektov A., Shekhtman L., Vorobyev V. Measurement of the forward energy flow in pp collisions at root s=7 TeV. // European Physical Journal C. - 2013. - Vol.73, №5. - P.2421.

[154] Aad G., ATLAS Collab., Anisenkov A.V., Beloborodova O.L., Bobrovnikov V.S., Bogdanchikov A.G., Kazanin V.F., Kolachev G.M., Korol A.A., Malyshev V.M., Maslennikov A.L., Maximov D.A., Peleganchuk S.V., Skovpen K.Yu., Soukharev A.M., Talyshev A.A., Tikhonov Yu.A. Search for a light charged Higgs boson in the decay channel $H^+ \to$ c(s)-bar in t(t)-bar events using pp collisions at root s=7 TeV with the ATLAS detector. // European Physical Journal C. - 2013. - Vol.73, №6. - P.2465.

[155] Aaij R., LHCb Collab., Bobrov A., Bondar A., Eidelman S., Krokovny P., Kudryavtsev V., Poluektov A., Shekhtman L., Vorobyev V. Measurements of the branching fractions of B+ $B^0_S \to$ p(p)-bar $K^{(+)}$ decays. // European Physical Journal C. - 2013. - Vol.73, №6. - P.2462.

[156] Abelev B., ALICE Collab., Pestov Yu. Measurement of inelastic, single- and double-diffraction cross sections in proton-proton collisions at the LHC with ALICE. // European Physical Journal C. - 2013. - Vol.73, №6. - P.2456.

[157] Bondar A., Dolgov A., Poluektov A., Vorobiev V. Effect of direct CP violation in charm on gamma extraction from $B^{\pm}$ $B^0_S \to DK^{\pm}$, $D \to K_S^{(0)}\ \pi^+\pi^-$ Dalitz plot analysis . // European Physical Journal C. - 2013. - Vol.73, №6. - P.2476.

[158] Abbas E., ALICE Collab., Pestov Yu. Mid-rapidity anti-baryon to baryon ratios in pp collisions at root s=0.9, 2.76 and 7 TeV measured by ALICE . // European Physical Journal C. - 2013. - Vol.73, №7. - P.2496.

[159] Aad G., ATLAS Collab., Anisenkov A.V., Beloborodova O.L., Bobrovnikov V.S., Bogdanchikov A.G., Kazanin V.F., Korol A.A., Malyshev V.M., Maslennikov A.L., Maximov D.A., Orlov I.O., Peleganchuk S.V., Schamov A.G., Skovpen K.Yu., Soukharev A.M., Talyshev A.A., Tikhonov Yu.A. Measurement of the inclusive jet cross-section in pp collisions at root s = 2.76 TeV and comparison to the inclusive jet cross-section at root s=7 TeV using the ATLAS detector. // European Physical Journal C. - 2013. - Vol.73, №8. - P.2509.

[160] Aad G., ATLAS Collab., Anisenkov A.V., Beloborodova O.L., Bobrovnikov V.S., Bogdanchikov A.G., Kazanin V.F., Kolachev G.M., Korol A.A., Malyshev V.M., Maslennikov A.L., Orlov I.O., Peleganchuk S.V., Schamov A.G., Skovpen K.Yu., Soukharev A.M., Talyshev A.A., Tikhonov Yu.A. Improved luminosity determination in pp collisions at root s=7 TeV using the ATLAS detector at the LHC. // European Physical Journal C. - 2013. - Vol.73, №8. - P.2518.

[161] E.M. Baldin. Checking lepton universality in decays of J/ψ mesons (in Russian). // Nuclear Physics. - 2013. - Vol.76, add. issue. - P.98-103

[162] K.A. Ten, E.R. Pruuel, L.A. Lukyanchikov, B.P. Tolochko, M.R. Sharafutdinov, A.N. Shmakov, Yu.A. Aminov, A.K. Muzyrya, O.V. Kostitsyn, E.B. Smirnov *In situ* analysis of TATB structure using SR diffraction methods (in Russian). // Scientific Bulletin of NSTU. - 2013. - N4(53). - P.105-112.

[163] O.P. Korobeinichev, A.D. Nikolenko, A.G. Shmakov, I.E. Gerasimov, A.M. Dmitriev, S.A. Yakimov, D.A. Knyazkov, L.V. Kuibida, P.S. Zavertkin, D.V. Ivlyushkin, M.R. Mashkovtsev, V.F. Pindyurin, A.E. Soldatov. Project of station for VUV synchrotron radiation for diagnostics of flame (in Russian). // Scientific Bulletin of NSTU. - 2013. – N4 (53). - P.86-95.

[164] Logachev P.V., Kuznetsov G.I., Korepanov A.A., Akimov A.V., Shiyankov S.V., Pavlov O.A., Starostenko D.A., Fat'kin G.A. // LIU-2 linear induction accelerator. // Instruments and Exp. Techniques. - 2013. - Vol.56, №6. - P.672-679 (2013. - №6. - P.42-49).

[165] A.N Agafonov, B.O. Volodkin, S.G. Volotovsky, A.K. Kaveev, B.A. Knyazev, G.I. Kropotov, K.N. Tukmakov, V.S. Paveliev, E.V. Tsygankova, D.I. Tsypishka, Yu.Yu. Choporova. Silicon optics for focusing terahertz laser radiation to gven two-dimensional areas (in Russian). // Computer Optics. - 2013. - Vol.37, №4. - P.464-470.

[166] V.I. Aleynik, A.A. Ivanov, A.S. Kuznetsov, I.N. Sorokin, S.Yu. Taskaev. Dark currents of the tandem accelerator with vacuum insulation (in Russian). // Instruments and Experimental Techniques. - 2013. - N5. - P.5-13.

[167] Barnyakov A.M., Chernousov Yu.D., Ivannikov V.I., Shebolaev I.V., Levichev A.E. Aerial type microwave entry. // Instruments and Experimental Techniques. - 2013. - №3. - P.72-76 (in Russian).

[168] A.E. Bondar, A.F. Buzulutskov, A.D. Dolgov, S.V. Peleganchuk, R.G. Snopkov, A.V. Sokolov, E.O. Shemyakina, L.I. Shekhtman. Project of two-phase cryogenic avalanche detector for dark matter search and low-energy neutrino detection (in Russian). // Bulletin of the Novosibirsk State University. Series: Physics. - 2013. - Vol.8, N6. - P.13-26.

[169] A.E. Bondar, A.F. Buzulutskov, A.V. Burdakov, E.S. Grishnyaev, A.D. Dolgov, A.N. Makarov, S.V. Polosatkin, AV Sokolov , S.Yu. Taskaev, L.I Shehtman. The project of neutron scattering systems for calibration of dark matter and low-energy neutrinos detector. // Bulletin of the Novosibirsk State University. Series: Physics. 2013. Vol.8. - N3. - P.27-38.

[170] E.S. Grishnyaev, A.D. Dolgov, S.V. Polosatkin. Numerical code for statistical simulation of neutron scattering in crio detector of weak interactive particles (in Russian). // Bulletin of Novosibirsk State University. Series: Physics. 2013. - Vol.8, N3. - P.39-45.

[171] L.I. Shechtman, A.D. Dolgov. Fast high-resolution gas position detectors. (in Russian) // Bulletin of Novosibirsk University. Series Physics. - 2013. - Vol.8, N3. -P.47-62.

[172] Bryazgin K.A., Domarov E.V., Korchagin A.I., Kuksanov N.K., Nemytov P.I., Salimov R.A., Fadeev S.N. Energy pulsations in electron accelerator ELV-4 for rapid-series X-ray tomography .– In Russian. // Vestnik NGU. - Vol.8. - №3. - 2013. - P.63-70.

[173] A.A. Legkodymov, A.V. Bryanskaya, R. Simon, V.R. Altapova, V.I. Kondratiev, M.R. Mashkovtsev, T.E. Aleshina, T.K. Malup, G.N. Kulipanov, S.E. Peltek. Analysis of chemical elements associated with microbial-tion communities using correlation of optical and X-ray images (in Russian). // Bulletin of the Russian Academy of Sciences. Physics. - 2013. - Vol.77, N9. - P.1363-1367.

[174] A.V. Darin, I.A. Kalugin, T.I. Markovich, A.V. Mordvinov, D.V. Ovchinnikov, Ya.V. Rakshun, D.S. Sorokoletov. Natural periodicity in sedimentation of Lake Teletskoe (the Altai Mountains) over the past 2,000 years using high-resolution scanning microanalysis on VEPP-3 (BINP) SR beams (in Russian). // Bulletin of the Russian Academy of Sciences. Series: Physics. - 2013. - Vol.77, N9. - P.1359-1362.

[175] A.V. Zorin, N.A. Mezentsev, V.M. Tsukanov. Fast measurement of deformation of the liner of superconducting wiggler in s-n transition (in Russian). // Bulletin of the Russian Academy of Sciences. Series: Physics. - 2013. - Vol.77, N9. - P.1354-1358.

[176] A.N. Gentselev, B.G. Goldenberg, A.G. Zelinsky, A.G. Lemzyakov, V.I. Kondratiev. X-ray patterns with titanium and polymer support membranes (in Russian). // Bulletin of the Russian Academy of Sciences. Series: Physics. - 2013. - Vol.77, N9. - P.1351-1353.

[177] T.V. Salikova. Monitoring of radiation level in the FEL accelerator hall (in Russian). // Bulletin of the Russian Academy of Sciences. Series: Physics. - 2013. - Vol.77, N9. - P.1349-1350.

[178] A.A. Vasiliev, E.I. Palchikov, V.V. Kubarev, E.N. Chesnokov, P.V. Koshlyakov, A.V. Dolgyh, I.Yu. Krasnikov, K.A. Ten. Exploration of stationary and non-stationary combustion waves in hydrogen-oxygen mixture at Novosibirsk terahertz free electron laser (in Russian). // Bulletin of the Russian Academy of Sciences. Series: Physics. - 2013. - V.77, N 9. - pp. 1345-1348.

[179] Aaij R., LHCb Collab., Bondar A., Eidelman S., Krokovny P., Kudryavtsev V., Poluektov A., Shekhtman L., Vorobyev V. Measurement of J/ψ polarization in pp collisions at root s=7 TeV. // European Physical Journal C. - 2013. - Vol.73, N11. - P.2631.

[180] Abbas E., ALICE Collab., Pestov Y. Charmonium and e^+e^- pair photoproduction at mid-rapidity inultra-peripheral Pb-Pb collisions at root s(NN)=2.76 TeV. // European Physical Journal C. - 2013. - Vol.73, N11. - P.2617.

[181] Aaij R., LHCb Collab., Bondar A., Eidelman S., Krokovny P., Kudryavtsev V., Poluektov A., Shekhtman L., Vorobyev V. Observation of $B_s^{(0)} \to \overline{B}_s^{(0)}$ mixing and measurementof mixing frequencies using semi-leptonic B decays. // European Physical Journal C. - 2013. - Vol.73, N12. - P.2655.

[182] Aad G., ATLAS Collab., Anisenkov A. V., Beloborodova O. L., Bobrovnikov V. S., Bogdanchikov

A. G., Kazanin V. F., Korol A. A., Malyshev V. M., Maslennikov A. L., Maximov D. A., Peleganchuk S. V., Skovpen K. Yu, Soukharev A. M., Talyshev A. A., Tikhonov Yu. A. Measurement of jet shapes in top-quark pair events at root s=7 TeV using the ATLAS detector. // European Physical Journal C. - 2013. - Vol.73, N12. - P.2676.

[183] Ablikim M., BESIII Collab., Achasov M.N., Muchnoi N.Yu, Nikolaev I.B. Observation of ηc decay into $\Sigma+\Sigma^{-}-$ and $\Xi-\Xi^{-}+$ final states. // Physical Review D. - 2013. - Vol.87, N1. - P.012003. [e-Print: arXiv:1210.2831 [hep-ex]].

[184] Lees J. P., BaBar Collab., Blinov V. E., Buzykaev A. R., Druzhinin V. P., Golubev V. B., Kravchenko E. A., Onuchin A. P., Serednyakov S. I., Skovpen Yu I., Solodov E. P., Todyshev K. Yu, Yushkov A. N. Measurement of D^0D^0-bar mixing and CP violation in two-body D^0 decays. // Physical Review D. - 2013. - Vol.87, N1. - P.012004. [arXiv:1209.3896 [hep-ex]].

[185] Aad G., Atlas Collab., Anisenkov A., Beloborodova O., Bobrovnikov V. S., Bogdanchikov A., Kazanin V. F., Kolachev G. M., Korol A., Malyshev V., Maslennikov A.L., Maximov D. A., Orlov I., Peleganchuk S. V., Schamov A. G., Skovpen K., Soukharev A., Talyshev A., Tikhonov Y. A., Zitoun R. Search for contact interactions and large extra dimensions indilepton events from pp collisions at root s=7 TeV with the ATLAS detector. // Physical Review D. - 2013. - Vol.87, N1. - P.015010.

[186] Ablikim M., BESIII Collab., Achasov M.N., Muchnoi N.Yu., Nikolaev I.B. Search for hadronic transition $\chi cJ \to \eta c\pi^{+}\pi^{-}$ and observation of $\chi cJ \to KK^{-}\pi\pi\pi$. // Physical Review D. - 2013. - Vol.87, N1. - P.012002. [e-Print: arXiv:1208.4805 [hep-ex]].

[187] Ablikim M., Achasov M. N., Muchnoi N. Yu., Nikolaev I. B. Measurements of $\psi' \to \bar{p}\, K+\Sigma 0$ and $\chi cJ \to \bar{p}\, K+\Lambda$. // Physical Review D. - 2013. - Vol.87, N1. - P.012007. [[e-Print: arXiv:1211.5631 [hep-ex]].

[188] Aad G., ATLAS Collab., Anisenkov A., Beloborodova O., Bobrovnikov V. B., Bogdanchikov A., Kazanin V. A., Kolachev G. M., Korol A., Malyshev V., Maslennikov A.L., Orlov I., Peleganchuk S. V., Schamov A. G., Skovpen K., Soukharev A., Talyshev A., Tikhonov Y. A. Search for squarks and gluinos with the ATLAS detector in final states with jets and missing transverse momentum using 4:7 $fb^{(-1)}$ of root s=7 TeV proton-proton collision data. // Physical Review D. - 2013. - Vol.87, N1. - P.012008.

[189] Ablikim M., BesIII Collab., Achasov M. N., Guan Y.H., Muchnoi N.Yu., Nikolaev I.B. Search for η and η' invisible decays in $J/\psi \to \varphi\eta$ and $\varphi\eta'$. // Physical Review D. - 2013. - Vol.87, N1. - P.012009. [e-Print: arXiv:1209.2469 [hep-ex]].

[190] Tamponi U., Belle Collab., Aulchenko V., Bondar A., Eidelman S., Epifanov D., Krokovny P., Kuzmin A., Shwartz B., Zhilich V., Zhulanov V. Study of the hadronic transitions $\Upsilon(2S) \to (\eta, \pi^0)\Upsilon(1S)$ at Belle. // Physical Review D. - 2013. - Vol.87, N 1. - P.011104.

[191] Aad G., ATLAS Collab., Anisenkov A., Beloborodova O., Bobrovnikov V. S., Bogdanchikov A., Kazanin V. F., Kolachev G. M., Korol A., Malyshev V., Maslennikov A.L., Orlov I., Peleganchuk S. V., Schamov A. G., Skovpen K., Soukharev A., Talyshev A., Tikhonov Y. A., Zaytsev A. Measurement of the $\Lambda^{(0)}_{(b)}$ lifetime and mass in the ATLAS experiment. // Physical Review D. - 2013. - Vol.87, N3. - P.032002.

[192] Ablikim M., BESIII Collab., Achasov M.N., Muchnoi N.Yu, Nikolaev I.B. Evidence for $\eta c \to \gamma\gamma$ and measurement of $J/\psi \to 3\gamma$. // Physical Review D. - 2013. - Vol.87, N3. - P.032003. [e-Print: arXiv:1208.1461 [hep-ex]].

[193] Esen S., Belle Collab., Eidelman S., Krokovny P., Shwartz B., Zhilich V., Zhulanov V. Precise measurement of the branching fractions for $B_s^0 \to D_s^{*(+)} D_s^{*(-)}$ and first measurement of the $D_s^{*(+)} D_s^{*(-)}$ polarization using $e^{+}e^{-}$ collisions. // Physical Review D. - 2013. - Vol.87, N3. - P.031101.

[194] Lees J.P., BaBbar Collab., Blinov V.E., Buzykaev A.R., Druzhinin V.P., Golubev V.B., Kravchenko E.A., Onuchin A.P., Serednyakov S.I., Skovpen Yu.I., Solodov E.P., Todyshev K.Yu., Yushkov A.N. Branching fraction measurement of $B^{+} \to \omega\, l^{+}\, \nu$ decays. // Physical Review D. - 2013. - Vol.87, N3. - P.032004. [arXiv:1205.6245 [hep-ex]].

[195] Ablikim M., BESIII Collab., Achasov M. N., Muchnoi N. Yu., Nikolaev I. B. Measurements of baryon pair decays of chi(cJ) mesons. // Physical Review D. - 2013. - Vol.87, N3. - P.032007. [e-Print: arXiv:1211.2283 [hep-ex]].

[196] Ablikim M., BESIII Collab., Achasov M. N., Muchnoi N. Yu., Nikolaev I. B. Search for η and $\eta' \to \pi^{+}e^{-}\ \bar{\nu}\ e^{+}$ c.c. decays in $J\psi \to \varphi\eta$ and $\varphi\eta'$. // Physical Review D. - 2013. - Vol.87, N3. - P.032006. [e-Print: arXiv:1211.3600 [hep-ex]].

[197] Lees J.P., BaBar Collab., Blinov V.E., Buzykaev A.R., Druzhinin V.P., Golubev V.B., Kravchenko E.A., Onuchin A.P., Serednyakov S.I., Skovpen Yu.I., Solodov E.P., Todyshev K.Yu., Yushkov A.N. Search for di-muon decays of a low-mass Higgs boson in radiative decays of the Upsilon(1S). // Physical Review D. - 2013. - Vol.87, N3. - P.031102.

[198] Duh Y. -T., Belle Collab., Aulchenko V., Bondar A., Eidelman S., Krokovny P., Kuzmin A., Shebalin V., Shwartz B., Vinokurova A., Zhilich V., Zhulanov V. Measurements of branching fractions and direct CP asymmetries for $B \to K\,\pi$, $B \to \pi\pi$ and $B \to KK$ decays. // Physical Review D. - 2013. - Vol.87, N 3. - P.031103.

[199] Ablikim M., BESIII Collab., Achasov M.N., Muchnoi N.Yu., Nikolaev I.B. Study of the near-threshold $\omega\varphi$ mass enhancement indoubly OZI-suppressed $J/\psi \to \gamma\omega\varphi$ decays. // Physical Review D. - 2013. -

Vol.87, N3. - P.032008. [e-Print:arXiv:1211.5668 [hep-ex]].

[200] Ablikim M, Achasov MN, Albayrak O, Ambrose DJ, An FF, An Q, Bai JZ, Ban Y, Becker J, Bennett JV, et al. Study of the near-threshold ωφ mass enhance-ment in doubly OZI suppressed $J/\psi \to \gamma\omega\varphi$ decays Phys. Rev. D87 (2013) 032008. e-Print: arXiv:1211.5668 [hep-ex]

[201] Aaij R., LHCb Collab., Bobrov A., Bondar A., Eidelman S., Krokovny P., Kudryavtsev V., Poluektov A., Shekhtman L., Vorobyev V. Analysis of the resonant components in B^0-bar - $J/\psi\ \pi^+\pi^-$. // Physical Review D. - 2013. - Vol.87, N5. - P.052001.

[202] Aad G., ATLAS Collab., Anisenkov A., Beloborodova O., Bobrovnikov V. S., Bogdanchikov A., Kazanin V. F., Kolachev G. M., Korol A., Malyshev V., Maslennikov A.L., Maximov D. A., Orlov I., Peleganchuk S. V., Schamov A. G., Skovpen K., Soukharev A., Talyshev A., Tikhonov Y. A. Search for new phenomena in events with three charged leptonsat root s=7 TeV with the ATLAS detector. // Physical Review D. - 2013. - Vol.87, N5. - P.052002.

[203] Aad G., ATLAS Collab., Anisenkov A., Beloborodova O., Bobrovnikov V. S., Bogdanchikov A., Kazanin V. F., Kolachev G. M., Korol A., Malyshev V., Maslennikov A.L., Maximov D. A., Orlov I., Peleganchuk S. V., Schamov A. G., Skovpen K., Soukharev A., Talyshev A., Tikhonov Y. A. Measurement of upsilon production in 7 TeV pp collisions at ATLAS. // Physical Review D. - 2013. - Vol.87, N5. - P.052004.

[204] Ablikim M., BESIII Collab., Achasov M.N., Muchnoi N.Yu., Nikolaev I.B. Evidence for ηc(2S) in $\psi(3686) \to \gamma K_S^0 K(+/-)\pi(-/+)\ \pi^+\pi^-$. // Physical Review D. - 2013. Vol.87, N5. - P.052005. [e-Print: arXiv:1301.1476 [hep-ex]].

[205] Ablikim M., BESIII Collab., Achasov M. N., Muchnoi N. Yu., Nikolaev I. B. Measurements of the branching fractions for J/ψ and $\psi' \to \Lambda\Lambda$-bar π^0 and $\Lambda\Lambda$-bar η. // Physical Review D. - 2013. - Vol.87, N5. - P.052007. [e-Print: arXiv:1211.4682 [hep-ex]].

[206] Lees J.P., BaBar Collab., Blinov V.E., Buzykaev A.R., Druzhinin V.P., Golubev V.B., Kravchenko E.A., Onuchin A.P., Serednyakov S.I., Skovpen Yu.I., Solodov E.P., Todyshev K.Yu., Yushkov A.N. Search for direct CP violation in singly Cabibbo-suppressed $D^\pm \to K^+K^-\pi^\pm$ decays. // Physical Review D. - 2013. - Vol.87, N5. - P.052010.

[207] Lees J. P., BaBar Collab., Blinov V. E., Buzykaev A. R., Druzhinin V. P., Golubev V. B., Kravchenko E. A., Onuchin A. P., Serednyakov S. I., Skovpen Yu. I., Solodov E. P., Todyshev K. Yu., Yushkov A. N. Measurement of CP asymmetries and branching fractions in charmless two-body B-meson decays to pions and kaons. // Physical Review D. - 2013. - Vol.87, N5. - P.052009. [arXiv:1206.3525 [hep-ex]].

[208] Lees J.P., Blinov V.E., Buzykaev A.R., Druzhinin V.P., Golubev V.B., Kravchenko E.A., Onuchin A.P., Serednyakov S.I., Skovpen Yu.I., Solodov E. P., Todyshev K. Yu., Yushkov A. N. Search for CP violation in the decays $D^\pm \to K_S K^\pm \to K^0, D_s \to K_S K^\pm \to K^0$, and $D_s^\pm \to K_S^0\ \pi^\pm$. // Physical Review D. - 2013. - Vol.87, N5. - P.052012.

[209] Wang X.L., Belle Collab., Aulchenko V., Eidelman S., Krokovny P., Lukin P., Usov Y., Zhilich V. Observation of psi(4040) and psi(4160) decay into η J/ψ. // Physical Review D. - 2013. - Vol.87, N5. - P.051101.

[210] Lees J.P., BaBar Collab., Blinov V.E., Buzykaev A.R., Druzhinin V.P., Golubev V.B., Kravchenko E. A., Onuchin A.P., Serednyakov S.I., Skovpen Yu.I., Solodov E.P., Todyshev K.Yu, Yushkov A.N. Observation of direct CP violation in the measurement of the Cabibbo-Kobayashi-Maskawa angle gamma with $B^\pm \to D_d^{(*)}\ K^{(*\pm)}$ decays. // Physical Review D. - 2013. - Vol.87, N5. - P.052015.

[211] Abelev B., ALICE Collab., Pestov Y. Charged kaon femtoscopic correlations in pp collisions at root s=7 TeV. // Physical Review D. - 2013. - Vol.87, N5. - P.052016.

[212] Aaij R., LHCb Collab., Bobrov A., Bondar A., Eidelman S., Krokovny P., Kudryavtsev V., Poluektov A., Shekhtman L., Vorobyev V. Amplitude analysis and branching fraction measurement of bar-$B_s^0 \to J/\psi\ K^+K^-$. // Physical Review D. - 2013. - Vol.87, N7. - P.072004.

[213] Liventsev D., Belle Collab., Arinstein K., Aulchenko V., Bondar A., Eidelman S., Epifanov D., Gabyshev N., Krokovny P., Kuzmin A., Matvienko D., Shwartz B., Usov Y., Vorobyev V., Zhilich V. Search for heavy neutrinos at Belle. // Physical Review D. - 2013. - Vol.87, N7. - P.071102.

[214] Aaij R., LHCb Collab., Bondar A., Eidelman S., Krokovny P., Kudryavtsev V., Poluektov A., Shekhtman L., Vorobyev V. Search for the decay $B_s^0 \to D^*(-+)\ \pi^\pm$.// Physical Review D. - 2013. - Vol.87, N7. - P.071101.

[215] Aaij R., LHCb Collab., Bondar A., Eidelman S., Krokovny P., Kudryavtsev V., Poluektov A., Shekhtman L., Vorobyev V. Observation of the decay $B_c^{(+)} \to \psi(2S)\ \pi^+$. // Physics Review D. - 2013. - Vol.87, N7. - P.071103.

[216] Oswald C., Belle Collab., Arinstein K., Bondar A., Eidelman S., Gabyshev N., Krokovny P., Matvienko D., Shiu J. -G., Zhilich V. Measurement of the inclusive semileptonic branching fraction B $B_s^0 \to X^-l^+$ ν(l) at Belle. // Physical Review D. - 2013. - Vol.87, N7. - P.072008.

[217] Aaij R., Bobrov A., Bondar A., Eidelman S., Krokovny P., Kudryavtsev V., Poluektov A., Shekhtman L., Vorobyev V. Study of $B^0 \to D^*(-)\ \pi^+\pi^-\pi^+$ and $B^0 \to D^*K^{-(+)}\ \pi^-\pi^+$ decays. // Physical Review D. - 2013. - Vol.87, N9. - P.092001.

[218] Lees J.P., BaBar Collab., Blinov V.E., Buzykaev A.R., Druzhinin V. P., Golubev V.B., Kravchenko E.A., Onuchin A.P., Serednyakov S.I., Skovpen Yu.I., Solodov E.P., Todyshev K.Yu., Yushkov A.N. Study of the decay B^0-bar $\to \Lambda_c^+$ p-bar $\pi^+\pi^-$ and its intermediate states. // Physical Review D. - 2013. - Vol.87, N.9. - P.092004. [arXiv:1302.0191 [hep-ex]].

[219] Lees J.P., BaBar Collab., Blinov V.E., Buzykaev A.R., Druzhinin V.P., Golubev V.B., Kravchenko E.A., Onuchin A.P., Serednyakov S.I., Skovpen Yu.I., Solodov E.P., Todyshev K.Yu., Yushkov A.N. Study of $e^+e^- \to$ pp-bar via initial-state radiation at BABAR. // Physical Review D. - 2013. - Vol.87, N9. - P.092005. [arXiv:1303.0571 [hep-ex]].

[220] Ablikim M., BESIII Collab., Achasov M.N., Muchnoi N.Yu., Nikolaev I.B. Study of $\psi(3686) \to \omega K K^-\pi$ decays. // Physical Review D. - 2013. - Vol.87, N9. - P.092006. [e-Print: arXiv:1303.6360 [hep-ex]].

[221] Gaur V., Belle Collab., Aulchenko V., Eidelman S., Gabyshev N., Lukin P., Matvienko D., Vorobyev V., Zhilich V. Evidence for the decay $B^0 \to K^+K^- \pi^0$. // Physical Review D. - 2013. - Vol.87, N9. - P.091101.

[222] Aaij R., LHCb Collab., Bondar A., Eidelman S., Krokovny P., Kudryavtsev V., Poluektov A., Shekhtman L., Vorobyev V. First observations of $\bar{B}_s^0 \to D^+D^-$, $D_s^+D^-$ and $D^0\bar{D}^0$ decays. // Physical Review D. - 2013. - Vol.87, N9. - P.092007.

[223] Ablikim M., BESIII Collab., Achasov M.N., Muchnoi N.Yu., Nikolaev I.B. Partial wave analysis of $J/\psi \to \gamma\eta\eta$. // Physical Review D. - 2013. - Vol.87, N9. - P.092009. [e-Print: arXiv:1301.0053 [hep-ex]].

[224] Ablikim M., BESIII Collab., Achasov M. N., Muchnoi N.Yu., Nikolaev I.B. Measurement of $\eta' \to \pi^+\pi^- e^+e^-$ and $\eta' \to \pi^+\pi^- \mu^+\mu^-$. // Physical Review D. - 2013. - Vol.87, N 9. - P.092011. [e-Print: arXiv:1303. 7360 [hep-ex]].

[225] Aad G., ATLAS Collab., Anisenkov A., Beloborodova O., Bobrovnikov V. S., Bogdanchikov A., Kazanin V. F., Kolachev G. M., Korol A., Malyshev V., Maslennikov A.L., Orlov I., Peleganchuk S. V., Schamov A. G., Skovpen K., Soukharev A., Talyshev A., Tikhonov Y. A. Measurement of W^+W^- production in pp collisions at root s=7 TeV with the ATLAS detector and limits on anomalous WWZ and WW gamma couplings. // Physical Review D. - 2013. - Vol.87, N11. - P.112001.

[226] Ablikim M., BESIII Collab., Achasov M. N., Muchnoi N. Yu., Nikolaev I. B. Study of $J/\psi \to \omega$pp-bar at BESIII. // Physical Review D. - 2013. - Vol.87, N11. - P.112004. [e-Print: arXiv:1303.3108 [hep-ex]].

[227] Aad G., ATLAS Collab., Anisenkov A., Beloborodova O., Bobrovnikov V. S., Bogdanchikov A., Kazanin V.F., Kolachev G.M., Korol A., Malyshev V., Maslennikov A.L., Maximov D.A., Peleganchuk S.V., Skovpen K., Soukharev A., Talyshev A., Tikhonov Y.A. Measurements of W gamma and Z gamma production in pp collisionsat root s=7 TeV with the ATLAS detector at the LHC. // Physical Review D. - 2013. - Vol.87, N11. - P.112003.

[228] Lees J.P., BABAR Collab., Blinov V.E., Buzykaev A.R., Druzhinin V.P., Golubev V.B., Kravchenko E.A., Onuchin A.P., Serednyakov S.I., Skovpen Yu.I., Solodov E.P., Todyshev K.Yu., Yushkov A.N. Search for $B^0 \to K(*)\ \nu\nu$-bar B $\to K(*)\ \nu\nu$-bar and invisible quarkonium decays. // Physical Review D. - 2013. - Vol.87, N11. - P.112005. [arXiv:1303.7465 [hep-ex]].

[229] Aad G., ATLAS Collab., Anisenkov A., Beloborodova O., Bobrovnikov V.S., Bogdanchikov A., Kazanin V.F., Kolachev G.M., Korol A., Malyshev V., Maslennikov A.L., Maximov D. A., Orlov I., Peleganchuk S.V., Schamov A.G., Skovpen K., Soukharev A., Talyshev A., Tikhonov Y.A. Search for resonant diboson production in the WW/WZ – lvjj decay channels with the ATLAS detector at root s=7 TeV. // Physical Review D. - 2013. - Vol.87, N11. - P.112006.

[230] Ablikim M., BesIII Collab., Achasov M.N., Muchnoi N.Yu., Nikolaev I.B. Search for the lepton flavor violation process $J/\psi \to e\mu$ at BESIII. // Physical Review D. - 2013. - Vol.87, N11. - P.112007. [[e-Print: arXiv:1304.3205 [hep-ex]].

[231] Aaij R., LHCb Collab., Bondar A., Eidelman S., Krokovny P., Kudryavtsev V., Poluektov A., Shekhtman L., Vorobyev V. Measurement of the branching fractions of the decays $B_s^0 \to$ bar-$D^0K^-\pi^+$ and B^0 – bar-$D^0\ K^+\pi^-$. // Physical Review D. - 2013. - Vol.87, N 11. - P.112009.

[232] Aaij R., LHCb Collab., Bondar A., Eidelman S., Krokovny P., Kudryavtsev V., Poluektov A., Shekhtman L., Vorobyev V. Measurement of CP violation and the B-s(0) meson decay widthdifference with $B_s^0 \to J/\psi\ K^+K^-$ and $B_s^0 \to J/\psi\ \pi^+\pi^-$ decays. // Physical Review D. - 2013. - Vol.87, N11. - P.112010.

[233] Ablikim M., BESIII Collab., Achasov M. N., Muchnoi N. Yu., Nikolaev I. B. Search for baryonic decays of c $\psi(3770)$ and $\psi(4040)$. // Physical Review D. - 2013. - Vol.87, N11. - P.112011. [[e-Print: arXiv: 1305.1782 [hep-ex]]].

[234] Lutz O., Belle Collab., Bondar A., Eidelman S., Gabyshev N., Krokovny P., Kuzmin A., Matvienko D., Shebalin V., Shwartz B., Usov Y., Vorobyev V., Zhilich V., Zhulanov V. Search for $B \to h^*\ \nu\nu$-bar with the full Belle Upsilon(4S) data sample. // Physical Review D. - 2013. - Vol.87, N 11. - P.111103.

[235] Aaij R., LHCb Collab., Bondar A., Eidelman S., Krokovny P., Kudryavtsev V., Poluektov A., Shekhtman L., Vorobyev V. Observation of $B_c^+ \to J/\psi\ D_s^+$ and $B_c^+ \to J/\psi\ D_s^{*+}$ decays. // Physical Review D. - 2013. - Vol.87, N11. - P.112012.

[236] Aad G., Anisenkov A., Beloborodova O., Bobrovnikov V.S., Bogdanchikov A., Kazanin V.F., Korol A., Malyshev V., Maslennikov A.L., Maximov

D.A., Peleganchuk S.V., Skovpen K., Soueid P., Talyshev A., Tikhonov Y.A. Search for nonpointing photons in the diphoton and E-T(miss) final state in root s=7 TeV proton-proton collisions using the ATLAS detector. // Physical Review D. - 2013. - Vol.88, N1. - P.012001.

[237] Lees J.P., BABAR Collab., Blinov V.E., Buzykaev A.R., Druzhinin V.P., Golubev V.B., Kravchenko E.A., Onuchin A.P., Serednyakov S.I., Skovpen Yu.I., Solodov E.P., Todyshev K.Yu., Yushkov A.N. Measurement of CP-violating asymmetries in $B^0 \to \rho\pi^0$ decays using a time-dependent Dalitz plot analysis. // Physical Review D. - 2013. - Vol.88, N1. - P.012003.

[238] Shen C.P., Belle Collab., Aulchenko V., Eidelman S., Gabyshev N., Krokovny P., Kuzmin A., Lukin P., Matvienko D., Shebalin V., Shwartz B., Vorobyev V., Zhilich V. Measurement of exclusive Upsilon(1S) and Upsilon(2S) decays into vector-pseudoscalar final states. // Physical Review D. - 2013. - Vol.88, N1. - P.011102.

[239] Aad G., ATLAS Collab., Anisenkov A., Beloborodova O., Bobrovnikov V. S., Bogdanchikov A., Kazanin V.F., Korol A., Malyshev V., Maslennikov A.L., Maximov D.A., Peleganchuk S. V., Skovpen K., Soukharev A., Talyshev A., Tikhonov Y.A. Search for t(t)over-bar resonances in the lepton plus jets final state with ATLAS using 4.7 fb^{-1} of pp collisions at root s=7 TeV. // Physical Review D. - 2013. - Vol.88, N1. - P.012004.

[240] Aad G., ATLAS Collab., Anisenkov A., Beloborodova O., Bobrovnikov V. S., Bogdanchikov A., Kazanin V. F., Kolachev G. M., Korol A., Malyshev V., Maslennikov A.L., Orlov I., Peleganchuk S. V., Schamov A. G., Skovpen K., Soukharev A., Talyshev A., Tikhonov Y. A. Measurement of charged-particle event shape variables ininclusive root(s)=7 TeV proton-proton interactions with the ATLAS detector. // Physical Review D. - 2013. - Vol.88, N3. - P.032004.

[241] Lees J.P., BaBar Collab., Blinov V.E., Buzykaev A. R., Druzhinin V.P., Golubev V.B., Kravchenko E.A., Onuchin A.P., Serednyakov S.I., Skovpen Yu.I., Solodov E.P., Todyshev K.Yu., Yushkov A.N. Search for a light Higgs boson decaying to two gluons or ss-bar in the radiative decays of Υ(1S). // Physical Review D. - 2013. - Vol.88, N3. - P.031701. [arXiv:1307.5306 [hep-ex]].

[242] Sibidanov A., Belle Collab., Aulchenko V., Eidelman S., Krokovny P., Kuzmin A., Lukin P., Matvienko D., Shebalin V., Vorobyev V., Zhilich V., Zhulanov V. Study of exclusive B → X(u)lv decays and extraction of vertical bar V → ub vertical bar using full reconstruction tagging at the Belle experiment. // Physical Review D. - 2013. - Vol.88, N3. - P.032005.

[243] Lees J.P., Blinov V.E., Buzykaev A.R., Druzhinin V.P., Golubev V.B., Kravchenko E.A., Onuchin A.P., Serednyakov S.I., Skovpen Yu.I., Solodov E.P., Todyshev K.Yu., Yushkov A.N. Evidence of $B^+ \to \tau^+\nu$ decays with hadronic B tags. // Physical Review D. - 2013. - Vol.88, N3. - P.031102.

[244] Ablikim M., BESIII Collab., Achasov M.N., Muchnoi N.Yu., Nikolaev I.B. Precision measurements of $B[\psi(3686) \to \pi^+\pi^- J/\psi]$ and $B[J/\psi \to l^+l^-]$. // Physical Review D. - 2013. - Vol.88, N3. - P.032007. [[e-Print: arXiv:1307.1189 [hep-ex]].

[245] Ablikim M., BESIII Collab., Achasov M.N., Muchnoi N.Yu., Nikolaev I.B. Partial wave analysis of $\psi(2S) \to p\ \bar{p}\ \eta$. // Physical Review D. - 2013. - Vol. 88, N 3. - P.032010. [e-Print: arXiv:1304.1973 [hep-ex]].

[246] Lees J.P., BABAR Collab., Blinov V.E., Buzykaev A.R., Druzhinin V.P., Golubev V.B., Kravchenko E.A., Onuchin A.P., Serednyakov S.I., Skovpen Yu.I., Solodov E.P., Todyshev K.Yu., Yushkov A.N. Production of charged pions, kaons, and protons in e^+e^- annihilations into hadrons at root s=10.54 GeV. // Physical Review D. - 2013. - Vol.88, N3. - P.032011. [arXiv:1306.2895 [hep-ex]].

[247] Lees J.P., BaBaR Collab., Blinov V.E., Buzykaev A.R., Druzhinin V.P., Golubev V.B., Kravchenko E.A., Onuchin A.P., Serednyakov S.I., Skovpen Yu.I., Solodov E.P., Todyshev K.Yu., Yushkov A.N. A search for the rare decays $B \to \pi\ l^+l^-$ and $B \to \eta\ l^+l^-$. // Physical Review D. - 2013. - Vol.88, N3. - P.032012. [arXiv:1303.6010 [hep-ex]].

[248] Lees J.P., BaBaR Collab., Blinov V.E., Buzykaev A.R., Druzhinin V.P., Golubev V.B., Kravchenko E.A., Onuchin A.P., Serednyakov S.I., Skovpen Yu.I., Solodov E.P., Todyshev K.Yu., Yushkov A.N. Precision measurement of the $e^+e^- \to K^+K^-(\gamma)$ crosssection with the initial-state radiation method at BABAR. // Physical Review D. - 2013. - Vol.88, N3. - P.032013. [arXiv:1306.3600 [hep-ex]].

[249] Aaij R., LHCB Collab., Bondar A., Eidelman S., Krokovny P., Kudryavtsev V., Poluektov A., Shekhtman L., Vorobyev V. Measurement of the polarization amplitudes in $B^0 \to J/\psi$ K*(892)(0) decays. // Physical Review D. - 2013. - Vol.88, N5. - P.052002.

[250] Achasov M.N., Aulchenko V.M., Barnyakov A.Yu., Beloborodov K.I., Berdyugin A.V., Bogdanchikov A.G., Botov A.A., Dimova T.V., Druzhinin V.P., Golubev V.B., Grevtsov K.A., Kardapoltsev L.V., Kharlamov A.G., Kovrizhin D.P., Koop I.A., Korol A.A., Koshuba S.V., Lysenko A.P., Martin K.A., Nesterenko .N., Obrazovsky A.E., Pakhtusova E.V., Perevedentsev E.A., Romanov A.L., Serednyakov S.I., Silagadze Z.K., Skovpen K.Yu., Skrinsky A.N., Surin I.K., Tikhonov Yu.A., Vasiljev A.V., Shatunov P.Yu., Shatunov Yu.M., Shtol D.A., Zemlyansky I.M. Study of $e^+e^- \to \omega\pi^0 \to \pi^0\pi^0\gamma$ in the energy range 1.05 - 2.00 GeV with the SND detector. // Physical Review D. - 2013. - Vol.88, №5. - P.054013.

[251] Lees J.P., Babar Collab., Blinov V.E., Buzykaev A.R., Druzhinin V.P., Golubev V.B., Kravchenko E.A., Onuchin A.P., Serednyakov S.I., Skovpen Yu.I., Solodov

E.P., Todyshev K.Yu., Yushkov A.N. Measurement of the $D^*(2010)^+$ natural linewidth and the $D^*(2010)^+ - D^0$ mass difference. // Physical Review D. - 2013. - Vol.88, N5. - P.052003. [arXiv:1304.5657 [hep-ex]].

[252] Aaij R., LHCb Collab., Bondar A., Eidelman S., Krokovny P., Kudryavtsev V., Poluektov A., Shekhtman L., Vorobyev V. Studies of the decays B+ → p(p)-bar ph^+ and observation of B+ → $\bar{\Lambda}$(1520)p. // Physical Review D. - 2013. - Vol.88, N5. - P.052015.

[253] Krokovny P., Belle Collab., Krokovny P., Bondar A., Arinstein K., Aulchenko V., Eidelman S., Gabyshev N., Garmash A., Kuzmin A., Lukin P., Matvienko D., Poluektov A., Shebalin V., Shwartz B., Vorobyev V., Zhilich V., Zhulanov V. First observation of the Z(b)(0)(10610) in a Dalitz analysis of Upsilon(10860) → Upsilon(nS) $\pi^0\pi^0$. // Physical Review D. - 2013. - Vol.88, N5. - P.052016.

[254] Shen C. P., Bondar A., Eidelman S., Gabyshev N., Krokovny P., Kuzmin A., Lukin P., Matvienko D., Shwartz B., Vinokurova A., Zhilich V., et al. Measurement of e^+e^- → $\omega\pi^0$, K*(892) $\bar{K}$ and K^2*(1430) $\bar{K}$ at root s near 10.6 GeV. // Physical Review D. - 2013. - Vol.88, N5. - P.052019.

[255] White E., Belle Collab., Aulchenko V., Eidelman S., Gabyshev N., Krokovny P., Kuzmin A., Lukin P., Matvienko D., Shwartz B., Vorobyev V., Zhilich V., Zhulanov V. Measurement of the wrong-sign decay D^0 → $K^+ \pi^- \pi^+\pi^-$. // Physical Review D. - 2013. - Vol.88, N5. - P.051101.

[256] Aad G., ATLAS Collab., Anisenkov A.V., Beloborodova O.L., Bobrovnikov V.S., Bogdanchikov A.G., Kazanin V.F., Korol A.A., Malyshev V.M., Maslennikov A.L., Maximov D.A., Peleganchuk S.V., Skovpen K.Yu., Soukharev A.M., Talyshev A.A., Tikhonov Yu.A. Search for microscopic black holes in a like-sign dimuon finalstate using large track multiplicity with the ATLAS detector. // Physical Review D. - 2013. - Vol.88, N7. - P.072001.

[257] Chistov R., Belle Collab., Aulchenko V., Bondar A., Eidelman S., Gabyshev N., Kuzmin A., Lukin P., Matvienko D., Shwartz B., Usov Y., Vinokurova A., Zhilich V., Zhulanov V. First observation of Cabibbo-suppressed Ξ^0_c decays. // Physical Review D. - 2013. - Vol.88, N7. - P.071103.

[258] Lees J.P., BABAR Collab., Blinov V.E., Buzykaev A.R., Druzhinin V.P., Golubev V.B., Kravchenko E.A., Onuchin A.P., Serednyakov S.I., Skovpen Yu.I., Solodov E.P., Todyshev K.Yu., Yushkov A.N. Search for a low-mass scalar Higgs boson decaying to a τ pair in single-photon decays of Y(1S). // Physical Review D. - 2013. - Vol.88, N7. - P.071102. [arXiv: 1210.5669 [hep-ex]].

[259] Prim M., Belle Collab., Eidelman S., Krokovny P., Lukin P., Matvienko D., Usov Y., Vorobyev V., Zhilich V. Angular analysis of B^0 → φK* decays and search for CP violation at Belle. // Physical Review D. - 2013. - Vol.88, N7. - P.072004.

[260] Aaij R., LHCb Collab., Bondar A., Eidelman S., Krokovny P., Kudryavtsev V., Poluektov A., Shekhtman L., Vorobyev V. First observation of $\bar{B}^0 \to J/\psi\ K^+K^-$ and search for $\bar{B}^0 \to J/\psi\ \varphi$ decays. // Physical Review D. - 2013. - Vol.88, N7. - P.072005.

[261] Lees J.P., BABAR Collab., Blinov V.E., Buzykaev A.R., Druzhinin V.P., Golubev V.B., Kravchenko E.A., Onuchin A.P., Serednyakov S.I., Skovpen Yu.I., Solodov E.P., Todyshev K.Yu., Yushkov A.N. Measurement of the $B^+ \to \omega\ l^+\ \nu$ branching fraction with semileptonically tagged B mesons. // Physical Review D. - 2013. - Vol.88, N7. - P.072006. [arXiv:1308.2589 [hep-ex]].

[262] Chilikin K., Belle Collab., Arinstein K., Aulchenko V., Bondar A., Eidelman S., Gabyshev N., Krokovny P., Kuzmin A., Lukin P., Matvienko D., Usov Y., Vinokurova A., Vorobyev V., Zhilich V., Zhulanov V. Experimental constraints on the spin and parity of the Z(4430)(+). // Physical Review D. - 2013. - Vol.88, N7. - P.074026.

[263] Lees J.P., Blinov V.E., Buzykaev A.R., Druzhinin V.P., Golubev V.B., Kravchenko E.A., Onuchin A.P., Serednyakov S.I., Skovpen Yu.I., Solodov E.P., Todyshev K.Yu., Yushkov A.N. Measurement of the $e^+e^- \to p\ \bar{p}$ cross section in the energy range from 3.0 to 6.5 GeV. // Physical Review D. - 2013. - Vol.88, N7. - P.072009. [arXiv:1308.1795 [hep-ex]].

[264] Lees J.P., BABAR Collab., Blinov V.E., Buzykaev A.R., Druzhinin V.P., Golubev V.B., Kravchenko E.A., Onuchin A.P., Serednyakov S.I., Skovpen Yu.I., Solodov E.P., Todyshev K.Yu., Yushkov A.N. Measurement of the mass of the D^0 meson. // Physical Review D. - 2013. - Vol.88, N7. - P.071104. [arXiv:1308.1151 [hep-ex]].

[265] Lees J.P., BaBar Collab., Blinov V.E., Buzykaev A.R., Druzhinin V.P., Golubev V.B., Kravchenko E.A., Onuchin A.P., Serednyakov S.I., Skovpen Yu.I., Solodov E.P., Todyshev K. Yu., Yushkov A.N. Measurement of an excess of $\bar{B} \to D^{(*)}\ \tau\nu$ decays and implications for charged Higgs bosons. // Physical Review D. - 2013. - Vol.88, N7. - P.072012. [arXiv:1303.0571 [hep-ex]].

[266] Ablikim M., BESIII Collab., Achasov M.N., Muchnoi N.Yu., Nikolaev I.B. Observation of a structure at 1.84 GeV/c2 in the $3(\pi^+\pi^-)$ mass spectrum in $J/\psi \to \gamma 3(\pi^+\pi^-)$ decays. // Physical Review D. - 2013. - Vol.88, N9. - P.091502. [[e-Print: arXiv:1307.1189 [hep-ex]].

[267] Nayak M., Belle Collab., Eidelman S., Gabyshev N., Krokovny P., Kuzmin A., Lukin P., Shwartz B., Zhilich V., Zhulanov V. Evidence for the suppressed decay $B^- \to DK^-$, $D \to K+ \pi^-\pi^0$. // Physical Review D. - 2013. - Vol.88, N9. - P.091104.

[268] Dalseno J., Belle Collab., Arinstein K., Aulchenko V., Bondar A., Eidelman S., Krokovny P.,

Kuzmin A., Lukin P., Matvienko D., Shwartz B., Vorobyev V., Zhilich V., Zhulanov V. Measurement of the CP violation parameters in $B^0 \to \pi^+\pi^-$ decays. // Physical Review D. - 2013. - Vol.88, N9. - P.092003.

[269] Thorne F., Belle Collab., Aulchenko V., Eidelman S., Ferber T., Gabyshev N., Krokovny P., Lukin P., Matvienko D., Shwartz B., Vorobyev V., Zhilich V. Measurement of the decays $B_s^0 \to J/\psi$ $\varphi(1020)$, $B_s^0 \to J/\psi$ f(2)'(1525) and $B_s^0 \to J/\psi$ K^+K^- at Belle. // Physical Review D. - 2013. - Vol.88 , N11. - P.114006.

[270] Aad G., ATLAS Collab., Anisenkov A. V., Beloborodova O.L., Bobrovnikov V.S., Bogdanchikov A.G., Kazanin V.F., Korol A.A., Malyshev V.M., Maslennikov A.L., Maximov D.A., Peleganchuk S.V., Skovpen K.Yu., Soukharev A.M., Talyshev A.A., Tikhonov Yu.A. Search for long-lived stopped R-hadrons decaying out of time with pp collisions using the ATLAS detector. // Physical Review D. - 2013. - Vol.88, N11. - P.112003.

[271] Ablikim M., BESlll Collab., Achasov M.N., Muchnoi N.Yu., Nikolaev I.B. Search for $\eta(c)(2S)h(c) \to p\ \bar{p}$ decays and measurements of the $\chi(cJ) \to p\ \bar{p}$ branching fractions. // Physical Review D. - 2013. - Vol.88, N11. - P.112001.

[272] Aad G., ATLAS Collab., Anisenkov A.V., Beloborodova O.L., Bobrovnikov V.S., Bogdanchikov A.G., Kazanin V.F., Korol A.A., Malyshev V.M., Maslennikov A.L., Maximov D.A., Peleganchuk S.V., Skovpen K.Yu., Soukharev A.M., Talyshev A.A., Tikhonov Yu.A. Search for charginos nearly mass degenerate with the lightest neutralino based on a disappearing-track signature in pp collisions at root(s)=8 TeV with the ATLAS detector. // Physical Review D. - 2013. - Vol.88, N11. - P.112006.

[273] Ablikim M., BESIII Collab., Achasov M.N., Muchnoi N.Yu., Nikolaev I.B. Observation of the decay $\psi(3686) \to \Lambda\ \bar{\Sigma}(+/-)\ \pi(-/+)$ + c.c. // Physical Review D. - 2013. - Vol.88, N11. - P.112007.

[274] Aad G., ATLAS Collab., Anisenkov A., Bobrovnikov V.B., Bogdanchikov A., Kazanin V.A., Kolachev G.M., Korol A., Malyshev V., Maslennikov A.L., Peleganchuk S.V., Schamov A.G., Skovpen K., Soukharev A., Talyshev A. Search for direct production of charginos and neutralinos in events with three leptons and missing transverse momentum in root s=7 TeV pp collisions with the ATLAS detector. // Physics Letters B. - 2013. - Vol.718, N3. - P.841-859.

[275] Aad G., ATLAS Collab., Anisenkov A., Beloborodova O., Bobrovnikov V. B., Bogdanchikov A., Kazanin V.A., Kolachev G.M., Korol A., Malyshev V., Maslennikov A.L., Orlov I., Peleganchuk S.V., Schamov A.G., Skovpen K., Soukharev A., Talyshev A., Tikhonov Y.A. Search for new phenomena in the WW - vertical bar v vertical bar ' v ' final state in pp collisions at root s=7 TeV with the ATLAS detector. // Physics Letters B. - 2013. - Vol.718, N3. - P.860-878.

[276] Aad G., ATLAS Collab., Anisenkov A., Beloborodova O., Bobrovnikov V. B., Bogdanchikov A., Kazanin V.A., Kolachev G.M., Korol A., Malyshevw V., Maslennikov A.L., Orov I., Peleganchuk S.V., Schamov A.G., Skovpen K., Soukharev A., Talyshev A., Tikhonov Y.A. Search for directs lepton and gaugino production in final states with two leptons and missing transverse momentum with the ATLAS detector in pp collisions at root s=7 TeV. // Physics Letters B. - 2013. - Vol.718, N3. - P.879-901.

[277] Aaij R., LHCb Collab., Bobrov A., Bondar A., Eidelman S., Krokovny P., Kudryavtsev V., Poluektov A., Shekhtman L., Vorobyev V. Measurement of the D(+/-) production asymmetry in 7 TeV pp collisions. // Physics Letters B. - 2013. - Vol.718, N3. - P.902-909.

[278] Abelev B., ALICE Collab., Pestov Y. Coherent J/psi photoproduction in ultra-peripheral Pb-Pb collisions at root s(NN)=2.76 TeV. // Physics Letters B. - 2013. - Vol.718, N4/5. - P.1273-1283.

[279] Aad G., ATLAS Collab., Anisenkov A., Beloborodova O., Bobrovnikov V.S., Bogdanchikov A., Kazanin V.F., Kolachev G.M., Korol A., Malyshev V., Maslennikov A.L., Maximov D.A., Orlov I., Peleganchuk S.V., Schamov A.G., Skovpen K., Soukharev A., Talyshev A., Tikhonov Y.A. Search for pair production of heavy top-like quarks decaying to a high-p(T) W boson and a b quark in the lepton plus jets final state at root s=7 TeV with the ATLAS detector. // Physics Letters B. - 2013. - Vol.718, N4/5. - P.1284-1302.

[280] Kharkov Y.A., Sokolov V.V. Elastic enhancement factor as a quantum chaos probe. // Physics Letters B. - 2013. - Vol.718, №4/5. - P.1562-1565.

[281] Abelev B., ALICE Collab., Pestov Y. Anisotropic flow of charged hadrons, pions and (anti-) protons measured at high transverse momentum in Pb-Pb collisions at root S-NN=2.76 TeV. // Physics Letters B. - 2013. - Vol.719, N1/3. - P.18-28.

[282] Abelev B., ALICE Collab., Pestov Yu. Long-range angular correlations on the near and away side inp-Pb collisions at root S-NN=5.02 TeV. // Physics Letters B. - 2013. - Vol.719, №1/3. - P.29-41.

[283] Aad G., ATLAS Collab., Anisenkov A., Beloborodova O., Bobrovnikov V. B., Bogdanchikov A., Kazanin V.A., Kolachev G.M., Korol A., Malyshev V., Maslennikov A.L., Orlov I., Peleganchuk S.V., Schamov A.G., Skovpen K., Soukharev A., Talyshev A., Tikhonov Y.A., Zaytsev A. Measurement of the jet radius and transverse momentum dependence of inclusive jet suppression in lead-lead collisions at root S-NN=2.76 TeV with the ATLAS detector. // Physics Letters B. - 2013. - Vol.719, N 4/5. - P.220-241.

[284] Aad G., Atlas Collab., Anisenkov A., Beloborodova O., Bobrovnikov V. S., Bogdanchikov A., Kazanin V.A., Kolachev G.M., Korol A., Malyshev V.,

Maslennikov A.L., Maximov D.A., Orlov I., Peleganchuk S.V., Schamov A.G., Skovpen K., Soukharev A., Talyshev A., Tikhonov Y.A. A search for high-mass resonances decaying to $\tau^+\tau^-$ in pp collisions at root s=7 TeV with the ATLAS detector. // Physics Letters B. - 2013 . - Vol.719, N4/5. - P 242-260.

[285] Aad G., Atlas Collab., Anisenkov A., Beloborodova O., Bobrovnikov V.S., Bogdanchikov A., Kazanin V.F., Kolachev G. M., Korol A., Malyshev V., Maslennikov A.L., Maximov D.A., Orlov I., Peleganchuk S.V., Schamov A.G., Skovpen K., Soukharev A., Talyshev A., Tikhonovh Y.A. Search for supersymmetry in events with photons, bottom quarks,and missing transverse momentum in proton-proton collisions at a centre-of-mass energy of 7 TeV with the ATLAS detector. // Physics Letters B. - 2013. - Vol.719, N4/5. - P.261-279.

[286] Aad G., ATLAS Collab., Anisenkov A., Beloborodova O., Bobrovnikov V. B., Bogdanchikov A., Kazanin V.A., Kolachev G.M., Korol A., Malyshev V., Maslennikov A.L., Orlov I., Peleganchuk S. V., Schamov A.G., Skovpen K., Soukharev A., Talyshev A., Tikhonov Y. A. Search for long-lived, heavy particles in final states with amuon and multi-track displaced vertex in proton-proton collisions at root s=7 TeV with the ATLAS detector. // Physics Letters B. - 2013. - Vol.719, N4/5. - P.280-298.

[287] Aad G., ATLAS Collab., Anisenkov A., Beloborodova O., Bobrovnikov V.S., Bogdanchikov A., Kazanin V.F., Kolachev G.M., Korol A., Malyshev V., Maslennikov A.L., Maximov D.A., Peleganchuk S.V., Skovpen K., Soukharev A., Talyshev A., Tikhonov Y.A. A search for prompt lepton-jets in pp collisions at root s=7 TeV with the ATLAS detector. // Physics Letters B. - 2013. - Vol.719, N4/5. - P.299-317.

[288] Aaij R., LHCb Collab., Bobrov A., Bondar A., Eidelman S., Krokovny P., Kudryavtsev V., Poluektov A., Shekhtman L., Vorobyev V. Measurement of the $B^0 \to \overline{B}^0$ oscillation frequency Δ m(d) with the decays $B^0 \to D\ \pi^+$ and $B^0 \to J/\psi\ K^*(0)$. // Physics Letters B. - 2013. - Vol.719, N4/5. - P.318-325.

[289] Miyazaki Y., Belle Collab., Aulchenko V., Eidelman S., Epifanov D., Gabyshev N., Garmash A., Krokovny P., Kuzmin A., Matvienko D., Shwartz B., Zhulanov V. Search for lepton-flavor and lepton-number-violating $\tau \to$ lhh' decay modes. // Physics Letters B. - 2013. - Vol.719, N4/5. - P.346-353.

[290] Aad G., ATLAS Collab., Anisenkov A., Beloborodova O., Bobrovnikov V.S., Bogdanchikov A., Kazanin V.A., Kolachev G.M., Korol A., Malyshev V., Maslennikov A.L., Orlov I., Peleganchuk S.V., Schamov A.G., Skovpen K., Soukharev A., Talyshev A., Tikhonov Y.A. Search for light top squark pair production in final states with leptons and b-jets with the ATLAS detector in root s=7 TeV proton-proton collisions. // Physics Letters B. - 2013. - Vol.720, N1/3. - P.13-31.

[291] Aad G., ATLAS Collab., Anisenkov A., Beloborodova O., Bobrovnikov V.S., Bogdanchikov A., Kazanin V. F., Kolachev G. M., Korol A., Malyshev V., Maslennikov A.L., Maximov D.A., Peleganchuk S.V., Skovpen K., Soukharev A., Talyshev A., Tikhonov Y.A. Measurement of angular correlations in Drell-Yan lepton pairsto probe Z/γ^* boson transverse momentum at root s=7 TeV with the ATLAS detector. // Physics Letters B. - 2013. - Vol.720, N1/3. - P.32-51.

[292] Abelev B., ALICE Collab., Pestov Y. Centrality dependence of charged particle production at large transverse momentum in Pb-Pb collisions at root s(NN)=2.76 TeV. // Physics Letters B. - 2013. - Vol.720, N1/3. – P.52-62.

[293] Aad G., ATLAS Collab., Anisenkov A., Beloborodova O., Bobrovnikov V.B., Bogdanchikov A., Kazanin V.A., Kolachev G.M., Korol A., Malyshev V., Maslennikov A.L., Orlov I., Peleganchuk S.V., Schamov A.G., Skovpen K., Soukharev A., Talyshev A., Tikhonov Y.A. Searches for heavy long-lived s leptons and R-hadrons with the ATLAS detector in pp collisions at root s=7 TeV. // Physics Letters B. - 2013. - Vol.720, N4/5. - P.277-308.

[294] Abelev B., ALICE Collab., Pestov Y. Measurement of electrons from beauty hadron decays in pp collisions at root s=7 TeV. // Physics Letters B. - 2013. - Vol.721, N1/3. - P.13-23.

[295] Aaij R., LHCB Collab., Bobrov A., Bondar A., Eidelman S., Krokovny P., Kudryavtsev V., Poluektov A., Shekhtman L., Vorobyev V. Measurement of the time-dependent CP asymmetry in $B^0 \to J/\psi\ K_S^0$ decays. // Physics Letters B. - 2013. - Vol.721, N1/3. - P.24-31.

[296] Aad G., ATLAS Collab., Anisenkov A., Beloborodova O., Bobrovnikov V.B., Bogdanchikov A., Kazanin V.A., Kolachev G.M., Korol A., Malyshev V., Maslennikov A.L., Orlov I., Peleganchuk S.V., Schamov A.G., Skovpen K., Soukharev A., Talyshev A., Tikhonov Y.A. Search for displaced muonic lepton jets from light Higgs boson decay in proton-proton collisions at root s=7 TeV with the ATLAS detector. // Physics Letters B. - 2013. - Vol.721, N1/3. - P.32-50.

[297] Aad G., ATLAS Collab., Anisenkov A., Beloborodova O., Bobrovnikov V.S., Bogdanchikov A., Kazanin V.F., Kolachev G.M., Korol A., Malyshev V., Maslennikov A.L., Maximov D.A., Peleganchuk S.V., Skovpen K., Soukharev A., Talyshev A., Tikhonov Y.A. Search for single b*-quark production with the ATLAS detector at root s=7 TeV. // Physics Letters B. - 2013. - Vol.721, N4/5. - P.171-189.

[298] Dmitriev V.F., Milstein A.I. Final state Coulomb interaction and asymmetry of pair production close to threshold in e^+e^- annihilation. // Physics Letters B. - 2013. - Vol.722, №1/3. - P.83-85.

[299] Abelev B., ALICE Collab., Pestov Y. Measurement of the inclusive differential jet cross section

in pp collisions at root s=2.76 TeV. // Physics Letters B. - 2013. - Vol.722, N4/5. - P.262-272.

[300] Aad G., ATLAS Collab., Anisenkov A., Beloborodova O., Bobrovnikov V.S., Bogdanchikov A., Kazanin V.F., Kolachev G.M., Korol A., Malyshev V., Maslennikov A.L., Maximov D.A., Orlov I., Peleganchuk S.V., Schamov A.G., Skovpen K., Soukharev A., Talyshev A., Tikhonov Y.A. Search for long-lived, multi-charged particles in pp collisions at root s=7 TeV using the ATLAS detector. // Physics Letters B. - 2013. - Vol.722, N4/5. - P. 305-323.

[301] Aad G., ATLAS Collab., Anisenkov A., Beloborodova O., Bobrovnikov V.S., Bogdanchikov A., Kazanin V.F., Kolachev G.M., Korol A., Malyshev V., Maslennikov A.L., Maximov D.A., Peleganchuk S.V., Skovpen K., Soukharev A., Talyshev A., Tikhonov Y.A. Search for a heavy narrow resonance decaying to e mu, e tau, or mu tau with the ATLAS detector in root s=7 TeV pp collisions at the LHC. // Physics Letters B. - 2013. - Vol.723, N1/3. - P. 15-32.

[302] Aaij R., LHCB Collab., Bondar A., Eidelman S., Krokovny P., Kudryavtsev V., Poluektov A., Shekhtman L., Vorobyev V. Search for direct CP violation in $D^0 \to h^-h^+$ modes using semileptonic B decays. // Physics Letters B. - 2013. - Vol.723, N1/3. - P.33-43.

[303] Aaij R., LHCb Collab., Bondar A., Eidelman S., Krokovny P., Kudryavtsev V., Poluektov A., Shekhtman L., Vorobyev V. Observation of the suppressed ADS modes $B(+/-) \to [\pi K(-+)\text{-}(-/+) \pi^+\pi^-]$ (D)K(+/-) and $B(+/-) \to [\pi K(+/-)(-/+)\pi^+\pi^-]$ (D) $\pi(+/-)$. // Physics Letters B. - 2013. - Vol.723, N1/3. - P.44-53.

[304] Akhmetshin R. R., Anisenkov A.V., Anokhin S. A., Aulchenko V.M., Banzarov V.S., Barkov L.M., Bashtovoy N.S., Berkaev D.E., Bondar A.E., Bragin A. V., Eidelman S.I., Epifanov D.A., Epshteyn L.B., Fedotovich G.V., Gayazov S.E., Grebenuk A.A., Grigoriev D.N., Gromov E.M., Ignatov F.V., Karpov S.V., Kazanin V.F., Khazin B.I., Koop I.A., Kozyrev A.N., Krokovny P.P., Kuzmenko A.E., Kuzmin A.S., Logashenko I.B., Lysenko A.P., Lukin P.A., Mikhailov K.Yu., Pestov Yu.N., Perevedentsev E.A., Pirogov S.A., Pivovarov S.G., Popov A.S., Popov Yu.S., Redin S.I., Rogovsky Yu.A., Romanov A.L., Ruban A.A., Ryskulov N.M., Ryzhenenkov A.E., Shebalin V.E., Shemyakin D.N., Shwartz B.A., Shwartz D.B., Sibidanov A.L., Shatunov P.Yu., Shatunov Yu.M., Snopkov I.G., Solodov E.P., Titov V.M., Talyshev A.A., Vorobiov A.I., Yudin Yu.V., Zaytsev A.S. Study of the process $e^+e^- \to 3\pi^+\pi^-$ in the c.m. energy range 1.5-2.0 GeV with the CMD-3 detector. // Physics Letters B. - 2013. - Vol.723, N1/3. - P.82-89. [e-print: arXiv:1302.0053 [hep-ex]].

[305] Abelev B., ALICE Collab., Pestov Y. Charge correlations using the balance function in Pb-Pb collisions at root s(NN)=2.76 TeV. // Physics Letters B. - 2013. - Vol.723, N4/5. - P.267-279.

[306] Aaij R., LHCb Collab., Bondar A., Eidelman S., Krokovny P., Kudryavtsev V., Poluektov A., Shekhtman L., Vorobyev V. Measurements of the $\Lambda(0)(b) \to J/\psi$ Lambda decay amplitudes and the $\Lambda(0)(b)$ polarisation in pp collisions at root s=7 TeV. // Physics Letters B. - 2013. - Vol.724, N1/3. - P.27-35.

[307] Aaij R., LHCb Collab., Bondar A., Eidelman S., Krokovny P., Kudryavtsev V., Poluektov A., Shekhtman L., Vorobyev V. Searches for violation of lepton flavour and baryon number in tau lepton decays at LHCb. // Physics Letters B. - 2013. - Vol.724, N1/3. - P.36-45.

[308] Aaij R., Bondar A., Eidelman S., Krokovny P., Kudryavtsev V., Poluektov A., Shekhtman L., Vorobyev V. Search for $D_s^+ \to \pi^+\mu^+\mu^-$ and $D_s^+ \to \pi^-\mu^+\mu^+$ decays. // Physics Letters B. - 2013. - Vol.724, N4/5. - P.203-212.

[309] Aaij R., LHCb Collab., Bondar A., Eidelman S., Krokovny P., Kudryavtsev V., Poluektov A., Shekhtman L., Vorobyev V. Search for the rare decay $D_0 \to \mu^+\mu^-$. // Physics Letters B. - 2013. - Vol.725, N1/3. - P.15-24.

[310] Aaij R., LHCb Collab., Bondar A., Eidelman S., Krokovny P., Kudryavtsev V., Poluektov A., Shekhtman L., Vorobyev V. Measurement of the differential branching fraction of the decay $\Lambda(0)(b) \to \Lambda\mu^+\mu^-$. // Physics Letters B. - 2013. - Vol.725, N1/3. - P.\ 25-35.

[311] Aad G., ATLAS Collab., Anisenkov A., Beloborodova O., Bobrovnikov V.S., Bogdanchikov A., Kazanin V.F., Korol A., Malyshev V., Maslennikov A. L., Maximov D.A., Peleganchuk S.V., Skovpen K., Soukharev A., Talyshev A., Tikhonov Y.A. Measurement with the ATLAS detector of multi-particle azimuthal correlations in p plus Pb collisions at root s(NN)=5.02 TeV. // Physics Letters B. - 2013. - Vol.725, N1/3. - P.60-78.

[312] Aad G., ATLAS Collab., Anisenkov A., Beloborodova O., Bobrovnikov V.S., Bogdanchikov A., Kazanin V.F., Korol A., Malyshev V., Maslennikov A.L., Maximov D.A., Peleganchuk S.V., Skovpen K., Soukharev A., Talyshev A., Tikhonov Y.A. Measurement of the high-mass Drell-Yan differential cross-section in pp collisions at root s=7 TeV with the ATLAS detector. // Physics Letters B. - 2013. - Vol.725, N4/5. - P.223-242.

[313] Aad G., ATLAS Collab., Anisenkov A. V., Beloborodova O.L., Bobrovnikov V.S., Bogdanchikov . G., Kazanin V.F., Korol A.A., Malyshev V.M., Maslennikov A.L., Maximov D.A., Peleganchuk S.V., Skovpen K.Yu., Soukharev A.M., Talyshev A.A., Tikhonov Yu.A. Measurements of Higgs boson production and couplings in diboson final states with the ATLAS detector at the LHC. // Physics Letters B. - 2013. - Vol.726, N1/3. - P.88-119.

[314] Aad G., ATLAS Collab., Anisenkov A.V., Beloborodova O.L., Bobrovnikov V.S., Bogdanchikov A.G., Kazanin V.F., Korol A.A., Malyshev V.M., Maslennikov A.L., Maximov D.A., Peleganchuk S.V., Skovpen K.Yu., Soukharev A.M., Talyshev A.A., Tikhonov Yu.A. Evidence for the spin-0 nature of the

Higgs boson using ATLAS data. // Physics Letters B. - 2013. - Vol.726, N1/3. - P.120-144.

[315] Aaij R., LHCb Collab., Bondar A., Eidelman S., Krokovny P., Kudryavtsev V., Poluektov A., Shekhtman L., Vorobyev V. Measurement of the CKM angle gamma from a combination of B+/- - Dh(+/-) analyses. // Physics Letters B. - 2013. - Vol.726, N 1/3. - P. 151-163.

[316] Abelev B., ALICE Collab., Pestov Y., et al. Long-range angular correlations of π, K and p in p-Pb collisions at root s(NN)=5.02 TeV. // Physics Letters B. - 2013. - Vol.726, N1/3. - P.164-177.

[317] Adlarson P., WASA-at-COSY Collab., Bondar A., Kuzmin A., Shwartz B. Search for a dark photon in the $\pi^0 \to e^+e^- \gamma$ decay. // Physics Letters B. - 2013. - Vol.726, N1/3. - P.187-193.

[318] Solovieva E., Belle Collab., Bondar A., Eidelman S., Krokovny P., Kuzmin A., Lukin P., Matvienko D., Shwartz B., Usov Y., Vinokurova A., Zhilich V., et al. Evidence for $\bar{B}_s^0 \to \Lambda^+_c \bar{\Lambda} \pi^-$. // Physics Letters B. - 2013. - Vol.726, N1/3. - P.206-210.

[319] Abbas E., ALICE Collab., Pestov Y. Centrality dependence of the pseudorapidity density distribution for charged particles in Pb-Pb collisions at root s(NN)=2.76 TeV. // Physics Letters B. - 2013. - Vol.726, N4/5. - P.610-622.

[320] Aaij R., LHCb Collab., Bondar A., Eidelman S., Krokovny P., Kudryavtsev V., Poluektov A., Shekhtman L., Vorobyev V. Model-independent search for CP violation in $D^0 K^-K^+ \pi^-\pi^+$ and $D^0 \to \pi^-\pi^+ \pi^+\pi^-$ decays. // Physics Letters B. - 2013. - Vol.726, N4/5. - P.623-633.

[321] Aaij R., LHCb Collab., Bondar A., Eidelman S., Krokovny P., Kudryavtsev V., Poluektov A., Shekhtman L., Vorobyev V. Branching fraction and CP asymmetry of the decays $B^+ \to K_S^0 \pi^+$ and $B^+ \to (K_SK^+) K^0$. // Physics Letters B. - 2013. - Vol.726, N4/5. - P.646-655.

[322] Abelev B., ALICE Collab., Pestov Y. Multiplicity dependence of the average transverse momentum in pp, p-Pb, and Pb-Pb collisions at the LHC. // Physics Letters B. - 2013. - Vol.727, N4/5. - P.371-380.

[323] Aaij R., Bondar A., Eidelman S., Krokovny R., Kudryavtsev V., Shekhtman L., Vorobyev V. Observation of the decay $B_s^0 \to \bar{D}^0 \varphi$. // Physics Letters B. - 2013. - Vol.727, N4/5. - P.403-411.

[324] Abelev B., ALICE Collab., Pestov Y. Charge separation relative to the reaction plane in Pb-Pb collisions at root s(NN)=2.76 TeV. // Physical Review Letters. - 2013. - Vol.110, N1. - P.012301.

[325] Aad G., ATLAS Collab. Anisenkov A., Beloborodova O., Bobrovnikov V.S., Bogdanchikov A., Kazanin V.F., Kolachev G.M., Korol A., Malyshev V., Maslennikov A.L., Orlov I., Peleganchuk S.V., Schamov A.G., Skovpen K., Soukharev A., Talyshev A., Tikhonov Y.A. Search for dark matter candidates and large extra dimensions in events with a photon and missing transverse momentum in pp collision data at root s=7 TeV with the ATLAS detector. // Physical Review Letters. - 2013. - Vol.110, N1. - P.011802.

[326] Aaij R., LHCb Collab., Bobrov A., Bondar A., Eidelman S., Krokovny P., Kudryavtsev V., Poluektov A., Shekhtman L., Vorobyev V. First Evidence for the decay $B_s^0 \to \mu^+\mu^-$ // Physical Review Letters. - 2013. - Vol.110, N 2. - P. 021801.

[327] Aad G., ATLAS Collab., Anisenkov A., Beloborodova O., Bobrovnikov V.S., Bogdanchikov A., Kazanin V.F., Kolachev G.M., Korol A., Malyshev V., Maslennikov A.L., Orlov I., Peleganchuk S.V., Schamov A.G., Skovpen K., Soukharev A., Talyshev A., Tikhonov Y.A. Measurement of Z Boson Production in Pb-Pb Collisions at root s(NN)=2.76 TeV with the ATLAS detector. // Physical Review Letters. - 2013. - Vol.110, N2. - P.022301.

[328] Ablikim M., BESIII Collab., Achasov M.N., Muchnoi N.Yu, Nikolaev I.B. Observation of two new N* resonances in the decay $\psi(3686) \to p \bar{p} \pi^0$. // Physical Review Letters. - 2013. - Vol.110, N 2. - P. 022001. [e-Print: arXiv:1207.0223 [hep-ex]].

[329] Aaij R., LHCb Collab., Bobrov A., Bondar A., Eidelman S., Krokovny P., Kudryavtsev V., Poluektov A., Shekhtman L., Vorobyev V. Measurement of the CP asymmetry in $B_s^0 \to K^*(0) \mu^+\mu^-$ decays. // Physical Review Letters. - 2013. - Vol.110, N3. - P.031801.

[330] Abelev B., ALICE Collab. Pestov Y. Pseudorapidity density of charged particles in p plus Pb collisions at root s(NN)=5.02 TeV. // Physical Review Letters. - 2013. - Vol.110, N 3. - P. 032301.

[331] Vinokurov N.A. Generating high-power short terahertz electromagnetic pulses with a multifoil radiator. // Physical Review Letters. - 2013. - Vol.110, N6. - P.064805.

[332] Abelev B., ALICE Collab., Pestov Yu. Transverse momentum distribution and nuclear modification factor of charged particles in p plus Pb collisions at root (NN)-N-s=5.02 TeV. // Physical Review Letters. - 2013. - Vol.110, N8. - P.082302.

[333] Aaij R., LHCb Collab., Bobrov A., Bondar A., Eidelman S., Krokovny P., Kudryavtsev V., Poluektov A., Shekhtman L., Vorobyev V. Observation of $D^0 \to \bar{D}^0$ oscillations. // Physical Review Letters. - 2013. - Vol.110, N10. - P.101802.

[334] Telnov V.I. Restriction on the Energy and Luminosity of e^+e^- storage rings due to beamstrahlung. // Physical Review Letters. - 2013. - Vol.110, N11. - P.114801. [arXiv:1203.6563 [physics.acc-ph]].

[335] Hara K., Belle Collab., Bondar A., Eidelman S., Epifanov D., Gabyshev N., Krokovny P., Kuzmin A., Matvienko D., Shwartz B., Usov Y., Vorobyev V., Zhilich ., Zhulanov V. Evidence for $B^- \to$ t(-)(v)over-bar(t) with a hadronic tagging method using the full data sample of Belle. // Physical Review Letters. - 2013. - Vol.110, N13. - P.131801.

[336] Abakumova E.V., Achasov M.N., Berkaev D.E., Kaminsky V.V., Muchnoi N.Yu., Perevedentsev E.A., Pyata E.E.,. Shatunov Yu.M. Backscattering of laser radiation on ultrarelativistic electrons in a transverse magnetic field: evidence of MeV-scale photon interference. // Physical Review Letters. - 2013. - Vol.110, №14. - P.140402. [e-Print: arXiv:1211.0103 [physics.acc-ph]].

[337] Aaij R., LHCb Collab., Bobrov A., Bondar A., Eidelman S., Krokovny P., Kudryavtsev V., Poluektov A., Shekhtman L., Vorobyev V. First observation of the decay B*(s2)(5840)(0) $\rightarrow$ B*K(+(-)) and studies of excited B_s^0 mesons. // Physical Review Letters. - 2013. - Vol.110, N15. - P.151803.

[338] Abelev B., ALICE Collab. Pestov Y. Net-Charge Fluctuations in Pb-Pb Collisions at root s(NN)=2.76 TeV. // Physical Review Letters. - 2013. - Vol.110, N15. - P.152301.

[339] Aad G., ATLAS Collab. Anisenkov A.V., Beloborodova O.L., Bobrovnikov V.S., Bogdanchikov A.G., Kazanin V.F., Korol A.A., Malyshev V.M., Maslennikov A.L., Maximov D.A., Peleganchuk S.V., Skovpen K.Yu., Soukharev A.M., Talyshev A.A., Tikhonov Yu.A. Observation of associated near-side and away-side long-range correlations in root S-NN=5.02 TeV proton-lead collisions with the ATLAS detector. // Physical Review Letters. - 2013. - Vol.110, N18. - 182302.

[340] Aaij R., LHCb Collab., Bobrov A., Bondar A., Eidelman S., Krokovny P., Kudryavtsev V., Poluektov A., Shekhtman L., Vorobyev V. Measurement of the Lambda(0)(b), Xi(-)(b), and Omega(-)(b) baryon masses. // Physical Review Letters. - 2013. - Vol.110, N18. - P.182001.

[341] Adam J., MEG Collab., Grigoriev D.N., Ignatov F., Khazin B.I., Khomotov N., Popov A., Yudin Yu.V. New constraint on the existence of the $\mu+ \rightarrow e+ \gamma$ decay. // Physical Review Letters. - 2013. - Vol.110, N20. - P.201801 [e-print: arXiv:1303.0754 [hep-ex]].

[342] Aaij R., LHCb Collab., Bobrov A., Bondar A., Eidelman S., Krokovny P., Kudryavtsev V., Poluektov A., Shekhtman L., Vorobyev V. Search for rare $B_s^0 \rightarrow \mu^+\mu^- \mu^+\mu^-$ decays. // Physical Review Letters. - 2013. - Vol.110, N21. - P.211801.

[343] Aaij R., LHCb Collab., Bondar A., Eidelman S., Krokovny P., Kudryavtsev V., Poluektov A., Shekhtman L., Vorobyev V. Determination of the X(3872) meson quantum numbers. // Physical Review Letters. - 2013. - Vol.110, N22. - P.222001.

[344] Aaij R., LHCb Collab., Affolder A., Bondar A., Eidelman S., Krokovny P., Kudryavtsev V., Poluektov A., Shekhtman L., Vorobyev V. First Observation of CP violation in the decays of B_s^0 mesons. // Physical Review Letters. - 2013. - Vol.110, N22. - P.221601.

[345] Kim B. H., Belle Collab., Aulchenko V., Eidelman S., Epifanov D., Krokovny P., Kuzmin A., Matvienko D., Shebalin V., Shwartz B., Usov Y., Vorobyev V., Zhilich V. Search for an H-dibaryon with a mass near 2m(Delta) in Y(1S) and Y(2S) decays. // Physical Review Letters. - 2013. - Vol.110, N22. - P222002.

[346] Aaij R., LHCb Collab., Bondar A., Eidelman S., Krokovny P., Kudryavtsev V., Poluektov A., Shekhtman L., Vorobyev V. First Measurement of the CP-violating phase in $B_s^0 \rightarrow \varphi \varphi$ decays. // Physical Review Letters. - 2013. - Vol.110, N24. - P.241802.

[347] Ablikim M., BESIII Collab., Achasov M.N., Muchnoi N.Yu., Nikolaev I.B. Observation of a charged charmoniumlike structure in $e^+e^- \rightarrow \pi^+\pi^- J/\psi$ at root s=4.26 GeV. // Physical Review Letters. - 2013. - Vol.110, N25. - P.252001. [e-Print: arXiv:1303.5949 [hep-ex]].

[348] Liu Z. Q., Belle Collab., Aulchenko V., Bondar A., Eidelman S., Gabyshev N., Krokovny P., Lukin P., Matvienko D., Shwartz B., Vorobyev V., Zhilich V. Study of $e^+e^- \rightarrow \pi^+\pi^- J/\psi$ and observation of a charged charmoniumlike state at Belle. // Physical Review Letters. - 2013. - Vol.110, N25. - P.252002.

[349] Bhardwaj V., Belle Collab., Aulchenko V., Bondar A., Eidelman S., Epifanov D., Gabyshev N., Krokovny P., Kuzmin A., Lukin P., Matvienko D., Shwartz B., Usov Yu.V., Vinokurova A., Zhilich V., Zhulanov V. Evidence of a new narrow resonance decaying to $\chi_{c1} \gamma$ in $B \rightarrow \chi_{c1} \gamma K$. // Physical Review Letters. - 2013. - Vol.111, N3. - P.032001.

[350] Leitgab M., Belle Collab., Aulchenko V., Bondar A., Eidelman S., Gabyshev N., Krokovny P., Matvienko D., Shwartz B., Usov Y., Vorobyev V., Zhilich V., Zhulanov V. Precision measurement of charged pion and kaon differential cross sections in e^+e^- annihilation at root s=10.52 GeV. // Physical Review Letters. - 2013. - Vol.111, N 6. - P. 062002.

[351] Aaij R., LHCb Collab., Bondar A., Eidelman S., Krokovny P., Kudryavtsev V., Poluektov A., Shekhtman L., Vorobyev V. Measurement of CP violation in the phase space of B(+/-) K(-/+) $\rightarrow \pi^+\pi^-$ and B(-/+) $\rightarrow$ (KK^+K^-) $\rightarrow$ K(-/+) decays. // Physical Review Letters. - 2013. - Vol.111, N10. - P.101801.

[352] Lees J.P., BaBar Collab., Blinov V.E., Buzykaev A.R., Druzhinin V.P., Golubev V.B., Kravchenko E.A., Onuchin A.P., Serednyakov S.I., Skovpen Yu.I., Solodov E.P., Todyshev K.Yu., Yushkov A.N. Search for CP violation in B^0B^0-bar mixing using partial reconstruction of $B^0 \rightarrow D^{*(-)} Xl^+ \nu$ and a kaon tag. // Physical Review Letters. - 2013. - Vol.111, N10. - P.101802. arXiv:1305.1575 [hep-ex]].

[353] Aaij R., LHCb Collab., Bondar A., Eidelman S., Krokovny P., Kudryavtsev V., Poluektov A., Shekhtman L., Vorobyev V. Measurement of the $B_s^0 \rightarrow \mu^+\mu^-$ branching fraction and search for $B_s^0 \rightarrow \mu^+\mu^-$ decays at the LHCb experiment. // Physical Review Letters. - 2013. - Vol.111, N10. - P.101805.

[354] Aaij R., LHCb Collab., Bondar A., Eidelman S., Krokovny P., Kudryavtsev V., Poluektov A., Shekhtman L., Vorobyev V. Precision measurement of the Lambda(0)(b) baryon lifetime. // Physical review Letters. - 2013. - Vol.111, N10. - P.102003.

[355] Abelev B., ALICE Collab., Pestov Y.N. Meson Elliptic flow in noncentral Pb-Pb collisions at root (S)(NN)=2.76 TeV. // Physical Review Letters. - 2013. - Vol.111, N10. - P.102301.

[356] Lees J.P., BaBar Collab., Blinov V.E., Buzykaev A.R., Druzhinin V.P., Golubev V.B., Kravchenko E.A., Onuchin A.P., Serednyakov S.I., Skovpen Yu.I., Solodov E.P., Todyshev K.Yu., Yushkov A.N. Measurement of the $D^*(2010)^+$ meson width and the $D^*(2010)(+/-)$ D^0 mass difference. // Physical Review Letters. - 2013. - Vol.111, N11. - P.111801. [arXiv:1304.5657 [hep-ex]].

[357] Sandilya S., Belle Collab., Bondar A., Eidelman S., Gabyshev N., Krokovny P., Kuzmin A., Lukin P., Matvienko D., Shwartz B., Vorobyev V., Zhilich V. Search for bottomonium states in exclusive radiative $\gamma(2S)$ decays. // Physical Review Letters. - 2013. - Vol.111, N11. - P.112001.

[358] Aaij R., LHCb Collab., Bondar A., Eidelman S., Krokovny P., Kudryavtsev V., Poluektov A., Shekhtman L., Vorobyev V. Observation of a resonance in $B^+ \to K^+\mu^+\mu^-$ decays at low recoil. // Physical Review Letters. - 2013. - Vol.111, N11. - P.112003.

[359] Aaij R., LHCb Collab., Bondar A., Eidelman S., Krokovny P., Kudryavtsev V., Poluektov A., Shekhtman L., Vorobyev V. Search for the lepton-flavor-violating decays $B_s^0 \to e(+/-)\mu(-/+)$ and $B^0 \to e(+/-)\mu(-/+)$. // Physical Review Letters. - 2013. - Vol.111, N14. - P.141801.

[360] Aaij R., Bondar A., Eidelman S., Krokovny P., Kudryavtsev V., Poluektov A., Shekhtman L., Vorobyev V. Measurement of the CP asymmetry in $B+ \to K^+ \mu^+\mu^-$ decays. // Physical Review Letters. - 2013. - Vol.111, N15. - P.151801.

[361] Aad G., ATLAS Collab., Anisenkov A.V., Beloborodova O.L., Bobrovnikov V.S., Bogdanchikov A.G., Kazanin V.F., Korol A.A., Malyshev V.M., Maslennikov A.L., Maximov D. A., Peleganchuk S.V., Skovpen K.Yu., Soukharev A.M., Talyshev A.A., Tikhonov Yu.A. Measurement of the azimuthal angle dependence of inclusive jet yields in Pb plus Pb collisions at root s(NN)=2.76 TeV with the ATLAS detector. // Physical Review Letters. - 2013. - Vol.111, N15. - P.152301.

[362] Abbas E., ALICE Collab., Pestov Y. J/ψ elliptic flow in Pb-Pb collisions at root s(NN)=2.76 TeV. // Physical Review Letters. - 2013. - Vol.111, N16. - P.162301.

[363] Aaij R., LHCb Collab., Bondar A., Eidelman S., Krokovny P., Kudryavtsev V., Poluektov A., Shekhtman L., Vorobyev V. Observation of the decay $B_c^+ \to B_s^0 \pi^+$. // Physical Review Letters. - 2013. - Vol.111, N18. - P.181801.

[364] Aaij R., LHCb Collab., Bondar A., Eidelman S., Krokovny P., Kudryavtsev V., Poluektov A., Shekhtman L., Vorobyev V. Measurement of form-factor-independent observables in the decay $B^0 \to K^*(0)\ \mu^+\mu^-$. // Physical Review Letters. - 2013. - Vol.111, N19. - P.191801.

[365] Abelev B., ALICE Collab., Pestov Y. K-S(0) and Lambda production in Pb-Pb collisions at root s(NN)=2: 76 TeV. // Physical Review Letters. - 2013. - Vol.111, N22. - P.222301.

[366] Aad G., ATLAS Collab., Anisenkov A. V., Beloborodova O. L., Bobrovnikov V. S., Bogdanchikov A. G., Kazanin V. F., Korol A. A., Malyshev V. M., Maslennikov A. L., Maximov D. A., Peleganchuk S. V., Skovpen K. Yu., Soukharev A. M., Talyshev A. A., Tikhonov Yu. A. Measurement of top quark polarization in top-antitop events from proton- proton collisions at root s=7 TeV using the ATLAS detector. // Physical Review Letters. - 2013. - Vol.111, N23. - P.232002.

[367] Ablikim M., BESIII Collab., Achasov M. N., Muchnoi N. Yu., Nikolaev I. B. Observation of a charged charmoniumlike structure Z_c (4020) and search for the Z_c (3900) in $e^+e^- \to \pi^+\pi^- h_c$. // Physical Review Letters. - 2013. - Vol.111, N24. - P.242001. [[e-Print: arXiv:1309.1896 [hep-ex]].

[368] Aaij R., LHCb Collab., Bondar A., Eidelman S., Krokovny P., Kudryavtsev V., Poluektov A., Shekhtman L., Vorobyev V. Measurement of D^0 $\bar{D}^0$ mixing parameters and search for CP violation using $D^0 \to K^+ \pi^-$ decays. // Physical Review Letters. - 2013. - Vol.111, N25. - P.251801.

[369] Aad G., ATLAS Collab., Anisenkov A., Beloborodova O., Bobrovnikov V. S., Bogdanchikov A., Kazanin V. F., Kolachev G. M., Korol A., Malyshev V., Maslennikov A.L., Maximov D. A., Orlov I., Peleganchuk S. V., Schamov A. G., Skovpen K., Soukharev A., Talyshev A., Tikhonov Y. A. Search for resonances decaying into top-quark pairs using fully hadronic decays in pp collisions with ATLAS at root s=7 TeV. // Journal of High Energy Physics. - 2013. - N1. - P.106.

[370] Aad G., ATLAS Collab., Anisenkov A., Beloborodova O., Bobrovnikov V.B., Bogdanchikov A., Kazanin V.A., Kolachev G.M., Korol A., Malyshev V., Maslennikov A.L., Orlov I., Peleganchuk S.V., Schamov A.G., Skovpen K., Soukharev A., Talyshev A., Tikhonov Y.A. Search for direct chargino production in anomaly-mediated supersymmetry breaking models based on a disappearing-track signature in pp collisions at root s=7 TeV with the ATLAS detector. // Journal of High Energy Physics. - 2013. - N1. - P.131.

[371] Aad G., ATLAS Collab., Anisenkov A., Beloborodova O., Bobrovnikov V.S., Bogdanchikov A., Kazanin V.F., Kolachev G.M., Korol A., Malyshev V.,

Maslennikov A.L., Maximov D.A., Orlov I., Peleganchuk S.V., Schamov A.G., Skovpen K., Soukharev A., Talyshev A., Tikhonov Y.A. Measurement of isolated-photon pair production in pp collisionsat root s=7 TeV with the ATLAS detector. // Journal of High Energy Physics. - 2013. - N1. - P.086.

[372] Aad G., ATLAS Collab., Anisenkov A., Beloborodova O., Bobrovnikov V. B., Bogdanchikov A., Kazanin V.A., Kolachev G.M., Korol A., Malyshev V., Maslennikov A.L., Maximov D.A., Orlov I., Peleganchuk S.V., Schamov A.G., Skovpen K., Soukharev A., Talyshev A., Tikhonov Y.A. ATLAS search for new phenomena in dijet mass and angular distributions using pp collisions at root s=7 TeV. // Journal of High Energy Physics. - 2013. - N1. - P.029.

[373] Aad G., ATLAS Collab., Anisenkov A., Beloborodova O., Bobrovnikov V.S., Bogdanchikov A., Kazanin V.F., Kolachev G.M., Korol A., Malyshev V., Maslennikov A.L., Maximov D.A., Peleganchuk S.V., Skovpen K., Soukharev A., Talyshev A., Tikhonov Y.A. Search for the neutral Higgs bosons of the minimal supersymmetric standard model in pp collisions at root s=7 TeV with the ATLAS detector. // Journal of High Energy Physics. - 2013. - №2. - P.095.

[374] Aaij R., LHCb Collab., Bobrov A., Bondar A., Eidelman S., Krokovny P., Kudryavtsev V., Poluektov A., Shekhtman L., Vorobyev V. Differential branching fraction and angular analysis of the B(+-) $K^+ \mu^+\mu^-$ decay. // Journal of High Energy Physics. - 2013. - N2. - P.105.

[375] Aaij R., LHCb Collab., Bobrov A., Bondar A., Eidelman S., Krokovny P., Kudryavtsev V., Poluektov A., Shekhtman L., Vorobyev V. Measurement of the cross-section for $Z \rightarrow e^+e^-$ production in pp collisions at root s=7 TeV. // Journal of High Energy Physics. - 2013. - N2. - P.106.

[376] Ko B. R., Belle Collab., Arinstein K., Bondar A., Eidelman S., Gabyshev N., Krokovny P., Kuzmin A., Zhilich V. Search for CP Violation in the Decay $D^+ \rightarrow (K_SK^+) K^0$. // Journal of High Energy Physics. - 2013. - N2. - P.098.

[377] Aaij R., LHCb Collab., Bobrov A., Bondar A., Eidelman S., Krokovny P., Kudryavtsev V., Poluektov A., Shekhtman L., Vorobyev V. First evidence for the annihilation decay mode $B^+ \rightarrow D_s^+ \varphi$. // Journal of High Energy Physics. - 2013. - N2. - P.043.

[378] Aaij R., LHCb Collab., Bobrov A., Bondar A., Eidelman S., Krokovny P., Kudryavtsev V., Poluektov A., Shekhtman L., Vorobyev V.Measurement of J/ψ production in pp collisions at root s=2.76 TeV. // Journal of High Energy Physics. - 2013. - N2. - P.041.

[379] Aad G., ATLAS Collab., Anisenkov A., Beloborodova O., Bobrovnikov V.S., Bogdanchikov A., Kazanin V.F., Kolachev G. M., Korol A., Malyshev V., Maslennikov A.L., Maximov D.A., Orlov I., Peleganchuk S.V., Schamov A.G., Skovpen K., Soukharev A., Talyshev A., Tikhonov Y.A. Search for charged Higgs bosons through the violation of lepton universality in t(t)over-bar events using pp collision data at root s=7 TeV with the ATLAS experiment. // Journal of High Energy Physics. - 2013. - N3. - P.076.

[380] Aaij R., LHCb Collab., Bobrov A., Bondar A., Eidelman S., Krokovny P., Kudryavtsev V., Poluektov A., Shekhtman L., Vorobyev V. Measurement of CP observables in $B^0 \rightarrow DK^*(0)$ with $D \rightarrow K^+K^-$. // Journal of High Energy Physics. - 2013. - N3. - P.067.

[381] Aad G., ATLAS Collab. Anisenkov A., Beloborodova O., Bobrovnikov V. S., Bogdanchikov A., Kazanin V.F., Kolachevl G.M., Korol A., Malyshev V., Maslennikov A.L., Maximov D.A., Orlov I., Peleganchuk S.V., Schamov A.G., Skovpen K., Soukharev A., Talyshev A., Tikhonov Y.A. Measurement of ZZ production in pp collisions at root s=7 TeV and limits on anomalous ZZZ and ZZ gamma couplings with the ATLAS detector. // Journal of High Energy Physics. - 2013. - N3. - P.128.

[382] Lee R. Marquard Peter, Smirnov Alexander V., Smirnov Vladimir A., Steinhauser Matthias. Four-loop corrections with two closed fermion loops to fermionself energies and the lepton anomalous magnetic moment. // Journal of High Energy Physics. - 2013. - №3. - P.162.

[383] Gerasimov R.E., Grabovsky A.V. Evolution equation for 3-quark Wilson loop operator. // Journal of High Energy Physics. - 2013. - №4. - P.102.

[384] Aad G., Anisenkov A., Beloborodova O., Bobrovnikov V.S., Bogdanchikov A., Kazanin V.F., Kolachev G.M., Korol A., Malyshev V., Masletinikov . L., Orlov I., Peleganchuk S. V., Skovpen K., Soukarev A., Tikhonov Y.A. Search for dark matter candidates and large extra dimensions inevents with a jet and missing transverse momentum with the ATLAS detector. // Journal of High Energy Physics. - 2013. - N4. - P.075.

[385] Aaij R., LHCb Collab., Bobrov A., Bondar A., Eidelman S., Krokovny P., Kudryavtsev V., Poluektov A., Shekhtman L., Vorobyev V. Measurement of the fragmentation fraction ratio f(s)/f(d) and its dependence on B meson kinematics. // Journal of High Energy Physics. - 2013. - N4. - P.001.

[386] Aaij R., LHCb Collab., Bondar A., Eidelman S., Krokovny P., Kudryavtsev V., Poluektov A., Shekhtman L., Vorobyev V. Limits on neutral Higgs boson production in the forward regionin pp collisions at root s=7 TeV. // Journal of High Energy Physics. - 2013. - N5. - P.132.

[387] Aaij R., Bondar A., Eidelman S., Krokovny P., Kudryavtsev V., Poluektov A., Shekhtman L., Vorobyev V. Measurement of the $B^0 \rightarrow K^*(0)$ e^+e^- branching fraction at low dilepton mass. // Journal of High Energy Physics. - 2013. - N5. - P.159.

[388] Aad G., ATLAS Collab., Anisenkov A., Beloborodova O., Bobrovnikov V.S., Bogdanchikov A., Kazanin V.F., Kolachev G.M., Korol A., Malyshev V., Maslennikov A.L., Maximov D.A., Peleganchuk S.V.,

Skovpen K., Soukharev A., Talyshev A., Tikhonov Y.A. Measurement of the cross-section for W boson production in association with b-jets in pp collisions at root s=7 TeV with the ATLAS detector. // Journal of High Energy Physics. - 2013. - N6. - P.084.

[389] Aaij R., LHCb Collab., Bondar A., Eidelman S., Krokovny P., Kudryavtsev V., Poluektov A., Shekhtman L., Vorobyev V. Production of J/psi and gamma mesons in pp collisions at root s=8 TeV. // Journal of High Energy Physics. - 2013. - N6. - P.064.

[390] Aaij R., Bondar A., Eidelman S., Krokovny P., Kudryavtsev V., Shekhtman L., Vorobyev V. Precision measurement of D meson mass differences. // Journal of High Energy Physics. - 2013. - N6. - P.065.

[391] Aaij R., Bondar A., Eidelman S., Krokovny P., Kudryavtsev V., Poluektov A., Shekhtman L., Vorobyev V. Search for CP violation in $D^+ \to \varphi\pi^+$ and $D_s^+ \to K_S^0 \pi^+$ decays. // Journal of High Energy Physics. - 2013. - N6. - P.112.

[392] Aad G., ATLAS Collab., Anisenkov A., Beloborodova O., Bobrovnikov V. S., Bogdanchikov A., Kazanin V.F., Kolachev G. M., Korol A., Malyshev V., Maslennikov A.L., Maximov D. A., Orlov I., Peleganchuk S.V., Schamov A.G., Skovpen K., Soukharev A., Talyshev A., Tikhonov Y.A. Search for third generation scalar leptoquarks in pp collisions at root s=7 TeV with the ATLAS detector. // Journal of High Energy Physics. - 2013. - N6. - P.033.

[393] Aad G., ATLAS Collab., Anisenkov A., Beloborodova O., Bobrovnikov V. S., Bogdanchikov A., Kazanin V.F., Korol A., Malyshev V., Maslennikov A. L., Maximov D.A., Peleganchuk S.V., Skovpen K., Soukharev A., Talyshev A., Tikhonov Y.A. Measurement of the production cross section of jets in association with a Z boson in pp collisions at root s=7 TeV with the ATLAS detector. // Journal of High Energy Physics. - 2013. - N7. - P.032.

[394] Aaij R., LHCb Collab., Bondar A., Eidelman S., Krokovny P., Kudryavtsev V., Poluektov A., Vorobyev V. Differential branching fraction and angular analysis of the decay $B_s^0 \to \varphi\mu^+\mu^-$. // Journal of High Energy Physics. - 2013. - N7. - P.084.

[395] Aaij R., LHCb Collab., Bondar A., Eidelman S., Krokovny P., Kudryavtsev V., Poluektov A., Shekhtman L., Vorobyev V. Differential branching fraction and angular analysis of the decay $B^0 \to K^*(0)\ \mu^+\mu^-$. // Journal of High Energy Physics. - 2013. - N8. - P.131.

[396] Aaij R., LHCB Collab., Bondar A., Eidelman S., Krokovny P., Kudryavtsev V., Poluektov A., Shekhtman L., Vorobyev V. Measurement of B meson production cross-sections in proton-proton collisions at root s=7 TeV. // Journal of High Energy Physics. - 2013. - N8. - P.117.

[397] Aaij R., LHCb Collab., Bondar A., Eidelman S., Krokovny P., Kudryavtsev V., Poluektov A., Shekhtman L., Vorobyev V. Searches for $B_s^0 \to J/\psi\ p\ \bar{p}$ and $B^+ \to J/\psi\ p\ \bar{p}\ \pi^+$ decays. // Journal of High Energy Physics. - 2013. - N9. - P.006.

[398] Abelev B., Pestov Y. Multiplicity dependence of two-particle azimuthal correlationsin pp collisions at the LHC. // Journal of High Energy Physics. - 2013. - N9. - P.049.

[399] Aad G., ATLAS Collab., Anisenkov A.V., Beloborodova O.L., Bobrovnikov V.S., Bogdanchikov A.G., Kazanin V.F., Korol A.A., Malyshev V.M., Maslennikov A.L., Maximov D.A., Peleganchuk S.V., Skovpen K.Yu., Soukharev A.M., Talyshev A.A., Tikhonov Yu.A. Performance of jet substructure techniques for large-R jets in proton-proton collisions at root s=7 TeV using the ATLAS detector. // Journal of High Energy Physics. - 2013. - N9. - P.076.

[400] Grabovsky A.V. On the solution to the NLO forward BFKL equation. // Journal of High Energy Physics. - 2013. - №9. - P.098.

[401] Grabovsky A.V. Connected contribution to the kernel of the evolution equationfor 3-quark Wilson loop operator. // Journal of High Energy Physics. - 2013. - №9. - P.141.

[402] Zupanc A., Belle Collab., Arinstein K., Eidelman S., Gabyshev N., Krokovny P., Kuzmin A., Lukin P., Shwartz B., Usov Y., Vinokurova A., Vorobyev V., Zhilich V., Zhulanov V. Measurements of branching fractions of leptonic and hadronic D_s^+ meson decays and extraction of the D_s^+ meson decay constant. // Journal of High Energy Physics. - 2013. - N9. - P.139.

[403] Aaij R., LHCb Collab., Bondar A., Eidelman S., Krokovny P., Kudryavtsev V., Poluektov A., Shekhtman L., Vorobyev V. Study of D-J meson decays to $D^+\pi^-$, $D^0\pi^+$ and $D^*(+)\ \pi^-$ final states in pp collisions. // Journal of High Energy Physics. - 2013. - N9. - P.145.

[404] Aaij R., Bondar A., Eidelman S., Krokovny P., Kudryavtsev V., Poluektov A., Shekhtman L., Vorobyev V. First evidence for the two-body charmless baryonic decay $B^0 \to p\ \bar{p}$. // Journal of High Energy Physics. - 2013. - N10. - P.005.

[405] Aad G., ATLAS Collab., Anisenkov A.V., Beloborodova O.L., Bobrovnikov V.S., Bogdanchikov A. G., Kazanin V.F., Korol A.A., Malyshev V.M., Maslennikov A.L., Maximov D.A., Peleganchuk S.V., Skovpen K.Yu., Soukharev A.M., Talyshev A.A., Tikhonov Yu.A. Measurement of the differential cross-section of B^+ meson production in pp collisions at root s=7 TeV at ATLAS. // Journal of High Energy Physics. - 2013. - N10. - P.042.

[406] Aaij R., LHCb Collab., Bondar A., Eidelman S., Krokovny P., Kudryavtsev V., Poluektov A., Shekhtman L., Vorobyev V. Measurement of the relative rate of prompt chi(c0,) chi(c1) and chi(c2) production at root s=7 TeV. // Journal of High Energy Physics. - 2013. - N10. - P.115.

[407] Aad G., ATLAS Collab., Anisenkov A.V., Beloborodova O.L., Bobrovnikov V.S., Bogdanchikov A.G., Kazanin V.F., Korol A.A., Malyshev V.M., Maslennikov A.L., Maximov D.A., Peleganchuk S.V., Skovpen K.Yu., Soukharev A.M., Talyshev A.A., Tikhonov Yu.A. Search for new phenomena in final states with large jet multiplicities and missing transverse momentum at root s=8 TeV proton-proton collisions using the ATLAS experiment. // Journal of High Energy Physics. - 2013. - N10. - P.130.

[408] Aaij R., LHCb Collab., Bondar A., Eidelman S., Krokovny P., Kudryavtsev V., Poluektov A., Shekhtman L., Vorobyev V. Study of $B_s^0 \to K_s^0 h^+h'^{(-)}$ decays with first observation of $B_s^0 \to (K_sK^{\pm}) K^0 \pi(-/+)$ and $B_s^0 \to K_s^0 \pi^+\pi^-$. // Journal of High Energy Physics. - 2013. - N10. - P.143.

[409] Aaij R., LHCb Collab., Bondar A., Eidelman S., Krokovny P., Kudryavtsev V., Poluektov A., Shekhtman L., Vorobyev V. First measurement of time-dependent CP violation in $B_s^0 \to K^+K^-$ decays. // Journal of High Energy Physics. - 2013. - N10. - P.183.

[410] Aad G., ATLAS Collab., Anisenkov A.V., Beloborodova O.L., Bobrovnikov V.S., Bogdanchikov A.G., Kazanin V.F., Korol A.A., Malyshev V.M., Maslennikov A.L., Maximov D.A., Peleganchuk S.V., Skovpen K.Yu., Soukharev A.M., Talyshev A.A., Tikhonov Yu.A. Search for direct third-generation squark pair production in final states with missing transverse momentum and two b-jets in root s=8 TeV pp collisions with the ATLAS detector. // Journal of High Energy Physics. - 2013. - N10. - P.189.

[411] Aad G., ATLAS Collab., Anisenkov A., Beloborodova O., Bobrovnikov V.S., Bogdanchikov A., Kazanin V.F., Korol A., Malyshev V., Maslennikov A.L., Maximov D.A., Peleganchuk S.V., Skovpen K., Soukharev A., Talyshev A., Tikhonov Y.A. Measurement of the top quark charge in pp collisions at root s=7 TeV with the ATLAS detector. // Journal of High Energy Physics. - 2013. - N11. - P.031.

[412] Aaij R., LHCb Collab., Bondar A., Eidelman S., Krokovny P., Kudryavtsev V., Poluektov A., Shekhtman L., Vorobyev V. Observation of the decay $\to$ J/psi K (+) K (-) pi (+). // Journal of High Energy Physics. - 2013. - N11. - P.094.

[413] Aaij R., Bondar A., Eidelman S., Krokovny P., Kudryavtsev V., Poluektov A., Shekhtman L., Vorobyev V. First observation of the decay B-s(0) $\to$ phi(K)over-bar*(0). // Journal of High Energy Physics. - 2013. - N11. - P.092.

[414] Lee R.N., Pomeransky A.A. Critical points and number of master integrals. // Journal of High Energy Physics. - 2013. - №11. - P.165.

[415] Khriplovich I. B. Gravitational four-fermion interaction and dynamics of the early Universe. // Journal of High Energy Physics. - 2013. - N11. - P.174.

[416] Aad G., ATLAS Collab., Anisenkov A., Beloborodova O., Bobrovnikov V.S., Bogdanchikov A., Kazanin V.F., Korol A., Malyshev V., Maslennikov A.L., Maximov D.A., Peleganchuk S.V., Skovpen K., Soukharev A., Talyshev A., Tikhonov Y.A. Measurement of the distributions of event-by-event flow harmonics in lead-lead collisions at root s(NN)=2.76 TeV with the ATLAS detector at the LHC. // Journal of High Energy Physics. - 2013. - N11. - P.183.

[417] Aaij R., LHCb Collab., Bondar A., Eidelman S., Krokovny P., Kudryavtsev V., Poluektov A., Shekhtman L., Vorobyev V. Search for the doubly charmed baryon Xi(+)(cc). // Journal of High Energy Physics. - 2013. - N12. - P.090.

[418] Aaij R., LHCb Collab., Bobrov A., Bondar A., Eidelman S., Krokovny P., Kudryavtsev V., Poluektov A., Shekhtman L., Vorobyev V. Search for the rare decay K-s(0) $\to$ mu(+)mu(-). // Journal of High Energy Physics. - 2013. - N1. - P.090.

[419] Aaij R., LHCb Collab., Bobrov A., Bondar A., Eidelman S., Krokovny P., Kudryavtsev V., Poluektov A., Shekhtman L., Vorobyev V. A study of the Z production cross-section in pp collisions at root s=7 TeV using tau final states. // Journal of High Energy Physics. - 2013. - N1. - P.111.

[420] Bobrov A.V., Bondar A.E. A search for $\tau \to \mu\gamma$ decay at Super c-τ factory (in Russian). // Bulletin of Novosibirsk State University. Series: Physics. - 2013. – Vol.8, N2. - P.19-35.

[421] A.N. Makarov, S.Yu. Taskaev. Beam of monoenergetic neutrons for the calibration of a dark-matter detector. // Letters to Journal of Experimental and Theoretical Physics. - 2013. - V.97, N 12. - P.667-669.

[422] A.V. Darin, Yu.V. Rakshun. Measurement procedure in determining the element content of rock samples by X-ray fluorescence analysis using VEPP-3 synchrotron radiation (in Russian). // Scientific Bulletin of NSTU. - 2013. - N2 (51). - P.112-118.

[423] A.V. Darin, Yu.V. Rakshun. Measurement procedure in XRF analysis using X-ray concentrating optics (polycapillary lenses) (in Russian). // Scientific Bulletin of NSTU. - 2013. - N2 (51). - P.119-129.

[424] Bondar A.E. Project of super-charm-tau factory in Novosibirsk (in Russian). // Nuclear Physics. - 2013. - Vol.76, N9. - P.1132-1145. - (On behalf of the Project of Super-charm-tau factory collab.).

[425] A.N. Gentselev, B.G. Goldenberg, A.D. Nikolenko, V.F. Pindyurin, I.V. Poletaev. Installation for soft X-ray lithography at VEPP-4M (in Russian). // Journal of Surface Investigation. - 2013. - N7. - P.96-102.

[426] S.E. Peltek, T.N. Goryachkovskaya, S.V. Bannikova, S.V. Shekhovtsov, B.G. Goldenberg, A.K. Potashnikov, V.M. Popik. Investigation into free immunodiffusion in channels of microfluidic module (in

Russian). // Bulletin of the Russian Academy of Science. Series: Physics. - 2013. - Vol.77, N9. - P.1341-1344.

[427] V.M. Popik, T.N. Goryachkovskaya, L.V. Kuibida, A.I. Semenov, M.A. Scheglov, S.E. Peltek. Modification of time-of-flight mass spectrometer for accurate measurement of nanoparticle masses using terahertz radiation (in Russian). // Bulletin of the Russian Academy of Sciences. Series: Physics - 2013. - Vol.77, N9. - P.1337-1340.

[428] V.V. Gerasimov, G.N. Zhizhin, B.A. Knyazev, I.A. Kotelnikov, N.A. Mitina, A.K. Nikitin. Diagnostics system for study of terahertz surfaces of plasmon polaritons at Novosibirsk free electron laser (in Russian). // Bulletin of the Russian Academy of Science. Series: Physics - 2013. - Vol.77, N9. - P.1333-1336.

[429] R.G. Valeev, V.V. Kryventsov, N.A. Mezentsev. EXAFS study of promising semiconductor Ga2Se3 (in Russian). // Bulletin of the Russian Academy of Science. Series: Physics - 2013. - Vol.77, N9. - P.1320-1322.

[430] R.G. Valeev, V.F. Kobziev, V.V. Kryventsov, N.A. Mezentsev. Synthesis and examination of the structure of gallium arsenide nanostructure arrays (in Russian). // Bulletin of the Russian Academy of Science. Series: Physics - 2013. - Vol.77, N9. - P.1323-1326.

[431] A.N. Agafonov, M.G. Vlasenko, B.O. Volodkin, V.V. Gerasimov, A.K. Kaveev, B.A. Knyazev, G.I. Kropotov, V.S. Paveliev, I.G. Palchikova, V.A. Soifer, M.F. Stupak, K.N. Tukmakov, E.V. Tsygankova, Yu.Yu. Choporova. Diffractive lenses for high-power beams of terahertz radiation (in Russian). // Bulletin of the Russian Academy of Sciences. Series: Physics - 2013. - Vol.77, N9. - P.1330-1332.

[432] A.V. Arzhannikov, N.S. Ginzburg, V.Yu. Zaslavsky, P.V. Kalinin, N.Yu. Peskov, A.S. Sergeev, S.L. Sinitsky, V. D. Stepanov, and M. Thumm. Generation of powerful narrow band 75-GHz radiation in a free-electron maser with two-dimensional distributed feedback. // Technical Physics Letters. – 2013. - Vol.39, N9. - P801-804 (2013. - Vol.39, N18. - P.8-16).

[433] N.A. Vinokurov, Ya.V. Getmanov, G.N. Kulipanov, O.A. Shevchenko. X-ray source on the basis of multi-turn energy recovery linac (in Russian). // Scientific Bulletin of NSTU. - 2013. - N1 (50). - P.112-118.

[434] Ya.V. Getmanov, N.A. Vinokurov, O.A. Shevchenko. Longitudinal stability in energy recovery linac with two accelerating structures (in Russian). // Scientific Bulletin of NSTU. - 2013. - N1 (50). - P.119-127.

[435] E.F. Reznikova, V.I. Kondratiev, B.G. Goldenberg. Wettability of LIGA polymers for microfluidic modules (in Russian). // Scientific Bulletin of NSTU. - 2013. - N2 (51). - P.136-143.

[436] K.A. Ten, V.M. Titov, E.R. Pruuel, L.A. Lukyanchikov, B.P. Tolochko, V.V. Zhulanov, L.I. Schechtman, Yu.A. Aminov, A.K. Muzyrya, O.V. Kostitsyn, E.B. Smirnov. Study of parameters of detonation wave and condensation processes in benzotrifuroxane by synchrotron methods (in Russian). // Scientific Bulletin of NSTU. - 2013. - N1 (50). - P.128-138

[437] K.A. Ten, E.R. Pruuel, L.A. Lukyanchikov, B.P. Efremov, E.V. Bespalov, B.P. Tolochko, V.V. Zhulanov, L.I. Schechtman. Shock compression of nanostructure porous materials (in Russian). // Scientific Bulletin of NSTU. - 2013. - N1 (50). - P.139-146.

[438] M.I. Bryzgunov, A.V. Ivanov, V.M. Panasyuk, V.V. Parkhomchuk, V.B. Reva. Efficiency improvement of an electron collector intended for Electron Cooling Systems using a wien filter (in Russian). // Technical Physics. - 2013. - Vol.83, N6. - P.139-146.

[439] A.E. Bondar, A.F. Buzulutskov, A.D. Dolgov, A.V. Sokolov, E.O. Shemyakina. Study of characteristics of two-phase cryogenic avalanche detector in argon with optical readout based on Geiger-mode avalanche photodiode arrays (in Russian). // Bulletin of Novosibirsk State University. Series: Physics. - 2013. - Vol.8, N2. - P.36-43.

[440] M.I. Bryzgunov, A.V. Ivanov, V.M. Panasyuk, V.V. Parkhomchuk, V.B. Reva. A High efficiency collector for a High Voltage Electron Cooler (in Russian). // Instruments and Experimental Techniques. - 2013. - N3. - P.12-20.

[441] P.S. Zagubisalo, A.G. Paulish, S.A. Kuznetsov, A.V. Arzhannikov, M.K.A. Thumm. Simulation of the thermophysical processes in the subterahertz imager based on a thin-film metamaterial converter // Radiophysics and Quantum Electronics. - 2013. - Vol.56. - P.20-35.

[442] A.N. Agafonov, B.O. Volodkin, A.K. Kaveev, B.A. Knyazev, G.I. Kropotov, V.S. Paveliev, V.A. Soifer, K.N. Tukmakov, E.V. Tsygankova, Yu.Yu. Choporova. Silicon diffractive optical elements for high-power monochromatic terahertz radiation (in Russian). // Optoelectronics. - 2013. - Vol.49, N2. - P.98-105.

[443] Rastigeev S.A., Frolov A.R., Goncharov A.D., Klyuev V.F., Konstantinov E.S., Kutnykova L.A., Parkhomchuk V.V., Petrozhitskii A.V. Accelerator mass-spectrometr SB RAS. // Problems of Atomic Science and Technology. - 2013. - № 6(88). - P.16-19.

[444] V.V. Anashin, V.M. Aulchenko, E.M. Baldin, A.K. Barladyan, A.Yu. Barnyakov, Barnyakov M.Yu., S.E. Baru, I.Yu. Basok, I.V. Bedny, O.L. Beloborodova, A.E. Blinov, V.E. Blinov, A.V. Bobrov, V.S. Bobrovnikov, A.E. Bondar, A.R. Buzykaev, A.I. Vorobiev, V.V. Gulevich, L.V. Dneprovsky, V.N. Zhylich, V.V. Zhulanov, G.V. Karpov, S.V. Karpov, S.A. Kononov, K.Yu. Kotov, E.A. Kravchenko, V.N. Kudryavtsev, A.S. Kuzmin, V.F. Kulikov, E.A. Cooper, E.B. Levichev, D.A. Maksimov, V.M. Malyshev, A.L. Maslennikov, A.S. Medvedko, N.Yu. Muchnoi, S.A.

Nikitin, I.B. Nikolaev, A.P. Onuchin, S.B. Oreshkin, I.O. Orlov, A.A. Osipov, S.V. Peleganchuk, S.G. Pivovarov, A.O. Poluektov, G.E. Pospelov, V.G. Prisekin, V.A. Rodyakin, A.A. Ruban, G.A. Savinov, Yu.I. Skovpen, A.N. Skrinsky, V.V. Smalyuk, R.G. Snopkov, A.V. Sokolov, A.M. Sukharev, A.A. Talyshev, V.A .Tayursky, V.I. Telnov, Yu.A. Tikhonov, K.Yu. Todyshev, Yu.V. Usov, T.A. Kharlamova, A.G. Shamov, B.A. Shwartz, L.I. Shekhtman, A.I. Shusharo, A.N. Yushkov. Detector KEDR (in Russian). // Physics of Elementary Particles and Atomic Nuclei. - 2013 . - V.44 , N 4 . - pp.1263 - 1345.

[445] Foot R., Silagadze Z.K. Thin disk of co-rotating dwarfs: A fingerprint of dissipative (mirror) dark matter? // Physics of the Dark Universe. - 2013. - Vol.2, №3. - P.163-165.

[446] Van Der Hoeven J., Grozin A., Gubinelli M., Lecerf G., Poulain F., Raux D. GNU TEXMACS: A scientific editing platform. // ACM Communications in Computer Algebra. - 2013. - Vol.47, № 1/2. - P. 59-61.

[447] Lee K., Jeong Y.U., Park S.H., Jang K.H., Miginsky S.V., Gudkov B.A., Cha Y.-H., Mun J., Kim K.N., Kim H.-N., Park S.J., Han B.-H., Bae S., Kim H., Vinokurov N.A. Development of advanced radiation sources at KAERI. // Bulletin of the Russian Academy of Sciences: Physics. - 2013. - Vol.77, № 2. - P. 166-168.

[448] E.I. Soldatkina. Gasdynamic trap device, transversal plasma confinement (in Russian). // LAP LAMBERT Academic Publishing GmbH & Co, Germany, ISBN 978-3-659-33540-2, 125p.

[449] P.A. Bagryansky, S.P. Demin, E.D. Gospodchikov, Yu.V. Kovalenko, V. I. Malygin, S.V. Murakhtin, V.Ya. Savkin, A.G. Shalashov, O.B. Smolyakova, A.L. Solomakhin, M. Thumm, D.V. Yakovlev. ECR heating system for the Gas Dynamic Trap. // Fusion Science and Technology, May 2013. - Vol.63, №1T. - P.40-45.

[450] P.A. Bagryansky, K.V. Zaytsev, A.V. Anikeev, A.S. Donin, Yu.V. Kovalenko, M.S. Korzhavina, A.A. Lizunov, A.N. Lozhkina, V.V. Maximov, E.I. Pinzhenin, V.V. Prikhodko, E.I. Soldatkina, A.L. Solomakhin, V.Ya. Savkin, S.V. Murakhtin, A.A. Ivanov. Advances in confinement study in the gas dynamic trap experiment. // Fusion Science and Technology. - May 2013. -Vol.63, N1T. - P.253-255.

[451] A.A. Ivanov, T.D. Akhmetov, A.D. Beklemishev, A.V. Burdakov, V.I. Davydenko, A.A. Lizunov, A.N. Lozhkina, V.V. Maximov, V.V. Mishagin, O.K. Myskin, V.V. Prikhodko, E.I. Soldatkina, V.Ya. Savkin, G.I. Shulzhenko, A.L. Solomakhin, M.A. Tiunov, Yu.A. Trunev, R.V. Voskoboinikov, K.V. Zaytsev. Auxiliary electron heating and plasma control in GDT device with electron beam: The results of initial experiments. // Fusion Science and Technology. - May 2013. - Vol.63, N1T. - P.289-291.

[452] D.V. Yurov, S.A. Brednikhin, S.A. Frolov, S.I. Lezhnin, V.V. Prikhodko, Yu.A. Tsidulko. Recent calculation results for a fission-fusion system with gas dynamic trap neutron source. // Fusion Science and Technology. - May 2013. - Vol.63, N1T. - P.313-315.

[453] K.V. Zaytsev, A.V. Anikeev, P.A. Bagryansky, A.S. Donin, Yu.V. Kovalenko, M.S. Korzhavina, A.A. Lizunov, A.N. Lozhkina, V.V. Maximov, E.I. Pinzhenin, V.V. Prikhodko, E.I. Soldatkina, A.L. Solomakhin, V.Ya. Savkin. Magnetic Measurements at the GDT facility. fusion science and technology. - May 2013. - Vol.63, N1T. - P.346-348.

[454] A. Beklemishev, A. Anikeev, V. Astrelin, P. Bagryansky, A. Burdakov, V. Davydenko, D. Gavrilenko, A. Ivanov, I. Ivanov, M. Ivantsivsky, I. Kandaurov, S. Polosatkin, V. Postupaev, S. Sinitsky, A. Shoshin, I. Timofeev, Yu. Tsidulko. Novosibirsk project of Gas-dynamic Multiple-Mirror Trap. // Fusion Science and Technology. - 2013. - Vol.63, No.1T. - P.46-51.

[455] A.D. Beklemishev et al. Novosibirsk Project of Gas-Dynamic Multiple-Mirror Trap. // Fusion Science and Technology, May 2013. - Vol.63, N1T. - P.46-51.

[456] Golkovski M.G. Relativistic electron beam hardening and alloying out off vacuum (in Russian). // LAP Lambert academic publishing. - 2013. - ISBN: 978-3-65931094-2, Saarbrucken. - P.318.

[457] Golkovski M.G., Bataev I.A., Bataev A.A., Krivizhenko D.S., Losinskaya A.A., Lenivtseva O.G. Structure of surface layers produced by non-vacuum electron beam boriding. // Applied Surface Science. - 2013. - Vol.284. - P.472-481.

[458] Lenivtseva O.G., Samoilenko V.V., Golkovski M.G., Bataev I.A., Dostovalov R.A. Preparation of wear-resistant coatings on titanium alloys by non-vakuum electron beam processing (in Russian). // Obrabotka metallov: tehnologiya, oborudovanie, instrumenty. - 2013. - № 3. - P.103-109.

[459] Mul' D.O., Samoilenko V.V., Lozhkin V.S., Drobyaz E.A., Chakin I.K., Dostovalov R.A. The structure and properties of the steel after non-vakuum electron beam alloying of titanium, tantalum, molybdenum and graphite powders (in Russian). // Obrabotka metallov: tehnologiya, oborudovanie, instrumenty. - 2013. - №3. - P.115-120. (Materialovedenie).

[460] Kuksanov N.K., Fadeev S.N., Kogut D.A. Improvement of uniformity of the electron beam treatment of the material by ELV-accelerator (in Russian). // Vestnik NGU. - February 2013. - Issue №1 (20). - P.94-99.

[461] Aaij R., LHCЬ Collab., Bondar A., Eidelman S., Krokovny P., Kudryavtsev V., Poluektov A., Shekhtman L., Vorobyev V. First observation of the decay $B_c^+ \to J/\psi K^+$. // Journal of High Energy Physics. - 2013. - N9. - P.075.

[462] P.S. Zagubisalo, A.G. Paulish, S.A. Kuznetsov, A.V. Arzhannikov, M.K.A. Thumm. Simulation of the thermophysical processes in the subterahertz imager based on a thin-film metamaterial converter. // Radiophysics and Quantum Electronics. 2013. – Vol.56. - №1. - P.20-35.

[463] N.K. Kuksanov, S.N. Fadeev, Yu.I. Golubenko, D.A. Kogut, A.I. Korchagin, A.V. Lavruhin, P.I. Nemytov, R.A. Salimov, A.V. Semenov. ELV-accelerator for industrial application (family of accelerators and tendency of development.) (in Russian). // Doklady AN VSh RF. - Tehnicheskie Nauki. - №1 (16). - January-June 2013. - P.94-99.

[464] A.N Aleshaev, V.V. Anashin, O.V. Anchugov, V.E. Blinov, A.V. Bogomyagkov, D.B. Burenkov, S.P. Vasichev, S.A. Glukhov, Yu.M. Glukhovchenko, O.P. Gordeev, G.A. Gusev, V.N. Yerokhov, K.V. Zolotarev, V.N. Zhilich, A.I. Zhmaka, A.N. Zhuravlev, V.V. Kaminsky, S.E. Karnaev, G.V. Karpov, V.A. Kiselev, E.A. Kravchenko, N.S. Kremnev, G.N. Kulipanov, E.A. Cooper, G.Ya. Kurkin, E.B. Levichev, A.S. Medvedko, O.I. Meshkov, L.A. Mironenko, S.I. Mishnev, I.I. Morozov, N.Yu. Muchnoi, V.V. Neufeld, I.B. Nikolaev, D.N. Nikolenko, I.N. Okunev, A.P. Onuchin, O.A. Pavlov, V.V. Petrov, P.A. Piminov, O.A. Plotnikov, A.V. Polyansky, Yu.A. Pupkov, E.A. Rotov, V.K. Sandyrev, V.V. Svischev, I.K. Sedlyarov, E.A. Simonov, S.V. Sinyatkin, A.N. Skrinsky, V.V. Smalyuk, E.V Starostina, D.P. Sukhanov, S.V. Tararyshkin, Yu.A. Tikhonov, D.K. Toporkov, G.M. Tumaikin, I.F. Utyupin, A.D. Khilchenko, V.M. Tsukanov, V.P. Cherepanov, A.G. Shamov, D.N. Shatilov, D.N. Shvedov, S.V. Shiyankov, E.I. Shubin, I.N. Churkin. Electron-positron collider VEPP-4M: Status and Prospects (in Russian). // Reports of the Russian Federation Higher Education Academy of Science. - Budker Institute of Nuclear Physics SB RAS, Novosibirsk, Russia - 2013 . - N1. - P.35 -46. (Proc of ERL2013: The 53th ICFA Advanced Beam Dynamics Workshop on Energy Recovery Linacs 9- 13 Sept., 2013).

[465] V.S. Burmasov, D.Yu. Dubov, M.V. Ivantsivsky, V.F. Klimkin, V.J. Madirbaev, O.I. Meshkov, A.V. Nartova, A.R. Nesterenko, I.N. Nesterenko, V.V. Postupaev, E.V. Starostina, A.T. Titov, D.K. Toporkov, N.V. Fateev. // Atomic Physics: Tutorial: Novosibirsk State University (in Russian). - Novosibirsk, 2013. - 440 pages.

[466] V.I. Yakovlev, A.G. Pogosov, S.L. Sinitsky, A.V. Bogomyagkov, L.S. Braginsky, V.A. Volodin, A.V. Zaitsev, M.I .Zakharov, P.V. Kalinin, M.S. Kotelnikova, D.A. Maksimov, A.V. Nenashev, P.L. Novikov, V.B. Reva, V.D. Stepanov, B.I. Khazin, V.S. Cherkassky, O.A. Shushakov. Examination and competion tasks in electrodynamics 2007-2012 (in Russian). // Tutorial. - Novosibirsk, Publishing House of NSU, 2013.

[467] D.B. Burenkov, P.P. Murzintsev, A.V. Polyansky, Yu.A. Pupkov, L.E. Serdakov. Geodetic monitoring of vertical deformations in tunnels of BINP accelerator complexes (in Russian). // Interexpo Geo-Siberia. - 2013. - Vol.1, N1. - P.128-131.

[468] M.K.A. Thumm, A.V. Arzhannikov, V.T. Astrelin, A.V. Burdakov, I.A. Ivanov, P.V. Kalinin, I.V. Kandaurov, V.V. Kurkuchekov, S.A. Kuznetsov, M.A. Makarov, K.I. Mekler, S.V. Polosatkin, S.A. Popov, V.V. Postupaev, A.F. Rovenskikh, S.L. Sinitsky, V.F. Sklyarov, V.D. Stepanov, Yu.A. Trunev, I.V. Timofeev, L.N. Vyacheslavov. Generation of High-Power Sub-THz Waves in Magnetized Turbulent Electron Beam Plasmas. // Journal of Infrared, Millimeter and Terahertz Waves. – [DOI 10.1007/s10762-013-9969-3].

[469] A.V. Arzhannikov, V.A. Bataev, I.A. Bataev, A.V. Burdakov, I.A. Ivanov, M.V. Ivantsivsky, K.N. Kuklin, K.I. Mekler, A.F. Rovenskikh, S.V. Polosatkin, V.V. Postupaev, S.L. Sinitsky, A.A. Shoshin. Surface modification and droplet formation of tungsten under hot plasma irradiation at the GOL-3. // Journal of Nuclear Materials. - 2013. - Vol.438. - P.S677-S680.

[470] A.V. Burdakov, A.A. Ivanov, E.P. Kruglyakov, A.D. Beklemishev. Axially symmetric magnetic mirrors: history of development and future prospects. // Fusion Science and Technology. – 2013. - Vol.63, N1T. – P.1-7.

[471] A.V. Burdakov, A. P. Avrorov, A.V. Arzhannikov, V.T. Astrelin, V.I. Batkin, A.D.Beklemishev, V.S. Burmasov, P.V. Bykov, G.E. Derevyankin, V.G. Ivanenko, I.A. Ivanov, M.V. Ivantsivsky, I.V. Kandaurov, A.A.Kasatov, S.A. Kuznetsov, V.V.Kurkuchekov, K.N. Kuklin, K.I. Mekler, S.V. Polosatkin, S.S. Popov, V.V. Postupaev, A.F. Rovenskikh, S.L. Sinitsky, V.D. Stepanov, A.V. Sudnikov, Yu.S. Sulyaev, I.V. Timofeev, Yu. A.Trunev, V.F. Sklyarov, N.V. Sorokina, A.A. Shoshin, and L.N. Vyacheslavov. Development of extended heating pulse operation mode at GOL-3. // Fusion Science and Technology. - 2013. - Vol.63, N1T. - P.29-34.

[472] A.V. Arzhannikov, A.V. Burdakov, V.S. Burmasov, P.V. Kalinin, S.A. Kuznetsov, M.A. Makarov, I.A. Ivanov, K.I. Mekler, S.S. Popov, V.V. Postupaev, A.F. Rovenskikh, S.L. Sinitsky, V.F. Sklyarov, V.D. Stepanov, I.V. Timofeev, M.K.A. Thumm, L.N. Vyacheslavov. Experimental and theoretical investigations of high power sub-millimeter wave emission at two-stream instability of high current REB. // Fusion Science and Technology. – 2013. - Vol.63, N1T. – P.82-87.

[473] S. Polosatkin, V.Astrelin, B.Bazylev, A. Beklemishev, A. Burdakov, D. Gavrilenko, A. Huber, A. Ivanov, I. Ivanov, P. Kalinin, I. Kandaurov, A. Kreter, I. Landman, V. Postupaev, S. Sinitsky, A. Shoshin, Yu. Trunev, M. Thumm, B. Unterberg. // GDMT-T: Superconducting linear device for PMI studies. // Fusion Science and Technology. - 2013. - Vol.63, N1T. - P.184-187.

[474] A. Huber, A. Burdakov, M. Zlobinski, M. Wirtz, J. Linke, Ph. Mertens, V. Philipps, G. Pintsuk, B.

Schweer, G. Sergienko, A. Shoshin, U. Samm, B. Unterberg. Investigation of the Impact on Tungsten of Transient Heat Loads induced by Laser Irradiation, Electron Beams and Plasma Guns. // Fusion Science and Technology. – 2013. - Vol.63, N1T. - P.197-200.

[475] A.V. Sudnikov, A.V. Burdakov, D.E. Gavrilenko, I.V. Kandaurov, V.V. Kurkuchekov, K.I. Mekler, A.F. Rovenskikh, S.V. Polosatkin, V.V. Postupaev, and Yu.A. Trunev. MHD activity in GOL-3 during injection of long-pulse electron beam. // Fusion Science and Technology. 2013. - Vol.63, N1T. - P.250-252.

[476] A.V. Burdakov, A.V. Arzhannikov, V.S. Burmasov, I.A. Ivanov, M.V. Ivantsivsky, I.V. Kandaurov, A.A. Kasatov, S.A. Kuznetsov, V.V. Kurkuchekov, K.N. Kuklin, K.I. Mekler, S.V. Polosatkin, S.S. Popov, V.V. Postupaev, A.F. Rovenskikh, V.F. Sklyarov, A.V. Sudnikov, M.K.A. Thumm, Yu.A. Trunev and L.N. Vyacheslavov. Microwave generation during 100 keV electron beam relaxation in GOL-3. // Fusion Science and Technology. – 2013. - Vol.63, N1T. - P.286-288.

[477] V.V. Kurkuchekov, V.T. Astrelin, A.P. Avrorov, A.V. Burdakov, P.V. Bykov, V.I. Davydenko, G.E. Derevyankin, A.A. Ivanov, I.V. Kandaurov, A.F. Rovenskikh, Yu.A. Trunev and V.A. Yarovoy. Novel injector of intense long pulse electron beam for linear plasma devices. // Fusion Science and Technology. – 2013. - Vol.63, N1T. - P.292-294.

[478] V.T. Astrelin. Features of solving a plasma emission electronics problems in CAD POISSON-2. // Advances of Applied Physics. - 2013, Vol.1, N5. - P.571-573.

[479] V.T. Astrelin, I.V. Kandaurov, V.M. Sveshnikov. Numerical simulation of transport and compression of electron beam by converging magnetic field during injection into multi-mirror trap GOL-3. // Advances of Applied Physics. - 2013. - Vol.1, N5. - P.574-579.

[480] O.N. Alyakrinsky, S.E. Baru, N.S. Dikansy, A.A. Kocheev, V.V. Leonov, V.V. Porosev. Multi-channel gas ionization chamber (in Russian). - Application for a patent N 2013109327. Date of receipt: 01.03.2013.

[481] D.A. Starostenko, P.V. Logachev, A.V. Akimov, A.A. Korepanov, P.A. Buck, et al. Results of LIA-2 operation in X-Ray mode (in Russian). // Letters to Particles and Nuclei, December 2013, passed to the editor.

[482] Chernousov Yu.D., Ivannikov V.I., Shebolaev I.V., Levichev A.E., Pavlov V.M. Accelerating structure with parallel coupling. - Patent No RU2472244C1, bulletin of inventions 10.01.2013, No 1) (in Russian).

[483] Barnyakov A.M., Chernousov Yu.D., Ivannikov V.I., Shebolaev I.V., Levichev A.E., Pavlov V.M. Accelerating structure with parallel coupling. - Patent No RU2479896C1, bulletin of inventions 20.04.2013, No 11.

[484] Kuno Y., Grigoriev D.N., Ignatov F., Khazin B.I., Khomotov N., Popov A., Yudin Yu.V., et al. A search for muon-to-electron conversion at J-PARC: the COMET experiment. // Prog. Theor. Exp. Phys. - 2013. - Vol.022C01. - P.1-43.

[485] L.I. Shekhtman, V.M. Aulchenko, V.S. Bobrovnikov, A.E. Bondar, A.D. Dolgov, G.V. Fedotovich, V.N. Kudryavtsev, D.M. Nikolenko, I.A. Rachek, V.N. Zhilich and V.V. Zhulanov. // Journal of Instrumentation. - 2013. - N8. - C12035.

[486] D.E. Berkaev, A.A. Borisov, G.A. Gusev, Yu.M. Zharinov, I.M. Zemlyansky, A.N. Kirpotin, I.A. Koop, V.S. Kuzminykh, A.P. Lysenko, I.N. Nesterenko, A.V. Otboev, O.A. Pavlov, E.A. Perevedentsev, Yu.A. Rogovsky, A.L. Romanov, A.N. Skrinsky, Yu.M. Shatunov, P.Yu. Shatunov, D.B. Shwartz. Status of electron-positron collider VEPP-2000 (in Russian). // Reports of the Russian Federation Higher Education Academy of Science - 2013. - N2 (21).

[487] K.Yu. Todyshev, Anashin, V.M., V.M. Aulchenko, E.M. Baldin, A.K. Barladyan, A.Yu. Barnyakov, M.Yu. Barnyakov, S.E. Baru, I.Yu. Basok, A.M. Batrakov, O.L. Rezanova, A.E. Blinov, V.E. Blinov, A.V. Bobrov, V.S. Bobrovnikov, A.V. Bogomyagkov, A.E. Bondar, A.R. Buzykaev, S.I. Eidelman, D.N. Grigoriev, V.R. Groshev, Yu.M. Glukhovchenko, V.V. Gulevich, D.V. Gusev, S.E. Karnaev, G.V. Karpov, S.V. Karpov, T.A. Kharlamova, V.A. Kiselev, V. Kolmogorov, S.A. Kononov, K.Yu. Kotov, E.A. Kravchenko, V.N. Kudryavtsev, V.F. Kulikov, G.Ya. Kurkin, E.A. Kuper, E. B. Levichev, D. A. Maksimov, V. M. Malyshev, A.L. Maslennikov, O.I. Meshkov, S.I. Mishnev, I.I. Morozov, N.Yu. Muchnoi, V.V. Neufeld, S.A. Nikitin, I.B. Nikolaev, I.N. Okunev, A.P. Onuchin, S.B. Oreshkin, I.O. Orlov, A.A. Osipov, S.V. Peleganchuk, S.G. Pivovarov, P.A. Piminov, V.V. Petrov, A.O. Poluektov, V.G. Prisekin, A.A. Ruban, V.K. Sandyrev, G.A. Savinov, A.G. Shamov, D.N. Shatilov, B.A. Shwartz, E.A. Simonov, S.V. Sinyatkin, A.N. Skrinsky, A.V. Sokolov, A.M. Sukharev, E.V. Starostina, A.A. Talyshev, V.A. Tayursky, V.I. Telnov, Yu.A. Tikhonov, G.M. Tumaikin, Yu.V. Usov, A.I. Vorobiov, A.N. Yushkov, V.N. Zhilich, V.V. Zhulanov, A.N. Zhuravlev, V.V. Results of measurement of $\psi(3770)$ parameters at KEDR/VEPP-4M. . // Yadernaya Fizika. - 2013. - Vol.76. - P.92-97.

[488] V. Aleynik, A. Bashkirtsev, A. Kuznetsov, A. Makarov, I. Sorokin, S. Taskaev, M. Tiunov, I. Schudlo. Optimizing of the beam transportation of negative hydrogen ions in the tandem accelerator with vacuum insulation (in Russian). Reports of Academy of Sciences of the Higher School of the Russian Federation. 2013. - №1(20). - P.47-55.

[489] A.G. Bashkirtsev, A.A. Ivanov, D.A. Kasatov, A.S. Kuznetsov, I.N. Sorokin, S.Yu. Taskaev, V.Ya. Chudaev. X-rays of high-voltage components of tandem accelerator with vacuum insulation (in Russian). //

Reports of the Russian Federation Higher Education Academy of Science. - 2013. - N1(20). - P.56-62.

[490] V.V. Kanygin, S.Yu. Taskaev. System of orthogonal neutron beam formation. The patent application. Registration number 2013105995 from 12.02.2013 (priority date).

[491] S.Yu. Taskaev. The gas stripping target. The patent application. Registration number 2013140568 from 02.09.2013 (priority date).

[492] A.N. Makarov, S.Yu. Taskaev. The method of determining the signal-to-noise ratio during the TOF measurement of the neutron energy spectrum. Know-how (NSU), № 19 dated 16.12.2013.

[493] P.P. Deichuli, V.P. Belov, A.S. Donin, A.G. Abdrashitov, N.V. Stupishin. Pulsed plasma gun for electrostatic magnetic trap WB-8 (in Russian). // XL Int. (Zvenigorod) Conference on Plasma Physics and CF, February 11 - 15 2013: Abstracts. - M.: PLAZMAIOFAN, 2013. - P.55.

[494] A.A. Ivanov. In commemoration of Edward P. Kruglyakov. Open traps: present and future (in Russian). // XL Int. (Zvenigorod) Conference on Plasma Physics and CF, February 11 - February 15, 2013, Zvenigorod: Abstracts. - M.: PLAZMAIOFAN, 2013. - p.7.

[495] P.P. Deichuli, V.P. Belov, A.A. Ivanov, V.V. Kolmogorov, V.V. Mishagin, A.V. Sorokin, N.V. Stupishin. High-power atomic injector with disitributed-arc-discharge plasma source (in Russian). // XL Int. (Zvenigorod) Conference on Plasma Physics and CF, February 11 - February 15, 2013, Zvenigorod: Abstracts. - M.: PLAZMAIOFAN, 2013. P.56.

[496] D.I. Skovorodin, A.D. Beklemishev. Instability of plasma stream in multiple-mirror trap (in Russian). // XL Int. (Zvenigorod) Conference on Plasma Physics and CF, February 11 - February 15, 2013, Zvenigorod: Abstracts. - M.: PLAZMAIOFAN, 2013. - P.66.

[497] I.S. Chernoshtanov, Yu.A. Tsidulko. Alfvén ion-cyclotron instability in a mirror trap with skew injection of neutral beams". // Int. (Zvenigorod) Conference on Plasma Physics and CF, February 11 - February 15, 2013, Zvenigorod: Abstracts. - M.: PLAZMAIOFAN, 2013. - P.67. (Fusion Science and Technology, v. 63, N1T, 2013, P. 319-321).

[498] A.A. Tkachev. The calculation of the power ion and atom beam's profile in the beam duct at arbitrary geometry of the accelerating ion-optical system. // XL Int. (Zvenigorod) Conference on Plasma Physics and CF, February 11 - February 15, 2013, Zvenigorod: Abstracts. - M.: PLAZMAIOFAN, 2013. - P.76.

[499] I.E. Karpov. Parameters of the plasma created by irradiation of a metal capillary by a laser pulse (in Russian). // XL Int. (Zvenigorod) Conference on Plasma Physics and CF, February 11 - February 15, 2013, Zvenigorod: Abstracts. - M.: PLAZMAIOFAN, 2013. - P.100.

[500] I.V. Timofeev. Features of modulation instability development in a strongly non-Maxwellian plasma (in Russian). // XL Int. (Zvenigorod) Conference on Plasma Physics and CF, February 11 - February 15, 2013, Zvenigorod: Abstracts. - M.: PLAZMAIOFAN, 2013. - P.98.

[501] Aad G., ATLAS Collab., Anisenkov A.V., Beloborodova O.L., Bobrovnikov V.S., Bogdanchikov A.G., Kazanin V.F., Korol A.A., Malyshev V.M., Maslennikov A.L., Maximov D.A., Peleganchuk S.V., Skovpen K.Yu., Soukharev A.M., Talyshev A.A., Tikhonov Yu.A. Search for excited electrons and muons in √s=8 TeV proton-proton collisions with the ATLAS detector. // New Journal of Physics. - 2013.- Vol. 15. - 093011.

[502] Aad G., ATLAS Collab., Anisenkov A.V., Beloborodova O.L., Bobrovnikov V.S., Bogdanchikov A.G., Kazanin V.F., Korol A.A., Malyshev V.M., Maslennikov A.L., Maximov D.A., Peleganchuk S.V., Skovpen K.Yu., Soukharev A.M., Talyshev A.A., Tikhonov Yu.A. Search for WH production with a light Higgs boson decaying to prompt electron-jets in proton-proton collisions at √s=7 TeV with the ATLAS detector. // New Journal of Physics. - 2013. - Vol. 15. - 043009.

[503] Aad G., ATLAS Collab., Anisenkov A.V., Beloborodova O.L., Bobrovnikov V.S., Bogdanchikov A.G., Kazanin V.F., Kolachev G.M., Korol A.A., Orlov I.O., Malyshev V.M., Maslennikov A.L., Maximov D.A., Peleganchuk S.V., Schamov A. G., Skovpen K.Yu., Soukharev A.M., Talyshev A.A., Tikhonov Yu.A. Search for extra dimensions in diphoton events from proton-proton collisions at √s=7 TeV in the ATLAS detector at the LHC. // New Journal of Physics. - 2013. - Vol. 15. - 043007.

[504] Aad G., ATLAS Collab., Anisenkov A.V., Beloborodova O.L., Bobrovnikov V.S., Bogdanchikov A.G., Kazanin V.F., Korol A.A., Malyshev V.M., Maslennikov A.L., Maximov D.A., Peleganchuk S.V., Skovpen K.Yu., Soukharev A.M., Talyshev A.A., Tikhonov Yu.A. Measurement of hard double-parton interactions in W $\rightarrow$ lv plus 2-jet events at √s=7 TeV with the ATLAS detector. // New Journal of Physics. – 2013. - Vol. 15. - 033038.

[505] Aad G., ATLAS Collab., Anisenkov A.V., Beloborodova O.L., Bobrovnikov V.S., Bogdanchikov A.G., Kazanin V.F., Korol A.A., Malyshev V.M., Maslennikov A.L., Maximov D.A., Peleganchuk S.V., Skovpen K.Yu., Soukharev A.M., Talyshev A.A., Tikhonov Yu.A. Single hadron response measurement and calorimeter jet energy scale uncertainty with the ATLAS detector at the LHC. // European Physical Journal C. - 2013. - Vol. 73. - 2305.

[506] E.A. Berendeev, A.V. Ivanov, G.G. Lazareva, A.V. Snytnikov. Supercomputer modeling of plasma electron dynamics in trap with inverse magnetic plugs and multipole magnetic walls (in Russian). // Numerical Methods and Programming. - 2013. - V.14. - P.149-154.

[507] G.I. Dimov, A.V. Ivanov. A plasma trap as a target for neutralization of the negative ion beam. // Transactions of the Fusion Science and Technology. - 2013. - 63, (1T May). - P.111-114.

[508] G.V. Karpov, A.S. Styuf. New system for beam position measuring for pre-injector of Injection Complex (in Russian). // Reports of the Russian Federation Higher Education Academy of Science. 2013. - N2. - P.110-117.

[509] M.G. Fedotov, M.V. Korobkov, S.G. Bugaeva, S.A. Treskov, A.S. Romanov, V.I. Yakovlev, et al (a total of 22 co-authors). Programs and tasks for 2013/2014 academic year (in Russian). Physics Department. 2nd year (3rd and 4th semesters), 137 pages. // Novosibirsk State Research University. Novosibirsk: NSU Physics Department, 2013. [http://www.phys.nsu.ru/courses/text/text_2013_2014/prog_2_kursa_fiz_FF_NGU_2013_2014.pdf].

[510] M.G. Fedotov, S.A. Treskov, O.V. Borodin, M.G. Paschenko, P.A. Kononova, N.L. Abasheeva. et al (a total of 17 co-authors). Programs and tasks for 2013/2014 academic year (in Russian). Physics Department. 2nd year (3rd and 4th semesters), 93 pages. // Novosibirsk State Research University. Novosibirsk: NSU Physics Department, 2013. [http:// www. phys.nsu. ru/ourses/text/text_2013_2014/prog_2_kursa_inf_FF_ NGU_2013_2014.pdf]].

[511] R. So (BaBar Collab.). Blinov V.E., Buzykaev A.R., Druzhinin V.P., Golubev V.B., Kravchenko E.A., Onuchin A.P., Serednyakov S.I., Skovpen Yu.I., Solodov E.P., Todyshev K.Yu, Yushkov A.N. Searches for a light Higgs and dark photons at BABAR. // J. Phys. Conf. Ser. - 2013. - 455. - 012040.

[512] B. Kowalewski (BaBar Collab.). Blinov V.E., Buzykaev A.R., Druzhinin V.P., Golubev V.B., Kravchenko E.A., Onuchin A.P., Serednyakov S.I., Skovpen Yu.I., Solodov E.P., Todyshev K.Yu, Yushkov A.N. Evidence for an excess of B 2192 $D^{(*)}$ $\tau\nu$ decays. // J. Phys. Conf. Ser. - 2013. - 455. - 012039.

[513] B. Oberhof (BaBar Collabor.), Blinov V.E., Buzykaev A.R., Druzhinin V.P., Golubev V.B., Kravchenko E.A., Onuchin A.P., Serednyakov S.I., Skovpen Yu.I., Solodov E.P., Todyshev K.Yu, Yushkov A.N., et al. Search for low-mass Higgs and dark bosons at BaBar. // Nucl. Phys. Proc. Suppl. 2013. - Vol.234. – P.37. [arXiv:1209.2666 [hep-ex]].

[514] J.P. Lees (BaBar Collabor.), Blinov V.E., Buzykaev A.R., Druzhinin V.P., Golubev V.B., Kravchenko E.A., Onuchin A.P., Serednyakov S.I., Skovpen Yu.I., Solodov E.P., Todyshev K.Yu, Yushkov A.N., et al. Branching fraction measurements of the color-suppressed decays B^0-bar $\rightarrow D^{(*)0}\pi^0$, $D^{*0}\eta$, $D^{(*)0}\omega$, and $D^{(*)0}\eta$' and measurement of the polarization in the decay B^0-bar \to $D^{*0}\omega$. // Phys. Rev. D. - 2013.- Vol.87, N3. - P.039901. [arXiv:1107.5751 [hep-ex]].

Reports on the conferences 2013

[515] Meng L., Parkhomchuk V.V., Reva V.B., et al. First recombination experiment of fluorine-like nickel ions at the main cooler storage ring. // (16th Intern. Conf. on the Physics of Highly Charged Ions, HCI 2012, Heidelberg, Germany, 2-7 Sept. 2012). - Physica Scripta. - 2013. - Vol.T156. - P.014044.

[516] Xiang R., Arnold A., Murcek P., Teichert J. (HZDR, Dresden, Germany); Volkov V. (BINP, Novosibirsk, Russia); Lu P., Vennekate H. (HZDR & Technische Universität Dresden, Germany), Barday R., Kamps T. (HZB, Berlin, Germany). Dark current measurements at the rossendorf SRF gun. // 35th Intern. Free-Electron Laser Conference, FEL 2013, New York, US, 26 - 30 Aug. 2013. - New York, 2013. - P.455-457.

[517] Lee C., Bogdanchikov A., Korol A., et al. ATLAS TDAQ system administration: an overview and evolution. // 2013 Intern. Symposium on Grids and Clouds, ISGC 2013, Taipei, Taiwan, 17 - 22 March 2013: Proc. of Science - 2013. - Art.nr 100840. -13p.

[518] Fadin V. S. Standard and quasi-conformal BFKL kernels. // 21st Intern. Workshop on Deep-Inelastic Scattering and Related Subjects, DIS 2013, Marseilles, France, 22 - 26 April 2013: Proc. of Science. - 2013. - 6p.

[519] Driscoll C.F., Kabantsev A.A., Dubin D.H.E., Tsidulko Yu.A. Transport, damping, and wave-couplings from chaotic and collisional neoclassical transport. // 10th Intern. Workshop on Non-neutral Plasmas, Greifswald, Germany, 27 - 30 Aug. 2012. - 2013. - P.15-25. - (AIP Conference Proc.; Vol.1521).

[520] Krokovny P. Bottomonium states. // 26th Les Rencontres de Physique de la Vallee d'Aoste. - Results and Perspectives in Particle Physics. - 26th Physics Conference in the Aosta Valley: Results and Perspectives in Particle Physics 2013, La Thuile, Aosta Valley, Italy, 26 Febr. - 2 March 2012: (Frascati Physics Series, Vol.57, Special Issue). - 2013. - P.223-229.

[521] B.P. Tolochko, K.A. Ten, E.R. Pruuel, N.Z. Lyakhov, V.M. Aulchenko. *In Situ* diffraction experiments with synchrotron radiation - from milliseconds to femtoseconds (in Russian). // 2nd All-Russian Scientific Conference "Methods of Investigation of Composition and Structure of Functional Materials" MISSFM 2013, 21 - 25 October. 2013, Novosibirsk: Book of abstracts. - Novosibirsk, 2013. - P.11-12.

[522] R.G. Valeev, A.N. Beltyukov, V.V. Kriventsov, N.A. Mezentsev. EXAFS spectroscopy in structure studies of semiconductor nanoparticles in matrices of porous Al_2O_3 (in Russian). // 2nd All-Russian Scientific Conference "Methods of Investigation of Composition and Structure of Functional Materials" MISSFM 2013, 21 - 25 October. 2013, Novosibirsk: Book of abstracts. - Novosibirsk, 2013. - p.268.

[523] R.G. Valeev, A.N. Beltyukov, V.V. Kriventsov, N.A. Mezentsev. EXAFS comparative examination of various-nature semiconductor nanocomposites based on

ZnS and ZnSe (in Russian). // 2nd All-Russian Scientific Conference "Methods of Investigation of Composition and Structure of Functional Materials" MISSFM 2013, 21 - 25 October. 2013, Novosibirsk: Book of abstracts. - Novosibirsk, 2013. - P.267.

[524] V.Ya. Prince, E.V. Naumova, S.V. Golod, A.A. Bocharov, V.V. Kubarev. Complex system based on chiral metamaterial for ultrafast control of radiation polarization (in Russian). // XI Russian Conference on Semiconductor Physics, St. Petersburg, 16 - 20 September 2013: Abstracts. - Ioffe Physico-Technical Inst. RAS, 2013. - P.88.

[525] Muggli P., Caldwell A., Reimann O., Oz E., Tarkeshian R., Bracco C., Gschwendtner E., Pardons A., Lotov K., Pukhov A., Wing M., Mandry S., Vieira J. Physics of the AWAKE project [Electronic resource]. // IPAC 2013: Proc. of the 4th Intern. Particle Accelerator Conference, 12 - 17 May 2013, Shanghai, China. - 2013. - P.1179-1181.

[526] Sinyatkin S., Dubrovin A., Gurov S., Levichev E., Pupkov Yu., Rouvinsky E., Sukhanov A. Design of NSLS-II booster dipoles with combined function magnetic field [Electronic resource]. // IPAC 2013: Proc. of the 4th Intern. Particle Accelerator Conference, 12 - 17 May 2013, Shanghai, China. - 2013. - P.3570-3572. - THPEA029.

[527] Korepanov A., Akimov A., Pachkov A., Panov A. Pulse power supplies for kicker magnets of NSLS-2 booster ring [Electronic resource]. // IPAC 2013: Proc. of the 4th Intern. Particle Accelerator Conference, 12 - 17 May 2013, Shanghai, China. - 2013. - P.720-722. - MOPWA027.

[528] Fliller III R.P., Blednykh A., Choi J., Davidsaver M., De Long J., Gao F., Gardner C., Hu Y., Jahnes G., Jew W., Klug J., Marino P., Padrazo D., Pharr L., Rainer R., Ramirez G., Ratzke P., Raynis R., Rose J., Santana M., Seletskiy S., Shah J., Shaftan T., Shen G., Singh O., Smaluk V., Sorrentino C., Vetter K., Wang G.-M., Weiner G., Yang X., Yu L.-H., Zeitler E. Results of NSLS-II Linac commissioning [Electronic resource]. // IPAC 2013: Proc. of the 4th Intern. Particle Accelerator Conference, 12 - 17 May 2013, Shanghai, China. - 2013. - P.2301-2303.

[529] Gurov S., Erokhin A., Karnaev S., Kiselev V., Levichev E., Polyansky A., Semenov A., Shiyankov S., Sinyatkin S., Smaluk V., BINP SB RAS, Novosibirsk, Russia; Shaftan T., Hseuh H., BNL, NY, USA, et al. Status of NSLS-II injector [Electronic resource]. // IPAC 2013: Proc. of the 4th Intern. Particle Accelerator Conference, 12 - 17 May 2013, Shanghai, China. - 2013. - P.273-275. - MOPEA053.

[530] Bernhard A., Huttel E., Peiffer P., Bragin A., Mezentsev N., Syrovatin V., Zolotarev K., Ferracin P. Preparations for beam tests of a CLIC damping wiggler prototype at ANKA [Electronic resource]. // IPAC 2013: Proc. of the 4th Intern. Particle Accelerator Conference, 12 - 17 May 2013, Shanghai, China. - 2013. - P.1568-1570.

[531] Erokhin A., Bulatov A., Gorchakov K., Gurov S., Kolmogorov V., Kremnev A., Pureskin D., Senkov D., Vakhrushev R. 2Hz ramping mode dipole power supply for testing the NSLSII booster dipole magnets [Electronic resource]. // IPAC 2013: Proc. of the 4th Intern. Particle Accelerator Conference, 12 - 17 May 2013, Shanghai, China. - 2013. - P.714-716. - MOPWA025.

[532] Erokhin A.I., Kolmogorov V.V., Medvedko A.S., Potapov S.I., Pureskin D.N., Senkov D.V. Power system for quadrupole magnets of NSLS-II 3 GeV booster [Electronic resource]. // IPAC 2013: Proc. of the 4th Intern. Particle Accelerator Conference, 12 - 17 May 2013, Shanghai, China. - 2013. - P.723-725. - MOPWA028.

[533] Shvedov D., Anchugov O., Kiselev V., Korepanov A., Sinyatkin S. Fast magnetic kickers for the NSLS-II booster synchrotron: design and test results [Electronic resource]. // IPAC 2013: Proc. of the 4th Intern. Particle Accelerator Conference, 12 - 17 May 2013, Shanghai, China, MOPWA026. - 2013. - P. 717-719.

[534] Gurov S., Erokhin A., Karnaev S., Kiselev V., Levichev E., Polyansky A., Semenov A., Shiyankov S., Sinyatkin S., Smaluk V. Status of NSLS-II booster [Electronic resource]. // IPAC 2013: Proc. of the 4th Intern. Particle Accelerator Conference, 12 - 17 May 2013, Shanghai, China. - 2013. - P.196-198. - MOPEA053.

[535] Koop I.A. Asymmetric energy colliding ion beams in the EDM storage ring [Electronic resource]. // IPAC 2013: Proc. of the 4th Intern. Particle Accelerator Conference, 12 - 17 May 2013, Shanghai, China. - 2013. - P.1961-1963.

[536] G.M. Zharkova, V.V. Syzrantsev, S.P. Bardakhanov, M.G. Golkovski. Dispersion of nanopowders in polymer-liquid-crystal films (in Russian). // Interaction of highly concentrated energy fluxes with materials in advanced technology and medicine: Reports of V All-Russian Conference, 26 - 29 March 2013, Novosibirsk, Russia. - Novosibirsk: Parallel, 2013. - Vol.2. - P.59-62.

[537] A.O. Lebedeva, Yu.V. Afonin, A.Yu. Demjanova, M.V. Korobeinikov, A.S. Yunoshev, A.A. Karpenko, I.V. Popova,, E.A. Pokushalov, A.E. Akulov, A.V. Romaschenko, P.P. Laktionov. Electron-beam treatment of electrospun vascular grafts (in Russian). // Interaction of highly concentrated energy fluxes with materials in advanced technology and medicine: Reports of V All-Russian. Conference, 26 - 29 March 2013, Novosibirsk, Russia. - Novosibirsk: Parallel, 2013. - Vol.2. - P.106-108.

[538] Kuznetsov A., Aleynik V., Bashkirtsev A., Kasatov D., Makarov A., Schudlo I., Sorokin I., Taskaev

S., Tiunov M. Raising the generating current in the VITA neutron source for BNCT [Electronic resource]. // IPAC 2013: Proc. of the 4th Intern. Particle Accelerator Conference, 12 - 17 May 2013, Shanghai, China. - 2013. - P.3693-3695.

[539] Cheblakov P., Derbenev A., Karnaev S., Serednyakov S., Davidsaver M., Tian Y. Software for power supplies control of the NSLS-II booster synchrotron [Electronic resource]. // IPAC 2013: Proc. of the 4th Intern. Particle Accelerator Conference, 12 - 17 May 2013, Shanghai, China. - 2013. - P.3213-3215. - THPEA032.

[540] De Maria R., Fartoukh S., Bogomyagkov A., Korostelev M. HLLHCV1.0: HL-LHC layout and optics models for 150 mm NB3SN triplets and local crab-cavities [Electronic resource]. // IPAC 2013: Proc. of the 4th Intern. Particle Accelerator Conference, 12 - 17 May 2013, Shanghai, China. - 2013. - P.1358-1350.

[541] Bogomyagkov A., De Maria R. Study of the IR2 and IR8 squeezeability for HL-LHC upgrade project [Electronic resource]. // IPAC 2013: Proc. of the 4th Intern. Particle Accelerator Conference, 12 - 17 May 2013, Shanghai, China. - 2013. - P. 1361-1363.

[542] Holzer B.J., De Maria R., Fartoukh S., Chance A., Dalena B., Payet J., Bogomyagkov A., Appleby R.B., Kelly S., Thomas M.B., Thompson L., Korostelev M., Hock K.M., Wolski A., Milardi C., Faus-Golfe A., Resta Lopes J. Optics design and lattice optimisation for the HL-LHC [Electronic resource]. // IPAC 2013: Proc. of the 4th Intern. Particle Accelerator Conference, 12 - 17 May 2013, Shanghai, China. - 2013. - P. 1385-1387.

[543] Bogomyagkov A., Levichev Eu.B., Piminov P.A., Chance A., Dalena B., Payet J., De Maria R., Fartoukh S., Giovannozzi M. Analysis of the non-linear fringe effects of large aperture triplets for the HL-LHC project. // IPAC 2013: Proc. of the 4th Intern. Particle Accelerator Conference, 12 - 17 May 2013, Shanghai, China. - 2013. - P.2615-2617. [http://accelconf.web.cern.ch/AccelConf/ IPAC2013/papers/wepea049.pdf].

[544] Wang G.M., Shaftan T., Bacha B., Blednykh A., Blum E., Cheng W.X., Choi J., Davidsaver M., De Long J., Dalesio L., Fliller R., George G., Guo W., Ha K., Hseuh H., Hu Y., Louie W., Maggipinto M., Padrazo D., Shen G., Singh O., Vetter K., Tian Y., Xu H., Yang L., Yang X., Willeke F., Smalyuk V., Karnaev S., Sinyatkin S., Gurov S., Erokhin A., Simonov E., Derbenev A., Cheblakov P., Kadyrov R. NSLS II injector integrated testing [Electronic resource]. // IPAC 2013: Proc. of the 4th Intern. Particle Accelerator Conference, 12 - 17 May 2013, Shanghai, China. - 2013. - P.3285-3287. - THPEA063.

[545] Blinov V., Bekhtenev E., Chabanov A., Gordeev O., Karpov G., Krutikhin S., Kurkin G., Mikaiylov A., Kiselev V., Levichev E., Meshkov O., Mishnev S., Neyfeld V., Nikitin S., Nikolaev I., Shatilov D., Tumaikin G. RF orbit separation for CPT-test experiment at VEPP-4M [Electronic resource]. // IPAC 2013: Proc. of the 4th Intern. Particle Accelerator Conference, 12 - 17 May 2013, Shanghai, China. - 2013. - P.1634-1636. [http://accelconf.web.cern.ch/AccelConf/ IPAC2013/papers/tupme028.pdf].

[546] Sinyatkin S., Baranov G., Batrakov A., Burdin P., Burenkov D., Gurov S., Kiselev V., Kobets V., Levichev E., Okunev I., Polyansky A., Pupkov Y., Serdakov L., Vobly P. Magnetic measurement results of the NSLS-II booster dipole magnets [Electronic resource]. // IPAC 2013: Proc. of the 4th Intern. Particle Accelerator Conference, 12 - 17 May 2013, Shanghai, China. - 2013. - P.3573-3575. - THPEA030.

[547] Pavlenko A., Batrakov A., Ilyin I. Electronics for precise measurements of accelerator pulsed magnets [Electronic resource]. // IPAC 2013: Proc. of the 4th Intern. Particle Accelerator Conference, 12 - 17 May 2013, Shanghai, China. - 2013. - P. 3216-3218. THPEA033.

[548] Okunev I., Kobets V., Batrakov A.M., Pavlenko A., Sinyatkin S., Kiselev V.A., Baranov G., Erokhin A., Vakhrushev R. Ramped magnetic measurement of NSLS-II booster dipoles [Electronic resource]. // IPAC 2013: Proc. of the 4th Intern. Particle Accelerator Conference, 12 - 17 May 2013, Shanghai, China. - 2013. - P.3576-3578. - THPEA031.

[549] Okunev I., Kobets V.V., Batracov A.M., Serdakov L., Baranov G., Burenkov D., Polyansky A., Sinyatkin S., Burdin P. Magnetic measurement of the NSLS-II booster dipole with combine functions [Electronic resource]. // IPAC 2013: Proc. of the 4th Intern. Particle Accelerator Conference, 12 - 17 May 2013, Shanghai, China. - 2013. - P.3579-3581. - THPME032.

[550] Zhuravlev A., Batrakov A., Chernyakin A., Kiselev V., Konstantinov V., Pavlenko A., Petrov V., Semenov E., Senkov D. Pulsed magnets for injection and extraction sections of NSLS-II 3 GeV booster [Electronic resource]. // IPAC 2013: Proc. of the 4th Intern. Particle Accelerator Conference, 12 - 17 May 2013, Shanghai, China. - 2013. - P.3582-3584. - THPEA033.

[551] Batrakov A.M., Chernyakin A.D., Kiselev V.A., Pavlenko A.V., Senkov D.V., Zhuravlev A.N. Pulse generators for septums and bumps of injection and extraction systems NSLS-II booster [Electronic resource]. // IPAC 2013: Proc. of the 4th Intern. Particle Accelerator Conference, 12 - 17 May 2013, Shanghai, China. - 2013. - P.726-728. - MOPWA029.

[552] Pinayev I., Belomestnykh S., Ben-Zvi I., Brown K., Brutus C., DeSanto L., Elizarov A., Folz C.M., Gassner D.M., Hao Y., Hulsart R., Jing Y., Kayran D., Lambiase R., Litvinenko V.N., Mahler G., Mapes M., Meng W., Michnoff R., Miller T.A., Minty M., Orfin P., Pendzik A., Randazzo F., Rao T., Roser T., Sandberg J., Sheehy B., Skaritka J., Smith K., Snydstrup L., Than R., Todd R.J., Tuozzolo J., Wang G., Weiss D., Willinski M.,

Xu W., Zaltsman A., Kholopov M.A., Vobliy P., Poelker M., Bell G.I., Cary J.R., Paul K., Schwartz B.T., Webb S.D., Boulware C., Grimm T., Jecks R., Miller N. Progress with coherent electron cooling proof-of-principle experiment [Electronic resource]. // IPAC 2013: Proc. of the 4th Intern. Particle Accelerator Conference, 12 - 17 May 2013, Shanghai, China. - 2013. - P.1535-1537.

[553] Knyazev B.A., Azarov I.A., Cherkassky V.S., Choporova Yu.Yu., Gerasimov V.V., Getmanov Ya.V., Grigorieva E.V., Dem'yanenko M.A., Esaev D.G., Kaveev A.K., Kotelnikov I.A., Kruchinin V.N., Kruchinina M.V., Kubarev V.V., Kulipanov G.N., Makarov S.N., Mitkov M.S., Mostovich L.A., Nikitin A.K., Nikitin P.A., Palchikova I.G., Pavelyev V.S., Rodionov D.G., Rykhlitsky S.V., Salikova T.V., Scheglov M.A., Shevchenko O.A., Shvets V.A., Serednyakov S.S., Skorokhod D.A., Stupak M.F., Vinokurov N.A., Vlasenko M.G., Volodkin B.O., Voloshinov V.B., Zavyalova M.A., Zhizhin G.N. Advances in the optics and photonics in the terahertz region at the SPIN workstation of Novosibirsk free electron laser facility. // Technical digest: MPLP'2013: IV Intern. Symposium "Modern Problems of Laser Physics", Novosibirsk, Russia, Aug. 25 - 31, 2013. - Novosibirsk: NSU, 2013. - P. 97-98.

[554] A.F. Brodnikov, V.Ya. Cherepanov. Modulation method for detection of melting-solidification phase transitions in miniature vials of reference points (in Russian). // IX Int. Scientific Congress and Exhibition Interexpo Geo-Siberia 2013; Int. Conference SibOptika 2013: collection of materials. - Novosibirsk: SCSA, 2013. - Vol.2. - P.75-78.

[555] Yu.Yu. Choporova, A.N. Agafonov, B.O. Volodkin, A.K. Kaveev, B.A. Knyazev, G.I. Kropotov, V.S. Paveliev, I.G. Palchikova, V.A. Soifer, M.F. Stupak, K.N. Tukmakov, E.V. Tsygankova, V.S. Cherkassky. Diffractive optical elements for high-power beams of terahertz radiation (in Russian). // IX All-Russian Workshop on Radiophysics of Millimeter and Submillimeter Wavelengths, February 26 - March 1, 2013, Nizhny Novgorod: Abstracts. - Nizhny Novgorod: Institute of Applied Physics, 2013. - P.18-19.

[556] Knyazev B.A., Cherkassky V.S., Choropova Yu.Yu., Gerasimov V.V., Kotelnikov I.A., Nikitin A.K., Rodionov D.G., Zhizhin G.N., Grigorieva E.V., Mostovich L.A. Application of terahertz-laser-launched evanescent waves to material study: surface plasmons on metal-dielectric interface and attenuated total reflection in circular dichroism spectrometer. // The 21th Annual Intern. Conference on Advanced Laser Technologies: ALT'13, Budva, Montenegro, Sept. 16 - 20, 2013: book of abstr. - Budva, 2013. - P.183.

[557] Shevchenko O.A., Arbuzov V.S., Dementyev E., Dovzhenko B., Getmanov Ya.V., Gorniker E.I., Knyazev B.A., Kolobanov E.I., Kondakov A.A., Kozak V., Kozyrev E., Krutikhin S.A., Kubarev V.V., Kulipanov G.N., Kuper E., Kuptsov I., Kurkin G.Ya., Medvedev L.E., Mironenko L., Ovchar V.K., Petrov V., Pilan A., Popik V.M., Repkov V.V., Salikova T.V., Scheglov M.A, Sedlyarov I., Serednyakov S.S., Skrinsky A., Tararyshkin S., Tcheskidov V.G., Tribendis A.G., Vlasenko M.G., Vobly P., Volkov V., Vinokurov N. Commissioning status and further development of the Novosibirsk multiturn ERL. // The 53th ICFA Advanced Beam Dynamics Workshop on Energy Recovery Linacs "ERL-2013", 9 - 13 Sept., 2013: ERL 2013: Abstr. book. - Novosibirsk: Budker Inst. of Nucl. Physics of SB RAS, 2013. - P.6-10.

[558] Salikova T.V., Petrichenkov M., Repkov A., Shevchenko O.A., Vinokurov N. Radiation monitoring at Novosibirsk FEL. // The 53th ICFA Advanced Beam Dynamics Workshop on Energy Recovery Linacs "ERL-2013", 9 - 13 Sept., 2013: ERL 2013: Abstr. book. - Novosibirsk: Budker Inst. of Nucl. Physics of SB RAS, 2013. - P.7.

[559] Kulipanov G.N., Kubarev V.V., Popik V.M., Scheglov M.A., Shevchenko O.A., Vinokurov N., Knyazev B.A. Novosibirsk ERL-based FEL as user facility. // The 53th ICFA Advanced Beam Dynamics Workshop on Energy Recovery Linacs "ERL-2013", 9 - 13 Sept., 2013: ERL 2013: Abstr. book. - Novosibirsk: Budker Inst. of Nucl. Physics of SB RAS, 2013. - P.7.

[560] Getmanov Ya.V., Shevchenko O.A., Vinokurov N. Longitudinal stability of multiturn ERL with split accelerating structure. // The 53th ICFA Advanced Beam Dynamics Workshop on Energy Recovery Linacs "ERL-2013", 9 - 13 Sept., 2013: ERL 2013: Abstr. book. - Novosibirsk: Budker Inst. of Nucl. Physics of SB RAS, 2013. - P.11.

[561] Volkov V., Arbuzov V.S., Gorniker E.I., Kolobanov E.I., Krutikhin S.A., Kuptsov I., Kurkiin G.Ya., Osipov V.N., Petrov V., Pilan A., Scheglov M.A., Sedlyarov I., Tribendis A.G., Vinokurov N. Beam diagnostic results of RF gun for the race-track microtron recuperator of BINP. // The 53th ICFA Advanced Beam Dynamics Workshop on Energy Recovery Linacs "ERL-2013", 9 - 13 Sept., 2013: ERL 2013: Abstr. book. - Novosibirsk: Budker Inst. of Nucl. Physics of SB RAS, 2013. - P.11.

[562] Salikova T.V. Modeling and optimization of orbit correction using fuzzy logic. // The 53th ICFA Advanced Beam Dynamics Workshop on Energy Recovery Linacs "ERL-2013", 9 - 13 Sept., 2013: ERL 2013: Abstr. book. - Novosibirsk: Budker Inst. of Nucl. Physics of SB RAS, 2013. - P.17.

[563] Serednyakov, S. S. Vinokurov N. The control system of Novosibirsk free electron laser. // The 53th ICFA Advanced Beam Dynamics Workshop on Energy Recovery Linacs "ERL-2013", 9 - 13 Sept., 2013: ERL 2013: Abstr. book. - Novosibirsk: Budker Inst. of Nucl. Physics of SB RAS, 2013. - P.18.

[564] Timko H., Argyropoulos T., Bartosik H., Bohl T., Muller J.E., Shaposhnikova E., Petrenko A. Short

high-intensity bunches for plasma wakefield experiment AWAKE in the CERN SPS [Electronic resource]. // IPAC 2013: Proc. of the 4th Intern. Particle Accelerator Conference, 12 - 17 May 2013, Shanghai, China. - 2013. - P.1820-1823.

[565] Meshkov O.I., Smalyuk V.V., Dorokhov V.L. SLM and flags for booster of NSLS-II [Electronic resource]. // IPAC 2013: Proc. of the 4th Intern. Particle Accelerator Conference, 12 - 17 May 2013, Shanghai, China, - 2013. - P.622-625. - MOMME064.

[566] Meshkov O. I. VEPP-4: application beyond the high energy physics. // IPAC 2013: Proc. of the 4th Intern. Particle Accelerator Conference, 12 - 17 May 2013, Shanghai, China. - 2013. - P.1637-1639.

[567] Lotov K. Simulation of self-modulating particle beams in plasma wakefield accelerators [Electronic resource]. // IPAC 2013: Proc. of the 4th Intern. Particle Accelerator Conference, 12 - 17 May 2013, Shanghai, China. - 2013. - P.1238-1241.

[568] Getmanov Ya.V., Shevchenko O.A., Atkinson T., Vinokurov N.A. Longitudinal stability of multiturn ERL with split accelerating structure [Electronic resource]. // IPAC 2013: Proc. of the 4th Intern. Particle Accelerator Conference, 12 - 17 May 2013, Shanghai, China. - 2013. - P.2226-2229.

[569] K.V. Lotov, A. Sosedkin, E. Mesyats. Simulation of Self-modulating Particle Beams in Plasma Wakefield Accelerators. // IPAC 2013: Proc. of the 4th Intern. Particle Accelerator Conference, 12 - 17 May 2013, Shanghai, China. - P.1238-1240.

[570] P. Muggli, C. Bracco, E. Gschwendtner, A. Pardons, A. Caldwell, K.V. Lotov, A.M. Pukhov, J. Vieira, M.Wing. Physics of the AWAKE Project. // IPAC 2013: 4th Intern. Particle Accelerator Conference, 12 - 17 May 2013, Shanghai, China. - Abstracts, p.67.

[571] K.V. Lotov, A. Sosedkin, E. Mesyats. Simulation of Self-modulating Particle Beams in Plasma Wakefield Accelerators. // IPAC 2013: the 4th Intern. Particle Accelerator Conference, 12 - 17 May 2013, Shanghai, China. - Abstracts, p.72.

[572] M.G. Kozlov. Multi regge amplitudes in non Abelian gauge theories. // Intern. Conference-Session of Section of Nuclear Physics of the Physical Sciences Division of the Russian Academy of Sciences, 5 - 8 Nov. 2013, BINP, Novosibirsk.

[573] Ya.A. Kharkov, V.V. Sokolov. Invited talk: Elastic Enhancement Factor as a Probe of Internal Chaos. // The 6th Intern. Workshop on "Quantum Chaos and Localization Phenomena", Warsaw, Poland, 24 - 26 May 2013.

[574] V.V. Sokolov. Invited talk: Mesoscopic quantum transport in presence of a weakly disordered background: time delay, decoherence and energy absorption. // Intern. 6th Workshop on "Quantum Chaos and Localization Phenomena". Warsaw, Poland, 24 - 26 May 2013.

[575] V.V. Sokolov. Plenary (Keynote) talk: Elastic Enhancement Factor as a Probe of Chaotic Quantum dynamics. // Intern. Conference CHAOS 2013: "Chaotic Modeling and Simulation". Istambul, Turkey, 11 - 14 June 2013.

[576] . I.B. Khriplovich, A.S. Rudenko Gravitational four-fermion interaction in the early Universe. // PINP Winter School, 2013, 25 - 28 February, Saint-Petersburg.

[577] I.B. Khriplovich, A.S. Rudenko. Gravitational four fermion interation in the early Universe. // Workshop on Fundamental Interactions PSI, 9 - 12 September, 2013, Zurich.

[578] I.B. Khriplovich, A.S. Rudenko. Gravitational four fermion interation in the early Universe. // II Russian-Spanish Congress: Particle and Nuclear Physics at all Scales and Cosmology, 1 - 4 October, 2013, Saint-Petersburg.

[579] M.N. Achasov, V.M. Aulchenko, A.Yu. Barnyakov, K.I. Beloborodov, A.V. Berdyugin, A.G. Bogdanchikov, A.A. Botov, A.V. Vasiljev, V.B. Golubev, T.V. Dimova, V.P. Druzhinin, D.P. Kovrizhin, I.A. Koop, A.A. Korol, S.V. Koshuba, A.E. Obrazovsky, E.V. Pakhtusova, S.I. Serednyakov, Z.K. Silagadze, A.G. Kharlamov, Yu.M. Shatunov, L.V. Kardapoltsev, A.S. Kupich, K.A. Martin, K.A. Grevtsov, I.K. Surin, K. Yu. Skovpen, D.A. Stohl, A.N. Skrinsky, Yu.A. Tikhonov, Yu.V. Usov, A. Yu. Barnyakov, D.E. Berkaev, D.B. Schwartz, Yu.A. Rogovsky, I.M. Zemlyansky. Results of experiments with SND detector on VEPP-2000 (in Russian). // Report at the session conference of the DPS RAS nuclear physics section, 5 - 8 November 2013, Protvino, Russia .

[580] M.N. Achasov, V.M. Aulchenko, A.Yu. Barnyakov, K.I. Beloborodov, A.V. Berdyugin, D.E. Berkaev, A.G. Bogdanchikov, A.A. Botov, T.V. Dimova, V.P. Druzhinin, V.B. Golubev, K.A. Grevtsov, L.V. Kardapoltsev, A.S. Kupich, A.G. Kharlamov, D.P. Kovrizhin, I.A. Koop, A.A. Korol, S.V. Koshuba, K.A. Martin, A.E. Obrazovsky, E.V. Pakhtusova, Yu.A. Rogovskii, S.I. Serednyakov, Z.K. Silagadze, K.Yu. Skovpen, A.N. Skrinsky, I.K. Surin, Yu.A. Tikhonov, A.V. Vasiljev, P.Yu. Shatunov, Yu.M. Shatunov, D.A. Shtol, D.B. Shwartz, Yu.M. Usov, I.M. Zemlyansky. Study of the process e+e– $\rightarrow$ π+π– π0π0 with SND at VEPP2000. // XV Intern. Conference on Hadron Spectroscopy, Hadron 2013, November 4 - 8, 2013, Nara, Japan, to be published in PoS. - Proc. of Science.

[581] M.N. Achasov, V.M. Aulchenko, A.Yu. Barnyakov, K.I. Beloborodov, A.V. Berdyugin, D.E. Berkaev, A.G. Bogdanchikov, A.A. Botov, T.V. Dimova, V.P. Druzhinin, V.B. Golubev, K.A. Grevtsov, L.V. Kardapoltsev, A.S. Kupich,A.G. Kharlamov, D.P. Kovrizhin, I.A. Koop, A.A. Korol, S.V. Koshuba, K.A. Martin, A.E. Obrazovsky, E.V. Pakhtusova, Yu.A. Rogovskii, S.I. Serednyakov, Z.K. Silagadze, K.Yu. Skovpen, A.N. Skrinsky, I.K. Surin, Yu.A. Tikhonov, A.V. Vasiljev, P.Yu. Shatunov, Yu.M. Shatunov, D.A.

Shtol, D.B. Shwartz, Yu.M. Usov, I.M. Zemlyansky. Measurement of the e+e– → η π+π– cross section with SND detector at VEPP2000 e+e–-collider in the energy range 1.08 - 2.00 GeV. // XV Intern. Conference on Hadron Spectroscopy, Hadron 2013, November 4 - 8, 2013, Nara, Japan, to be published in PoS. - Proc. of Science.

[582] M.N. Achasov, V.M. Aulchenko, A.Yu. Barnyakov, K.I. Beloborodov, A.V. Berdyugin, D.E. Berkaev, A.G. Bogdanchikov, A.A. Botov, T.V. Dimova, V.P. Druzhinin, V.B. Golubev, K.A. Grevtsov, L.V. Kardapoltsev, A.S. Kupich,A.G. Kharlamov, D.P. Kovrizhin, I.A. Koop, A.A. Korol, S.V. Koshuba, K.A. Martin, A.E. Obrazovsky, E.V. Pakhtusova, Yu.A. Rogovskii, S.I. Serednyakov, Z.K. Silagadze, K.Yu. Skovpen, A.N. Skrinsky, I.K. Surin, Yu.A. Tikhonov, A.V. Vasiljev, P.Yu. Shatunov, Yu.M. Shatunov, D.A. Shtol, D.B. Shwartz, Yu.M. Usov, I.M. Zemlyansky. Measurement of the neutron time like form factor in the process e+e– → n $\bar{n}$. // Report at the Session Conference Section of the DPS RAS uclear Physics Section. IHEP, 5 - 8 November, 2013, Protvino.

[583] M.N. Achasov, V.M. Aulchenko, A.Yu. Barnyakov, K.I. Beloborodov, A.V. Berdyugin, D.E. Berkaev, A.G. Bogdanchikov, A.A. Botov, T.V. Dimova, V.P. Druzhinin, V.B. Golubev, K.A. Grevtsov, L.V. Kardapoltsev, A.S. Kupich, A.G. Kharlamov, D.P. Kovrizhin, I.A. Koop, A.A. Korol, S.V. Koshuba, K.A. Martin, A.E. Obrazovsky, E.V. Pakhtusova, Yu.A. Rogovskii, S.I. Serednyakov, Z.K. Silagadze, K.Yu. Skovpen, A.N. Skrinsky, I.K. Surin, Yu.A. Tikhonov, A.V. Vasiljev, P.Yu. Shatunov, Yu.M. Shatunov, D.A. Shtol, D.B. Shwartz, Yu.M. Usov, I.M. Zemlyansky. Measurement of the e+e– → π0π0γ cross section with SND detector at VEPP2000 e+e– -collider in the energy range 1 - 2 GeV. // XV Intern. Conference on Hadron Spectroscopy, Hadron 2013, November 4 – 8, 2013, Nara, Japan, to be publ. in PoS. Proc. of Science.

[584] V.V. Anashin, V.M. Aulchenko, E.M. Baldin, A.K. Barladyan, A.Yu. Barnyakov, M.Yu. Barnyakov, S.E. Baru, I.Yu. Basok, O.L. Rezanova, A.E. Blinov, V.E. Blinov, A.V. Bobrov, V.S. Bobrov, A.V. Bogomyagkov, A.E. Bondar, A.R. Buzykaev, A.I. Vorobiev, Yu.M. Glukhovchenko, D.N. Grigoriev, V.V. Gulevich, D.V. Gusev, V.N. Zhylich, V.V. Zhulanov, A.N. Zhuravlev, S.E. Karnaev, G.V. Karpov, S.V. Karpov, V.A. Kiselev, V.V. Kolmogorov, S.A. Kononov, K.Yu. Kotov, E.A. Kravchenko, V.N. Kudryavtsev, V.F. Kulikov, G.Ya. Kurkin, E.A. Cooper, E.B. Levichev, D.A. Maksimov, V.M. Malyshev, A.L. Maslennikov, A.S. Medvedko, O.I. Meshkov, S.I. Mishnev, I.I. Morozov, N.Yu. Muchnoi, V.V. Neufeld, S.A. Nikitin, I.B. Nikolaev, I.N. Okunev, A.P. Onuchin, S.B. Oreshkin, I.O. Orlov, A.A. Osipov, S.V. Peleganchuk, V.V. Petrov, S.G. Pivovarov, P.A. Piminov, A.O. Poluektov, V.G. Prisekin, AA. Ruban, G.A. Savinov, V.K. Sandyrev, E.A. Simonov, S.V. Sinyatkin, A.N. Skrinsky, V.V. Smalyuk, A.V. Sokolov, E.V. Starostina, A.M. Sukharev, A.A. Talyshev, V.A. Tayursky, V.I. Telnov, Yu.A. Tikhonov, K.Yu. Todyshev, G.M. Tumaikin, Yu.V Usov, T.A. Kharlamova, A.G. Shamov, D.N. Shatilov, B.A. Schwartz, S.I. Eidelman, A.N. Yushkov. Overview of KEDR detector results (in Russian). // Report at the Session Conference of the DPS RAS Nuclear Physics Section, 5 - 8 November 2013, Protvino, Russia .

[585] V.V. Anashin, V.M. Aulchenko, E.M. Baldin, A.K. Barladyan, A.Yu. Barnyakov, M.Yu. Barnyakov, S.E. Baru, I.Yu. Basok, O.L. Rezanova, A.E. Blinov, V.E. Blinov, A.V. Bobrov, V.S. Bobrov, A.V. Bogomyagkov, A.E. Bondar, A.R. Buzykaev, A.I. Vorobiev, Yu.M. Glukhovchenko, D.N. Grigoriev, V.V. Gulevich, D.V. Gusev, V.N. Zhylich, V.V. Zhulanov, A.N. Zhuravlev, S.E. Karnaev, G.V. Karpov, S.V. Karpov, V.A. Kiselev, V.V. Kolmogorov, S.A. Kononov, K.Yu. Kotov, E.A. Kravchenko, V.N. Kudryavtsev, V.F. Kulikov, G.Ya. Kurkin, E.A. Cooper, E.B. Levichev, D.A. Maksimov, V.M. Malyshev, A.L. Maslennikov, A.S. Medvedko, O.I. Meshkov, S.I. Mishnev, I.I. Morozov, N.Yu. Muchnoi, V.V. Neufeld, S.A. Nikitin, I.B. Nikolaev, I.N. Okunev, A.P. Onuchin, S.B. Oreshkin, I.O. Orlov, A.A. Osipov, S.V. Peleganchuk, V.V. Petrov, S.G. Pivovarov, P.A. Piminov, A.O. Poluektov, V.G. Prisekin, AA. Ruban, G.A. Savinov, V.K. Sandyrev, E.A. Simonov, S.V. Sinyatkin, A.N. Skrinsky, V.V. Smalyuk, A.V. Sokolov, E.V. Starostina, A.M. Sukharev, A.A. Talyshev, V.A. Tayursky, V.I. Telnov, Yu.A. Tikhonov, K.Yu. Todyshev, G.M. Tumaikin, Yu.V Usov, T.A. Kharlamova, A.G. Shamov, D.N. Shatilov, B.A. Schwartz, S.I. Eidelman, A.N. Yushkov. Measurement of the Гее·Bh J/ψ-meson (in Russian). // Report at the Session Conference Section of the DPS RAS uclear Physics Section. IHEP, 5 - 8 November, 2013, Protvino.

[586] V.V. Anashin, V.M. Aulchenko, E.M. Baldin, A.K. Barladyan, A.Yu. Barnyakov, M.Yu. Barnyakov, S.E. Baru, I.Yu. Basok, O.L. Rezanova, A.E. Blinov, V.E. Blinov, A.V. Bobrov, V.S. Bobrov, A.V. Bogomyagkov, A.E. Bondar, A.R. Buzykaev, A.I. Vorobiev, Yu.M. Glukhovchenko, D.N. Grigoriev, V.V. Gulevich, D.V. Gusev, V.N. Zhylich, V.V. Zhulanov, A.N. Zhuravlev, S.E. Karnaev, G.V. Karpov, S.V. Karpov, V.A. Kiselev, V.V. Kolmogorov, S.A. Kononov, K.Yu. Kotov, E.A. Kravchenko, V.N. Kudryavtsev, V.F. Kulikov, G.Ya. Kurkin, E.A. Cooper, E.B. Levichev, D.A. Maksimov, V.M. Malyshev, A.L. Maslennikov, A.S. Medvedko, O.I. Meshkov, S.I. Mishnev, I.I. Morozov, N.Yu. Muchnoi, V.V. Neufeld, S.A. Nikitin, I.B. Nikolaev, I.N. Okunev, A.P. Onuchin, S.B. Oreshkin, I.O. Orlov, A.A. Osipov, S.V. Peleganchuk, V.V. Petrov, S.G. Pivovarov, P.A. Piminov, A.O. Poluektov, V.G. Prisekin, AA. Ruban, G.A. Savinov, V.K. Sandyrev, E.A. Simonov, S.V. Sinyatkin, A.N. Skrinsky, V.V. Smalyuk, A.V. Sokolov, E.V. Starostina, A.M. Sukharev, A.A. Talyshev, V.A. Tayursky, V.I. Telnov, Yu.A. Tikhonov, K.Yu. Todyshev, G.M.

Tumaikin, Yu.V Usov, T.A. Kharlamova, A.G. Shamov, D.N. Shatilov, B.A. Schwartz, S.I. Eidelman, A.N. Yushkov. Measurement of the ratio of the Γee/Γμμ widths of J/ψ meson (in Russian). // Report at the Session Conference Section of the DPS RAS uclear Physics Section. IHEP, 5 - 8 November, 2013, Protvino.

[587] V.V. Anashin, V.M. Aulchenko, E.M. Baldin, A.K. Barladyan, A.Yu. Barnyakov, M.Yu. Barnyakov, S.E. Baru, I.Yu. Basok, O.L. Rezanova, A.E. Blinov, V.E. Blinov, A.V. Bobrov, V.S. Bobrov, A.V. Bogomyagkov, A.E. Bondar, A.R. Buzykaev, A.I. Vorobiev, Yu.M. Glukhovchenko, D.N. Grigoriev, V.V. Gulevich, D.V. Gusev, V.N. Zhylich, V.V. Zhulanov, A.N. Zhuravlev, S.E. Karnaev, G.V. Karpov, S.V. Karpov, V.A. Kiselev, V.V. Kolmogorov, S.A. Kononov, K.Yu. Kotov, E.A. Kravchenko, V.N. Kudryavtsev, V.F. Kulikov, G.Ya. Kurkin, E.A. Cooper, E.B. Levichev, D.A. Maksimov, V.M. Malyshev, A.L. Maslennikov, A.S. Medvedko, O.I. Meshkov, S.I. Mishnev, I.I. Morozov, N.Yu. Muchnoi, V.V. Neufeld, S.A. Nikitin, I.B. Nikolaev, I.N. Okunev, A.P. Onuchin, S.B. Oreshkin, I.O. Orlov, A.A. Osipov, S.V. Peleganchuk, V.V. Petrov, S.G. Pivovarov, P.A. Piminov, A.O. Poluektov, V.G. Prisekin, AA. Ruban, G.A. Savinov, V.K. Sandyrev, E.A. Simonov, S.V. Sinyatkin, A.N. Skrinsky, V.V. Smalyuk, A.V. Sokolov, E.V. Starostina, A.M. Sukharev, A.A. Talyshev, V.A. Tayursky, V.I. Telnov, Yu.A. Tikhonov, K.Yu. Todyshev, G.M. Tumaikin, Yu.V Usov, T.A. Kharlamova, A.G. Shamov, D.N. Shatilov, B.A. Schwartz, S.I. Eidelman, A.N. Yushkov. Measurement of the branching of the J/ψ → γηc decay and ηc parameters at KEDR (in Russian). // Measuring Γee·Brμμ of ψ(2S) meson (in Russian).

[588] V.V. Anashin, V.M. Aulchenko, E.M. Baldin, A.K. Barladyan, A.Yu. Barnyakov, M.Yu. Barnyakov, S.E. Baru, I.Yu. Basok, O.L. Rezanova, A.E. Blinov, V.E. Blinov, A.V. Bobrov, V.S. Bobrov, A.V. Bogomyagkov, A.E. Bondar, A.R. Buzykaev, A.I. Vorobiev, Yu.M. Glukhovchenko, D.N. Grigoriev, V.V. Gulevich, D.V. Gusev, V.N. Zhylich, V.V. Zhulanov, A.N. Zhuravlev, S.E. Karnaev, G.V. Karpov, S.V. Karpov, V.A. Kiselev, V.V. Kolmogorov, S.A. Kononov, K.Yu. Kotov, E.A. Kravchenko, V.N. Kudryavtsev, V.F. Kulikov, G.Ya. Kurkin, E.A. Cooper, E.B. Levichev, D.A. Maksimov, V.M. Malyshev, A.L. Maslennikov, A.S. Medvedko, O.I. Meshkov, S.I. Mishnev, I.I. Morozov, N.Yu. Muchnoi, V.V. Neufeld, S.A. Nikitin, I.B. Nikolaev, I.N. Okunev, A.P. Onuchin, S.B. Oreshkin, I.O. Orlov, A.A. Osipov, S.V. Peleganchuk, V.V. Petrov, S.G. Pivovarov, P.A. Piminov, A.O. Poluektov, V.G. Prisekin, AA. Ruban, G.A. Savinov, V.K. Sandyrev, E.A. Simonov, S.V. Sinyatkin, A.N. Skrinsky, V.V. Smalyuk, A.V. Sokolov, E.V. Starostina, A.M. Sukharev, A.A. Talyshev, V.A. Tayursky, V.I. Telnov, Yu.A. Tikhonov, K.Yu. Todyshev, G.M. Tumaikin, Yu.V Usov, T.A. Kharlamova, A.G. Shamov, D.N. Shatilov, B.A. Schwartz, S.I. Eidelman, A.N. Yushkov. Measurement of the Γee·Brμμ of ψ(2S) meson (in Russian). // Report at the Session Conference Section of the DPS RAS uclear Physics Section. IHEP, 5 - 8 November, 2013, Protvino.

[589] K.Yu. Todyshev, A.G. Shamov. Joint experimental data processing of BaBar, Belle, BES, CLEO and KEDR in the range of ψ(3770) (in Russian). // Report at the Session Conference section of the DPS RAS nuclear Physics Section. IHEP, 5 - 8 November 2013, Protvino.

[590] A.Yu. Barnyakov, M.Yu. Barnyakov, V.S. Bobrovnikov, A.R. Buzykaev, S.A. Kononov, E.A. Kravchenko, A.P. Onuchin. Test beam experiments with FARICH prototype (in Russian). // Report at the Session Conference Section of the DPS RAS uclear Physics Section. IHEP, 5 - 8 November, 2013, Protvino.

[591] V.V. Anashin, V.M. Aulchenko, E.M. Baldin, A.K. Barladyan, A.Yu. Barnyakov, M.Yu. Barnyakov, S.E. Baru, I.Yu. Basok, O.L. Rezanova, A.E. Blinov, V.E. Blinov, A.V. Bobrov, V.S. Bobrovnikov, A.V. Bogomyagkov, A.E. Bondar, A.R. Buzykaev, S.I. Eidelman, D.N. Grigoriev, Yu.M. Glukhovchenko, V.V. Gulevich, D.V. Gusev, S.E. Karnaev, G.V. Karpov, S.V. Karpov, T.A. Kharlamova, V.A. Kiselev, V.V. Kolmogorov, S.A. Kononov, K.Yu. Kotov, E.A. Kravchenko, V.F. Kulikov, G.Ya. Kurkin, E.A. Kuper, E.B. Levichev, D.A. Maksimov, V.M. Malyshev, A.L. Maslennikov, A.S. Medvedko, O.I. Meshkov, S.I. Mishnev, I.I. Morozov, N.Yu. Muchnoi, V.V. Neufeld, S.A. Nikitin, I.B. Nikolaev, I.N. Okunev, A.P. Onuchin, S.B. Oreshkin, I.O. Orlov, A.A. Osipov, S.V. Peleganchuk, S.G. Pivovarov, P.A. Piminov, V.V. Petrov, A.O. Poluektov, V.G. Prisekin, A.A. Ruban, V.K. Sandyrev, G.A. Savinov, A.G. Shamov, D.N. Shatilov, B.A. Shwartz, E.A. Simonov, S.V. Sinyatkin, A.N. Skrinsky, V.V. Smaluk, A.V. Sokolov, A.M. Sukharev, E.V. Starostina, A.A. Talyshev, V.A. Tayursky, V.I. Telnov, Yu.A. Tikhonov, K.Yu. Todyshev, G.M. Tumaikin, Yu.V. Usov, A.I. Vorobiov, A.N. Yushkov, V.N. Zhilich, V.V. Zhulanov, A.N. Zhuravlev. Test of leptonic universality in J/ψ decays. // The 2013 European Physical Society Conference on High Energy Physics (EPSHEP 2013), 18 - 24 July, 2013, Stockholm, Sweden.

[592] V.V. Anashin, V.M. Aulchenko, E.M. Baldin, A.K. Barladyan, A.Yu. Barnyakov, M.Yu. Barnyakov, S.E. Baru, I.Yu. Basok, O.L. Rezanova, A.E. Blinov, V.E. Blinov, A.V. Bobrov, V.S. Bobrovnikov, A.V. Bogomyagkov, A.E. Bondar, A.R. Buzykaev, S.I. Eidelman, D.N. Grigoriev, Yu.M. Glukhovchenko, V.V. Gulevich, D.V. Gusev, S.E. Karnaev, G.V. Karpov, S.V. Karpov, T.A. Kharlamova, V.A. Kiselev, V.V. Kolmogorov, S.A. Kononov, K.Yu. Kotov, E.A. Kravchenko, V.F. Kulikov, G.Ya. Kurkin, E.A. Kuper, E.B. Levichev, D.A. Maksimov, V.M. Malyshev, A.L. Maslennikov, A.S. Medvedko, O.I. Meshkov, S.I. Mishnev, I.I. Morozov, N.Yu. Muchnoi, V.V. Neufeld, S.A. Nikitin, I.B. Nikolaev, I.N. Okunev, A.P. Onuchin, S.B. Oreshkin, I.O. Orlov, A.A. Osipov, S.V. Peleganchuk, S.G. Pivovarov, P.A. Piminov, V.V. Petrov,

A.O. Poluektov, V.G. Prisekin, A.A. Ruban, V.K. Sandyrev, G.A. Savinov, A.G. Shamov, D.N. Shatilov, B.A. Shwartz, E.A. Simonov, S.V. Sinyatkin, A.N. Skrinsky, V.V. Smaluk, A.V. Sokolov, A.M. Sukharev, E.V. Starostina, A.A. Talyshev, V.A. Tayursky, V.I. Telnov, Yu.A. Tikhonov, K.Yu. Todyshev, G.M. Tumaikin, Yu.V. Usov, A.I. Vorobiov, A.N. Yushkov, V.N. Zhilich, V.V. Zhulanov, A.N. Zhuravlev. Results from KEDR on charmonium spectroscopy. // VIII Intern. Workshop of QWG, April 22 – 26 2013, Beijing, China.

[593] V.V. Anashin, V.M. Aulchenko, E.M. Baldin, A.K. Barladyan, A.Yu. Barnyakov, M.Yu. Barnyakov, S.E. Baru, I.Yu. Basok, O.L. Rezanova, A.E. Blinov, V.E. Blinov, A.V. Bobrov, V.S. Bobrovnikov, A.V. Bogomyagkov, A.E. Bondar, A.R. Buzykaev, S.I. Eidelman, D.N. Grigoriev, Yu.M. Glukhovchenko, V.V. Gulevich, D.V. Gusev, S.E. Karnaev, G.V. Karpov, S.V. Karpov, T.A. Kharlamova, V.A. Kiselev, V.V. Kolmogorov, S.A. Kononov, K.Yu. Kotov, E.A. Kravchenko, V.F. Kulikov, G.Ya. Kurkin, E.A. Kuper, E.B. Levichev, D.A. Maksimov, V.M. Malyshev, A.L. Maslennikov, A.S. Medvedko, O.I. Meshkov, S.I. Mishnev, I.I. Morozov, N.Yu. Muchnoi, V.V. Neufeld, S.A. Nikitin, I.B. Nikolaev, I.N. Okunev, A.P. Onuchin, S.B. Oreshkin, I.O. Orlov, A.A. Osipov, S.V. Peleganchuk, S.G. Pivovarov, P.A. Piminov, V.V. Petrov, A.O. Poluektov, V.G. Prisekin, A.A. Ruban, V.K. Sandyrev, G.A. Savinov, A.G. Shamov, D.N. Shatilov, B.A. Shwartz, E.A. Simonov, S.V. Sinyatkin, A.N. Skrinsky, V.V. Smaluk, A.V. Sokolov, A.M. Sukharev, E.V. Starostina, A.A. Talyshev, V.A. Tayursky, V.I. Telnov, Yu.A. Tikhonov, K.Yu. Todyshev, G.M. Tumaikin, Yu.V. Usov, A.I. Vorobiov, A.N. Yushkov, V.N. Zhilich, V.V. Zhulanov, A.N. Zhuravlev. Parameters of charmonium states from KEDR. // Conference “From phi to psi”, September 9 - 12, Rome, Italy. [arXiv:1311.7530 [hep-ex]].

[594] V.V. Anashin, V.M. Aulchenko, E.M. Baldin, A.K. Barladyan, A.Yu. Barnyakov, M.Yu. Barnyakov, S.E. Baru, I.Yu. Basok, O.L. Rezanova, A.E. Blinov, V.E. Blinov, A.V. Bobrov, V.S. Bobrovnikov, A.V. Bogomyagkov, A.E. Bondar, A.R. Buzykaev, S.I. Eidelman, D.N. Grigoriev, Yu.M. Glukhovchenko, V.V. Gulevich, D.V. Gusev, S.E. Karnaev, G.V. Karpov, S.V. Karpov, T.A. Kharlamova, V.A. Kiselev, V.V. Kolmogorov, S.A. Kononov, K.Yu. Kotov, E.A. Kravchenko, V.F. Kulikov, G.Ya. Kurkin, E.A. Kuper, E.B. Levichev, D.A. Maksimov, V.M. Malyshev, A.L. Maslennikov, A.S. Medvedko, O.I. Meshkov, S.I. Mishnev, I.I. Morozov, N.Yu. Muchnoi, V.V. Neufeld, S.A. Nikitin, I.B. Nikolaev, I.N. Okunev, A.P. Onuchin, S.B. Oreshkin, I.O. Orlov, A.A. Osipov, S.V. Peleganchuk, S.G. Pivovarov, P.A. Piminov, V.V. Petrov, A.O. Poluektov, V.G. Prisekin, A.A. Ruban, V.K. Sandyrev, G.A. Savinov, A.G. Shamov, D.N. Shatilov, B.A. Shwartz, E.A. Simonov, S.V. Sinyatkin, A.N. Skrinsky, V.V. Smaluk, A.V. Sokolov, A.M. Sukharev, E.V. Starostina, A.A. Talyshev, V.A. Tayursky, V.I. Telnov, Yu.A. Tikhonov, K.Yu. Todyshev, G.M. Tumaikin, Yu.V. Usov, A.I. Vorobiov, A.N. Yushkov, V.N. Zhilich, V.V. Zhulanov, A.N. Zhuravlev. Study of $\psi(2S) \to \mu^+\mu^-$ decay with KEDR detector. // From phi to psi, September 9 - 12, Rome, Italy.

[595] V.V. Anashin, V.M. Aulchenko, E.M. Baldin, A.K. Barladyan, A.Yu. Barnyakov, M.Yu. Barnyakov, S.E. Baru, I.Yu. Basok, O.L. Rezanova, A.E. Blinov, V.E. Blinov, A.V. Bobrov, V.S. Bobrovnikov, A.V. Bogomyagkov, A.E. Bondar, A.R. Buzykaev, S.I. Eidelman, D.N. Grigoriev, Yu.M. Glukhovchenko, V.V. Gulevich, D.V. Gusev, S.E. Karnaev, G.V. Karpov, S.V. Karpov, T.A. Kharlamova, V.A. Kiselev, V.V. Kolmogorov, S.A. Kononov, K.Yu. Kotov, E.A. Kravchenko, V.F. Kulikov, G.Ya. Kurkin, E.A. Kuper, E.B. Levichev, D.A. Maksimov, V.M. Malyshev, A.L. Maslennikov, A.S. Medvedko, O.I. Meshkov, S.I. Mishnev, I.I. Morozov, N.Yu. Muchnoi, V.V. Neufeld, S.A. Nikitin, I.B. Nikolaev, I.N. Okunev, A.P. Onuchin, S.B. Oreshkin, I.O. Orlov, A.A. Osipov, S.V. Peleganchuk, S.G. Pivovarov, P.A. Piminov, V.V. Petrov, A.O. Poluektov, V.G. Prisekin, A.A. Ruban, V.K. Sandyrev, G.A. Savinov, A.G. Shamov, D.N. Shatilov, B.A. Shwartz, E.A. Simonov, S.V. Sinyatkin, A.N. Skrinsky, V.V. Smaluk, A.V. Sokolov, A.M. Sukharev, E.V. Starostina, A.A. Talyshev, V.A. Tayursky, V.I. Telnov, Yu.A. Tikhonov, K.Yu. Todyshev, G.M. Tumaikin, Yu.V. Usov, A.I. Vorobiov, A.N. Yushkov, V.N. Zhilich, V.V. Zhulanov, A.N. Zhuravlev. Joint analysis of the data in the $\psi(3770)$ energy range. // From phi to psi, September 9 - 12, Rome, Italy.

[596] V.V. Anashin, V.M. Aulchenko, E.M. Baldin, A.K. Barladyan, A.Yu. Barnyakov, M.Yu. Barnyakov, S.E. Baru, I.Yu. Basok, O.L. Rezanova, A.E. Blinov, V.E. Blinov, A.V. Bobrov, V.S. Bobrov, A.V. Bogomyagkov, A.E. Bondar, A.R. Buzykaev, A.I. Vorobiev, Yu.M. Glukhovchenko, D.N. Grigoriev, V.V. Gulevich, D.V. Gusev, V.N. Zhylich, V.V. Zhulanov, A.N. Zhuravlev, S.E. Karnaev, G.V. Karpov, S.V. Karpov, V.A. Kiselev, V.V. Kolmogorov, S.A. Kononov, K.Yu. Kotov, E.A. Kravchenko, V.N. Kudryavtsev, V.F. Kulikov, G.Ya. Kurkin, E.A. Cooper, E.B. Levichev, D.A. Maksimov, V.M. Malyshev, A.L. Maslennikov, A.S. Medvedko, O.I. Meshkov, S.I. Mishnev, I.I. Morozov, N.Yu. Muchnoi, V.V. Neufeld, S.A. Nikitin, I.B. Nikolaev, I.N. Okunev, A.P. Onuchin, S.B. Oreshkin, I.O. Orlov, A.A. Osipov, S.V. Peleganchuk, V.V. Petrov, S.G. Pivovarov, P.A. Piminov, A.O. Poluektov, V.G. Prisekin, AA. Ruban, G.A. Savinov, V.K. Sandyrev, E.A. Simonov, S.V. Sinyatkin, A.N. Skrinsky, V.V. Smalyuk, A.V. Sokolov, E.V. Starostina, A.M. Sukharev, A.A. Talyshev, V.A. Tayursky, V.I. Telnov, Yu.A. Tikhonov, K.Yu. Todyshev, G.M. Tumaikin, Yu.V Usov, T.A. Kharlamova, A.G. Shamov, D.N. Shatilov, B.A. Schwartz, S.I. Eidelman, A.N. Yushkov. KEDR detector results (in Russian). // VI All-Russian Meeting on Fundamental Constants and

Precision Measurements, October 7 - 11, St. Petersburg, Russia

[597] V.V. Anashin, V.M. Aulchenko, E.M. Baldin, A.K. Barladyan, A.Yu. Barnyakov, M.Yu. Barnyakov, S.E. Baru, I.Yu. Basok, O.L. Rezanova, A.E. Blinov, V.E. Blinov, A.V. Bobrov, V.S. Bobrovnikov, A.V. Bogomyagkov, A.E. Bondar, A.R. Buzykaev, S.I. Eidelman, D.N. Grigoriev, Yu.M. Glukhovchenko, V.V. Gulevich, D.V. Gusev, S.E. Karnaev, G.V. Karpov, S.V. Karpov, T.A. Kharlamova, V.A. Kiselev, V.V. Kolmogorov, S.A. Kononov, K.Yu. Kotov, E.A. Kravchenko, V.F. Kulikov, G.Ya. Kurkin, E.A. Kuper, E.B. Levichev, D.A. Maksimov, V.M. Malyshev, A.L. Maslennikov, A.S. Medvedko, O.I. Meshkov, S.I. Mishnev, I.I. Morozov, N.Yu. Muchnoi, V.V. Neufeld, S.A. Nikitin, I.B. Nikolaev, I.N. Okunev, A.P. Onuchin, S.B. Oreshkin, I.O. Orlov, A.A. Osipov, S.V. Peleganchuk, S.G. Pivovarov, P.A. Piminov, V.V. Petrov, A.O. Poluektov, V.G. Prisekin, A.A. Ruban, V.K. Sandyrev, G.A. Savinov, A.G. Shamov, D.N. Shatilov, B.A. Shwartz, E.A. Simonov, S.V. Sinyatkin, A.N. Skrinsky, V.V. Smaluk, A.V. Sokolov, A.M. Sukharev, E.V. Starostina, A.A. Talyshev, V.A. Tayursky, V.I. Telnov, Yu.A. Tikhonov, K.Yu. Todyshev, G.M. Tumaikin, Yu.V. Usov, A.I. Vorobiov, A.N. Yushkov, V.N. Zhilich, V.V. Zhulanov, A.N. Zhuravlev. Results from e+e- colliders in Novosibirsk. // Intern. Symposium on Lepton and Hadron Physics at Meson, Factories, October 13 - 15, Messina, Italy.

[598] V.V. Anashin, V.M. Aulchenko, E.M. Baldin, A.K. Barladyan, A.Yu. Barnyakov, M.Yu. Barnyakov, S.E. Baru, I.Yu. Basok, O.L. Rezanova, A.E. Blinov, V.E. Blinov, A.V. Bobrov, V.S. Bobrovnikov, A.V. Bogomyagkov, A.E. Bondar, A.R. Buzykaev, S.I. Eidelman, D.N. Grigoriev, Yu.M. Glukhovchenko, V.V. Gulevich, D.V. Gusev, S.E. Karnaev, G.V. Karpov, S.V. Karpov, T.A. Kharlamova, V.A. Kiselev, V.V. Kolmogorov, S.A. Kononov, K.Yu. Kotov, E.A. Kravchenko, V.F. Kulikov, G.Ya. Kurkin, E.A. Kuper, E.B. Levichev, D.A. Maksimov, V.M. Malyshev, A.L. Maslennikov, A.S. Medvedko, O.I. Meshkov, S.I. Mishnev, I.I. Morozov, N.Yu. Muchnoi, V.V. Neufeld, S.A. Nikitin, I.B. Nikolaev, I.N. Okunev, A.P. Onuchin, S.B. Oreshkin, I.O. Orlov, A.A. Osipov, S.V. Peleganchuk, S.G. Pivovarov, P.A. Piminov, V.V. Petrov, A.O. Poluektov, V.G. Prisekin, A.A. Ruban, V.K. Sandyrev, G.A. Savinov, A.G. Shamov, D.N. Shatilov, B.A. Shwartz, E.A. Simonov, S.V. Sinyatkin, A.N. Skrinsky, V.V. Smaluk, A.V. Sokolov, A.M. Sukharev, E.V. Starostina, A.A. Talyshev, V.A. Tayursky, V.I. Telnov, Yu.A. Tikhonov, K.Yu. Todyshev, G.M. Tumaikin, Yu.V. Usov, A.I. Vorobiov, A.N. Yushkov, V.N. Zhilich, V.V. Zhulanov, A.N. Zhuravlev. Recent results from the KEDR detector. // XV Intern. Conference on Hadron Spectroscopy, Hadron 2013, November 4 - 8, 2013, Nara, Japan.

[599] V.V. Anashin, V.M. Aulchenko, E.M. Baldin, A.K. Barladyan, A.Yu. Barnyakov, M.Yu. Barnyakov, S.E. Baru, I.Yu. Basok, O.L. Rezanova, A.E. Blinov, V.E. Blinov, A.V. Bobrov, V.S. Bobrovnikov, A.V. Bogomyagkov, A.E. Bondar, A.R. Buzykaev, S.I. Eidelman, D.N. Grigoriev, Yu.M. Glukhovchenko, V.V. Gulevich, D.V. Gusev, S.E. Karnaev, G.V. Karpov, S.V. Karpov, T.A. Kharlamova, V.A. Kiselev, V.V. Kolmogorov, S.A. Kononov, K.Yu. Kotov, E.A. Kravchenko, V.F. Kulikov, G.Ya. Kurkin, E.A. Kuper, E.B. Levichev, D.A. Maksimov, V.M. Malyshev, A.L. Maslennikov, A.S. Medvedko, O.I. Meshkov, S.I. Mishnev, I.I. Morozov, N.Yu. Muchnoi, V.V. Neufeld, S.A. Nikitin, I.B. Nikolaev, I.N. Okunev, A.P. Onuchin, S.B. Oreshkin, I.O. Orlov, A.A. Osipov, S.V. Peleganchuk, S.G. Pivovarov, P.A. Piminov, V.V. Petrov, A.O. Poluektov, V.G. Prisekin, A.A. Ruban, V.K. Sandyrev, G.A. Savinov, A.G. Shamov, D.N. Shatilov, B.A. Shwartz, E.A. Simonov, S.V. Sinyatkin, A.N. Skrinsky, V.V. Smaluk, A.V. Sokolov, A.M. Sukharev, E.V. Starostina, A.A. Talyshev, V.A. Tayursky, V.I. Telnov, Yu.A. Tikhonov, K.Yu. Todyshev, G.M. Tumaikin, Yu.V. Usov, A.I. Vorobiov, A.N. Yushkov, V.N. Zhilich, V.V. Zhulanov, A.N. Zhuravlev. Recent results from the KEDR detector. // Development of MCP PMT for aerogel Cherenkov counters at BINP. // 4th Asian Forum for Accelerators and Detectors. 25 - 26 February 2013, Novosibirsk, Russia.

[600] V.V. Anashin, V.M. Aulchenko, E.M. Baldin, A.K. Barladyan, A.Yu. Barnyakov, M.Yu. Barnyakov, S.E. Baru, I.Yu. Basok, O.L. Rezanova, A.E. Blinov, V.E. Blinov, A.V. Bobrov, V.S. Bobrovnikov, A.V. Bogomyagkov, A.E. Bondar, A.R. Buzykaev, S.I. Eidelman, D.N. Grigoriev, Yu.M. Glukhovchenko, V.V. Gulevich, D.V. Gusev, S.E. Karnaev, G.V. Karpov, S.V. Karpov, T.A. Kharlamova, V.A. Kiselev, V.V. Kolmogorov, S.A. Kononov, K.Yu. Kotov, E.A. Kravchenko, V.F. Kulikov, G.Ya. Kurkin, E.A. Kuper, E.B. Levichev, D.A. Maksimov, V.M. Malyshev, A.L. Maslennikov, A.S. Medvedko, O.I. Meshkov, S.I. Mishnev, I.I. Morozov, N.Yu. Muchnoi, V.V. Neufeld, S.A. Nikitin, I.B. Nikolaev, I.N. Okunev, A.P. Onuchin, S.B. Oreshkin, I.O. Orlov, A.A. Osipov, S.V. Peleganchuk, S.G. Pivovarov, P.A. Piminov, V.V. Petrov, A.O. Poluektov, V.G. Prisekin, A.A. Ruban, V.K. Sandyrev, G.A. Savinov, A.G. Shamov, D.N. Shatilov, B.A. Shwartz, E.A. Simonov, S.V. Sinyatkin, A.N. Skrinsky, V.V. Smaluk, A.V. Sokolov, A.M. Sukharev, E.V. Starostina, A.A. Talyshev, V.A. Tayursky, V.I. Telnov, Yu.A. Tikhonov, K.Yu. Todyshev, G.M. Tumaikin, Yu.V. Usov, A.I. Vorobiov, A.N. Yushkov, V.N. Zhilich, V.V. Zhulanov, A.N. Zhuravlev. Recent results from the KEDR detector. // HEP data analysis at BINP using the virtualized HPC infrastructure of the Novosibirsk Scientific Center. // 4th Asian Forum for Accelerators and Detectors. 25 - 26 February 2013, Novosibirsk, Russia.

[601] S.A. Kononov. Beam test of FARICH prototype with DPC (dSiPM). // 13th Vienna Conference on

Instrumentation (VCI 2013), February 2013, Vienna, Austria.

[602] E.A. Kravchenko. Tests of FARICH prototype with fine photon position detection. // 8th Intern. Workshop on Ring Imaging Cherenkov Detectors (RICH 2013), December 2013, Japan.

[603] A.A. Anikeev, P.A. Bagryansky, A.D. Beklemishev, K.V. Zaitsev, A.A. Ivanov, Yu.V. Kovalenko, M.S. Korzhavina, A.A. Lizunov, V.V. Maksimov, S.V. Murakhtin, E.I. Pinzhenin, V.V. Prikhodko, V.Ya. Savkin, E.I. Soldatkina, A.L. Solomakhin, D.V. Yurov. Results of experiments to support the project of neutron source based on axisymmetric open-type magnetic trap (in Russian), XL Int. (Zvenigorod) conference on plasma physics and CF, 11 - 15 February, 2013, Zvenigorod: Abstracts. - M.: PLAZMAIOFAN, 2013. - P.13.

[604] E.I. Soldatkina, A.S. Arakcheev, P.A. Bagryansky, V.V. Maximov, Gas-dynamic trap as a stand for study of plasma-surface interaction (in Russian). // XL Int. (Zvenigorod) conference on plasma physics and CF, February 11 - February 15, 2013, Zvenigorod: Abstracts. - M.: PLAZMAIOFAN, 2013. - P.33

[605] A.L. Solomakhin, P.A. Bagryansky, P.V. Kalinin, Yu.V. Kovalenko, V.Ya. Savkin, M. Thumm, D.V. Yakovlev. The first results on the ECR plasma heating at the GDL device. // XL Intern. Zvenigorod Conference on Plasma Physics and Controlled Fusion, Zvenigorod, - 15 February 2013: Abstracts. - M.: PLASMAIOFAN, 2013. - P.32.

[606] D.V. Yakovlev, P.A. Bagryansky, P.V. Kalinin, Yu.V. Kovalenko, S.A. Kuznetsov, V.Ya. Savkin, A.L. Solomakhin, M. Thumm. ECR heating system on the GDL device. // XL Intern. Zvenigorod Conference on Plasma Physics and Controlled Fusion, 11 - 15 February 2013 Zvenigorod: Abstracts. - M.: PLASMAIOFAN, 2013. - P.72.

[607] Bagryansky, S.A. Brednikhin, S.I. Lezhnin, V.V. Prikhodko, S.A. Frolov, Yu.A. Tsidulko D.V. Yurov. Simulation of plasma neutron processes in subcritical hybrid system with an open-trap based on source (in Russian). // XL Int. (Zvenigorod) conference on plasma physics and CF, 11 – 15 February, 2013 Zvenigorod: Abstracts. - M.: PLAZMAIOFAN, 2013. - P.74.

[608] O.A. Korobeinikova, S.V. Murahtin. Microinstability influence on longitudinal loss of fast ions in the GDT device (in Russian). // XL Int. (Zvenigorod) conference on plasma physics and CF, 11 - 15 February, 2013, Zvenigorod: Abstracts. - M.: PLAZMAIOFAN, 2013. - P.47.

[609] A.A. Lizunov, A.S. Donin, A.A. Ivanov, A.N. Kvashnin, A.D. Khilchenko. MSE spectral diagnostics to measure spatial profiles of magnetic field in GDT plasma (in Russian). // Abstracts of XV National Conference on high-temperature plasma diagnostics, 3 -7 June, 2013, Zvenigorod, Moscow region. - P.49.

[610] P.A. Bagryansky, K.V. Zaitsev, M.S. Korzhavina, A.A. Lizunov, V.V. Prikhodko. Diagnostics of kinetic plasma instabilities at the GDT facility (in Russian). // Abstracts of XV National Conference on high-temperature plasma diagnostics, 3 – 7 June, 2013, Zvenigorod, Moscow region. - P.99.

[611] E.I. Pinzhenin, V.V. Maximov. Multi-channel system for detection of nuclear fusion products at the gas dynamic trap facility (in Russian). // Abstracts of XV National Conference on high-temperature plasma diagnostics, 3 - 7 June, 2013, Zvenigorod, Moscow region., P.121.

[612] A.V. Anikeev, P.A. Bagryansky, S.A. Brednikhin, S.A. Frolov, S.I. Lezhnin, V.V. Prikhodko, Yu.A. Tsidulko and D.V. Yurov. A neutron source based on gas dynamic trap for fusion-fission hybrid systems. // 40th European Physical Society Conference on Plasma Physics, 1 - 5 July 2013, Espoo, Finland.

[613] A.V. Anikeev, P.A. Bagryansky, A.S. Donin, A.A. Ivanov, M.S. Korzhavina, Yu.V. Kovalenko, A.A. Lizunov, V.V. Maximov, S.V. Murakhtin, E.I. Pinzhenin, V.V. Prikhodko, V.Ya. Savkin, E.I. Soldatkina, A.L. Solomakhin, K.V. Zaytsev. Experimental results in support of the neutron source based on an axisymmetric mirror trap. // 40th European Physical Society Conference on Plasma Physics, 1 - 5 July 2013, Espoo, Finland.

[614] P. Bagryansky, S. Ivanenko, A. Khilchenko, Yu. Kovalenko, A. Kvashnin, A. Lizunov, A. Solomakhin, V. Savkin. Perfomance analysis of a dispersion interferometer based on CO2 laser and roadmap for near-term development. // 40th European Physical Society Conference on Plasma Physics, 1 - 5 July 2013, Espoo, Finland.

[615] A. Khilchenko, V. Khilchenko, A. Kvashnin, A. Lizunov, P. Zubarev. Multipoint spectral motional Stark effect diagnostic for measurements of a local pressure-driven magnetic field variation in a plasma in the gas dynamic trap. // 40th European Physical Society Conference on Plasma Physics, 1 - 5 July 2013, Espoo, Finland.

[616] O.A. Korobeinikova. Microinstability influence on longitudinal loss of fast ions at the GDT facility (in Russian). // The 51th Int. Student Scientific Conference "Student and Scientific-Technical Progress", 12 - 18 April, 2013. BINP, Novosibirsk.

[617] Lenivtseva O.G., Butylenkova O.A., Golovin E.D., Golkovsky M.G. High-energy electron beam cladding of titanium and carbon on titanium alloy. // The 8 Intern. Forum on Strategic Technologies (IFOST 2013): proc. - Mongolia, Ulaanbaatar, 28 June - 1 July 2013. – Ulaanbaatar, 2013. - Vol.1. - P.152-155.

[618] Mul D.O., Golkovskii M.G., Bataev V.A., Krivezhenko D.S. // The 8 Intern. Forum on Strategic Technologies (IFOST 2013): Proc. - Mongolia,

Ulaanbaatar, 28 June - 1 July 2013. – Ulaanbaatar, 2013. - Vol.1. – P.147-149.

[619] S.P.Bardakhanov, I.K. Chakin, A.P.Zavyalov, K.V.Zobov, A.V.Nomoev. - Nanopowder production by electron beam technology. // Abstract, CD-ROM, Proc. of Intern. Congress on Particle Technology (PARTEC), 23 - 25 April, 2013. - Nurnberg, Germany. - 1 page. Oral statement.

[620] Cherepkov V.G., Golubenko Yu.I., Fadeev S.N., Korchagin A.I., Kuksanov N.K., Lavruhin A.V., Nemytov P.I., Salimov R.A., Semenov A.V. New development of HV ELV accelerators for Industrial applications and Research Experiments (Family of accelerators and development trends). // Shanghai 17th Intern. Meeting on Radiation Processing (IMRP 2013), 4 - 8 November. - 2013. - Handbook IMRP 17. - Programme and abstracts. - TC-139. - P. 235.

[621] Abd. Halim Baijan, Muhammad Zahidee Taat, Abu Bakar Ghazali, Sergey Fadeev, Mohd Rizal Md Chulan, Rokiah Mohd Sabri, Leo Kwee Wah, Mohd Rizal. cooling system for baby EBM scanning device. // NTC'09. Nuclear Malaysia Complex, Bangi, 6 - 8 October 2009. - Nada Nuclear Malaysia. - №1. - 2013. - P.22-23.

[622] Fadeev S.V. Electron beam accelerator technologies, principle and application. // Proc. of Workshop on Electron Beam Accelerator Technology, 25 November - 6 December 2013 - Malaysian Nuclear Agency Handbook. - Kuala Lumpur, Malaysia, 2013.

[623] A. Bogomyagkov, E. Levichev, D. Shatilov. Another look at IP parameters and luminosity of TLEP. // 6th TLEP Workshop, 16 - 18 October 2013, CERN.

[624] A. Bogomyagkov, E. Levichev, P. Piminov, S. Sinyatkin, K.Zolotarev. Design of a storage ring with diffraction limited emittance and large dynamic aperture. // 3rd Low Emittance Ring Workshop, 8 - 10 July, Oxford UK.

[625] A. Valishev, D. Shatilov, T. Pieloni. Beam-beam studies for HL-LHC. // Proc. of NA Particle Accelerator Conference (PAC'13), 29 September - 4 October 2013, Pasadena, USA.

[626] A. Valishev, S. Nagaitsev, D. Shatilov, V. Danilov, Beam-beam limit in an integrable system. // Proc. of NA Proc. of NA Particle Accelerator Conference (PAC'13), 29 September - 4 October 2013, Pasadena, USA.

[627] A.D. Beklemishev, A.V. Burdakov. Physical basis of the project fusion reactor based on open trap. // XL Intern. Zvenigorod Conference on Plasma Physics and Controlled Fusion, Zvenigorod, 11 - 15 February, 2013: Abstracts. - P.8.

[628] V.V. Postupaev, A.P. Avrorov, A.V. Arzhannikov, V.T. Astrelin, V.I. Batkin, A.V. Burdakov, V.S. Burmasov, L.N. Vyacheslavov, I.A. Ivanov, M.V. Ivantsivsky, I.V. Kandaurov, A.A. Kasatov, S.A. Kuznetsov, K.N. Kuklin, V.V. Kurkuchekov, K.I. Mekler, S.V. Polosatkin, S.S. Popov, A.F. Rovenskikh, V.F. Sklyarov, A.V. Sudnikov, Yu.S. Sulyaev, Yu.A. Trunev, A.A. Shoshin. Experiments with 100-mks electron beam on GOL-3 facility. // XL Intern. Zvenigorod Conference on Plasma Physics and Controlled Fusion, Zvenigorod, 11 - 15 February 2013: Abstracts. - M.: PLASMAIOFAN, 2013. - P.13.

[629] I.V. Kandaurov, V.V. Postupaev, A.P. Avrorov, V.T. Astrelin, V.I. Batkin, A.V. Burdakov, P.V. Bykov, G.E. Derevyankin, I.A. Ivanov, I.E. Karpov, V.V. Kurkuchekov, K.I. Mekler, S.V. Polosatkin, A.F. Rovenskikh, Yu.A. Trunev, V.A. Yarovoy. High power, long pulse electron beam source with plasma emitter designed for injection into linear plasma systems. // XL Intern. Zvenigorod Conference on Plasma Physics and Controlled Fusion, Zvenigorod, 11 - 15 February 2013: Abstracts. - M.: PLASMAIOFAN, 2013. - P.222.

[630] A.V. Sudnikov, A.V. Burdakov, D.E. Gavrilenko, I.V. Kandaurov, V.V. Kurkuchekov, S.V. Polosatkin, V.V. Postupaev, A.F. Rovenskikh, Yu.A. Trunev. Plasma magnetic activity during the injection of a long-pulse electron beam. // Abstracts of XL Intern. Zvenigorod Conference on Plasma Physics and Controlled Fusion, 11 - 15 February 2013. Zvenigorod: Abstracts. – M.: PLASMAIOFAN. - P.49.

[631] V.F. Sklyarov, A.V. Arzhannikov, A.V. Burdakov, V.S. Burmasov, L.N. Vyacheslavov, I.A. Ivanov, I.V. Kandaurov, S.A. Kuznetsov, V.V. Kurkuchekov, K.I. Mekler, S.V. Polosatkin, S.S. Popov, V.V. Postupaev, A.F. Rovenskikh, Yu.A. Trunev, M.K.A. Thumm. Generation of microwave radiation during relaxation of 100 keV electron beam in a plasma on the GOL-3. // XL Intern. Zvenigorod Conference on Plasma Physics and Controlled Fusion, 11 - 15 February, Zvenigorod: Abstracts. - M.: PLASMAIOFAN, 2013. - P.259.

[632] A.V. Arzhannikov, M.K.A. Thumm. Development of Investigations in LPIMTI NSU in Millimeter and Sub-Millimeter Wave Bands. // Abstracts of IX All-Russian Seminar on Radio Physics of Millimeters and Sub-Millimeters Waves, Nizhni-Novgorod, Institute of Applied Physics, 26 February - 1 March, 2013. - P.40.

[633] S.A. Kuznetsov, M.A. Astafiev, A.V. Arzhannikov, A.G. Paulish, A.V. Gelfand. Spectrum-Selective Bolometric Detectors and Visualizators of Radiation Beams for Millimeter and Sub-Millimeter Wave Band. // Abstracts of IX All-Russian Seminar on Radio Physics of Millimeters and Sub-Millimeters Waves, Nizhni-Novgorod, Institute of Applied Physics, 26 February - 1 March, 2013. - P.104.

[634] A.A. Shoshin, A.V. Burdakov, D.E. Gavrilenko, A. Huber, I.A. Ivanov, K.N. Kuklin, K.I. Mekler, A.A. Medvedeva, S.V. Polosatkin, V.V. Postupaev, S.L. Sinitsky and A.A. Vasilyev. Modification of preheated tungsten surface after irradiation at the GOL-3. // Book of

Abstracts 14th Intern. Conference on Plasma-Facing Materials and Components for Fusion Applications, May 13 - 17, 2013, Forschungszentrum Juelich, Germany. - P.78.

[635] A. Huber, M. Wirtz, B. Schweer, G. Sergienko, M. Zlobinski, I. Steudel, A. Arakcheev, A. Burdakov, J.W. Coenen, A. Kreter, J. Linke, Ph. Mertens, V. Philipps, G. Pintsuk, M. Reinhart, U. Samm, A. Shoshin, B. Unterberg. Investigation of the Impact on Tungsten of Transient Heat Loads applied by Laser Irradiation. // Book of Abstracts 14th Intern. Conference on Plasma-Facing Materials and Components for Fusion Applications, May 13 - 17, 2013, Forschungszentrum Juelich, Germany. - P.96.

[636] V.T. Astrelin, I.V. Kandaurov, V.M. Sveshnikov. Numerical simulation of transport and compression of electron beam by converging magnetic field during injection into multi-mirror trap GOL-3. // Papers of 11th All-Russian Seminar "Problems of Electron and Ion Optics", May 28 - 30, 2013, Moscow, Russia: Publisher SSC RF JSC "Orion". - P.20-24.

[637] V.T. Astrelin. Features of solving a plasma emission electronics problems in CAD POISSON-2. // Papers of 11th All-Russian Seminar "Problems of Electron and Ion Optics", May 28 - 30, 2013, Moscow, Russia: Publisher SSC RF JSC "Orion". - P.107-111.

[638] S.V. Polosatkin. On the interpretation of the results of the doppler spectroscopy of atomic beams. // Abstracts of the XV All-Russian Conference "Diagnostics of High-Temperature Plasma", Zvenigorod, June 3 - 7, 2013, P.51-53.

[639] V.F. Sklyarov, A.V. Arzhannikov, A.V. Burdakov, I.A. Ivanov, S.A. Kuznetsov, K.I. Mekler, S.V. Polosatkin, V.V. Postupaev, A.F. Rovenskikh, S.L. Sinitsky, M.A. Makarov. The Polarization of the Sub-Terahertz Radiation Exited by Collective Plasma Heating. // Abstracts of the XV All-Russian Conference "Diagnosis of High-Temperature Plasma", Zvenigorod, June 3 - 7, 2013, P.108-109.

[640] A.S. Arakcheev, A.A. Burdakov, A.A. Shoshin, A. Huber, M. Wirtz, G. Sergienko, I. Steudel, J.W. Coenen, A. Kreter, J. Linke, Ph. Mertens, V. Philipps, G. Pintsuk, M. Reinhart, U. Samm, B. Schweer, B. Unterberg, M. Zlobinski. Model of cracks formation in tungsten after heat loads. // 4th IEA Intern. Workshop on Plasma Material Interaction Facilities for Fusion Research (PMIF 2013), joint with the Plasma Facing Components 2013 Meeting (PFC 2013). 9 - 13 September 2013 in Oak Ridge, Tennessee, USA. [http://www.ornl.gov/sci/fed/PMIF13/PMIF-PFC13_404.pdf].

[641] A. Huber, M. Wirtz, B. Unterberg, G. Sergienko, I. Steudel, M. Zlobinski, A. Arakcheev, A. Burdakov, J.W. Coenen, A. Kreter, J. Linke, Ch. Linsmeier, Ph. Mertens, V. Philipps, G.Pintsuk, M. Reinhart, B. Schweer, A. Shoshin, A. Terra. Investigation of the impact on tungsten of transient heat loads applied by laser irradiation. // 4th IEA Intern. Workshop on Plasma Material Interaction Facilities for Fusion Research (PMIF 2013), joint with the Plasma Facing Components 2013 Meeting (PFC 2013). 9 - 13 September 2013 in Oak Ridge, Tennessee, USA. [http://www.ornl.gov/sci/fed/PMIF13/PMIF-PFC13_205.pdf].

[642] V.V. Postupaev, A.V. Burdakov, I.A. Ivanov, V.F. Sklyarov, A.V. Arzhannikov, D.Ye. Gavrilenko, I.V. Kandaurov, A.A. Kasatov, V.V. Kurkuchekov, K.I. Mekler, S.V. Polosatkin, S.S. Popov, A.F. Rovenskikh, A.V. Sudnikov, Yu.S. Sulyaev, Yu.A. Trunev, and L.N. Vyacheslavov. Temporal structure of 2ωp emission at plasma heating by long-pulse electron beam. // 40th EPS Conference on Plasma Physics, Vol.37D, ISBN 2-914771-84-3, 1 - 5 July 2013, Espoo, Finland, P5.409. [http://ocs.ciemat.es/EPS2013PAP/pdf/P5.409.pdf].

[643] I.A. Ivanov, A.V. Arzhannikov, M.A. Astafyev, A.V. Burdakov, S.A. Kuznetsov, K.I. Mekler, V.V. Postupaev, A.F. Rovenskikh, V.F. Sklyarov, M.K.A. Thumm. Sub-THz spectrally-selective quasi-optical system. // 40th EPS Conference on Plasma Physics, Vol.37D, ISBN 2-914771-84-3, 1 - 5 July 2013, Espoo, Finland, P6.008, [http://ocs.ciemat.es/EPS2013PAP/pdf/P6.008.pdf].

[644] Kuznetsov G.I., Batazova M.A. Electron - optical system of LIU-2 induction accelerator. // Proc. of the 10th Intern. Seminar on Particle Accelerator Problem, September 2013, Alushta, Crimea, Ukraine.

[645] S. Gurov, V. Kiselev, S. Sinyatkin. Current induced in vacuum chamber during NSLS-II booster ramp. // Proc of NA Particle Accelerator Conference (PAC'13), 29 September - 4 October 2013, Pasadena, USA. - MOPBA01.

[646] C. Bracco, E. Gschwendtner, A. Petrenko, H. Timko, T. Argyropoulos, H. Bartosik, T. Bohl, J. E. Muller, B. Goddard, M. Meddahi, A. Pardons, E. Shaposhnikova, F. M. Velotti, H. Vincke. Beam studies and experimental facility for the AWAKE experiment at CERN. // 1st European Advanced Accelerator Concepts Workshop (EAAC'2013), June 2 - 7, 2013, Elba, Italy.

[647] A. Petrenko, et. al. Electron injection into proton driven plasma wake-field for the AWAKE experiment at CERN. // 1st European Advanced Accelerator Concepts Workshop (EAAC'2013), June 2 - 7, 2013, Elba, Italy.

[648] Belchenko Yu.I., Gorbovsky A.I., Ivanov A.A., Konstantinov S.G., Sanin A.L., Shikhovtsev I.V., Tiunov M.A. Multiaperture negative ion source. // Third Intern. Symposium on Negative Ions, Beams and Sources (NIBS 2012), Jyvaskyla, Finland, Sept. 03-07, 2012. - Jyvaskyla, 2013. - P.167-176. - (AIP Conference Proc.; Vol.1515).

[649] Ivanov A.A., Abdrashitov G.F., Anashin V.V., Belchenko Yu.I., Burdakov A.V., Davydenko V.I., Deichuli P.P., Dimov G.I., Dranichnikov A.N., Kapitonov V.A., Kolmogorov V.V., Kondakov A.A., Popov S.S., Sanin A.L., Shikhovtsev I.V., Sorokin A.V., Stupishin N.V., Tiunov M.A., Belov V.P., Gorbovsky

A.I., Kobets V.V., Binderbauer M., Putvinski S., Smirnov A., Sevier L., et al. Development of a negative ion-based neutral beam injector in Novosibirsk. // Third Intern. Symposium on Negative Ions, Beams and Sources (NIBS 2012), Jyvaskyla, Finland, Sept. 3 - 7, 2012. - Jyvaskyla, 2013. - P.197-206. - (AIP Conference Proc.; Vol.1515).

[650] Belchenko Yu.I., Gorbovsky A.I., Ivanov A.A., Sanin A.L., Savkin V.Y., Tiunov M.A. Upgrade of CW negative hydrogen ion source. // Third Intern. Symposium on Negative Ions, Beams and Sources (NIBS 2012), Jyvaskyla, Finland, Sept. 03-07, 2012. - 2013. - P.448-455. - (AIP Conference Proc.; Vol.1515).

[651] Romanov, D. Berkaev, A. Kasaev, I. Koop, A. Kyrpotin, A. Lysenko, E. Perevedentsev, V. Prosvetov, Yu. Rogovsky, A. Senchenko, P. Shatunov, Yu. Shatunov, D. Shwartz, A. Skrinsky, I. Zemlyansky, Yu. Zharinov. Status of the electron-positron collider VEPP-2000. // Proc. of NA Particle Accelerator Conference (PAC'13), 29 September - 4 October 2013, Pasadena, USA.

[652] A. Romanov, I. Koop, E. Perevedentsev, D. Shwartz. Luminosity estimation and beam phase space analysis at VEPP-2000. // Proc. of NA Particle Accelerator Conference (PAC'13), 29 September - 4 October 2013, Pasadena, USA.

[653] V. Smaluk, O. Meshkov, G. Karpov, E. Bekhtenev, S. Karnaev BINP, Novosibirsk, Russia; O. Singh, D. Padrazo, K. Vetter, G. Wang, BNL, Upton, USA. Status of beam diagnostics for NSLS-II booster. // Second International Beam Instrumentation Conference, IBIC 2013, 16 - 19 September 2013, Oxford, UK.

[654] G.M. Wang, T. Shaftan, B. Bacha, A. Blednykh, E. Blum, W.X. Cheng, J. Choi, M. Davidsaver, J.De Long, L. Dalesio, R. Fliller, M. Fulkerson, G. George, W. Guo, K. Ha, H. Hseuh, Y. Hu, W. Louie, M. Maggipinto, J. Mead, D. Padrazo, G. Shen, K. Shroff, O. Singh, K. Vetter; Y. Tian, H. Xu, L. Yang, X. Yang, F. Willeke, BNL, New York, USA; V. Smalyuk, S. Karnaev, S. Sinyatkin, S. Gurov, A. Erokhin, E. Simonov, A. Derbenev, P. Cheblakov, R. Kadyrov, BINP, Novosibirsk, Russia. NSLS-II commissioning tools. // Proc. of NA Particle Accelerator Conference (PAC'13), 29 September - 4 October 2013, Pasadena, USA, MOPHO17.

[655] R. Kadyrov, P. Cheblakov, A. Derbenev, S. Karnaev, S. Serednyakov, E. Simonov, BINP, Novosibirsk, Russia; Scott Buda, Hsiao-Chaun Hseuh BNL, New York, USA; NSLS-II Booster interlock system. // The Intern. Conference on Accelerator and Large Experimental Physics Control Systems: ICALEPCS'13, October 6 - 11, 2013, San-Francisco, USA, MOPPC051.

[656] S. Karnaev, P. Cheblakov, A. Derbenev, R. Kadyrov, S. Serednyakov, E. Simonov, BINP, Novosibirsk, Russia; J. De Long, BNL, New York, USA. Status of the NSLS-II Booster Control System // The Intern. Conference on Accelerator and Large Experimental Physics Control Systems: ICALEPCS'13, October 6 - 11, 2013, San-Francisco, USA, MOPPC108.

[657] P. Cheblakov, D. Bolkhovityanov, R. Kadyrov, S. Karnaev, A. Makeev, BINP, Novosibirsk, Russia. Configuration system of the NSLS-II booster control system electronics. // The Intern. Conference on Accelerator and Large Experimental Physics Control Systems: ICALEPCS'13, October 6 - 11, 2013, San-Francisco, USA, MOPPC021.

[658] A. Derbenev, P. Cheblakov, R. Kadyrov, S. Karnaev, S. Serednyakov, E. Simonov, BINP, Novosibirsk, Russia; M. Davidsaver, BNL, New York, USA. Monitoring and archiving of NSLS-II booster synchrotron parameters. // The Intern. Conference on Accelerator and Large Experimental Physics Control Systems: ICALEPCS'13, October 6 - 11, 2013, San-Francisco, USA, TUPPC021.

[659] P. Cheblakov, A. Derbenev, R. Kadyrov, S. Karnaev, S. Serednyakov, E. Simonov, BINP, Novosibirsk, Russia; T. Shaftan, Y. Tian, BNL, New York, USA. NSLS-II booster ramp handling. // The Intern. Conference on Accelerator and Large Experimental Physics Control Systems: ICALEPCS'13, October 6 - 11, 2013, San-Francisco, USA, THPPC053.

[660] S. Taskaev. A new method for generating monoenergetic neutrons using accelerator. // NEUDOS-12 program: 3 - 7 June 2013, Aix-en-Provence, France, P.53.

[661] V.I. Aleinik, Z.Sh. Annaev, A.G. Bashkirtsev, A.V. Burdakov, N.V. Gubanova, V.V. Kanygin, D.A. Kasatov, A.I. Kichigin, a.S. Kuznetsov, A.N. Makarov, R.A. Morozov, I.N. Sorokin, S.Yu. Taskaev, I.M. Schudlo. Studies on innovative tandem accelerator with vacuum insulation. // Scientific and Practical Workshop "Accelerators for Russia's Future", 24 - 25 June 2013. - Abstracts: Moscow, MSU, P.28-31.

[662] V. Aleynik, Z. Annayev, N. Gubanova, V. Kanygin, D. Kasatov, A. Kichigin, A. Kiskayev, A. Kuznetsov, A. Makarov, R. Morozov, S. Taskaev, I. Shchudlo. Conducting of the biological research at the accelerator-based epithermal neutron source. // 7th Young Researchers' Boron Neutron Capture Therapy Meeting, 22 - 26 September 2013, Granada, Spain: Book of Abstracts, P.15.

[663] V. Aleynik, N. Gubanova, D. Kasatov, A. Kuznetsov, A. Makarov, R. Morozov, S. Taskaev, I. Shchudlo. VITA neutron source for BNCT - Status and Prospects. // 7th Young Researchers' Boron Neutron Capture Therapy Meeting, 22 - 26 September, Granada, Spain: Book of Abstracts, P.16.

[664] V. Aleynik, D. Kasatov, A. Kuznetsov, A. Makarov, S. Sinitskiy, S. Taskaev, I. Shchudlo. Neutron spectrum measurement on the tandem accelerator for BNCT using a new time-of-flight method. // 7th Young Researchers' Boron Neutron Capture Therapy Meeting,

22 - 26 September, Granada, Spain: Book of Abstracts, P.53.

[665] V.B. Reva, N.I. Alinovskiy, T.V. Bedareva, E.B., O.V. Belikov, V.N. Bocharov, V.V. Borodich, M.I. Bryzgunov, A.V. Bubley, V. Chekavinskiy, V. Cheskidov, B. Dovzhenko, A. Erokhin, M. Fedotov, A.D. Goncharov, K. Gorchakov, V.K. Gosteev, I. Gusev, A.V. Ivanov, G. Karpov, Yu. Koisin, M. Kondaurov, V. Kozak, A. Kruchkov, A. Lisitsyn, I. Lopatkin, V. Mamkin, A.S. Medvedko, V.M. Panasyuk, V.V. Parkhomchuk, I. Poletaev, V. Polukhin, A. Protopopov, D. Pureskin, A. Putmakov, P.A. Selivanov, E. Semenov, D. Senkov, D.N. Skorobogatov, N.P. Zapiatkin. Commissioning COSY cooler with electron beam at Novosibirsk. // COOL'13, TUPM2HA01, 10 - 14 June 2013, Murren, Switzerland: Proceedings. - P.79-83.

[666] M. Bryzgunov, A. Bubley, V. Panasyuk, V. Parkhomchuk, V. Reva. Matching of magnetic field with energy of electrons in 2 MeV COSY Cooler. // COOL'13, TUPM2HA01, 10 - 14 June 2013, Murren, Switzerland.

[667] M.I. Bryzgunov, A.V. Bubley, V.A. Chekavinskiy, I.A. Gusev, A.V. Ivanov, M.N. Kondaurov, V.M. Panasyuk, V.V. Parkhomchuk, D.N. Pureskin, A.A. Putmakov, V.B. Reva, D.V. Senkov, D.N. Skorobogatov. Collector for Electron cooling systems with suppression of reflected electron flux. // COOL'13, TUPM2HA01, 10 - 14 June 2013, Murren, Switzerland.

[668] M. Bryzgunov, A. Bubley, V. Cheskidov, M. Fedotov, V. Gosteev, O. Meshkov, V. Panasyuk, V. Parkhomchuk, V. Reva, BINP, Novosibirsk, Russia. V. Kamerdzhiev, G. Langenberg FZJ, Jülich, Germany. Compass for measuring the magnetic lines straightness at the cooling section in vacuum. // COOL'13, TUPM2HA01, 10 - 14 June, 2013, Murren, Switzerland.

[669] S.A. Rastigeev, A.D. Goncharov, V.F. Klyuev, E.S. Konstantinov, L.A. Kutnyakova, V.V. Parchkomchuk, A.V. Petrozhitskii, A.R. Frolov. Accelerator mass-spectrometer SB RAS. // XXIII Intern. Workshop on Charged Particle Accelerators (IWCPA) (Sarantsev memory), 3 - 7 September 2013, Ukraine.

[670] S.A. Rastigeev, A.D. Goncharov, V.F. Klyuev, E.S. Konstantinov, L.A. Kutnyakova, V.V. Parkhomchuk, A.V. Petrozhitsky, A.R. Frolov. Adaptation of BINP AMS to biomedical applications (in Russian). // X Int. Seminar on Charged Particle Accelerators in Commemoration of V.P. Sarantsev, 3 - 7 September 2013, Alushta, Ukraine.

[671] O.A. Shevchenko, V.S. Arbuzov, E.N. Dementyev, B.A. Dovzhenko, Ya.V. Getmanov, E.I. Gorniker, B.A. Knyazev, E.I. Kolobanov, A.A. Kondakov, V.R. Kozak, E.V. Kozyrev, S.A. Krutikhin, V.V. Kubarev, G.N. Kulipanov, E.A. Kuper, I.V. Kuptsov, G.Ya. Kurkin, L.E. Medvedev, L.A. Mironenko, V.K. Ovchar, V.M. Petrov, A.M. Pilan, V.M. Popik, V.V. Repkov, T.V. Salikova, M.A. Scheglov, I.K. Sedlyarov, S.S. Serednyakov, A.N. Skrinsky, S.V. Tararyshkin, V.G. Tcheskidov, A.G. Tribendis, N.A. Vinokurov, M.G. Vlasenko, P.D. Vobly, V.N. Volkov, BINP, Novosibirsk, Russia. // COOL'13, TUPM2HA01, 10 - 14 June 2013, Murren, Switzerland: Proceedings.

[672] V.I. Telnov. Issues with current designs of e+e- and γγ colliders. // Talk at PHOTON-2013: Intern. Conf. on the Structure and the Interactions of the Photon, May 20 - 24, 2013, Paris.

[673] V.I. Telnov. Crossing angle and beamdump at PLC. // Talk at LCWS-2013: Intern. Workshop on Future Linear Colliders, November 11 - 15 2013, Tokyo.

[674] V.I. Telnov, Problems of charge compensation in a ring e+e- Higgs factory. Talk at 5th TLEP Workshop, TLEP, Physics and Technology, July 25 – 26, FNAL, USA.

[675] V.I. Telnov. Photon collider Higgs factories. // Talk at European Linear Collider Workshop, LC-ECFA-2013, May 27-31, DESY, Hamburg, Germany.

[676] V.I. Telnov. Photon collider: summary. // Talk at European Linear Collider Workshop, LC-ECFA-2013, May 27 - 31, DESY, Hamburg, Germany.

[677] S. Dawson, A. Gritsan, V.I. Telnov, et al. Higgs Working Group Report of the Snowmass 2013 Community Planning Study. // Intern. Conference "Snowmass on the Mississippi", July 29 - August 6, 2013, Minneapolis, USA. [E-print:arXiv:1310.8361 [hep-ex]].

[678] V.I. Telnov. Comments on photon colliders for Snowmass 2013. // Intern. Conference "Snowmass on the Mississippi", July 29 - August 6, 2013, Minneapolis, USA. [arXiv:1308.4868 [physics.acc-ph]].

[679] I.A. Prokhorov, G.F. Abdrashitov, I.I. Averbukh, V.P. Belov, V.I. Davydenko, A.A. Ivanov, V.A. Kapitonov, V.V. Kolmogorov, A.A. Kondakov, I.V. Shikhovtsev, A.V. Sorokin, A.A. Tkachev. Ion source for 10 sec diagnostic neutral beam. // Transactions of Fusion Science and Technology. - 2013. - Vol.63, No1T. - P.349-351.

[680] A.A. Ivanov, V.I. Davydenko, I.A. Kotelnikov, A. Kreter, V.V. Mishagin, I.A. Prokhorov, I.V. Shikovtsev, B. Unterberg. High efficiency helicon plasma source for PMI studies. // Transactions of Fusion Science and Technology, 2013. - Vol.63, No1T. - P.217-220.

[681] T. Richert, J. Baldzuhn, V.I. Davydenko, U. Herbst, A.A. Ivanov, V.V. Kolmogorov, P. McNeely, M. Sauer, B. Schweer, I.V. Shikhovtsev. Diagnostic Neutral Beam Injector for WENDELSTEIN W7-X. // Abstracts of 25th Symposium on Fusion Engineering, June 10 - 14, 2013, San Francisco, California, paper 1416.

[682] A.A. Ivanov, V.I. Davydenko, V.A. Kapitonov, A.V. Sorokin, I.V. Shikhovtsev, V.P. Belov, A.A. Tkachev. A project of multi-aperture ion-optical system of quasi-stationary ion source. // Proc. of the 11th All-Russian Seminar "Problems of Theoretical Electron and Ion optics", 28 - 30 May 2013, Moscow, Russia, publ. SSC RF JSC "Orion", p.130-133.

[683] A. Listopad, Y. Belchenko, V. Davydenko, A. Ivanov, I. Ivanov, V. Kolmogorov, V. Mishagin, S. Putvinsky, G. Shulzhenko, A. Smirnov. Arc plasma generator for atomic driver in steady-state negative ion source. // The 15th Intern. Conference on Ion Sources ICIS-13, September 9 - 13, 2013, Chiba, Japan: Absracts, p.73.

[684] A.V. Kolmogorov, Grigor Atoian, Vladimir I. Davydenko, Alexander A. Ivanov, John Ritter, Nikolay V. Stupishin, Anatoli N.Zelenski. Production, Formation and transport of high-brightness atomic hydrogen beam studies for the RHIC polarized source upgrade. // The 15th Intern. Conference on Ion Sources ICIS-13, September 9 - 13, 2013, Chiba, Japan: Absracts, p.273.

[685] A. Zelenski, G. Atoian, J. Fite, D. Raparia, J. Ritter, D. Steski, V. Klenov, V. Zubets , V. Davydenko, A. Ivanov, A. Kolmogorov. The RHIC Polarized Source Upgrade. North American Particle Accelerator Conference, September 29 - October 4, Pasadena, California, USA, http://jacow.web.psi.ch/conf/pac13/prepress/MOOBA2.PDF.

[686] Ruktuev A. A., Golkovski M. G., Samoilenko V. V., Popelyuh A. I., Plotnikova N. V., Belousova N. S.- Multi-layer electron-beam welding of tantalum powder mixtures onto titanium BT1-0 blank (in Russian). // Obrabotka metallov: tehnologija, oborudovanie, instrumenty. - 2013. - №4. - P.43-48 - (Materialovedenie).

[687] Ruktuev A. A., Golkovski M. G., Samoilenko V. V., Popelyuh A.I., Plotnikova N.V., Belousova N.S. Multi-layer electron-beam welding of tantalum powder mixtures onto titanium BT1-0 blank (in Russian). // Obrabotka metallov: tehnologija, oborudovanie, instrumenty. - 2013. - №4. - P.43-48 - (Materialovedenie).

[688] K.V. Zaitsev, A.V. Anikeev, P.A. Bagryansky, A.S. Donin, O.A. Korobeinikova, M.S. Korzhavina, Yu.V. Kovalenko, A.A. Lizunov, V.V. Maximov, E.I. Pinzhenin, V.V. Prikhodko, E.I. Soldatkina, A.L. Solomakhin, V.Ya. Savkin and D.V. Yakovlev. Kinetic instabilities observations in the Gas Dynamic Trap. // Intern. Conference on Research and Applications of Plasmas, 2 - 6 September, 2013, Warsaw, Poland.

Preprints 2013

1. V.I. Kaplin. A.N. Kvashnin, E.B. Levichev, O.A. Plotnikova Programmable 32-channel temperature controller containing relays being controlled. // Preprint INP 2013-1, 18p. - Novosibirsk, 2013 (in Russian).

2. V.S. Fadin, R. Fiore, L.N. Lipatov, A. Papa. Mobius invariant BFKL equation for the adjoint representation in N=4 SUSY. // Preprint Budker INP 2013-6, 19p. - Novosibirsk, 2013 (in Russian).

3. D.S. Gurov, V.V. Zuev, P.V. Martyshkin, V.V. Petrov, M. Masuzawa (KEK). Development of Super B-factory correctors KEK. // Preprint INP 2013-8, 16p. - Novosibirsk, 2013 (in Russian).

4. A. Bondar, A. Buzulutskov, A. Dolgov, S. Peleganchuk R. Snopkov, A. Sokolov, E. Shemyakina, L. Shekhtman. Proposal for two-phase cryogenic avalanche detector for dark matter search and low-energy neutrino detection. // Preprint INP 2013-10, 22p. - Novosibirsk, 2013 (in Russian).

5. M.N. Achasov, V.M. Aulchenko, A.Yu. Barnyakov, K.I. Beloborodov, A.V. Berdyugin, D.E. Berkaev, A.G. Bogdanchikov, A.A. Botov, A.V. Vasiljev, V.B. Golubev, K.A. Grevtsov, T.V. Dimova, V.P. Druzhinin, I.M. Zemliansky, L.V. Kardapoltsev, A.S. Kasaev, A.N. Kirpotin, I.A. Koop, D.P. Kovrizhin, A.A. Korol, S.V. Koshuba, A.P. Lysenko, K.A. Martin, A.E. Obrazovsky, E.V. Pakhtusova, Yu.A. Rogovsky, A.L. Romanov, S.I. Serednyakov, Z.K. Silagadze, K.Yu. Skovpen, A.N. Skrinsky, I.K. Surin, Yu.A. Tikhonov, Yu.V. Usov, A.G. Kharlamov, P.Yu. Shatunov, Yu.M. Shatunov, D.A. Shtol, D.B. Shwartz. Status of e+ e– $\rightarrow$ n $\bar{n}$ process analysis using SND detector data from VEPP-2000 collider. // Preprint INP 2013-11, 19p. - Novosibirsk, 2013 (in Russian).

6. V.E. Blinov, E.A. Bekhtenev, A.P. Chabanov , O.P. Gordeev, S.A. Krutikhin, V.A. Kiselev, G.Ya. Kurkin, E.B. Levichev, O.I. Meshkov, A.I. Mikaiylov, V.V. Neifeld, S.A. Nikitin, I.B. Nikolaev, D.N. Shatilov G.M. Tumaikin, A.I. Zhmaka. RF system for electron and positron beams orbit separation at VEPP-4M. // Preprint INP 2013-12, 17p. - Novosibirsk, 2013 (in Russian).

7. V.M. Aulchenko, M.N. Achasov, A.Yu. Barnyakov, K.I. Beloborodov, A.V. Berdyugin, D.E. Berkaev, A.G. Bogdanchikov, A.A. Botov, A.V. Vasiljev, V.M. Vesenev, V.B. Golubev, K.A. Grevtsov, T.V. Dimova, V.P. Druzhinin, I.M. Zemlyansky, L.V. Kardapoltsev, A.S. Kasaev, A.N. Kirpotin, D.P. Kovrizhin, I.A. Koop, A.A. Korol, S.V. Koshuba, E.A. Kravchenko, A.Yu. Kulpin, A.S. Kupich, A.P. Lysenko, K.A. Martin, N.A. Melnikova, N.Yu. Muchnoi, A.E. Obrazovsky, A.P. Onuchin, E.V. Pakhtusova, E.A. Perevedentsev, K.V. Pugachev, Yu.A. Rogovsky, E.V. Rogozina, A.L. Romanov, A.I. Senchenko, S.I. Serednyakov, Z.K. Silagadze, A.A. Sirotkin, K.Yu. Skovpen, A.N. Skrinskii, I.K. Surin, A.I. Tekutev, Yu.A. Tikhonov, Yu.V. Usov, A.G. Kharlamov, Yu.M. Zharinov, Yu.M. Shatunov, P.Yu. Shatunov, D.B. Shwartz, D.A. Shtol, A.N. Shukaev. Experiments with the SND detector at the e+ e– collider VEPP-2000. // Preprint INP 2013-13, 23p. - Novosibirsk, 2013 (in Russian).

8. A. Bondar, A. Buzulutskov, A. Burdakov, E. Grishnyaev, A. Dolgov, A. Makarov, S. Polosatkin, A. Sokolov, S. Taskaev, L. Shekhtman. Proposal for neutron scattering systems for calibration of dark matter search and low-energy neutrino detectors. // Preprint INP 2013-14, 22p. - Novosibirsk, 2013 (in Russian).

9. I.Yu. Basok. Mechanical stability of wire structure of the KEDR drift chamber. // Preprint INP 2013-16, 35p. - Novosibirsk, 2013 (in Russian).

10. I. Balitsky and A.V. Grabovsky. NLO evolution of 3-quark Wilson loop operator. // Preprint Budker INP 2013-25, 52p. - Novosibirsk, 2013.

11. A.B. Bogomyagkov. K.V. Zolotarev, E.B. Levichev, P.A. Piminov, S.V. Sinyatkin. The electron storage ring project with the emittance limited by the diffraction limit and large dynamic aperture. // Preprint INP 2013-28, 38p. - Novosibirsk, 2013 (in Russian).

12. D.S. Gurov, P.V. Martyshkin, M. Masuzawa, V.V. Petrov, V.V. Zuev. Steering magnets for the upgrade of KEK B-factory. // Preprint Budker INP 2013-31, 15p. - Novosibirsk, 2013.

***

13. A. Caldwell, E. Gschwendtner, K. Lotov, P. Muggli, M. Wing, et al. (AWAKE Collab.). AWAKE Design Report: A Proton-Driven Plasma Wakefield Acceleration Experiment at CERN. // E-print: CERN-SPSC-2013-013; SPSC-TDR-003.

14. K. Lotov. Simulation of wakefield excitation and electron acceleration for AWAKE experiment. // E-print: CERN EDMS No.1276926.

15. S. Jolly, J. Bauche, E. Gschwendtner, D. Hall, G.le Godec, K. Lotov, S. Mandry, P. Muggli, A. Petrenko, and M. Wing. Design of the AWAKE Spectrometer. // E-print: CERN EDMS No. 1275622.

16. L. Yi, B. Shen, K. Lotov, L. Ji, X. Zhang, W. Wang, X. Zhao, Y. Yu, J. Xu, X. Wang, Y. Shi, L. Zhang, T. Xu, Z. Xu. Scheme for proton-driven plasma-wakefield acceleration of positively charged particles in a hollow plasma channel. // E-print: arXiv:1306.1613 [physics.plasm-ph].

17. K.V. Lotov. Excitation of two-dimensional plasma wakefields by trains of equidistant particle bunches. // E-print: arXiv:1307.3812 [physics.plasm-ph].

18. L. Yi, B. Shen, , L. Ji, K. Lotov, A. Sosedkin, X. Zhang, W. Wang, J. Xu, Y. Shi, L. Zhang, and Z. Xu. Positron acceleration in a hollow plasma channel up to TeV regime. // E-print: arXiv:1309.5691 [physics.plasm-ph].

19. V.L. Chernyak. Mass spectra in N=1 super-symmetric QCD with additional fields. III. // E-print: arXiv: 1308.5863 [hep-th].

20. A.G. Grozin. Introduction to effective field theories, 3. Bloch--Nordsieck effective theory, HQET. // arXiv:1305.4245 [hep-ph].

21. A.G. Grozin. Effective weak Lagrangians in the Standard Model and B decays. // arXiv:1311.0550 [hep-ph].

22. Valentin V. Sokolov, Oleg V. Zhirov. Chaotic Interference and Quantum-Classical Correspondence: Mechanisms of Decoherence and State Mixing. // arXiv:1311.1953 [quant-ph].

23. V.F. Dmitriev, A.I. Milstein, S.G. Salnijov. Isoscalar amplitude dominance in e+e- annihilation to $N\bar{N}$ pair close to the threshold. // arXiv: 1307.0936 [hep-ph].

24. V.M. Khatsymovsky. On the Faddeev gravity on the piecewise flat manifold. // arXiv:1312.7116[gr-qc], p.1-10, (2013).

25. R.N Lee. LiteRed 1.4: a powerful tool for the reduction of the multiloop integrals. // arXiv: 1310.1145.

26. V.M. Katkov. On structure of the polarization operator in a magnetic field. // arXiv:1311.6205v1 [hep-ph].

27. V.V. Anashin, V.M. Aulchenko, E.M. Baldin, A.K. Barladyan, A.Yu. Barnyakov, M.Yu. Barnyakov, S.E. Baru, I.Yu. Basok, O.L. Rezanova, A.E. Blinov, V.E. Blinov, A.V. Bobrov, V.S. Bobrovnikov, A.V. Bogomyagkov, A.E. Bondar, A.R. Buzykaev, S.I. Eidelman, D.N. Grigoriev, Yu.M. Glukhovchenko, V.V. Gulevich, D.V. Gusev, S.E. Karnaev, G.V. Karpov, S.V. Karpov, T.A. Kharlamova, V.A. Kiselev, V.V. Kolmogorov, S.A. Kononov, K.Yu. Kotov, E.A. Kravchenko, V.F. Kulikov, G.Ya. Kurkin, E.A. Kuper, E.B. Levichev, D.A. Maksimov, V.M. Malyshev, A.L. Maslennikov, A.S. Medvedko, O.I. Meshkov, S.I. Mishnev, I.I. Morozov, N.Yu. Muchnoi, V.V. Neufeld, S.A. Nikitin, I.B. Nikolaev, I.N. Okunev, A.P. Onuchin, S.B. Oreshkin, I.O. Orlov, A.A. Osipov, S.V. Peleganchuk, S.G. Pivovarov, P.A. Piminov, V.V. Petrov, A.O. Poluektov, V.G. Prisekin, A.A. Ruban, V.K. Sandyrev, G.A. Savinov, A.G. Shamov, D.N. Shatilov, B.A. Shwartz, E.A. Simonov, S.V. Sinyatkin, A.N. Skrinsky, V.V. Smaluk, A.V. Sokolov, A.M. Sukharev, E.V. Starostina, A.A. Talyshev, V.A. Tayursky, V.I. Telnov, Yu.A. Tikhonov, K.Yu. Todyshev, G.M. Tumaikin, Yu.V. Usov, A.I. Vorobiov, A.N. Yushkov, V.N. Zhilich, V.V. Zhulanov, A.N. Zhuravlev. Measurement of the ratio of the leptonic widths $\Gamma_{ee}/\Gamma_{\mu\mu}$ for the J/ψ meson. // E-print: arXiv:1311.5005v2 [hep-ex]].

28. Adam, …, F.V. Ignatov, B.I. Khazin, A.S. Popov, Yu.V. Yudin (MEG Collaboration) Measurement of polarized muon radiative decay. // E-print: arXiv:1312.3217 [hep-ex].

29. A. Baldini, …, F.V. Ignatov, B.I. Khazin, A.S. Popov, Yu.V. Yudin (MEG Collaboration) MEG Upgrade Proposal. e-Print: arXiv:1301:7225 [physics.ins-det].

30. A. Bogomyagkov, E. Levichev, D. Shatilov. Beam-beam effects investigation and parameters optimization for a circular e+e- collider TLEP to study the Higgs boson. // arXiv:1311.1580 [physics.acc-ph] (or arXiv:1311.1580v1 [physics.acc-ph] for this version).

31. E.V Abakumova, M.N. Achasov, D.E. Berkaev, V.V. Kaminsky, I.A. Koop, A.A. Korol, S.V. Koshuba, A.A. Krasnov, N.Yu. Muchnoi, E.A. Perevedentsev, E.E. Pyata, P.Yu. Shatunov, Yu.M. Shatunov, D.B. Shwartz. A system of beam energy measurement based on the

Compton backscattered laser photons for the VEPP-2000 electron-positron collider. // E-print: arXiv:1310.7764.

32. M. Ablikim, M.N. Achasov, N.Yu. Muchnoi, I.B. Nikolaev, et al. Search for $\eta c(2S)$ and hc decays into pp^- . // E-print: arXiv:1310.6099 [hep-ex].

33. M. Ablikim, M.N. Achasov, N.Yu. Muchnoi, I.B. Nikolaev, et al. Observation of the decay $\psi(3686) \to \Lambda\Sigma\pm \pi^{-+}$ +c.c. // E-print: arXiv:1310.5826 [hep-ex].

34. M. Ablikim, M.N. Achasov, N.Yu. Muchnoi, I.B. Nikolaev, et al. Observation of $e+e- \to \gamma X(3872)$ at BESII. // E-print: arXiv:1310.4101 [hep-ex].

35. M. Ablikim, M.N. Achasov, N.Yu. Muchnoi, I.B. Nikolaev, et al. Observation of a charged $(D\ \bar{D})^-$ mass peak in $e^+e^- \to \pi^+ (D\ \bar{D})^-$ at Ecm = 4.26 GeV. // E-print: arXiv:1310.1163 [hep-ex].

36. M. Ablikim, M.N. Achasov, N.Yu. Muchnoi, I.B. Nikolaev, et al. Observation of a charged charmoniumlike structure in e+e− → (D*D¯*) ± π^{-+} at √s = 4.26 GeV. // E-print: arXiv:1308.2760 [hep-ex].

37. M. Baszczyk, P. Dorosz, J. Kolodziej, M.Yu. Barnyakov, V.E. Blinov, A.A. Botov, V.P. Druzhinin, V.B. Golubev, S.A. Kononov, E.A. Kravchenko, E.B. Levichev, A.P. Onuchin, S.I. Serednyakov, D.A. Shtol, Y.I. Skovpen, E. P. Solodov, et al. SuperB Technical Design Report. Jun 24, 2013. 495p. INFN-13-01-PI, LAL-13-01, SLAC-R-1003. e-Print: arXiv:1306.5655 [physics.ins-det].

38. M.N. Achasov, V.M. Aulchenko, A.Yu. Barnyakov, K.I. Beloborodov, A.V. Berdyugin, A.G. Bogdanchikov, A.A. Botov, T.V. Dimova, V.P. Druzhinin, V.B. Golubev K.A. Grevtsov, L.V. Kardapoltsev, A.G. Kharlamov, D.P. Kovrizhin, I.A. Koop, A.A. Korol, S.V. Koshuba, A.P. Lysenko, K.A. Martin, A.E. Obrazovsky, E.V. Pakhtusova, E.A. Perevedentsev, A.L. Romanov, S.I. Serednyakov, Z.K. Silagadze, A.N. Skrinsky, I.K. Surin, Yu. A. Tikhonov, A.V. Vasiljev, P.Yu. Shatunov, Yu. M. Shatunov, D.A. Shtol. Study of the process $e^+e^- \to \eta\gamma$ in the center-of-mass energy range 1.07–2.00 GeV. // E-print: arXiv:1312.7078.

39. M. Bicer, H.D. Yildiz, …, V.I. Telnov, et al. First look at the physics case of TLEP. // E-print: arXiv:1308.6176 [hep-ex].

40. V.I. Telnov. Higgs factories. // E-print: arXiv:1307.3893.

41. V.I. Telnov. Limitation on the luminosity of e+e– storage rings due to beamstrahlung. // E-print: arXiv:1307.3915 [physics.acc-ph].

42. D. Bernard (on behalf of the BaBar Collab.), Blinov V.E., Buzykaev A.R., Druzhinin V.P., Golubev V.B., Kravchenko E.A., Onuchin A.P., Serednyakov S.I., Skovpen Yu.I., Solodov E.P., Todyshev K.Yu, Yushkov A.N., et al. Measurement of e^+e^- to hadrons cross sections at BABAR, and implication for the muon g-2. // PoS Hadron 2013. 126. [arXiv:1402.0618 [hep-ex]].

43. J.P. Lees (BaBar Collab.), Blinov V.E., Buzykaev A.R., Druzhinin V.P., Golubev V.B., Kravchenko E.A., Onuchin A.P., Serednyakov S.I., Skovpen Yu.I., Solodov E.P., Todyshev K.Yu, Yushkov A.N., et al. Search for the decay B^0-bar $\to \Lambda^+_c\ \bar{p}\ p\ \bar{p}$. // [arXiv:1312.6800 [hep-ex]].

44. J.P. Lees (BaBar Collab.), Blinov V.E., Buzykaev A.R., Druzhinin V.P., Golubev V.B., Kravchenko E.A., Onuchin A.P., Serednyakov S.I., Skovpen Yu.I., Solodov E.P., Todyshev K.Yu, Yushkov A.N., et al. Measurement of the $B \to Xs\ l^+l^-$ branching fraction from a sum of exclusive final states. // arXiv: 1312.5364 [hep-ex].

45. J.P. Lees, (BaBar Collabor.), Blinov V.E., Buzykaev A.R., Druzhinin V.P., Golubev V.B., Kravchenko E.A., Onuchin A.P., Serednyakov S.I., Skovpen Yu.I., Solodov E.P., Todyshev K.Yu, Yushkov A.N., et al. Evidence for the decay $B^0 \to \omega\omega$ and search for $B^0 \to \omega\varphi$. // arXiv:1312.0056 [hep-ex].

46. V. Santoro (BaBar Collabor.), Blinov V.E., Buzykaev A.R., Druzhinin V.P., Golubev V.B., Kravchenko E.A., Onuchin A.P., Serednyakov S.I., Skovpen Yu.I., Solodov E.P., Todyshev K.Yu, Yushkov A.N., et al. Studies of charmonium production at BaBar. // arXiv:1311.7531 [hep-ex].

47. V.P. Druzhinin (on behalf of the BABAR Collaboration). Measurement of the proton electromagnetic form factors at BABAR. // arXiv:1311.7517 [hep-ex].

48. J.P. Lees, (BaBar Collabor.), Blinov V.E., Buzykaev A.R., Druzhinin V.P., Golubev V.B., Kravchenko E.A., Onuchin A.P., Serednyakov S.I., Skovpen Yu.I., Solodov E.P., Todyshev K.Yu, Yushkov A.N., et al. Search for lepton-number violating $B^+ \to X^-\ l^+\ l'^+$ decays. // [arXiv:1310.8238 [hep-ex]].

49. E.M.T.I. Puccio (BaBar Collabor.), Blinov V.E., Buzykaev A.R., Druzhinin V.P., Golubev V.B., Kravchenko E.A., Onuchin A.P., Serednyakov S.I., Skovpen Yu.I., Solodov E.P., Todyshev K.Yu, Yushkov A.N., et al. Lepton-number violation in B decays at BaBar. // arXiv:1310.0876 [hep-ex].

50. J.P.Lees (BaBar Collabor.), Blinov V.E., Buzykaev A.R., Druzhinin V.P., Golubev V.B., Kravchenko E.A., Onuchin A.P., Serednyakov S.I., Skovpen Yu.I., Solodov E.P., Todyshev K.Yu, Yushkov A.N., et al. Measurement of Collins asymmetries in inclusive production of charged pion pairs in e^+e^- annihilation at BABAR. // arXiv:1309.5278 [hep-ex].

51. G. Eigen (BaBar Collabor.), Blinov V.E., Buzykaev A.R., Druzhinin V.P., Golubev V.B., Kravchenko E.A., Onuchin A.P., Serednyakov S.I., Skovpen Yu.I., Solodov E.P., Todyshev K.Yu, Yushkov A.N., et al. Radiative penguin decays at e^+e^- colliders. // arXiv:1309.1327 [hep-ex].

52. RM. White (BaBar Collabor.), Blinov V.E., Buzykaev A.R., Druzhinin V.P., Golubev V.B.,

Kravchenko E.A., Onuchin A.P., Serednyakov S.I., Skovpen Yu.I., Solodov E.P., Todyshev K.Yu, Yushkov A.N., et al. Search for CP Violation in Charm at e^+e^- colliders. // arXiv:1308.0080 [hep-ex].

53. A.P. Perez (BaBar Collabor.), Blinov V.E., Buzykaev A.R., Druzhinin V.P., Golubev V.B., Kravchenko E.A., Onuchin A.P., Serednyakov S.I., Skovpen Yu.I., Solodov E.P., Todyshev K.Yu, Yushkov A.N., et al. Recent results on T and CP violation at BABAR. // arXiv:1307.2759.

54. A.P. Perez (BaBar Collabor.), Blinov V.E., Buzykaev A.R., Druzhinin V.P., Golubev V.B., Kravchenko E.A., Onuchin A.P., Serednyakov S.I., Skovpen Yu.I., Solodov E.P., Todyshev K.Yu, Yushkov A.N., et al. Light Higgs and dark photon searches at BABAR. // arXiv:1307.2758.

55. J.P. (BaBar Collabor.), Blinov V.E., Buzykaev A.R., Druzhinin V.P., Golubev V.B., Kravchenko E.A., Onuchin A.P., Serednyakov S.I., Skovpen Yu.I., Solodov E.P., Todyshev K.Yu, Yushkov A.N., et al. Study of the K^+ K^- invariant-mass dependence of CP asymmetry in $B^+ \rightarrow K^+K^- K^+$ decays. // arXiv:1305.4218 [hep-ex].

56. A. Denig (BaBar Collabor.), Blinov V.E., Buzykaev A.R., Druzhinin V.P., Golubev V.B., Kravchenko E.A., Onuchin A.P., Serednyakov S.I., Skovpen Yu.I., Solodov E.P., Todyshev K.Yu, Yushkov A.N., et al. Measurement of the π^0, $\eta\eta'$ transition form factors at BaBar. // Nucl. Phys. Proc. Suppl.- 2013. Vol.234. - P.283.

57. E.M.T.I. Puccio (BaBar Collabor.), Blinov V.E., Buzykaev A.R., Druzhinin V.P., Golubev V.B., Kravchenko E.A., Onuchin A.P., Serednyakov S.I., Skovpen Yu.I., Solodov E.P., Todyshev K.Yu, Yushkov A.N., et al. Direct CP violation in charmless B decays at BaBar. // arXiv:1301.5668 [hep-ex].

58. E.Ben-Haim (BaBar Collabor.), Blinov V.E., Buzykaev A.R., Druzhinin V.P., Golubev V.B., Kravchenko E.A., Onuchin A.P., Serednyakov S.I., Skovpen Yu.I., Solodov E.P., Todyshev K.Yu, Yushkov A.N., et al. Results on β from BABAR. // arXiv:1301.4133 [hep-ex].

59. D. Derkach (BaBar Collabor.), Blinov V.E., Buzykaev A.R., Druzhinin V.P., Golubev V.B., Kravchenko E.A., Onuchin A.P., Serednyakov S.I., Skovpen Yu.I., Solodov E.P., Todyshev K.Yu, Yushkov A.N., et al. Combination of gamma measurements from BaBar. // arXiv:1301.3283 [hep-ex].

60. J.L. Ritchie (BaBar Collabor.), Blinov V.E., Buzykaev A.R., Druzhinin V.P., Golubev V.B., Kravchenko E.A., Onuchin A.P., Serednyakov S.I., Skovpen Yu.I., Solodov E.P., Todyshev K.Yu, Yushkov A.N., et al. Angular Analysis of $B \rightarrow K^*l^+l^-$ in BABAR. // arXiv:1301.1700 [hep-ex].

61. R.F. Cowan (BaBar Collabor.), Blinov V.E., Buzykaev A.R., Druzhinin V.P., Golubev V.B., Kravchenko E.A., Onuchin A.P., Serednyakov S.I., Skovpen Yu.I., Solodov E.P., Todyshev K.Yu, Yushkov A.N., et al. Observation of Time-reversal Violation at BABAR. // arXiv:1301. 1372 [hep-ex].

62. A. Rossi (BaBar Collabor.), Blinov V.E., Buzykaev A.R., Druzhinin V.P., Golubev V.B., Kravchenko E.A., Onuchin A.P., Serednyakov S.I., Skovpen Yu.I., Solodov E.P., Todyshev K.Yu, Yushkov A.N., et al. Search for $B \rightarrow \nu\nu$-bar and related modes with the BABAR detector. // arXiv:1301.1179 [hep-ex].

63. J.L. Ritchie (BaBar Collabor.), Blinov V.E., Buzykaev A.R., Druzhinin V.P., Golubev V.B., Kravchenko E.A., Onuchin A.P., Serednyakov S.I., Skovpen Yu.I., Solodov E.P., Todyshev K.Yu, Yushkov A.N., et al. BABAR results on $B \rightarrow Xs\ \gamma$. // arXiv:1301.0836 [hep-ex].

Authorial papers 2013

1. LEE R.N. Quasiclassical approach to the description of the QED processes in the field of a heavy atom. // 01.04.01 - instruments and methods of experimental physics, Author. papers of thesis for the degree of doctor of phys.-math. science: Novosibirsk, 2013, BINP, SB RAS.

2. TIMOFEEV I.V. Excitation of small-scale turbulence and electromagnetic emission in a magnetized plasma with an electron beam. // 01.04.08 - physics of plasma Author. papers of thesis for the degree of doctor of phys.-math. science: Novosibirsk, 2013, BINP, SB RAS.

3. ACHASOV M.N. Study of light vector mesons in the hadron processes in e+e− annihilation. Study of light vector mesons in the processes of hadron production in e+e - annihilation // 01.04.16 - elementary particle physics, and atomic nuclear physics, Author. papers of thesis for the degree of doctor of phys.-math. science: Novosibirsk, 2013, BINP, SB RAS.

4. KOLMOGOROV V.V. Power supply systems of neutral beam injectors for plasma diagnostic and heating. // 01.04.20 – physics of charged particle beams and accelerator techniques, Author. papers of thesis for the degree of doctor of technical science: Novosibirsk, 2013, BINP, SB RAS.

5. GERASIMOV V.V. Methods for surface study using terahertz radiation of free-electron laser. // 01.04.01 - instruments and methods of experimental physics, Author. papers of thesis for the degree of candidate of phys.-math. science: Novosibirsk, 2013, BINP, SB RAS.

6. SALNIKOV S.S. Spin effects in electron-proton and nucleon-antinucleon interaction // 01.04.02 - theoretical physics, Author. papers of thesis for the degree of candidate of phys.-math. science: Novosibirsk, 2013, BINP, SB RAS.

7. KOZLOV M.G. Multi Regge amplitudes in non Abelian gauge theories. // 01.04.02 - theoretical physics,

Author. papers of thesis for the degree of candidate of phys.-math. science: Novosibirsk, 2013, BINP, SB RAS.

8. ARAKCHEEV A.S. Behabiour of materials under high power plasma load. // 01.04.08 - physics of plasma, Author. papers of thesis for the degree of candidate of phys.-math. science: Novosibirsk, 2013, BINP, SB RAS.

9. LIZUNOV A.A. Spatial profiles of anisotropic plasma pressure in the gas dynamic trap. // 01.04.08 - physics of plasma, Author. papers of thesis for the degree of candidate of phys.-math. science: Novosibirsk, 2013, BINP, SB RAS.

10. SUDNIKOV A.V. Spatial structure of the plasma in multi-mirror trap with the longitudinal current. // 01.04.08 - physics of plasma, Author. papers of thesis for the degree of candidate of phys.-math. science: Novosibirsk, 2013, BINP, SB RAS.

11. KARDAPOLTSEV L.V. Measurement of the cross-section process of $e^+e^-\to\omega\pi \to \pi^0\pi^0\gamma$ in the energy range 1.05–2.00 GeV with SND. // 01.04.16 - elementary particle physics, and atomic nuclear physics, Author. papers of thesis for the degree of candidate of phys.-math. science: Novosibirsk, 2013, BINP, SB RAS

12. AKIMOV A.V. A high-voltage pulse power supply of the linear induction accelerator LIU-2. // 01.04.20 - physics of charged particle beams and accelerator techniques, Author. papers of thesis for the degree of candidate of technical science: Novosibirsk, 2013, BINP, SB RAS.

13. BRYZGUNOV M.I. Electron collector for high-voltage cooling system for COSY. // 01.04.20 - physics of charged particle beams and accelerator techniques, Author. papers of thesis for the degree of candidate of phys.-math. science: Novosibirsk, 2013, BINP, SB RAS

14. SHWARTZ D.B. Round beams at VEPP-2000 collider. // 01.04.20 - physics of charged particle beams and accelerator techniques, Author. papers of thesis for the degree of candidate of phys.-math. science: Novosibirsk, 2013, BINP, SB RAS.

15. SHATILOV D.N. Beam-beam simulations for circular colliders. // 01.04.20 - physics of charged particle beams and accelerator techniques, Author. papers of thesis for the degree of candidate of phys.-math. science: Novosibirsk, 2013, BINP, SB RAS.

Participation in conferences 2013

1. XL International Zvenigorod Conference on Plasma Physics and Controlled Fusion, 11 - 15 February 2013 Zvenigorod, Russia.

2. 4th Asian Forum for Accelerators and Detectors, 25 - 26 February 2013, Novosibirsk, Russia.

3. PINP Winter School, 2013, 25 - 28 February, Saint-Petersburg, Russia.

4. IX All-Russian Seminar on Radio Physics of Millimeters and Sub-Millimeters Waves, Institute of Applied Physics, 26 February - 1 March, Nizhni-Novgorod.

5. 13th Vienna Conference on Instrumentation, VCI 2013, February, 2013, Vienna, Austria.

6. 2013 International Symposium on Grids and Clouds, ISGC 2013, 17 - 22 March, 2013, Taipei, Taiwan.

7. V All-Russian Conference, 26 - 29 March 2013, Novosibirsk, Russia.

8. 51th International Student Scientific Conference "Student and Scientific-Technical Progress", 12 - 18 April, 2013. BINP, Novosibirsk, Russia.

9. VIII International Workshop of QWG, April 22 - 26 2013, Beijing, China.

10. 21st International Workshop on Deep-Inelastic Scattering and Related Subjects, DIS 2013, 22 - 26 April, 2013, Marseilles, France.

11. International Congress on Particle Technology, PARTEC 2013, 23 - 25 April, 2013, Nurnberg, Germany.

12. 4th International Particle Accelerator Conference, IPAC 2013, 12 - 17 May 2013, Shanghai, China.

13. 14th International Conference on Plasma-Facing Materials and Components for Fusion Applications, May 13 - 17, 2013, Forschungszentrum Juelich, Germany.

14. International Conference on the Structure and the Interactions of the Photon, PHOTON-2013, May 20 - 24, 2013, Paris.

15. 6th International Workshop on "Quantum Chaos and Localization Phenomena", 24 - 26 May, 2013, Warsaw, Poland.

16. European Linear Collider Workshop, LC-ECFA-2013, May 27-31, 2013, DESY, Hamburg, Germany.

17. 11th All-Russian Seminar "Problems of Electron and Ion Optics", May 28 - 30, 2013, Moscow, Russia.

18. XV National Conference on High-Temperature Plasma Diagnostics, 3 - 7 June, 2013, Zvenigorod.

19. COOL'13, 10 - 14 June 2013, Murren, Switzerland.

20. 25th Symposium on Fusion Engineering, June 10 - 14, 2013, San Francisco, California, USA.

21. International Conference "Chaotic Modeling and Simulation", CHAOS 2013, 11- 14 June, 2013, Istambul, Turkey.

22. Scientific and Practical Workshop "Accelerators for Russia's Future", 24 - 25 June 2013, Moscow, Russia.

23. 8 International Forum on Strategic Technologies, IFOST 2013, 28 June - 1 July, 2013, Ulaanbaatar, Mongolia.

24. 40th European Physical Society Conference on Plasma Physics, 1 - 5 July, 2013, Espoo, Finland.

25. 1st European Advanced Accelerator Concepts Workshop, EAAC'2013, June 2 - 7, 2013, Elba, Italy.

26. 3rd Low Emittance Ring Workshop, 8 - 10 July, Oxford UK.

27. 2013 European Physical Society Conference on High Energy Physics, EPSHEP 2013, 18 - 24 July, 2013, Stockholm, Sweden.

28. 5th TLEP Workshop, TLEP, Physics and Technology, July 25 - 26 FNAL, USA.

29. International Conference “Snowmass on the Mississippi”, July 29 - August 6, 2013, Minneapolis, USA.

30. IV International Symposium "Modern Problems of Laser Physics", MPLP'2013, August 25 - 31, 2013, Novosibirsk, Russia.

31. 35th International Free-Electron Laser Conference, FEL 2013, 26 - 30 August, 2013, New York, US.

32. International Conference on Research and Applications of Plasmas, 2 - 6 September, 2013, Warsaw, Poland.

33. X International Seminar on Charged Particle Accelerators in Commemoration of V.P. Sarantsev, 3 - 7 September 2013, Alushta, Ukraine.

34. Conference “From phi to psi”, September 9 - 12, Rome, Italy.

35. Workshop on Fundamental Interactions PSI, 9 - 12 September, 2013, Zurich.

36. 53th ICFA Advanced Beam Dynamics Workshop on Energy Recovery Linacs, ERL-2013, 9 - 13 September, 2013, Novosibirsk, INP, Russia.

37. 4th IEA International Workshop on Plasma Material Interaction Facilities for Fusion Research, PMIF 2013, joint with the Plasma Facing Components 2013 Meeting, PFC 2013, 9 - 13 September 2013, Tennessee, USA.

38. Second International Beam Instrumentation Conference, IBIC 2013, 16 - 19 September 2013, Oxford, UK.

39. 15th International Conference on Ion Sources ICIS-13, September 9 - 13, 2013, Chiba, Japan.

40. XI Russian Conference on Semiconductor Physics, 16 - 20 September, 2013, St. Petersburg, Russia.

41. 21th Annual International Conference on Advanced Laser Technologies, ALT'13, September, 16 - 20, 2013, Budva, Montenegro.

42. 7th Young Researchers' Boron Neutron Capture Therapy Meeting, 22 - 26 September, 2013, Granada, Spain.

43. North American Particle Accelerator Conference, September 29 - October 4, Pasadena, California, USA.

44. International Conference on Accelerator and Large Experimental Physics Control Systems, ICALEPCS’13, October 6 - 11, 2013, San-Francisco, USA.

45. VI All-Russian Meeting on Fundamental Constants and Precision Measurements, October 7 - 11, St. Petersburg, Russia.

46. International Symposium on Lepton and Hadron Physics at Meson, Factories, October 13 - 15, Messina, Italy.

47. 6th TLEP Workshop, 16 - 18 October 2013, CERN.

48. 2nd All-Russian Scientific Conference "Methods of Investigation of Composition and Structure of Functional Materials" MISSFM 2013, 21 - 25 October. 2013, Novosibirsk, Russia.

49. 17th International Meeting on Radiation Processing, IMRP 2013, 4 - 8 November, 2013, Shanghai.

50. XV International Conference on Hadron Spectroscopy, Hadron 2013, November 4 - 8, 2013, Nara, Japan.

51. Internernational Conference-Session of Section of Nuclear Physics of the Physical Sciences Division of the Russian Academy of Sciences, 5 - 8 November, 2013, BINP, Novosibirsk, Russia.

52. session conference of the DPS RAS nuclear physics section, 5 - 8 November 2013, Protvino, Russia.

53. International Workshop on Future Linear Colliders, LCWS-2013, November 11 - 15, 2013, Tokyo.

54. Workshop on Electron Beam Accelerator Technology, 25 November - 6 December, 2013, Kuala Lumpur, Malaysia.

55. 8th International Workshop on Ring Imaging Cherenkov Detectors (RICH 2013), December 2013, Japan.

56. IX International Scientific Congress and Exhibition Interexpo Geo-Siberia 2013; Int. Conference SibOptika 2013: Collection of Materials, Novosibirsk, Russia.

List of Collaboration Agreements between the Budker INP and Foreign Laboratories

Name of Laboratory		Title or Field of Collaboration	Dates	Principal Investigators
№	*1*	*2*	*3*	*4*
1	*Daresbury (England)*	Generation and utilization of SR.	1977	*G. Kulipanov (INP); I. Munro (Daresbury)*
2	*BESSY (Germany)*	Development of the wigglers for BESSY-2.	1993	*A. Skrinsky, N. Mezentsev (INP); E. Jaeschke (BESSY)*
3	*Research Centre Rossendorf (Germany)*	Physical foundations of a plasma neutron source.	1994	*E. Kruglyakov, A. Ivanov (INP); K. Noack (Germany)*
4	*Nuclear Centre "Karlsruhe" (Germany)*	1. Development of conceptual project and data base for neutron source on the basis of GDT device. 2. Simulation of processes in diverter of ITER device.	1994	*E. Kruglyakov, A. Ivanov, A. Burdakov (INP); G. Kessler (Germany)*
5	*GSI (Germany)*	Collaboration in the field of accelerator physics: electron cooling; electron-ion colliders.	1995	*Yu. Shatunov, V. Parkhomchuk (INP); H. Eickhoff (GSI)*
6	*DESY (Germany)*	Elementary-particle physics, synchrotron radiation, accelerator physics and technology, electronics and experimental equipment.	1995	*A. Skrinsky, G. Kulipanov (INP); A. Vagner, K. Scherff (DESY)*
7	*CIEMAT (Spain)*	Accelerator technology and plasma physics.	2007	*E. Levichev (INP), J. Rubio (CIEMAT)*
8	*CELLS (Spain)*	Collaboration in the field of application of new equipment for SR sources.	2008	*E. Levichev (INP); Joan Bordas and Orpinell (CELLS)*
9	*INFN (Italy)*	Development of intense source for radioactive ion beams for experiments in nuclear physics	1984	*P. Logachev (INP); L. Techio (INFN)*
10	*University of Milan (Italy)*	Theoretical and numerical studies of dynamic chaos in classic and quantum mechanics.	1991	*A. Skrinsky, V. Sokolov (INP); T. Montegazza, J. Kasati (Italy)*
11	*INFN-LNF (Italy)*	Development of collider project DAFNE-II	2004	*E. Levichev (INP); S. Biscari (INFN-LNF)*
12	*University of Padua (Italy)*	Development of cryogenic detectors for experiments in neutrino physicist.	2008	*Yu. Tikhonov, A. Bondar (INP); A. Gudlielmi (Italy)*

№	*1*	*2*	*3*	*4*
13	*National Nuclear Center. Park of Nuclear Technology (Kazakhstan)*	Development and application of industrial accelerators, generation and utilization of neutron beams, development of SR sources, RF-generators.	2007	*G. Kulipanov (INP); K. Kadyrzhanov, A. Kusainov (Kazakhstan)*
14	*National Nuclear Center. Al-Farabi National University (Kazakhstan)*	Creation and development of a multi-purpose research complex of radiation technology and terahertz radiation.	2009	*G. Kulipanov (INP); K. Kadyrzhanov, B. Zhumagulov (Kazakhstan)*
15	*Institute of Morden Physics and Techniques, Lanchzou (China)*	Collaboration in the field of accelerator physics: electron cooling. .	2000	*V. Parkhomchuk (INP); S. Yang (PRC)*
16	*WOER Company, Shenzhen, (China))*	Using of electron accelerator ILU-10, exchanging of personal, information and experimental equipment.	2005	*A. Bryazgin (INP); Leo Li (WOER)*
17	*SINAP Shanghai, (China)*	Researching in field of industrial electron accelerators.	2006	*A. Bryazgin (INP); Hu Hounku (SINAP)*
18	*IHEP (China)*	Work of Chinese scientists on BINP installations, work of BINP scientists on IHEP installations.	2007	*A. Skrinsky (INP); H. Chen (IHEP)*
19	*Industrial and Technological Center of Cooperation with Russia and Belorussia of Heilongjiang Province (P.R.C) (China)*	Exchange of information about BINP-developed devices and the technology and product demand of the Chinese factories.	2009	*D. Grigoriev (INP); Zhan Hun-Vei (PRC)*
20	*POSTECH (Korea)*	Creation of beam accelerators, add-on devices, SR experiments.	1992	*A. Skrinsky, N. Mezentsev (INP); H. Kim (POSTECH)*
21	*KAERI (Korea)*	Development of FEL and accelerator-recuperator.	1999	*N. Vinokurov (INP); B.Ch. Lee (KAERI)*
22	*BNL, Brookhaven (USA)*	1. Measurement of the magnetic muon anomaly. 2. Joint research of RHIC spin.	1991 1993	*L. Barkov (INP); J. Bunse (BNL)* *Yu. Shatunov (INP); S. Ozaki (BNL)*
23	*ANL, Argonn (USA)*	1. Experiments with polarized gas jet target at VEPP-3. 2. SR instrumentation.	1988 1993	*L. Barkov (INP); R. Holt (ANL)* *G. Kulipanov, A. Skrinsky (INP); G. Shenoy (USA)*

№	*1*	*2*	*3*	*4*
24	*University of Pittsburgh (USA)*	Experiments on VEPP-2M and ϕ-factory.	1989	*S. Eidelman, E. Solodov (INP); V. Savinov (USA)*
25	*University of Duke (USA)*	Free electron lasers.	1992	*N. Vinokurov (INP); J. Wu (Duke)*
26	*BNL, Brookhaven (USA)*	Collaboration on electron-ion colliders.	1993	*V. Parkhomchuk (INP); I. Benzvi (USA)*
27	*FERMILAB (USA)*	Collaboration in the field of accelerator physics: electron cooling; conversion system.	1995	*V. Parkhomchuk (INP); O. Finli (FERMILAB)*
28	*FERMILAB (USA)*	Exchange of scientists and engineers for scientific research.	2005	*A. Skrinsky (INP); P. Oddone (FERMILAB)*
29	*SLAC, Stanford (USA)*	Obtainment of submicron beams and intensive positron beams, development of B-factory elements, detectors, RF-generators based on magnicons.	1994	*A. Skrinsky (INP); Persis Drel (SLAC)*
30	*Institute of Plasma Physics ASCR (Czech Republic)*	Collaboration in the field of plasma physics and plasma diagnostics research.	2008	*A. Ivanov (INP); P. Hruška (Czech Republic)*
31	*CERN (Switzerland)*	1. Research and development of the detectors for LHC. 2. Development of the LHC elements.	1992 1996	*A. Bondar, Yu. Tikhonov (INP); T. Nakada, P. Yenni (CERN) V. Anashin (INP); L. Evans (CERN)*
32	*Paul Scherrer Institute (Switzerland)*	Collaboration in the field of particle physics.	2009	*D. Grigoriev (INP); D. Mecom (Paul Scherrer Institute)*
33	*CERN (Switzerland)*	Research and development of micro-pattern detector technology..	2009	*Yu. Tikhonov (INP); S. Bertolucci (CERN)*
34	*CERN (Switzerland)*	Collaboration in the development of the electron-positron colliders with super-high luminosity.	2009	*E. Levichev (INP); S. Myers (CERN)*
35	*RIKEN Spring-8 (Japan)*	Collaboration in the field of accelerator physics and synchrotron radiation	1996	*G. Kulipanov (INP); H. Kamitsubo (Japan)*
36	*KEK (Japan)*	Research in accelerator physics and allied fields, development of elementary particle detectors.	1995	*A. Skrinsky (INP); A. Suzuki (KEK)*
37	*Center of Plasma Research, Tsukuba (Japan)*	Collaboration on Open traps.	2007	*A. Ivanov (INP); T. Imai (Japan)*

Research Personnel

Members of Russian Academy of Science

Academicians:

Barkov Lev Mitrofanovich
Dikansky Nikolai Sergeevich
Kulipanov Gennady Nikolaevich
Skrinsky Alexandr Nikolaevich

Corresponding members:

Bondar Alexandr Evgenievich
Vinokurov Nikolai Alexandrovich
Dimov Gennady Ivanovich
Logachev Pavel Vladimirovich
Parkhomchuk Vasily Vasilievich
Khriplovich Iosif Bentsionovich
Shatunov Yury Michailovich

Director Board

Director:

Skrinsky Alexandr Nikolaevich

Adviser RAN:

Kulipanov Gennady Nikolaevich

Scientific Secretary:

Vasiljev Alexei Vladimirovich

Deputy Director (scientific):

Bondar Alexandr Evgenievich
Burdakov Alexandr Vladimirovich
Ivanov Alexandr Alexandrovich
Levichev Evgeny Borisovich
Logachev Pavel Vladimirovich
Mezentsev Nikolai Alexandrovich
Tikhonov Yury Anatoljevich

Scientific Council

1. Academician, Chairman	Skrinsky A.N.
2. Corr. member RAS, Co-Chairman	Bondar A.E.
3. Corr. member RAS, Co-Chairman	Burdakov A.V.
4. Doctor of phys.-math. science	Ivanov A.A.
5. Doctor of phys.-math. science	Levichev E.B.
6. Corr. member RAS, Co-Chairman	Logachev P.V.
7. Doctor of phys.-math. science, Co-Chairman	Mezentsev N.A.
8. Doctor of phys.-math. science, Professor	Tikhonov Yu.A.
9. Candidate of phys.-math. science, Sci. Secretary	Vasiljev A.V.
10. Doctor of phys.-math. science	Bagryansky P.A.
11. Doctor of techn. science	Batrakov A.M
12. Candidate of phys.-math. science	Beklemishev A.D.
13. Doctor of phys.-math. science	Blinov V.E.
14. Candidate of techn. science	Bryazgin A.A.
15. Corr. member RAS	Vinokurov N.A.
16. Academician	Dikansky N.S.

17. Corr. member RAS	Dimov G.I.
18. Doctor of phys.-math. science	Druzhinin V.P.
19. Candidate of phys.-math. science	Zolotarev K.V.
20. Candidate of phys.-math. science	Kardapoltsev L.V. – Chairman of Council of Young scientists
21. Doctor of techn. science	Kolmogorov V.V.
22. Doctor of phys.-math. science	Koop I.A.
23. Candidate of phys.-math. science	Krasnov A.A.
24. Doctor of techn. science	Kuksanov N.K.
25. Academician	Kulipanov G.N.
26. Doctor of phys.-math. science	Lotov K.V.
27. Doctor of phys.-math. science	Meshkov O.I.
28. Doctor of phys.-math. science, Professor	Milstein A.I.
29. Corr. Member RAS	Parkhomchuk V.V.
30. Candidate of phys.-math. science	Rakshun Ya.V. – Chairman of Council of Young scientists
31. Doctor of phys.-math. science, Professor	Serednyakov S.I.
32. Candidate of phys.-math. science	Starostenko A.A.
33. Doctor of phys.-math. science, Professor	Fadin V.S.
34. Doctor of phys.-math. science	Khazin B.I.
35. Corr. Member RAS	Khriplovich I.B.
36. Corr. Member RAS	Shatunov Yu.M.
37. Candidate of techn. science	Shiyankov S.V.
38. Doctor of phys.-math. science	Eidelman S.I.

Specialized Sections of Scientific Council

Accelerators for Applied Purposes

Kulipanov G.N. (Chrmn.)
Gorbunov V.A. (Secr.)
Anashin V.V.
Antokhin E.I.
Batrakov A.M.
Bondar A.E.
Bryazgin A.A.
Chernyakin A.D.
Churkin I.N.
Dikansky N.S.
Erokhin A.I.
Fadeev S.N.
Goldenberg B.G.
Gurov D.S.
Ivanov A.A.
Karpov G.V.
Knyazev B.A.
Kolmogorov V.V.
Korchagin A.I.
Kuksanov N.K.
Kuper E.A.
Kuper K.E.
Kurkin G.Ya.
Levichev E.B.
Logachev P.V.
Medvedko A.S.
Mezentsev N.A.
Mishnev S.I.
Nemytov P.I.
Nikolenko A.D.
Onuchin A.P.
Parkhomchuk V.V.
Petrichenkov M.V.
Petrov V.M.
Pindyurin V.F.
Pyata E.E.
Rakshun Ya.V.
Salimov R.A.
Shatunov Yu.M.
Shevchenko O.A.
Shkaruba V.A.
Skrinsky A.N.
Tribendis A.G.
Tumaikin G.M.
Vinokurov N.A.
Vostrikov V.A.
Zolotarev K.V.

Plasma Physics and Controlled Fusion Problems

Ivanov A.A. (Chrmn)
Kandaurov I.V. (Secr.)
Anikeev A.V.
Akhmetov T.D.
Arzhannikov A.V.
Astrelin V.T.
Bagryansky P.A.
Beklemishev A.D.
Belchenko Yu.I.
Burdakov A.V.
Burmasov V.S.
Dimov G.I.
Davydenko V.I.
Ivanov I.A.
Kapitonov V.A.
Khilchenko A.D.
Konstantinov S.G.
Kotelnikov I.A.
Kulipanov G.N.
Kuznetsov A.S.
Lizunov A.A.
Lotov K.V.
Mekler K.I.
Murakhtin S.V.
Polosatkin S.V.
Popov S.S.
Postupaev V.V.
Prikhodko V.V.
Sanin A.L.
Sinitsky S.L.
Skrinsky A.N.
Soldatkina E.I.
Solomakhin A.L.
Sorokin A.V.
Sulyaev Yu.S.
Taskaev S.Yu.
Timofeev I.V.
Shiyankov S.V.
Volosov V.I.
Vasiljev A.V.
Voskoboinikov P.V.
Vyacheslavov L.N.

Colliding Beams

Parkhomchuk V.V. (Chrmn)
Petrov V.V. (Secr.)
Anashin V.V.
Barkov L.M.
Batrakov A.M.
Berkaev D.E.
Blinov V.E.
Bondar A.E.
Bryazgin A.A.
Dikansky N.S.
Erokhin A.I.
Gorbunov V.A.
Gurov S.M.
Khazin B.I.
Kiselev V.A.
Kolmogorov V.V.
Koop I.A.
Krasnov A.A.
Kulipanov G.N.
Kuksanov N.K.
Kuper E.A.
Kurkin G.Ya.
Levichev E.B.
Logachev P.V.
Medvedko A.S.
Meshkov O.I.
Mezentsev N.A.
Mishnev S.I.
Nikitin S.A.
Onuchin A.P.
Perevedentsev E.A.
Pestrikov D.V.
Petrov V.M.
Reva V.B.
Salimov R.A.
Shatilov D.N.
Shatunov P.Yu.
Shatunov Yu.M.
Shevchenko O.A.
Shiyankov S.V.
Simonov E.A.
Skrinsky A.N.
Solodov E.P.
Starostenko A.A.
Shwartz D.B.
Tikhonov Yu.A.
Tumaikin G.M.
Vasiljev A.V.
Vinokurov N.A.
Vobly P.D.
Zolotarev K.V.

Physics of Elementary Particles

Bondar A.E. (Chrmn.)
Tayursky V.A. (Secr.)
Achasov M.N.
Aulchenko V.M.
Barkov L.M.
Baru S.E.
Berkaev D.E.
Blinov A.E.
Blinov V.E.
Buzulutskov A.F
Chernyak V.L.
Dimova T.V.
Dmitriev V.F.
Druzhinin V.P.
Eidelman S.I.
Fadin V.S.
Fedotovich G.V.
Garmash A.Yu.
Golubev V.B.
Grebenyuk A.A.
Grigoriev D.N.
Groshev V.R.
Grozin A.G.
Ignatov F.V.
Katkov V.M.
Kharlamov A.G.
Khazin B.I.
Khriplovich I.B.
Kononov S.A.
Koop I.A.
Kravchenko E.A.
Krokovny P.P.
Kuzmin A.S.
Lee R.N.
Levichev E.B.
Logachev P.V.
Logashenko I.B.
Lukin P.A.
Malyshev V.M.
Maslennikov A.L.
Milshtein A.I.
Muchnoi N.Yu.
Nikolaev I.B.
Nikolenko D.M.
Obrazovsky A.E.
Onuchin A.P.
Pakhtusova E.V.
Peleganchuk S.V.
Parkhomchuk V.V.
Pestov Yu.N.
Pivovarov S.G.
Pomeransky A.A.
Popov A.S.
Rachek I.A.
Redin S.I.
Ryskulov N.M.
Serednyakov S.I.
Shamov A.G.
Shatunov Yu.M.
Shekhtman L.I.
Shwartz B.A.
Shwartz D.B.
Silagadze Z.K.
Skovpen Yu.I.
Skrinsky A.N.
Sokolov A.V.
Sokolov V.V.
Solodov E.P.
Telnov V.I.
Terekhov I.S.
Todyshev K.Yu.
Tikhonov Yu.A.
Toporkov D.K.
Vasiljev A.V.
Vorob'ev A.I.
Zhilich V.N.

Automation

Tikhonov Yu.A. (Chrmn)
Kuper E.A. (Co-Chrmn)
Baldin E.M. (Secr.)
Dubrov S.V. (Secr.)
Aleshaev A.N.
Amosov S.A.
Aulchenko V.M.
Banzarov V.Sh.
Batrakov A.M.
Belov S.D.
Berkaev D.E.
Bolkhovityanov D.Yu.
Buzykaev A.R.
Cheblakov P.B.
Faktorovich B.P.
Grozin A.G.
Kaplin V.I.
Khilchenko A.D.
Kolmogorov V.V.
Koop I.A.
Korol A.A.
Kovalenko Yu.V.
Kupchik V.I.
Kurilin O.Yu.
Kuzin M.V.
Kvashnin A.N.
Levichev E.B.
Logashenko I.B.
Maximova S.V.
Medvedko A.S.
Nekhanevich E.L.
Shatunov Yu.M.
Shuvalov B.N.
Solodov E.P.
Sukharev A.M.
Tararyshkin S.V.
Tsukanov V.M.
Vasiljev A.V.

SIBERIAN BRANCH OF RUSSIAN ACADEMY OF SCIENCES
BUDKER INSTITUTE OF NUCLEAR PHYSICS

ANNUAL REPORT
2013

Cover E.D. Bender

Ответственный за выпуск А.В. Васильев
Работа поступила 14.05. 2014 г.

Сдано в набор 15.06. 2014 г.
Подписано в печать 30.07. 2014 г.
Формат 60x90 1/16 Объем 14,4 печ.л., 11,5 уч.-изд.л.
Тираж 100 экз. Бесплатно. Заказ № 13

Обработано на РС и отпечатано
на ротапринте «ИЯФ им. Г.И. Будкера» СО РАН,
Новосибирск, 630090, пр. Академика Лаврентьева, 11